

RICHARD HERRMANN

FRACTIONAL CALCULUS

AN INTRODUCTION FOR PHYSICISTS

2ND EDITION



FRACTIONAL CALCULUS

AN INTRODUCTION FOR PHYSICISTS

2ND EDITION

This page intentionally left blank

FRACTIONAL CALCULUS

AN INTRODUCTION FOR PHYSICISTS

2ND EDITION



RICHARD HERRMANN

GigaHedron, Germany



NEW JERSEY • LONDON • SINGAPORE • BEIJING • SHANGHAI • HONG KONG • TAIPEI • CHENNAI

Published by

World Scientific Publishing Co. Pte. Ltd.

5 Toh Tuck Link, Singapore 596224

USA office: 27 Warren Street, Suite 401-402, Hackensack, NJ 07601

UK office: 57 Shelton Street, Covent Garden, London WC2H 9HE

Library of Congress Cataloging-in-Publication Data

Herrmann, Richard, author.

Fractional calculus : an introduction for physicists / Richard Herrmann, GigaHedron, Germany. -- 2nd edition.

pages cm

Includes bibliographical references and index.

ISBN 978-9814551076 (hardcover : alk. paper)

1. Fractional calculus. I. Title.

QC20.7.F75H4775 2014

515'.83--dc23

2013048544

British Library Cataloguing-in-Publication Data

A catalogue record for this book is available from the British Library.

Copyright © 2014 by World Scientific Publishing Co. Pte. Ltd.

All rights reserved. This book, or parts thereof, may not be reproduced in any form or by any means, electronic or mechanical, including photocopying, recording or any information storage and retrieval system now known or to be invented, without written permission from the publisher.

For photocopying of material in this volume, please pay a copying fee through the Copyright Clearance Center, Inc., 222 Rosewood Drive, Danvers, MA 01923, USA. In this case permission to photocopy is not required from the publisher.

In-house Editor: Rhaimie Wahap

Printed in Singapore

Intentio vero nostra est
manifestare in hoc libro
ea, que sunt, sicut sunt,
et ad artis certitudinem redigere,
quorum nullus scientiam habuit
hactenus neque artem.

Fridericus Romanorum Imperator Secundus (1194–1250)
De arte venandi cum avibus

This page intentionally left blank

Preface to the Second Edition

We are pleased that the first edition of *Fractional Calculus - An Introduction for Physicists* and its reprint has found many friends among students and scientists.

With the necessity for a second edition arising, we used the opportunity to implement several improvements, expansions and explanatory remarks, which enhance comprehensibility and are a reflection of helpful discussions and hints from colleagues and readers all over the world.

This new, extended edition reflects the broadening range of developments and demonstrations of the fractional approach in different branches of physics, in particular:

Image processing - presenting a fractional approach resulting in a stable algorithm for 3D-shape recovery from sequences of aperture afflicted slides obtained in confocal microscopy or autofocus algorithms.

Folded potentials in cluster physics, where a new interpretation of the Riesz fractional integral is given in terms of a smooth transition from Coulomb to Yukawa-potentials.

Infrared spectroscopy, with a first practical application of the fractional quantum harmonic oscillator to describe rot-vib spectra in diatomic molecules from a generalized point of view.

Numerical solutions of the fractional Schrödinger equation show the influence of nonlocal concepts in quantum mechanics.

Triaxiality as a ground state property of nuclei is investigated using an analytical fractional model.

Local aspects for alternative fractional derivative definitions and consequences are discussed.

Fractional calculus with variable order is discussed and the impact of genetic strategies based on evolutionary differential equations to describe cosmological models is investigated.

As a new feature we present exercises with elaborated solutions, which help to get acquainted with presented strategies and allow for a direct investigation and application of new concepts developed within the framework of fractional calculus. We discuss questions, which help to gain a deeper understanding of general aspects of the theory. This book will also be a valuable addition for courses devoted to this subject.

We hope, that this new edition will motivate students and scientists to explore the fascinating, still mysterious world of fractional calculus and apply these new ideas in their own research area, too.

We thank Anke Friedrich for her continuous support and the publishing team of World Scientific for their help.

Richard Herrmann
Dreieich, Germany
Autumn, 2013

Preface to the First Edition

Theoretical physics has evolved into a multi-faceted science. The sheer amount of knowledge accumulated over centuries forces a lecturer to focus on the mere presentation of derived results. The presentation of strategies or the long path to find appropriate tools and methods often has been neglected.

As a consequence, from a students point of view, theoretical physics seems to be a construct of axiomatic completeness, where apparently is no space left for speculations and new approaches. The limitations of presented concepts and strategies are not obvious until these tools are applied to new problems.

Especially the creative process of research, which evolves beyond the state of mere reception of already known interrelations is a particular ambition of most students.

One prerequisite to reach that goal is a permanent readiness, to question even well-established results and check the validity of common statements time and time again. Already Roger Bacon in his *opus majus* pointed out, that the main causes of error are the belief in false authority, the force of habit, the ignorance of others and pretended knowledge [Bacon (1267)].

New concepts and new methods depend on each other. The unified theory of electro-magnetism by James Clerk Maxwell was motivated by Faraday's experiments. The definite formulation was then realized in terms of a new theory of partial differential equations. Einstein's general relativity is based on experiments on the constancy of the speed of light; the elegant presentation was made possible with Riemann's tensor calculus.

This book too takes up an at first simple idea: due to the fact that differential equations play such a central role in physics since the times of Newton and since the first and second derivative denote such fundamental

properties as velocity and acceleration, does it make sense, to investigate the physical meaning of a half, a π -th and an imaginary derivative?

This interesting question has been raised since the days of Leibniz and has been discussed by all mathematicians of their times. But for centuries no practical applications could be imagined.

During the last years fractional calculus has developed rapidly. This process is still going on, but we can already recognize, that within the framework of fractional calculus new concepts and strategies emerge, which make it possible, to obtain new challenging insights and surprising correlations between different branches of physics.

This is the basic purpose of this book: to present a concise introduction to the basic methods and strategies in fractional calculus and to enable the reader to catch up with the state of the art on this field and to participate and contribute in the development of this exciting research area.

In contrast to other monographs on this subject, which mainly deal with the mathematical foundations of fractional calculus, this book is devoted to the application of fractional calculus on physical problems. The fractional concept is applied to subjects in classical mechanics, group theory, quantum mechanics, nuclear physics, hadron spectroscopy up to quantum field theory and will surprise the reader with new intriguing insights.

This book provides a skilful insight into a vividly growing research area and opens the reader's mind to a world yet completely unexplored. It encourages the reader to participate in the exciting quest for new horizons of knowledge.

Richard Herrmann
Dreieich, Germany
Summer, 2010

Acknowledgments

As a young student, I had the opportunity to attend the Nobel Laureate Meeting at Lindau/Germany in 1982. Especially Paul Dirac's talk [Dirac (1963); Dirac (1984); Farmelo (2009)] was impressive and highly inspiring and affirmed my aspiration to focus my studies on theoretical physics.

I joined the Institute for Theoretical Physics in Frankfurt/Germany. Working on the fission properties of super heavy elements, I suggested to linearise the collective Schrödinger equation used in nuclear collective models and to introduce a new collective degree of freedom, the collective spin. Within this project, my research activities concentrated on the field theoretical implications, which follow from linearized wave equations. As a direct consequence the question of the physical interpretation of multi-factorized wave equations and of a fractional derivative came up.

I achieved a breakthrough in my research program in 2005: I found that a specific realization of the fractional derivative suffices to describe the properties of a fractional extension of the standard rotation group $SO(n)$. This was the key result to start an investigation of symmetries of fractional wave equations and the concept of a fractional group theory could be successfully realized. Up to now, this concept has led to a vast amount of intriguing and valuable results.

This success would not have been possible without the permanent enduring loving support of my family and friends.

I am grateful to all those who shared their knowledge with me and made suggestions reflected in this book. Special thanks go to Anke Friedrich and Günter Plunien for their encouragement and their valuable contributions.

I also want to emphasize, that fractional calculus is a world wide activity. I benefited immensely from international support and communication. Suggestions from, discussions and correspondence with Elsayed Ahmed,

Eberhard Engel, Ervin Goldfain, Cezar Ionescu, Virginia Kiryakova, Swee Cheng Lim, Yuri Luchko, Ahmad-Rami El-Nabulsi, Manuel Ortigueira, Dirk Troltenier and Volker Schneider were particularly useful.

Finally I want to express my gratitude to the publishing team of World Scientific for their support.

Contents

<i>Preface to the Second Edition</i>	vii
<i>Preface to the First Edition</i>	ix
<i>Acknowledgments</i>	xi
<i>List of Exercises</i>	xix
1. Introduction	1
2. Functions	7
2.1 Gamma function	8
2.2 Mittag-Leffler functions	9
2.3 Hypergeometric functions	11
2.4 Miscellaneous functions	12
3. The Fractional Derivative	15
3.1 Basics	15
3.2 The fractional Leibniz product rule	20
3.3 The fractional derivative in terms of finite differences - the Grünwald-Letnikov derivative	22
3.4 Discussion	24
3.4.1 Orthogonal polynomials	24
3.4.2 Differential representation of the Riemann and Caputo fractional derivative	26
4. Friction Forces	33

4.1	Classical description	33
4.2	Fractional friction	36
5.	Fractional Calculus	43
5.1	The Fourier transform	44
5.2	The fractional integral	45
5.2.1	The Liouville fractional integral	46
5.2.2	The Riemann fractional integral	46
5.3	Correlation of fractional integration and differentiation	47
5.3.1	The Liouville fractional derivative	48
5.3.2	The Riemann fractional derivative	49
5.3.3	The Liouville fractional derivative with inverted operator sequence - the Liouville-Caputo fractional derivative	50
5.3.4	The Riemann fractional derivative with inverted operator sequence - the Caputo fractional derivative	52
5.4	Fractional derivative of second order	53
5.4.1	The Riesz fractional derivative	54
5.4.2	The Feller fractional derivative	56
5.5	Fractional derivatives of higher orders - the Marchaud fractional derivative	58
5.6	Erdélyi-Kober operators of fractional integration	61
5.7	Geometric interpretation of the fractional integral	62
5.8	Low level fractionality	63
5.9	Discussion	66
5.9.1	Semi-group property of the fractional integral . .	66
6.	The Fractional Harmonic Oscillator	69
6.1	The fractional harmonic oscillator	70
6.2	The harmonic oscillator according to Fourier	70
6.3	The harmonic oscillator according to Riemann	72
6.4	The harmonic oscillator according to Caputo	74
7.	Wave Equations and Parity	77
7.1	Fractional wave equations	77
7.2	Parity and time-reversal	78
7.3	Solutions of the free regularized fractional wave equation .	80
8.	Nonlocality and Memory Effects	87

8.1	A short history of nonlocal concepts	87
8.2	From local to nonlocal operators	90
8.3	Memory effects	100
9.	Fractional Calculus in Multidimensional Space — 2D-Image Processing	107
9.1	The generalized fractional derivative	108
9.2	Shape recovery - the local approach	110
9.3	Shape recovery - the nonlocal approach	114
10.	Fractional Calculus in Multidimensional Space — 3D-Folded Potentials in Cluster Physics	121
10.1	Folded potentials in fragmentation theory	122
10.2	The Riesz potential as smooth transition between Coulomb and folded Yukawa potential	126
10.3	Discussion	134
10.3.1	Calculation of a fission yield	134
11.	Quantum Mechanics	141
11.1	Canonical quantization	143
11.2	Quantization of the classical Hamilton function and free solutions	144
11.3	Temperature dependence of a fission yield and determina- tion of the corresponding fission potential	147
11.4	The fractional Schrödinger equation with an infinite well potential	150
11.5	Radial solutions of the fractional Schrödinger equation . .	156
12.	The Fractional Schrödinger Equation with the Infinite Well Potential — Numerical Results using the Riesz Derivative	161
12.1	The problem - analytic part	161
12.2	The solution - numerical part	170
13.	Uniqueness of a Fractional Derivative — the Riesz and Regularized Liouville Derivative as Examples	173
13.1	Uniqueness on a global scale - the integral representation of the Riesz derivative	174
13.2	Uniqueness on a local scale - the differential representation of the Riesz derivative	178

13.3	Manifest covariant differential representation of the Riesz derivative on \mathbb{R}^N	182
13.4	The integral representation of the regularized Liouville derivative	185
13.5	Differential representation of the regularized Liouville derivative	188
13.6	Manifest covariant differential representation of the regularized Liouville derivative on \mathbb{R}^N	190
13.7	Generalization of a fractional derivative	191
14.	Fractional Spin — A Property of Particles Described with the Fractional Schrödinger Equation	193
14.1	Spin - the classical approach	194
14.2	Fractional spin	195
15.	Factorization	199
15.1	The Dirac equation	200
15.2	Linearization of the collective Schrödinger equation	202
15.3	The fractional Dirac equation	206
15.4	The fractional Pauli equation	208
16.	Symmetries	213
16.1	Characteristics of fractional group theory	214
16.2	The fractional rotation group SO_N^α	216
17.	The Fractional Symmetric Rigid Rotor	223
17.1	The spectrum of the fractional symmetric rigid rotor	223
17.2	Rotational limit	227
17.3	Vibrational limit	227
17.4	Davidson potential - the so called γ -unstable limit	229
17.5	Linear potential limit	230
17.6	The magic limit	232
17.7	Comparison with experimental data	235
18.	q-deformed Lie Algebras and Fractional Calculus	245
18.1	q-deformed Lie algebras	246
18.2	The fractional q-deformed harmonic oscillator	248
18.3	The fractional q-deformed symmetric rotor	253

18.4	Half integer representations of the fractional rotation group $SO^\alpha(3)$	255
19.	Infrared Spectroscopy of Diatomic Molecules	259
19.1	The fractional quantum harmonic oscillator	260
19.2	Numerical solution of the fractional quantum harmonic oscillator	262
19.3	The infrared-spectrum of HCl	268
20.	Fractional Spectroscopy of Hadrons	279
20.1	Phenomenology of the baryon spectrum	280
20.2	Charmonium	285
20.3	Phenomenology of meson spectra	291
20.4	Metaphysics: about the internal structure of quarks	300
21.	Magic Numbers in Atomic Nuclei	305
21.1	The four decompositions of the mixed fractional $SO^\alpha(9)$	306
21.2	Notation	308
21.3	The 9-dimensional fractional Caputo-Riemann-Riemann symmetric rotor	311
21.4	Magic numbers of nuclei	312
21.5	Ground state properties of nuclei	315
21.6	Fine structure of the single particle spectrum - the extended Caputo-Riemann-Riemann symmetric rotor	320
21.7	Triaxiality	325
21.8	Discussion	328
21.8.1	Curvature interaction in the collective Riemannian space	328
22.	Magic Numbers in Metal Clusters	339
22.1	The Caputo-Caputo-Riemann symmetric rotor - an analytic model for metallic clusters	340
22.2	Binding energy of electronic clusters	343
22.3	Metaphysics: magic numbers for clusters bound by weak and gravitational forces respectively	346
23.	Fractors — Fractional Tensor Calculus	353
23.1	Covariance for fractional tensors	353

23.2	Singular fractional tensors	354
24.	Fractional Fields	357
24.1	Fractional Euler-Lagrange equations	358
24.2	The fractional Maxwell equations	361
24.3	Discussion	364
24.3.1	Lagrangian density for a space fractional Schrödinger equation	364
25.	Gauge Invariance in Fractional Field Theories	369
25.1	Gauge invariance in first order of the coupling constant \bar{g}	370
25.2	The fractional Riemann-Liouville-Zeeman effect	374
26.	On the Origin of Space	379
26.1	The interplay between matter and space	380
26.2	Fractional calculus with time dependent α in the adiabatic limit	383
26.3	The model and possible consequences for an application in cosmology	386
26.4	On the detectability of dynamic space evolution	389
26.5	Meta physics: on the connection between dark matter and dark energy	390
27.	Outlook	395
Appendix A	Solutions to exercises	397
<i>Bibliography</i>		439
<i>Index</i>		473

List of exercises

Exercise 2.1 <i>Fractional binomials</i>	14
Exercise 2.2 <i>Solution of the cubic equation in terms of hypergeometric functions</i>	14
Exercise 3.1 <i>The Riemann derivative of $x^\alpha/(1-x)$</i>	31
Exercise 3.2 <i>The Riemann derivative of $x^p/(1-x)$</i>	31
Exercise 3.3 <i>Eigenvalues and eigenfunctions of the Caputo fractional derivative</i>	31
Exercise 3.4 <i>Asymptotic behavior of the the Grünwald-Letnikov fractional derivative</i>	32
Exercise 4.1 <i>Eigenfunctions for a first order fractional differential equation with purely imaginary fractional coefficient α</i>	42
Exercise 5.1 <i>The Laplace transform of the Mittag-Leffler function</i>	68
Exercise 5.2 <i>The Caputo derivative of $\ln(1+x)$</i>	68
Exercise 5.3 <i>Low level fractionality for $\ln(1+x)$</i>	68
Exercise 6.1 <i>Eigenfunctions of the m-th order Caputo differential operator</i>	76
Exercise 8.1 <i>A linear delay differential equation</i>	105
Exercise 9.1 <i>A geometric interpretation of a generalized nonlocal integral</i>	118
Exercise 10.1 <i>Momentum dependence of nonlocal potentials</i>	140
Exercise 13.1 <i>The differential representation of the fractional Schrödinger equation in spherical coordinates</i>	192
Exercise 15.1 <i>Commutation relations for the matrix-representation of $U(d)$</i>	211
Exercise 15.2 <i>Linearization of a $2\lambda+1$ dimensional free collective Schrödinger equation</i>	212
Exercise 16.1 <i>Invariant commutation relations of canonically conjugated operators</i>	222
Exercise 16.2 <i>Asymptotic expansion of the eigenvalue spectrum of the fractional $SO^\alpha(2)$ and $SO^\alpha(3)$</i>	222
Exercise 18.1 <i>Fractional Euler polynomials</i>	257

This page intentionally left blank

Chapter 1

Introduction

During recent years the interest of physicists in nonlocal field theories has been steadily increasing. The main reason for this development is the expectation that the use of these field theories will lead to a much more elegant and effective way of treating problems in particle and high-energy physics as it has been possible up to now with local field theories.

Nonlocal effects may occur in space and time. For example in the time domain the extension from a local to a nonlocal description becomes manifest as a memory effect, which roughly states that the actual behaviour of a given object is not only influenced by the actual state of the system but also by events, which happened in the past.

In a first approach this could be interpreted as an ability of the object to collect or memorize previous events, an idea going back to the physics of Aristotle and perpetuated until the post-scholastic era. But this concept already irritated Descartes [Descartes (1664)] and seems obsolete since the days of Newton.

In order to allow a better understanding of nonlocal effects, we consider as a simple example the motion of a classical particle in a dilute gas. On the left side of figure 1.1 we illustrate the free field case which is characterized by the absence of any boundaries. In that case, with a given collision rate $\psi(t)$, the dynamics of the system is determined by a local theory.

Let us now introduce some walls or boundaries, where the gas molecules bounce off.

This situation is schematically sketched on the right of figure 1.1. In that case, at the time $t - \tau$ a fixed rate of gas molecules is scattered, but in contrast to the free field case, at the time $t - \tau/2$ they collide with the boundaries and are reflected. At the time t the dynamics of the system is then characterized by a source term which besides $\psi(t)$ contains an

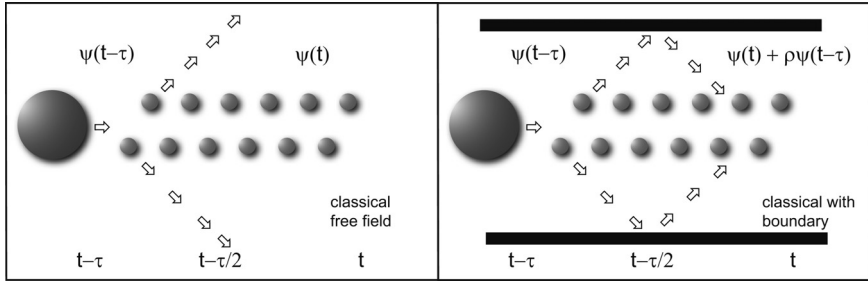


Fig. 1.1 A possible geometric interpretation of a memory effect. The boundary free case shown on the left side is described by a local theory (characterized by a source term $\psi(t)$), while the same case including boundaries may be described by a nonlocal theory (characterized by a source term $\psi(t) + \rho\psi(t - \tau)$ with ρ being a proportionality factor).

additional nonlocal term proportional to $\psi(t - \tau)$. This is a simple geometric interpretation of a nonlocal theory. Neither the described particle nor the surrounding medium memorize previous events. There is no intelligence in the system. The boundaries generate a delayed reaction of the medium, which results in a memory effect.

In a more sophisticated scenario, we may assert to every point in space a complex reflection coefficient and are lead to Huygens' principle which states that each point of an advancing wave front is in fact the source of a new set of waves.

In that sense a nonlocal theory may be interpreted as a construct which allows a smooth transition between a local (Newtonian) and a full quantum theory of motion.

A particular subgroup of nonlocal field theories plays an increasingly important role and may be described with operators of fractional nature and is specified within the framework of fractional calculus.

From a historical point of view fractional calculus may be described as an extension of the concept of a derivative operator from integer order n to arbitrary order α , where α is a real or complex value or even more complicated a complex valued function $\alpha = \alpha(x, t)$:

$$\frac{d^n}{dx^n} \rightarrow \frac{d^\alpha}{dx^\alpha} \quad (1.1)$$

Despite the fact that this concept is being discussed since the days of Leibniz [Leibniz (1695)] and since then has occupied the great mathematicians of their times, no other research area has resisted a direct application for centuries. Abel's treatment of the tautochrone problem [Abel (1823)] from

1823 stood for a long time as a singular example for an application of fractional calculus.

Not until the works of Mandelbrot [Mandelbrot (1982)] on fractal geometry in the early 1980's was the interest of physicists attracted by this subject, and a first wave of publications in the area of fractional Brownian motion and anomalous diffusion processes was created. But these works lead only to possibly a handful of useful applications and did not produce results of far-reaching consequences [Kilbas *et al.* (2003)].

The situation changed drastically by the progress made in the area of fractional wave equations during the last years. Within this process, new questions in fundamental physics have been raised, which cannot be formulated adequately using traditional methods. Consequently a new research area has emerged, which allows for new insights and intriguing results using new methods and approaches.

The interest in fractional wave equations was amplified in 2000 with a publication by Raspini [Raspini (2000)]. He deduced a SU(3) symmetric wave equation, which turned out to be of fractional nature. In contrast to this formal derivation a standard Yang-Mills theory is merely a recipe for coupling any phenomenologically deduced symmetry. Zavada [Zavada (2000)] has generalized Raspini's result: he demonstrated, that a n-fold factorization of the d'Alembert operator automatically leads to fractional wave equations with an inherent SU(n) symmetry.

In 2002, Laskin [Laskin (2002)] on the basis of the Riesz definition [Riesz (1949)] of the fractional derivative presented a Schrödinger equation with fractional derivatives and gave a proof of Hermiticity and parity conservation of this equation.

In 2005, the Casimir operators and multiplets of the fractional extension of the standard rotation group SO(n) were calculated algebraically [Herrmann (2005a)]. A mass formula was derived, which successfully described the ground state masses of the charmonium spectrum. This may be interpreted as a first approach to investigate a fractional generalization of a standard Lie algebra, a first attempt to establish a fractional group theory and the first non trivial application of fractional calculus in multi-dimensional space.

In 2006, Goldfain [Goldfain (2006)] demonstrated, that the low level fractional dynamics [Tarasov and Zaslavsky (2006)] on a flat Minkowski metric most probably describes similar phenomena as a field theory in curved Riemann space time. In addition, he proposed a successful mechanism to quantize fractional free fields. Lim [Lim (2006a)] proposed a

quantization description for free fractional fields of Klein-Gordon-type and investigated the temperature dependence of those fields.

In 2007, we [Herrmann (2007a)] applied the concept of local gauge invariance to fractional free fields and derived the exact interaction form in first order of the coupling constant. The fractional analogue of the normal Zeeman-effect was calculated and as a first application a mass formula was presented, which yields the masses of the baryon spectrum with an accuracy better than 1%. It has been demonstrated, that the concept of local gauge invariance determines the exact form of interaction, which in lowest order coincides with the derived group chain for the fractional rotation group.

Since then the investigation of the fractional rotation group alone within the framework of fractional group theory has led to a vast amount of interesting results, e.g. a theoretical foundation of magic numbers in atomic nuclei and metallic clusters.

Besides group theoretical methods, the application of fractional derivatives on multi dimensional space \mathbb{R}^N and the increasing importance of numerical approaches are major developments within the last years [Herrmann (2012a); Herrmann (2013c)].

Furthermore, as long as the fractional derivative has been considered as the inverse of a fractional integral, which *per se* is nonlocal its nonlocality was a common paradigm. But recent years have seen an increasing number of alternative approaches, which are not necessarily founded on nonlocality [Samko *et al.* (1993b); Tarasov (2008b); Herrmann (2013b)].

Another increasing area of research is the investigation of genetic differential equations with variable order fractional derivatives based on an idea of Samko and Ross [Samko and Ross (1993a)], where the form and type of a differential operator changes with time or space respectively emphasizing evolutionary aspects of dynamic behavior.

Covering the above mentioned subjects, this book is an invitation to the interested student and to the professional researcher as well. It presents a thorough introduction to the basics of fractional calculus and routes the reader up to the current state of the art of a physical interpretation.

What makes this textbook unique is its application oriented approach. A large body of literature already covers the mathematical aspects of fractional calculus and the classical aspects of fractional calculus like anomalous diffusion and fractional Brownian motion (e.g. [Oldham and Spanier (1974); Samko *et al.* (1993b); Miller and Ross (1993); Kiryakova (1994); Gorenflo and Mainardi (1997); Podlubny (1999); Hilfer (2000); Hilfer (2008); Mainardi (2010); Monje *et al.* (2010); Klafter *et al.* (2011); Ortigueira

(2011a); Tarasov (2011); Baleanu *et al.* (2012); Torres and Malinowska (2012); Uchaikin (2012); Ibe (2013); Jumarie (2014)].

This book is explicitly devoted to the practical consequences of a use of fractional calculus in different branches of physics from classical mechanics up to quantum fields.

The book may be divided into two parts. Chapters 2 to 10 give a step by step introduction to the techniques and methods derived in fractional calculus and their application to classical problems. Chapters 11 to 26 are devoted to a concise introduction of fractional calculus in the area of quantum mechanics of multi-particle systems. The application of group theoretical methods will lead to new and unexpected results. The reader is directly led to the actual state of research. All derived results are directly compared to experimental findings. As a consequence, the reader is guided on a solid basis and is encouraged to apply the fractional calculus approach in his research area, too.

It will be demonstrated, that the viewpoint of fractional calculus leads to new insights and surprising interrelations of classical fields of research that remain unconnected until now.

This page intentionally left blank

Chapter 2

Functions

What is number?

When the Pythagoreans believed that everything is number they had in mind primarily integer numbers or ratios of integers [Burkert (1972)]. The discovery of additional number types, first ascribed to Hippasus of Metapontum, at that time must have been both, a deeply shocking as well as an extremely exciting experience which in the course of time helped to gain a deeper understanding of mathematical problems.

The increasing commercial success and volume of trade in the North Italian city states commencing on the reign of the Stauffian emperors promoted the progress of practical mathematics and gave a first application of the negative numbers in terms of a customer's debts [Fibonacci (1204)].

The general solutions of cubic and quartic equations [Cardano (1545)] forced an interpretation of imaginary numbers [Bombelli (1572)], which were finally accepted as useful quantities, when Gauss gave a general interpretation of the fundamental theorem of algebra [Gauß (1799)] not until 1831.

If we consider a number as a scalar object, we may proceed and introduce a vector, a matrix or a general tensor as objects with increasing level of complexity regarding their transformation properties. Therefore we have a well defined sequence of number definitions with increasing complexity.

Furthermore we have nice examples for a successful extension of the scope of functions e.g. from integer to real values. Let us begin with two stories of success: we present the gamma and Mittag-Leffler functions, which turn out to be well established extensions of the factorial and the exponential function. These functions play an important role for practical applications of the fractional calculus.

2.1 Gamma function

The gamma function is the example par excellence for a reasonable extension of the scope of a function from integer to real up to imaginary numbers.

For natural numbers the factorial $n!$ is defined by

$$n! = 1 \times 2 \times 3 \times \dots \times n = \prod_{j=1}^n j \quad (2.1)$$

with the following essential properties

$$1! = 1 \quad (2.2)$$

$$n! = n(n - 1)! \quad (2.3)$$

Now we define the gamma function on the set of complex numbers z

$$\Gamma(z) = \lim_{n \rightarrow \infty} \frac{n! n^z}{z(z + 1)(z + 2)\dots(z + n)} \quad (2.4)$$

or alternatively

$$\frac{1}{\Gamma(z)} = z e^{\gamma z} \prod_{n=0}^{\infty} \left(1 + \frac{z}{n}\right) e^{-z/n} \quad (2.5)$$

where $\gamma = 0.57721\dots$ denotes the Euler constant.

The scope of both definitions extends on the field of complex numbers z .

In case $\operatorname{Re}(z) > 0$ the integral representation

$$\Gamma(z) = \int_0^\infty t^{z-1} e^{-t} dt \quad (2.6)$$

is valid.

From integration by parts it follows

$$\Gamma(1 + z) = z\Gamma(z) \quad (2.7)$$

and by direct integration $\Gamma(1) = 1$. Therefore we associate:

$$\Gamma(1 + n) = n! \quad (2.8)$$

Hence the gamma function may be considered a reasonable extension of the factorial.

Within the framework of fractional calculus, as we shall see later, the zeroes of the reciprocal value of the gamma function are of particular interest:

$$\frac{1}{\Gamma(z)} = 0 \quad z = -n \quad n = 0, 1, 2, 3\dots \quad (2.9)$$

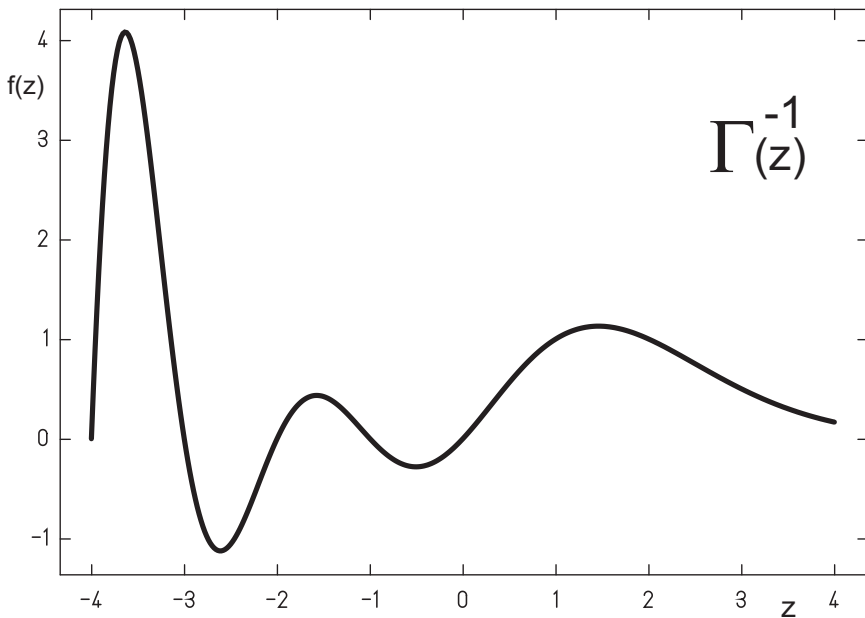


Fig. 2.1 The inverse gamma function $f(z) = \frac{1}{\Gamma(z)}$.

Furthermore we may extend the definition of the Binomial coefficients:

$$\binom{z}{v} = \frac{z!}{v!(z-v)!} = \frac{\Gamma(1+z)}{\Gamma(1+v)\Gamma(1+z-v)} \quad (2.10)$$

In addition the reflection formula

$$\Gamma(z)\Gamma(1-z) = \frac{\pi}{\sin(\pi z)} \quad (2.11)$$

will be used.

2.2 Mittag-Leffler functions

Besides the gamma function Euler has brought to light an additional important function, the exponential:

$$e^z = \sum_{n=0}^{\infty} \frac{z^n}{n!} \quad (2.12)$$

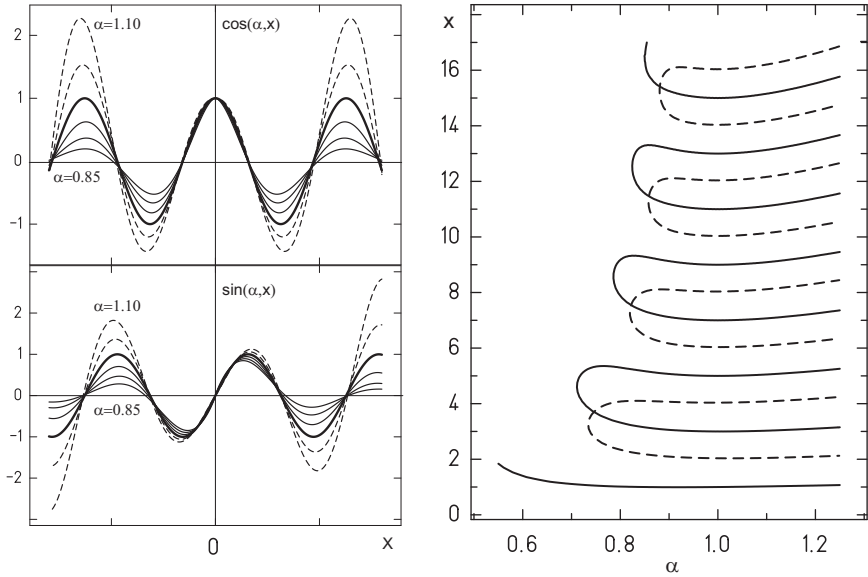


Fig. 2.2 Solutions and zeroes of the Caputo-wave equation are the fractional pendant of the trigonometric functions and special cases of the Mittag-Leffler function $\cos(\alpha, x) = E_{2\alpha}(-x^{2\alpha})$ and the generalized Mittag-Leffler function $\sin(\alpha, x) = x^\alpha E_{2\alpha, 1+\alpha}(-x^{2\alpha})$. The graph is given for different α near $\alpha = 1$. Units are given as multiples of $\pi/2$.

According to our remarks made in the previous section we may replace the factorial by the gamma function:

$$e^z = \sum_{n=0}^{\infty} \frac{z^n}{\Gamma(1+n)} \quad (2.13)$$

Without difficulty this definition may be extended, where one option is given by:

$$E_\alpha(z) = \sum_{n=0}^{\infty} \frac{z^n}{\Gamma(1+n\alpha)} \quad (2.14)$$

where we have introduced an arbitrary real number $\alpha > 0$. The properties of this function $E_\alpha(z)$ were first investigated systematically in the year 1903 by Mittag-Leffler and consequently it is called Mittag-Leffler function [Mittag-Leffler (1903)]. In the area of fractional calculus this function is indeed of similar importance as is the exponential function in standard mathematics and is subject of actual research [Gorenflo and Mainardi (1996); Mainardi and Gorenflo (2000); Hilfer and Seybold (2006);

Kilbas *et al.* (2013)]. An extensive collection of standard functions are special cases of the Mittag-Leffler function :

$$E_2(-z^2) = \cos(z) \quad E_{1/2}(z^{1/2}) = e^z \left(1 + \operatorname{erf}(z^{1/2})\right) \quad (2.15)$$

where the error function $\operatorname{erf}(z)$ is given by

$$\operatorname{erf}(z) = \frac{2}{\sqrt{\pi}} \int_0^z e^{-t^2} dt \quad (2.16)$$

An extended version of the Mittag-Leffler function is given by

$$E_{\alpha,\beta}(z) = \sum_{n=0}^{\infty} \frac{z^n}{\Gamma(n\alpha + \beta)} \quad (2.17)$$

This function is named generalized Mittag-Leffler function [Wiman (1905); Seybold and Hilfer (2005); Hilfer and Seybold (2006); Seybold and Hilfer (2008)]. It is one of the many reasonable extensions of the exponential function. A large number of simple functions are special cases of the generalized Mittag-Leffler function, for example:

$$E_{1,2}(z) = \frac{e^z - 1}{z} \quad E_{2,2}(z^2) = \frac{\sinh(z)}{z} \quad (2.18)$$

2.3 Hypergeometric functions

Hypergeometric functions contain many particular special functions as special cases and are used extensively within the framework of fractional calculus. From the definition

$${}_pF_q(\{a_i\}; \{b_j\}; z) = \frac{\prod_{j=1}^q \Gamma(b_j)}{\prod_{i=1}^p \Gamma(a_i)} \sum_{n=0}^{\infty} \frac{\prod_{i=1}^p \Gamma(a_i + n)}{\prod_{j=1}^q \Gamma(b_j + n)} \frac{z^n}{n!} \quad (2.19)$$

follows for the derivative

$$\frac{d}{dz} {}_pF_q(\{a_i\}; \{b_j\}; z) = \frac{\prod_{i=1}^p \Gamma(a_i)}{\prod_{j=1}^q \Gamma(b_j)} {}_pF_q(\{a_i + 1\}; \{b_j + 1\}; z) \quad (2.20)$$

Beyond many other special cases hypergeometric functions include the Gauss' s hypergeometric series ${}_2F_1(a, b; c; z)$ and the confluent hypergeometric series ${}_1F_1(a; b; z)$ which is a solution of Kummer's differential equation.

2.4 Miscellaneous functions

Fractional calculus not only extends our view on physical processes. It also breaks into regions of mathematics, which in general are neglected in B. Sc.-physics. Since we will derive in the course of this book some exotic results, an alphabetic listing of functions and their notation is given here:

complementary error function [Wolfram (2013)]

$$\operatorname{erfc}(z) = 1 - \operatorname{erf}(z) \quad (2.21)$$

cosine integral [Abramowitz and Stegun (1965)]

$$\operatorname{Ci}(z) = - \int_z^\infty \frac{\cos(t)}{t} dt = \gamma + \ln(z) + \int_0^z \frac{\cos(t) - 1}{t} dt \quad (2.22)$$

digamma function [Abramowitz and Stegun (1965)]

$$\Psi(z) = \frac{d}{dz} \ln(\Gamma(z)) \quad (2.23)$$

Euler γ constant [Wolfram (2013)]

$$\gamma = 0.577215\dots \quad (2.24)$$

exponential integral Ei [Spanier *et al.* (2008)]

$$\operatorname{Ei}(z) = - \int_{-z}^\infty \frac{e^{-t}}{t} dt \quad (2.25)$$

exponential integral E_n [Wolfram (2013)]

$$\operatorname{E}_n(z) = - \int_1^\infty \frac{e^{-zt}}{t^n} dt \quad (2.26)$$

harmonic number [Wolfram (2013)]

$$H_z = \gamma + \Psi(z+1) = z_3 F_2(1, 1, 1-z, 2, 2, 1) \quad (2.27)$$

Hurwitz function [Hurwitz (1882)]

$$\zeta(s, z) = \sum_{k=0}^{\infty} (k+z)^{-s} \quad (2.28)$$

incomplete gamma function [Wolfram (2013)]

$$\Gamma(a, z) = \int_z^\infty t^{a-1} e^{-t} dt \quad (2.29)$$

Meijer G-function [Meijer (1941); Prudnikov *et al.* (1990)]

$$G_{p,q}^{m,n} \left(z \middle| \begin{matrix} a_1, \dots, a_p \\ b_1, \dots, b_q \end{matrix} \right) = \frac{1}{2\pi i} \int_{\gamma L} \frac{\left(\prod_{j=1}^m \Gamma(b_j + s) \right) \left(\prod_{j=1}^n \Gamma(1 - a_j - s) \right)}{\left(\prod_{j=n+1}^p \Gamma(a_j + s) \right) \left(\prod_{j=m+1}^q \Gamma(1 - b_j - s) \right)} z^{-s} ds \quad (2.30)$$

where the contour γL lies between the poles of $\Gamma(1 - a_j - s)$ and $\Gamma(b_j + s)$.

polygamma function [Abramowitz and Stegun (1965)]

$$\Psi^{(n)}(z) = \frac{d^n}{dz^n} \Psi(z) = \frac{d^{n+1}}{dz^{n+1}} \ln(\Gamma(z)) \quad (2.31)$$

sine integral [Abramowitz and Stegun (1965)]

$$\text{Si}(z) = \int_0^z \frac{\sin(t)}{t} dt \quad (2.32)$$

Exercise 2.1

Fractional binomials

Problem: Prove the identity

$$(-1)^j \binom{j-q-1}{j} = \binom{q}{j} \quad q \in \mathbb{R} \wedge q \notin \mathbb{N}, j \in \mathbb{N} \quad (2.33)$$

Exercise 2.2

Solution of the cubic equation in terms of hypergeometric functions

Problem: A general solution of the cubic equation

$$x^3 + ax^2 + bx + c = 0 \quad (2.34)$$

given in radicals was first published by Cardano (1545).

An alternative approach, which is more appropriate in view of a generalization to higher order equations, gives the solutions in terms of hypergeometric functions:

Applying a Tschirnhausen transformation [Tschirnhausen (1683)] of type

$$x \Rightarrow \alpha x + \beta \quad (2.35)$$

the cubic equation may be transformed to an equivalent, but easier to handle form:

$$x^3 - x - q = 0, \quad q = \left(\frac{2a^3}{27} - \frac{ab}{3} + c \right) / \sqrt{\left(b - \frac{a^3}{3} \right)^3} \quad (2.36)$$

where the general solutions x_i with $i \in \{1, 2, 3\}$ are a function of only one variable $x_i = f_i(q)$.

Prove that one solution of (2.36) is given by:

$$x_1(q) = -q {}_2F_1(1/3, 2/3; 3/2; \frac{27}{4}q^2) \quad (2.37)$$

Chapter 3

The Fractional Derivative

The historical development of fractional calculus begins with a step by step introduction of the fractional derivative for special function classes. We follow this path and present these functions and the corresponding derivatives.

In addition we will present alternative concepts to introduce a fractional derivative definition, e.g. a series expansion in terms of the standard derivative. Furthermore we introduce the fractional extension of the Leibniz product rule and we will demonstrate, that an application of this rule will extend the range of function classes, a fractional derivative may be defined for.

The strategies we present for an appropriate extension of the standard derivative definition may be applied uniquely in areas of mathematical sciences, where similar concepts are valid.

As one example we mention the important field of orthogonal polynomials, which is a vivid and actual research area.

3.1 Basics

If we consider an application of differential or integral calculus simply as a mapping from a given function set f onto another set g e.g.

$$g(x) = \frac{d}{dx} f(x) \quad (3.1)$$

then in general from this relation we cannot deduce any valid information on a possible similarity of a function and its derivative.

Therefore it is surprising and remarkable that for particular function classes we observe a very simple relationship in respect of their derivatives.

For the exponential function we obtain

$$\frac{d}{dx} e^{kx} = k e^{kx} \quad (3.2)$$

for trigonometric functions we have

$$\begin{aligned} \frac{d}{dx} \sin(kx) &= k \cos(kx) = k \sin(kx + \frac{\pi}{2}) \\ \frac{d}{dx} (k \cos(kx)) &= \frac{d^2}{dx^2} \sin(kx) = -k^2 \sin(kx) = k^2 \sin(kx + \pi) \\ \frac{d}{dx} (-k^2 \sin(kx)) &= \frac{d^3}{dx^3} \sin(kx) = -k^3 \cos(kx) = k^3 \sin(kx + \frac{3\pi}{2}) \\ \frac{d}{dx} (-k^3 \cos(kx)) &= \frac{d^4}{dx^4} \sin(kx) = k^4 \sin(kx) = k^4 \sin(kx + 2\pi) \end{aligned} \quad (3.3)$$

or for powers

$$\frac{d}{dx} x^k = k x^{k-1} \quad (3.4)$$

We deduce a simple rule which we can easily write in a generalized form valid for all $n \in \mathbb{N}$:

$$\frac{d^n}{dx^n} e^{kx} = k^n e^{kx} \quad (3.5)$$

$$\frac{d^n}{dx^n} \sin(kx) = k^n \sin(kx + \frac{\pi}{2}n) \quad (3.6)$$

$$\frac{d^n}{dx^n} x^k = \frac{k!}{(k-n)!} x^{k-n} \quad (3.7)$$

For arbitrary order n apparently a kind of self similarity emerges, e.g. all derivatives of the exponential lead to exponentials, all derivatives of trigonometric functions lead to trigonometric functions. Since the derivative is given in this closed form it is straightforward to extend this rule from integer derivative coefficients $n \in \mathbb{N}$ to real and even imaginary coefficients α and postulate a fractional derivative as:

$$\frac{d^\alpha}{dx^\alpha} e^{kx} = k^\alpha e^{kx} \quad k \geq 0 \quad (3.8)$$

$$\frac{d^\alpha}{dx^\alpha} \sin(kx) = k^\alpha \sin(kx + \frac{\pi}{2}\alpha) \quad k \geq 0 \quad (3.9)$$

$$\frac{d^\alpha}{dx^\alpha} x^k = \frac{\Gamma(1+k)}{\Gamma(1+k-\alpha)} x^{k-\alpha} \quad x \geq 0, k \neq -1, -2, -3, \dots \quad (3.10)$$

We restrict to $k \geq 0$ and $x \geq 0$ respectively to ensure the uniqueness of the fractional derivative definition. This intuitive approach follows the historical path along which the fractional calculus has evolved. The definition of

the fractional derivative of the exponential function was given by Liouville [Liouville (1832)]. The corresponding derivative of trigonometric functions has first been proposed by Fourier [Fourier (1822)]. The fractional derivative for powers was studied systematically by Riemann [Riemann (1847)]; first attempts to solve this problem were already made by Leibniz and Euler [Euler (1738)].

The fractional derivative of a constant function is given according to Riemann's definition (3.10) by:

$$\frac{d^\alpha}{dx^\alpha} \text{const} = \frac{d^\alpha}{dx^\alpha} x^0 = \frac{1}{\Gamma(1 - \alpha)} x^{-\alpha} \quad (3.11)$$

which is an at first unexpected behavior. Hence as an additional postulate Caputo [Caputo (1967)] has introduced

$$\frac{d^\alpha}{dx^\alpha} \text{const} = 0 \quad (3.12)$$

which allows for a more familiar definition of e.g. series expansions, as will be demonstrated in the following.

As a consequence we obtain four different definitions of a fractional derivative. However they share common aspects. On one hand all definitions fulfil a correspondence principle:

$$\lim_{\alpha \rightarrow n} \frac{d^\alpha}{dx^\alpha} f(x) = \frac{d^n}{dx^n} f(x), \quad n = 0, 1, 2, \dots \quad (3.13)$$

In addition the following rules are valid:

$$\frac{d^\alpha}{dx^\alpha} cf(x) = c \frac{d^\alpha}{dx^\alpha} f(x) \quad (3.14)$$

$$\frac{d^\alpha}{dx^\alpha} (f(x) + g(x)) = \frac{d^\alpha}{dx^\alpha} f(x) + \frac{d^\alpha}{dx^\alpha} g(x) \quad (3.15)$$

These are very important properties, since we can define, in analogy to the well known Taylor series expansion series on these four different function classes and specify the corresponding fractional derivatives:

For the fractional derivative according to Liouville:

$$f(x) = \sum_{k=0}^{\infty} a_k e^{kx} \quad (3.16)$$

$$\frac{d^\alpha}{dx^\alpha} f(x) = \sum_{k=0}^{\infty} a_k k^\alpha e^{kx} \quad (3.17)$$

the fractional derivative according to Fourier:

$$f(x) = a_0 + \sum_{k=1}^{\infty} a_k \sin(kx) + \sum_{k=1}^{\infty} b_k \cos(kx) \quad (3.18)$$

$$\frac{d^\alpha}{dx^\alpha} f(x) = \sum_{k=1}^{\infty} a_k k^\alpha \sin(kx + \frac{\pi}{2}\alpha) + \sum_{k=1}^{\infty} a_k k^\alpha \cos(kx - \frac{\pi}{2}\alpha) \quad (3.19)$$

the fractional derivative according to Riemann:

$$f(x) = x^{\alpha-1} \sum_{k=0}^{\infty} a_k x^{k\alpha} \quad (3.20)$$

$$\frac{d^\alpha}{dx^\alpha} f(x) = x^{\alpha-1} \sum_{k=0}^{\infty} a_{k+1} \frac{\Gamma((k+2)\alpha)}{\Gamma((k+1)\alpha)} x^{k\alpha} \quad (3.21)$$

and for the fractional derivative according to Caputo:

$$f(x) = \sum_{k=0}^{\infty} a_k x^{k\alpha} \quad (3.22)$$

$$\frac{d^\alpha}{dx^\alpha} f(x) = \sum_{k=0}^{\infty} a_{k+1} \frac{\Gamma(1+(k+1)\alpha)}{\Gamma(1+k\alpha)} x^{k\alpha} \quad (3.23)$$

A given analytic function may therefore be expanded in a series and the fractional derivative may then be calculated.

With this result we can prove whether the four different definitions of a fractional derivative are equivalent. Do we obtain similar results for the fractional derivative for a given function?

We choose the exponential function as an example and calculate the fractional derivative according to Caputo:

$$\frac{d^\alpha}{dx^\alpha} e^x = \frac{d^\alpha}{dx^\alpha} \sum_{n=0}^{\infty} \frac{x^n}{n!} \quad (3.24)$$

$$= \sum_{n=1}^{\infty} \frac{x^{n-\alpha}}{\Gamma(1+n-\alpha)} \quad (3.25)$$

$$= x^{1-\alpha} E_{1,2-\alpha}(x) \quad (3.26)$$

In contrast to Liouville's definition the fractional derivative according to Caputo's definition is obviously not an exponential function any more but a generalized Mittag-Leffler function (2.17).

We obtain the disturbing result, that the proposed definitions of a fractional derivative are not interchangeable, but will lead to different results if

applied to the same function. Up to now there is no ultimate definition of a fractional derivative, even worse over time some additional definitions have been proposed which we will discuss extensively in the following chapters.

For practical applications of fractional calculus this leads to a situation, that e.g. the solutions of a fractional differential equation are unique, but will show different behavior depending on the specific definition of the fractional derivative used. From a mathematical point of view all these definitions are equally well-founded. But in contrast to mathematicians physicists are in an advantageous position. Since they intend to describe natural phenomena they have the opportunity to compare theoretical results with experimental data.

In the following chapters we will therefore lay particular emphasis on the application of derived results and we will present evidence for the validity of one or the other formal definition of a fractional derivative. Nevertheless we have to admit that until now there is no unique candidate which explains all experimental data. Instead, depending on the specific problem, one of the fractional derivatives will lead to better agreement with the experiment.

A substantial progress in the theory of fractional calculus without doubt would be achieved if an extended formulation of a fractional derivative would be proposed, which was valid for more or less different function classes simultaneously.

A step in this direction is based on the idea, to deduce a series expansion of the fractional derivative in terms of the standard derivative. For that purpose we start with the well known series expansion:

$$(a+b)^n = \sum_{k=0}^n \binom{n}{k} a^{n-k} b^k = \sum_{k=0}^n \binom{n}{k} a^n b^{n-k} \quad (3.27)$$

which is valid for $n \in \mathbb{N}$. Using the fractional extension of the Binomial coefficient (2.10) we propose the following generalization which is valid for arbitrary powers α :

$$(a+b)^\alpha = \sum_{k=0}^{\infty} \binom{\alpha}{k} a^{\alpha-k} b^k = \sum_{k=0}^{\infty} \binom{\alpha}{k} a^k b^{\alpha-k} \quad (3.28)$$

Hence we may present a definition of a fractional derivative as a series expansion:

$$\left(\frac{d}{dx} + \omega \right)^\alpha = \sum_{k=0}^{\infty} \binom{\alpha}{k} \omega^{\alpha-k} \frac{d^k}{dx^k} \quad (3.29)$$

where ω is an arbitrary, but infinitesimally small number.

At first sight this result seems nothing else but one more definition of a fractional derivative. But at least for the fractional derivative according to Liouville the relation

$$\left(\frac{d}{dx} + \omega\right)^\alpha f(x) = e^{-\omega x} \frac{d^\alpha}{dx^\alpha} e^{\omega x} f(x) \quad (3.30)$$

holds.

We therefore obtain the encouraging result, that both definitions are strongly related.

In addition, the series expansion of the fractional derivative gives a first impression of the nonlocal properties of this operation. Since the sum of derivatives is infinite, we obtain an infinite series of derivative values which is equivalent to determine the full Taylor series of a given function. Depending on the convergence radius of this Taylor series this implies, that a knowledge about the exact behavior of the function considered is necessary in order to obtain its fractional derivative.

In the following chapters we will demonstrate, that a large number of problems may already be solved using the proposed definitions of a fractional derivative (3.8)-(3.12).

3.2 The fractional Leibniz product rule

In the previous section we have presented a simple approach to fractional derivatives. But we want to state clearly that well-established techniques used in ordinary differential calculus may not be transferred thoughtlessly and without proof to the field of fractional calculus.

A typical example is the Leibniz rule in its familiar form

$$\frac{d}{dx}(\psi \chi) = \left(\frac{d}{dx}\psi\right)\chi + \psi\left(\frac{d}{dx}\chi\right) \quad (3.31)$$

It could be carelessly assumed, that in the case of fractional calculus the relation

$$\frac{d^\alpha}{dx^\alpha}(\psi \chi) = \left(\frac{d^\alpha}{dx^\alpha}\psi\right)\chi + \psi\left(\frac{d^\alpha}{dx^\alpha}\chi\right) \quad (3.32)$$

will hold.

A simple counter-example using e.g. the Liouville definition of a fractional derivative will do:

$$\frac{d^\alpha}{dx^\alpha}(e^{k_1 x} e^{k_2 x}) = \frac{d^\alpha}{dx^\alpha} e^{(k_1+k_2)x} \quad (3.33)$$

$$= (k_1 + k_2)^\alpha e^{(k_1+k_2)x} \quad (3.34)$$

On the other hand with (3.32) we obtain:

$$\frac{d^\alpha}{dx^\alpha}(e^{k_1 x} e^{k_2 x}) = (k_1^\alpha + k_2^\alpha)(e^{k_1 x} e^{k_2 x}) \quad (3.35)$$

Therefore the Leibniz product rule according to (3.32) is not valid for fractional derivatives.

In order to derive an extension of this product rule which is valid for fractional derivatives too, let us first note the rule for higher derivatives:

$$\begin{aligned} \frac{d}{dx}(\psi \chi) &= \left(\frac{d}{dx} \psi \right) \chi + \psi \left(\frac{d}{dx} \chi \right) \\ \frac{d^2}{dx^2}(\psi \chi) &= \left(\frac{d^2}{dx^2} \psi \right) \chi + 2 \left(\frac{d}{dx} \psi \right) \left(\frac{d}{dx} \chi \right) + \psi \left(\frac{d^2}{dx^2} \chi \right) \\ \frac{d^3}{dx^3}(\psi \chi) &= \left(\frac{d^3}{dx^3} \psi \right) \chi + 3 \left(\frac{d^2}{dx^2} \psi \right) \left(\frac{d}{dx} \chi \right) + 3 \left(\frac{d}{dx} \psi \right) \left(\frac{d^2}{dx^2} \chi \right) + \psi \left(\frac{d^3}{dx^3} \chi \right) \end{aligned} \quad (3.36)$$

using the abbreviation

$$\partial_x^\alpha = \frac{d^\alpha}{dx^\alpha} \quad (3.37)$$

we obtain for arbitrary integers:

$$\partial_x^n(\psi \chi) = \sum_{j=0}^n \binom{n}{j} (\partial_x^{n-j} \psi) (\partial_x^j \chi) \quad n \in \mathbb{N} \quad (3.38)$$

According to (3.28) this expression may be extended to arbitrary α :

$$\partial_x^\alpha(\psi \chi) = \sum_{j=0}^{\infty} \binom{\alpha}{j} (\partial_x^{\alpha-j} \psi) (\partial_x^j \chi) \quad (3.39)$$

Indeed this form of the Leibniz product rule is valid for fractional derivatives too.

On a first glance, the symmetry between ψ and χ is lost when extending $\alpha \in \mathbb{N}$ to $\alpha \in \mathbb{C}$. Hence Watanabe [Watanabe (1931)] and Osler [Osler (1970)] have derived a generalized Leibniz product rule for a fractional derivative, which emphasizes the interchangeability of ψ and χ

$$\partial_x^\alpha(\psi \chi) = \sum_{j=-\infty}^{\infty} \binom{\alpha}{\gamma + j} (\partial_x^{\alpha-\gamma-j} \psi) (\partial_x^{\gamma+j} \chi) \quad (3.40)$$

where γ may be chosen arbitrarily.

Of course there are many other known rules which are common in standard calculus e.g. the chain rule. As demonstrated, a direct transfer of any standard rule to fractional calculus is hazardous, instead in every case the validity of a rule used in fractional calculus must be checked carefully.

Therefore we have demonstrated, that a useful strategy for a satisfactory fractionalization scheme is given as a two step procedure:

- Derive a rule which is valid for all $n \in \mathbb{N}$.
- Replace n by $\alpha \in \mathbb{C}$.

3.3 The fractional derivative in terms of finite differences - the Grünwald-Letnikov derivative

Extending a general rule from $n \in \mathbb{N}$ to $\alpha \in \mathbb{C}$ is a very helpful recipe to establish another definition of a fractional derivative in terms of a limit of finite differences.

Starting with the definition of the first derivative as

$$\partial_x f(x) = \lim_{h \rightarrow 0} \frac{\Delta f(x)}{h} = \lim_{h \rightarrow 0} \frac{f(x) - f(x-h)}{h} \quad (3.41)$$

where h is an arbitrary small value $h < \epsilon$, $h \geq 0$ and Δ is the backward difference operator, we obtain for higher derivatives:

$$\begin{aligned} \partial_x^2 f(x) &= \lim_{h \rightarrow 0} \frac{\Delta^2 f(x)}{h^2} = \lim_{h \rightarrow 0} \frac{\Delta(f(x) - f(x-h))}{h^2} \\ &= \lim_{h \rightarrow 0} \frac{f(x) - 2f(x-h) + f(x-2h)}{h^2} \end{aligned} \quad (3.42)$$

$$\begin{aligned} \partial_x^3 f(x) &= \lim_{h \rightarrow 0} \frac{\Delta^3 f(x)}{h^3} = \lim_{h \rightarrow 0} \frac{\Delta^2(f(x) - f(x-h))}{h^3} \\ &= \lim_{h \rightarrow 0} \frac{\Delta(f(x) - 2f(x-h) + f(x-2h))}{h^3} \\ &= \lim_{h \rightarrow 0} \frac{f(x) - 3f(x-h) + 3f(x-2h) - f(x-3h)}{h^3} \end{aligned} \quad (3.43)$$

Therefore we deduce the following closed formula for an integer derivative with $n \in \mathbb{N}$:

$$\partial_x^n f(x) = \lim_{h \rightarrow 0} \frac{\Delta^n f(x)}{h^n} = \lim_{h \rightarrow 0} \left(\sum_{m=0}^n \binom{n}{m} (-1)^m f(x-mh) \right) / h^n \quad (3.44)$$

Replacing n by $\alpha \in \mathbb{C}$ yields the following definition of a fractional derivative, which is a special case of the Grünwald-Letnikov fractional derivative [Grünwald (1867); Diaz and Osler (1974); Podlubny (1999); Ortigueira and Coiti (2004)]:

$$\partial_x^\alpha f(x) = \lim_{h \rightarrow 0} \frac{\Delta^\alpha f(x)}{h^\alpha} = \lim_{h \rightarrow 0} \left(\sum_{m=0}^{\infty} \binom{\alpha}{m} (-1)^m f(x-mh) \right) / h^\alpha \quad (3.45)$$

As an application, for $f(x) = \exp(kx)$ we obtain:

$$\partial_x^\alpha \exp(kx) = \lim_{h \rightarrow 0} \left(\sum_{m=0}^{\infty} \binom{\alpha}{m} (-1)^m \exp(k(x-mh)) \right) / h^\alpha \quad (3.46)$$

$$= \exp(kx) \lim_{h \rightarrow 0} \left(\sum_{m=0}^{\infty} \binom{\alpha}{m} (-1)^m \exp(-mkh) \right) / h^\alpha \quad (3.47)$$

$$= \exp(kx) \lim_{h \rightarrow 0} \left(\sum_{m=0}^{\infty} \binom{\alpha}{m} (-1)^m \exp(-kh)^m \right) / h^\alpha \quad (3.48)$$

Using the binomial formula (3.27)

$$(1-z)^\alpha = \sum_{m=0}^{\infty} \binom{\alpha}{m} (-1)^m z^m \quad (3.49)$$

which converges for $|z| \leq 1$ and therefore for all $k \geq 0$ in a next step we evaluate the sum in (3.48), which yields

$$\partial_x^\alpha \exp(kx) = \exp(kx) \lim_{h \rightarrow 0} (1 - \exp(-hk))^\alpha / h^\alpha \quad k \geq 0 \quad (3.50)$$

$$= \exp(kx) \lim_{h \rightarrow 0} \left(1 - \sum_{j=0}^{\infty} (-1)^j \frac{(hk)^j}{j!} \right)^\alpha / h^\alpha \quad (3.51)$$

$$= \exp(kx) \lim_{h \rightarrow 0} \left(- \sum_{j=1}^{\infty} (-1)^j h^{j-1} \frac{k^j}{j!} \right)^\alpha \quad (3.52)$$

$$= \exp(kx) \lim_{h \rightarrow 0} \left(k - h \frac{k^2}{2!} + h^2 \frac{k^3}{3!} \dots \right)^\alpha \quad (3.53)$$

$$= k^\alpha \exp(kx) \quad (3.54)$$

which nicely coincides with the Liouville definition of a fractional derivative. Hence with (3.45) we have presented a first unique definition of a fractional derivative, which is valid for any analytic function, as long as the series converges.

The presented definition of a fractional derivative in terms of a infinite sum over function values at points $p = x - mh$ gives a first impression of the nonlocal aspects (for space-like coordinates) or memory effects (for time-like coordinates) of a fractional derivative.

Interpreting the variable x as a time like coordinate, especially the required knowledge of the complete history of a given process may cause difficulties in practical applications. Therefore in his original work Grünwald introduced the idea of a finite lower cutoff u by the requirement:

$$u \leq x - nh \quad \Rightarrow \quad N = \lfloor \frac{x-u}{h} \rfloor \quad N \in \mathbb{N} \quad (3.55)$$

where $\lfloor x \rfloor = \text{floor}(x)$ is the integer part of a real number. Thus we have

$$\partial_x^\alpha f(x) = \lim_{h \rightarrow 0} \left(\sum_{m=0}^N \binom{\alpha}{m} (-1)^m f(x - mh) \right) / h^\alpha \quad (3.56)$$

$$= \lim_{h \rightarrow 0} \left(\sum_{m=0}^{\infty} \binom{\alpha}{m} (-1)^m H(x - mh - u) f(x - mh) \right) / h^\alpha \quad (3.57)$$

with the Heaviside step function $H(x)$ [Hunt (2012)]

$$H(x) = \begin{cases} 0 & x < 0 \\ 1 & x \geq 0 \end{cases} \quad (3.58)$$

3.4 Discussion

3.4.1 Orthogonal polynomials

question:

You have presented a procedure to generalize

- a) a function like factorial $n!$,
- b) the concept of a derivative or
- c) the Leibniz product rule

from integer values n to arbitrary α . There is another area in mathematical physics where integers play an important role in counting orthogonal polynomials. Will the proposed fractionalization procedure lead to sets of fractional orthogonal polynomials?

answer:

The proposed fractionalization mechanism may indeed be applied to orthogonal polynomials leading to generalized polynomials of fractional order. We present an elementary example:

The Laguerre polynomials $L_n(x)$ are explicitly given by

$$L_n(x) = \sum_{m=0}^n (-1)^m \binom{n}{n-m} \frac{1}{m!} x^m \quad (3.59)$$

$$= {}_1F_1(-n; 1; x) \quad (3.60)$$

They obey the differential equation:

$$x \frac{d^2}{dx^2} L_n(x) + (1-x) \frac{d}{dx} L_n(x) + n L_n(x) = 0 \quad , n \in \mathbb{N} \quad (3.61)$$

and the orthogonality relation is given by

$$\int_0^\infty e^{-x} L_n(x) L_m(x) dx = \delta_{nm} \quad (3.62)$$

As a generalization from integer n to arbitrary α we propose

$$L_\alpha(x) = \sum_{m=0}^\infty (-1)^m \binom{\alpha}{\alpha-m} \frac{1}{m!} x^m \quad (3.63)$$

$$= {}_1F_1(-\alpha; 1; x) \quad (3.64)$$

Indeed it can be proven, that the fractional Laguerre polynomials $L_\alpha(x)$ fulfil the differential equation

$$x \frac{d^2}{dx^2} L_\alpha(x) + (1-x) \frac{d}{dx} L_\alpha(x) + \alpha L_\alpha(x) = 0 \quad , \alpha \in \mathbb{C} \quad (3.65)$$

which is nothing else but a generalization of (3.61). On the other hand the orthogonality relation (3.62) is not valid in general with the simple weight function e^{-x} :

$$\int_0^\infty e^{-x} L_\alpha(x) L_\beta(x) dx \neq \delta_{\alpha\beta} \quad (3.66)$$

Hence the concept of orthogonality within the framework of fractional order polynomials is still an open question and needs further investigations [Abbott (2000)].

But it is indeed remarkable, that many well known formulas generating orthogonal polynomials may be extended using similar techniques as proposed for a generalization of the fractional derivative, e.g. the integral representation of Hermite polynomials H_n

$$H_n(x) = e^{x^2} \frac{2^{n+1}}{\sqrt{\pi}} \int_0^\infty e^{-t^2} t^n \cos(2xt - \frac{\pi}{2}n) dt \quad , n \in \mathbb{N} \quad (3.67)$$

may be extended to a definition of fractional order Hermite polynomials H_α via

$$H_\alpha(x) = e^{x^2} \frac{2^{\alpha+1}}{\sqrt{\pi}} \int_0^\infty e^{-t^2} t^\alpha \cos(2xt - \frac{\pi}{2}\alpha) dt \quad , \alpha \in \mathbb{C} \quad (3.68)$$

The recurrence relations for Legendre polynomials P_n :

$$(n+1)P_{n+1}(x) = (2n+1)xP_n(x) - nP_{n-1}(x) \quad , n \in \mathbb{N} \quad (3.69)$$

remains valid for P_α if we extend the definition for $n \in \mathbb{N}$

$$P_n(x) = {}_2F_1(-n, n+1; 1; \frac{1-x}{2}) \quad (3.70)$$

to $\alpha \in \mathbb{C}$

$$P_\alpha(x) = {}_2F_1(-\alpha, \alpha+1; 1; \frac{1-x}{2}) \quad (3.71)$$

and is then given by:

$$(\alpha+1)P_{\alpha+1}(x) = (2\alpha+1)xP_\alpha(x) - \alpha P_{\alpha-1}(x) \quad , \alpha \in \mathbb{C} \quad (3.72)$$

3.4.2 Differential representation of the Riemann and Caputo fractional derivative

question:

You have proposed a series expansion as a strategy to extend the scope of the fractional derivative types presented. Will the fractional Leibniz product rule serve as a promising tool to determine the exact form of such an extension?

answer:

Yes, the fractional Leibniz product rule (3.39) allows for an appropriate generalization of a given fractional derivative definition for a special function class and leads to a differential representation of this general definition. Starting e.g. with the Riemann-Euler definition of a fractional derivative of x^β and using the fractional extension of the Leibniz product rule indeed leads to a series expansion of the Riemann fractional derivative which is valid for analytic functions $f(x)$.

To derive the explicit form, we write the analytic function $f(x)$ as a general product:

$$f(x) = x^\beta g(x) \quad \beta, x \geq 0 \quad (3.73)$$

We now apply the Leibniz product rule

$$\begin{aligned} \partial_x^\alpha f(x) &= \partial_x^\alpha (x^\beta g(x)) \\ &= \sum_{j=0}^{\infty} \binom{\alpha}{j} (\partial_x^{\alpha-j} x^\beta) (\partial_x^j g(x)) \\ &= \sum_{j=0}^{\infty} \binom{\alpha}{j} \frac{\Gamma(1+\beta)}{\Gamma(1+\beta-\alpha+j)} x^{\beta-\alpha+j} (\partial_x^j g(x)) \\ &= \Gamma(1+\beta) x^{\beta-\alpha} \sum_{j=0}^{\infty} \binom{\alpha}{j} \frac{1}{\Gamma(1+\beta-\alpha+j)} x^j (\partial_x^j g(x)) \\ &= \Gamma(1+\beta) x^{\beta-\alpha} \sum_{j=0}^{\infty} (-1)^j \binom{j-\alpha-1}{j} \frac{1}{\Gamma(1+\beta-\alpha+j)} x^j (\partial_x^j g(x)) \end{aligned} \quad (3.74)$$

We now introduce the Euler-operator $J_e = x\partial_x$ and define the symbol $\mathbf{:}$ as a normal order operator

$$\mathbf{:} J_e^n := \mathbf{:} (x\partial_x)^n := x^n \partial_x^n \quad (3.75)$$

It then follows

$$\begin{aligned}
\partial_x^\alpha f(x) &= \Gamma(1 + \beta)x^{\beta - \alpha} \sum_{j=0}^{\infty} \binom{j - \alpha - 1}{j} \frac{1}{\Gamma(1 + \beta - \alpha + j)} : (-x\partial_x)^j : g(x) \\
&= \Gamma(1 + \beta)x^{\beta - \alpha} \sum_{j=0}^{\infty} \frac{\Gamma(j - \alpha)}{\Gamma(-\alpha)\Gamma(1 + j)\Gamma(1 + \beta - \alpha + j)} : (-J_e)^j : g(x) \\
&= \frac{\Gamma(1 + \beta)}{\Gamma(1 + \beta - \alpha)} x^{\beta - \alpha} \sum_{j=0}^{\infty} \frac{\Gamma(j - \alpha)}{\Gamma(-\alpha)} \frac{\Gamma(1 + \beta - \alpha)}{\Gamma(1 + \beta - \alpha + j)} \frac{1}{j!} : (-J_e)^j : g(x) \\
&= \frac{\Gamma(1 + \beta)}{\Gamma(1 + \beta - \alpha)} x^{\beta - \alpha} : {}_1F_1(-\alpha; 1 + \beta - \alpha; -J_e) : g(x)
\end{aligned} \tag{3.76}$$

For $\beta = 0$ this reduces to

$$\partial_x^\alpha f(x) = \frac{1}{\Gamma(1 - \alpha)} x^{-\alpha} : {}_1F_1(-\alpha; 1 - \alpha; -J_e) : f(x) \quad x \geq 0 \tag{3.77}$$

Interpreting the hypergeometric function ${}_1F_1$ as a series expansion, equation (3.77) represents the differential representation of the Riemann fractional derivative for an analytic function, as long as this series is convergent. It should be noted, that the knowledge of all derivatives $\partial_x^n f(x)$ is necessary to obtain the exact result. This amount of necessary information is equivalent to a full Taylor series expansion of the given function. This is a first hint for the nonlocality of the fractional derivative.

Furthermore equation (3.77) may be intuitively extended to negative x -values. We propose as a possible generalization:

$${}_{\text{R}}\partial_x^\alpha f(x) = \frac{1}{\Gamma(1 - \alpha)} \text{sign}(x)|x|^{-\alpha} : {}_1F_1(-\alpha; 1 - \alpha; -J_e) : f(x) \quad x \in \mathbb{R} \tag{3.78}$$

where $|x|$ denotes the absolute value of x and the index ${}_{\text{R}}$ denotes the Riemann fractional derivative.

As an example, the fractional derivative of the exponential function according to the Riemann definition is given as

$${}_{\text{R}}\partial_x^\alpha e^{kx} = \frac{1}{\Gamma(1 - \alpha)} \text{sign}(x)|x|^{-\alpha} {}_1F_1(-\alpha; 1 - \alpha; -kx) e^{kx} \tag{3.79}$$

$$= \frac{1}{\Gamma(1 - \alpha)} \text{sign}(x)|x|^{-\alpha} {}_1F_1(1; 1 - \alpha; kx) \tag{3.80}$$

$$= \text{sign}(x)(\text{sign}(x)k)^\alpha e^{kx} \left(1 - \frac{\Gamma(-\alpha, kx)}{\Gamma(-\alpha)}\right) \tag{3.81}$$

$$= \text{sign}(x)|x|^{-\alpha} E_{1,1-\alpha}(kx) \tag{3.82}$$

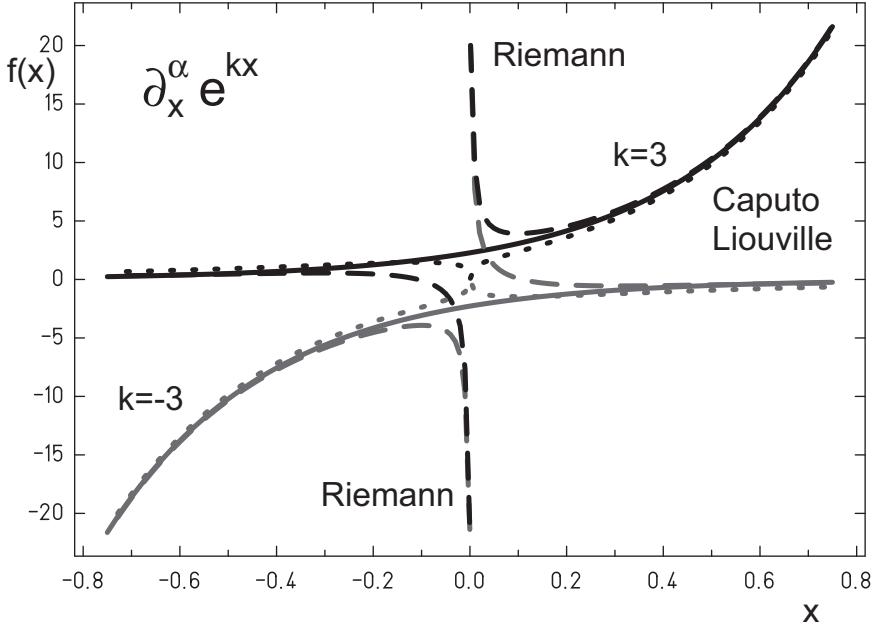


Fig. 3.1 Comparison of different fractional derivative definitions. For $\alpha = 0.75$ the fractional derivative of the exponential e^{kx} is plotted for $k = 3$ (black lines) and $k = -3$ (light gray lines). Thick lines indicate the Liouville fractional derivative, which is extended to negative k -values setting $L\partial_x^\alpha e^{kx} = \text{sign}(k)|k|^\alpha e^{kx}$, dashed lines represent the Riemann fractional derivative according to (3.78), dotted lines correspond to the Caputo derivative according to (3.86). Asymptotic behavior is similar for all derivatives considered. Only near $x = 0$ there are differences: The Riemann fractional derivative is divergent at the origin for $\alpha < 1$, the graph for the Caputo derivative touches the origin, the Liouville derivative yields a smooth behavior near the origin. In the limit $\alpha = 1$ all three definitions coincide with the standard derivative $\partial_x e^{kx} = ke^{kx}$.

where $\Gamma(a, z)$ is the incomplete gamma function and $E_{\alpha, \beta}(z)$ is the generalized Mittag-Leffler function. The result is valid and well behaved for all $k, x \in \mathbb{R}$.

In order to derive a differential representation of the Caputo fractional derivative ${}_C\partial_x^\alpha$ we have to fulfill as an additional condition

$${}_C\partial_x^\alpha \text{const} = 0 \quad (3.83)$$

which is ensured extending the fractional derivative to a two step procedure:

$$\partial_x^\alpha = \partial_x^{\alpha-1} \partial_x \quad (3.84)$$

With (3.77) it follows

$${}_C\partial_x^\alpha f(x) = \frac{1}{\Gamma(2-\alpha)} x^{1-\alpha} :_1 F_1(1-\alpha; 2-\alpha; -J_e) : \partial_x f(x) \quad x \geq 0 \quad (3.85)$$

and an appropriate extension to negative x values is given by

$${}_C\partial_x^\alpha f(x) = \frac{1}{\Gamma(2-\alpha)} |x|^{1-\alpha} :_1 F_1(1-\alpha; 2-\alpha; -J_e) : \partial_x f(x) \quad x \in \mathbb{R} \quad (3.86)$$

As an example, the fractional derivative of the exponential function according to the Caputo definition is given as

$${}_C\partial_x^\alpha e^{kx} = \frac{1}{\Gamma(2-\alpha)} |x|^{1-\alpha} :_1 F_1(1-\alpha; 2-\alpha; -J_e) : \partial_x e^{kx} \quad (3.87)$$

$$= \frac{1}{\Gamma(2-\alpha)} |x|^{1-\alpha} {}_1 F_1(1-\alpha; 2-\alpha; -kx) k e^{kx} \quad (3.88)$$

$$= k|x|^{1-\alpha} \frac{1}{\Gamma(2-\alpha)} {}_1 F_1(1; 2-\alpha; kx) \quad (3.89)$$

$$= \text{sign}(x)(\text{sign}(x)k)^\alpha e^{kx} \left(1 - \frac{\Gamma(1-\alpha, kx)}{\Gamma(1-\alpha)}\right) \quad (3.90)$$

$$= k|x|^{1-\alpha} E_{1,2-\alpha}(kx) \quad (3.91)$$

where $\Gamma(a, z)$ is the incomplete gamma function and $E_{\alpha,\beta}(z)$ is the generalized Mittag-Leffler function. The result is valid and well behaved for all $k, x \in \mathbb{R}$.

Finally, extending the Liouville fractional derivative definition to negative k -values via

$${}_L\partial_x^\alpha e^{kx} = \text{sign}(k)|k|^\alpha e^{kx} \quad (3.92)$$

we compare the behavior of the Liouville-, Riemann- and Caputo fractional derivative applied to the exponential function in figure 3.1. We may deduce, that the major differences occur for small values x , while for large x -values the different definitions for a fractional derivative lead to similar results.

It is remarkable, that we have used methods, which were available already in the first half of the eighteenth century [Euler (1738)] to derive a differential form of the Riemann and Caputo fractional derivative valid for all those analytic functions, where this series converge. In that sense, fractional calculus may be considered eighteenth century mathematics.

Sad enough, these differential representations did not play any role in the historic development of fractional calculus, while the integral representations of the same fractional derivatives, which will be presented in

detail in Chapter 5, were derived not until the mid-nineteenth century by Riemann [Riemann (1847)] and not until the mid-twentieth century by Caputo [Caputo (1967)] and therefore globally applicable fractional calculus methods became available just about 50 years ago.

Exercise 3.1**The Riemann derivative of $x^\alpha/(1-x)$**

Problem: Calculate the fractional derivative according to Riemann for

$$f(x) = \frac{x^\alpha}{1-x} \quad |x| < 1 \quad (3.93)$$

Exercise 3.2**The Riemann derivative of $x^p/(1-x)$**

Problem: Calculate the fractional derivative according to Riemann for

$$f(x) = \frac{x^p}{1-x} \quad |x| < 1, p \in \mathbb{R}, p > -1 \quad (3.94)$$

Exercise 3.3**Eigenvalues and eigenfunctions of the Caputo fractional derivative**

Problem: The eigenvalues $s(k)$ and the eigenfunctions $\Psi(k, t)$ of the Caputo derivative ${}_C\partial_t$ are solutions of the differential equation

$${}_C\partial_t\Psi(k, t) = s(k)\Psi(k, t) \quad (3.95)$$

Show that the solution of this differential equation for $t \geq 0$ and $k \geq 0$ is given by the Mittag-Leffler function (2.14)

$$\Psi(k, t) = E_\alpha(k^\alpha t^\alpha) \quad (3.96)$$

and the eigenvalues are given by

$$s(k) = k^\alpha \quad (3.97)$$

Exercise 3.4**Asymptotic behavior of the the Grünwald-Letnikov fractional derivative**

Problem: Prove that the asymptotic behavior of the weights in the Grünwald-Letnikov derivative

$$\partial_x^\alpha f(x) = \lim_{h \rightarrow 0} \frac{\Delta^\alpha f(x)}{h^\alpha} = \lim_{h \rightarrow 0} \left(\sum_{m=0}^{\infty} \binom{\alpha}{m} (-1)^m f(x - mh) \right) / h^\alpha \quad (3.98)$$

is approximately given by:

$$(-1)^m \binom{\alpha}{m} \sim \frac{-\alpha}{\Gamma(1-\alpha)} \frac{1}{m^{1+\alpha}} \quad m \rightarrow \infty \quad (3.99)$$

Chapter 4

Friction Forces

To start with a practical application of the fractional calculus on problems in the area of classical physics we will investigate the influence of friction forces on the dynamical behavior of classical particles. Within the framework of Newtonian mechanics friction phenomena are treated mostly schematically. Therefore a description using fractional derivatives may lead to results of major importance.

There are two reasons to start with this subject. This is a nice example, where fractional calculus may be applied on a very early entry level in physics. In addition, for a thorough treatment of fractional friction forces it is not necessary to use an exceptionally difficult mathematical framework, the hitherto presented mathematical tools are sufficient. It is also the first example, that an analytic approach using the methods developed in fractional calculus leads to results, which in general reach beyond the scope of a classical treatment. More examples will be presented in the following chapters.

First we will recapitulate the classical approach and will then discuss the solutions of Newton's equations of motion including fractional friction.

It will be demonstrated, that the viewpoint of fractional calculus leads to new insights and surprising interrelations of until now unconnected classical fields of research.

4.1 Classical description

We owe Sir Isaac Newton the first systematic application of differential calculus. Newton's mechanics abstracts from real complex physical processes introducing an idealized dimensionless point mass. Its dynamical behavior is completely specified giving the position $x(t)$ and the velocity

$v(t) = \dot{x}(t) = \frac{d}{dt}x(t)$ as a function of time t .

The dynamic development of these quantities caused by an external force F is determined by Newton's second law:

$$F = ma = m\ddot{x}(t) = m\frac{d^2}{dt^2}x(t) \quad (4.1)$$

This is an ordinary second order differential equation for $x(t)$ depending on the time variable t . In absence of external forces $F = 0$ the general solution of this equation follows from twofold integration of $\ddot{x} = 0$:

$$x(t) = c_1 + c_2 t \quad (4.2)$$

with two at first arbitrary constants of integration c_1 and c_2 , which may be determined defining appropriately chosen initial conditions.

For a given initial position x_0 and initial velocity v_0

$$x(t=0) = x_0 \quad (4.3)$$

$$v(t=0) = v_0$$

it follows

$$c_1 = x_0 \quad (4.4)$$

$$c_2 = v_0 \quad (4.5)$$

and therefore

$$x(t) = x_0 + v_0 t \quad (4.6)$$

$$\dot{x}(t) = v_0 \quad (4.7)$$

Hence we conclude, that a point mass keeps its initial velocity forever in absence of external forces. This statement is known as Newton's first law.

The observation of everyday motion contradicts this result. Sooner or later every kind of motion comes to rest without outer intervention. A wheel stops spinning. The ball will not roll any more, but will lie still in the grass. If we stop rowing, a boat will not glide forward any more.

All these observed phenomena have different physical causes. Within the framework of Newton's theory they are summarized as friction forces F_R . To be a little bit more specific we consider as friction forces all kinds of forces which point in the opposite direction of the velocity of a particle.

Therefore an ansatz for friction forces is a simple power law:

$$F_R = -\mu \operatorname{sign}(v)|v|^\alpha \quad (4.8)$$

with an arbitrarily chosen real exponent α .

The following special cases are:

$\alpha \approx 0$ is observed for static and kinetic friction for solids

$\alpha = 1$ Stokes friction in liquids with high viscosity

$\alpha = 2$ is a general trend for high velocities

In reality both gases and liquids show a behavior which only approximately corresponds to these special cases. For a more realistic treatment a superposition of these different cases leads to better results.

In the following we want to discuss the solutions for an equation of motion including the friction force of type (4.8). We have to solve the following differential equation:

$$m\ddot{x} = -\mu \operatorname{sign}(v)|\dot{x}|^\alpha \quad (4.9)$$

Within the mks unit-system the mass m is measured in [kg] and the friction coefficient μ is given as [$kg/s^{2-\alpha}$]. Assuming $v(t) > 0$ equation (4.9) reduces to

$$m\ddot{x} = -\mu\dot{x}^\alpha \quad \dot{x} > 0 \quad (4.10)$$

Despite the fact that this is a nonlinear differential equation, it may be solved directly with an appropriately chosen ansatz. We start with:

$$x(t) = c_1 + c_2(1+bt)^\alpha \quad (4.11)$$

Using the initial conditions (4.3) we obtain the general solution for (4.10):

$$x(t) = x_0 + \frac{mv_0^{2-\alpha}}{\mu(2-\alpha)} - \frac{m \left((\alpha-1) \left(-\frac{v_0^{1-\alpha}}{1-\alpha} + \frac{\mu}{m}t \right) \right)^{\frac{2-\alpha}{1-\alpha}}}{\mu(2-\alpha)} \quad (4.12)$$

This equation determines the motion of a point mass influenced by a velocity dependent friction force with arbitrary α . The well known special cases $\alpha = 0$, $\alpha = 1$ and $\alpha = 2$ are included as limiting cases:

$$\lim_{\alpha \rightarrow 0} x(t) = x_0 + v_0 t - \frac{1}{2} \frac{\mu}{m} t^2 \quad (4.13)$$

$$\lim_{\alpha \rightarrow 1} x(t) = x_0 + \frac{m}{\mu} v_0 (1 - e^{-\frac{\mu}{m}t}) \quad (4.14)$$

$$\lim_{\alpha \rightarrow 2} x(t) = x_0 + \frac{m}{\mu} \log(1 + \frac{\mu}{m} v_0 t) \quad (4.15)$$

A series expansion of (4.12) up to second order in t results in:

$$x(t) \approx x_0 + v_0 t - \frac{1}{2} \frac{\mu}{m} v_0^\alpha t^2 \quad (4.16)$$

Therefore the point mass is subject to a negative acceleration or deceleration proportional to v_0^α .

4.2 Fractional friction

We will now discuss friction phenomena within the framework of fractional calculus. According to the classical results presented in the previous section we propose the following fractional friction force:

$$F_R = -\mu \frac{d^\alpha}{dt^\alpha} x(t) \quad \dot{x}(t) > 0 \quad (4.17)$$

Here we have introduced a fractional derivative coefficient α which is an arbitrary real number and the fractional friction coefficient μ in units $[kg/s^{2-\alpha}]$ which parametrizes the strength of the fractional friction force.

For the special case $\alpha = 1$ classical and fractional friction force coincide. But for all other cases we have

$$\dot{x}^\alpha = \left(\frac{d}{dt} x(t) \right)^\alpha \neq \frac{d^\alpha}{dt^\alpha} x(t) \quad (4.18)$$

and hence we expect a dynamic behavior which differs from the classical result. We define the following fractional differential equation

$$m\ddot{x} = -\mu \frac{d^\alpha}{dt^\alpha} x(t) \quad \dot{x}(t) > 0 \quad (4.19)$$

with initial conditions (4.3), which determines the dynamical behavior of a classical point mass object to a fractional friction force.

A solution of this equation may be realized with the ansatz

$$x(t) = e^{\omega t} \quad (4.20)$$

and applying the Liouville definition of the fractional derivative

$$\frac{d^\alpha}{dt^\alpha} e^{\omega t} = \omega^\alpha e^{\omega t} \quad (4.21)$$

Inserting this ansatz into the differential equation the general solution of the equation may be obtained, if the complete set of solutions for the polynomial

$$\omega^2 = -\frac{\mu}{m} \omega^\alpha \quad (4.22)$$

is determined.

The trivial solution $\omega = 0$ for $\alpha > 0$ describes a constant, time independent function $x(t) = \text{const}$ and is a consequence of the fact, that the differential equation is built from derivatives of $x(t)$ only.

Additional solutions of the polynomial equation are formally given by

$$\omega = (-1)^{\frac{1}{2-\alpha}} \left| \frac{\mu}{m} \right|^{\frac{1}{2-\alpha}} \quad (4.23)$$

The actual number of different solutions depends on the numerical value of α .

If α is in the range of $0 < \alpha < 1$ two different conjugate complex solutions exist. Using the abbreviation

$$\kappa = \left| \frac{\mu}{m} \right|^{\frac{1}{2-\alpha}} \quad (4.24)$$

these solutions are given as:

$$\omega_1 = \kappa \left(\cos\left(\frac{\pi}{2-\alpha}\right) + i \sin\left(\frac{\pi}{2-\alpha}\right) \right) \quad (4.25)$$

$$\omega_2 = \kappa \left(\cos\left(\frac{\pi}{2-\alpha}\right) - i \sin\left(\frac{\pi}{2-\alpha}\right) \right) \quad (4.26)$$

Hence we obtain the general solution of the fractional differential equation (4.19):

$$x(t) = c_1 + c_2 e^{\omega_1 t} + c_3 e^{\omega_2 t} \quad 0 < \alpha < 1 \quad (4.27)$$

A first remarkable result of our investigation is the fact, that there are three different constants c_i , where two of these may be determined independently using the initial conditions (4.3). Consequently we are free to specify an additional reasonable initial condition. This clearly indicates that the fractional differential equation (4.19) describes a broader range of phenomena than the classical equation of motion.

One possible choice for an additional initial condition results from the series expansion (4.16) of the equation of motion including classical friction. For the second derivative of the fractional differential equation we demand:

$$\ddot{x}(t=0) = -\frac{\mu}{m} v_0^\alpha \quad (4.28)$$

This leads to the following set of determining equations for the three different coefficients c_i :

$$\begin{pmatrix} 1 & 1 & 1 \\ 0 & \omega_1 & \omega_2 \\ 0 & \omega_1^2 & \omega_2^2 \end{pmatrix} \begin{pmatrix} c_1 \\ c_2 \\ c_3 \end{pmatrix} = \begin{pmatrix} x_0 \\ v_0 \\ -\frac{\mu}{m} v_0^\alpha \end{pmatrix} \quad (4.29)$$

As a consequence the solutions of the fractional differential equation agree up to second order in t with solutions obtained for the Newtonian equation of motion including the classical friction term (4.8).

$$x(t) \approx x_0 + v_0 t - \frac{1}{2} \frac{\mu}{m} v_0^\alpha t^2 + o(t^3) \quad (4.30)$$

From figure 4.1 we may deduce, that indeed the difference of classical and fractional solution becomes manifest only for $t \gg 1$.

Remarkably enough there is an alternative choice for the additional initial condition. Let us assume that the initial velocity of a mass point

decelerates under the influence of a fractional friction force. In other words during all stages of motion the initial velocity is maximal and therefore at least a local extremum of the velocity graph.

Besides the initial conditions (4.3) we therefore define as an additional condition:

$$\dot{v}(t = 0) = \ddot{x}(t = 0) = 0 \quad (4.31)$$

This leads to the following set of determining equations for the coefficients c_i :

$$\begin{pmatrix} 1 & 1 & 1 \\ 0 & \omega_1 & \omega_2 \\ 0 & \omega_1^2 & \omega_2^2 \end{pmatrix} \begin{pmatrix} c_1 \\ c_2 \\ c_3 \end{pmatrix} = \begin{pmatrix} x_0 \\ v_0 \\ 0 \end{pmatrix} \quad (4.32)$$

The complete solution of the fractional differential equation including a fractional friction force is then given by:

$$x(t) = x_0 + \frac{v_0}{\kappa \sin(\frac{\pi}{2-\alpha})} \left(e^{\kappa \cos(\frac{\pi}{2-\alpha}) t} \sin(\frac{2\pi}{2-\alpha} - \kappa \sin(\frac{\pi}{2-\alpha}) t) - \sin(\frac{2\pi}{2-\alpha}) \right) \quad (4.33)$$

This solution is valid from $t = 0$ up to a final time t_0 where the motion of the mass point comes to rest and then remains at the final position. t_0 is determined by:

$$t_0 = \frac{\pi}{(2-\alpha)\kappa \sin(\frac{\pi}{2-\alpha})} \quad (4.34)$$

Special cases of the general solution (4.33) are solutions for $\alpha = 0$ and $\alpha = 1$ respectively:

$$x(t, \alpha = 0) = x_0 + \frac{v_0}{\kappa} \sin(\kappa t) \quad (4.35)$$

$$x(t, \alpha = 1) = x_0 + \frac{v_0}{\kappa} (2 - 2e^{-\kappa t} - \kappa t e^{-\kappa t}) \quad (4.36)$$

Obviously this is a completely new function type. The initial velocity v_0 becomes less important and merely acts as a scaling parameter. The time evolution of the solutions may be understood much better in terms of free ($\alpha = 0$) and damped ($0 < \alpha \leq 1$) oscillations, if we consider the first quarter period for a description of a fractional friction process.

In order to investigate this aspect of fractional friction, for reasons of completeness we first present the solutions of the classical harmonic oscillator.

The differential equation for the damped harmonic oscillator is given by:

$$m\ddot{x}(t) = -kx(t) - \gamma\dot{x}(t) \quad (4.37)$$

For a mass m with the damping coefficient γ and the spring constant k . The ansatz

$$x(t) = e^{\omega t} \quad (4.38)$$

leads to a quadratic equation for the frequencies ω :

$$\omega^2 = -\frac{\gamma}{m}\omega - \frac{k}{m} \quad (4.39)$$

which leads to two solutions:

$$\omega_{1,2} = -\frac{\gamma}{2m} \pm \sqrt{\frac{\gamma^2}{4m^2} - \frac{k}{m}} \quad (4.40)$$

Depending on the value of γ and of the discriminant $D = \frac{\gamma^2}{4m^2} - \frac{k}{m}$ we distinguish the cases

$\gamma = 0$ leads to a free oscillation

$\gamma > 0$ and $D < 0$ leads to a damped oscillation.

$\gamma > 0$ and $D = 0$ There is no oscillatory contribution any more. The system returns to equilibrium as quickly as possible. This case is called the critically damped case.

$\gamma > 0$ and $D > 0$ In this case too there is no oscillatory component any more. The system exponentially decays. This case is called the overdamped case. The equilibrium position is reached for $t \rightarrow \infty$.

Now we can compare the frequencies ω_i from the fractional differential equation (4.25) to the frequencies for the damped harmonic oscillator (4.40).

We obtain the following relations for the parameter set $\{\gamma, k\}$ which determines the behavior of the classical damped harmonic oscillator and the parameter set $\{\alpha, \mu\}$, which describes the behavior of the solutions of the fractional friction differential equation:

$$\frac{k}{m} = \left(\frac{\mu}{m}\right)^{\frac{2}{2-\alpha}} \quad (4.41)$$

$$\frac{\gamma}{m} = -2 \left(\frac{\mu}{m}\right)^{\frac{1}{2-\alpha}} \cos\left(\frac{\pi}{2-\alpha}\right) \quad (4.42)$$

From the above follows a unique relation between γ/\sqrt{km} and the fractional derivative coefficient α :

$$\frac{\gamma}{\sqrt{km}} = -2 \cos\left(\frac{\pi}{2-\alpha}\right) \quad (4.43)$$

$$\approx \frac{\pi}{2}\alpha \quad \text{for } \alpha \approx 0 \quad (4.44)$$

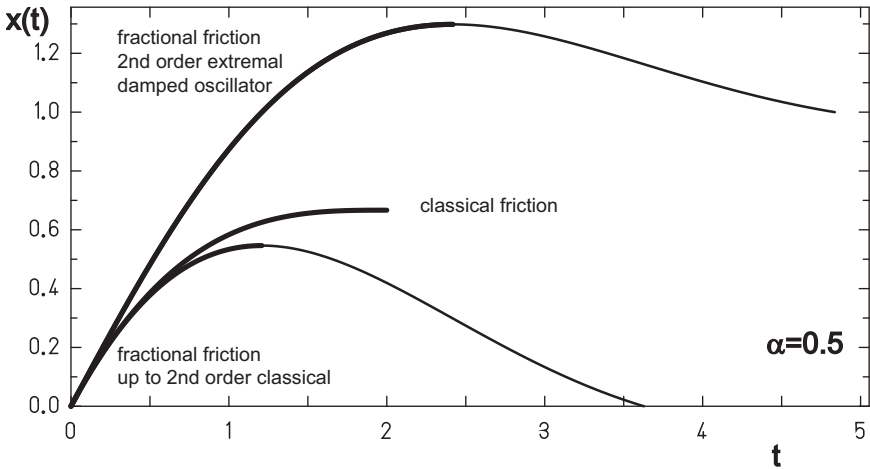


Fig. 4.1 For $\alpha = 0.5$ different solutions of equations of motion are plotted. In the middle the classical solution of the Newtonian differential equation (4.12) is presented, below the corresponding fractional solution with the additional initial condition (4.28) is shown. Up to second order in t both solutions coincide. A difference may be observed only at the end of the motion period. The upper line indicates the fractional solution using the additional initial condition (4.31). Thick lines describe the motion valid until the body comes to rest. In addition, for both fractional solutions the plot range is extended to t -values $t > t_0$ (thin lines), which is beyond the physically valid region.

We have derived a first physical interpretation for the at first abstractly introduced fractional derivative coefficient α . Obviously the ratio γ/\sqrt{km} and the fractional derivative coefficient α are directly correlated.

We may conclude, that fractional friction may be interpreted in the limit $\alpha \rightarrow 0$ in analogy to the harmonic oscillator more and more as a damping term.

On the other hand, if we examine the region $\alpha \approx 2$ the fractional friction force may be understood as an additional contribution to the acceleration term. For the ideal case $\alpha = 2$ we obtain the differential equation

$$(m + \mu)\ddot{x} = 0 \quad (4.45)$$

which obviously describes an increase of mass. The point mass moves freely with an increased mass $m' = m + \mu$.

The variation of the fractional friction coefficient α within the interval $2 \geq \alpha \geq 0$ therefore describes acceleration- velocity- and position dependent classical force types from a generalized point of view as fractional friction.

We want to emphasize two aspects of our investigations performed so far.

Using the fractional equivalent to the Newtonian equation of motion with a classical friction term, we may describe a much broader area of application than it is possible with the classical approach. For an appropriately chosen set of fractional initial conditions we are able to describe damped oscillations. From the point of view of fractional calculus the harmonic oscillator is just one more example for a fractional friction phenomenon. In other words, while in a classical picture friction and damping are described using different approaches, the fractional picture allows for an unified description.

This is a general aspect of a fractional approach. Different phenomena, which seem to be unrelated in a classical description, now appear as different realizations of a general aspect in a fractional theory. This leads to intriguing, sometimes surprising new insights. We will demonstrate, that this is a common aspect of all applications of fractional calculus, as we will verify in the following chapters.

One more important observation is a rather technical remark. The fractional differential equation (4.19) merges two different classical types of a differential equation. On the one hand the solutions of a nonlinear differential equation, which is in general a quite complicated type of equation and on the other hand solutions of a simple second order differential equation with constant coefficients result from the same fractional equation.

This aspect is of general nature and nourishes the hope, that a wide range of complex problems may be solved analytically with minimal effort using fractional calculus, while a solution within the framework of a classical theory may be difficult. In the following chapters we will present some examples, to illustrate this point.

Exercise 4.1

Eigenfunctions for a first order fractional differential equation with purely imaginary fractional coefficient α

Problem: We know that an exponential growth may be modeled by the standard first order differential equation:

$$\partial_t f(t) = kf(t) \quad (4.46)$$

where the solution is given by $f(t) = e^{kt}$.

This ansatz was extended by Liouville for fractional derivatives

$$\partial_t^\alpha f(t) = k^\alpha f(t), \quad k > 0, t > 0, \alpha \in \mathbb{C} \quad (4.47)$$

with the same eigenfunction $f(t) = e^{kt}$, which may be interpreted from a physicists point of view as the fractional generalization of exponential growth, which seems a natural explanation as long as $\alpha \in \mathbb{R}$.

But what are the characteristics of the eigenfunctions of the following purely imaginary fractional differential equation with $\alpha = i = \sqrt{-1}$

$$\partial_t^i f(t) = kf(t), \quad k > 0, t > 0 \quad (4.48)$$

Hint: Use the Liouville definition of a fractional derivative and the Moivre formula:

$$e^{i\phi} = \cos(\phi) + i \sin(\phi) \quad (4.49)$$

Chapter 5

Fractional Calculus

Up to now we have introduced a fractional derivative definition for special simple function classes. In the following section we will present common generalizations for arbitrary analytic functions. As a starting point we will use Cauchy's formula for repeated integration which will be extended to fractional integrals. Having derived a fractional integral I^α properly we will obtain a satisfying definition of a fractional derivative, if we assume

$$\frac{d^\alpha}{dx^\alpha} = I^{-\alpha} \quad (5.1)$$

which is equivalent to demand, that a fractional integral is the inverse of a fractional derivative.

As a consequence, the complexity level and difficulties of calculating the fractional derivative for a given function will turn out to be similar to integral calculus. This is in contrast to a standard classical derivative, which, in general, is much easier to calculate than a corresponding integral.

First we will discuss possible generalizations for the first derivative, namely, the Liouville, Liouville-Caputo, Riemann- and Caputo fractional derivative definition on the basis of the different possible sequences of applying operators for the fractional integral and the derivative. This approach has the advantage, that it may be easily extended to more complex operator types, e.g. space dependent derivatives.

We will also show, that higher order derivatives may be directly generalized on the basis of the Riesz-definition of the fractional derivative.

We will present Podlubny's [Podlubny (2001)] geometric interpretation of a fractional integral and will demonstrate, that we may establish a smooth transition from standard derivative ($\alpha = n$) via low level fractionality ($\alpha = n + \epsilon$) up to arbitrary fractional derivative following an idea proposed by Tarasov [Tarasov and Zaslavsky (2006)].

Finally we will present a derivation of the semi-group property

$$I^\alpha I^\beta f(x) = I^{\alpha+\beta} f(x) \quad \alpha, \beta \geq 0 \quad (5.2)$$

which is the defining property for a nonlocal derivative operator of fractional type.

5.1 The Fourier transform

A direct approach for a general fractional derivative had been proposed by Fourier in the early 19th century [Fourier (1822)]. Therefore we will present his idea first:

In the interval $[-L/2 \leq x \leq L/2]$ a function may be expanded in a Fourier series:

$$f(x) = \frac{1}{\sqrt{L}} \sum_{k=-\infty}^{k=+\infty} g_k e^{-ik\frac{2\pi}{L}x} \quad (5.3)$$

where the complex valued coefficients g_k are given by

$$g_k = \frac{1}{\sqrt{L}} \int_{-L/2}^{+L/2} f(x) e^{ik\frac{2\pi}{L}x} dx \quad (5.4)$$

Extending the interval length to infinity, the discrete spectrum g_k changes to a continuous one $g(k)$.

The Fourier transform $g(k)$ is then given by

$$g(k) = \frac{1}{\sqrt{2\pi}} \int_{-\infty}^{+\infty} f(x) e^{ikx} dx \quad (5.5)$$

and the inverse is given as

$$f(x) = \frac{1}{\sqrt{2\pi}} \int_{-\infty}^{+\infty} g(k) e^{-ikx} dk \quad (5.6)$$

The derivative of a function results as

$$\frac{d^n}{dx^n} f(x) = \frac{1}{\sqrt{2\pi}} \int_{-\infty}^{+\infty} g(k) (-ik)^n e^{-ikx} dk \quad (5.7)$$

This result may be directly extended to a fractional derivative definition:

$$\frac{d^\alpha}{dx^\alpha} f(x) = \frac{1}{\sqrt{2\pi}} \int_{-\infty}^{+\infty} g(k) (-ik)^\alpha e^{-ikx} dk \quad (5.8)$$

Equations (5.5) and (5.8) define the fractional derivative according to Fourier. This definition is quite simple but very elegant. The only condition is the existence of the Fourier transform $g(k)$ and its fractional inverse

Table 5.1 Some special functions and their fractional derivative according to Fourier.

$f(x)$	$\frac{d^\alpha}{dx^\alpha} f(x)$
e^{ikx}	$(ik)^\alpha e^{ikx}$
$\sin(kx)$	$k^\alpha \sin(kx + \frac{\pi}{2}\alpha)$
$\cos(kx)$	$k^\alpha \cos(kx + \frac{\pi}{2}\alpha)$
e^{-kx^2}	$\frac{2^\alpha}{\sqrt{\pi}} k^{\alpha/2} (\cos(\frac{\pi}{2}\alpha)\Gamma(\frac{1+\alpha}{2})_1F_1(\frac{1+\alpha}{2}; \frac{1}{2}; -kx^2) - \sqrt{k}\alpha \sin(\frac{\pi}{2}\alpha)\Gamma(\frac{\alpha}{2})_1F_1(\frac{2+\alpha}{2}; \frac{3}{2}; -kx^2))$
$\text{erf}(kx)$	$\frac{2^\alpha}{\sqrt{\pi}} k^\alpha (2kx \cos(\frac{\pi}{2}\alpha)\Gamma(\frac{1+\alpha}{2})_1F_1(\frac{1+\alpha}{2}; \frac{3}{2}; -k^2x^2) + \sin(\frac{\pi}{2}\alpha)\Gamma(\frac{\alpha}{2})_1F_1(\frac{\alpha}{2}; \frac{1}{2}; -k^2x^2))$
$\log(x)$	$\frac{\Gamma(\alpha)}{2 x ^\alpha} (e^{i\pi\alpha} + 1 + \text{sign}(x)(e^{i\pi\alpha} - 1))$
$ x ^{-k}$	$\frac{\Gamma(k+\alpha)}{\Gamma(k)} x ^{-k-\alpha} \quad x < 0$

for a given function. In addition, the fractional derivative parameter α may be chosen arbitrarily.

In particular the real part of α may also be a negative number. In this case we call (5.8) a fractional integral definition.

In table 5.1 we have listed some special functions and the corresponding fractional derivative according to Fourier.

5.2 The fractional integral

If we use the abbreviation $_aI$ for the integral operator

$$_aIf = \int_a^x f(\xi) d\xi \quad (5.9)$$

integration of a function may be considered as the inverse operation of differentiation:

$$\left(\frac{d}{dx} \right) (_aI)f = f \quad (5.10)$$

Hence it is reasonable to investigate the method of fractional integration first and based on this investigation in a next step to make statements on the fractional derivative of analytic functions in general.

Let us start with the observation, that the multiple integral

$$_aI^n f = \int_a^{x_n} \int_a^{x_{n-1}} \dots \int_a^{x_1} f(x_0) dx_0 \dots dx_{n-1} \quad (5.11)$$

using Cauchy's formula of repeated integration may be reduced to a single integral

$$_aI^n f(x) = \frac{1}{(n-1)!} \int_a^x (x-\xi)^{n-1} f(\xi) d\xi \quad (5.12)$$

This formula may be easily extended to the fractional case [Krug (1890)]:

$${}_aI_+^\alpha f(x) = \frac{1}{\Gamma(\alpha)} \int_a^x (x - \xi)^{\alpha-1} f(\xi) d\xi \quad (5.13)$$

$${}_bI_-^\alpha f(x) = \frac{1}{\Gamma(\alpha)} \int_x^b (\xi - x)^{\alpha-1} f(\xi) d\xi \quad (5.14)$$

The first of these two equations is valid for $x > a$, the second one is valid for $x < b$. The constants a, b determine the lower and upper boundary of the integral domain and may at first be arbitrarily chosen. To distinguish the two cases, we call them the left- and right-handed case respectively. This may be understood from a geometrical point of view. The left-handed integral collects weighted function values for $\xi < x$, which means left from x . The right-handed integral collects weighted function values for $\xi > x$, which means right from x . If x is a time-like coordinate, then the left-handed integral is causal, the right handed integral is anti-causal.

The actual value of the integral obviously depends on the specific choice of the two constants (a, b) .

This will indeed be the remarkable difference for the two mostly used different definitions of a fractional integral:

5.2.1 *The Liouville fractional integral*

We define the fractional integral according to Liouville setting $a = -\infty$, $b = +\infty$:

$${}_L I_+^\alpha f(x) = \frac{1}{\Gamma(\alpha)} \int_{-\infty}^x (x - \xi)^{\alpha-1} f(\xi) d\xi \quad (5.15)$$

$${}_L I_-^\alpha f(x) = \frac{1}{\Gamma(\alpha)} \int_x^{+\infty} (\xi - x)^{\alpha-1} f(\xi) d\xi \quad (5.16)$$

5.2.2 *The Riemann fractional integral*

The fractional integral according to Riemann is given by setting $a = 0$, $b = 0$:

$${}_R I_+^\alpha f(x) = \frac{1}{\Gamma(\alpha)} \int_0^x (x - \xi)^{\alpha-1} f(\xi) d\xi \quad (5.17)$$

$${}_R I_-^\alpha f(x) = \frac{1}{\Gamma(\alpha)} \int_x^0 (\xi - x)^{\alpha-1} f(\xi) d\xi \quad (5.18)$$

What is the difference between the definition according to Liouville (5.15), (5.16) and according to Riemann (5.17), (5.18) ? Let us apply both integral definitions to the special function $f(x) = e^{kx}$. We obtain:

$$_L I_+^\alpha e^{kx} = k^{-\alpha} e^{kx} \quad k, x > 0 \quad (5.19)$$

$$_L I_-^\alpha e^{kx} = (-k)^{-\alpha} e^{kx} \quad k < 0 \quad (5.20)$$

$$_R I_+^\alpha e^{kx} = k^{-\alpha} e^{kx} \left(1 - \frac{\Gamma(\alpha, kx)}{\Gamma(\alpha)} \right) \quad x > 0 \quad (5.21)$$

$$_R I_-^\alpha e^{kx} = (-k)^{-\alpha} e^{kx} \left(1 - \frac{\Gamma(\alpha, kx)}{\Gamma(\alpha)} \right) \quad x < 0 \quad (5.22)$$

where $\Gamma(\alpha, x)$ is the incomplete gamma function.

Using the Liouville fractional integral definition the function e^{kx} vanishes for $k > 0$ at the lower boundary of the integral domain. Consequently there is no additional contribution. On the other hand with the Riemann definition we obtain an additional contribution, since at $a = 0$ the exponential function does not vanish.

5.3 Correlation of fractional integration and differentiation

In the last section we have presented the Riemann and Liouville version of a fractional integral definition. But actually we are interested in a useful definition of a fractional derivative. Using the abbreviation

$$\frac{d^\alpha}{dx^\alpha} = D^\alpha \quad (5.23)$$

we will demonstrate, that the concepts of fractional integration and fractional differentiation are closely related. Let us split up the fractional derivative operator

$$D^\alpha = D^m D^{\alpha-m} \quad m \in \mathbb{N} \quad (5.24)$$

$$= \frac{d^m}{dx^m} {}_a I^{m-\alpha} \quad (5.25)$$

This means that a fractional derivative may be interpreted as a fractional integral followed by an ordinary standard derivative. Once a definition of the fractional integral is given the fractional derivative is determined too.

The inverted sequence of operators

$$D^\alpha = D^{\alpha-m} D^m \quad m \in \mathbb{N} \quad (5.26)$$

$$= {}_a I^{m-\alpha} \frac{d^m}{dx^m} \quad (5.27)$$

leads to an alternative decomposition of the fractional derivative into an ordinary standard derivative followed by a fractional integral.

Both decompositions (5.24) and (5.26) of course lead to different results.

With these decompositions we are able to understand the mechanism, how nonlocality enters the fractional calculus. The standard derivative of course is a local operator, but the fractional integral certainly is not. The fractional derivative must be understood as the inverse of fractional integration, which is a nonlocal operation. As a consequence, fractional differentiation and fractional integration yield the same level of difficulty.

In the last section we have given two different definitions of the fractional integral from Liouville and Riemann. For each of these definitions according to the two different decompositions given above follow two different realizations of a fractional derivative definition, which we will present in the following.

5.3.1 The Liouville fractional derivative

For the simple case $0 < \alpha < 1$ we obtain for the Liouville definition of a fractional derivative using (5.15), (5.16) and operator sequence (5.24)

$${}_L D_+^\alpha f(x) = \frac{d}{dx} {}_L I_+^{1-\alpha} f(x) \quad (5.28)$$

$$= \frac{d}{dx} \frac{1}{\Gamma(1-\alpha)} \int_{-\infty}^x (x-\xi)^{-\alpha} f(\xi) d\xi \quad (5.29)$$

$${}_L D_-^\alpha f(x) = \frac{d}{dx} {}_L I_-^{1-\alpha} f(x) \quad (5.30)$$

$$= \frac{d}{dx} \frac{1}{\Gamma(1-\alpha)} \int_x^{+\infty} (\xi-x)^{-\alpha} f(\xi) d\xi \quad (5.31)$$

In table 5.2 we have listed some special functions and their Liouville fractional derivative.

Table 5.2 The fractional derivative ${}_L D_+^\alpha$ according to Liouville for some special functions.

$f(x)$	$\frac{d^\alpha}{dx^\alpha} f(x)$
e^{kx}	$k^\alpha e^{kx} \quad k \geq 0$
$\sin(kx)$	$k^\alpha \sin(kx + \frac{\pi}{2}\alpha)$
$\cos(kx)$	$k^\alpha \cos(kx + \frac{\pi}{2}\alpha)$
$\text{erf}(kx)$	divergent
e^{-kx^2}	$\frac{k^{\frac{\alpha}{2}}}{\Gamma(1-\alpha)} (\Gamma(1 - \frac{\alpha}{2}) {}_1F_1(\frac{1}{2} + \frac{\alpha}{2}; \frac{1}{2}; -kx^2) - \sqrt{k}\alpha x \Gamma(\frac{1}{2} - \frac{\alpha}{2}) {}_1F_1(1 + \frac{\alpha}{2}; \frac{3}{2}; -kx^2)) - 2\sqrt{k}\alpha x \Gamma(\frac{3}{2} - \frac{\alpha}{2}) {}_1F_1(\frac{1}{2} + \frac{\alpha}{2}; \frac{3}{2}; -kx^2) - \frac{2}{3}k(1 - \alpha^2)x^2 \Gamma(\frac{1}{2} - \frac{\alpha}{2}) {}_1F_1(\frac{3}{2} + \frac{\alpha}{2}; \frac{5}{2}; -kx^2))$
${}_p F_q(\{a_i\}; \{b_j\}; kx)$	$k^\alpha \prod_{i=1}^p \frac{\Gamma(a_i + \alpha)}{\Gamma(a_i)} \prod_{j=1}^q \frac{\Gamma(b_j)}{\Gamma(b_j + \alpha)} {}_p F_q(\{a_i + \alpha\}; \{b_j + \alpha\}; kx)$
$ x ^{-k}$	$\frac{\Gamma(k+\alpha)}{\Gamma(k)} x ^{-k-\alpha} \quad x < 0$

5.3.2 The Riemann fractional derivative

For the Riemann fractional derivative we obtain using (5.17), (5.18) and operator sequence (5.24):

$${}_R D_+^\alpha f(x) = \frac{d}{dx} {}_R I_+^{1-\alpha} f(x) \quad (5.32)$$

$$= \frac{d}{dx} \frac{1}{\Gamma(1-\alpha)} \int_0^x (x-\xi)^{-\alpha} f(\xi) d\xi \quad (5.33)$$

$${}_R D_-^\alpha f(x) = \frac{d}{dx} {}_R I_-^{1-\alpha} f(x) \quad (5.34)$$

$$= \frac{d}{dx} \frac{1}{\Gamma(1-\alpha)} \int_x^0 (\xi-x)^{-\alpha} f(\xi) d\xi \quad (5.35)$$

In table 5.3 we have listed some special functions and their Riemann fractional derivative.

Table 5.3 Some special functions and their fractional derivative ${}_R D^\alpha$ according to the Riemann definition.

$f(x)$	$\frac{d^\alpha}{dx^\alpha} f(x)$
e^{kx}	$\text{sign}(x) x ^{-\alpha} E(1, 1 - \alpha, kx)$
$\sin(kx)$	$\frac{(2-\alpha) k \text{sign}(x) x ^{-\alpha} x}{(2-3\alpha+\alpha^2)\Gamma(1-\alpha)} {}_1F_2(1; \frac{3}{2} - \frac{\alpha}{2}, 2 - \frac{\alpha}{2}; -\frac{1}{4}k^2 x^2) -$ $\frac{k^3 \text{sign}(x) x ^{-\alpha} x^3}{(\frac{3}{2} - \frac{\alpha}{2})(2 - \frac{\alpha}{2})(2-3\alpha+\alpha^2)\Gamma(1-\alpha)} {}_1F_2(2; \frac{5}{2} - \frac{\alpha}{2}, 3 - \frac{\alpha}{2}; -\frac{1}{4}k^2 x^2)$
$\cos(kx)$	$\text{sign}(x) \frac{ x ^{-\alpha}}{\Gamma(4-\alpha)}$ $((\alpha-1)(\alpha-2)(\alpha-3) {}_1F_2(1; 1 - \frac{\alpha}{2}, \frac{3}{2} - \frac{\alpha}{2}; -\frac{1}{4}k^2 x^2) +$ $+ 2k^2 x^2 {}_1F_2(2; 2 - \frac{\alpha}{2}, \frac{5}{2} - \frac{\alpha}{2}; -\frac{1}{4}k^2 x^2))$
$\text{erf}(kx)$	$-2^{-1+\alpha} k \text{sign}(x) x ^{-\alpha}$ $\left((a-2) {}_2F_2(\frac{1}{2}, 1; \frac{3}{2} - \frac{\alpha}{2}, 2 - \frac{\alpha}{2}; -k^2 x^2) + \right.$ $\left. k^2 x^2 {}_2F_2(\frac{3}{2}, 2; \frac{5}{2} - \frac{\alpha}{2}, 3 - \frac{\alpha}{2}; -k^2 x^2) \right)$
$p F_q(\{a_i\}; \{b_j\}; kx)$	$\text{sign}(x) x ^{-\alpha} \frac{1}{\Gamma(1-\alpha)} p+1 F_{q+1}(\{1, 1+a_i\}; \{b_j, 2-\alpha\}; kx) +$ $k \text{sign}(x) x ^{-\alpha} x \frac{1}{(1-\alpha)(2-\alpha)\Gamma(1-\alpha)} \prod_{i=1}^p a_i \prod_{j=1}^q \frac{1}{b_j} \times$ $p+1 F_{q+1}(\{2, 1+a_i\}; \{1+b_j, 3-\alpha\}; kx)$
$\log(x)$	$\frac{x^{-\alpha}}{\Gamma(2-\alpha)} (1 - (1-\alpha)(H_{1-\alpha} + \log(x))) \quad x > 0$
x^k	$\frac{\Gamma(1+k)}{\Gamma(1+k-\alpha)} \text{sign}(x) x ^{-\alpha} x^k$

5.3.3 The Liouville fractional derivative with inverted operator sequence - the Liouville-Caputo fractional derivative

In case we invert the operator sequence according to (5.26) we obtain on the basis of the Liouville fractional integral definition (5.15), (5.16):

$${}_{LC} D_+^\alpha f(x) = {}_L I_+^{1-\alpha} \frac{d}{dx} f(x) \quad (5.36)$$

$$= \frac{1}{\Gamma(1-\alpha)} \int_{-\infty}^x (x-\xi)^{-\alpha} \frac{df(\xi)}{d\xi} d\xi \quad (5.37)$$

$$= \frac{1}{\Gamma(1-\alpha)} \int_{-\infty}^x (x-\xi)^{-\alpha} f'(\xi) d\xi \quad (5.38)$$

$${}_{LC} D_-^\alpha f(x) = {}_L I_-^{1-\alpha} \frac{d}{dx} f(x) \quad (5.39)$$

$$= \frac{1}{\Gamma(1-\alpha)} \int_x^{+\infty} (\xi-x)^{-\alpha} \frac{df(\xi)}{d\xi} d\xi \quad (5.40)$$

$$= \frac{1}{\Gamma(1-\alpha)} \int_x^{+\infty} (\xi-x)^{-\alpha} f'(\xi) d\xi \quad (5.41)$$

This definition of a fractional derivative has no special name nor did we find any mention in the mathematical literature. At first it could be assumed, that both derivatives (5.28) and (5.36) lead to similar results. But with the special choice $f(x) = \text{const}$, it follows immediately that the Liouville fractional derivative definition (5.28) leads to a divergent result, while with (5.36) the result vanishes.

As a general remark, the conditions for analytic functions which lead to a convergent result for the Liouville fractional derivative are much more restrictive than for the Liouville fractional derivative with inverted operator sequence.

As a convergence condition for the Liouville derivative definition we obtain for an analytic function

$$\lim_{x \rightarrow \pm\infty} f(x) = O(|x|^{-\alpha-\epsilon}), \quad \epsilon > 0 \quad (5.42)$$

while for the Liouville derivative with inverted operator sequence the same behavior is required only for the derivative.

The idea to define a fractional derivative with an inverted operator sequence was first proposed by Caputo and was used for a reformulation of the Riemann fractional derivative. Hence we will call the fractional derivative according to Liouville with inverted operator sequence as Liouville-Caputo derivative.

As long as both integrals (5.28) and (5.36) are convergent for a given function, the Liouville and the Liouville-Caputo derivative definition lead to similar results.

Later in chapter 8 we will demonstrate, that both definitions will lead to different results when extended to describe general nonlocal operators.

In table 5.4 some functions and the corresponding Liouville-Caputo derivative are listed.

A comparison with table 5.2 demonstrates, that both definitions lead to similar results, as long as the integrals (5.28) and (5.36) converge.

On the other hand, the error function $\text{erf}(x)$ is a nice example for the different convergence requirements of the Liouville and Liouville-Caputo fractional derivative definition.

In the sense of Liouville the fractional derivative integral (5.28) applied to the error function is divergent and therefore the error function is not differentiable. For the Liouville-Caputo definition of a fractional derivative the integral (5.36) converges and therefore the error function is differentiable.

Table 5.4 Some special functions and the corresponding Liouville-Caputo derivative ${}_{LC}D_+$.

$f(x)$	$\frac{d^\alpha}{dx^\alpha} f(x)$
e^{kx}	$k^\alpha e^{kx} \quad k \geq 0$
$\sin(kx)$	$k^\alpha \sin(kx + \frac{\pi}{2}\alpha)$
$\cos(kx)$	$k^\alpha \cos(kx + \frac{\pi}{2}\alpha)$
e^{-kx^2}	$\frac{k^{\frac{\alpha}{2}}}{\Gamma(1-\alpha)} (\Gamma(1-\frac{\alpha}{2}) {}_1F_1(\frac{1}{2} + \frac{\alpha}{2}; \frac{1}{2}; -kx^2) - \sqrt{k}\alpha x \Gamma(\frac{1}{2} - \frac{\alpha}{2}) {}_1F_1(1 + \frac{\alpha}{2}; \frac{3}{2}; -kx^2))$
$\text{erf}(kx)$	$-\frac{k^{\alpha}}{\pi^{3/2}} \sin(\pi\alpha) (kx\Gamma(-\frac{\alpha}{2})\Gamma(1+\alpha) {}_1F_1(\frac{1}{2} + \frac{\alpha}{2}; \frac{3}{2}; -k^2x^2) - \Gamma(\frac{1}{2} - \frac{\alpha}{2})\Gamma(\alpha) {}_1F_1(\frac{\alpha}{2}; \frac{1}{2}; -k^2x^2))$
${}_pF_q(\{a_i\}; \{b_j\}; kx)$	$k^\alpha \prod_{i=1}^p \frac{\Gamma(a_i + \alpha)}{\Gamma(a_i)} \prod_{j=1}^q \frac{\Gamma(b_j)}{\Gamma(b_j + \alpha)} {}_pF_q(\{a_i + \alpha\}; \{b_j + \alpha\}; kx)$

5.3.4 The Riemann fractional derivative with inverted operator sequence - the Caputo fractional derivative

The inverted operator sequence (5.26) using the Riemann fractional integral definition (5.17), (5.18) leads to:

$${}_{C}D_+^\alpha f(x) = {}_R I_+^{1-\alpha} \frac{d}{dx} f(x) \quad (5.43)$$

$$= \frac{1}{\Gamma(1-\alpha)} \int_0^x (x-\xi)^{-\alpha} \frac{df(\xi)}{d\xi} d\xi \quad (5.44)$$

$$= \frac{1}{\Gamma(1-\alpha)} \int_0^x (x-\xi)^{-\alpha} f'(\xi) d\xi \quad (5.45)$$

$${}_{C}D_-^\alpha f(x) = {}_R I_-^{1-\alpha} \frac{d}{dx} f(x) \quad (5.46)$$

$$= \frac{1}{\Gamma(1-\alpha)} \int_x^0 (\xi-x)^{-\alpha} \frac{df(\xi)}{d\xi} d\xi \quad (5.47)$$

$$= \frac{1}{\Gamma(1-\alpha)} \int_x^0 (\xi-x)^{-\alpha} f'(\xi) d\xi \quad (5.48)$$

This definition is known as the Caputo fractional derivative. The difference between Riemann and Caputo fractional derivative may be demonstrated using $f(x) = \text{const}$.

For the Riemann fractional derivative it follows

$${}_{R}D_+^\alpha \text{const} = \frac{\text{const}}{\Gamma(1-\alpha)} x^{-\alpha} \quad (5.49)$$

Table 5.5 Some special functions and their Caputo derivative ${}_C D^\alpha$.

$f(x)$	$\frac{d^\alpha}{dx^\alpha} f(x)$
e^{kx}	$k x ^{1-\alpha} E(1, 2-\alpha, kx)$
x^p	$\frac{\Gamma(1+p)}{\Gamma(1+p-\alpha)} \text{sign}(x) x ^{-\alpha} x^p \quad p > -1$ $0 \quad p = 0$
$\sin(kx)$	$\frac{k \text{sign}(x) x ^{-\alpha} x}{\Gamma(1-\alpha/2) \Gamma(3/2-\alpha/2) \Gamma(2-\alpha)} {}_1F_2(1; 1 - \frac{\alpha}{2}, \frac{3}{2} - \frac{\alpha}{2}; -\frac{1}{4} k^2 x^2)$
$\cos(kx)$	$\frac{-k^2 \text{sign}(x) x ^{-\alpha} x^2}{\Gamma(3/2-\alpha/2) \Gamma(2-\alpha/2) \Gamma(3-\alpha)} {}_1F_2(1; \frac{3}{2} - \frac{\alpha}{2}, 2 - \frac{\alpha}{2}; -\frac{1}{4} k^2 x^2)$
e^{-kx^2}	$\frac{-2kx^{2-\alpha}}{\Gamma(3-\alpha)} {}_2F_2(1, \frac{3}{2}; \frac{3}{2} - \frac{\alpha}{2}, 2 - \frac{\alpha}{2}; -kx^2)$
$\text{erf}(kx)$	$\frac{2k \text{sign}(x) x ^{-\alpha} x}{\Gamma(2-\alpha) \sqrt{\pi}} {}_2F_2(\frac{1}{2}, 1; 1 - \frac{\alpha}{2}, \frac{3}{2} - \frac{\alpha}{2}; -k^2 x^2)$
$p F_q(\{a_i\}; \{b_j\}; kx)$	$k \text{sign}(x) x ^{-\alpha} x \prod_{i=1}^p a_i \prod_{j=1}^q \Gamma(b_j) \times$ $p+1 F_{q+1}(\{1, 1+a_i\}; \{b_j, 2-\alpha\}; kx)$

while applying the Caputo derivative we obtain

$${}_C D_+^\alpha \text{const} = 0 \quad (5.50)$$

In table 5.5 we have listed some special functions and the corresponding Caputo derivative.

Therefore in this section we have presented all standard definitions of a fractional derivative, which satisfy the condition

$$\lim_{\alpha \rightarrow 1} D^\alpha f(x) = \frac{df(x)}{dx} \quad (5.51)$$

5.4 Fractional derivative of second order

For the case $0 \leq \alpha \leq 1$ we have presented fractional derivative definitions. The four different definitions namely the Liouville, Riemann, Liouville-Caputo and Caputo derivatives are direct generalizations of the standard first order derivative to fractional values α .

Derivatives of higher order may be generated by multiple application of a first order derivative:

$$\frac{d^n}{dx^n} = \frac{d}{dx} \frac{d}{dx} \cdots \frac{d}{dx} \quad \text{n-fold} \quad (5.52)$$

This strategy is valid for fractional derivatives of higher order too:

$$D_\pm^\alpha f(x) = \begin{cases} \pm(D^m {}_a I_\pm^{m-\alpha}) f(x) & m-1 < \alpha \leq m, \quad m \text{ odd}, \\ (D^m {}_a I_\pm^{m-\alpha}) f(x) & m-1 < \alpha \leq m, \quad m \text{ even} \end{cases} \quad (5.53)$$

An alternative approach is based on the idea, to extend a derivative of higher order directly. In this section we will investigate the behavior of fractional derivatives with the property

$$\lim_{\alpha \rightarrow 2} D^\alpha = \frac{d^2}{dx^2} \quad (5.54)$$

which of course not necessarily implies the similarity of the first derivative and the fractional derivative for $\alpha = 1$. There are well known strategies for a numerical solution of an ordinary differential equation which in a similar way approximate the second derivative directly (e.g. the Störmer-method).

5.4.1 The Riesz fractional derivative

For a fractional derivative definition which fulfills condition (5.54) the most prominent representative is the Riesz definition of a fractional derivative [Riesz (1949)].

Starting point is a linear combination of both fractional Liouville integrals (5.15) and (5.16)

$${}_{RZ} I^\alpha f(x) = \frac{{}^L I_+^\alpha + {}^L I_-^\alpha}{2 \cos(\pi\alpha/2)} f(x) \quad (5.55)$$

$$= \frac{1}{2\Gamma(\alpha) \cos(\pi\alpha/2)} \int_{-\infty}^{+\infty} |x - \xi|^{\alpha-1} f(\xi) d\xi, \quad (5.56)$$

$$0 < \alpha \leq 1$$

where $||$ denotes the absolute value, which defines the so called Riesz potential or the fractional Riesz integral respectively.

In order to derive the explicit form of the Riesz fractional derivative we first present the left- and right-handed Liouville derivative (5.15) and (5.16) in an alternative form:

$${}_L D_+^\alpha f(x) = \frac{\alpha}{\Gamma(1-\alpha)} \int_0^\infty \frac{f(x) - f(x-\xi)}{\xi^{\alpha+1}} d\xi \quad (5.57)$$

$${}_L D_-^\alpha f(x) = \frac{\alpha}{\Gamma(1-\alpha)} \int_0^\infty \frac{f(x) - f(x+\xi)}{\xi^{\alpha+1}} d\xi \quad (5.58)$$

Table 5.6 Special functions and their Riesz fractional derivative ${}_{RZ}D_+^\alpha$.

$f(x)$	$\frac{d^\alpha}{dx^\alpha} f(x)$
e^{ikx}	$- k ^\alpha e^{ikx}$
$\sin(kx)$	$- k ^\alpha \sin(kx)$
$\cos(kx)$	$- k ^\alpha \cos(kx)$
e^{-kx^2}	$\frac{k^{\alpha/2}}{\pi} \sin(\frac{\pi\alpha}{2}) \Gamma(-\alpha/2) \Gamma(1+\alpha) {}_1F_1(\frac{1+\alpha}{2}; \frac{1}{2}; -kx^2) \quad k \geq 0$
${}_pF_q(\{a_i\}; \{b_j\}; kx)$	divergent

which follows from (5.28) by partial integration:

$${}_L D_+^\alpha f(x) = {}_L I_+^{-\alpha} f(x) = + \frac{\partial}{\partial x} {}_L I_+^{1-\alpha} f(x) \quad (5.59)$$

$$= \frac{1}{\Gamma(1-\alpha)} \frac{\partial}{\partial x} \int_{-\infty}^x (x-\xi)^{-\alpha} f(\xi) d\xi \quad (5.60)$$

$$= \frac{1}{\Gamma(1-\alpha)} \frac{\partial}{\partial x} \int_0^\infty \xi^{-\alpha} f(x-\xi) d\xi \quad (5.61)$$

$$= \frac{1}{\Gamma(1-\alpha)} \int_0^\infty \xi^{-\alpha} \left(-\frac{\partial}{\partial \xi} f(x-\xi) \right) d\xi \quad (5.62)$$

$$= \frac{\alpha}{\Gamma(1-\alpha)} \left(\int_0^\infty \frac{f(x)}{\xi^{\alpha+1}} d\xi - \int_0^\infty \frac{f(x-\xi)}{\xi^{\alpha+1}} d\xi \right) \quad (5.63)$$

and similarly for (5.30)

$${}_L D_-^\alpha f(x) = {}_L I_-^{-\alpha} f(x) = - \frac{\partial}{\partial x} {}_L I_-^{1-\alpha} f(x) \quad (5.64)$$

$$= - \frac{1}{\Gamma(1-\alpha)} \frac{\partial}{\partial x} \int_x^\infty (\xi-x)^{-\alpha} f(\xi) d\xi \quad (5.65)$$

$$= - \frac{1}{\Gamma(1-\alpha)} \frac{\partial}{\partial x} \int_0^\infty \xi^{-\alpha} f(\xi+x) d\xi \quad (5.66)$$

$$= - \frac{1}{\Gamma(1-\alpha)} \int_0^\infty \xi^{-\alpha} \left(\frac{\partial}{\partial \xi} f(\xi+x) \right) d\xi \quad (5.67)$$

$$= \frac{\alpha}{\Gamma(1-\alpha)} \left(\int_0^\infty \frac{f(x)}{\xi^{\alpha+1}} d\xi - \int_0^\infty \frac{f(\xi+x)}{\xi^{\alpha+1}} d\xi \right) \quad (5.68)$$

Applying the reflection formula (2.11) we obtain for the factor

$$\frac{\alpha}{\Gamma(1-\alpha)} = \Gamma(1+\alpha) \frac{\sin(\pi\alpha)}{\pi} \quad (5.69)$$

With the definition of the fractional derivative according to Riesz

$${}_{RZ} D^\alpha = - \frac{{}_L D_-^\alpha + {}_L D_+^\alpha}{2 \cos(\pi\alpha/2)} \quad (5.70)$$

we explicitly obtain

$${}_{\text{RZ}}D^{\alpha}f(x) = \Gamma(1 + \alpha) \frac{\sin(\pi\alpha/2)}{\pi} \int_0^{\infty} \frac{f(x + \xi) - 2f(x) + f(x - \xi)}{\xi^{\alpha+1}} d\xi \quad 0 < \alpha < 2 \quad (5.71)$$

In table 5.6 we have listed some examples for functions and their corresponding Riesz derivative. For $\alpha = 2$ the given fractional derivatives coincide with the standard second order derivative for the given functions.

An important property of the fractional Riesz derivative is the invariance of the scalar product

$$\int_{-\infty}^{\infty} ({}_{\text{RZ}}D^{\alpha*}f^*(x)) g(x) dx = \int_{-\infty}^{\infty} f(x)^* ({}_{\text{RZ}}D^{\alpha}g(x)) dx \quad (5.72)$$

where $*$ designates complex conjugation.

5.4.2 The Feller fractional derivative

A possible generalization for the Riesz fractional derivative was proposed by Feller [Feller (1952)]. He suggested a general superposition of both fractional Liouville integrals:

$${}_F I_{\theta}^{\alpha} = c_{-}(\theta, \alpha) {}_L I_{+}^{\alpha} + c_{+}(\theta, \alpha) {}_L I_{-}^{\alpha} \quad (5.73)$$

introducing a free parameter $0 < \theta < 1$ which is a measure for the influence of both components:

$$c_{-}(\theta, \alpha) = \frac{\sin((\alpha - \theta)\pi/2)}{\sin(\pi\theta)} \quad (5.74)$$

$$c_{+}(\theta, \alpha) = \frac{\sin((\alpha + \theta)\pi/2)}{\sin(\pi\theta)} \quad (5.75)$$

The fractional Feller derivative is then given as

$${}_F D_{\theta}^{\alpha} = - (c_{+}(\theta, \alpha) D_{+}^{\alpha} + c_{-}(\theta, \alpha) D_{-}^{\alpha}) \quad (5.76)$$

For the special case $\theta = 0$ we obtain

$$c_{-}(\theta = 0, \alpha) = c_{+}(\theta = 0, \alpha) = \frac{1}{2 \cos(\alpha\pi/2)} \quad (5.77)$$

which exactly corresponds to the definition of the Riesz derivative (5.71).

There is an additional special case for $\theta = 1$

$$c_{-}(\theta = 1, \alpha) = -c_{+}(\theta = 1, \alpha) = \frac{1}{2 \sin(\alpha\pi/2)} \quad (5.78)$$

Table 5.7 Some functions and the corresponding Feller derivative for $\theta = 1$, or ${}_F D_1^\alpha$.

$f(x)$	$\frac{d^\alpha}{dx^\alpha} f(x)$
$\sin(kx)$	$\text{sign}(k) k ^\alpha \cos(kx)$
$\cos(kx)$	$-\text{sign}(k) k ^\alpha \sin(kx)$
e^{-kx^2}	$-\frac{k^{\frac{1+\alpha}{2}}}{\pi} x \cos(\pi\alpha/2) \Gamma(\frac{1-\alpha}{2}) \Gamma(1+\alpha) {}_1F_1(\frac{2+\alpha}{2}; \frac{3}{2}; -kx^2) \quad k \geq 0$
${}_p F_q(\{a_i\}; \{b_j\}; kx)$	divergent

which leads to a very simple realization of a fractional derivative:

$${}_F D_1^\alpha f(x) = \frac{{}_L D_+^\alpha - {}_R D_-^\alpha}{2 \sin(\alpha\pi/2)} f(x) \quad (5.79)$$

$$= \Gamma(1+\alpha) \frac{\cos(\alpha\pi/2)}{\pi} \int_0^\infty \frac{f(x+\xi) - f(x-\xi)}{\xi^{\alpha+1}} d\xi \quad (5.80)$$

$0 \leq \alpha < 1$

Since this derivative is a symmetric combination of the left- and right-handed Liouville derivative (5.28), (5.30) it may be interpreted as a regularized Liouville derivative.

The Feller derivative therefore may be written as a linear combination of ${}_F D_1^\alpha$ and ${}_{RZ} D^\alpha$:

$${}_F D_\theta^\alpha = A_1(\theta, \alpha)(D_+^\alpha - D_-^\alpha) + A_2(\theta, \alpha)(D_+^\alpha + D_-^\alpha) \quad (5.81)$$

with coefficients

$$A_1(\theta, \alpha) = -\frac{1}{2} (c_+(\theta, \alpha) - c_-(\theta, \alpha)) = -\frac{\sin(\theta\pi/2)}{2 \sin(\alpha\pi/2)} \quad (5.82)$$

$$A_2(\theta, \alpha) = -\frac{1}{2} (c_+(\theta, \alpha) + c_-(\theta, \alpha)) = -\frac{\cos(\theta\pi/2)}{2 \cos(\alpha\pi/2)} \quad (5.83)$$

Hence we obtain:

$${}_F D_\theta^\alpha = \sin(\theta\pi/2) {}_F D_1^\alpha + \cos(\theta\pi/2) {}_{RZ} D^\alpha \quad (5.84)$$

or more accurately

$${}_F D_\theta^\alpha = \begin{cases} \sin(\theta\pi/2) {}_F D_1^\alpha + \cos(\theta\pi/2) {}_{RZ} D^\alpha & 0 < \alpha < 1 \\ \sin(\theta\pi/2) \frac{d}{dx} {}_F D_1^{\alpha-1} + \cos(\theta\pi/2) {}_{RZ} D^\alpha & 1 \leq \alpha < 2 \\ \sin(\theta\pi/2) \frac{d^2}{dx^2} {}_F D_1^{\alpha-2} + \cos(\theta\pi/2) \frac{d^2}{dx^2} {}_{RZ} D^{\alpha-2} & 2 \leq \alpha < 3 \\ \vdots & \end{cases} \quad (5.85)$$

Having derived the Feller derivative in this form, the parameter θ may be understood as a rotation parameter. In addition we can use this form for an extension of this concept to fractional derivatives of higher orders.

5.5 Fractional derivatives of higher orders - the Marchaud fractional derivative

Second order differential equations play a central role in physics, e.g. the description of oscillations, waves or the whole area of quantum mechanics. But there are subjects and problems which are better described using higher order derivatives.

A remarkable example for a nonlinear third order differential equation is the Korteweg-de Vries equation [Korteweg and de Vries (1895)]:

$$\left(\frac{\partial}{\partial t} + \frac{\partial^3}{\partial x^3} - 6u \frac{\partial}{\partial x} \right) u(t, x) = 0 \quad (5.86)$$

The stationary solutions of this equation play an important role in the description of the behavior of solitons.

Typical applications of fourth order differential equations are given in elasticity theory e.g. for elastic deflection under load of a rod we have to solve:

$$\left(\frac{\partial^4}{\partial x^4} + N \frac{\partial^2}{\partial x^2} \right) u(x) = q(x) \quad (5.87)$$

An example for a fifth order differential equation is the extended Korteweg-de Vries equation [Marchant and Smyth (1990); Khanal *et al.* (2012)]:

$$\left(\frac{\partial}{\partial t} + u \frac{\partial}{\partial x} - \frac{\partial^5}{\partial x^5} \right) u(t, x) = 0 \quad (5.88)$$

We have demonstrated that a large number of physical processes may be adequately described using differential equations of higher order. Since we interpret higher order derivatives as entities, which should directly correspond to a fractional extended pendant, we should present higher order fractional derivatives too.

Our derivation of the Riesz and Feller fractional derivative presented in the previous section provides a direct hint to the construction principle of higher fractional derivatives. Especially Feller's fractional first derivative (5.79) and Riesz's fractional second derivative (5.71) may be easily interpreted as integrals over differential approximations of the standard first and second order derivative. Using the basic properties of the central difference operators $\delta_{\frac{1}{2}}$ and δ_1

$$\delta_{\frac{1}{2}}\phi(x) = \phi(x + \frac{1}{2}\xi) - \phi(x - \frac{1}{2}\xi) \quad (5.89)$$

$$\delta_1\phi(x) = \frac{1}{2}(\phi(x + \xi) - \phi(x - \xi)) \quad (5.90)$$

Table 5.8 Some special functions and the corresponding fractional derivatives according to ${}_3D^\alpha$. In the limit $\alpha \rightarrow 3$ the fractional derivatives coincide with the standard third order derivative.

$f(x)$	$\frac{d^\alpha}{dx^\alpha} f(x)$
e^{ikx}	$-i\text{sign}(k) k ^\alpha e^{ikx}$
$\sin(kx)$	$- k ^\alpha \cos(kx)$
$\cos(kx)$	$- k ^\alpha \sin(kx)$
e^{-kx^2}	$\frac{2^\alpha k^{\frac{1+\alpha}{2}} \sqrt{\pi\alpha}}{\sin(\pi\alpha/2)\Gamma(\frac{1-\alpha}{2})} {}_1F_1(\frac{2+\alpha}{2}; \frac{3}{2}; -kx^2) \quad k \geq 0$
${}_pF_q(\{a_i\}; \{b_j\}; kx)$	divergent

we define the central difference operator \mathfrak{D}^k of order k

$$\mathfrak{D}^k f(x) = \begin{cases} \delta_{\frac{1}{2}}^k f(x) & k \text{ even} \\ \delta_1 \delta_{\frac{1}{2}}^{k-1} f(x) & k \text{ odd} \end{cases} \quad (5.91)$$

or explicitly, using (5.89) and (5.90):

$$\mathfrak{D}^k \phi(x) = \sum_{n=0}^{2[(k+1)/2]} a_n^k \phi(x - ((k+1)/2) - n)\xi \quad (5.92)$$

with the summation coefficients

$$a_n^k = (-1)^n \begin{cases} \binom{k}{n} & k \text{ even} \\ \frac{1}{2} \left\{ \binom{k-1}{n} - \binom{k-1}{n-2} \right\} & k \text{ odd} \end{cases} \quad (5.93)$$

The renormalized fractional derivative is known as Marchaud fractional derivative [Marchaud (1927)] and is then given as:

$${}_k D^\alpha \phi(x) = \frac{1}{N_k} \int_0^\infty \frac{d\xi}{\xi^{\alpha+1}} \mathfrak{D}^k \phi(x) \quad (5.94)$$

with the normalization factor:

$$N_k = \frac{\Gamma(1+\alpha)}{\pi} \left(2 \sum_{n=0}^{[(k+1)/2]} a_n^k (k-n-1)^\alpha \right)^{-1} \times \begin{cases} (-1)^{\frac{k+2}{2}} \sin(\pi\alpha/2) & k \text{ even} \\ (-1)^{\frac{k+1}{2}} \cos(\pi\alpha/2) & k \text{ odd} \end{cases} \quad (5.95)$$

Table 5.9 Some special functions and the corresponding fractional derivatives according to ${}_4D^\alpha$. In the limit $\alpha \rightarrow 4$ the fractional derivatives coincide with the standard fourth order derivative.

$f(x)$	$\frac{d^\alpha}{dx^\alpha} f(x)$
e^{ikx}	$ k ^\alpha e^{ikx}$
$\sin(kx)$	$ k ^\alpha \sin(kx)$
$\cos(kx)$	$ k ^\alpha \cos(kx)$
e^{-kx^2}	$\frac{k^{\frac{\alpha}{2}} \Gamma(-\alpha/2)}{2 \cos(\pi\alpha/2) \Gamma(-\alpha)} {}_1F_1(\frac{1+\alpha}{2}; \frac{1}{2}; -kx^2) \quad k \geq 0$
${}_pF_q(\{a_i\}; \{b_j\}; kx)$	divergent

With (5.94) based on the Liouville definition of the fractional derivative (5.28) we therefore have given all fractional derivatives, which extend the ordinary derivative of order k :

$$\lim_{\alpha \rightarrow k} {}_k D^\alpha = \frac{d^k}{dx^k} \quad (5.96)$$

In addition, for these derivatives the invariance of the scalar product follows:

$$\int_{-\infty}^{\infty} ({}_k D^{\alpha*} f^*(x)) g(x) dx = (\pm)^k \int_{-\infty}^{\infty} f(x)^* ({}_k D^\alpha g(x)) dx \quad (5.97)$$

The first four fractional derivative definitions according to (5.94) follow as:

$${}_1 D^\alpha f(x) = \Gamma(1 + \alpha) \frac{\cos(\alpha\pi/2)}{\pi} \int_0^\infty \frac{f(x + \xi) - f(x - \xi)}{\xi^{\alpha+1}} d\xi \quad 0 \leq \alpha < 1 \quad (5.98)$$

$${}_2 D^\alpha f(x) = \Gamma(1 + \alpha) \frac{\sin(\alpha\pi/2)}{\pi} \int_0^\infty \frac{f(x + \xi) - 2f(x) + f(x - \xi)}{\xi^{\alpha+1}} d\xi \quad 0 \leq \alpha < 2 \quad (5.99)$$

$$\begin{aligned} {}_3 D^\alpha f(x) &= \Gamma(1 + \alpha) \frac{\cos(\alpha\pi/2)}{\pi} \frac{1}{2^\alpha - 2} \\ &\times \int_0^\infty \frac{-f(x + 2\xi) + 2f(x + \xi) - 2f(x - \xi) + f(x - 2\xi)}{\xi^{\alpha+1}} d\xi \end{aligned} \quad 0 \leq \alpha < 3 \quad (5.100)$$

$$\begin{aligned} {}_4 D^\alpha f(x) &= \Gamma(1 + \alpha) \frac{\sin(\alpha\pi/2)}{\pi} \frac{1}{2^\alpha - 4} \\ &\times \int_0^\infty \frac{-f(x + 2\xi) + 4f(x + \xi) - 6f(x) + 4f(x - \xi) - f(x - 2\xi)}{\xi^{\alpha+1}} d\xi \end{aligned} \quad 0 \leq \alpha < 4 \quad (5.101)$$

These definitions are valid for $0 \leq \alpha < k$. Setting $\alpha > k$

$${}_k D^\alpha = \frac{d^{nk}}{dx^{nk}} {}_k D^{\alpha-nk} \quad n \in \mathbb{N} \quad (5.102)$$

and choosing n so that $0 \leq \alpha - nk < k$ the definitions given are valid for all $\alpha > 0$.

In the same manner the Feller fractional derivative definition may be extended to fractional derivatives of higher order.

We introduce hyperspherical coordinates on the unit sphere on \mathbb{R}^n :

$$x_1 = \cos(\theta_{n-1}) \quad (5.103)$$

$$x_2 = \sin(\theta_{n-1}) \cos(\theta_{n-2}) \quad (5.104)$$

...

$$x_{n-1} = \sin(\theta_{n-1}) \sin(\theta_{n-2}) \dots \cos(\theta_1) \quad (5.105)$$

$$x_n = \sin(\theta_{n-1}) \sin(\theta_{n-2}) \dots \sin(\theta_1) \quad (5.106)$$

With these coordinates the Feller definition of a fractional derivative may be extended to

$${}_F D_{\{\theta_k\}}^\alpha = \sum_{k=1}^n x_k {}_k D^\alpha \quad (5.107)$$

5.6 Erdélyi-Kober operators of fractional integration

Another area of active research are generalizations of the fractional integral definition.¹ Until now we discussed different realizations of a fractional integral, depending on one parameter α . A possible generalization takes into account more than one parameter, which allows to model multi-parameter fractional integrals.

Common members of this family of fractional operators are the so-called Erdélyi-Kober operators of fractional integration, as is the recently universally adopted notion, in Kiryakova [Kiryakova (1994)] but also in many other authors. They are extensions of the Riemann-Liouville right- and left-handed fractional integrals, depending not only on the order $\alpha > 0$ but

¹We are grateful for help from Virginia Kiryakova while preparing this text.

also on weight $\gamma \in \mathbb{R}$ and an additional parameter $\beta > 0$ as follows:

$$I_{+;\beta}^{\gamma,\alpha} f(x) = x^{\beta(\gamma+\alpha)} \int_0^x \frac{(x^\beta - \tau^\beta)^{\alpha-1}}{\Gamma(\alpha)} \tau^{\beta\gamma} f(\tau) d\tau^\beta \quad (5.108)$$

$$= \int_0^1 \frac{(1-\sigma)^{\alpha-1} \sigma^\gamma}{\Gamma(\alpha)} f(x\sigma^{1/\beta}) d\sigma \quad (5.109)$$

$$I_{-;\beta}^{\gamma,\alpha} f(x) = x^{\beta\gamma} \int_x^\infty \frac{(\tau^\beta - x^\beta)^{\alpha-1}}{\Gamma(\alpha)} \tau^{-\beta(\gamma+\alpha)} f(\tau) d\tau^\beta \quad (5.110)$$

$$= \int_1^\infty \frac{(\sigma-1)^{\alpha-1} \sigma^{-(\gamma+\alpha)}}{\Gamma(\alpha)} f(x\sigma^{1/\beta}) d\sigma \quad (5.111)$$

If we take the special case $\beta = 1$ and change the initial point 0 to $-\infty$ in (5.108), the resulting modifications of the Erdélyi-Kober operators can be written as follows

$$\tilde{I}_+^{\gamma,\alpha} f(x) = x^{\gamma+\alpha} \int_{-\infty}^x \frac{(x-\tau)^{\alpha-1}}{\Gamma(\alpha)} \tau^\gamma f(\tau) d\tau, \quad (5.112)$$

$$\tilde{I}_-^{\gamma,\alpha} f(x) = x^\gamma \int_x^\infty \frac{(\tau-x)^{\alpha-1}}{\Gamma(\alpha)} \tau^{-\gamma-\alpha} f(\tau) d\tau. \quad (5.113)$$

which clearly shows the analogy to the fractional Riemann-Liouville integral definitions.

These operators of the so-called “Erdélyi-Kober type” with numerous applications [Sneddon (1966); Sneddon (1975)] are the base on which the generalized fractional calculus of Kiryakova [Kiryakova (1994)] has been developed. In Chapter 9 we will discuss a possible geometric interpretation, but let us first present a geometric interpretation of the standard fractional integrals.

5.7 Geometric interpretation of the fractional integral

A geometric interpretation of a fractional integral has first been proposed by Podlubny [Podlubny (2001)].

We illustrate his idea using the left-handed fractional Riemann integral (5.17).

$${}_R I_+^\alpha f(x) = \frac{1}{\Gamma(\alpha)} \int_0^x (x-\xi)^{\alpha-1} f(\xi) d\xi \quad (5.114)$$

Introducing an auxiliary function $g_x(\xi)$ we can write the integral as

$${}_{\text{R}}I_{+}^{\alpha}f(x) = \frac{1}{\Gamma(\alpha)} \int_0^x f(\xi) dg_x(\xi) \quad (5.115)$$

with

$$g_x(\xi) = \frac{1}{\Gamma(1 + \alpha)} (x^{\alpha} - (x - \xi)^{\alpha}) \quad (5.116)$$

For a given upper limit x of the integral (5.114) we define a three dimensional coordinate system with coordinates $\{\xi, g, f\}$. In the (ξ, g) -plane or, as illustrated in figure 5.1 on the floor, we first draw the function $g_x(\xi)$ in the region $0 \leq \xi \leq x$. Along this path we draw $f(\xi)$, in this way we construct a fence (light gray color). The upper boundary of the fence is a three dimensional curve $(\xi, g_x(\xi), f(\xi))$ in the interval $0 \leq \xi \leq x$. This fence may now be projected to two different planes: A first projection onto the (ξ, f) -plane generates the area below the curve $f(\xi)$, which corresponds to the standard integral

$${}_{\text{R}}I_{+}^1 f(x) = \int_0^x f(\xi) d\xi \quad (5.117)$$

This area is dark gray in figure 5.1.

A second projection onto the (g, f) -plane, which corresponds to the area of the integral (5.115) is colored black in figure 5.1. Therefore the black area is a geometric representation for the fractional integral.

In the special case $\alpha = 1$ $g_x(\xi) = \xi$ and both projections are of similar form. Hence we have a smooth transition from a standard to a fractional integral.

A variation of the upper bound x results in a change of the path $g_x(\xi)$ and consequently the shape of projections is changed. On the left side of figure 5.2 we have drawn different paths and on the right side the corresponding projections onto the (g, f) -plane are given, which directly correspond to the value of the fractional integral for increasing x .

The change of the projected area in shape and size with increasing x gives a direct geometric picture of the change of the fractional integral as a function of x .

5.8 Low level fractionality

In this chapter so far we have presented several commonly used definitions of the fractional derivative parametrized via an arbitrary derivative parameter

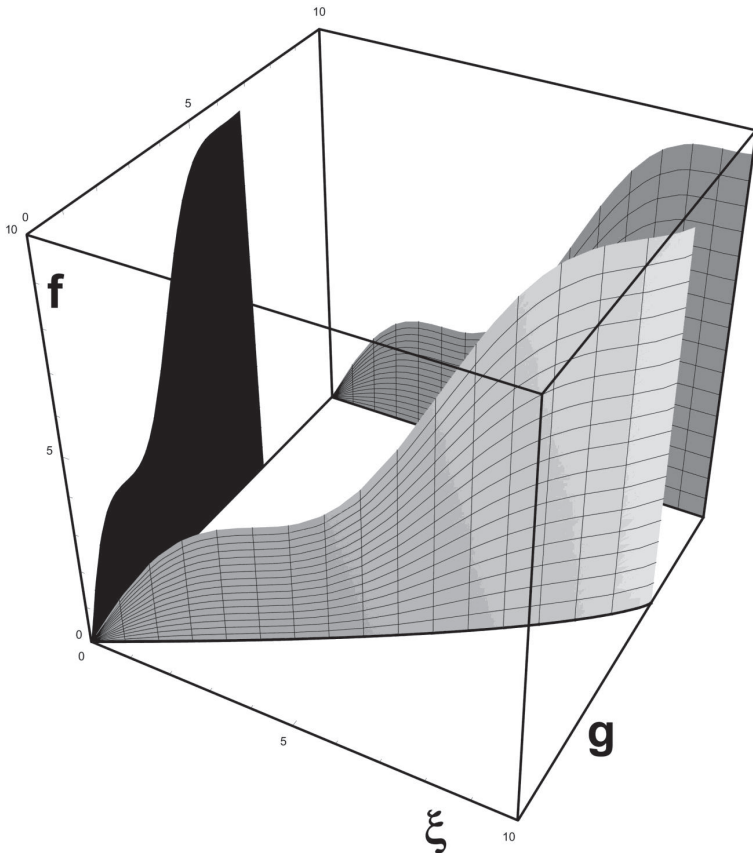


Fig. 5.1 The fence and its projections. The geometric interpretation of an integral is given in terms of a projected area of the light gray fence. In the back in dark gray the standard integral. On the left plane the fractional integral is given as the black area from the fence projection.

α . It is interesting to investigate cases where α only minimally deviates from an integer value.

$$\alpha = n - \epsilon \quad (5.118)$$

For $\epsilon \ll 1$ the behavior of the fractional derivative is called low level fractionality and was considered e.g. by Tarasov [Tarasov and Zaslavsky (2006)].

For demonstrative purposes we will investigate low level fractionality for the left-handed Caputo derivative (5.43) for the simple case $\alpha = 1 - \epsilon$.

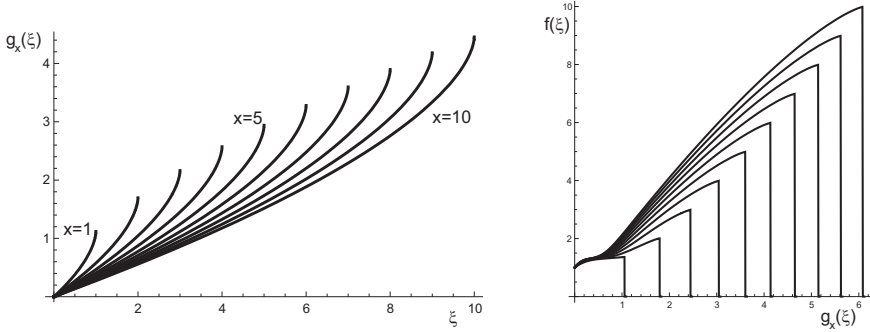


Fig. 5.2 The fence path and projection of the fractional integral. For $\alpha = 0.6$, on the left the function $g_x(\xi)$ projected onto the (g, ξ) -plane is plotted for different $x = 1, 2, \dots, 10$, which corresponds to the view of the fence from above. On the right the corresponding projections onto the (g, f) -plane of the fractional integral are given for $f(\xi) = \xi + e^{-\xi^2}$.

It follows

$${}_c D_+^{1-\epsilon} f(x) = \frac{1}{\Gamma(\epsilon)} \int_0^x (x - \xi)^{\epsilon-1} f'(\xi) d\xi \quad (5.119)$$

and partial integration leads to:

$${}_c D_+^{1-\epsilon} f(x) = \frac{f'(0)x^\epsilon}{\Gamma(1+\epsilon)} + \frac{1}{\Gamma(1+\epsilon)} \int_0^x (x - \xi)^\epsilon f''(\xi) d\xi \quad (5.120)$$

A Taylor series expansion leads to:

$$\begin{aligned} \frac{1}{\Gamma(1+\epsilon)} (x - \xi)^\epsilon &= 1 + \epsilon (\gamma + \ln(x - \xi)) \\ &+ \epsilon^2 \left(\frac{\gamma^2}{2} - \frac{\pi^2}{12} + \gamma \ln(x - \xi) + \frac{1}{2} \ln^2(x - \xi) \right) \end{aligned} \quad (5.121)$$

where $\gamma = 0.577\dots$ denotes Euler's constant.

In lowest order in ϵ therefore for the fractional derivative follows:

$${}_c D_+^{1-\epsilon} f(x) = f'(x) + \epsilon \left(f'(0) \ln(x) + \gamma f'(x) + \int_0^x f''(\xi) \ln(x - \xi) d\xi \right) \quad (5.122)$$

For $\epsilon \ll 1$ we obtain the result:

$${}_c D_+^{1-\epsilon} f(x) = f'(x) + \epsilon D_1^1 + \dots \quad (5.123)$$

with

$$D_1^1 = f'(0) \ln(x) + \gamma f'(x) + \int_0^x f''(\xi) \ln(x - \xi) d\xi \quad (5.124)$$

in the limit $\lim \epsilon \rightarrow 0$ we obtain:

$$\lim_{\epsilon \rightarrow 0} {}_c D_+^{1-\epsilon} = f'(x) \quad (5.125)$$

Hence we have demonstrated that there is a smooth transition between fractional, low level and ordinary derivatives.

As an example we obtain for $f(x) = \cos(x)$:

$${}_c D_+^{1-\epsilon} \cos(x) = -\sin(x) + \epsilon (\cos(x) \text{Si}(x) - \sin(x) \text{Ci}(x)) \quad (5.126)$$

where Ci and Si are the cosine- (2.22) and sine integral (2.32).

5.9 Discussion

5.9.1 Semi-group property of the fractional integral question:

How can I prove the semi-group property of the fractional integral

$${}_a I_+^\alpha {}_a I_+^\beta f(x) = {}_a I_+^{\alpha+\beta} f(x) \quad \alpha, \beta \geq 0 \quad (5.127)$$

where ${}_a I_+^\alpha$ is given by (5.13)?

answer:

To solve that problem, we will use the definition of the beta function:

$$\int_0^1 d\xi \xi^{\alpha-1} (1-\xi)^{\beta-1} = \frac{\Gamma(\alpha)\Gamma(\beta)}{\Gamma(\alpha+\beta)} \quad (5.128)$$

and the Dirichlet formula, which is given by [Whittaker and Watson (1965)]

$$\begin{aligned} & \int_a^x d\xi (x-\xi)^{\alpha-1} \int_a^\xi d\phi (\xi-\phi)^{\beta-1} g(\xi, \phi) \\ &= \int_a^x d\phi \int_\phi^x d\xi (x-\xi)^{\alpha-1} (\xi-\phi)^{\beta-1} g(\xi, \phi) \end{aligned} \quad (5.129)$$

which reduces for $g(\xi, \phi) = g(\xi)f(\phi)$ for the simplified case $g(\xi) = 1$ to:

$$\begin{aligned} & \int_a^x d\xi (x-\xi)^{\alpha-1} \int_a^\xi d\phi (\xi-\phi)^{\beta-1} f(\phi) \\ &= \int_a^x d\phi f(\phi) \int_\phi^x d\xi (x-\xi)^{\alpha-1} (\xi-\phi)^{\beta-1} \end{aligned} \quad (5.130)$$

Therefore we obtain

$${}_a I_+^\alpha {}_a I_+^\beta f(x) = \frac{1}{\Gamma(\alpha)} \frac{1}{\Gamma(\beta)} \int_a^x d\phi \int_a^\phi d\xi (x-\xi)^{\alpha-1} (\xi-\phi)^{\beta-1} f(\phi) \quad (5.131)$$

according to (5.130) this is equivalent to

$${}_aI_{+a}^\alpha I_{+}^\beta f(x) = \frac{1}{\Gamma(\alpha)\Gamma(\beta)} \int_a^x d\phi f(\phi) \int_\phi^x d\xi (x-\xi)^{\alpha-1} (\xi-\phi)^{\beta-1} \quad (5.132)$$

The inner integral $k(x, \phi)$ in (5.132) may be interpreted as the kernel of the external convolution integral. With the substitution

$$u = \frac{\xi - \phi}{x - \phi} \quad (5.133)$$

which leads to $\xi = \phi + u(x - \phi)$ and $d\xi = (x - \phi)du$ we obtain

$$k(x, \phi) = \int_\phi^x d\xi (x-\xi)^{\alpha-1} (\xi-\phi)^{\beta-1} \quad (5.134)$$

$$= (x - \phi)^{\alpha+\beta-1} \int_0^1 du (1-u)^{\alpha-1} u^{\beta-1} \quad (5.135)$$

$$= (x - \phi)^{\alpha+\beta-1} \frac{\Gamma(\alpha)\Gamma(\beta)}{\Gamma(\alpha + \beta)} \quad (5.136)$$

In the last step we used the definition of the beta function. Inserting this result into (5.132) completes the proof.

$${}_aI_{+a}^\alpha I_{+}^\beta f(x) = \frac{1}{\Gamma(\alpha + \beta)} \int_a^x d\phi (x-\xi)^{\alpha+\beta-1} f(\phi) \quad (5.137)$$

$$= {}_aI_{+}^{\alpha+\beta} f(x) \quad (5.138)$$

A similar procedure may be used for the right-handed integrals ${}_aI_-^\alpha$ too. Furthermore, since the derivation is valid for an arbitrary $a < x$, we have proven the validity of the semi-group property for the Liouville and the Riemann fractional integral definition as well.

Exercise 5.1**The Laplace transform of the Mittag-Leffler function**

Problem: The Laplace transform of a function $f(t)$ is given by:

$$\mathcal{F}(s) = \int_0^\infty dt e^{-st} f(t) \quad s \in \mathbb{R}^+ \quad (5.139)$$

What is the Laplace transform of the Mittag-Leffler function $E_\alpha(\nu t^\alpha)$, $\nu \in \mathbb{R}^+$?

Exercise 5.2**The Caputo derivative of $\ln(1 + x)$**

Problem: Calculate the fractional derivative according to Caputo for

$$f(x) = \ln(1 + x) \quad |x| < 1 \quad (5.140)$$

Hint: Use a Taylor series expansion

Exercise 5.3**Low level fractionality for $\ln(1 + x)$**

Problem: For $f(x) = \ln(1 + x)$ compare the low level fractional derivative of Caputo type with the exact solution from exercise (5.2).

Hint: The following integral might be of help [Gradshteyn and Ryzhik (1980)]:

$$\int d\xi \frac{\ln(x - \xi)}{(1 + \xi)^2} = -\frac{(x - \xi) \ln(x - \xi) + (1 + \xi) \ln(1 + \xi)}{(1 + x)(1 + \xi)} \quad (5.141)$$

Chapter 6

The Fractional Harmonic Oscillator

There are only few problems which may be solved analytically in full generality. The solutions of the differential equation of the harmonic oscillator

$$\left(m \frac{d^2}{dt^2} + k \right) x(t) = 0 \quad (6.1)$$

which are given by

$$x(t) = c_1 \cos(\omega t) + c_2 \sin(\omega t) \quad (6.2)$$

play a dominant role in theoretical physics. Furthermore this differential equation has a wide range of applications.

In the field of classical mechanics the equation (6.1) describes free oscillations and in general is a harmonic approximation for an arbitrary potential minimum. If appropriate boundary conditions are given this equation is a useful tool for describing of a vibrating string or a rectangular membrane as a spatial solution of a wave equation:

$$\left(\frac{d^2}{dx^2} + \frac{d^2}{dy^2} + \frac{d^2}{dz^2} - \frac{1}{c^2} \frac{d^2}{dt^2} \right) \psi(x, y, z, t) = 0 \quad (6.3)$$

In quantum mechanics the same differential equation results as a special solution of the stationary Schrödinger equation

$$-\frac{\hbar^2}{2m} \left(\frac{d^2}{dx^2} + \frac{d^2}{dy^2} + \frac{d^2}{dz^2} \right) \psi(x) = E\psi(x) \quad (6.4)$$

for a particle confined to a bounded region of space.

Therefore it is of fundamental importance to study the fractional pendant of the harmonic oscillator and to discuss the specific properties of its solutions.

It will turn out, that the solutions for the fractional harmonic oscillator and the solutions for fractional friction forces given in the previous chapter show a similar behavior. This similarity may be understood, if we consider the corresponding characteristic polynomials, which determine the solutions.

6.1 The fractional harmonic oscillator

We define the following fractional differential equation

$$\left(m \frac{d^{2\alpha}}{dt^{2\alpha}} + k \right) x(t) = 0 \quad (6.5)$$

we are free to adjust the dimensions and meaning of the parameters m and k respectively or both m, k .

With the settings

$$\left(\frac{d^{2\alpha}}{dt^{2\alpha}} + \frac{k}{m} \right) x(t) = 0 \quad (6.6)$$

in units of the mks-system $[k/m]$ is given as $1/s^{2\alpha}$.

In the following we will present the solutions of this fractional differential equation for different types of the fractional derivative and will investigate the specific differences of the obtained solutions.

6.2 The harmonic oscillator according to Fourier

With the ansatz

$$x(t) = e^{\omega t} \quad (6.7)$$

the solution of the fractional oscillator is reduced to the examination of the zeros of the polynomial

$$\omega^{2\alpha} + \frac{k}{m} = 0 \quad (6.8)$$

In the region $1/2 < \alpha \leq 3/2$ are exactly two complex conjugated solutions:

$$\omega_{1,2} = \left| \frac{k}{m} \right|^{\frac{1}{2\alpha}} \left(\cos\left(\frac{\pi}{2\alpha}\right) \pm i \sin\left(\frac{\pi}{2\alpha}\right) \right) \quad (6.9)$$

For $\alpha = 1$ we obtain two purely imaginary solutions, which corresponds to a free, undamped oscillation. If α is decreased, an increasing negative real

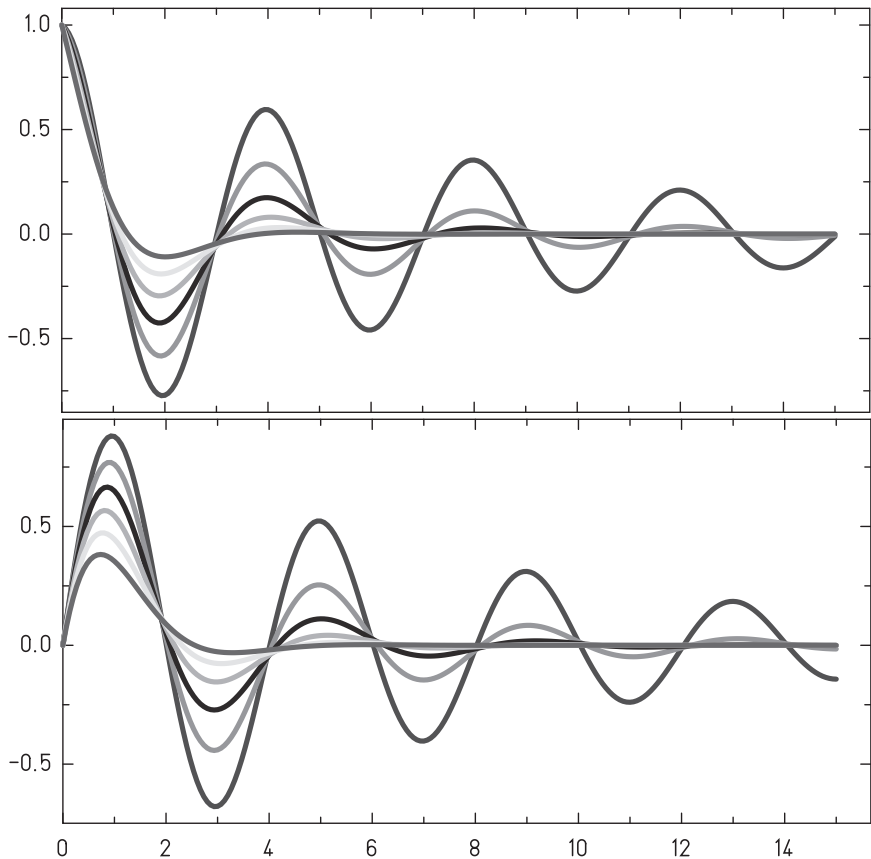


Fig. 6.1 Solutions $F \cos(\alpha, t)$ and $F \sin(\alpha, t)$ of the fractional harmonic oscillator using the Fourier derivative with $\alpha = 0.95, 0.90, 0.85, 0.80, 0.75, 0.70$.

part occurs which from a classical point of view may be interpreted as an increasing damping. For $\alpha > 1$ we obtain an increasing positive real part which corresponds to an increasing excitation.

A direct comparison with the classical solutions (4.40) of an harmonic oscillator including friction leads to:

$$-\frac{\gamma}{2m} = \left| \frac{k}{m} \right|^{\frac{1}{2\alpha}} \cos\left(\frac{\pi}{2\alpha}\right) \quad (6.10)$$

$$\approx \left| \frac{k}{m} \right|^{\frac{1}{2\alpha}} \frac{1}{2}\pi(\alpha - 1) \quad \text{for } \alpha \approx 1 \quad (6.11)$$

Near $\alpha \approx \frac{1}{2}$ there is no oscillating contribution any more. The evolution in time for this system is dominated by an exponential decay. On the other hand $\alpha > 1$ corresponds to a negative classical friction coefficient. Consequently we obtain the surprising result, that the behavior of the free solutions of the fractional harmonic oscillator under variation of the fractional derivative parameter α may be interpreted from a classical point of view as damping and excitation phenomena respectively.

In order to simplify a comparison for the solutions for different types of fractional derivatives we introduce the following initial conditions:

$$x(t=0) = x_0 \quad (6.12)$$

$$D^\alpha x(t)|_{t=0} = \tilde{v}(t=0) = \tilde{v}_0 \quad (6.13)$$

Only for $\alpha = 1$ these initial conditions correspond to the classical initial conditions. For all other cases at first we leave the physical interpretation of a fractional velocity \tilde{v} an open question.

But with these settings we can reformulate the solutions of the fractional harmonic oscillator: a first set with the fractional initial conditions $x_0 = 1$, $\tilde{v}_0 = 0$ may be considered as a fractional extension of the standard cosine function, while the fractional initial conditions $x_0 = 0$, $\tilde{v}_0 = 1$ characterize the fractional pendant to the sine function:

$${}_{\text{F}} \sin(\alpha, t) = \frac{1}{2i} \left(e^{\frac{1}{2}e^{\frac{i\pi}{2\alpha}}\pi t} - e^{\frac{1}{2}e^{-\frac{i\pi}{2\alpha}}\pi t} \right) \quad (6.14)$$

$${}_{\text{F}} \cos(\alpha, t) = \frac{1}{2} \left(e^{\frac{1}{2}e^{\frac{i\pi}{2\alpha}}\pi t} + e^{\frac{1}{2}e^{-\frac{i\pi}{2\alpha}}\pi t} \right) \quad (6.15)$$

An appropriately chosen linear combination of these two extended trigonometric functions will again fulfill the classical initial conditions (4.3).

In figure 6.1 we present a graphical representation of these solutions (12.3) and (12.1) for different α .

6.3 The harmonic oscillator according to Riemann

In order to solve the harmonic oscillator differential equation based on the Riemann definition of the fractional derivative we use a series expansion according to (3.20).

Since

$${}_{\text{R}} D^\alpha t^{n\alpha} = \frac{\Gamma(1+n\alpha)}{\Gamma(1+(n-1)\alpha)} t^{(n-1)\alpha} \quad (6.16)$$

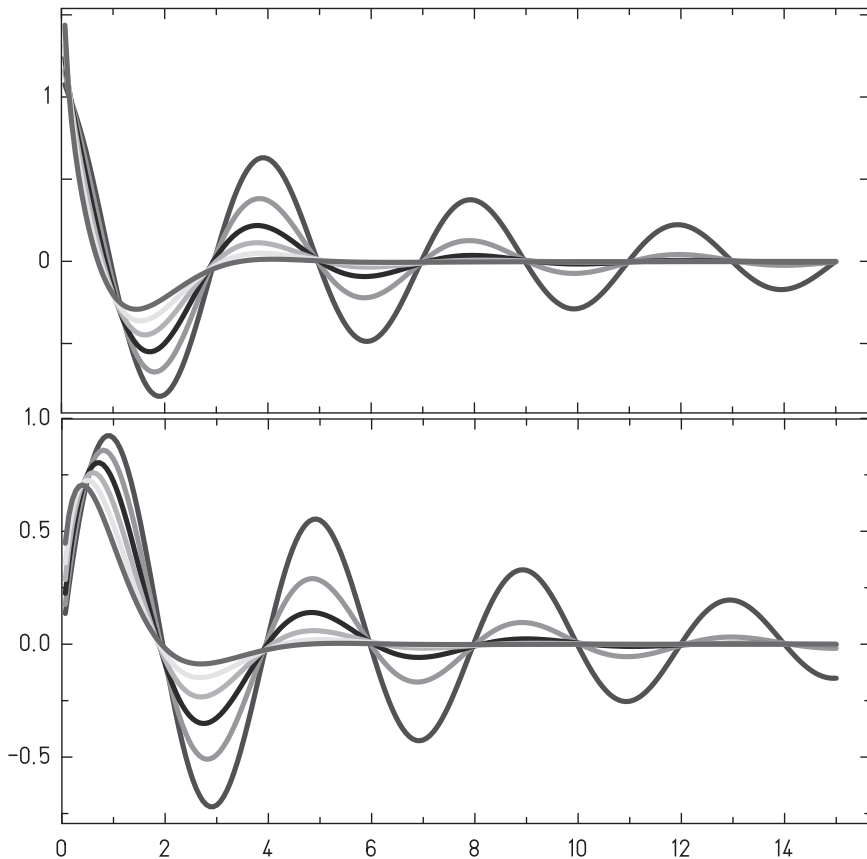


Fig. 6.2 Solutions ${}_R \cos(\alpha, t)$ and ${}_R \sin(\alpha, t)$ of the harmonic oscillator with Riemann derivative for $\alpha = 0.95, 0.90, 0.85, 0.80, 0.75, 0.70$.

we obtain two different linearly independent solutions, which we call in analogy to the trigonometric functions ${}_R \sin(\alpha, t)$ and ${}_R \cos(\alpha, t)$,

$${}_R \sin(\alpha, t) = t^{\alpha-1} \sum_{n=0}^{\infty} (-1)^n \frac{t^{(2n+1)\alpha}}{\Gamma((2n+2)\alpha)} \quad (6.17)$$

$${}_R \cos(\alpha, t) = t^{\alpha-1} \sum_{n=0}^{\infty} (-1)^n \frac{t^{2n\alpha}}{\Gamma((2n+1)\alpha)} \quad (6.18)$$

with the property

$${}_R D^\alpha {}_R \sin(\alpha, \omega t) = \omega^\alpha {}_R \cos(\alpha, \omega t) \quad (6.19)$$

$${}_R D^\alpha {}_R \cos(\alpha, \omega t) = -\omega^\alpha {}_R \sin(\alpha, \omega t) \quad (6.20)$$

These functions are related to the Mittag-Leffler function (2.17) :

$$_R \sin(\alpha, t) = t^{2\alpha-1} E_{2\alpha, 2\alpha}(-t^{2\alpha}) \quad (6.21)$$

$$_R \cos(\alpha, t) = t^{\alpha-1} E_{2\alpha, \alpha}(-t^{2\alpha}) \quad (6.22)$$

For $\alpha < 1$

$$\lim_{t \rightarrow 0} {}_R \cos(\alpha, \omega t) = \infty \quad (6.23)$$

holds, which means, that we cannot give a nonsingular solution, which fulfills the general initial conditions (6.12). At a first glance, this seems to be a serious drawback for a practical application of the Riemann fractional derivative. But we should keep in mind that the solutions presented may be helpful for problems which are not determined by initial conditions but are formulated in terms of boundary conditions, which is the case for example for solutions of a wave equation.

6.4 The harmonic oscillator according to Caputo

The solution of the differential equation of the harmonic oscillator with Caputo derivative definition may be written according to (3.22) as a series. The Caputo derivative for a power is given as

$${}_C D^\alpha t^{n\alpha} = \begin{cases} \frac{\Gamma(1+n\alpha)}{\Gamma(1+(n-1)\alpha)} t^{(n-1)\alpha} & n > 0, \\ 0 & n = 0 \end{cases} \quad (6.24)$$

Therefore we obtain two linearly independent solutions which we call in analogy to the trigonometric functions as ${}_C \sin(\alpha, t)$ and ${}_C \cos(\alpha, t)$:

$${}_C \sin(\alpha, t) = \sum_{n=0}^{\infty} (-1)^n \frac{t^{(2n+1)\alpha}}{\Gamma(1 + (2n+1)\alpha)} \quad (6.25)$$

$${}_C \cos(\alpha, t) = \sum_{n=0}^{\infty} (-1)^n \frac{t^{2n\alpha}}{\Gamma(1 + 2n\alpha)} \quad (6.26)$$

The major property of these series is:

$${}_C D^\alpha {}_C \sin(\alpha, \omega t) = \omega^\alpha {}_C \cos(\alpha, \omega t) \quad (6.27)$$

$${}_C D^\alpha {}_C \cos(\alpha, \omega t) = -\omega^\alpha {}_C \sin(\alpha, \omega t) \quad (6.28)$$

They are directly related to the Mittag-Leffler function (2.17):

$${}_C \sin(\alpha, t) = t^\alpha E_{2\alpha, 1+\alpha}(-t^{2\alpha}) \quad (6.29)$$

$${}_C \cos(\alpha, t) = E_{2\alpha}(-t^{2\alpha}) \quad (6.30)$$

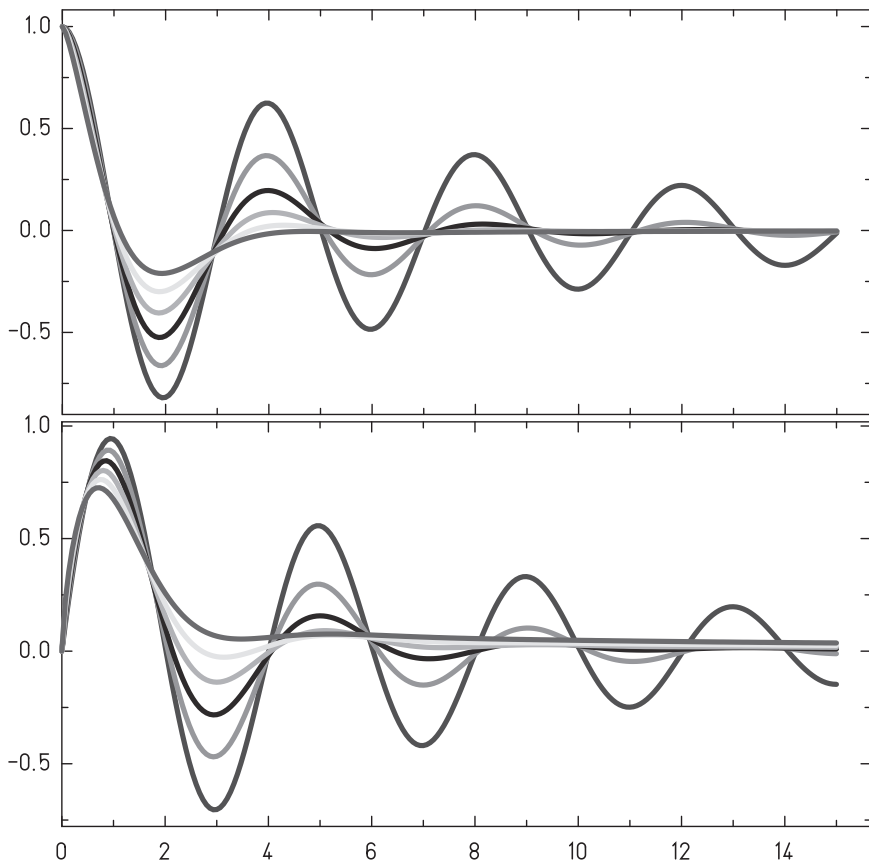


Fig. 6.3 Solutions $c \cos(\alpha, t)$ and $c \sin(\alpha, t)$ of the harmonic oscillator differential equation with Caputo derivative with $\alpha = 0.95, 0.90, 0.85, 0.80, 0.75, 0.70$.

In figure 6.3 we have sketched a graphical representation.

Let us compare the derived solutions of the harmonic oscillator differential equation for different definitions of the fractional derivative. First we observe a surprising similarity of the presented solutions. All of them decay exponentially for $\alpha < 1$ which may be interpreted from a classical point of view as a damping phenomenon.

Furthermore the frequency of these damped oscillations for a given $\alpha \approx 1$ are quite similar for the different fractional derivative definitions presented and therefore may be regarded as a definition-independent property.

The main difference for the different solutions is the number of zeros. This will be an important observation for solutions of fractional wave-equations when appropriate boundary conditions are imposed.

In general the fractional harmonic oscillator behaves like a damped harmonic oscillator for $\alpha < 1$. The damping is intrinsic to the fractional oscillator and not due to external influences such as friction [Mainardi (1996); Gorenflo and Mainardi (1996); Tofighi (2003); Stanislavsky (2006a); Stanislavsky (2006b); Yonggang Xiu'e (2010)]. Nevertheless, there is a correspondence of the solutions of the fractional oscillator with solutions of a classical particle with fractional friction, which becomes obvious, if we compare the determining polynomials (6.8) and (4.22).

A physical interpretation for the fractional harmonic oscillator has been given by Stanislavsky [Stanislavsky (2004)] in terms of a statistical multi-particle interpretation: He interprets the fractional oscillator as an ensemble average of ordinary harmonic oscillators governed by a stochastic time arrow. The intrinsic absorption of the fractional oscillator results from the full contribution of the harmonic oscillator ensemble: these oscillators differ a little from each other in frequency so that each response is compensated by an antiphase response of another harmonic oscillator.

The solutions of the classical fractional harmonic oscillator will turn out to be helpful solving the free fractional Schrödinger equation in chapter 11.

Exercise 6.1

Eigenfunctions of the m-th order Caputo differential operator

Problem: For the m-th order differential equation

$$(\partial_t^\alpha)^m x(t) = -\omega^{m\alpha} x(t) \quad (6.31)$$

give the m different solutions in terms of the Mittag-Leffler functions.

Chapter 7

Wave Equations and Parity

The classical field of application for wave equations is the determination of the eigenfrequencies and eigenfunctions of vibrating systems.

Obviously there is a close analogy with the differential equation of the harmonic oscillator.

Therefore an extension of wave equations to the fractional case will benefit from solutions presented in the previous chapter.

A new aspect is the use of boundary conditions in contrast to initial conditions. Furthermore, since a wave equation besides the time dependence also contains a spatial part, we are forced to consider the behavior of solutions for negative arguments.

For free solutions, this problem may be solved by the additional requirement, that these solutions should be eigenfunctions of the parity operator, too.

7.1 Fractional wave equations

A possible extension of a classical wave equation (6.3) to the fractional case is given by

$$\left(\frac{d^{2\alpha}}{dx^{2\alpha}} + \frac{d^{2\alpha}}{dy^{2\alpha}} + \frac{d^{2\alpha}}{dz^{2\alpha}} - \mu^2 \frac{d^2}{dt^2} \right) \psi(x, y, z, t) = 0 \quad (7.1)$$

Here we have extended only the spatial contribution to the fractional case, while the time derivative remains unchanged being of second order. The dimension of the parameter μ is determined in the mks-system by $[s/m^\alpha]$.

Because (3.14) holds, a separation of variables is possible using the product ansatz:

$$\psi(x, y, z, t) = X(x)Y(y)Z(z)T(t) \quad (7.2)$$

The partial differential equation (7.1) is therefore transformed into a system of uncoupled ordinary differential equations:

$$\frac{d^{2\alpha}}{dx^{2\alpha}}X = -\kappa_x^2 X \quad (7.3)$$

$$\frac{d^{2\alpha}}{dx^{2\alpha}}Y = -\kappa_y^2 Y \quad (7.4)$$

$$\frac{d^{2\alpha}}{dx^{2\alpha}}Z = -\kappa_z^2 Z \quad (7.5)$$

$$\frac{d^2}{dx^2}T = \frac{\omega^2}{\mu^2}T \quad (7.6)$$

The separation constants $\omega, \kappa_x, \kappa_y, \kappa_z$ fulfill the condition

$$\omega = \mu \sqrt{\kappa_x^2 + \kappa_y^2 + \kappa_z^2} \quad (7.7)$$

A solution of this system of fractional differential equations may be determined, if an appropriate set of boundary conditions (Dirichlet, Neumann, mixed) at the boundaries of a given domain is known.

The simple case of a vibrating string with length $L = 2a$, which is fixed at its ends for example is described classically by a one dimensional wave equation for the oscillation $X(x)$ and is uniquely determined by the Dirichlet boundary conditions:

$$X(-a) = X(a) = 0 \quad (7.8)$$

The differential equation for a vibrating string is equivalent to the differential equation for the harmonic oscillator, where from the homogeneous set of all possible solutions those are selected, which obey the boundary conditions (7.8).

This strategy may also be directly applied in the case of a fractional wave equation. But this implies, that we are forced to make statements on the behavior of solutions for negative argument too. Until now, for the fractional harmonic oscillator we have only presented solutions as a function of the variable x for $x > 0$.

We will solve this problem by introducing additional assumptions on the behavior of solutions under space inversion.

7.2 Parity and time-reversal

The transition of variables and derivatives from integer to fractional values

$$\left\{ x^n, \frac{d^n}{dx^n} \right\} \rightarrow \left\{ x^\alpha, \frac{d^\alpha}{dx^\alpha} \right\} \quad (7.9)$$

makes it necessary to consider the behavior of functions under space inversions.

We present a simple example to clarify the problem: The function

$$f(x) = x \quad (7.10)$$

behaves under space inversions as

$$f(-x) = -x = -f(x) \quad (7.11)$$

and therefore has negative parity or in other words is an odd function. If we choose the simple substitution $x \rightarrow x^\alpha$, we obtain for the fractional function

$$f(x) = x^\alpha \quad (7.12)$$

$$f(-x) = (-x)^\alpha = (-1)^\alpha |x|^\alpha \quad (7.13)$$

a multi-valent value (e.g. for the semi-derivative $\alpha = 1/2$ we have two different purely imaginary function values $\pm i|x|^{\frac{1}{2}}$). The parity property is lost.

If we intend to conserve the parity properties of normal functions for the corresponding fractional generalization, we must specify the parity behavior for the variable x .

With the ansatz

$$x \rightarrow \text{sign}(x)|x|^\alpha = \hat{x}^\alpha \quad (7.14)$$

$$\frac{d}{dx} \rightarrow \frac{d^\alpha}{d\hat{x}^\alpha} = \hat{D}_x^\alpha \quad (7.15)$$

this problem is solved.

Instead of (7.1) we will therefore use

$$\left(\left(\frac{d^\alpha}{d\hat{x}^\alpha} \right)^2 + \left(\frac{d^\alpha}{d\hat{y}^\alpha} \right)^2 + \left(\frac{d^\alpha}{d\hat{z}^\alpha} \right)^2 - \mu^2 \frac{d^2}{dt^2} \right) \psi(x, y, z, t) = 0 \quad (7.16)$$

as a regularized fractional wave equation. The free solutions of this wave equation show then a similar behavior under parity transformations for arbitrary α as in the limiting case $\alpha = 1$.

This regularization procedure is equivalent to the use of the left and right handed fractional derivative definitions according to Riemann and Caputo, because these are distinguished at $x = 0$. For Liouville type derivative definitions the regularization is an additional requirement, since from the original definition for left- and right-handed Liouville type derivatives the point $x = 0$ is not distinguished.

Until now we have only discussed the spatial part of a fractional equation. If we allow a fractional derivative for the time variable too, a similar problem arises for time-reversal.

With the ansatz

$$t \rightarrow \text{sign}(t)|t|^\alpha = \hat{t}^\alpha \quad (7.17)$$

$$\frac{d}{dt} \rightarrow \frac{d^\alpha}{d\hat{t}^\alpha} = \hat{D}_t^\alpha \quad (7.18)$$

the function $g(t) = (\hat{t}^\alpha)^{2n}$ behaves as

$$g(-t) = (\text{sign}(-t)|-t|^\alpha)^{2n} = (-1)^{2n}(\text{sign}(t)|t|^\alpha)^{2n} = g(t) \quad (7.19)$$

and the function $u(t) = (\hat{t}^\alpha)^{2n+1}$ behaves as

$$u(-t) = (\text{sign}(-t)|-t|^\alpha)^{2n+1} = (-1)^{2n+1}(\text{sign}(t)|t|^\alpha)^{2n+1} = -u(t) \quad (7.20)$$

and consequently $g(t)$ and $u(t)$ are eigenfunctions of the time-reversal operator. Free solutions of such a regularized time fractional derivative equation show a similar behavior under time-reversal as for $\alpha = 1$.

A simultaneous conservation of parity and time-reversal may be achieved, if space and time coordinates are treated similarly. Of course, these are symmetries, which are intentionally imposed. Interrelations between the non conservation properties of parity, time reversal, and charge conjugation are discussed e.g. in [Lee *et al.* (1957)].

7.3 Solutions of the free regularized fractional wave equation

The solutions of the free regularized one dimensional fractional wave equation

$$\left(\left(\frac{d^\alpha}{d\hat{x}^\alpha} \right)^2 + \kappa_x^2 \right) X(x) = 0 \quad (7.21)$$

are given in the sense of (7.14) using the regularized fractional derivative according to Fourier as the solutions for the fractional harmonic oscillator (12.3) and (12.1) extended to negative arguments:

$${}_{\text{F}} \sin(\alpha, x) = \text{sign}(x) \frac{1}{2i} \left(e^{\frac{1}{2}e^{\frac{i\pi}{2\alpha}}|x|} - e^{\frac{1}{2}e^{-\frac{i\pi}{2\alpha}}|x|} \right) \quad (7.22)$$

$${}_{\text{F}} \cos(\alpha, x) = \frac{1}{2} \left(e^{\frac{1}{2}e^{\frac{i\pi}{2\alpha}}|x|} + e^{\frac{1}{2}e^{-\frac{i\pi}{2\alpha}}|x|} \right) \quad (7.23)$$

For the fractional derivative according to Riemann solutions are given as a spatial extension of (6.21) and (6.22):

$${}_{\text{R}} \sin(\alpha, x) = \text{sign}(x)|x|^{2\alpha-1} E_{2\alpha, 2\alpha}(-|x|^{2\alpha}) \quad (7.24)$$

$${}_{\text{R}} \cos(\alpha, x) = |x|^{\alpha-1} E_{2\alpha, \alpha}(-|x|^{2\alpha}) \quad (7.25)$$

For the fractional Caputo derivative the regularized solutions are given as a spatial extension of (6.29) and (6.30):

$${}_{\text{C}} \sin(\alpha, x) = \text{sign}(x)|x|^{\alpha} E_{2\alpha, 1+\alpha}(-|x|^{2\alpha}) \quad (7.26)$$

$${}_{\text{C}} \cos(\alpha, x) = E_{2\alpha}(-|x|^{2\alpha}) \quad (7.27)$$

Application of the regularized fractional derivative leads to:

$$\hat{D}_{\text{F}, \text{R}, \text{C}}^{\alpha} \sin(\alpha, \kappa_x x) = \text{sign}(\kappa_x)|\kappa_x|^{\alpha} {}_{\text{F}, \text{R}, \text{C}} \cos(\alpha, \kappa_x x) \quad (7.28)$$

$$\hat{D}_{\text{F}, \text{R}, \text{C}}^{\alpha} \cos(\alpha, \kappa_x x) = -\text{sign}(\kappa_x)|\kappa_x|^{\alpha} {}_{\text{F}, \text{R}, \text{C}} \sin(\alpha, \kappa_x x) \quad (7.29)$$

Obviously the function $\sin(\alpha, x)$ is odd while $\cos(\alpha, x)$ is an even function:

$${}_{\text{F}, \text{R}, \text{C}} \sin(\alpha, -x) = -{}_{\text{F}, \text{R}, \text{C}} \sin(\alpha, x) \quad (7.30)$$

$${}_{\text{F}, \text{R}, \text{C}} \cos(\alpha, -x) = {}_{\text{F}, \text{R}, \text{C}} \cos(\alpha, x) \quad (7.31)$$

Therefore parity is conserved even for $\alpha \neq 1$.

For a given set of boundary conditions of type (7.8) it is of fundamental importance to determine the zeros of the proposed solutions:

The zeros for the solutions of the one dimensional wave equation with fractional derivative according to Fourier are given by:

$${}_{\text{F}} x_0(n, \alpha) = \frac{(n+1)}{\sin(\frac{\pi}{2\alpha})} \frac{\pi}{2} \quad n = 0, 1, 2, 3, \dots \quad (7.32)$$

The zeros for solutions based on the Riemann and Caputo derivative can only be determined numerically and are listed in tables 7.1 and 7.2.

In figure 7.1 we have plotted the zeros of the functions ${}_{\text{F}, \text{R}, \text{C}} \sin(\alpha, x)$ and ${}_{\text{F}, \text{R}, \text{C}} \cos(\alpha, x)$. While position differences of the zeros for $\alpha > 1$ are minimal, they are steadily increasing for $\alpha < 1$.

The solutions for the Fourier derivative in the case $\alpha < 1$ are equidistant and countable infinite, for the solutions based on the Riemann and Caputo derivative definition there exist only a finite number of zeros. For $\alpha < 0.65$ using the Riemann derivative there exists only one zero for the lowest even and odd solution. For the Caputo derivative in this region there exists only a single zero for the lowest even solution.

If we apply our results to the example of a vibrating string, for solutions of the fractional wave equation using the Fourier definition of a fractional

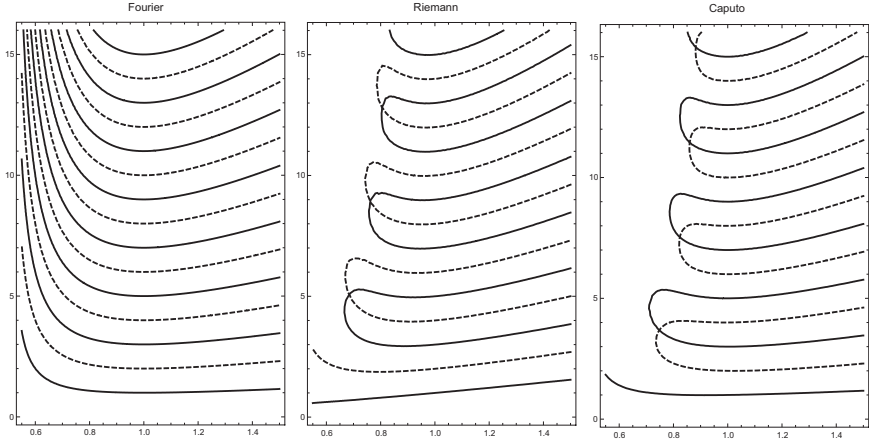


Fig. 7.1 Zeros of solutions of the fractional one dimensional wave equation with good parity for $0.55 \leq \alpha \leq 1.5$ in units $\pi/2$. Thick lines indicate the zeros of $\cos(\alpha, \pi x/2)$. Dashed lines indicate the zeros of $\sin(\alpha, \pi x/2)$. From left to right results are given for the Fourier-, Riemann- and Caputo fractional derivative.

derivative an arbitrary number of overtones is possible and the corresponding spectrum differs only by a multiplicative constant from the case $\alpha = 1$. Using the Riemann- and Caputo derivative for $\alpha < 1$ there is only a limited number of overtones.

For $\alpha > 1$ there is no limitation for the number of zeros any more. In figure 7.3 the solutions for $\alpha = 1.1$ are presented. We observe, that the graphs do not differ too much for a specific choice of a fractional derivative.

A comparison of the solutions with the standard trigonometric functions sine and cosine respectively leads to the result, that for $\alpha > 1$ the solutions are concentrated at the boundaries of a given domain, while for $\alpha < 1$ the solutions are centered within a given domain.

Since wave equations play a dominant role in many different branches of physics, the results derived for the classical harmonic oscillator are of general interest and give a first insight into the structure of solutions of fractional wave equations.

Until now, we have presented solutions which fulfill boundary conditions (7.8) which are synonymous to a determination of zeros. In the next section we will demonstrate, that in the case of a fractional differential equation a given set of boundary conditions determines the behavior of the solution not only within a given domain, but on $-\infty < x < +\infty$ in general.

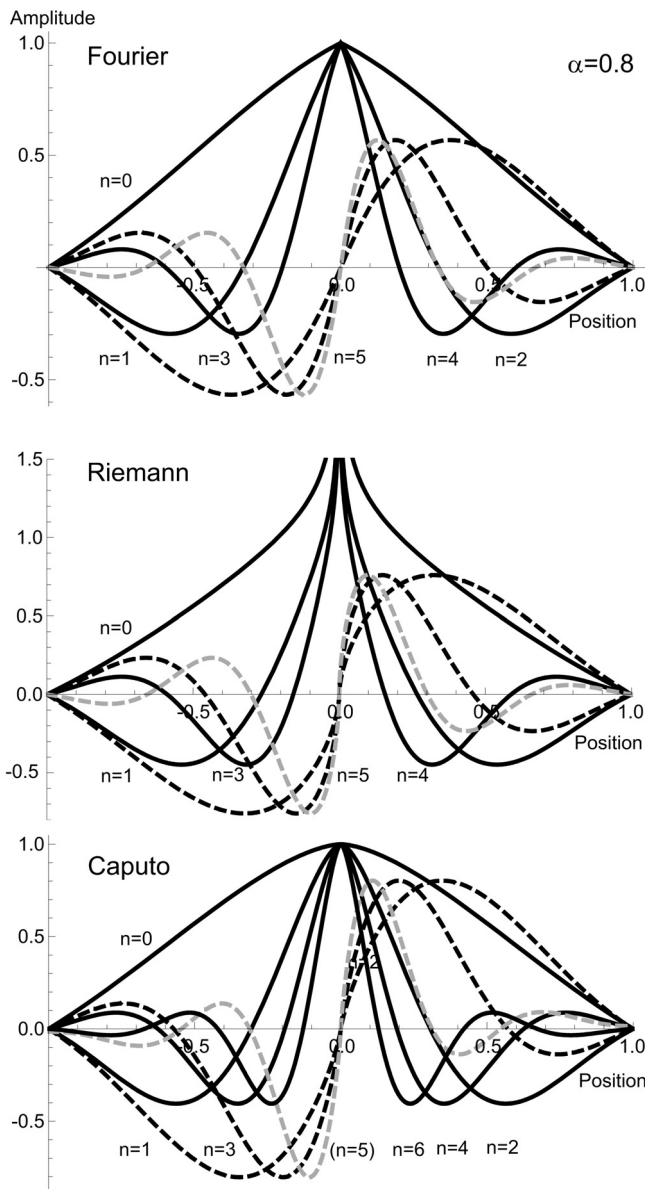


Fig. 7.2 A plot of the solutions of the fractional one dimensional wave equation with good parity for $\alpha = 0.8$. Even parity solutions using the Riemann derivative are singular at $x = 0$ for $\alpha < 1$.

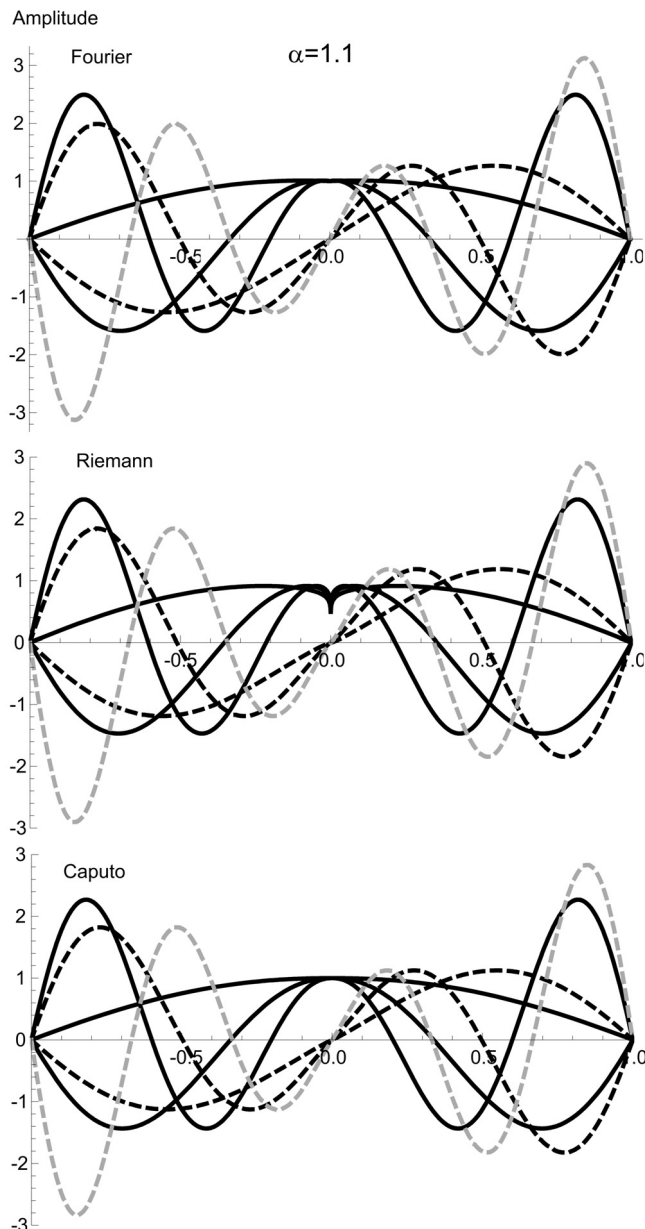


Fig. 7.3 A plot of the solutions of the fractional one dimensional wave equation with good parity for $\alpha = 1.1$. Solutions with even parity using the Riemann derivative for $\alpha > 1$ are passing the origin.

Table 7.1 The first eight zeros for the solutions of the fractional one dimensional wave equation for Fourier-, Riemann- and Caputo fractional derivative in units $\pi/2$ and given parity P .

α	n^P	${}_F D^\alpha$	${}_R D^\alpha$	${}_C D^\alpha$
1.50	0 ⁺	1.154700538379252	1.548108822078692	1.177627403143068
	1 ⁻	2.309401076758503	2.694943399235297	2.301485321060443
	2 ⁺	3.464101615137755	3.848714543680542	3.463996739874055
	3 ⁻	4.618802153517006	5.003699546069677	4.619242495665932
	4 ⁺	5.773502691896258	6.158416296644961	5.773503146252100
	5 ⁻	6.928203230275509	7.313103421812020	6.928165237760808
	6 ⁺	8.082903768654761	8.467802994810423	8.082903766685844
	7 ⁻	9.237604307034012	9.622504486441429	9.237608301057787
1.05	0 ⁺	1.002804043493139	1.052253594892194	1.009958990475784
	1 ⁻	2.005608086986279	2.054540724669651	1.999991857976986
	2 ⁺	3.008412130479418	3.055565373242182	3.007066283126732
	3 ⁻	4.011216173972558	4.058770424328503	4.013845158692073
	4 ⁺	5.014020217465697	5.061991096397526	5.014455210596974
	5 ⁻	6.016824260958837	6.064630851634081	6.015386179509487
	6 ⁺	7.019628304451976	7.067285327409207	7.019447308205646
	7 ⁻	8.022432347945116	8.070165889316242	8.023291113388379
0.95	0 ⁺	1.003427212662145	0.9485556666012389	0.993859584618117
	1 ⁻	2.006854425324291	1.951901826622405	2.016808715223814
	2 ⁺	3.010281637986436	2.958778776731958	3.013531854799109
	3 ⁻	4.013708850648581	3.961514062563152	4.005581101580363
	4 ⁺	5.017136063310727	4.963512298155291	5.015252693943481
	5 ⁻	6.020563275972872	5.967460183652009	6.028145383626639
	6 ⁺	7.023990488635017	6.971778811065169	7.025360849700859
	7 ⁻	8.027417701297163	7.974782024819545	8.019755900608110
0.90	0 ⁺	1.015426611885745	0.8980152822603107	0.992867116474696
	1 ⁻	2.030853223771490	1.912155183357559	2.058922060350698
	2 ⁺	3.046279835657235	2.937527595269366	3.056838785757390
	3 ⁻	4.061706447542980	3.951145368700498	4.030496394327696
	4 ⁺	5.077133059428725	4.960898498175122	5.068657771501075
	5 ⁻	6.092559671314470	5.978282565552790	6.132627214952245
	6 ⁺	7.107986283200215	6.998570670133788	7.116479023856850
	7 ⁻	8.123412895085960	8.011784466949399	8.069174049919944
0.85	0 ⁺	1.039689477087815	0.8484878274219066	0.999017046724642
	1 ⁻	2.079378954175631	1.883577115729535	2.142709963565060
	2 ⁺	3.119068431263446	2.945613974533191	3.146224716035916
	3 ⁻	4.158757908351262	3.981809920418118	4.061459296682879
	4 ⁺	5.198447385439077	5.003256218558363	5.167273413970680
	5 ⁻	6.238136862526893	6.048766968061488	6.432265275042531
	6 ⁺	7.277826339614708	7.110941545600579	7.323330098304986
	7 ⁻	8.317515816702523	8.140938806638054	7.988816945315072

Table 7.2 The first eight zeros for the solutions of the fractional one dimensional wave equation for Fourier-, Riemann- and Caputo fractional derivative in units $\pi/2$ and given parity P .

α	n^P	${}_F D^\alpha$	${}_R D^\alpha$	${}_C D^\alpha$	
0.80	0 ⁺	1.082392200292394	0.800099199204332	1.015444980477658	
	1 ⁻	2.164784400584788	1.870526110148884	2.306905904794297	
	2 ⁺	3.247176600877182	3.000266309334720	3.315190114494079	
	3 ⁻	4.329568801169576	4.076964366870888	4.036685978528044	
	4 ⁺	5.411961001461970	5.100970116743314	5.297651744717252	
	5 ⁻	6.494353201754364	6.199703886212465	-	
	6 ⁺	7.576745402046758	7.395685854947899	7.880345808692397	
0.75	7 ⁻	8.659137602339152	8.431716117739785	-	
	0 ⁺	1.154700538379252	0.752995286892762	1.047385229126909	
	1 ⁻	2.309401076758503	1.880162355069878	2.709953761138090	
	2 ⁺	3.464101615137755	3.138735906150366	3.6565566552063427	
	3 ⁻	4.618802153517006	4.286558874580779	3.712844196718815	
	4 ⁺	5.773502691896258	5.236318730295013	5.332625953261004	
	5 ⁻	6.928203230275509	6.434022212906170	-	
0.70	6 ⁺	8.082903768654761	-	-	
	7 ⁻	9.237604307034012	9.299965066401486	-	
	0 ⁺	1.279048007689933	0.707345469167315	1.104302891625908	
	1 ⁻	2.558096015379865	1.925218737937735	-	
	2 ⁺	3.837144023069798	3.474330055900506	-	
	3 ⁻	5.116192030759730	4.761391703578645	-	
	4 ⁺	6.395240038449663	5.221510825017026	-	
2/3	5 ⁻	7.674288046139596	6.564387392917614	-	
	6 ⁺	8.953336053829528	-	-	
	7 ⁻	10.23238406151946	-	-	
	0 ⁺	1.414213562373095	0.677815951504878	1.164837741928043	
	1 ⁻	2.828427124746190	1.986468690765288	-	
	2 ⁺	4.242640687119285	4.330846158230810	-	
	3 ⁻	5.656854249492380	-	-	
0.50	4 ⁺	7.071067811865475	4.475249390687474	-	
	5 ⁻	8.485281374238570	-	-	
	6 ⁺	9.899494936611665	-	-	
	7 ⁻	11.31370849898476	-	-	
	0 ⁺	-	0.5436940754380249	-	
	0.45	0 ⁺	2.923804400163087	0.5088985086845058	-
	2 ⁺	8.771413200489262	-	-	
0.40	0 ⁺	1.414213562373095	0.4771904074047175	-	
	2 ⁺	4.242640687119285	-	-	
0.35	0 ⁺	1.025716863272554	0.4488898520770091	-	
	2 ⁺	3.077150589817662	-	-	
0.30	0 ⁺	1.154700538379252	0.4242668293935616	-	
	2 ⁺	3.464101615137755	-	-	

Chapter 8

Nonlocality and Memory Effects

Now we will embed the concept of fractional calculus into a broader theory of nonlocal operators. This strategy will lead to a successful generalization of the fractional derivative operator and will result in a promising concept for a deduction of a covariant fractional derivative calculus on the Riemann space in the future.

We will demonstrate the influence of a memory effect for a distinguished set of histories presenting a full analytic solution for a simple nonlocal model for a metal hydride battery.

8.1 A short history of nonlocal concepts

The concept of nonlocality and memory effects has a long historical tradition in physics.

Figure 8.1 illustrates a first example for nonlocal concepts. A woodcut from the 1551 edition of *Rudimenta mathematica* [Münster (1551)] is reproduced showing the ballistic curve of a canon ball, which at that time was determined on the basis of the impetus theory, which was the fundamental pre-Newtonian dynamic theory of motion for more than 1000 years [Philoponus (~530)].

According to Leonardo da Vinci impetus “is the impression of local movement transmitted from the mover to the mobile object and maintained by the air or by the water as they move to prevent a vacuum” [Vinci (1488)]. A logical consequence of this definition is the prediction of a curved movement of a mobile object, if this object moves in a circle and is released in the course of this motion, which is known as circular impetus. In terms of a modern nonlocal theory such a behavior was a direct consequence of a memory effect: The actual state of the object contains a circular component

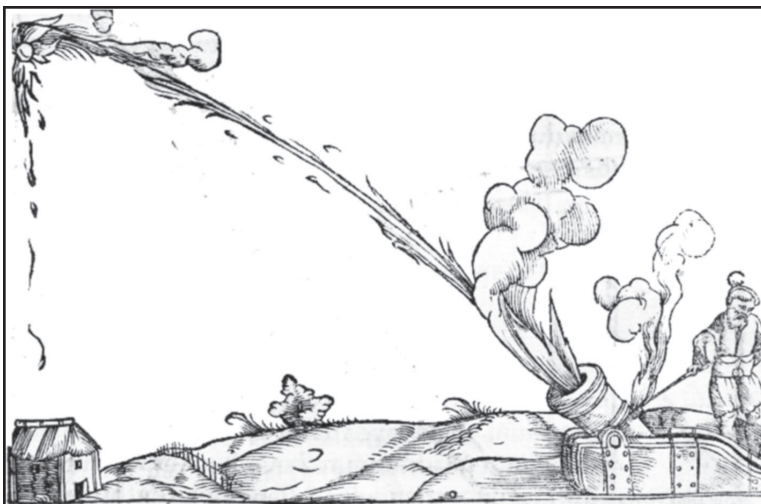


Fig. 8.1 The flight of a canon ball according to impetus theory [Münster (1551)].

since it is influenced by an earlier circular state in the past. Following Newton, this conclusion is wrong and in course of Newton's theory's continued success the medieval impetus theory was dead.

But at the beginning of the twentieth century atomic and subatomic physics caused an unexpected triumphant return of nonlocal concepts in terms of quantum mechanics.

A prominent example is the tunnel effect, which cannot be explained within the framework of classical physics. A typical application is spontaneous fission, where a nucleus disintegrates into two or more large fragments. The fission process in general was first proposed by Ida Noddack [Noddack (1934)] as an alternative interpretation of Fermi's experimental results [Fermi (1934)]. The spontaneous fission of uranium was first observed by Flerov [Flerov and Petrzhak (1940)].

In figure 8.2 this process is illustrated schematically. As a function of the total elongation of the nucleus (Δz) a collective potential is shown. The state of the nucleus is determined solving the collective Schrödinger equation including this potential. The meta stable ground state of the nucleus is located at a given ground state deformation β_0 which determines a local minimum in the potential function. From a classical point of view, the nucleus could stay there for ever.

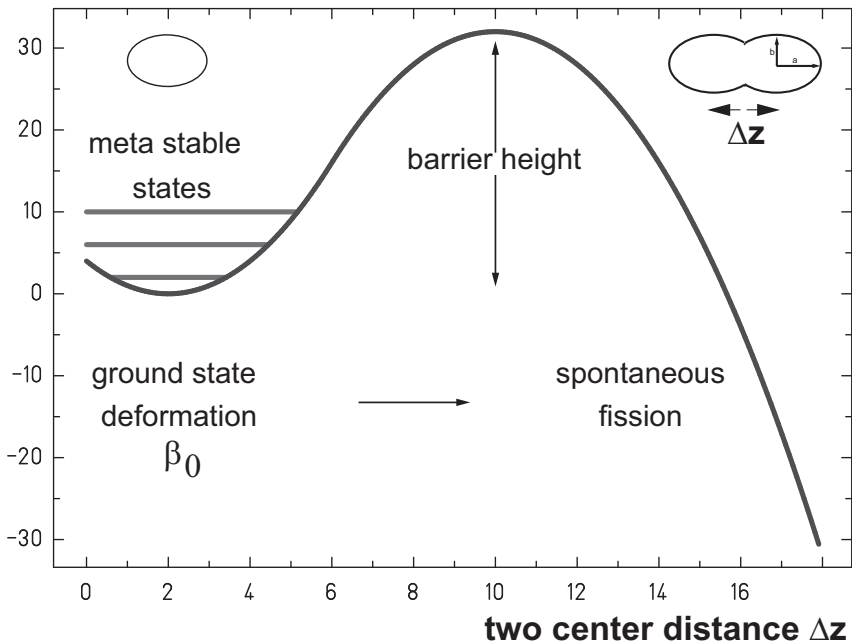


Fig. 8.2 Schematic view of the tunnel effect.

But as a consequence of Heisenberg's uncertainty relation there is a nonvanishing probability for a separated configuration beyond the finite potential barrier. As a result there is a finite lifetime T for the compound nucleus which is given in WKB-approximation [Martin (2006)] as

$$\log(T) \approx \frac{2}{\hbar} \int d(\Delta z) \sqrt{2mE - V(\Delta z)} \quad (8.1)$$

In view of a nonlocal theory, the time development of the meta-stable ground state is influenced by the fission potential characteristics for large Δz values, which are not accessible from a classical point of view.

Consequently, the figures presented in 8.1 and 8.2 illustrate a remarkable historical development of nonlocal concepts in physics. And finally, modern string theory could be reckoned as one more nonlocal extension of a point particle dynamics. Within that context, fractional calculus is a revival, sublimation and continuation of nonlocal concepts developed in the past.

Until now we have proceeded with the presentation of the conceptual basis of fractional calculus along a historical path, which started with the realization of the fractional derivative for special function classes followed

by an extension to general analytic function sets based on Cauchy's integral formula.

Now we intend to embed the fractional calculus into a much broader context of a theory of nonlocal extensions of standard operators.

We will first present a gradual classification scheme of different levels of nonlocality. We will then investigate some of the general properties of a certain class of normalizable nonlocal operators and we will determine their relation to fractional operators. Finally we will apply the concept of nonlocality to demonstrate the influence of memory effects on the solution of nonlocal differential equations.

8.2 From local to nonlocal operators

In the following we present a concept of nonlocality, which is based on the increasing amount of information which has to be gathered in the neighbourhood of a given local quantity to obtain a specific realization of the corresponding nonlocal quantity.

The position of a point mass is given in terms of classical mechanics according to Newton for a given time t as $x(t)$. It is given in the mks-system in units of $[m]$. This implies that there exists a reference position, e.g. a zero-point of a space coordinate system. The position of a point mass is measured with respect to this reference position. Since the position for a given time t is independent from a position at $t+\delta t$ and $t-\delta t$ respectively, we call $x(t)$ a purely local quantity or in other words a zero-nonlocal quantity, because information within a circle of radius $r = 0$ centered at $x(t)$ suffices to determine the position (neglecting the work of the geometer who devoted his life to establish a precisely gauged coordinate system). Besides the position are many more variables of this locality type, e.g. temperature, pressure, field strength etc.

The velocity of a point mass is given according to Newton by the first derivative of the position $x(t)$ with respect to t .

Following Weierstraß the first derivative may be defined as

$$v(t) = \frac{d}{dt}x(t) = \begin{cases} \lim_{h \rightarrow 0} \frac{x(t)-x(t-h)}{h} & \text{left, causal} \\ \lim_{h \rightarrow 0} \frac{x(t+h)-x(t-h)}{2h} & \text{symmetric} \\ \lim_{h \rightarrow 0} \frac{x(t+h)-x(t)}{h} & \text{right, anti-causal, } h < \epsilon, h \geq 0 \end{cases} \quad (8.2)$$

where ϵ is an arbitrary small positive real value.

As long as $x(t)$ is an analytic smooth function of t the three given definitions seem to be equivalent. As long as t is interpreted as a space-like coordinate, the definitions indicate that position information is gathered from the left only, from the right only or from both sides simultaneously.

If t is interpreted as a time-like coordinate, the first definition of (8.2) obeys the causality principle, which roughly states, that the current state of a physical object may only be influenced by events, which already happened in the past (concepts of past, future, causality and locality are discussed e.g. in [Kant (1781); Wells (1895); Einstein *et al.* (1935); Weizsäcker (1939); Treder (1983); Beecham (1947); Todd and Lantham (1992); Rowling (1999); Svensmark (2012)]).

The last of definitions (8.2) clearly violates the principle of causality within the framework of a classical context. Of course, in the area of quantum mechanics we may adopt Stückelberg's [Stückelberg (1941)] and Feynman's [Feynman (1949)] view and recall their idea, that anti-particles propagate backwards in time. Therefore this definition is appropriate to describe e.g. the velocity of an anti-particle.

Finally the second definition in (8.2) of a derivative is a mixture of causal and anti-causal propagation, which indicates, that a single particle interpretation may lead to difficulties. Therefore it should be considered, if this definition could be used to describe the velocity of a particle anti-particle pair.

Though for ordinary derivatives this discussion sounds somewhat sophisticated and artificial, since whatever definition we use, a violation of the causality principle is only of order ϵ , in case of really nonlocal quantities these considerations become important.

Since we need information within a radius of $r < \epsilon$ centered at $x(t)$ in order to determine the standard derivative we call such a quantity to be ϵ -nonlocal. In standard textbooks the ordinary derivative is classified as a local quantity, since ϵ is arbitrarily close to zero. Therefore we may use the terms ϵ -nonlocal and local simultaneously, as long as $\epsilon \approx 0$.

Besides velocity there are many more variables of this locality type, e.g. currents, flux densities and last not least all variables, which are determined by a differential equation. As a next step we will reformulate the ordinary derivative in terms of an integral form

$$v(t) = \frac{d}{dt}x(t) = \begin{cases} 2 \int_0^\infty dh \delta(h) v(t-h) & \text{left, causal} \\ 2 \int_0^\infty dh \delta(h) \frac{v(t+h)+v(t-h)}{2} & \text{symmetric} \\ 2 \int_0^\infty dh \delta(h) v(t+h) & \text{right, anti-causal} \end{cases} \quad (8.3)$$

where $\delta(t)$ is the Dirac-delta function which has the property [Lighthill (1958)]:

$$\int_{-\infty}^{\infty} dh \delta(h) f(h) = f(0) \quad (8.4)$$

and is defined as a class of all equivalent regular sequences of good functions $w(a, t)$

$$\delta(t) = \lim_{a \rightarrow 0} w(a, t) \quad (8.5)$$

where a is a smooth parameter with $a \geq 0$.

Following [Lighthill (1958)] a good function is one, which is everywhere differentiable any number of times and such, that it and all its derivatives are $O(|t|^{-N})$ as $|t| \rightarrow \infty$ for all N . Furthermore a sequence $w(a, t)$ of good functions is called regular, if, for any good function $f(t)$ the limit

$$\lim_{a \rightarrow 0} \int_{-\infty}^{+\infty} w(a, t) f(t) dt \quad (8.6)$$

exists. Finally two regular sequences of good functions are called equivalent if, for any good function $f(t)$ whatever, the limit (8.6) is the same for each sequence.

Typical examples for such sequences of good functions are

$$w(a, t) = \begin{cases} \exp^{-(|t|/a)^p} & \text{exponential, } p \in \mathbb{R}_+ \\ \text{Ai}(|t|/a) & \text{Airy} \\ \frac{1}{t} \sin(|t|/a) & \text{sine} \end{cases} \quad (8.7)$$

In figure 8.3 we have collected some graphs of good functions.

If the smooth parameter a is close to zero, the relations

$$\lim_{a \rightarrow 0} 2 \int_0^{\infty} dh w(a, h) v(t \pm h) \approx \lim_{a \rightarrow 0} 2 \int_0^{\epsilon} dh w(a, h) v(t \pm h) = v(t) \quad (8.8)$$

become valid and therefore definition (8.3) is equivalent to (8.2) for $a < \epsilon$. Consequently for this case we need information within a radius $r < \epsilon$ centered at $x(t)$ and the definition (8.3) leads to a ϵ -nonlocality.

But if we allow that a may be any finite real value, we have to gather information within a radius of arbitrary size, therefore

$$\frac{d}{dt} \text{nonlocal} x(t) = \begin{cases} \frac{1}{N} \int_0^{\infty} dh w(a, h) v(t - h) & \text{left, causal} \\ \frac{1}{N} \int_0^{\infty} dh w(a, h) \frac{v(t+h) + v(t-h)}{2} & \text{symmetric} \\ \frac{1}{N} \int_0^{\infty} dh w(a, h) v(t + h) & \text{right, anti-causal} \end{cases} \quad (8.9)$$

with

$$\lim_{a \rightarrow 0} w(a, t) = \delta(t) \quad (8.10)$$

and a normalization constant N which is determined by the condition

$$\frac{1}{N} \int_0^\infty dh w(a, h) = 1 \quad (8.11)$$

is a reasonable extension from the local operator $\frac{d}{dt}$ to a nonlocal version of the same operator.

Let us introduce a set of shift operators $\hat{s}(h)$ which acts on an analytic function $f(x)$ like:

$$\hat{s}_+ f(x) = f(x + h) \quad (8.12)$$

$$\hat{s}_- f(x) = f(x - h) \quad (8.13)$$

$$\frac{1}{2}(\hat{s}_+ + \hat{s}_-)f(x) = \frac{1}{2}(f(x + h) + f(x - h)) \quad (8.14)$$

$$\frac{1}{2h}(\hat{s}_+ - \hat{s}_-)f(x) = \frac{1}{2h}(f(x + h) - f(x - h)) = \frac{\Delta f}{\Delta x} \quad (8.15)$$

where the last operation is equivalent to the secant approximation of the first derivative of $f(x)$.

A possible generalization of the proposed procedure for an arbitrary local operator $\hat{O}_{\text{local}}(x)$ to the corresponding nonlocal representation $\hat{O}_{\text{nonlocal}}(x)$ is then given according to (8.9) by:

$$\hat{O}_{\text{nonlocal}}(x) f(x) = \frac{1}{N} \int_0^\infty dh w(a, h) \hat{s}(h) \hat{O}_{\text{local}}(x) f(x) \quad (8.16)$$

Therefore the transition from a local representation of a given operator to a reasonable nonlocal representation of the same operator is given by 3 operations:

An application of

- a) the local version of the operator \hat{O}_{local}
- b) a shift operation \hat{s} and
- c) an averaging procedure \hat{A} with an appropriately chosen weight function $w(a, h)$

$$\langle f(a) \rangle = \hat{A}(a, h) f(h) = \frac{1}{N} \int_0^\infty dh w(a, h) f(h) \quad (8.17)$$

For these 3 operations exist 6 optional permutations, which result in 6 equally reasonable realizations of nonlocality:

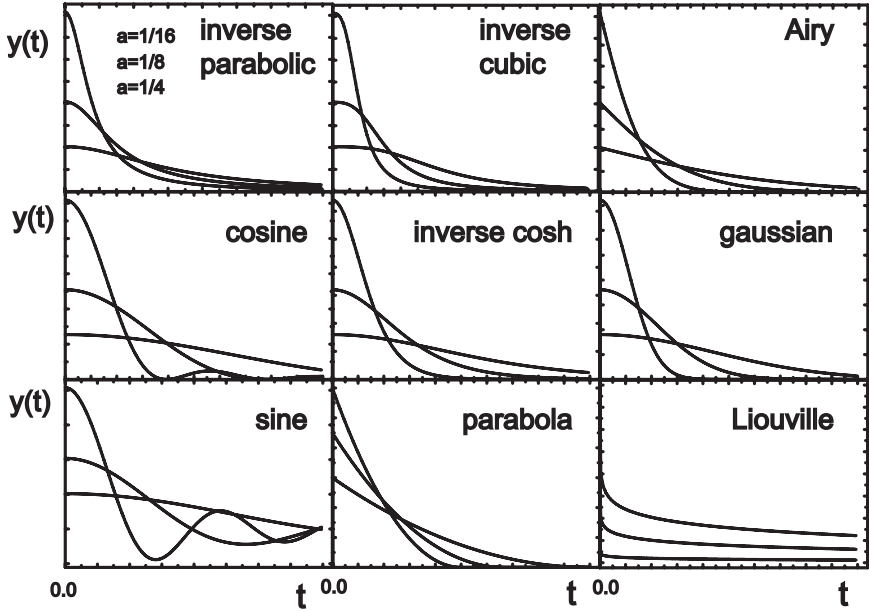


Fig. 8.3 Weight functions $w(a, t)$ listed in table 8.1 for different values of a .

A first set with $\hat{A} \hat{s}$ sequence:

$${}_1\hat{O}_{\text{nonlocal}}(x) f(x) = \hat{O}_{\text{local}} \hat{A} \hat{s} f(x) \quad (8.18)$$

$$= \frac{1}{N} \hat{O}_{\text{local}} \int_0^\infty dh w(a, h) \hat{s} f(x) \quad (8.19)$$

$${}_2\hat{O}_{\text{nonlocal}}(x) f(x) = \hat{A} \hat{O}_{\text{local}} \hat{s} f(x) \quad (8.20)$$

$$= \frac{1}{N} \int_0^\infty dh w(a, h) \hat{O}_{\text{local}} \hat{s} f(x) \quad (8.21)$$

$${}_3\hat{O}_{\text{nonlocal}}(x) f(x) = \hat{A} \hat{s} \hat{O}_{\text{local}} f(x) \quad (8.22)$$

$$= \frac{1}{N} \int_0^\infty dh w(a, h) \hat{s} \hat{O}_{\text{local}} f(x) \quad (8.23)$$

and a second set with $\hat{s} \hat{A}$ sequence:

$${}_4\hat{O}_{\text{nonlocal}}(x) f(x) = \hat{s} \hat{A} \hat{O}_{\text{local}} f(x) \quad (8.24)$$

$$= \frac{1}{N} \hat{s} \int_0^\infty dh w(a, h) \hat{A} \hat{O}_{\text{local}} f(x) \quad (8.25)$$

$$= \hat{s} \hat{O}_{\text{local}} f(x) \quad (8.26)$$

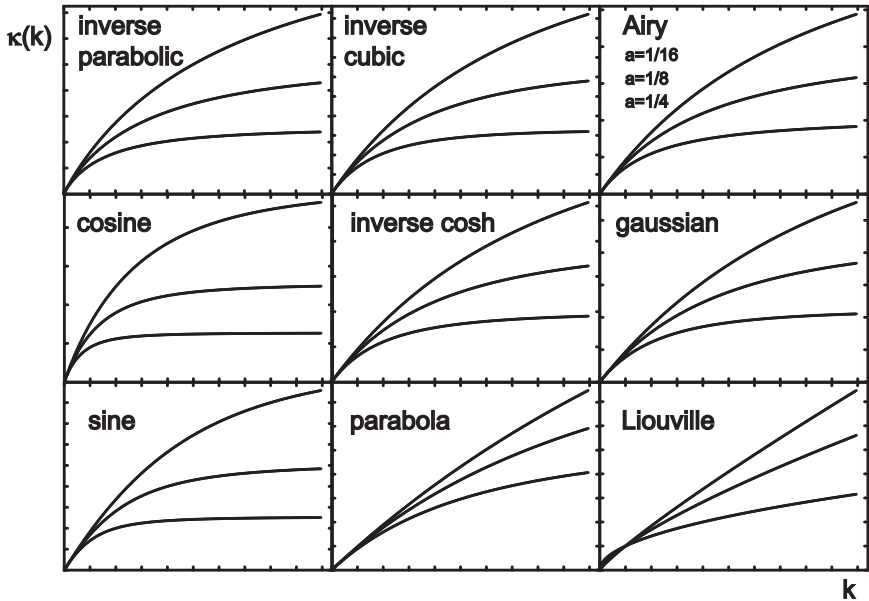


Fig. 8.4 Eigenvalue spectrum (8.49) of the nonlocal first order differential equation (8.44) for different weight functions $w(a, t)$ for different values of a . Function names are listed in table 8.1.

$$5 \hat{O}_{\text{nonlocal}}(x) f(x) = \hat{s} \hat{O}_{\text{local}} \hat{A} f(x) \quad (8.27)$$

$$= \frac{1}{N} \hat{s} \hat{O}_{\text{local}} \int_0^\infty dh w(a, h) f(x) \quad (8.28)$$

$$= \hat{s} \hat{O}_{\text{local}} f(x) \quad (8.29)$$

$$6 \hat{O}_{\text{nonlocal}}(x) f(x) = \hat{O}_{\text{local}} \hat{s} \hat{A} f(x) \quad (8.30)$$

$$= \frac{1}{N} \hat{O}_{\text{local}} \hat{s} \int_0^\infty dh w(a, h) f(x) \quad (8.31)$$

$$= \hat{O}_{\text{local}} \hat{s} f(x) \quad (8.32)$$

In the presentation of the last 3 realizations of a nonlocal operator we made use of the normalizability of the weight-function. These realizations may be interpreted as simple models of a delayed response of a physical system.

For example for the local differential equation

$$\frac{d}{dt} y(t) = -ky(t) \quad (8.33)$$

the nonlocal pendant is given according to (8.24) and (8.27) as

$$\hat{s} \frac{d}{dt} y(t) = -ky(t) \quad (8.34)$$

A multiplication from the left with the inverse of the shift operator (e.g. for the case $\hat{s}_\pm^{-1} = \hat{s}_\mp$) leads to

$$\hat{s}^{-1}\hat{s}\frac{d}{dt}y(t) = -k\hat{s}^{-1}y(t) \quad (8.35)$$

$$\frac{d}{dt}y(t) = -ky(t \mp h) \quad (8.36)$$

A similar treatment for (8.30) leads to

$$\frac{d}{dt}\hat{s}y(t) = -ky(t) \quad (8.37)$$

$$\frac{d}{dt}y(t \pm h) = -ky(t) \quad (8.38)$$

Such a behavior could be called discontinuous nonlocality. A promising field of application might be in signal theory, where the parameter h determines a fixed time delay for a reaction of a given system [May (1975)]. This is just a simple example for functional differential equations, where the rate of change of a given quantity depends not only on values at the same time, but also time values in the past:

$$\frac{d}{dt}y(t) = f(t, y(t), y(t - \tau)) \quad (8.39)$$

where τ is a constant delay. It should be noted, that this equation cannot be treated as an initial value problem, because on the initial point t_0 the derivative depends on the value of $y(t_0 - \tau)$. Therefore it is necessary to specify the value of y on an initial interval $[t_0 - \tau, t_0]$ [Butcher (2008)].

The amount of information necessary to solve the delay differential equation is of the same order as in the case of fractional differential equations.

The first two realizations of a nonlocal operator (8.18), (8.20) are equivalent which follows from:

$$[\hat{O}_{\text{local}}(x), \hat{A}(a, h)] = 0 \quad (8.40)$$

In other words, the weight procedure \hat{A} and the local operator \hat{O} commute, as long as the weight procedure is independent of x .

The equivalence ${}_2\hat{O}_{\text{nonlocal}}(x) = {}_3\hat{O}_{\text{nonlocal}}(x)$ follows, as long as the local operator is a pure derivative, e.g. $\hat{O}_{\text{local}} = d/dx$, from

$$[\hat{O}_{\text{local}}(x), \hat{s}] = 0 \quad (8.41)$$

or in other words, as long as $\hat{O}_{\text{nonlocal}}(x)$ commutes with the shift operator \hat{s} , which is true for a pure derivative operator.

As a first intermediate result we may conclude, that our presentation of a nonlocal generalization of a local operator in the special case of the local

derivative leads to only one reasonable definition which according to (8.18) is given by:

$$\frac{d}{dx}_{\text{nonlocal}} f(x) = \frac{1}{N} \frac{d}{dx} \int_0^\infty dh w(a, h) \hat{s}f(x) \quad (8.42)$$

This definition allows for a generalization of simple differential equations.

As an example, the first order differential equation

$$\frac{d}{dx} f(x) = \kappa f(x) \quad (8.43)$$

may be extended to the causal nonlocal case

$$\frac{d}{dx}_{\text{nonlocal}} f(x) = \frac{1}{N} \frac{d}{dx} \int_0^\infty dh w(a, h) f(x - h) = \kappa f(x) \quad (8.44)$$

With the ansatz

$$f(x) = e^{kx} \quad (8.45)$$

we obtain

$$\frac{d}{dx}_{\text{nonlocal}} e^{kx} = \frac{1}{N} \frac{d}{dx} \int_0^\infty dh w(a, h) e^{k(x-h)} \quad (8.46)$$

$$= \frac{1}{N} \int_0^\infty dh w(a, h) k e^{k(x-h)} \quad (8.47)$$

$$= e^{kx} \frac{1}{N} \int_0^\infty dh w(a, h) k e^{-kh} \quad (8.48)$$

Therefore the exponential function (8.45) indeed is an eigenfunction of the nonlocal differential equation (8.44) and the eigenvalue spectrum is given by

$$\kappa(k) = k \frac{1}{N} \int_0^\infty dh w(a, h) e^{-kh} \quad (8.49)$$

In table 8.1 this spectrum is calculated analytically for different weight functions and the corresponding graphs are given in figure 8.4. Despite the fact, that the analytic solutions cover a wide range of exotic functions for different weights, the graphs differ not very much and show a similar behavior: For finite values of a the eigenvalue spectrum increases weaker than $\kappa(k) = k$ for the local limit $a \rightarrow 0$.

At this point of discussion we may now try to determine the connection between nonlocal operators and fractional calculus. For that purpose, we will weaken our requirements for the weight function and will first give up

the requirement of normalizability (8.11). In addition, we allow for weakly singular weight functions. In that case, we may consider:

$$w(a, h) = h^{a-1} \quad 0 < a < 1 \quad (8.50)$$

$$N = \Gamma(a) \quad (8.51)$$

With these settings (8.42) is nothing else but the Liouville definition of a fractional derivative. To be more specific, depending on our choice of the shift operator, the four cases (8.12) lead to

$${}_1\hat{O}(\hat{s}_-) f(x) = \frac{1}{\Gamma(a)} \frac{d}{dx} \int_0^\infty dh h^{a-1} f(x-h) \quad (8.52)$$

$$= \frac{1-a}{\Gamma(a)} \int_0^\infty dh h^{a-1} \frac{f(x) - f(x-h)}{h} \quad (8.53)$$

$${}_1\hat{O}(\hat{s}_+) f(x) = \frac{1}{\Gamma(a)} \frac{d}{dx} \int_0^\infty dh h^{a-1} f(x+h) \quad (8.54)$$

$$= \frac{1-a}{\Gamma(a)} \int_0^\infty dh h^{a-1} \frac{f(x+h) - f(x)}{h} \quad (8.55)$$

$${}_1\hat{O}\left(\frac{\hat{s}_+ + \hat{s}_-}{2}\right) f(x) = \frac{1}{\Gamma(a)} \frac{d}{dx} \int_0^\infty dh h^{a-1} \frac{f(x+h) + f(x-h)}{2} \quad (8.56)$$

$$= \frac{1-a}{\Gamma(a)} \int_0^\infty dh h^{a-1} \frac{f(x+h) - f(x-h)}{2h} \quad (8.57)$$

$${}_1\hat{O}\left(\frac{\hat{s}_+ - \hat{s}_-}{2h}\right) f(x) = \frac{1}{\Gamma(a)} \frac{d}{dx} \int_0^\infty dh h^{a-1} \frac{f(x+h) - f(x-h)}{2h} \quad (8.58)$$

$$= \frac{2-a}{2\Gamma(a)} \int_0^\infty dh h^{a-1} \frac{f(x+h) - 2f(x) + f(x-h)}{h^2} \quad (8.59)$$

which correspond to the left-Liouville and right-Liouville (5.57), Feller ${}_F D_1^\alpha (\theta = 1)$ (5.79) and Riesz (5.71) definition of a fractional derivative. Hence these four different definitions of a fractional derivative operator may be understood within the framework of a nonlocal theory as a result of left, right, symmetric and antisymmetric shift operations.

In addition we want to emphasize the smooth transition from normalizable, nonsingular weights to not normalizable, weakly-singular weight functions, as long as the eigenvalue spectrum for a nonlocal differential equation is considered. In figure 8.4 we have plotted the eigenvalues of the solutions of the first order differential equation (8.49) for the left-sided Liouville fractional derivative, which are simply given as $\kappa(k) = k^{1-a}$. For $k > 1$ they show a similar behavior as the nonlocal solutions using a normalizable weight.

The fractional derivative definition may be considered as a convolution integral with a weakly singular kernel [Gorenflo *et al.* (2008)] and the concept of a fractional derivative may be embedded as a special case into a general theory of nonlocal operators.

The presented theory of nonlocal operators is not restricted to pure derivative operators but may be applied to any coordinate dependent local operator. If we intend to apply the fractional calculus to arbitrary curvilinear coordinate systems, the concept of fractional calculus has to be extended to arbitrary space dependent operators.

It should be emphasized, that space dependent local operators will not commute with the shift operator in general:

$$[\hat{O}_{\text{local}}(x), \hat{s}] \neq 0 \quad (8.60)$$

We therefore have two equivalent extensions of a fractional generalization of an arbitrary operator, namely \hat{O}_1 and \hat{O}_3 which according to (8.18) and (8.22) are given by:

$$\hat{O}_{LR} f(x) = \frac{1}{\Gamma(a)} \hat{O}_{\text{local}}(x) \int_0^\infty dh h^{a-1} \hat{s} f(x) = \hat{O}^a f(x) \quad (8.61)$$

We call \hat{O}_{LR} as the Liouville-Riemann or covariant \hat{O}^a fractional extension for an arbitrary coordinate dependent local operator \hat{O} and

$$\hat{O}_{LC} f(x) = \frac{1}{\Gamma(a)} \int_0^\infty dh h^{a-1} \hat{s} \hat{O}_{\text{local}}(x) f(x) = \hat{O}_a f(x) \quad (8.62)$$

we call \hat{O}_{LC} as the Liouville-Caputo or \hat{O}_a contravariant fractional extension for an arbitrary coordinate dependent local operator \hat{O} .

With (8.61) and (8.62) we have expanded the concept of fractional calculus from an extension of the standard derivative operator d/dx to a specific nonlocal generalization of an arbitrary local operator.

Within the framework of nonlocal operator calculus we may now discuss problems like coordinate transformations or an extension to higher-dimensional Riemannian spaces from a general point of view. For example an explicit and complete derivation of fractional operators in spherical coordinates is still an open task, despite the fact, that there have been several attempts in the past [Goldfain (2006); Tarasov (2008a); Roberts (2009); Li *et al.* (2010)].

Besides a geometric interpretation of the fractional integral in terms of a given area of projection of a curved fence presented in chapter 5.7 proposed by Podlubny [Podlubny (2001)], in this chapter we gave an alternative interpretation in terms of an averaging weight procedure for a given function.

This is in close analogy to possible interpretations of the standard integral, which may be interpreted geometrically as the calculation of an area under a given curve and a function average in a given interval respectively.

8.3 Memory effects

The solutions of a differential equation may be given in general, but for a specific application they have to obey additional initial or boundary conditions. If the differential equation is defined in terms of local operators, e.g. the Newtonian equations of motion, the knowledge of an initial position and the initial velocity determines a solution completely. The solutions of the general wave equation for a vibrating string may be determined, assuming the string is fixed at both ends. In both cases a specific solution of a local differential equation is completely determined by local conditions. As a consequence, more complex problems may be solved by piecewise solution in different areas, which later are combined to obtain a smooth general solution.

Typical examples are scattering problems. The Mie solutions of the Maxwell equations [Mie (1908)] e.g. describe the scattering of plane electromagnetic waves with spheres. For that purpose, the incoming wave, the scattered wave and the wave inside the sphere are expanded in spherical vector functions, which at first are independent of each other, but are combined employing the boundary conditions given on the surface of the sphere.

Another example is the penetration of a double humped fission barrier [Cramer and Nix (1970)]. The complex double humped potential is separated into different regions of space, where the potential takes the simple form of a harmonic oscillator. The Schrödinger equation is solved in these different regions and finally the different solutions are combined to obtain a smooth, differentiable general solution.

All these strategies are well established techniques to obtain solutions for a local differential equation. But they all will fail if applied to nonlocal theories.

The reason of the failure of the above mentioned techniques is of course the nonlocality of the operators used. The averaging procedure \hat{A} spreads out over the full region of space.

In the following we will demonstrate, how nonlocality influences the behavior of solutions and how the actual state of a system is influenced by it's history.

We will demonstrate this memory effect investigating the properties of an idealized model for a battery, which is discharged via a resistor [West-erlund (1991)]. First we present the classical local solution. Then we will solve the corresponding nonlocal differential equation and investigate the implicit and explicit influence of memory.

- In a classical approach, the discharging of a battery may simply be described as an RC-circuit with resistance R and capacity C , which yields a local first order differential equation for the charge Q :

$$\frac{d}{dt}Q(t) = -\frac{1}{RC}Q(t) \quad t \geq 0 \quad (8.63)$$

with the ansatz $Q(t) = Q_0 e^{-kt}$ a solution is given by:

$$k = \frac{1}{RC} \quad (8.64)$$

$$Q(t=0) = Q_0 \quad (8.65)$$

where k is called the decay constant and Q_0 is the charge amount for the battery at $t = 0$, which is given by $Q_0 = U_0 C$, where U_0 is the battery (capacitor) voltage at $t = 0$.

This is the classical description of the process. There is no information necessary on the number of charge-cycles or the age of the battery. In contrast to this idealized result, in practice a lowered capacity after repeated charge/discharge cycles has been reported for alkaline batteries [Hullmeine *et al.* (1989); Tarascon *et al.* (1996); Sato *et al.* (2001)]. We want to incorporate such memory effects into our idealized local model. Hence a promising strategy might be the step from a local to a nonlocal description:

- In the next step we will solve the corresponding nonlocal differential equation:

$$\frac{d}{dt}_{\text{nonlocal}} Q(t) = -\frac{1}{RC}Q(t) \quad t \geq 0 \quad (8.66)$$

With (8.42) we obtain using the causal translation operator \hat{s}_-

$$\frac{d}{dt}_{\text{nonlocal}} Q(t) = \frac{1}{N} \frac{d}{dt} \int_0^\infty dh w(a, h) Q(t-h) = -\frac{1}{RC}Q(t) \quad (8.67)$$

We will use the following weight-function

$$w(a, t) = e^{-t/a} \quad (8.68)$$

$$N = a \quad (8.69)$$

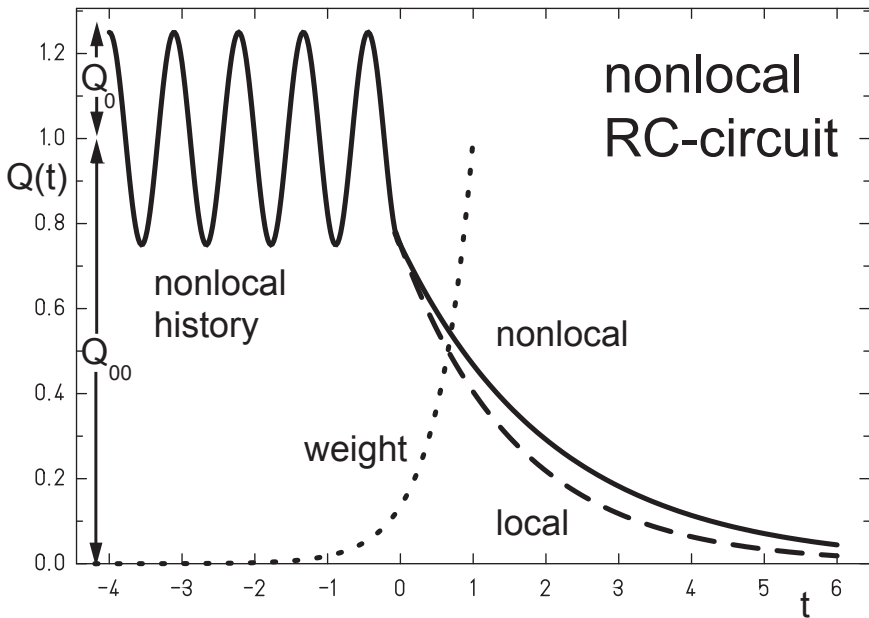


Fig. 8.5 Solutions of the nonlocal differential equation (8.74). Thick lines indicate the nonlocal solution (8.73), dashed line denotes the corresponding local solution ($a = 0$). The dotted line is a plot of the weight function $w(a, t)$ at $t = 1$ to give an impression about the influence of the memory effect.

which has the advantage, that all following results are obtained analytically. Inserting the ansatz

$$Q(t) = Q_0 e^{-kt} \quad -\infty \leq t \leq +\infty \quad (8.70)$$

into (8.67) we obtain the conditions

$$k = \frac{1}{RC + a} \quad (8.71)$$

$$Q(0) = Q_0 \quad (8.72)$$

The decay constant k for a given fixed set Q_0, R, C is reduced compared to the local case.

Despite the fact, that the differential equation is valid for $t > 0$ only, we had to give additional information on $Q(t)$ in the range $-\infty < t < 0$ in order to evaluate the integral (8.67). The eigenfunction (8.70) makes an implicit assumption about the development of the solution in the past.

But $Q(t) = Q_0 e^{-kt}$ is not a very realistic history, especially for $t \ll 0$.

- Let us therefore take into account a more realistic charge/discharge history of the battery. We will try

$$Q(t) = \begin{cases} Q_{00} + Q_0 \cos(\omega t) & t < 0 \\ (Q_{00} + Q_0)e^{-kt} & t \geq 0 \end{cases} \quad (8.73)$$

which is an idealized model for a charge history for $t < 0$, where Q_{00} is the average over all charge cycles, Q_0 is the amplitude of a harmonic oscillating charge/discharge cycle and ω is the cycle frequency.

Inserting this ansatz into (8.67) we obtain

$$\frac{d}{dt}_{\text{nonlocal}} Q(t) = \frac{1}{a} \frac{d}{dt} \int_0^\infty dh e^{-h/a} Q(t) \quad (8.74)$$

$$= \frac{1}{a} \frac{d}{dt} \int_0^t dh e^{-h/a} (Q_{00} + Q_0)e^{-k(t-h)} \quad (8.75)$$

$$+ \frac{1}{a} \frac{d}{dt} \int_t^\infty dh e^{-h/a} (Q_{00} + Q_0 \cos(\omega(t-h))) \\ = (Q_{00} + Q_0) \left(e^{-kt} \frac{k}{-1 + ak} + e^{-t/a} \frac{1}{a - a^2 k} \right) \\ - e^{-t/a} \frac{Q_0 + Q_{00}(1 + a^2 \omega^2)}{a + a^3 \omega^2} \quad (8.76)$$

$$= -\frac{1}{RC} Q(t) \quad t \geq 0 \quad (8.77)$$

A term by term comparison leads to the conditions

$$e^{-kt} \frac{k}{-1 + ak} = -\kappa e^{-kt} \quad (8.78)$$

$$e^{-t/a} \left(\frac{Q_0 + Q_{00}}{a - a^2 k} - \frac{Q_0 + Q_{00}(1 + a^2 \omega^2)}{a + a^3 \omega^2} \right) = 0 \quad (8.79)$$

From the first condition we obtain

$$k = \frac{1}{RC + a} \quad (8.80)$$

which coincides with (8.71).

For the solution of the local differential equation the behavior for $t < 0$ was arbitrary. Now for the nonlocal case we derived two solutions which are identical for $t \geq 0$, but differ in the past $t < 0$.

The second condition (8.79) yields:

$$\frac{1}{RC} = \frac{-Q_0}{Q_0 + Q_{00}} \frac{a\omega^2}{1 + a\omega^2} \quad (8.81)$$

from which we deduce, that an exponential discharge is only possible for $Q_0 < 0$. This implies, that $Q(0)$ is the minimum value of the oscillating part. Hence we have found only a special solution for a given set of a, Q_{00}, Q_0, ω values. For value sets, which do not fulfill condition (8.81) therefore the solution is not simply an exponential function any more, but of a rather more general function type.

We may conclude, that a memory effect may be modeled with nonlocal differential equations. We presented an idealized model to describe the behavior of a discharged battery. Indeed we found, that the discharge speed is reduced, if a memory effect ($a > 0$) is present. Consequently this simple model may be useful in biophysics, since it demonstrates, that training has a positive impact on fatigue behavior.

The most surprising news is, that the knowledge of the full past ($-\infty < t \leq 0$) of a given system does not uniquely determine the future development. As we have just demonstrated, an oscillatory and an exponential decay behavior respectively both may lead to the same exponential decay rate in the future. As a consequence, a given behavior in the future $t > 0$ may be the result of different histories. This is just the inverted concept of bifurcation theory, which states, that despite an identical behavior in the past, a minimal parameter change may cause a drastic change in the future development of a system.

We may easily understand the reason for this behavior: A nonlocal operator is not determined by the function values directly; by definition only a weighted integral over all past function values is necessary. Of course this may yield the same integral value at e.g. $t = 0$ for different functions. Therefore the concept of nonlocality, in analogy to Heisenberg's uncertainty principle, introduces a new quality of uncertainty into deterministic physical systems. It should also be clear now, that the method of a piecewise solution will not be applicable in general for nonlocal problems [Jeng *et al.* (2008)], but will only work for very special scenarios.

In addition a covariant formulation of a fractional derivative is necessarily based on a global concept of nonlocality, which is valid for space dependent derivative operators too.

Exercise 8.1**A linear delay differential equation**

Problem: Give an analytic solution for $y(t)$ in the interval $t \in [0, 4a]$ of the following delay differential equation

$$\partial_t y(t) = -y(t - a), \quad t > 0, a \in \mathbb{R} \quad (8.82)$$

where $y(t)$ is given by

$$y(t) = 1, t \leq 0 \quad (8.83)$$

For reasons of simplicity set the interval length to $a = 1$.

Table 8.1 A listing of possible weight functions $w(a, h)$ with name, definition, norm, and eigenvalue spectrum for the first order differential equation $\frac{d^a}{dx^a}y(x) = \kappa(k)y(x)$. In the last column function names according to chapter 2 are used.

name	$w(a, h)$	N	$\kappa(k)$
inverse parabolic	$\frac{1}{1+(h/a)^2}$	$\frac{a\pi}{2}$	$\frac{k}{\pi}(2\sin(ak)\text{Ci}(ak) + \cos(ak)(\pi - 2\text{Si}(ak)))$
inverse cubic	$\frac{1}{1+(h/a)^3}$	$\frac{2\pi}{3\sqrt[3]{a}}$	$\frac{3k}{4\pi^2}G_{1,4}^{4,1}\left(\frac{a^3 k^3}{27} \middle 0, \frac{1}{3}, \frac{2}{3}, \frac{2}{3}\right)$
Airy	$\text{Ai}(x/a)$	$\frac{a}{3}$	$-\frac{ak^2}{23^{5/6}\pi}e^{-a^3 k^3/3}(\text{Ei}_{2/3}(-(ka)^3/3)\Gamma(-1/3) + 3^{2/3}ak\text{Ei}_{1/3}(-(ka)^3/3)\Gamma(1/3))$
cosine	$\frac{1}{h^2}(1 - \cos(h/a))$	$\frac{\pi}{2a}$	$\frac{k}{\pi}(2\text{ArcCot}(ak) - ak\log(1 + \frac{1}{ka}))$
inverse cosh	$\cosh(h/a)^{-2}$	a	$\frac{k}{2}(2 + ak(\text{H}_{(ak-2)/4} - \text{H}_{ak/4}))$
exponential	$e^{-(h/a)}$	a	$\frac{k}{1+ka}$
gaussian	$e^{-(h/a)^2}$	$a\Gamma(3/2)$	$ke^{k^2 a^2/4}\text{erfc}(ak/2)$
sine	$\frac{1}{h}\sin(h/a)$	$\frac{\pi}{2}$	$\frac{2k}{\pi}\text{ArcCot}(ak)$
Liouville	h^{a-1}	$\frac{1}{\Gamma(a)}$	k^{1-a}
constant	$\theta(a - h)$	a	$\frac{1-e^{-ka}}{a}$
linear	$(a - h)\theta(a - h)$	$\frac{a^2}{2}$	$\frac{2}{a^2 k}(ak - (1 - e^{-ka}))$
parabola	$(a - h)^2\theta(a - h)$	$\frac{a^3}{3}$	$\frac{6}{a^3 k^2}(\frac{1}{2}ak(ak - 2) + (1 - e^{-ka}))$
Caputo	$h^{a-1}\theta(x - h)$	$\frac{1}{\Gamma(a)}$	$k^{1-a} \left(1 - \frac{\Gamma(a, kx)}{\Gamma(a)}\right)$ (not an eigenfunction)

Chapter 9

Fractional Calculus in Multidimensional Space — 2D- Image Processing

Until now, we have presented only one dimensional applications of fractional calculus. This is appropriate, as long as we confine ourselves to time-dependent problems. But space is a multi-dimensional construct and therefore we have to extend the proposed definitions to the multi-dimensional case in order to solve fractional space dependent problems.

Therefore in this chapter we will present a covariant, multi-dimensional generalization of the fractional derivative definition, which may be applied to any bound operator on the Riemannian space.

In the last chapter we have demonstrated, that we may consider fractional calculus as a specific prescription to extend the definition of a local operator to the nonlocal case. Of course, we are aware of the fact, that non-locality is a concept, which in general makes physicists shiver. Therefore it is important to present a simple and clear perception of this concept.

Hence as a first application of a covariant fractional extension of a higher dimensional operator, we will investigate the fractional analogue to the modified local Laplace-operator, which is widely used in problems of image processing. We will especially compare the local to the nonlocal approach for 3D-shape recovery from a set of 2D aperture afflicted slide sequences, which may be obtained e.g. in confocal microscopy or auto focus algorithms [Zernike (1935); Spencer (1982)].

It will turn out, that nonlocality has an evident meaning within the framework of image processing and may be easily interpreted as a blur effect.

9.1 The generalized fractional derivative

We start with the Liouville definition of the left and right fractional integral [Liouville (1832)]:

$${}_L I^\alpha f(x) = \begin{cases} (I_+^\alpha f)(x) = \frac{1}{\Gamma(\alpha)} \int_{-\infty}^x d\xi (x - \xi)^{\alpha-1} f(\xi) \\ (I_-^\alpha f)(x) = \frac{1}{\Gamma(\alpha)} \int_x^\infty d\xi (\xi - x)^{\alpha-1} f(\xi) \end{cases} \quad (9.1)$$

With a slight modification of the fractional parameter $\alpha = 1 - a$, where α is in the interval $0 \leq \alpha \leq 1$. Consequently for the limiting case $\alpha = 0$ I_+ and I_- both coincide with the unit-operator and for $\alpha = 1$ I_+ and I_- both correspond to the standard integral operator.

I_+ and I_- may be combined to define a regularized Liouville integral:

$$I^\alpha f(x) = \left(\frac{1}{2} (I_+^\alpha + I_-^\alpha) f \right)(x) \quad (9.2)$$

$$= \frac{1}{\Gamma(\alpha)} \int_0^\infty d\xi \xi^{\alpha-1} \frac{f(x + \xi) + f(x - \xi)}{2} \quad (9.3)$$

$$= \frac{1}{\Gamma(\alpha)} \int_0^\infty d\xi \xi^{\alpha-1} \hat{s}(\xi) f(x) \quad (9.4)$$

where we have introduced the symmetric shift-operator:

$$\hat{s}(\xi) f(x) = \frac{f(x + \xi) + f(x - \xi)}{2} \quad (9.5)$$

The regularized fractional Liouville-Caputo derivative may now be defined as:

$$\partial_x^\alpha f(x) = I^\alpha \partial_x f(x) \quad (9.6)$$

$$= \left(\frac{1}{\Gamma(\alpha)} \int_0^\infty d\xi \xi^{\alpha-1} \hat{s}(\xi) \right) \partial_x f(x) \quad (9.7)$$

$$= \frac{1}{\Gamma(\alpha)} \int_0^\infty d\xi \xi^{\alpha-1} \frac{f'(x + \xi) + f'(x - \xi)}{2} \quad (9.8)$$

$$= \frac{1 - \alpha}{\Gamma(\alpha)} \int_0^\infty d\xi \xi^{\alpha-1} \frac{f(x + \xi) - f(x - \xi)}{2\xi} \quad (9.9)$$

with the abbreviation $\partial_x f(x) = f'(x)$. This definition of a fractional derivative coincides with Feller's definition ${}_F \partial_x(\theta)$ for the special case $\theta = 1$.

We may interpret I^α as a nonlocalization operator, which is applied to the local derivative operator to determine a specific nonlocal extension of the same operator. Therefore the fractional extension of the derivative operator is separated into a sequential application of the standard derivative followed by a nonlocalization operation. The classical interpretation of a

fractional integral is changed from the inverse operation of a fractional derivative to a more general interpretation of a nonlocalization procedure, which may be easily interpreted in the area of image processing as a blur effect.

This is a conceptual new approach, since it may be easily extended to other operators e.g. higher order derivatives or space dependent operators, e.g. for ∂_x^2 we obtain:

$$(\partial_x^2)^\alpha f(x) = I^\alpha \partial_x^2 f(x) \quad (9.10)$$

$$= \left(\frac{1}{\Gamma(\alpha)} \int_0^\infty d\xi \xi^{\alpha-1} \hat{s}(\xi) \right) \partial_x^2 f(x) \quad (9.11)$$

$$= \frac{1}{\Gamma(\alpha)} \int_0^\infty d\xi \xi^{\alpha-1} \frac{f''(x+\xi) + f''(x-\xi)}{2} \quad (9.12)$$

$$= \frac{1-\alpha}{\Gamma(\alpha)} \int_0^\infty d\xi \xi^{\alpha-1} \frac{f'(x+\xi) - f'(x-\xi)}{2\xi} \quad (9.13)$$

$$= \frac{2-\alpha}{2\Gamma(\alpha)} \int_0^\infty d\xi \xi^{\alpha-1} \frac{f(x+\xi) - 2f(x) + f(x-\xi)}{\xi^2} \quad (9.14)$$

which is nothing else but the Riesz definition of a fractional derivative.

Therefore we define the following fractional extension of a local operator ${}_{\text{local}}\hat{O}$ to the nonlocal case

$${}_{\text{nonlocal}}\hat{O}^\alpha f(x) = I^\alpha {}_{\text{local}}\hat{O} f(x) \quad (9.15)$$

as the covariant generalization of the Liouville-Caputo fractional derivative to arbitrary operators on \mathbb{R} .

This definition may be easily extended to the multi-dimensional case, interpreting the variable ξ as a measure of distance.

In two dimensions, with

$$\xi = \sqrt{\xi_1^2 + \xi_2^2} \quad (9.16)$$

and with

$$\hat{s}(\xi_1, \xi_2) f(x, y) = \hat{s}(\xi_1) \hat{s}(\xi_2) f(x, y) \quad (9.17)$$

$$= \frac{1}{4} (f(x+\xi_1, y+\xi_2) + f(x-\xi_1, y+\xi_2) + f(x+\xi_1, y-\xi_2) + f(x-\xi_1, y-\xi_2)) \quad (9.18)$$

$I^\alpha(x, y)$ explicitly reads:

$$\begin{aligned}
I^\alpha(x, y) = & \frac{1}{2^{a-2}\Gamma(\alpha/2)^2 \sin(a\pi/2)} \\
& \times \int_0^\infty d\xi_1 \int_0^\infty d\xi_2 (\xi_1^2 + \xi_2^2)^{\frac{1}{2}(\alpha-2)} \hat{s}(\xi_1, \xi_2) \\
& 0 \leq \alpha \leq 2
\end{aligned} \tag{9.19}$$

which is normalized such, that the eigenvalue spectrum for:

$$I^\alpha f(x, y) = \kappa f(x, y) \tag{9.20}$$

with the eigenfunctions $f(x, y) = \exp^{ik_1x+ik_2y}$ follows as:

$$\kappa = (k_1^2 + k_2^2)^{-\alpha/2} \tag{9.21}$$

It should be noted, that the validity range for α spans from $0 \leq \alpha \leq 2$, since we deal with a two dimensional problem. Obviously within the framework of signal processing, the nonlocalization operator may be interpreted as a low-pass filter.

In the following sections, we will use this operator for a well defined extension of the standard algorithm used for 3D-shape recovery from aperture afflicted 2D-slide sequences to a generalized, fractional nonlocal version, which results in a very stable procedure with drastically reduced errors.

We will first present the minimal standard method and its limitations in the next section.

9.2 Shape recovery - the local approach

In a set $\{p_i(z_i), i = 1, \dots, N\}$ of N 2D-slides with increasing focal distance z_i , $\{z_i, \forall z_i : z_{\min} \leq z_i \leq z_{\max}, i = 1, \dots, N\}$ every slide contains areas with focused as well as defocused parts of the specimen considered. In the first row of figure 9.1 we present two examples from a slide-sequence of a spherical object with radius $r = 1$ located at $z = 0$ in the x,y-plane, where the focal plane was chosen to be $z = 0.45$ and $z = 0.8$ respectively.

For a 3D-shape recovery in a first step for a given slide the parts being in focus have to be extracted. For a textured object, areas in focus are dominated by a larger amount of high frequency contributions, while for out of focus parts mainly the low frequency amount of texture survives.

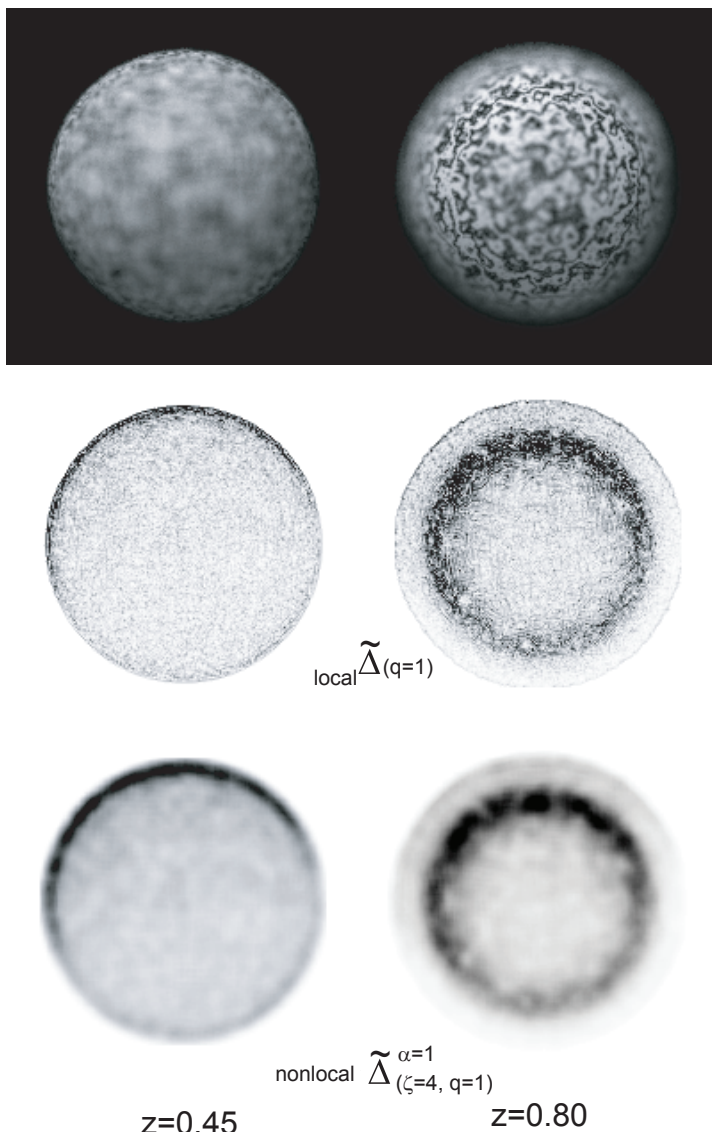


Fig. 9.1 Application of the local and nonlocal modified Laplace-operator to 2 different original slides (left column $z = 0.45$ and right column $z = 0.8$) from a 2D-slide sequence $z \in \{0, 1\}$. From top to bottom original slide, result of local modified Laplacian from (9.24) $\tilde{\Delta}_{\text{local}}(q = 1)$ and result of nonlocal operator (9.29) are shown.

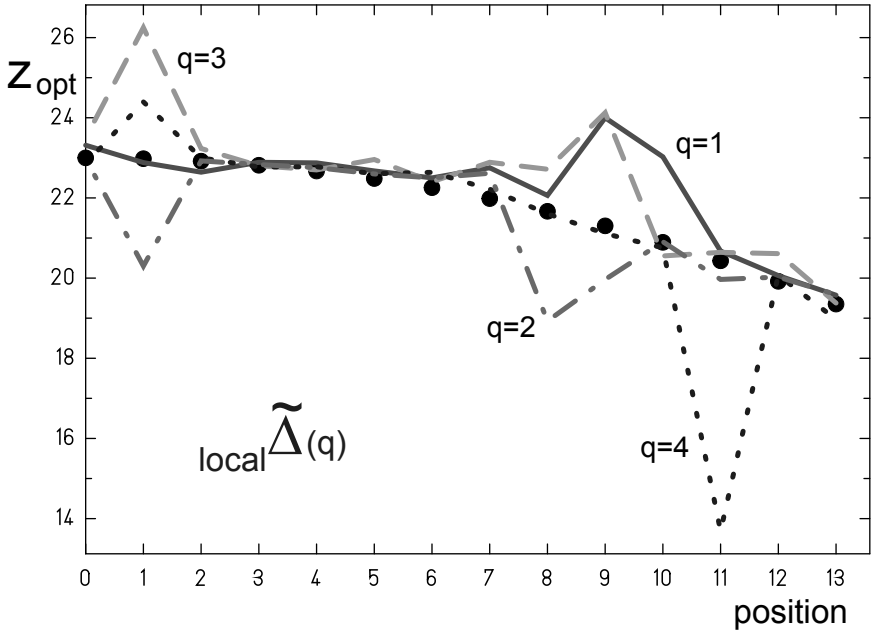


Fig. 9.2 Comparison of recovered positions with original height positions for a set of points along the y-axis. Black circles mark the correct positions, lines represent recovered positions based on the local modified Laplacian ${}_{\text{local}}\tilde{\Delta}(q)$ from (9.24) for different values of step-size q . It should be noted, that there is no fixed value of q , which uniquely may be used to determine all positions. There are drop outs for every curve. Errors are listed in Table 9.1.

Consequently an appropriate operator to determine the high-frequency domains is the modified Laplacian ${}_{\text{local}}\tilde{\Delta}$ given e.g. by:

$$({}_{\text{local}}\tilde{\Delta} f)(x, y) = \left(\left| \frac{\partial^2}{\partial x^2} \right| + \left| \frac{\partial^2}{\partial y^2} \right| \right) f(x, y) \quad (9.22)$$

where \parallel denotes the absolute value.

In the discrete case with a symmetrically discretized function f_{ij} on a rectangular domain $x_{\min} \leq x \leq x_{\max}$ and $y_{\min} \leq y \leq y_{\max}$:

$$f_{ij} = f(x_{\min} + ih, y_{\min} + jh) \quad (9.23)$$

$$i = 0, \dots, i_{\max}, j = 0, \dots, j_{\max}$$

with stepsize h in both x- and y-direction, the same operator is given by:

$$\begin{aligned} ({}_{\text{local}}\tilde{\Delta}(q) f)_{ij} &= \left| \frac{f_{i+q,j} - 2f_{i,j} + f_{i-q,j}}{(qh)^2} \right| + \left| \frac{f_{i,j+q} - 2f_{i,j} + f_{i,j-q}}{(qh)^2} \right| \\ i &= q, \dots, i_{\max} - q, j = q, \dots, j_{\max} - q \end{aligned} \quad (9.24)$$

and 0 elsewhere, where the free parameter q has to be chosen according to the Nyquist-Shannon sampling theorem [Shannon (1949)] to be of order of the inverse average wavelength ω of the texture applied to the object considered

$$qh \approx 2/\omega \quad (9.25)$$

a requirement, which can be fulfilled only locally for random generated textures and for regular textures on curved surfaces respectively.

An application of the modified Laplacian to every slide in a set $\{p_k(z_k)\}$ leads to a set of intensity values $\{\rho_{ij}(q, z_k)\}$ at a given pixel-position at ij :

$$_{\text{local}}\tilde{\Delta}(q)\{p_{ij,k}(z_k)\} = \{\rho_{ij}(q, z_k)\} \quad (9.26)$$

In the second row of figure 9.1 the result of an application of the discrete modified Laplacian with $q = 1$ to the original slides presented in the first row, is demonstrated.

It is assumed, that for a fixed q a maximum exists in $\rho_{ij}(q, z_k)$ for a given \tilde{k} . A parabolic fit of $\{\rho_{ij}(q, z_k)\}$ near \tilde{k} helps to determine the position $_{\text{opt}}z(q)$, where $\rho_{ij}(q, z)$ is maximal:

$$_{\text{opt}}z(q) = \tilde{k} - \frac{1}{2} \frac{\rho_{ij}(q, z_{\tilde{k}+1}) - \rho_{ij}(q, z_{\tilde{k}-1})}{2\rho_{ij}(q, z_{\tilde{k}+1}) - 2\rho_{ij}(q, z_{\tilde{k}}) + \rho_{ij}(q, z_{\tilde{k}-1})} \quad (9.27)$$

In the center row of figure 9.1 we present the result of the application of (9.24) onto the original slides. The gray-level indicates the intensity values $\{\rho_{ij}(q, z_k)\}$ for $z_k = 0.45$ and $z_k = 0.8$ respectively. In figure 9.2 recovered $z_{\text{opt}}(q)$ along the positive y-axis are compared for different q-values with the original height-values.

Obviously there is no unique optimum choice for q , which works for all positions simultaneously. The proposed simple local approach is not very effective, instead it generates drop outs as a result of an interference of varying texture scaling with the fixed step size q . For a realistic treatment of 3D-shape recovery a more sophisticated procedure is necessary.

Consequently a nonlocal approach, which weights the different contributions for a varying step size is a promising and well defined approach. Indeed it will enhance the quality of the results significantly, as will be demonstrated in the next section.

9.3 Shape recovery - the nonlocal approach

The generalized fractional approach extends the above presented local algorithm. The nonlocal modified Laplacian according to (9.15) is given by:

$$\begin{aligned} \text{nonlocal } \tilde{\Delta}^\alpha(q) f(x, y) &= (I^\alpha_{\text{local}} \tilde{\Delta}(q)) f(x, y) \\ &= \frac{1}{2^{a-2} \Gamma(\alpha/2)^2 \sin(a\pi/2)} \\ &\times \int_0^\infty d\xi_1 \int_0^\infty d\xi_2 (\xi_1^2 + \xi_2^2)^{\frac{1}{2}(\alpha-2)} \hat{s}(\xi_1, \xi_2)_{\text{local}} \tilde{\Delta}(q) f(x, y) \end{aligned} \quad (9.28)$$

Therefore we obtain a well defined two step procedure. First, the local operator is applied, followed by the nonlocalization integral.

In the discrete case, applying the nonlocal Laplacian to every slide in a slide set, the first step is therefore identical with (9.26) and yields the same set of intensity values $\{\rho_{ij}(q, z_k)\}$ at a given pixel-position at ij . An application of the discrete version of I^α then leads to:

$$\text{nonlocal } \tilde{\Delta}^\alpha(\zeta, q) p_{ij,k}(z_k) = I^\alpha(\zeta)_{\text{local}} \tilde{\Delta}(q) p_{ij,k}(z_k) \quad (9.29)$$

$$= I^\alpha(\zeta) \rho_{ij}(q, z_k) \quad (9.30)$$

$$\begin{aligned} &= \frac{1}{2^{a-2} \Gamma(\alpha/2)^2 \sin(a\pi/2)} \\ &\times \int_0^\zeta d\xi_1 \int_0^\zeta d\xi_2 (\xi_1^2 + \xi_2^2)^{\frac{1}{2}(\alpha-2)} \hat{s}(\xi_1, \xi_2) \rho_{ij}(q, z_k) \end{aligned} \quad (9.31)$$

$$= \tilde{\rho}_{ij}^\alpha(\zeta, q, z_k) \quad (9.32)$$

where we have introduced a cutoff ζ , which limits the integral on the finite domain of pixel values. If we interpret the intensity values as constant function values at position ij with size h , the integration may be performed fully analytically.

The resulting nonlocal intensities $\tilde{\rho}_{ij}^\alpha(\zeta, q, z_k)$ are presented in the lower row of figure 9.1. The nonlocal approach reduces the granularity of the local operator and a more smooth behavior of intensities results.

Since this is the only modification of the local approach, the recovery of the height information for every pixel is similar to (9.27)

$$\text{opt } z(\alpha, \zeta, q) = \tilde{k} - \frac{1}{2} \frac{\tilde{\rho}_{ij}^\alpha(\zeta, q, z_{\tilde{k}+1}) - \tilde{\rho}_{ij}^\alpha(\zeta, q, z_{\tilde{k}-1})}{\tilde{\rho}_{ij}^\alpha(\zeta, q, z_{\tilde{k}+1}) - 2\tilde{\rho}_{ij}^\alpha(\zeta, q, z_{\tilde{k}}) + \tilde{\rho}_{ij}^\alpha(\zeta, q, z_{\tilde{k}-1})} \quad (9.33)$$

In figure 9.3 results are plotted for different values of α .

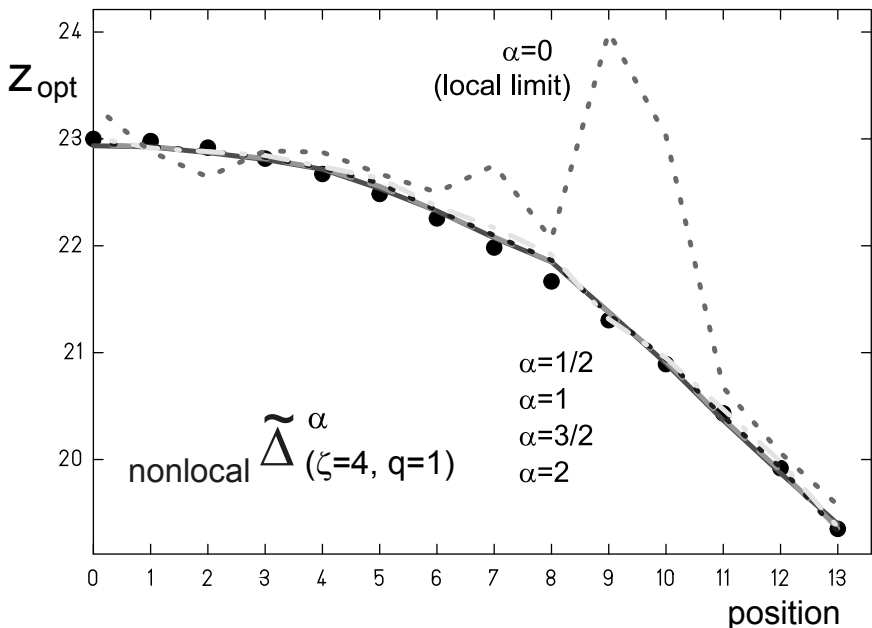


Fig. 9.3 Comparison of recovered positions with original height positions for a set of points along the y -axis. Black circles mark the correct positions, lines represent recovered positions based on the nonlocal modified Laplacian $\tilde{\Delta}^\alpha(\zeta, q)$ from (9.29) for different values of the fractional parameter α . The algorithm is very stable against a variation of α . In the limit $\alpha = 0$ the nonlocal approach reduces to the local scenario. Errors are listed in Table 9.1.

In Table 9.1 a listing of errors is given for the local and the nonlocal algorithm presented.

The discrete version of the nonlocalization operator $I^\alpha(\zeta)$ from (9.29) may be interpreted as a matrix operation $M(\alpha)$ on f_{ij} :

$$I^\alpha(\zeta)f_{ij} = M(\alpha)f_{ij} \quad (9.34)$$

$M(\alpha)$ is a quadratic $(2\zeta+1) \times (2\zeta+1)$ matrix with the symmetry properties

$$M(\alpha)_{i,j} = M(\alpha)_{-i,j} = M(\alpha)_{-i,-j} = M(\alpha)_{i,-j} = M(\alpha)_{j,i} \quad (9.35)$$

$$i, j \leq \zeta$$

Setting the normalization condition $M(\alpha)_{00} = 1$ the integral may be solved analytically for stepwise constant pixel values p_{ij} . As an example,

Table 9.1 Comparison of rms-errors in % for nonlocal modified Laplacian $\tilde{\Delta}^\alpha(\zeta, q = 1)$ from (9.29) for different α to local approach from (9.26) with varying q in the last column.

ζ	$\alpha = 2.0$	$\alpha = 1.5$	$\alpha = 1.0$	$\alpha = 0.5$	$\alpha = 0.0$	q
1	0.277	0.265	0.263	0.405	1.929	1.929
2	0.227	0.225	0.225	0.301	1.929	2.496
3	0.211	0.211	0.216	0.272	1.929	3.702
4	0.182	0.187	0.198	0.251	1.929	2.919
5	0.145	0.151	0.172	0.235	1.929	3.945
6	0.134	0.136	0.158	0.223	1.929	6.131
7	0.137	0.138	0.155	0.215	1.929	2.832
8	0.146	0.143	0.154	0.205	1.929	4.228

we present the fourth quadrant of $M(\alpha)$ for $\zeta = 4$ in units h^2 :

$$M(0) = \begin{pmatrix} 1. & 0. & 0. & 0. & 0. \\ 0. & 0. & 0. & 0. & 0. \\ 0. & 0. & 0. & 0. & 0. \\ 0. & 0. & 0. & 0. & 0. \\ 0. & 0. & 0. & 0. & 0. \end{pmatrix} \quad (9.36)$$

$$M(1/2) = \begin{pmatrix} 1. & 0.116147 & 0.038486 & 0.020685 & 0.013374 \\ 0.116147 & 0.066866 & 0.032440 & 0.019096 & 0.012776 \\ 0.038486 & 0.032440 & 0.022637 & 0.015652 & 0.011301 \\ 0.020685 & 0.019096 & 0.015652 & 0.012237 & 0.009550 \\ 0.013374 & 0.012776 & 0.011301 & 0.009550 & 0.007929 \end{pmatrix} \quad (9.37)$$

$$M(1) = \begin{pmatrix} 1. & 0.294441 & 0.143268 & 0.094982 & 0.071095 \\ 0.294441 & 0.205559 & 0.127951 & 0.090073 & 0.068963 \\ 0.143268 & 0.127951 & 0.100830 & 0.078927 & 0.063559 \\ 0.094982 & 0.090073 & 0.078927 & 0.067014 & 0.056825 \\ 0.071095 & 0.068963 & 0.063559 & 0.056825 & 0.050208 \end{pmatrix} \quad (9.38)$$

$$M(3/2) = \begin{pmatrix} 1. & 0.570351 & 0.400990 & 0.326971 & 0.283027 \\ 0.570351 & 0.478687 & 0.379117 & 0.318443 & 0.278761 \\ 0.400990 & 0.379117 & 0.336822 & 0.298160 & 0.267640 \\ 0.326971 & 0.318443 & 0.298160 & 0.274801 & 0.253092 \\ 0.283027 & 0.278761 & 0.267640 & 0.253092 & 0.237922 \end{pmatrix} \quad (9.39)$$

$$M(2) = \begin{pmatrix} 1. & 1. & 1. & 1. & 1. \\ 1. & 1. & 1. & 1. & 1. \\ 1. & 1. & 1. & 1. & 1. \\ 1. & 1. & 1. & 1. & 1. \\ 1. & 1. & 1. & 1. & 1. \end{pmatrix} \quad (9.40)$$

Obviously there is a smooth transition from a local ($\alpha = 0$) to a more and more nonlocal operation, which in the limiting case ($\alpha = 2$) may be interpreted as the result of the use of a pinhole camera with finite hole radius ζ .

From the presented results we may conclude, that the nonlocal approach is very robust and stable in a wide range of α and ζ values respectively. We gain one order of magnitude in accuracy using the nonlocal modified Laplacian. An additional factor 2 in accuracy is obtained if we chose the optimal fractional $\{\alpha, \zeta\}$ parameter set.

Furthermore we have given an additional direct geometric interpretation of a fractional integral within the framework of image processing as a blur effect.

Exercise 9.1

A geometric interpretation of a generalized nonlocal integral

Problem: We may consider a fractional integral in \mathbb{R}^2 as a blur operator in two dimensions; a subject we have just discussed. We had demonstrated that for increasing α in the limiting case of $\lim \alpha \rightarrow 2$ the Riesz fractional integral may be interpreted physically as a synonym for a pinhole camera with finite more and more increasing circular cut off radius a . Since the camera pinhole is circular, the result of acting to any function $f(x, y)$ is invariant under rotations of the camera objective.

The two-dimensional approach may also be useful for a geometric interpretation of a generalized fractional calculus, where the fractional integral

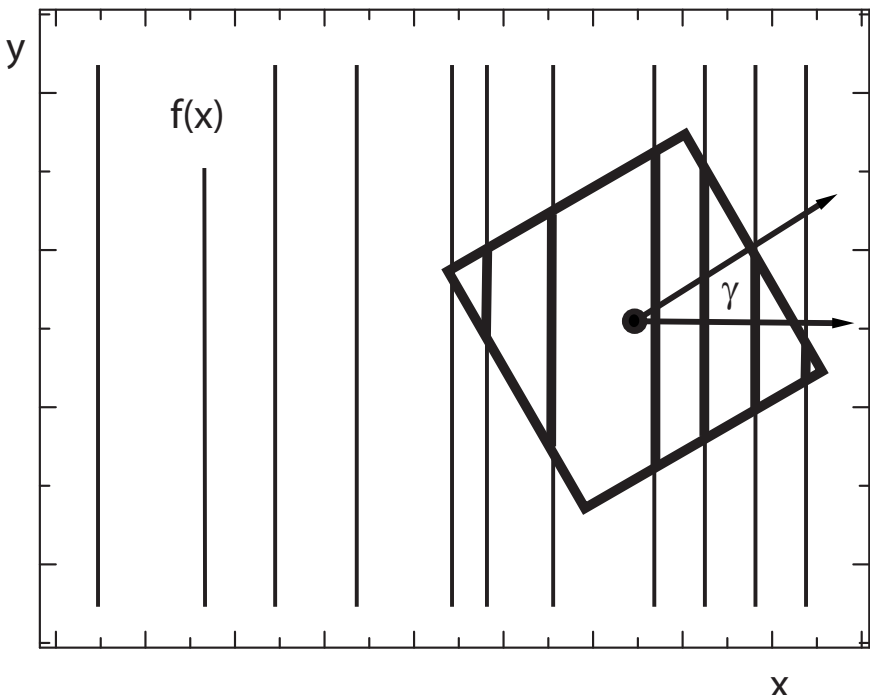


Fig. 9.4 Area of integration for a quadratic pinhole of size a rotated by the angle γ . Vertical lines sketch the contours of a given function $f(x)$. Thick lines indicate the interior of the integration area.

depends on more than one parameter:

$$I^\alpha f(x) \Rightarrow I^{\alpha,\gamma} f(x) \quad (9.41)$$

Typical examples of this class of fractional operators are the Erdélyi-Kober operators (5.108), (5.110).

We choose the pinhole camera as a model for a nonlocal operator (with the simple weight function $w(h) = H(a/2 - |h|)$, $H(x)$ being the Heaviside step function), which has the advantage to be fully analytically solvable. Investigating the case of a pinhole camera with quadratic pinhole shape of size a , introduces an additional parameter γ , which may be interpreted as an rotation angle γ , see figure 9.4.

In this case, such an operator acting on a function $f(x, y)$ has the form

$$\begin{aligned} I(a, \gamma)f(x, y) &= \frac{1}{a^2} \int_{-a/2}^{+a/2} dh_x \int_{-a/2}^{+a/2} dh_y \\ &\times f(x + \cos(\gamma)h_x + \sin(\gamma)h_y, y - \sin(\gamma)h_x + \cos(\gamma)h_y) \end{aligned} \quad (9.42)$$

Acting on a function depending on only one variable $f(x, y) = f(x)$ the integral is simply given by:

$$I(a, \gamma)f(x) = \frac{1}{a^2} \int_{-a/2}^{+a/2} dh_x \int_{-a/2}^{+a/2} dh_y f(x + \cos(\gamma)h_x + \sin(\gamma)h_y) \quad (9.43)$$

indeed may be interpreted as a generalized nonlocal integral depending on an additional parameter γ with a well defined geometric meaning.

Prove that $f(x) = \cos(kx)$ is an eigenfunction of this operator and determine the eigenvalues $\kappa(\alpha, \gamma)$.

Compare the result with the rotationally invariant pinhole camera with circular cutoff R_0 , which is given by:

$$I^0(a)f(x) = \frac{1}{\pi R_0^2} \int_{-R_0}^{+R_0} dh_x \int_{-\sqrt{R_0^2 - h_x^2}}^{+\sqrt{R_0^2 - h_x^2}} dh_y f(x + h_x) \quad (9.44)$$

This page intentionally left blank

Chapter 10

Fractional Calculus in Multidimensional Space — 3D-Folded Potentials in Cluster Physics - a Comparison of Yukawa and Coulomb Potentials with Riesz Fractional Integrals

Convolution integrals of the type

$$F(x) = \int_{-\infty}^{\infty} d\xi f(x - \xi)w(\xi) = \int_{-\infty}^{\infty} d\xi f(\xi)w(x - \xi) \quad (10.1)$$

play a significant role in the areas of signal- and image processing or in the solution of differential equations.

In classical physics the first contact with the 3D-generalization of a convolution integral occurs within the framework of gravitation and electromagnetic theory respectively in terms of a volume integral to determine the potential V of a given charge density distribution ρ :

$$V(\vec{x}) = \int_{R^3} d^3\xi \frac{\rho(\vec{\xi})}{|\vec{x} - \vec{\xi}|} \quad (10.2)$$

where the weight w

$$w(|\vec{x} - \vec{\xi}|) = \frac{1}{|\vec{x} - \vec{\xi}|} \quad (10.3)$$

is interpreted as the gravitational or electromagnetic field of a point charge [Jackson (1998); Kibble and Berkshire (2004)].

In nuclear physics collective phenomena like fission or cluster-radioactivity, where many nucleons are involved, are successfully described introducing the concept of a collective single-particle potential, based on folded potentials of, e.g. Woods-Saxon type. Several weight functions have been investigated in the past.

In order to give a direct physical interpretation of a multi-dimensional fractional integral, we will demonstrate, that the previously presented Riesz-potential which extends the weight function introducing the fractional parameter α

$$w(|\vec{x} - \vec{\xi}|) = \frac{1}{|\vec{x} - \vec{\xi}|^\alpha} \quad (10.4)$$

serves as a serious alternative for commonly used Nilsson- [Nilsson (1955)], Woods-Saxon [Eisenberg and Greiner (1987)] and folded Yukawa potentials [Bolsterli et al. (1972); Möller and Nix (1981)], modeling the single particle potential widely applied in nuclear physics as well as in electronic cluster physics.

Hence we give a direct physical interpretation of a multi-dimensional fractional integral within the framework of fragmentation theory, which is the fundamental tool to describe the dynamic development of clusters in nuclear and atomic physics [Fink et al. (1974); Sandulescu et al. (1976); Maruhn et al. (1980); Depta et al. (1985); Iwamoto and Herrmann (1991); Möller et al. (1993); Greiner et al. (1995); Poenaru et al. (2010a); Knight et al. (1984); Clemenger (1985); Martin et al. (1991); Brack (1993); Engel et al. (1993); Reinhard and Suraud (2004); Chowdhury et al. (2006); Sobczewski and Pomorski (2007); Poenaru and Plonski (2008); Poenaru et al. (2010a)].

10.1 Folded potentials in fragmentation theory

The use of collective models for a description of collective aspects of nuclear motion has proven considerably successful during the past decades.

Calculating life-times of heavy nuclei [Myers and Swiatecki (1966); Grumann et al. (1969); Staszczak et al. (2012)], fission yields [Lustig et al. (1980)], giving insight into phenomena like cluster-radioactivity [Poenaru and Greiner (2010b)], bimodal fission [Hulet et al. (1986); Herrmann et al. (1988)] or modeling the ground state properties of triaxial nuclei [Möller et al. (2008)] - remarkable results have been achieved by introducing an appropriate set of collective coordinates, like length, deformation, neck or mass-asymmetry [Maruhn and Greiner (1972)] for a given nuclear shape and investigating its dynamic properties.

As an example, in figure 10.1 the parametrization of the 3-sphere model is sketched. It determines the geometry of a given cluster shape by two intersecting spheres, which are smoothly connected via a third sphere, which models a neck depending on the size of the radius r_3 .

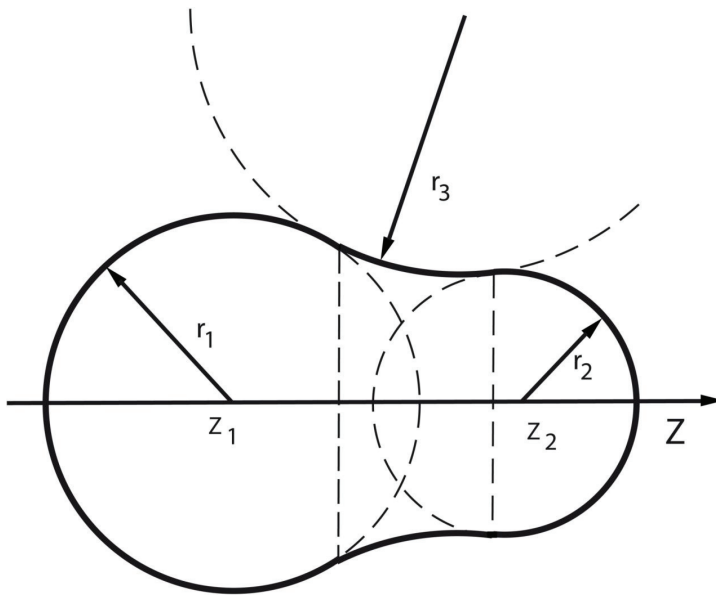


Fig. 10.1 The parametrization of the 3-sphere model.

The corresponding set of collective coordinates $\{q^i, i = 1, \dots, 4\}$ is given by [Deptà *et al.* (1990)]:

the two center distance	$\Delta z = z_2 - z_1$
the mass asymmetry	$\eta_A = (A_1 - A_2)/(A_1 + A_2)$
the charge asymmetry	$\eta_Z = (Z_1 - Z_2)/(Z_1 + Z_2)$
the neck	$c_3 = 1/r_3$

where A_1, Z_1 and A_2, Z_2 are the number of nucleons and protons in the two daughter nuclei.

This choice of collective coordinates allows to describe a wide range of nuclear shapes involved in collective phenomena from a generalized point of view [Herrmann *et al.* (1986)], e.g. a simultaneous description is made possible of general fission properties and the cluster-radioactive decay of radium



which was predicted by Sandulescu, Poenaru and Greiner and later experimentally verified by Rose and Jones [Sandulescu *et al.* (1980); Rose and Jones (1984)].

In order to describe the properties and dynamics of such a process, we start with the classical collective Hamiltonian function

$$H_{\text{coll}} = T_{\text{coll}} + V_{\text{coll}} \quad (10.6)$$

introducing a collective potential V_{coll} (see e.g. figure 8.2), depending on the collective coordinates,

$$V_{\text{coll}}(q^i) = E_{\text{macro}}(q^i) + E_{\text{mic}}(q^i) \quad (10.7)$$

with a macroscopic contribution E_{macro} based on e.g. the liquid drop model and a microscopic contribution E_{mic} , which mainly contains the shell and pairing energy based on a single particle potential $V_{s.p.}$ and the classical kinetic energy T_{coll}

$$T_{\text{coll}} = \frac{1}{2} B_{ij}(q^i) \dot{q}^i \dot{q}^j \quad (10.8)$$

with collective mass parameters B_{ij} .

There are several common methods to generate the collective mass parameters B_{ij} , e.g. the cranking model [Inglis (1954); Schneider *et al.* (1986)] or irrotational flow models [Werner and Wheeler (1958); Kelson (1964); Wu *et al.* (1985)] are used.

Quantization of the classical Hamiltonian [Podolsky (1928); Pauli (1933)] results in the collective Schrödinger equation

$$\hat{S}_{\text{coll}} \Psi(q^i, t) = \left(-\frac{\hbar^2}{2} \frac{1}{\sqrt{B}} \partial_i B^{ij} \sqrt{B} \partial_j - i\hbar \partial_t + V_{\text{coll}} \right) \Psi(q^i, t) = 0 \quad (10.9)$$

with $B = \det B_{ij}$ is the determinant of the mass tensor. This is the central starting point for a discussion of nuclear collective phenomena.

For a specific realization of the single particle potential $V_{s.p.}$, for protons and neutrons respectively a Woods-Saxon type potential may be used. The advantages of such a potential are a finite potential depth and a given surface thickness. Furthermore arbitrary geometric shapes may be treated similarly by a folding procedure, which yields smooth potential values for such shapes.

For the 3-sphere model, in order to define a corresponding potential, a Yukawa-function is folded with a given volume V , which is uniquely determined within the model:

$$V_Y(\vec{r}) = -\frac{V_0}{4\pi a^3} \int_V d^3 r' \frac{\exp^{-|\vec{r}-\vec{r}'|/a}}{|\vec{r}-\vec{r}'|/a} \quad (10.10)$$

with the parameters potential depth V_0 and surface thickness a .

For protons, in addition the Coulomb-potential has to be considered, which is given for a constant density ρ_0

$$V_C(\vec{r}) = \frac{\rho_0}{a} \int_V d^3 r' \frac{1}{|\vec{r} - \vec{r}'|/a} \quad (10.11)$$

where the charge density is given by

$$\rho_0 = \frac{Ze}{\frac{4}{3}\pi R_0^3} \quad (10.12)$$

Both potentials may be written as general convolutions in R^3 of type:

$$V_{\text{type}}(\vec{r}) = C_{\text{type}} \int_{R^3} d^3 r' \rho(\vec{r}') w_{\text{type}}(|\vec{r} - \vec{r}'|) \quad (10.13)$$

with the weights

$$w_Y(d) = \frac{\exp^{-d/a}}{d/a} \quad (10.14)$$

$$w_C(d) = \frac{1}{d/a} \quad (10.15)$$

where d is a measure of distance on R^3 and a density, which is constant inside the nucleus

$$\rho(\vec{r}) = \begin{cases} \rho_0 & \vec{r} \text{ inside the nucleus} \\ 0 & \vec{r} \text{ outside the nucleus} \end{cases} \quad (10.16)$$

Therefore the single particle potential $V_{s.p.}$ is given by

$$V_{s.p.} = V_Y + (\frac{1}{2} + t_3)V_C + \kappa \vec{\sigma}(\nabla V_Y \times \vec{p}) \quad (10.17)$$

with t_3 is the eigenvalue of the isospin operator with $+\frac{1}{2}$ for protons and $-\frac{1}{2}$ for neutrons, which guarantees that the Coulomb potential V_C only acts on protons. The last term is the spin-orbit term with the Pauli-matrices $\vec{\sigma}$, \vec{p} is the momentum operator and the strength is parametrized with κ . This term is necessary to split up the degeneracy of energy levels with different angular momentum and to generate the experimentally observed magic shell closures [Elsasser (1933); Goeppert-Mayer (1948)].

In the original Nilsson oscillator potential an additional \vec{l}^2 term was necessary to lower the higher angular momentum levels in agreement with experiment. For Woods-Saxon type potentials such a term is not necessary. Whether Riesz potentials are a realistic alternative, will be investigated in the next section.

The solutions of the single particle Schrödinger equation with the potential $V_{s.p.}$ yield the single particle energy levels, which are used to calculate the microscopic part of the total potential energy and contains two major parts, the shell and pairing corrections.

$$E_{\text{mic}}(q^i) = E_{\text{shell}}(q^i) + E_{\text{pair}}(q^i) \quad (10.18)$$

10.2 The Riesz potential as smooth transition between Coulomb and folded Yukawa potential

Let us reinterpret the Riesz potential

$$V_{RZ}(\vec{r}) = C_{RZ} \int_{R^3} d^3 r' \rho(\vec{r}') w_{RZ}(|\vec{r} - \vec{r}'|) \quad (10.19)$$

with the weight

$$w_{RZ}(d) = \frac{1}{(d/a)^\alpha} \quad 0 \leq \alpha < 3 \quad (10.20)$$

as the 3D-version of Riesz integral (5.55) applied to a scalar function $\rho(\vec{r})$, where the Riesz integral is given as a symmetric superposition of the right- (${}_+ I_+^\alpha$) and left (${}_- I_-^\alpha$) Liouville integrals (5.55):

$${}_{RZ} I^\alpha f(x) = \frac{{}_+ I_+^\alpha + {}_- I_-^\alpha}{2 \cos(\pi\alpha/2)} f(x) \quad (10.21)$$

$$\begin{aligned} &= \frac{1}{2 \cos(\pi\alpha/2)} \left(\frac{1}{\Gamma(\alpha)} \int_x^{+\infty} (\xi - x)^{\alpha-1} f(\xi) d\xi \right. \\ &\quad \left. + \frac{1}{\Gamma(\alpha)} \int_{-\infty}^x (x - \xi)^{\alpha-1} f(\xi) d\xi \right) \end{aligned} \quad (10.22)$$

$$= \frac{1}{2\Gamma(\alpha) \cos(\pi\alpha/2)} \int_{-\infty}^{+\infty} |x - \xi|^{\alpha-1} f(\xi) d\xi, \quad (10.23)$$

$$0 < \alpha < 1$$

and with the fractional parameter $\alpha \in \mathbb{R}$, which allows for a smooth transition between $0 < \alpha < 3$, as a consequence we may treat and interpret the Coulomb ($\alpha = 1$), Riesz- and Yukawa potentials similarly from a generalized point of view.

In the following we will investigate the behavior of the Riesz potential with varying α , and compare its properties with the cases of Coulomb and Yukawa weight functions. In a way, the parameter α in the Riesz potential may be interpreted as a global screening of the Coulomb weight, such that the effect of the Yukawa exponential is partly modeled.

$$w_C(d) = \frac{1}{d/a} \quad (10.24)$$

$$w_{RZ}(d) = \frac{1}{(d/a)^{\alpha-1}} \frac{1}{d/a} \quad (10.25)$$

$$w_Y(d) = \exp^{-d/a} \frac{1}{d/a} \quad (10.26)$$

Therefore the Riesz potential could be an interesting alternative to the Yukawa potential in the case $\alpha \gg 1$. In a way, we expect the screening properties of the Riesz potential for increasing α to result in an interpolation between Coulomb and Yukawa limit.

Hence the fragmentation potentials used in a dynamic description of fission or cluster emission processes are an ideal framework to discuss and understand the properties of the Riesz integral.

The integral (10.13) with the weights (10.24)-(10.26) may be evaluated analytically for a spherical nucleus with radius R_0 and uniform density

$$\rho(r) = \rho_0 H(R_0 - r) \quad (10.27)$$

with the Heaviside step function H .

In this case we have, using spherical coordinates $\{r, \theta, \phi\}$:

$$V_{\text{type}}^{\text{sphere}}(r) = C_{\text{type}} \rho_0 \int_0^{R_0} r'^2 dr' \int_0^\pi \sin(\theta') d\theta' \int_0^{2\pi} d\phi' w_{\text{type}}(|\vec{r} - \vec{r}'|) \quad (10.28)$$

with

$$|\vec{r} - \vec{r}'| = \sqrt{r^2 + r'^2 - 2rr' \cos(\theta')} \quad (10.29)$$

With the substitution u

$$u = \sqrt{r^2 + r'^2 - 2rr' \cos(\theta')} \quad (10.30)$$

we end up with a double integral for spherical shapes:

$$V_{\text{type}}^{\text{sphere}}(r) = 2\pi C_{\text{type}} \rho_0 \int_0^{R_0} dr' r'/r \int_{\sqrt{(r-r')^2}}^{\sqrt{(r+r')^2}} du u w_{\text{type}}(u) \quad (10.31)$$

$$= 2\pi \rho_0 \frac{C_{\text{type}}}{r} \int_0^{R_0} dr' r' \int_{|r-r'|}^{r+r'} du u w_{\text{type}}(u) \quad (10.32)$$

This integral is valid for any analytic weight $w(u)$ and may be easily solved for the Coulomb, Riesz and Yukawa weight functions. We obtain:

$$V_C^{\text{sphere}}(r) = aC_C \begin{cases} \frac{Ze}{R_0} \left(\frac{3}{2} - \frac{r^2}{2R_0^2} \right) & r \leq R_0 \\ \frac{Ze}{r} & r \geq R_0 \end{cases} \quad (10.33)$$

$$V_{\text{RZ}}^{\text{sphere}}(r) = a^\alpha C_{\text{RZ}} \frac{2\pi}{(\alpha-2)(\alpha-3)(\alpha-4)} \frac{1}{r} \times \begin{cases} (r+R_0)^{3-\alpha}(r-(3-\alpha)R_0) + \\ (R_0-r)^{3-\alpha}(r+(3-\alpha)R_0) & r \leq R_0 \\ (r+R_0)^{3-\alpha}(r-(3-\alpha)R_0) - \\ (r-R_0)^{3-\alpha}(r+(3-\alpha)R_0) & r \geq R_0 \end{cases} \quad (10.34)$$

$$V_Y^{\text{sphere}}(r) = 4\pi a^3 C_Y \times \begin{cases} \left(1 - \left(1 + \frac{R_0}{a} \right) e^{-R_0/a} \frac{\sinh(r/a)}{r/a} \right) & r \leq R_0 \\ \frac{e^{-r/a}}{r/a} \left(\frac{R_0}{a} \cosh\left(\frac{R_0}{a}\right) - \sinh\left(\frac{R_0}{a}\right) \right) & r \geq R_0 \end{cases} \quad (10.35)$$

In figure 10.2 a sequence of these potentials is plotted for a spherical nucleus, ranging from Coulomb ($\alpha = 1.00$) and Riesz potential with increasing α up to the Yukawa potential with parameter settings according to [Bolsterli *et al.* (1972)].

For large $\alpha > 2.00$ the Riesz potential as well as the Yukawa potential model a finite surface thickness. where in the limiting case $\alpha \rightarrow 3$ the surface thickness vanishes and according to (10.34) we obtain

$$\lim_{\alpha \rightarrow 3} V_{\text{RZ}}^{\text{sphere}}(r) \sim \rho(r) = \begin{cases} \text{const} & r \leq R_0 \\ 0 & r > R_0 \end{cases} \quad (10.36)$$

A remarkable difference between both potentials follows for small z . In this area, the Yukawa potential models a more Woods-Saxon type potential, while the Riesz potential may be compared with an harmonic oscillator potential. But this behavior is restricted only to the lowest energy levels; for realistic calculations the energy region near the Fermi-level is much more relevant. In this region, both potential types show a similar behavior for $2.00 < \alpha < 2.50$.

Nevertheless, both potentials seem interesting candidates for generation of realistic single particle energy levels.

For cylinder symmetric configurations the integral (10.13) cannot be solved analytically. Instead we switch to cylinder coordinates $\{\rho, z, \phi\}$. With the distance

$$d_{\text{cyl}} = \sqrt{\rho^2 + \rho'^2 - 2\rho\rho' \cos(\phi') + (z-z')^2} \quad (10.37)$$

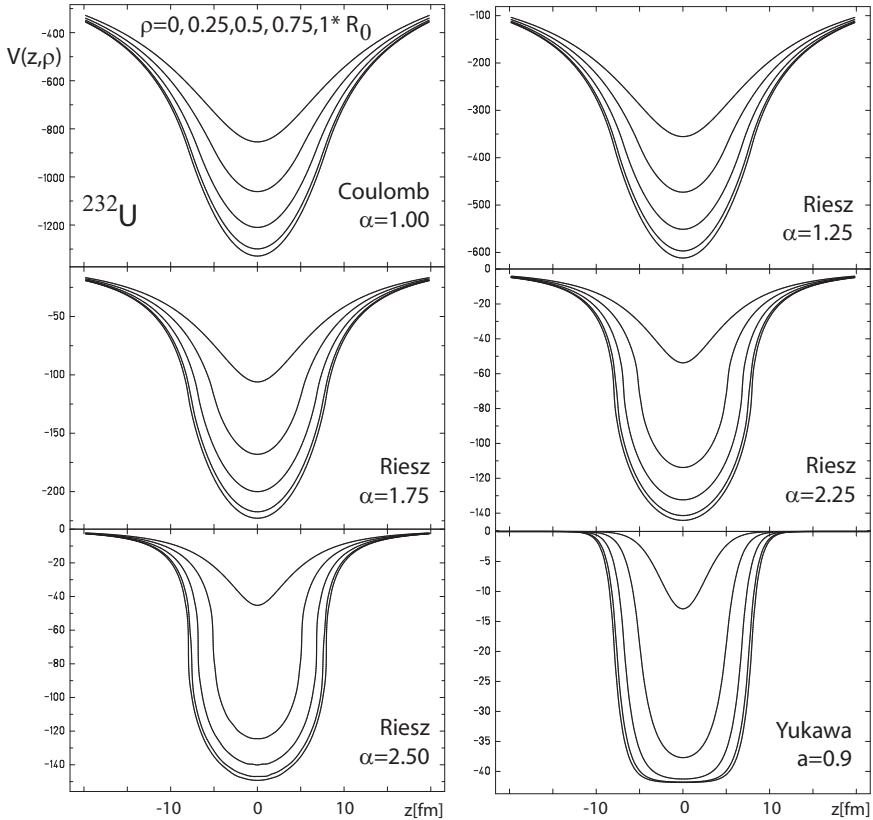


Fig. 10.2 For a spherical assumed shape (here ^{232}U) the potential for different weight functions is drawn. From top to bottom: Coulomb ($\alpha = 1.00$), Riesz ($\alpha = 1.25, 1.75, 2.25, 2.50$) and Yukawa (with $a = 0.9[\text{fm}]$ weight). In order to compare the plots with cylinder symmetric shapes, the potential curves are drawn in cylinder coordinates (z, ρ) for a sequence of $\rho = 0.00, 0.25, 0.50, 0.75, 1.00 \times R_0$. $R_0(^{232}\text{U}) = 8.26[\text{fm}]$.

we have to solve the integral

$$V_{\text{type}}(\rho, z) = C_{\text{type}} \int_V d\rho' \rho' dz' d\phi' \rho(\rho', z') w_{\text{type}}(d_{\text{cyl}}) \quad (10.38)$$

numerically.

In figure 10.3 we have solved (10.38) and compare the three different weights for the strong asymmetric cluster decay



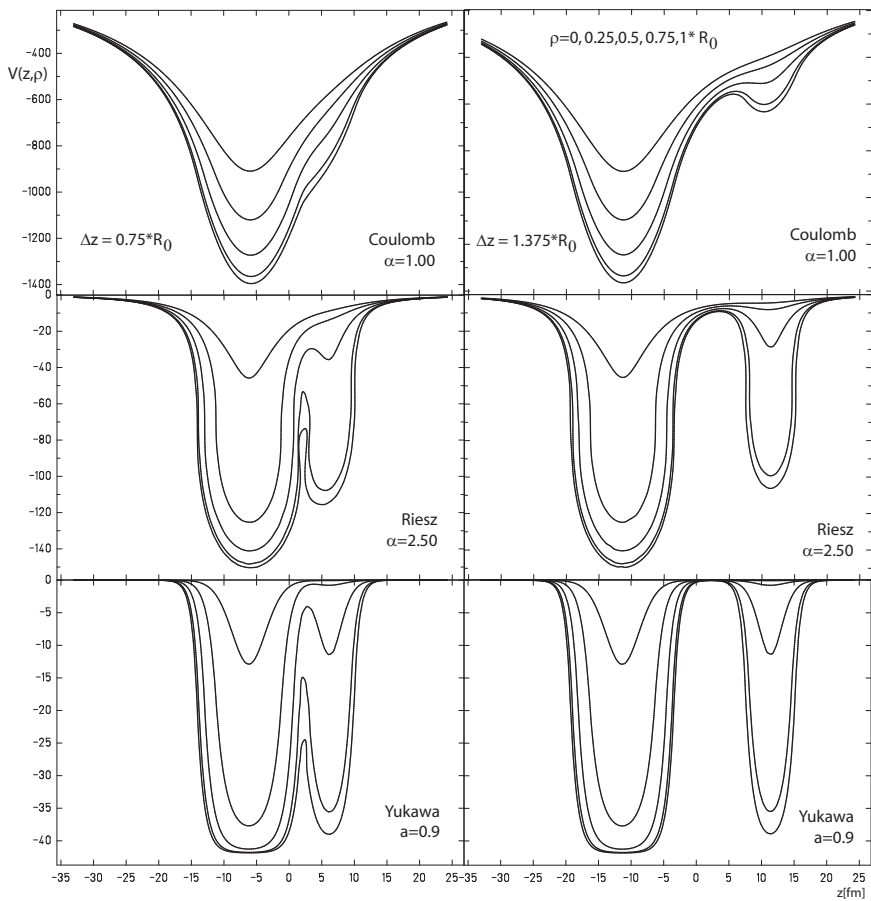


Fig. 10.3 For the configuration $^{232}\text{U} \rightarrow ^{208}\text{Pb} + ^{24}\text{Ne}$ the Coulomb, Riesz ($\alpha = 2.50$) and Yukawa ($a = 0.9[\text{fm}]$) potential is plotted for $\Delta z = 0.75R_0$ (left column) and $\Delta z = 1.375R_0$ (right column). $R_0(^{232}\text{U}) = 8.26[\text{fm}]$.

The Riesz potential allows for a smooth transition between the Coulomb case and the Yukawa limit by varying α . Hence we obtain a direct geometric interpretation of the fractional parameter α .

Up to now, we discussed the properties of the single particle potential, which is the starting point for a calculation of the microscopic part of the collective potential.

The self energy of a given configuration contributes to the macroscopic part of the nuclear potential as the Coulomb- and surface or more sophisti-

cated Yukawa energy term in a macroscopic energy formula, historically first used in Weizsäcker's famous liquid drop mass formula [Weizsäcker (1935)]:

$$E_{\text{macro}} = a_v A + a_s A^{2/3} - a_c Z A^{-1/3} + a_{\text{sym}} (N - Z) A^{-1} + a_{\text{pair}} A^{-1/2} \quad (10.40)$$

as a function of the nucleon number $A = r_0 R_0^3$ containing a volume, surface, Coulomb, symmetry and pairing term.

The self energy for a given charge type E_{type} is defined as the volume integral over the potential restricted on the volume of a given shape

$$E_{\text{type}}(\vec{r}) = \frac{1}{2} C_{\text{type}} \int_V d^3 r \rho(\vec{r}) \int_{R^3} d^3 r' \rho(\vec{r}') w_{\text{type}}(|\vec{r} - \vec{r}'|) \quad (10.41)$$

or

$$E_{\text{type}}(\vec{r}) = \frac{1}{2} C_{\text{type}} \int_V \int_{V'} d^3 r d^3 r' \rho(\vec{r}) \rho(\vec{r}') w_{\text{type}}(|\vec{r} - \vec{r}'|) \quad (10.42)$$

For the three different weights (10.24)-(10.26) we obtain for the simplest case of a sphere with radius R_0 and unit charge ($Z e = 1$) and a surface thickness $a > 0$:

$$E_C = \frac{3}{5} \frac{a}{R_0} \quad (10.43)$$

$$E_{RZ} = \frac{9 \times 2^{2-\alpha}}{(3-\alpha)(4-\alpha)(6-\alpha)} \left(\frac{a}{R_0} \right)^\alpha \quad 0 \leq \alpha < 3 \quad (10.44)$$

$$E_Y = \frac{3}{4} (3 - 3(R_0/a)^2 + 2(R_0/a)^3 - 3e^{-2R_0/a} (1 + (R_0/a))^2) \left(\frac{a}{R_0} \right)^6 \quad (10.45)$$

We obtain the important result that the Riesz self energy behaves like

$$E_{RZ} \sim \frac{1}{R_0^\alpha} \quad (10.46)$$

which scales with the nucleon number $A \sim R_0^3$ as

$$E_{RZ} \sim A^{-\alpha/3} \quad (10.47)$$

and therefore allows us to model the influence of a screened Coulomb like charge contribution to the total energy.

In figure 10.4 we compare the R_0 dependence for the 3 different types of self energy. Depending on the size of the spherical nucleus e.g. $R_0(^{208}\text{Pb}) = 7.25[\text{fm}]$ the behavior of the Yukawa self energy is covered by the Riesz self energy for α within the range $2 \leq \alpha \leq 2.5$ and therefore the Riesz self energy covers the full range of relevant categories.

In addition it should be mentioned, that for the case $\alpha = 3/2$ the Riesz self energy behaves like $A^{-1/2}$ which emulates the pairing term and

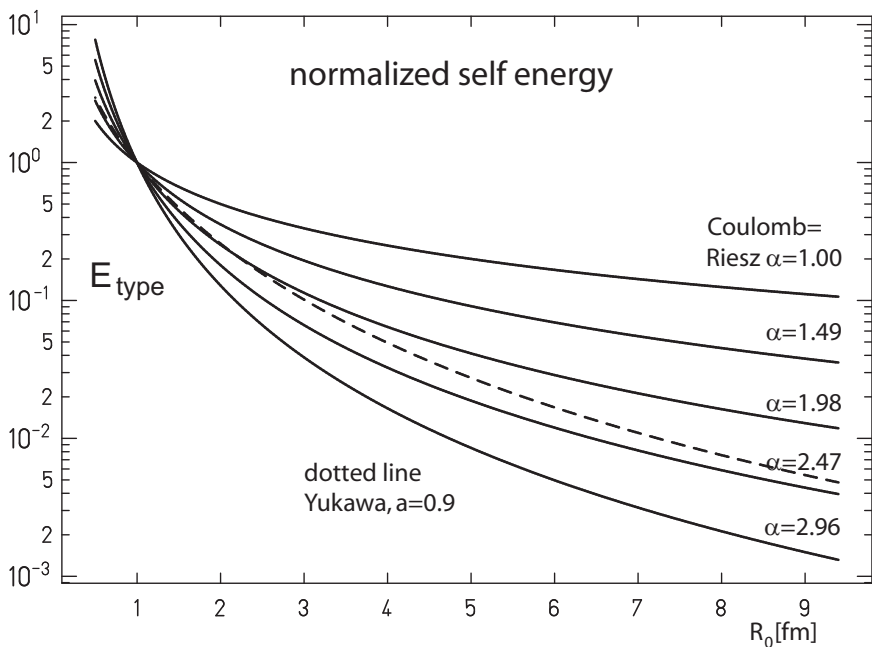


Fig. 10.4 For a spherical shape the self energy as a function of the sphere radius R_0 [fm] is plotted for the Coulomb, the Riesz ($\alpha = 1.49, 1.98, 2.47, 2.96$) and the Yukawa ($a = 0.9$ [fm]) weight. To compare all different types, all energies are normalized to $E_{\text{type}}(R_0 = 1) = 1$. Depending on R_0 , the Yukawa self energy lies is covered by the Riesz self energy within a range of $2.0 \leq \alpha \leq 2.5$ values.

for $\alpha = 3$ the Riesz self energy behaves like A^{-1} which is equivalent to the behavior of the proton-neutron symmetry term in the Weizsäcker mass formula.

Therefore the macroscopic pairing-, symmetry- and Coulomb contributions to the total energy content of a nucleus may be treated from a generalized view as different realizations of the same Riesz potential and are all determined in the same way for a given shape.

As a consequence, there is a one to one correspondence between a given change in the shape geometry and the dynamic behavior of these energy contributions. On the other hand, the hitherto abstract fractional coefficient α now may be interpreted within the context of cluster physics as a smooth order parameter with a well defined physical meaning for distinct α values.

The combination of concepts and methods developed in different branches of physics, here demonstrated for the case of fractional calculus and cluster physics, has always led to new insights and improvements. As an additional step based on this concept, which marks a possible direction for future research, we may emphasize the convolution aspect of the Riesz integral, which may be interpreted within the framework of linear system theory, leading to new insights in large amplitude collective motion.

From all these presented results we may draw the conclusion, that the Riesz potential may be considered as a promising alternative approach to folded potentials, which are widely used to describe nuclear dynamics within the framework of a collective shell model.

Of course, these potentials are only an alternative starting point to calculate fragmentation potentials based on a fractional integral definition. In the next chapters we will present other powerful alternative methods to calculate single particle spectra based on fractional group theoretical methods.

Therefore we gave one more physical interpretation of the fractional parameter α in R^3 as a surface thickness of a homogeneous cluster shape. In the geometric picture, presented in the last chapter, we interpreted a fractional integral as a blurring procedure for a pixel in a 2D picture, it now becomes the blur of an at first sharp voxel in 3D, which could also be interpreted as the time average of the position of a particle in a heat bath.

We also conclude, that nonlocality is a common phenomenon in cluster physics and widely accepted, even though it is not explicitly stated. While for electromagnetic and gravitational fields, nonlocality is mostly interpreted as the outcome of an effective interaction, in nuclear physics the same phenomenon becomes very fundamental and therefore a description of properties of nuclear or more general hadronic matter and strongly interacting particles respectively in terms of fractional calculus methods could be a promising alternative approach, as we will point out in the following chapters.

10.3 Discussion

10.3.1 Calculation of a fission yield

question:

How to calculate a fission yield and what is it's connection with the collective potential $V(q^i)$?

answer:

The fission yield is defined as the number of fission fragments for a given mass asymmetry with respect to the total of fission products for a given reaction and is given in %. In fragmentation theory, the starting point to calculate the fission yield is the classical total energy of the fissioning system.

The classical total energy of the nuclear system is dominated by two degrees of freedom, the two center distance Δz and the mass-asymmetry

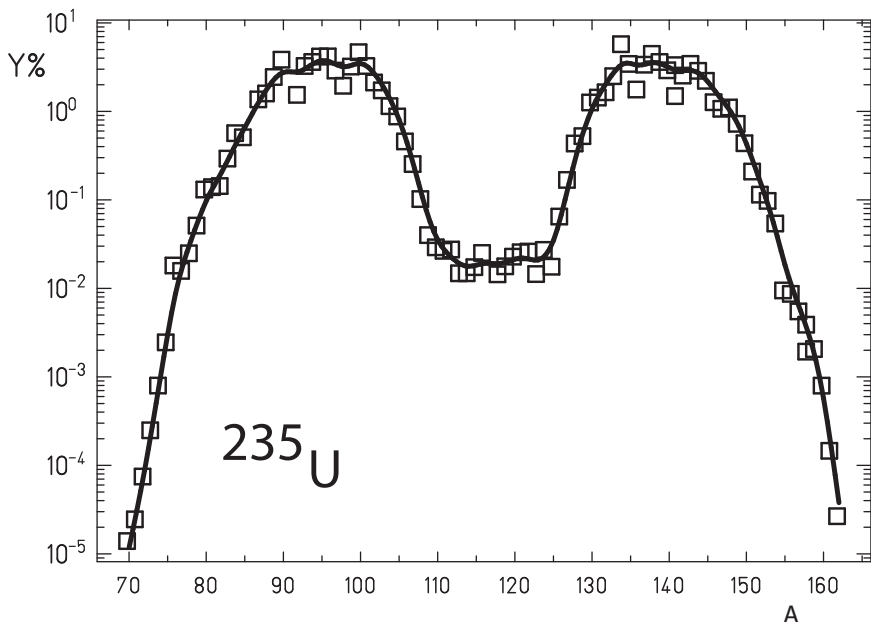


Fig. 10.5 The first systematic study of the distribution of fission fragments as a function of mass number of the daughter nuclei was performed for ^{235}U within the Plutonium project [Plutonium Project (1946)] and since then has been steadily improved until today. Squares indicate the experimental values [England and Rider (1994)], thick line represents a fit.

η_A and is given by:

$$H(\Delta z, \eta_A) = \frac{1}{2}B_{\Delta z \Delta z}\Delta \dot{z}^2 + B_{\Delta z \eta_A}\Delta \dot{z}\dot{\eta}_A + \frac{1}{2}B_{\eta_A \eta_A}\dot{\eta}_A^2 + V(\Delta z, \eta_A) \quad (10.48)$$

The collective mass parameters B_{ij} may be calculated using the cranking-formula in the BCS formalism [Inglis (1954); Belyaev (1959); Schneider *et al.* (1986)]:

$$B_{ij} = 2\hbar^2 \sum_{\mu, \nu} \frac{\langle \nu | \partial_i | \mu \rangle \langle \mu | \partial_j | \nu \rangle}{\tilde{\epsilon}_\mu + \tilde{\epsilon}_\nu} (u_\nu v_\mu + v_\nu u_\mu)^2 + \hbar^2 \sum_\nu \frac{1}{v_\nu^2 \epsilon_\nu} (\partial_i u_\nu)(\partial_j u_\nu) \quad (10.49)$$

where $v_\nu^2 = 1 - u_\nu^2$ is the BCS occupation probability of the ν -th single particle level and $\tilde{\epsilon}_\nu = \sqrt{(\epsilon_\nu - \lambda)^2 + \Delta^2}$ is the quasi-particle energy, depending on the Fermi energy λ and the gap-parameter Δ .

From practical calculations follows that the mixing mass is small:

$$B_{\Delta z \eta_A} \ll B_{\Delta z \Delta z} B_{\eta_A \eta_A} \quad (10.50)$$

During the fission process, in a first step the nucleus will tunnel through the fission barrier (see figure 8.1 for a schematic picture of the fission potential $V(\Delta z)$ in Δz -direction). For a given elongation Δz_0 the tunneling process is finished and the kinetic energy is positive once again.

At that time, the velocity $\Delta \dot{z}$ is small and therefore Δz may be treated as a parameter. With this assumption and ignoring the the mixing mass $B_{\Delta z \eta_A}$ the total energy reduces to:

$$H(\eta_A; \Delta z_0) = \frac{1}{2}B_{\eta_A \eta_A}\dot{\eta}_A^2 + V(\eta_A; \Delta z_0) \quad (10.51)$$

This classical Hamiltonian is quantized according to the prescription of Pauli [Pauli (1933)] and Podolsky [Podolsky (1928)] and leads to a one dimensional collective Schrödinger equation:

$$\left(-\frac{\hbar^2}{2} \frac{1}{\sqrt{B}} \partial_{\eta_A} \frac{1}{\sqrt{B}} \partial_{\eta_A} + V(\eta_A; \Delta z_0) \right) \Psi_{\Delta z_0}^n = E_{\Delta z_0}^n \Psi_{\Delta z_0}^n \quad (10.52)$$

where B is a short-hand notation for $B_{\eta_A \eta_A}(\eta_A; \Delta z_0)$.

The eigenfunctions for a given elongation Δz_0 are normalized to

$$\int_{-1}^{+1} \Psi_{\Delta z_0}^{m*} \Psi_{\Delta z_0}^n \sqrt{B} d\eta_A = \delta_{mn} \quad (10.53)$$

If we consider spontaneous fission as a completely adiabatic process with no internal excitations, only the ground state ($n = 0$) should be occupied and the yield, normalized to 200% simply results as:

$$Y(A) = |\Psi_{\Delta z_0}^0|^2 \sqrt{B} \frac{400}{A_0} \quad (10.54)$$

where A_0 is the mass of the fissioning nucleus.

In case of neutron induced fission the system fissions from an excited state. There may also be a coupling between elongation and mass-asymmetry which introduces some heat into the system. As a consequence, we introduce a nuclear temperature T , which is connected with the system's excitation energy E^* via:

$$E^* = \frac{T^2}{10\text{MeV}} A_0 \quad (10.55)$$

Assuming a Boltzmann distribution of the occupation probability on the vibrational states n the yield results as:

$$Y(A) = \frac{\sum_{n=0}^{\infty} |\Psi_{\Delta z_0}^n|^2 e^{-E^n/T} \sqrt{B} \frac{400}{A_0}}{\sum_{n=0}^{\infty} e^{-E^n/T}} \quad (10.56)$$

In figures 10.6 and 10.7 we have sketched a typical fission potential $V(\eta_A)$ and inserted the calculated eigenvalues. The corresponding solutions are listed in clockwise direction. For a temperature of $T = 1[\text{MeV}]$ the logarithm of the fission yield is plotted.

The minima in the potential result from the microscopic shell- and pairing contributions to the total energy and mark energetically favored daughter nuclei combinations. These correspond to closed shells in the nuclei at magic neutron and proton numbers respectively; an observation, first published by Goeppert-Mayer [Goeppert-Mayer (1948)]. These minima correspond directly to the maxima in the fission yield.

Therefore within the framework of fragmentation theory the full variety of different fission phenomena may be understood and calculated quantitatively. The question arises, if collective phenomena like fission may also be described using alternative methods. In case of high excitation energies methods developed in the area of statistical mechanics may be useful.

Let us consider fission as an aspect of collective motion of a multi-particle system, where its constituents obey the laws of classical mechanics. One point in collective phase space is then characterized giving a set of collective parameters, which determines a specific nuclear shape and its conjugated momenta.

Instead of investigating the dynamical development of every possible classical trajectory in this space and extracting interesting properties by a time dependent averaging, we will consider the change of a statistical distribution function f directly.

In the one dimensional case, the time development of the distribution function $f(q, v, t)$ on a phase space, spanned by the collective coordinate

q and the velocity v is described by the Fokker-Planck-equation [Nix *et al.* (1984)]:

$$\partial_t f = -v \partial_q f + \frac{1}{m} (\partial_q V)(\partial_v f) + \frac{\eta}{m} \partial_v(vf) + \frac{\eta T}{m^2} \partial_v^2 f \quad (10.57)$$

where we have introduced a constant collective mass m , a constant dissipation coefficient η and a constant nuclear temperature T , which is assumed high enough to justify the statistical approach.

The first two terms in (10.57) are the well known Poisson-bracket:

$$\{f, H\} = v \partial_q f - \frac{1}{m} (\partial_q V)(\partial_v f) \quad (10.58)$$

with

$$H = \frac{1}{2} v^2 + V(q) \quad (10.59)$$

and the last two terms may be interpreted as damping term or in terms of a Boltzmann equation as a collective collision term.

For stationary, momentum independent solutions a set of simplifications results: First we integrate the Fokker-Planck equation over all velocities and obtain a continuity equation

$$\partial_t \bar{f}(q, t) + \nabla j(q, t) = 0 \quad (10.60)$$

with a current j and

$$\bar{f}(q, t) = \int f(q, v, t) dv \quad (10.61)$$

$$j(q, t) = \int vf(q, v, t) dv \quad (10.62)$$

In the stationary case it follows immediately

$$\partial_q j(q) = 0 \quad (10.63)$$

As long as the current j vanishes at the boundaries of integration, we set an ansatz for a solution of the stationary Fokker-Planck equation

$$f(q, v, t) = \frac{1}{N} e^{-H/T} \quad (10.64)$$

and obtain for the stationary distribution function

$$\bar{f}(q) = \frac{1}{N'} e^{-V(q)/T} \quad (10.65)$$

In the left lower part of figure 10.6 we have sketched the logarithm of this distribution function, which may be interpreted as the logarithm of the fission yield obtained with statistical methods.

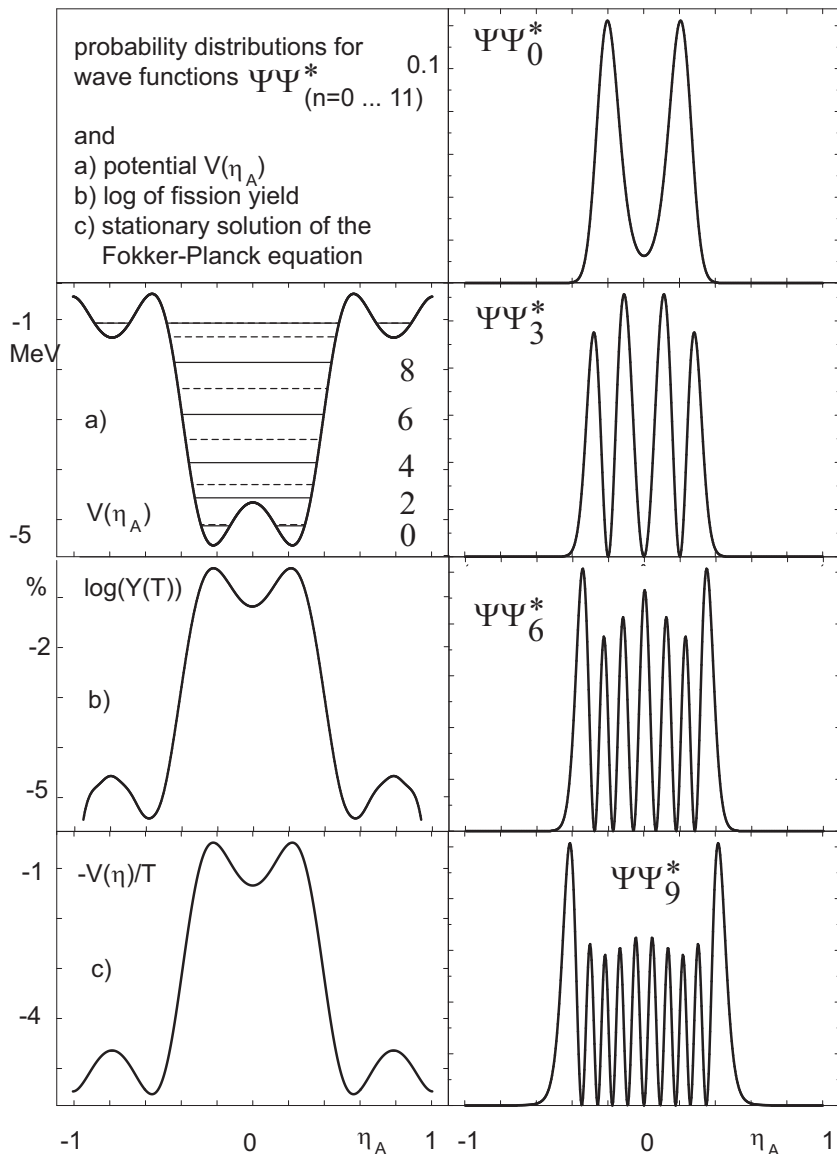


Fig. 10.6 Solution of the collective Schrödinger equation with a model potential (part 1). Wave functions (clockwise), potential $V(\eta_A)$ a), logarithmic fission-yield b) and $-V(\eta_A)/T$ c).

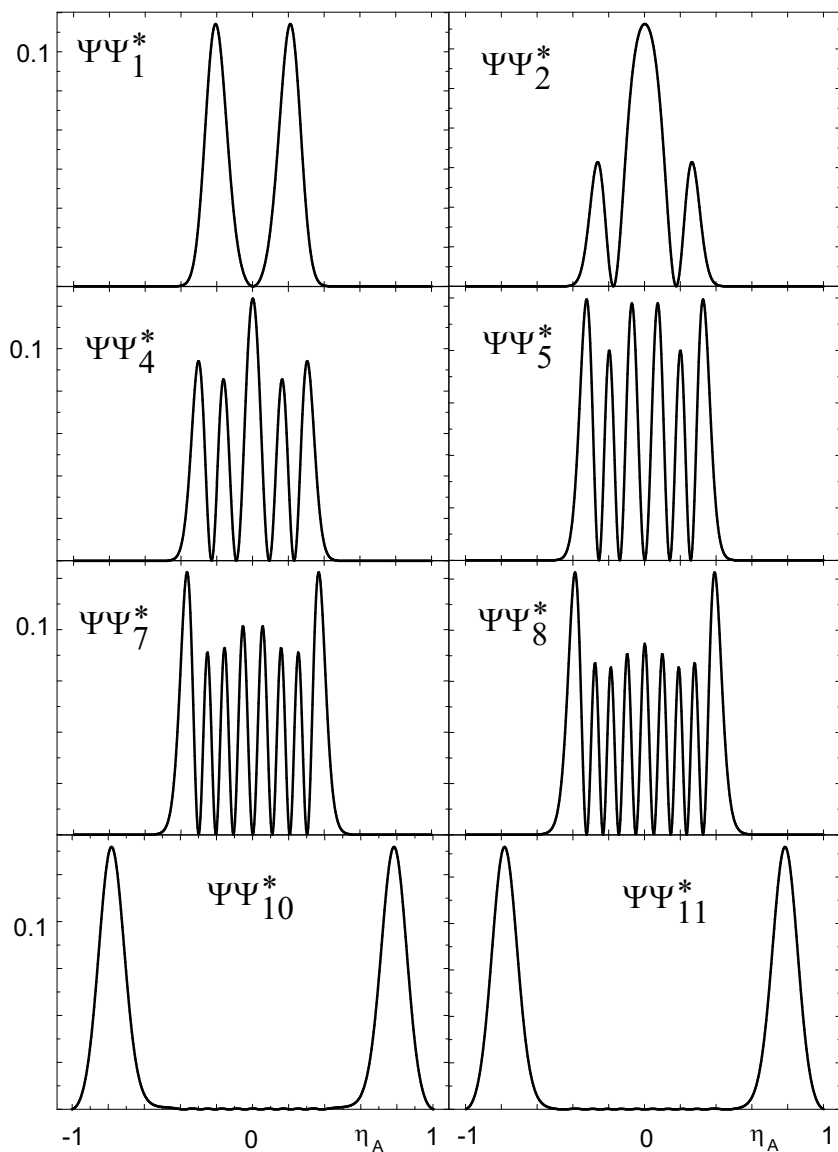


Fig. 10.7 Solution of the collective Schrödinger equation with a model potential (part 2). Wave functions (clockwise), potential $V(\eta_A)$ a), logarithmic fission-yield b) and $-V(\eta_A)/T$ c).

Exercise 10.1**Momentum dependence of nonlocal potentials**

Problem: Nonlocal potentials play an important role in nuclear physics. Show that nonlocality and momentum dependence of potentials are equivalent concepts.

Hint: Expand the wave function in a Taylor series.

Chapter 11

Quantum Mechanics

So far we have presented several methods to extend the definition of a standard derivative from integer value n to arbitrary α values:

$$\frac{d^n}{dx^n} \rightarrow \frac{d^\alpha}{dx^\alpha} \quad (11.1)$$

Indeed we may argue, that nearly all fractional extensions of classical problems are based on this ansatz. But of course, the proposed fractional extensions of a derivative operator leave the role of the corresponding coordinates untouched. This is one of the reasons of the difficulties to determine the fractional extension of a derivative e.g. in spherical coordinates and one of the reasons that nearly all the results of publications are derived in Cartesian coordinates.

A simple Fourier-transform of (11.1) using (5.8) results in

$$\frac{d^n}{dx^n} \rightarrow k^n \quad (11.2)$$

$$\frac{d^\alpha}{dx^\alpha} \rightarrow k^\alpha \quad (11.3)$$

and leads to the conclusion, that in the frequency domain

$$k^n \rightarrow k^\alpha \quad (11.4)$$

is an equivalent formulation of fractional calculus.

It is indeed remarkable, that many problems of fractional calculus may be easily solved applying a simple Fourier transform or alternatively for initial value problems by a Laplace-transformation.

On the other hand, any theory which works with fractional derivatives only and neglects an adequate treatment of coordinates, may be transformed into an equivalent standard differential theory with fractional powers

$$\{x^n, \frac{d^\alpha}{dx^\alpha}\} \equiv \{\frac{d^n}{dk^n}, k^\alpha\} \quad (11.5)$$

and consequently leads to results, which may be derived with standard methods without knowledge of fractional calculus.

A possible realization of this concept is the transition from integer space dimension n to arbitrary space dimension α . A geometrical interpretation could be given in terms of the volume of a hyper cube in such a space.

If we reduce the concept of fractal geometry to the introduction of arbitrary space dimensions, which of course is an oversimplification, fractional calculus and fractal geometry are indeed convertible via a simple Fourier transform and therefore are equivalent. Some aspects about a relationship between fractional calculus and fractals are discussed in [Nigmatullin (1992); Tatom (1995)].

The transition from classical mechanics to quantum mechanics may be interpreted as a transition from independent coordinate space and momentum space to a Hilbert space, in which space and momentum operators are treated similarly.

Consequently one postulate of quantum mechanics states, that derived results must be independent of the specific choice of e.g. a space or momentum representation. This is the mathematical manifestation of wave-particle-duality: The use of an operator e.g. either position \vec{x} or wave vector \vec{k} describes the same quantum object completely.

This implies, that a successful fractional extension of quantum mechanics has to treat coordinates and conjugated momenta equivalently:

$$\{x^n, \frac{d^n}{dx^n}\} \rightarrow \{x^\alpha, \frac{d^\alpha}{dx^\alpha}\} \quad (11.6)$$

This simultaneous treatment is the major difference between a classical and a quantum mechanical treatment. Furthermore this is the key information needed to quantize any classical quantity like a Hamilton function or angular momentum.

In the following we will apply the method of canonical quantization to the classical Hamilton function to obtain a fractional extension of the standard Schrödinger equation and will investigate some of its properties.

One surprising result will be the observation, that confinement is a natural outcome of the use of a fractional wave equation.

Especially the transformation properties under rotations will lead to the conclusion, that the behavior of a fractional Schrödinger equation should be directly compared to a standard Pauli equation.

A fractional Schrödinger equation describes particles with a complex internal structure, which we call fractional spin.

11.1 Canonical quantization

The transition from classical mechanics to quantum mechanics may be performed by canonical quantization [Dirac (1930); Herrmann (2005b)], path-integrals [Feynman (1949); Laskin (2002)], Weyl phase-space quantization [Weyl (1927); Tarasov (2008a)] or stochastic quantization [Parisi and Wu (1981); Lim and Tao (2008)].

To emphasize the similarity of a space or momentum representation, we will use the classical procedure, proposed by Dirac:

The classical canonically conjugated observables x and p are replaced by quantum mechanical observables \hat{x} and \hat{p} , which are introduced as derivative operators on a Hilbert space of square integrable wave functions f . The space coordinate representations of these operators are:

$$\hat{x}f(x) = xf(x) \quad (11.7)$$

$$\hat{p}f(x) = -i\hbar\partial_x f(x) \quad (11.8)$$

where \hat{x} and \hat{p} fulfill the commutation relation

$$[\hat{x}, \hat{p}] = i\hbar \quad (11.9)$$

We will now describe a generalization of these operators from integer order derivative to arbitrary order derivative.

According to our comments on parity conservation (7.14) we introduce two canonically conjugated operators in space representation:

$$\hat{X} f(\hat{x}^\alpha) = \left(\frac{\hbar}{mc} \right)^{(1-\alpha)} \hat{x}^\alpha f(\hat{x}^\alpha) \quad (11.10)$$

$$\hat{P} f(\hat{x}^\alpha) = -i \left(\frac{\hbar}{mc} \right)^\alpha mc \hat{D}^\alpha f(\hat{x}^\alpha) \quad (11.11)$$

The attached factors $(\hbar/mc)^{(1-\alpha)}$ and $(\hbar/mc)^\alpha mc$ ensure correct length and momentum units. For the special case $\alpha = 1$ these definitions correspond to the classical limits (11.7) and (11.8). The Hilbert space of square integrable functions f, g is based on the scalar product

$$\langle f | g \rangle = \int dx f^* g \quad (11.12)$$

Expectation values of an operator \hat{O} may be calculated with

$$\langle f | \hat{O} | g \rangle = \int dx f^* \hat{O} g \quad (11.13)$$

11.2 Quantization of the classical Hamilton function and free solutions

With definitions (11.10),(11.11) for the space and momentum operator we may now quantize the classical Hamilton function of a nonrelativistic particle.

The classical nonrelativistic N particle Hamilton function H_c depends on the classical moments and coordinates $\{p_i, x^i\}$:

$$H_c = \sum_{i=1}^{3N} \frac{p_i^2}{2m} + V(x^1, \dots, x^i, \dots, x^{3N}) \quad (11.14)$$

Following the canonical quantization method the classical observables are replaced by quantum mechanical operators. Hence we obtain the fractional Hamiltonian H^α :

$$H^\alpha = \sum_{i=1}^{3N} \frac{\hat{P}_i^2}{2m} + V(\hat{X}^1, \dots, \hat{X}^i, \dots, \hat{X}^{3N}) \quad (11.15)$$

$$= -\frac{1}{2}mc^2 \left(\frac{\hbar}{mc} \right)^{2\alpha} \hat{D}^{\alpha i} \hat{D}_i^\alpha + V(\hat{X}^1, \dots, \hat{X}^i, \dots, \hat{X}^{3N}) \quad (11.16)$$

Thus, a time dependent Schrödinger type equation for fractional derivative operators results

$$\begin{aligned} H^\alpha \Psi &= i\hbar \frac{\partial}{\partial t} \Psi \\ &= \left(-\frac{1}{2}mc^2 \left(\frac{\hbar}{mc} \right)^{2\alpha} \hat{D}^{\alpha i} \hat{D}_i^\alpha + V(\hat{X}^1, \dots, \hat{X}^i, \dots, \hat{X}^{3N}) \right) \Psi \end{aligned} \quad (11.17)$$

where we have introduced Einstein's summation convention $\sum_{i=1}^N x_i^2 = x^i x_i$. For $\alpha = 1$ this reduces to the classical Schrödinger equation.

A stationary Schrödinger equation results with the product ansatz $\Psi(\hat{X}^i, t) = \psi(\hat{X}^i)T(t)$ and a separation constant E :

$$\begin{aligned} H^\alpha \psi(\hat{X}^i) &= \left(-\frac{1}{2}mc^2 \left(\frac{\hbar}{mc} \right)^{2\alpha} \hat{D}^{\alpha i} \hat{D}_i^\alpha + V(\hat{X}^1, \dots, \hat{X}^i, \dots, \hat{X}^{3N}) \right) \psi(\hat{X}^i) \\ &= E\psi(\hat{X}^i) \end{aligned} \quad (11.18)$$

We will investigate the simple case of a free one dimensional fractional Schrödinger equation:

$$H_{\text{free}}^\alpha \psi = -\frac{1}{2}mc^2 \left(\frac{\hbar}{mc} \right)^{2\alpha} \hat{D}^\alpha \hat{D}^\alpha \psi = E\psi \quad (11.19)$$

This fractional differential equation is equivalent to the fractional regularized wave equation (7.21).

For $\alpha = 1$ solutions are given as plane waves:

$$\psi^+(x) = \cos(kx) \quad (11.20)$$

$$\psi^-(x) = \sin(kx) \quad (11.21)$$

If we apply the fractional derivative definition according to Fourier, the solutions of the free fractional Schrödinger equation are given by (7.22), for the Riemann definition by (7.24) and for the Caputo definition by (7.26).

In addition a valid solution of the fractional Schrödinger equation must be normalizable, so that a probabilistic interpretation is possible. In the region $\alpha < 1$ this may be realized easily:

For the Fourier fractional derivative the norm may be calculated analytically:

$$\int_{-\infty}^{\infty} dx_F \sin(\alpha, x)_F \sin(\alpha, x) = \frac{(-1 + \cos(\frac{\pi}{\alpha}))}{4\pi \cos(\frac{\pi}{2\alpha})} \quad (11.22)$$

$$\int_{-\infty}^{\infty} dx_F \sin(\alpha, x)_F \cos(\alpha, x) = 0 \quad (11.23)$$

$$\int_{-\infty}^{\infty} dx_F \cos(\alpha, x)_F \cos(\alpha, x) = -\frac{(3 + \cos(\frac{\pi}{\alpha}))}{4\pi \cos(\frac{\pi}{2\alpha})} \quad (11.24)$$

For $\alpha \geq 1$ this integral is divergent. In analogy to classical quantum mechanics we hence propose a box normalization in this region, where the dimensions of the box should be chosen large enough.

A similar procedure is necessary for the solutions according to Riemann and Caputo. In this case the solutions correspond to solutions for a Schrödinger equation in an infinitely deep potential well. This is equivalent to a search for zeroes for these solutions and may be easily performed numerically.

A graphical representation of the solutions of the free fractional Schrödinger equation is given in figure 11.1.

For a physical interpretation it is important to recognize, that the solutions for $\alpha < 1$ are more and more located at the origin.

This is in contrast to the solutions for free particles, which are described by the ordinary Schrödinger equation as free waves which are spread out on the whole space and therefore are located everywhere with a similar probability (this is a direct consequence of Heisenberg's uncertainty relation, since the momentum of the free particle is known exactly, we may not make a statement of the position).

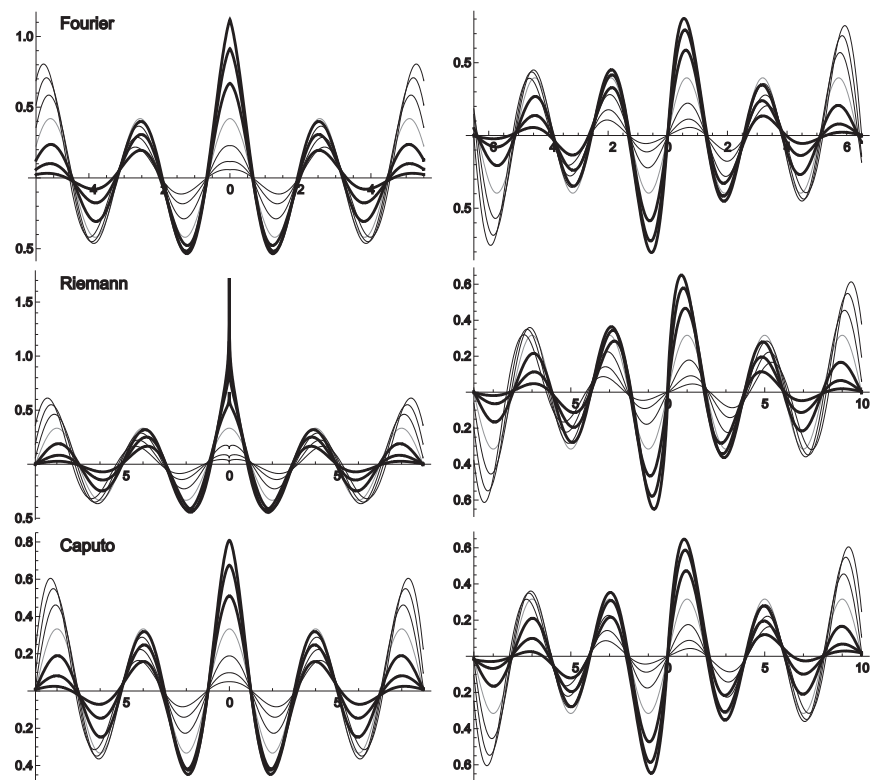


Fig. 11.1 Normalized solutions of the free fractional Schrödinger equation with good parity (even on the left and odd on the right side) for different fractional derivative parameters (thick lines $\alpha < 1$ and thin lines $\alpha \geq 1$) according to Fourier, Riemann and Caputo: Solutions in the region $\alpha \geq 1$ are box normalizable. Solutions for $\alpha < 1$ are localized at $x = 0$ and decrease very fast for large x -values.

If Bohr's concept of a probability interpretation is valid for the solution of the fractional Schrödinger equation for a fractional particle we obtain the remarkable result, that a fractional particle will not be equally spaced, but instead is located at the origin.

As a first reaction, we could call this behavior nonphysical and might discard a fractional Schrödinger equation. On the other hand we know about particles, which undoubtedly exist but have not been observed as free particles until now. These particles are called quarks and the problem, that they have not been observed as free quarks until now, is called quark confinement and is a direct consequence of the specific nature of strong interaction.

Hence, we will not discard the fractional Schrödinger equation, but will compare our predictions with results which have been derived by using traditional methods for a description of hadronic interaction.

Of course it would be a nice success of fractional calculus, if we could derive a fractional theory of quark dynamics, which was more elegant and successful than the usually applied methods.

A phenomenological strategy to model quark confinement is a classical description in terms of an ad hoc postulated potential. The most prominent example is a linear ansatz [Eichten *et al.* (1975)]:

$$V(x) \sim \text{const} |x| \quad (11.25)$$

In the next section we want to find out, whether we can reproduce the behavior of the free solutions of the fractional Schrödinger equation (11.19) if we assume, that similar solutions of the standard ($\alpha = 1$) Schrödinger equation with an additional phenomenological potential term exist.

$$H_{\text{free}}^{\alpha} \psi = E\psi \approx \left(-\frac{\hbar^2}{2m} \partial_x^2 + V(x) \right) \psi \quad (11.26)$$

We will show, that the explicit form of such an additional potential term may indeed be derived, using methods, originally developed to describe the fission yields of excited nuclei for a given potential energy surface.

11.3 Temperature dependence of a fission yield and determination of the corresponding fission potential

We will investigate the problem, whether we can estimate the original form of a given potential, if a complete set of eigenfunctions and corresponding energy values of the standard Schrödinger equation with a potential term are known.

For that purpose, we will use methods developed within the framework of fragmentation theory [Fink *et al.* (1974); Sandulescu *et al.* (1976); Maruhn *et al.* (1980); Herrmann *et al.* (1988); Greiner *et al.* (1995)], which originally were used for an explanation of the fission yields of heavy nuclei [Lustig *et al.* (1980)]. We will show, that the temperature dependence of a fission yield and the corresponding potential are indeed connected. For reasons of simplicity, we will present the analytically solvable example of the harmonic oscillator.

The stationary solutions of the Schrödinger equation

$$\left(-\frac{\hbar^2}{2m}\partial_x^2 + V(x)\right)\psi = E\psi \quad (11.27)$$

with the model potential of the harmonic oscillator

$$V(x) = \frac{1}{2}m\omega^2x^2 \quad (11.28)$$

using the abbreviation

$$\beta = \sqrt{\frac{m\omega}{\hbar}} \quad (11.29)$$

lead to a set of eigenfunctions (H_n denotes the Hermite polynomial)

$$\psi_n(x) = \sqrt{\frac{\beta}{\pi^{\frac{1}{2}}2^n n!}} H_n(\beta x)e^{-\frac{1}{2}\beta^2 x^2} \quad (11.30)$$

and eigenvalues:

$$E_n = \hbar\omega(n + \frac{1}{2}) \quad (11.31)$$

The temperature dependent fission yield is given by a Boltzmann-like occupation of excited states [Maruhn *et al.* (1980)]:

$$Y(x, T) = \frac{\sum_n \psi_n(x)\psi_n^*(x)e^{-\frac{E_n}{T}}}{\sum_n e^{-\frac{E_n}{T}}} \quad (11.32)$$

Inserting energies (11.31) and eigenfunctions (11.30) using the abbreviation

$$q = e^{-\frac{\hbar\omega}{T}} \quad (11.33)$$

lead to:¹

$$\begin{aligned} Y(x, T) &= (1 - q) \frac{\beta}{\pi^{\frac{1}{2}}} e^{-\beta^2 x^2} \sum_n H_n^2(\beta x) \frac{q^n}{2^n n!} \\ &= (1 - q) \frac{\beta}{\pi^{\frac{1}{2}}} e^{-\beta^2 x^2} \frac{1}{\sqrt{1 - q^2}} e^{-\frac{2\beta^2 x^2 q}{1+q}} \end{aligned} \quad (11.34)$$

For the limiting case of high temperatures

$$q \approx 1 - \frac{\hbar\omega}{T} \quad (11.35)$$

¹A nice derivation is presented in: Greiner, W., Neise, L. and Stöcker, H. (2001) *Thermodynamics and statistical mechanics* Springer, New York, USA. exercise 10.7, pp. 280–284

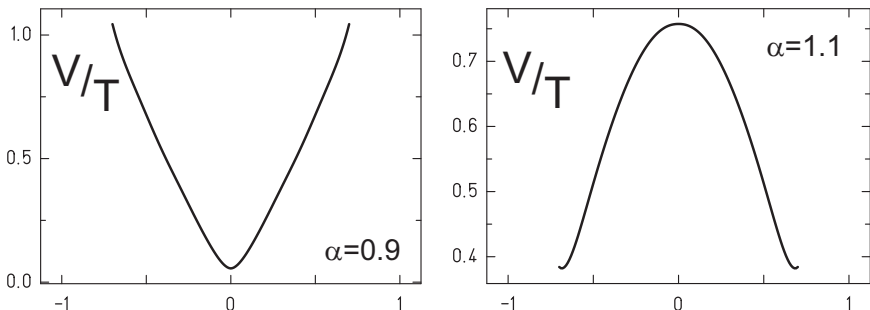


Fig. 11.2 Graph of the potential $V(x)$ which is necessary to simulate the behavior of eigenfunctions and solutions of the free fractional Schrödinger equation (11.19) in terms of the ordinary Schrödinger equation according to (11.26). For $\alpha < 1$ the potential is dominated by a linear term $V \sim \text{const} |x|$. For $\alpha > 1$ the potential is of the type $V \sim \text{const}(1 - x^2)$.

we obtain:

$$Y(x, T) = \frac{\beta}{\pi^{\frac{1}{2}}} \sqrt{\frac{\hbar\omega}{2T}} e^{-\frac{m\omega^2 x^2}{2T}} = \sqrt{\frac{m\omega^2}{2\pi T}} e^{-\frac{V}{T}} \quad (11.36)$$

or finally

$$\frac{\sum_n \psi_n(x) \psi_n^*(x) e^{-\frac{E_n}{T}}}{\sum_n e^{-\frac{E_n}{T}}} = Y(x, T) = \sqrt{\frac{m\omega^2}{2\pi T}} e^{-\frac{V}{T}} \quad (11.37)$$

We obtain the important result, that we may deduce the general form of the potential energy $V(x)$ from a temperature dependent fission yield using (11.37). Once eigenfunctions and energy levels are known, we may determine this potential.

With this information we may calculate the regularized solutions of the free fractional Schrödinger equation using the Caputo derivative, normalize these solutions in a box of size $L = 2$ and apply the boundary conditions $\psi(\alpha, x = -1) = 0$ and $\psi(\alpha, x = +1) = 0$. The corresponding eigenvalues are determined numerically.

With these results in a next step we calculate the fission yield (11.32) and deduce the potential according to (11.37). The result is presented in figure 11.2.

In the vicinity of $\alpha \approx 1$ we distinguish three cases:

$$V(x) = \begin{cases} c_1 + c_2|x| & \alpha < 1 \\ 0 & \alpha = 1 \\ c_1(1 - c_2x^2) & \alpha > 1 \end{cases} \quad (11.38)$$

- For the case $\alpha < 1$ the behavior of the solutions of the free fractional Schrödinger equation corresponds to the behavior of solutions of the standard Schrödinger equation with a dominant linear potential contribution.
- For the case $\alpha = 1$ both free solutions are identical.
- In order to model the behavior of the fractional solutions in the case $\alpha > 1$ a potential of type $V \sim c_1(1 - c_2x^2)$ has to be inserted into the standard Schrödinger equation. In three dimensional space this potential is identical to the potential inside a homogeneously charged sphere.

From a classical point of view the behavior of a particle described by a free fractional Schrödinger equation for $\alpha > 1$ corresponds to the behavior of a classical charged particle in a homogeneously charged background medium.

On the other hand for $\alpha < 1$ we may conclude, that from a classical point of view, there is a charged background too, which is described by a linear potential term instead of a quadratic term in case of a homogeneously charged sphere.

This is a further indication, that the use of a phenomenological linear potential, necessary for an approximate description for the hadron excitation spectrum in classical models, is obsolete in a fractional theory or in other words, this behavior is already incorporated in a fractional theory.

In order to clarify this result, in the next section we will present the energy spectrum of the fractional Schrödinger equation with an infinite well potential.

11.4 The fractional Schrödinger equation with an infinite well potential

The one dimensional infinite well potential is defined as:

$$V(x) = \begin{cases} 0 & |x| \leq a \\ \infty & |x| > a \end{cases} \quad (11.39)$$

From a classical point of view, the solutions of the standard Schrödinger equation with this potential therefore correspond to the solutions of the classical wave equation for a fixed vibrating string. The reason for this equivalence is based on the fact, that the solution of the standard

Schrödinger equation for the infinite potential well may be split as

$$\psi(x) = \begin{cases} \psi_0(x) & |x| \leq a \\ 0 & |x| > a \end{cases} \quad (11.40)$$

Therefore the solution in the interior region $|x| \leq a$ is equivalent to the solution of a free wave equation with boundary conditions $\psi_0(\pm a) = 0$.

Such a piecewise solution is valid only in the case of a standard derivative.

- If we apply a fractional derivative in the sense of Liouville or Fourier, according to our statements on nonlocality and memory effects in the previous chapter, the behavior of the wave function in the outside region influences the behavior in the inside region. Consequently the use of solutions for the fractional wave equation obtained for a vibrating string will be considered as approximate solutions for the fractional infinite well potential, which are valid only for $\alpha \approx 1$.
- On the other hand, for the Riemann- and Caputo fractional derivative definition, the interior solutions $\psi_0(x)$ for the infinite potential well and for the vibrating string are identical. Indeed, according to (5.32) and (5.43) the fractional integral in this case is confined to the region from 0 to $|x|$ and therefore, the functional behavior inside the infinite potential well is independent of the exterior region. But if the potential well has a finite depth or is not located at the origin, this equivalence of solutions is lost. The translation invariance of the fractional Schrödinger equation is lost for the Riemann- and Caputo fractional derivative definition.

Therefore until now there is no exact analytic solution for the fractional infinite depth potential well, which is valid for all types of fractional derivatives.

A correct solution was indeed given by a free fractional Schrödinger equation (11.19)

$$H^\alpha \psi = -\frac{1}{2} mc^2 \left(\frac{\hbar}{mc} \right)^{2\alpha} \hat{D}^\alpha \hat{D}^\alpha \psi = E\psi \quad (11.41)$$

where ψ must obey the conditions (11.40).

Instead we will use the boundary conditions

$$\psi(-a) = \psi(a) = 0 \quad (11.42)$$

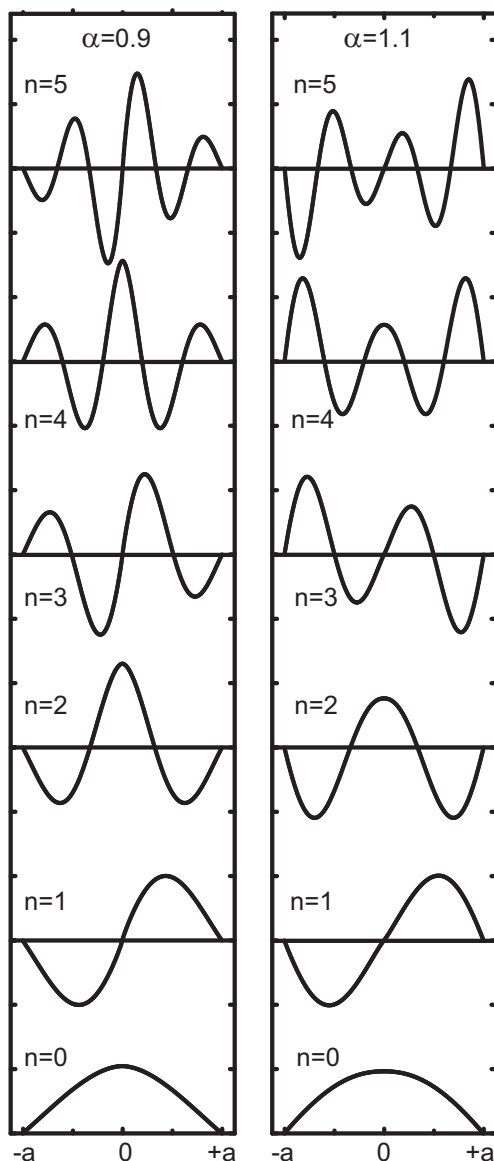


Fig. 11.3 The six lowest eigenfunctions for the one dimensional fractional Schrödinger equation with the infinite square well potential (11.39) based on the Caputo fractional derivative (5.43), with $\alpha = 0.9$ on the left and $\alpha = 1.1$ on the right side.

Conditions (11.40) and (11.42) are only equivalent for the infinite square well potential using the Riemann- and Caputo fractional derivative. They may be considered a crude approximation only in case of the Fourier, Liouville or Riesz fractional derivative.

With these boundary conditions we may indeed use the solutions of the free fractional Schrödinger equation, which for example are given approximately for the Fourier fractional derivative according to (7.22) by

$${}_{\text{F}} \sin(\alpha, x) = \text{sign}(x) \frac{1}{2i} \left(e^{\frac{1}{2}e^{\frac{i\pi}{2\alpha}}|x|} - e^{\frac{1}{2}e^{-\frac{i\pi}{2\alpha}}|x|} \right) \quad (11.43)$$

$${}_{\text{F}} \cos(\alpha, x) = \frac{1}{2} \left(e^{\frac{1}{2}e^{\frac{i\pi}{2\alpha}}|x|} + e^{\frac{1}{2}e^{-\frac{i\pi}{2\alpha}}|x|} \right) \quad (11.44)$$

the zeroes of these solutions are known analytically (7.32):

$${}_{\text{F}} x_0(n, \alpha) = \frac{(n+1)}{\sin(\frac{\pi}{2a})} \frac{\pi}{2} \quad n = 0, 1, 2, 3, \dots \quad (11.45)$$

Therefore approximate solutions of the fractional Schrödinger equation according to Fourier for the infinite depth potential well, which fulfill the boundary conditions (11.42) are given as

$$\psi(\alpha, x) = \begin{cases} {}_{\text{F}} \cos(\alpha, x/x_0(n, \alpha)) & n = 0, 2, 4, \dots \\ {}_{\text{F}} \sin(\alpha, x/x_0(n, \alpha)) & n = 1, 3, 5, \dots \end{cases} \quad (11.46)$$

and the corresponding energy levels follow according to (7.28) as:

$$E(\alpha, n) = \frac{1}{2} mc^2 \left(\frac{\hbar}{mc} \right)^{2\alpha} \left(\frac{\pi}{2 \sin(\frac{\pi}{2a})} \right)^{2\alpha} (n+1)^{2\alpha} \quad (11.47)$$

This result may easily be extended to the three dimensional case:

$$E(\alpha, n_x, n_y, n_z) = \frac{1}{2} mc^2 \left(\frac{\hbar}{mc} \right)^{2\alpha} \left(\frac{\pi}{2 \sin(\frac{\pi}{2a})} \right)^{2\alpha} \times ((n_x + 1)^{2\alpha} + (n_y + 1)^{2\alpha} + (n_z + 1)^{2\alpha}) \quad (11.48)$$

In figure 11.4 the lowest energy levels of the fractional infinite three dimensional potential well are presented for different α . Magic numbers for shell closures are given.

Although these results are approximate, since we have ignored the non-local character of the fractional derivative operator, we may deduce, that the spectrum of the fractional infinite potential well (11.48) in the limit $\alpha \rightarrow \frac{1}{2}$ coincides with the spectrum of the classical harmonic oscillator:

$$\lim_{\alpha \rightarrow \frac{1}{2}} E(\alpha, n_x, n_y, n_z) = \frac{\hbar c}{2} \frac{\pi}{2 \sin(\frac{\pi}{2a})} (n_x + n_y + n_z + 3) \quad (11.49)$$

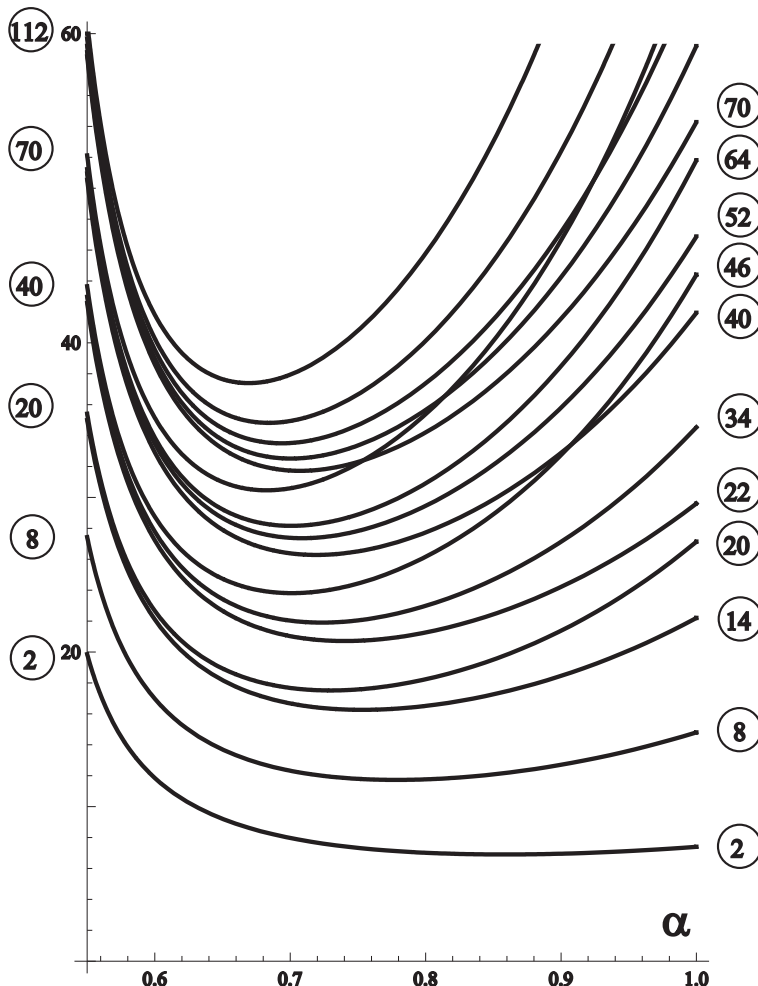


Fig. 11.4 Approximate level spectrum for the three dimensional fractional infinite potential well according to Fourier. Occupation numbers are given in circles. For the semi-derivative $\alpha \approx 0.5$ the spectrum more and more coincides with the spectrum of the standard harmonic oscillator.

In view of phenomenological shell models the fractional derivative parameter α allows a smooth analytic transition from a box- to a spherical symmetry.

If we interpret the degeneracy as a measure for the symmetry of a system, we obtain the result, that the symmetry of the fractional potential well is increasing for decreasing α .

A typical area of application for the fractional potential well within the framework of nuclear physics is the use as a model potential for a shell model of nuclei. In Chapters 21 and 22 we will use fractional potentials to reproduce the ground state properties of clusters in nuclear and atomic physics.

The results, derived so far for the fractional potential well according to Fourier may be used in the case of the Riemann- and Caputo definition too.

The zeros k_n^0 of the free solutions must be obtained in this case numerically. The eigenfunctions for the infinite potential well are then given by

$$\psi_{2n}^{(+)}(x) = {}_{\text{R,C}} \cos(\alpha, k_{2n}^0 \frac{x}{a}) \quad (11.50)$$

$$\psi_{2n+1}^{(-)}(x) = {}_{\text{R,C}} \sin(\alpha, k_{2n+1}^0 \frac{x}{a}) \quad (11.51)$$

And the corresponding eigenvalues are then given by:

$$e_n = \frac{1}{2} \left(\frac{\hbar}{mc} \right)^{2\alpha} mc^2 |\frac{k_n^0}{a}|^{2\alpha} \quad (11.52)$$

The extension to the multi-dimensional case reads:

$$\Psi_{n_1 n_2 \dots n_N}(x^1, x^2, \dots, x^N) = \prod_{i=1}^N \psi_{n_i}(x^i) \quad (11.53)$$

and the corresponding levels result as:

$$E_{n_1 n_2 \dots n_N} = \frac{1}{2} \left(\frac{\hbar}{mc} \right)^{2\alpha} mc^2 \sum_{i=1}^N |\frac{k_{n_i}^0}{a_i}|^{2\alpha} \quad (11.54)$$

For $\alpha \approx 1$ the difference of the numerically determined energy spectrum and the analytic spectrum according to Fourier is small, as long as $\alpha \approx 1$.

When α becomes smaller, there is only a finite number of zeros of the free fractional Schrödinger equation (see figure 7.1). As a consequence the energy spectrum is finite. For $\alpha < 0.65$ we obtain only one even and one odd solution for the Riemann-derivative, so we may occupy only the ground state and the first excited state of the spectrum. For the Caputo derivative we obtain only one solution and therefore only one energy level. Consequently, the number of particles, which may occupy the levels of the infinite potential well is limited. Of course, shell models used in nuclear physics, which intend to model a realistic behavior, show a similar behavior e.g. the Woods-Saxon-potential.

Hence we have presented exact solutions for the fractional Schrödinger equation with a potential term for the infinite well with Riemann- and

Caputo derivative, which as a major result for $\alpha < 1$ generate only a finite number of energy levels. On the other hand the approximate solutions according to Fourier generate an infinite number of energy levels similar to the classical case.

The integral representation of a fractional derivative is a nonlocal operator and consequently a fractional Schrödinger equation is a nonlocal wave equation. It should be mentioned, that in the literature there are several presentations of so called exact solutions of the fractional Schrödinger equation with Coulomb potential [Laskin (2000)], potential wells [Laskin (2010)] and solved scattering problems [Guo and Xu (2006); Dong and Xu (2007); Bayin (2012a); Bayin (2012b); Dong (2013)], which completely ignore the nonlocality of the fractional derivative and therefore should be considered merely as approximations valid for $\alpha \approx 1$ only [Jeng *et al.* (2008); Hawkins and Schwarz (2012)].

For the Riesz-derivative definition we will explicitly present the solutions of the corresponding fractional Schrödinger equation with an infinite potential well potential in the next chapter.

11.5 Radial solutions of the fractional Schrödinger equation

In the case of fractional derivative operators up to now no general theory of covariant coordinate transformations exists. Hence in the following we will only collect some arguments about aspects of a coordinate transform and make some remarks on radial solutions, which are independent of angular variables.

We intend to perform a coordinate transformation from Cartesian to hyperspherical coordinates in \mathbb{R}^N

$$f(x_1, x_2, \dots, x_N) = f(r, \phi_1, \phi_2, \dots, \phi_{N-1}) \quad (11.55)$$

The invariant line element in the case $\alpha = 1$

$$ds^2 = g_{ij} dx^i dx^j \quad i, j = 1, \dots, N \quad (11.56)$$

for arbitrary fractional derivative coefficient α may be generalized to

$$ds^{2\alpha} = g_{ij}^\alpha dx^{i\alpha} dx^{j\alpha} \quad i, j = 1, \dots, N \quad (11.57)$$

Consequently a reasonable definition of the radial coordinate is given by

$$r^{2\alpha} = \sum_{i=1}^N x_i^{2\alpha} \quad (11.58)$$

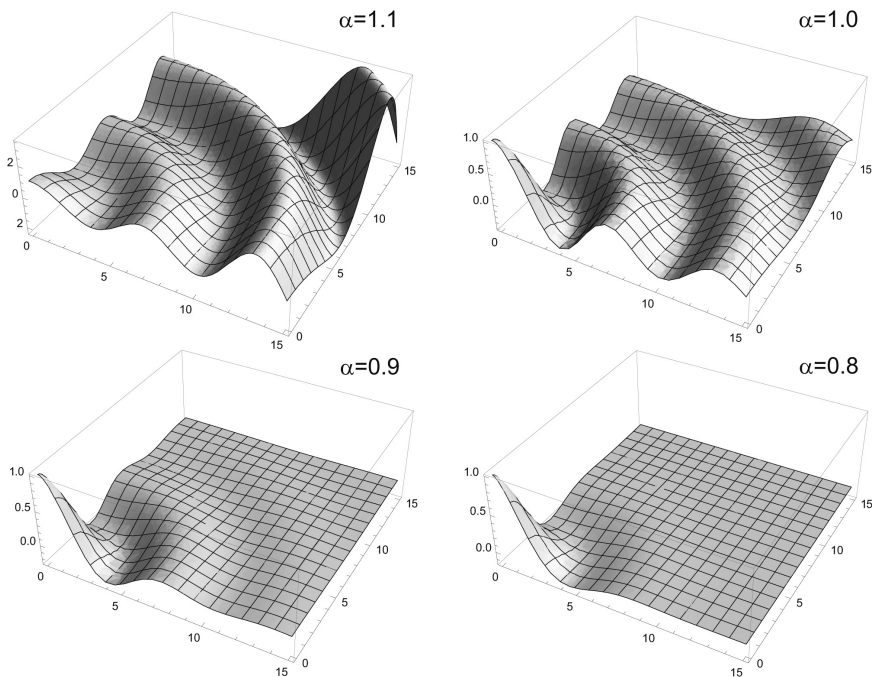


Fig. 11.5 Radial symmetric ground state solutions ($s = 0$) of the free fractional Schrödinger equation for different α .

A radial symmetric solution is a function which only depends on the radial variable r . For fractional coordinates this does not imply, that this function is rotational symmetric.

But for a spherical ground state we require the following symmetry properties: We assume the spherical ground state to be independent of the angular variables, square integrable and of positive parity. If we apply the Caputo definition of the fractional derivative, therefore an appropriate ansatz is:

$$g(N, \alpha, kr) = \sum_{n=0}^{\infty} (-1)^n a_n(N, \alpha) (|k|r)^{2\alpha n} \quad (11.59)$$

or in Cartesian coordinates

$$g(N, \alpha, kx_1, \dots, kx_N) = \sum_{n=0}^{\infty} (-1)^n a_n(N, \alpha) \left(\sum_{i=1}^N |kx_i|^{2\alpha} \right)^n \quad (11.60)$$

where the coefficients a_n depend on the explicit form of the potential.

For a free particle, a solution on \mathbb{R}^N is given with the abbreviation

$$\eta_j = \Gamma(1 + 2\alpha j)/\Gamma(1 + 2\alpha(j - 1)) \quad (11.61)$$

by the recurrence relation

$$\begin{aligned} a_0 &= 1 \\ a_j &= a_{j-1} / ((N - 1) j \eta_1 + \eta_j) \quad j = 1, 2, \dots \end{aligned} \quad (11.62)$$

Following the naming conventions in atomic- and nuclear physics we call these solutions fractional s-waves. For the limit $\alpha = 1$ this solution reduces to a simple Bessel function.

Once these solutions are derived, the ground state solutions for a spherical potential well with infinite depth may be deduced accordingly:

An infinite spherical well is described by the potential

$$V(r) = \begin{cases} 0 & r \leq r_0 \\ \infty & r > r_0 \end{cases} \quad (11.63)$$

The corresponding boundary condition for the ground state wave function $g(N, \alpha, r)$ is:

$$g(N, \alpha, r_0) = 0 \quad (11.64)$$

Let k_{sph}^0 be the first zero of the free particle ground state wave function, the ground state wave function for the spherical infinite well potential is given by

$$g(N, \alpha, k_{\text{sph}}^0 r/r_0) \quad (11.65)$$

and the ground state energy is then given by

$$e_0(N, \alpha) = \frac{1}{2} mc^2 \left(\frac{\hbar}{mc} \frac{k_{\text{sph}}^0}{r_0} \right)^{2\alpha} \quad (11.66)$$

If there are more than one zeros, we may calculate the wave functions and energy values for higher (ns)-states.

From figure 11.5 we observe, that the radial symmetric solutions of the fractional Schrödinger equation and the behavior of one-dimensional solutions in Cartesian coordinates show a similar behavior. In both cases the solutions show an increasing behavior for $\alpha > 1$, while for $\alpha < 1$ they are located at the origin of the coordinate system.

We draw the conclusion, that coordinate transformations at the current state of the art are not an appropriate tool to investigate symmetry properties of fractional wave equations. As long as there is no general theory

for fractional coordinate transformations, we should restrict investigations to Cartesian coordinate systems.

Since we are interested in fractional symmetry properties we apply a much more powerful tool: the fractional group theory. Indeed we will demonstrate in the following chapters the strength of a group theoretical approach and will use the concept of fractional group theory to investigate the properties of the fractional rotation group.

This page intentionally left blank

Chapter 12

The Fractional Schrödinger Equation with the Infinite Well Potential — Numerical Results using the Riesz Derivative

Wave equations play a significant role in the description of the dynamic development of particles and fields; e.g. the Maxwell-equations describe the behavior of the electromagnetic field in terms of coupled partial differential equations. In quantum mechanics a particle may be described by the non-relativistic Schrödinger wave equation, where the kinetic term is given by the Laplace-operator.

Fractional calculus introduces the concept of nonlocality to arbitrary hitherto local operators. This is a new property, which only recently attracted attention on a broader basis. The interest in a nonlocal dynamic description of e.g. quantum systems has been steadily increasing, because it is expected, that quantum phenomena may be treated more elegantly from a generalized point of view.

Within this context, it is helpful to investigate fundamental properties of a fractional wave equation and to study general features of its solution.

In the last section, we interpreted the solutions of the fractional Schrödinger equation with infinite potential well using the Caputo/Riemann fractional derivative. In this section, we present the main results for the same problem using the Riesz derivative [Herrmann (2012b); Luchko (2013)]:

12.1 The problem - analytic part

Let the one dimensional fractional stationary Schrödinger equation in scaled canonical form be defined as

$$-\mathcal{D}_\alpha \Delta^{\alpha/2} \Psi(x) = (E - V(x)) \Psi(x) \quad (12.1)$$

where \mathcal{D}_α is a constant in units [MeV m $^\alpha$ s $^{-\alpha}$] and $\Delta^{\alpha/2}$ is the fractional Laplace-operator.

The definition of a fractional order derivative is not unique, several definitions e.g. the Riemann, Caputo, Liouville, Riesz, Feller fractional derivative coexist and are equally well suited for an extension of the standard derivative.

In order to preserve Hermiticity for the fractional extension of the Laplace-operator[Laskin (2002)], we will explicitly apply the Riesz fractional derivative

$$\begin{aligned} \Delta^{\alpha/2} f(x) &\equiv {}_{RZ}^{\infty} D^\alpha f(x) \\ &= \Gamma(1 + \alpha) \frac{\sin(\pi\alpha/2)}{\pi} \int_0^\infty \frac{f(x + \xi) - 2f(x) + f(x - \xi)}{\xi^{\alpha+1}} d\xi \\ &\quad 0 < \alpha < 2 \end{aligned} \quad (12.2)$$

where the left superscript in ${}_{RZ}^{\infty} D^\alpha$ emphasizes the fact, that the integral domain is the full space \mathbb{R} .

Since the eigenfunctions of the Riesz derivative operator are given as

$${}_{RZ}^{\infty} D^\alpha \cos(kx) = -|k|^\alpha \cos(kx) \quad (12.3)$$

$${}_{RZ}^{\infty} D^\alpha \sin(kx) = -|k|^\alpha \sin(kx) \quad (12.4)$$

the eigenfunctions of the potential free ($V(x) = 0$) fractional Schrödinger equation using the Riesz fractional derivative follow as

$${}_{RZ} \Psi^+(k, x) = \cos(kx) \quad (12.5)$$

$${}_{RZ} \Psi^-(k, x) = \sin(kx) \quad (12.6)$$

where the \pm -sign indicates the parity and the corresponding continuous energy spectrum follows as:

$$E_k^{\text{free}} = |k|^\alpha \quad k \in \mathbb{R} \quad (12.7)$$

Since the integrals $\int_{-\infty}^{+\infty} dx \cos(kx)$ and $\int_{-\infty}^{+\infty} dx \sin(kx)$ respectively are divergent, the eigenfunctions are not normalizable on the full domain \mathbb{R} .

In the case $\alpha = 2$, which corresponds to the classical quantum mechanics, of course we may apply the classical box-normalization, which means we make a statement on the behavior of the wave-function isolated in a box of size e.g. $2q$ of the form:

$$\int_{-q}^{+q} \cos(kx) dx < \infty \quad (12.8)$$

$$\int_{-q}^{+q} \sin(kx) dx < \infty \quad (12.9)$$

According to (12.3) and (12.4) a special feature of the Riesz derivative is that the type of the eigenfunctions of the free fractional Schrödinger equation does not change for arbitrary α . Hence the question arises, whether box-normalization is a legal procedure in the case of nonlocal differential equations. At least, the physical meaning of box-normalization may be different.

To avoid these interpretative difficulties we will switch on a potential $V(x)$, such that the eigenfunctions vanish at infinity. An ideal candidate for such a potential is the infinite potential well, centered at the origin with finite size $2q$, which is explicitly given by:

$$V(x) = \begin{cases} 0 & |x| \leq q \\ \infty & |x| > q \end{cases} \quad (12.10)$$

A reasonable ansatz for the corresponding eigenfunction follows as:

$${}^{\square}\Psi(x) = \begin{cases} {}^{\infty}\Psi(x) & |x| \leq q \\ 0 & |x| > q \end{cases} \quad (12.11)$$

Where the superscript ${}^{\square}\Psi(x)$ emphasizes the fact, that the wave-function per definitionem is now confined inside the infinite potential well and vanishes outside. The superscript ${}^{\infty}\Psi(x)$ indicates, that this function may at first be defined on the whole domain, but is used only inside the bounded domain of the infinite potential well.

The normalization condition for ${}^{\square}\Psi(x)$ is now given by:

$$\int_{-\infty}^{+\infty} dx {}^{\square}\Psi(x) = \int_{-q}^{+q} dx {}^{\infty}\Psi(x) = 1 \quad (12.12)$$

As a consequence, we may interpret ${}^{\square}\Psi(x)$ physically as a normalizable wave-function and its absolute value ${}^{\square}\Psi(x){}^{\square}\Psi(x)^*$ as a probability measure.

In the classical, local case ($\alpha = 2$) we obtain immediately

$${}^{\square}\Psi^{\pm}(x) = \begin{cases} \cos \frac{k\pi}{2q}x & |x| \leq q \text{ and } k = 1, 3, 5, \dots \\ \sin \frac{k\pi}{2q}x & |x| \leq q \text{ and } k = 2, 4, 6, \dots \\ 0 & |x| > q \end{cases} \quad (12.13)$$

and the continuous energy spectrum changes to a discrete one, since $k \in \mathbb{N}$ is an integer now.

$$E_k^{\text{local}} = \left(\frac{\pi}{2q}\right)^2 k^2 \quad k = 1, 2, 3, \dots \quad (12.14)$$

In order to solve the fractional Schrödinger equation of the infinite potential well for arbitrary α , we have to apply the Riesz derivative operator to ${}^{\square}\Psi(x)$.

For the positive semi-axis $x \geq 0$ we obtain for $x \leq q$:

$$\begin{aligned} {}_{\text{RZ}}^{\infty}D^{\alpha}({}^{\square}\Psi(x)) &= \Gamma(1+\alpha) \frac{\sin(\pi\alpha/2)}{\pi} \\ &\quad \times \int_0^{\infty} \frac{{}^{\square}\Psi(x-\xi) - 2{}^{\square}\Psi(x) + {}^{\square}\Psi(x+\xi)}{\xi^{\alpha+1}} d\xi \\ &= \Gamma(1+\alpha) \frac{\sin(\pi\alpha/2)}{\pi} \\ &\quad \times \left\{ \int_0^{q-x} \frac{{}^{\infty}\Psi(x-\xi) - 2{}^{\infty}\Psi(x) + {}^{\infty}\Psi(x+\xi)}{\xi^{\alpha+1}} d\xi \right. \\ &\quad + \int_{q-x}^{q+x} \frac{{}^{\infty}\Psi(x-\xi) - 2{}^{\infty}\Psi(x)}{\xi^{\alpha+1}} d\xi \\ &\quad \left. + \int_{q+x}^{\infty} \frac{-2{}^{\infty}\Psi(x)}{\xi^{\alpha+1}} d\xi \right\} \\ &= {}_{\text{RZ}}^{\square}D^{\alpha}({}^{\infty}\Psi(x)) \quad 0 \leq x \leq q \end{aligned} \quad (12.15)$$

In addition, for $x > q$ due to the nonlocal character of the Riesz derivative operator we obtain a nonvanishing finite term

$${}_{\text{RZ}}^{\infty}D^{\alpha}({}^{\square}\Psi(x)) = \Gamma(1+\alpha) \frac{\sin(\pi\alpha/2)}{\pi} \times \int_{x-q}^{x+q} \frac{{}^{\infty}\Psi(x-\xi)}{\xi^{\alpha+1}} d\xi \quad x > q \quad (12.16)$$

which is negligible only in the special case of the infinite potential well discussed here.

The corresponding equations for $x \leq 0$ just interchange the roles of ${}^{\infty}\Psi(x-\xi)$ and ${}^{\infty}\Psi(x+\xi)$. Since parity is conserved for the infinite potential well, we may restrict to (12.15) without loss of generality.

We can write (12.15) in short-hand notation:

$${}_{\text{RZ}}^{\infty}D^{\alpha}({}^{\square}\Psi(x)) = {}_{\text{RZ}}^{\square}D^{\alpha}({}^{\infty}\Psi(x)) \quad (12.17)$$

This may be interpreted as a modification of the Riesz-operator, which now only covers the inside region of the potential well. Obviously both operators differ significantly.

$${}_{\text{RZ}}^{\infty}D^{\alpha} \neq {}_{\text{RZ}}^{\square}D^{\alpha} \quad (12.18)$$

This is a general feature of all fractional derivative definitions, which span over the full \mathbb{R} e.g. Liouville's, Weyl's and Feller's definition.

Only for the Riemann ${}_R D^\alpha$ and the Caputo ${}_C D^\alpha$ definition of a fractional derivative and only for the very special case of an infinite potential well centered at the origin the operator is not altered:

$${}_{\text{R}}^{\infty} D^\alpha = {}_{\text{R}}^{\square} D^\alpha \quad (12.19)$$

$${}_{\text{C}}^{\infty} D^\alpha = {}_{\text{C}}^{\square} D^\alpha \quad (12.20)$$

because the corresponding derivative definitions only cover the inside region of the potential well $0 \leq x \leq q$.

As a direct consequence, eigenfunctions of the free fractional Schrödinger equation based on the Riemann and Caputo derivative definition automatically determine the eigenfunctions of the same Schrödinger equation with infinite potential well fulfilling the additional constraint, that the functions should vanish at the boundaries of the infinite well.

These eigenfunctions ${}_{\text{R,C}}^{\infty} \Psi^{\pm}(x, \alpha)$ are known analytically, normalizable on \mathbb{R} for $\alpha < 2$ and are given in terms of the Mittag-Leffler functions $E_\alpha(z)$ and $E_{\alpha,\beta}(z)$ as:

$${}_{\text{R}}^{\infty} \Psi^+(x, \alpha) = x^{\frac{\alpha}{2}-1} E_{\alpha, \frac{\alpha}{2}}(-x^\alpha) \quad (12.21)$$

$${}_{\text{R}}^{\infty} \Psi^-(x, \alpha) = x^{\alpha-1} E_{\alpha, \alpha}(-x^\alpha) \quad (12.22)$$

$${}_{\text{C}}^{\infty} \Psi^+(x, \alpha) = E_\alpha(-x^\alpha) \quad (12.23)$$

$${}_{\text{C}}^{\infty} \Psi^-(x, \alpha) = x^{\frac{\alpha}{2}} E_{\alpha, 1+\frac{\alpha}{2}}(-x^\alpha) \quad 0 \leq \alpha \leq 2 \quad (12.24)$$

which reduce to the trigonometric functions for $\alpha = 2$ and the corresponding eigenvalues are determined from the zeros of these functions.

In contrast to this simple classical behavior we now consider the case of the fractional Schrödinger equation for the infinite potential well based on the Riesz definition of a fractional derivative. The following questions arise:

- are plain waves still a solution for the infinite potential well?
- if not, are they at least a good approximation?
- what do the exact solutions look like?

To answer these questions, we rearrange terms in the integral-operators I_n of the modified Riesz-operator ${}_{\text{RZ}}^{\square} D^\alpha$:

$$\left({}_{\text{RZ}}^{\square} D^\alpha (\infty \Psi) \right)(x) = \left(\Gamma(1 + \alpha) \frac{\sin(\pi\alpha/2)}{\pi} (I_1 + I_2 + I_3) \infty \Psi \right)(x) \quad (12.25)$$

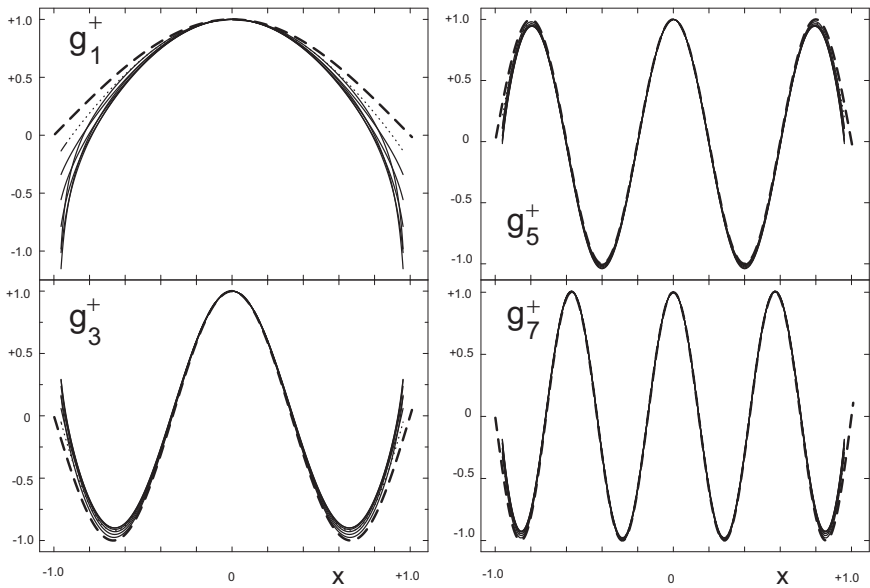


Fig. 12.1 The lowest solutions of ${}_{RZ}^{\square}D^{\alpha} \cos(\frac{k\pi}{2q}x) = Eg_k(\alpha, x)$ for $q = 1$ in the range (dashed line) $2 \geq \alpha \geq 0.25$ (dotted line) in $\Delta\alpha = 0.25$ steps. For the classical, local case $\alpha = 2$ the solution is indeed an eigenfunction, but for decreasing α deviations from $\cos(\frac{k\pi}{2q}x)$ become more and more pronounced. On the other hand, for large k the error becomes smaller and $\cos(\frac{k\pi}{2q}x)$ becomes a good first guess for the exact eigenfunction.

where I_n are given explicitly:

$$I_1\Psi(x) = \int_0^{q-x} \frac{\Psi(x+\xi) - 2\Psi(x) + \Psi(x-\xi)}{\xi^{\alpha+1}} d\xi \quad (12.26)$$

$$I_2\Psi(x) = \int_{q-x}^{q+x} \frac{\Psi(x-\xi)}{\xi^{\alpha+1}} d\xi \quad (12.27)$$

$$I_3\Psi(x) = \int_{q-x}^{\infty} \frac{-2\Psi(x)}{\xi^{\alpha+1}} d\xi = -2\Psi(x) \int_{q-x}^{\infty} \frac{1}{\xi^{\alpha+1}} d\xi \quad (12.28)$$

Using the test functions $\Psi^+(x) = \cos(\frac{k\pi}{2q}x)$ and $\Psi^-(x) = \sin(\frac{k\pi}{2q}x)$ we obtain with the help of [Abramowitz and Stegun (1965); Erdélyi et

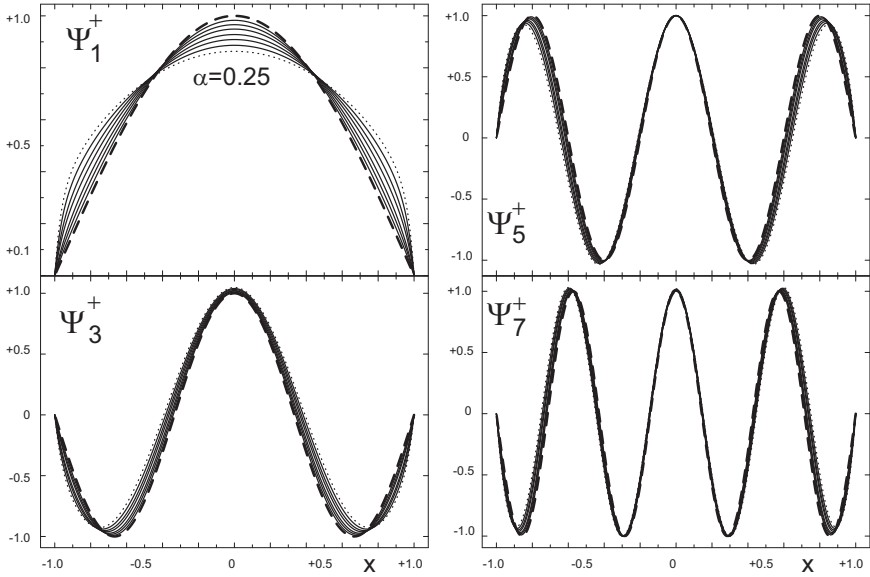


Fig. 12.2 The lowest numerically determined eigenfunctions $\Psi_k^+(\alpha, x)$ for $q = 1$ with positive parity for (dashed line) $2 \geq \alpha \geq 0.25$ (dotted line) in $\Delta\alpha = 0.25$ steps. Only in the limit $\Psi_k^+(\alpha \rightarrow 2, x) = \cos(\frac{k\pi}{2q}x)$ holds.

al. (1953)] and a cup of tea:

$$I_1 \begin{cases} \cos(\frac{k\pi}{2q}x) \\ \sin(\frac{k\pi}{2q}x) \end{cases} = \frac{(q-x)^{-\alpha}}{2\alpha} \left(\frac{k^2\pi^2}{\alpha-2} \left(\frac{q-x}{q} \right)^2 {}_1F_2 \left(1 - \frac{\alpha}{2}; \frac{3}{2}, 2 - \frac{\alpha}{2}; -k^2\pi^2 \left(\frac{q-x}{4q} \right)^2 \right) + 8 \sin^2 \left(k\pi \frac{q-x}{4q} \right) \right) \times \begin{cases} \cos(\frac{k\pi}{2q}x) \\ \sin(\frac{k\pi}{2q}x) \end{cases} \quad (12.29)$$

$$I_2 \begin{cases} \cos(\frac{k\pi}{2q}x) \\ \sin(\frac{k\pi}{2q}x) \end{cases} = \left(\frac{k\pi}{2q} \right)^\alpha \times \begin{cases} \operatorname{Re}(\Upsilon(x)) \\ -\operatorname{Im}(\Upsilon(x)) \end{cases} \quad (12.30)$$

$$I_3 \begin{cases} \cos(\frac{k\pi}{2q}x) \\ \sin(\frac{k\pi}{2q}x) \end{cases} = \frac{-2(q-x)^{-\alpha}}{\alpha} \times \begin{cases} \cos(\frac{k\pi}{2q}x) \\ \sin(\frac{k\pi}{2q}x) \end{cases} \quad (12.31)$$

with ${}_1F_2(a; b, c; x)$ is the hypergeometric function, $\operatorname{Re}(\Upsilon(x))$ is the real part and $\operatorname{Im}(\Upsilon(x))$ is the imaginary part of the complex function $\Upsilon(x)$ given by

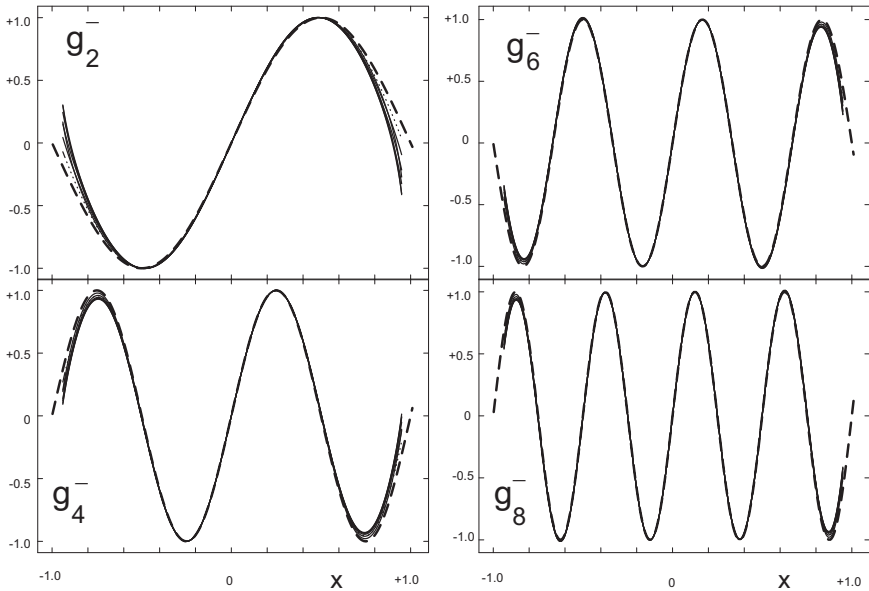


Fig. 12.3 The lowest solutions of ${}_{\text{RZ}}^{\square} D^{\alpha} \sin(\frac{k\pi}{2q}x) = E g_k(\alpha, x)$ for $q = 1$ in the range (dashed line) $2 \geq \alpha \geq 0.25$ (dotted line) in $\Delta\alpha = 0.25$ steps. For the classical, local case $\alpha = 2$ the solution is indeed an eigenfunction, but for decreasing α deviations from $\sin(\frac{k\pi}{2q}x)$ become more and more pronounced. On the other hand, for large k the error becomes smaller and $\sin(\frac{k\pi}{2q}x)$ becomes a good first guess for the exact eigenfunction.

$$\Upsilon(x) = e^{-i\frac{\pi}{2}(a+kx/q)} \left(\Gamma(-\alpha, -ik\pi \frac{q-x}{2q}) - \Gamma(-\alpha, -ik\pi \frac{q+x}{2q}) \right) \quad (12.32)$$

where $\Gamma(a, z)$ denotes the incomplete Γ -function on the complex plane.

The kinetic part of the fractional Schrödinger equation may therefore be calculated analytically and may be written with the test functions ${}^{\infty}\Psi^+(x) = \cos(\frac{k\pi}{2q}x)$ and ${}^{\infty}\Psi^-(x) = \sin(\frac{k\pi}{2q}x)$:

$${}_{\text{RZ}}^{\square} D^{\alpha} \cos(\frac{k\pi}{2q}x) = E g_k(x) \quad k = 1, 3, 5, \dots \quad (12.33)$$

$${}_{\text{RZ}}^{\square} D^{\alpha} \sin(\frac{k\pi}{2q}x) = E g_k(x) \quad k = 2, 4, 6, \dots \quad (12.34)$$

We define a pseudo-normalization condition

$$g_k(x=0) = 1 \quad k = 1, 3, 5, \dots \quad (12.35)$$

$$g_k(x=1/k) = 1 \quad k = 2, 4, 6, \dots \quad (12.36)$$

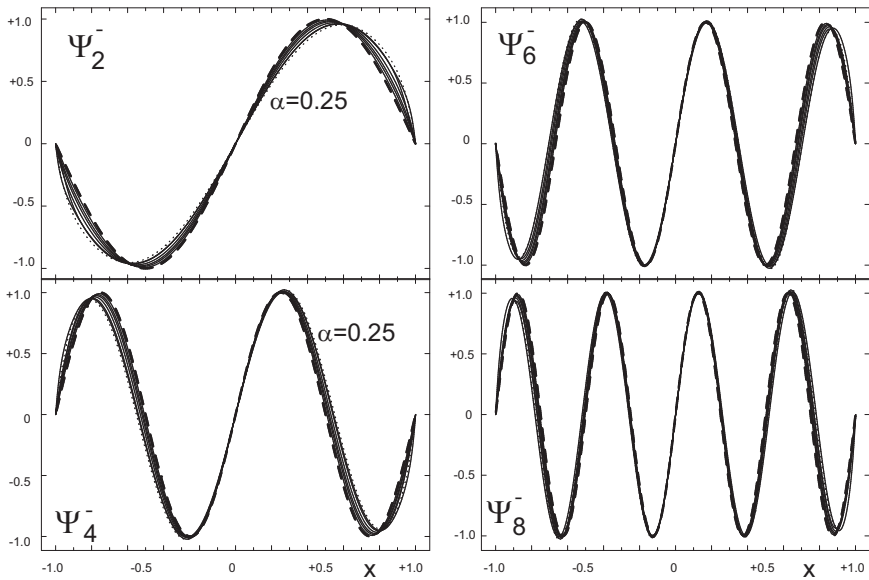


Fig. 12.4 The lowest numerically determined eigenfunctions $\Psi_k^-(\alpha, x)$ with negative parity for $q = 1$ in the range (dashed line) $2 \geq \alpha \geq 0.25$ (dotted line) in $\Delta\alpha = 0.25$ steps. Only in the limit $\Psi_k^-(\alpha \rightarrow 2, x) = \sin(\frac{k\pi}{2q}x)$ holds.

which allows to compare $g_k(x)$ with the trigonometric functions.

In figures 12.1 and 12.3 the results are sketched. The bad news is, that neither $g_k(x) = \cos(\frac{k\pi}{2q}x)$ nor $g_k(x) = \sin(\frac{k\pi}{2q}x)$ holds. Consequently the solutions of the free fractional Schrödinger equation based on the Riesz derivative definition are no eigenfunctions of the same fractional Schrödinger equation with infinite potential well. This answers the first question.

The good news is, that the deviations become more and more negligible for $k \gg 1$. This answers the second question: For large k , in the vicinity of $\alpha \approx 2$ and for $x \approx 0$ the trigonometric functions seem to be a good first guess.

As a consequence of the pseudo-normalization condition (12.35), we can give an analytic expression for the approximate energy spectrum. With

$${}_{\text{RZ}}^{\square} D^\alpha \cos\left(\frac{k\pi}{2q}x\right)|_{x=0} = E_k^{\sim}(\alpha) \quad k = 1, 3, 5, \dots \quad (12.37)$$

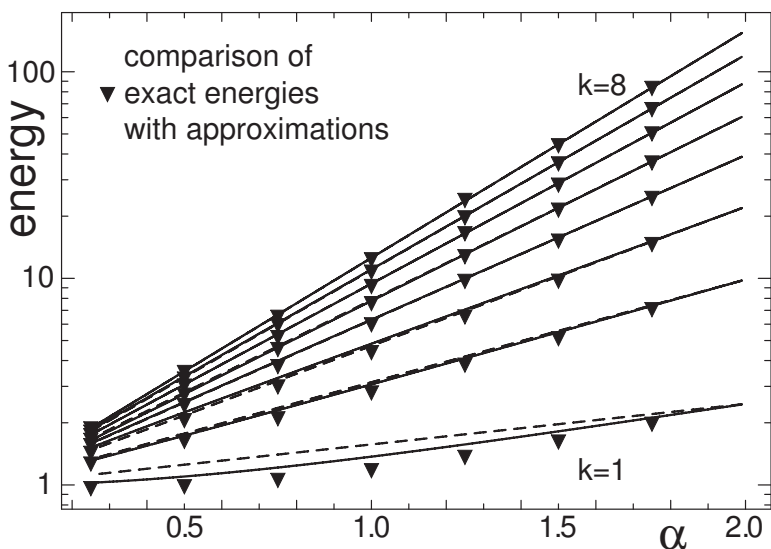


Fig. 12.5 A comparison of the numerically determined energy values (triangles) with approximate formulas $E_k^{\sim}(\alpha)$ from (12.38) (solid line) and $E_k^{\text{free}}(\alpha)$ from (12.7) (dashed line) normalized to $q = 1$.

we obtain (since I_2 vanishes for $x = 0$):

$$E_k^{\sim}(\alpha) = \frac{1}{2} q^{-\alpha} \Gamma(\alpha) \frac{\sin(\frac{\pi}{2}\alpha)}{\pi} \times \left(\frac{k^2 \pi^2}{2 - \alpha} {}_1F_2 \left(1 - \frac{\alpha}{2}; \frac{3}{2}, 2 - \frac{\alpha}{2}; -\frac{1}{16} k^2 \pi^2 \right) - 4 \cos \left(k \frac{\pi}{2} \right) \right) \quad (12.38)$$

which according to the above mentioned criteria will turn out to be a good approximation of the exact energy eigenvalues for large k in the vicinity of $\alpha \approx 2$.

12.2 The solution - numerical part

Since we have shown by explicit analytic evaluation of the fractional derivative, that the trigonometric functions are no eigenfunctions of the infinite potential well, but only good approximations, we will calculate the exact solutions numerically.

For that purpose, we expand the exact solution $\Psi_k^\pm(x)$ in a Taylor series

$$\Psi_k^+(x) = \lim_{N \rightarrow \infty} \sum_{n=0}^N a_{2n} x^{2n} \quad (12.39)$$

$$\Psi_k^-(x) = \lim_{N \rightarrow \infty} \sum_{n=0}^N a_{2n+1} x^{2n+1} \quad (12.40)$$

and insert it into the fractional Schrödinger equation for the infinite well potential:

$$-\frac{\square}{\text{RZ}} D^\alpha \Psi_k^\pm(x) = E_k \Psi_k^\pm(x) \quad (12.41)$$

The integrals on the left may be evaluated analytically and lead to transcendental functions in x , which then are expanded up to order N in a Taylor-series too. This leads to

$$\sum_{n=0}^N b_{2n} x^{2n} = E_k \sum_{n=0}^N a_{2n} x^{2n} \quad (12.42)$$

$$\sum_{n=0}^N b_{2n+1} x^{2n+1} = E_k \sum_{n=0}^N a_{2n+1} x^{2n+1} \quad (12.43)$$

A term by term comparison results in a system of nonlinear equations of the type $\{E_k a_n = b_n(a_n)\}$ on the set of variables $\{a_n, E_k\}$, which is solved numerically. For practical calculations we set $N = 20$, which yields an accuracy of the calculated energy levels of about 0.25% for the ground state.

Results are presented in figures 12.2 and 12.4. For $\alpha = 2$ we obtain the classical trigonometric functions. For decreasing α the eigenfunctions show a increasing tendency to shift towards the walls. This is exactly the behavior, which is not modeled by the trigonometric test functions presented in the last section. In figure 12.5 we compare the determined energy levels with the presented energy formulas. Especially $E_k^\sim(\alpha)$ from (12.38) is a useful approximation.

We have demonstrated, that the nonlocal character of the fractional operators used in the fractional Schrödinger equation indeed needs special attention. Concepts like box normalization, WKB-approximation or piecewise solution may work well in a classical local approach, but cause errors when applied to nonlocal problems.

On the other hand, we have shown, that such local strategies may lead to useful approximations e.g. in low-level ($\alpha = 2 - \epsilon$) fractional problems.

This may be understood from

$$\lim_{q \rightarrow \infty} {}^{\text{L}}_{\text{RZ}} D^{\alpha} = {}^{\infty}_{\text{RZ}} D^{\alpha} \quad (12.44)$$

as a consequence of the specific weight $w(\xi) = \frac{1}{\xi^{\alpha+1}}$ in the integral definition of the Riesz fractional derivative definition (13.2) with the property

$$\lim_{\xi \rightarrow \infty} w(\xi) = 0 \quad (12.45)$$

The infinite potential well serves as a helpful tool to demonstrate the consequences of different approaches.

Chapter 13

Uniqueness of a Fractional Derivative — the Riesz and Regularized Liouville Derivative as Examples

The concept of action-at-a-distance has dominated the interpretation of physical dynamic behavior in the early years of classical mechanics at the times of Kepler [Kepler (1609)] and Newton [Newton (1692)]. In the second half of the 19th century the introduction of a field, first successfully applied in the electromagnetic theory of Maxwell [Maxwell (1873)], has led to a change of paradigm away from the previously accepted nonlocal view to an emphasis of local aspects of a given interaction. This development found its culmination in the case of gravitational interaction with Einstein's geometric interpretation in terms of a space deformation [Adler et al. (1975)].

On the other hand, the increasing success of quantum theory since the beginning of the 20th century may be interpreted as a renaissance of nonlocal concepts in physics and at the time present the interest in nonlocal field theories is steadily growing.

A nonrelativistic description of quantum particles may be given using the Schrödinger wave equation. In this case, a new facet of nonlocality may be introduced extending the standard local Laplace operator by its nonlocal fractional pendant. Fractional calculus introduces the concept of nonlocality to arbitrary hitherto local operators. This is a new property, which only recently attracted attention on a broader basis.

Let the one dimensional fractional stationary Schrödinger equation in scaled canonical form be defined as

$$-\mathcal{D}_{\alpha/2} \Delta^{\alpha/2} \Psi(x) = (E - V(x)) \Psi(x) \quad (13.1)$$

where $\mathcal{D}_{\alpha/2}$ is a constant in units [$\text{MeV m}^\alpha \text{ s}^{-\alpha}$] and $\Delta^{\alpha/2}$ is the fractional Laplace-operator. The definition of a fractional order derivative is not

unique, several definitions e.g. the Riemann[Riemann (1847)], Caputo[Caputo (1967)], Riesz [Riesz (1949)], Feller[Feller (1952)] coexist and are equally well suited for an extension of the standard derivative.

In order to preserve Hermiticity for the fractional extension of the Laplace-operator [Laskin (2002)], we will explicitly consider the Riesz fractional derivative [Riesz (1949); Herrmann (2011)]:

$$\begin{aligned} \Delta^{\alpha/2} f(x) &\equiv {}_{RZ}^{\infty}\partial_x^{\alpha} f(x) & (13.2) \\ &= \Gamma(1 + \alpha) \frac{\sin(\pi\alpha/2)}{\pi} \int_0^{\infty} \frac{f(x + \xi) - 2f(x) + f(x - \xi)}{\xi^{\alpha+1}} d\xi \\ &\quad 0 < \alpha < 2 & (13.3) \end{aligned}$$

where the left superscript in ${}_{RZ}^{\infty}\partial_x^{\alpha}$ emphasizes the fact, that the integral domain is the full space \mathbb{R} and therefore explicitly denotes the nonlocal aspect of this definition.

Within this chapter we will investigate the uniqueness of this definition.

There is a common sense, that all the different definitions of fractional derivatives have certain common properties, e.g. a fractional derivative has to be an inverse operator to the corresponding fractional integral.

Within the following discourse we will choose a different approach: We will present differential representations of a fractional derivative, which are derived from binomial expansions of standard derivative operators.

We will show, that the eigenvalue spectrum of these fractional derivatives are equivalent to the one of the Riesz derivative, and therefore may be considered from a pragmatic point of view as local pendants of the standard integral representations.

Furthermore, these new definitions may be considered as a legitimization of e.g. piecewise solution of a fractional wave equation.

13.1 Uniqueness on a global scale - the integral representation of the Riesz derivative

In order to investigate the uniqueness of a definition of a fractional derivative we will consider the Riesz derivative as an example. In this section, we will investigate a set of generalized integral representations.

We may determine the Riesz derivative as a specific symmetrized nonlocal generalization of the standard second order derivative. We have

$${}_{\text{RZ}}^{\infty} \partial_x^{\alpha} f(x) = I^{\alpha} \partial_x^2 f(x) = I^{\alpha} f''(x) \quad (13.4)$$

$$= 2\Gamma(\alpha - 1) \frac{\sin(\pi\alpha/2)}{\pi} \int_0^{\infty} d\xi \xi^{1-\alpha} \frac{f''(x + \xi) + f''(x - \xi)}{2} \quad (13.5)$$

$$= 2\Gamma(\alpha) \frac{\sin(\pi\alpha/2)}{\pi} \int_0^{\infty} d\xi \xi^{1-\alpha} \frac{f'(x + \xi) - f'(x - \xi)}{2\xi} \quad (13.6)$$

$$= \Gamma(1 + \alpha) \frac{\sin(\pi\alpha/2)}{\pi} \int_0^{\infty} d\xi \xi^{1-\alpha} \frac{f(x + \xi) - 2f(x) + f(x - \xi)}{\xi^2} \quad (13.7)$$

which indeed looks as a unique definition for the Riesz fractional derivative. The eigenfunctions of this operator are the trigonometric functions and the eigenvalues are given by

$${}_{\text{RZ}}^{\infty} \partial_x^{\alpha} \sin(kx) = -|k|^{\alpha} \sin(kx) \quad (13.8)$$

$${}_{\text{RZ}}^{\infty} \partial_x^{\alpha} \cos(kx) = -|k|^{\alpha} \cos(kx) \quad (13.9)$$

Since (13.7) is nothing else but a weighted sum of the simplest central difference approximation of the second derivative:

$$f''(x) = \frac{f(x + \xi) - 2f(x) + f(x - \xi)}{\xi^2} + o(\xi^4) \quad (13.10)$$

we may consider more sophisticated definitions of the Riesz derivative as a result of using higher order accuracy approximations of the standard second order derivative, which are given as a finite series over $2N + 1$ elements

$$f''(x) = \frac{1}{\xi^2} \sum_{n=-N}^N a_n f(x + n\xi) + o(\xi^{2N+2}) \quad (13.11)$$

with the properties, resulting from the requirement of a vanishing second derivative for a constant function and invariance under parity transformation $\Pi(\pm\xi)$ with positive parity:

$$\sum_{n=-N}^N a_n = 0, \quad a_{-n} = a_n \quad (13.12)$$

In table 13.1 we have compiled the lowest representations of these finite series for $N = 1, \dots, 11$.

Therefore we may define the following generalization of the Riesz fractional derivative ${}_{\text{RZ}}^{\infty} \partial_x^{\alpha}$:

$${}_{\text{RZ}}^{\infty} \partial_x^{\alpha} f(x) = \Gamma(1 + \alpha) \frac{\sin(\pi\alpha/2)}{\pi} \int_0^{\infty} d\xi \xi^{1-\alpha} \sum_{n=-N}^N a_n f(x + n\xi) \frac{1}{\xi^2} \quad (13.13)$$

which at a first glance looks like a new family of fractional derivatives.

Table 13.1 Coefficients a_n for a central difference approximation of the second derivative of the form $\sum_{n=-N}^N a_n f(x + n\xi)$, from [Fornberg (1988)].

N	a_0	$a_{\pm 1}$	$a_{\pm 2}$	$a_{\pm 3}$	$a_{\pm 4}$	$a_{\pm 5}$	$a_{\pm 6}$	$a_{\pm 7}$	$a_{\pm 8}$	$a_{\pm 9}$	$a_{\pm 10}$	$a_{\pm 11}$
1	-2	1										
2	$-\frac{5}{2}$	$\frac{4}{3}$	$-\frac{1}{12}$									
3	$-\frac{49}{18}$	$\frac{3}{2}$	$-\frac{3}{20}$	$\frac{1}{90}$								
4	$-\frac{205}{72}$	$\frac{8}{5}$	$-\frac{1}{5}$	$\frac{8}{315}$	$-\frac{1}{560}$							
5	$-\frac{5269}{1800}$	$\frac{5}{3}$	$-\frac{5}{21}$	$\frac{5}{126}$	$-\frac{5}{1008}$	$\frac{1}{3150}$						
6	$-\frac{5369}{1800}$	$\frac{12}{7}$	$-\frac{15}{56}$	$\frac{10}{189}$	$-\frac{1}{112}$	$\frac{2}{1925}$	$-\frac{1}{16632}$					
7	$-\frac{266681}{88200}$	$\frac{7}{4}$	$-\frac{7}{24}$	$\frac{7}{108}$	$-\frac{7}{528}$	$\frac{7}{3300}$	$-\frac{7}{30888}$	$\frac{1}{84084}$				
8	$-\frac{1077749}{352800}$	$\frac{16}{9}$	$-\frac{14}{45}$	$\frac{112}{1485}$	$-\frac{7}{396}$	$\frac{112}{32175}$	$-\frac{2}{3861}$	$\frac{16}{315315}$	$-\frac{1}{411840}$			
9	$-\frac{9778141}{3175200}$	$\frac{9}{5}$	$-\frac{18}{55}$	$\frac{14}{165}$	$-\frac{63}{2860}$	$\frac{18}{3575}$	$-\frac{2}{2145}$	$\frac{9}{70070}$	$-\frac{9}{777920}$	$\frac{1}{1969110}$		
10	$-\frac{1968329}{635040}$	$\frac{20}{11}$	$-\frac{15}{44}$	$\frac{40}{429}$	$-\frac{15}{572}$	$\frac{24}{3575}$	$-\frac{5}{3432}$	$\frac{30}{119119}$	$-\frac{5}{155584}$	$\frac{10}{3741309}$	$-\frac{1}{9237800}$	
11	$-\frac{239437889}{76839840}$	$\frac{11}{6}$	$-\frac{55}{156}$	$\frac{55}{546}$	$-\frac{11}{364}$	$\frac{11}{1300}$	$-\frac{11}{5304}$	$\frac{55}{129948}$	$-\frac{55}{806208}$	$\frac{11}{1360476}$	$-\frac{11}{17635800}$	$\frac{1}{42678636}$

We will choose a pragmatic point of view and will investigate the eigenvalue spectrum of this set of operators. For that purpose, we use the following properties of the trigonometric functions [Abramowitz and Stegun (1965)]:

$$\sin(z_1 \pm z_2) = \sin(z_1) \cos(z_2) \pm \cos(z_1) \sin(z_2) \quad (13.14)$$

$$\cos(z_1 \pm z_2) = \cos(z_1) \cos(z_2) \mp \sin(z_1) \sin(z_2) \quad (13.15)$$

For $f(x) = \cos(kx)$ it follows with (13.12)

$$\sum_{n=-N}^N a_n \cos(k(x + n\xi)) = a_0 \cos(kx) \quad (13.16)$$

$$\begin{aligned} &+ \sum_{n=1}^N a_n (\cos(k(x - n\xi)) + \cos(k(x + n\xi))) \\ &= \cos(kx) (a_0 + 2 \sum_{n=1}^N a_n \cos(kn\xi)) \end{aligned} \quad (13.17)$$

as a consequence, $\cos(kx)$ is an eigenfunction of the generalized Riesz derivative operator ${}_{\text{N}}^{\infty} \partial_x^{\alpha}$. The same statement also holds for $\sin(kx)$. It follows:

$${}_{\text{N}}^{\infty} \partial_x^{\alpha} \exp(ikx) = \kappa \exp(ikx) \quad (13.18)$$

$${}_{\text{N}}^{\infty} \partial_x^{\alpha} \cos(kx) = \kappa \cos(kx) \quad (13.19)$$

$${}_{\text{N}}^{\infty} \partial_x^{\alpha} \sin(kx) = \kappa \sin(kx) \quad (13.20)$$

with the eigenvalue spectrum κ :

$$\kappa = \Gamma(1 + \alpha) \frac{\sin(\pi\alpha/2)}{\pi} \int_0^\infty d\xi \xi^{-1-\alpha} (a_0 + 2 \sum_{n=1}^N a_n \cos(kn\xi)) \quad (13.21)$$

For $n = 1$ we obtain the Riesz result $\kappa = -|k|^{\alpha}$.

For $n > 1$ since the integral covers the whole \mathbb{R}^+ , we may apply a coordinate transformation of the type $\nu\xi = \hat{\xi}$ to each term in the sum above. It then follows:

$$\kappa = \Gamma(1 + \alpha) \frac{\sin(\pi\alpha/2)}{\pi} \int_0^\infty d\xi \xi^{-1-\alpha} (a_0 + 2 \sum_{n=1}^N n^{\alpha} a_n \cos(k\xi)) \quad (13.22)$$

$$\begin{aligned} &= \Gamma(1 + \alpha) \frac{\sin(\pi\alpha/2)}{\pi} |k|^{\alpha} \int_0^\infty d\xi \xi^{-1-\alpha} (a_0 + 2 \sum_{n=1}^N n^{\alpha} a_n \cos(\xi)) \\ &= |k|^{\alpha} (a_0 + \sum_{n=1}^N n^{\alpha} a_n), \quad 0 < \alpha < 2 \end{aligned} \quad (13.23)$$

or in short hand notation:

$$\kappa = -\zeta_0(\alpha, N)|k|^\alpha \quad (13.24)$$

Up to a scaling constant $\zeta_0(\alpha, N) = -(a_0 + \sum_{n=1}^N n^\alpha a_n)$ the eigenvalue spectrum is identical with the original Riesz derivative eigenvalue spectrum (13.8)-(13.9) and may be absorbed by proper normalization of the generalized Riesz derivative definition. Therefore all generalized derivative definitions of type (13.13), which obey conditions (13.12) are equivalent and lead to same results. In that sense, the Riesz definition of a second order fractional derivative is indeed unique and emphasizes the nonlocal aspects of a fractional derivative.

It should be emphasized, that alternative realizations of the fractional Riesz derivative in terms of e.g. a central differences representation of Grünwald-Letnikov type are equivalent to the above integral representation in their nonlocal behavior [Ortigueira (2006); Ortigueira and Trujillo (2012)].

In the next section we will investigate the differential representation of the Riesz derivative and will demonstrate in a similar way as in the case of the integral representations that different approaches lead to the same result.

13.2 Uniqueness on a local scale - the differential representation of the Riesz derivative

Differential representations of the Riemann and Caputo fractional derivative in terms of a series expansion of integer derivatives are commonly known [Samko and Ross (1993a); Tarasov (2007); Tarasov (2008b)]. This approach emphasizes the local aspects of a fractional derivative, where we use a modified concept of locality determined in the following.

A corresponding series expansion for the Riesz derivative would lead to a differential representation of the same fractional derivative, which emphasizes local aspects too and therefore may be considered as a new definition of a local fractional derivative.

Indeed there are several strategies to derive a differential representation of the Riesz derivative. Let us begin with the fractional extension of the binomial series [Abramowitz and Stegun (1965); Liu (2010)]:

$$\partial_x^\alpha = \lim_{\omega \rightarrow 0} (\partial_x + \omega)^\alpha = \lim_{\omega \rightarrow 0} \sum_{j=0}^{\infty} \binom{\alpha}{j} \omega^{\alpha-j} \partial_x^j \quad \alpha \in \mathbb{R} \quad (13.25)$$

where ω is an arbitrary real number. We consider this operator as well defined, as long as the series is convergent in the limit $\omega \rightarrow 0$ on a specific function class. It is not a trivial task, to determine general function classes, which fulfill this requirement, but in the following we will demonstrate, that at least for the important case of the trigonometric functions $\cos(\omega t)$ and $\sin(\omega t)$ series of this type lead to reasonable results.

In case of convergence, series of this type may be called local in the following sense:

For a given $M \in \mathbb{N}$ for the M -th term in the above series expansion the integer derivative is defined as a finite sum of e.g. backward differences (with Δ is the backward difference operator):

$$\partial_x^M f(x) = \lim_{h \rightarrow 0} \frac{\Delta^M f(x)}{h^M} = \lim_{h \rightarrow 0} \left(\sum_{m=0}^M \binom{M}{m} (-1)^m f(x - mh) \right) / h^M \quad (13.26)$$

which for all $h < \epsilon/M$ is located within an area of size ϵ and therefore may be considered as a local quantity. Therefore (13.25) is considered in the case $M \rightarrow \infty$ as an infinite sum of local terms which itself determines a definition of locality, which is used in the following.

Of course, the collected information is equivalent to a full Taylor series expansion of $f(x)$ and therefore equivalent to the knowledge of the function $f(x)$ within the whole region of convergence, which may be considered nonlocal in a classical sense.

Motivated by the correspondence

$$\lim_{\alpha \rightarrow 2} {}_{RZ} \partial_x^\alpha = \partial_x^2 \quad (13.27)$$

which holds for the Riesz derivative, we extend the above binomial series to

$$\overset{\triangle}{2} \partial_x^\alpha = \lim_{\omega \rightarrow 0} (\partial_x^2 + \omega^2)^{\alpha/2} \quad (13.28)$$

$$= \lim_{\omega \rightarrow 0} \sum_{j=0}^{\infty} \binom{\alpha/2}{j} (\omega^2)^{\alpha/2-j} \partial_x^{2j} \quad (13.29)$$

$$= \lim_{\omega \rightarrow 0} |\omega|^\alpha \sum_{j=0}^{\infty} \binom{\alpha/2}{j} |\omega|^{-2j} \partial_x^{2j} \quad \alpha \in \mathbb{R} \quad (13.30)$$

where the superscript $\overset{\triangle}{2}$ emphasizes the differential representation of an hitherto integral representation of a fractional derivative operator ∂_x^α .

Applying this operator to the exponential function leads to:

$${}_2^{\triangle} \partial_x^\alpha \exp(kx) = \lim_{\omega \rightarrow 0} \sum_{j=0}^{\infty} \binom{\alpha/2}{j} (\omega^2)^{\alpha/2-j} k^{2j} \exp(kx) \quad (13.31)$$

$$= \lim_{\omega \rightarrow 0} (k^2 + \omega^2)^{\alpha/2} \exp(kx) \quad (13.32)$$

$$= |k|^\alpha \exp(kx) \quad \alpha \in \mathbb{R} \quad (13.33)$$

Consequently we interpret this operator as the hyperbolic Riesz derivative, since it works for $k \in \mathbb{R}$, while the original Riesz derivative in its integral form is divergent for $\exp(kx)$ but converges for $\exp(ikx)$.

Therefore in an heuristic approach we obtain as a differential representation of the Riesz derivative:

$${}_{\text{RZ}}^{\triangle} \partial_x^\alpha = \lim_{\omega \rightarrow 0} -|\omega|^\alpha \sum_{j=0}^{\infty} \binom{\alpha/2}{j} |\omega|^{-2j} (i\partial_x)^{2j} \quad (13.34)$$

$$= \lim_{\omega \rightarrow 0} -|\omega|^\alpha \sum_{j=0}^{\infty} \binom{\alpha/2}{j} |\omega|^{-2j} (-1)^j \partial_x^{2j} \quad (13.35)$$

which we call a valid realization of the differential form of the Riesz fractional derivative.

Indeed it follows in accordance with (13.8)-(13.9):

$${}_{\text{RZ}}^{\triangle} \partial_x^\alpha \exp(ikx) = -|k|^\alpha \exp(ikx) \quad (13.36)$$

$${}_{\text{RZ}}^{\triangle} \partial_x^\alpha \cos(kx) = -|k|^\alpha \cos(kx) \quad (13.37)$$

$${}_{\text{RZ}}^{\triangle} \partial_x^\alpha \sin(kx) = -|k|^\alpha \sin(kx) \quad \alpha \in \mathbb{R} \quad (13.38)$$

Since we have realized the differential form of the Riesz derivative as the limit of a series we will answer the question if other series may yield the same result.

As a demonstration, we use the fractional extension of the Leibniz product rule [Watanabe (1931); Osler (1970)]

$$\partial_x^\alpha (u(x)v(x)) = \sum_{j=0}^{\infty} \binom{\alpha}{j} (\partial_x^{\alpha-j} u(x)) (\partial_x^j v(x)) \quad (13.39)$$

and rewrite the analytic function $f(x) = u(x)v(x)$ as

$$f(x) = \lim_{\omega \rightarrow 0} \cos(\omega x) f(x) \quad (13.40)$$

With (13.9) we first calculate:

$${}_{\text{RZ}}\partial_x^{\alpha-j} \lim_{\omega \rightarrow 0} \cos(\omega x) = \lim_{\omega \rightarrow 0} (\partial_x^{-j} {}_{\text{RZ}}\partial_x^\alpha) \cos(\omega x) \quad (13.41)$$

$$= \lim_{\omega \rightarrow 0} -|\omega|^\alpha \partial_x^{-j} \cos(\omega x) \quad (13.42)$$

$$= \lim_{\omega \rightarrow 0} -|\omega|^\alpha \omega^{-j} \cos(\omega x - \frac{\pi}{2} j) \quad (13.43)$$

$$= \lim_{\omega \rightarrow 0} -|\omega|^\alpha \omega^{-j} \cos(-\frac{\pi}{2} j) \quad (13.44)$$

$$= \lim_{\omega \rightarrow 0} -|\omega|^\alpha \omega^{-j} \begin{cases} 0 & j \text{ odd} \\ (-1)^{j/2} & j \text{ even} \end{cases} \quad (13.45)$$

Using the Leibniz product rule we hence obtain:

$${}_{\text{2}}\triangle \partial_x^\alpha = \lim_{\omega \rightarrow 0} \sum_{j=0}^{\infty} \binom{\alpha}{j} (\partial_x^{\alpha-j} \cos(\omega x)) \partial_x^j \quad (13.46)$$

$$= -\lim_{\omega \rightarrow 0} |\omega|^\alpha \sum_{j=0}^{\infty} \binom{\alpha}{2j} \omega^{-2j} (-1)^j \partial_x^{2j} \quad (13.47)$$

$$= -\lim_{\omega \rightarrow 0} |\omega|^\alpha {}_2F_1\left(\frac{1}{2} - \frac{\alpha}{2}, -\frac{\alpha}{2}; \frac{1}{2}; -\frac{1}{\omega^2} \partial_x^2\right) \quad (13.48)$$

Lets apply this operator to the exponential function:

$$\begin{aligned} {}_{\text{2}}\triangle \partial_x^\alpha \exp(kx) &= -\lim_{\omega \rightarrow 0} |\omega|^\alpha {}_2F_1\left(\frac{1}{2} - \frac{\alpha}{2}, -\frac{\alpha}{2}; \frac{1}{2}; -\frac{k^2}{\omega^2}\right) \exp(kx) \\ &= -|k|^\alpha \cos(\alpha\pi/2) \exp(kx) \end{aligned} \quad (13.49)$$

where we have used (15.3.7) and (15.1.8) from [Abramowitz and Stegun (1965)].

Once again, we may consider this operator as an alternative realization of a hyperbolic Riesz derivative, since it works for $k \in \mathbb{R}$, while the original Riesz derivative in its integral form is divergent for $\exp(kx)$ but converges for $\exp(ikx)$.

Therefore we define a differential representation of the Riesz derivative heuristically:

$${}_{\text{RZ}}\partial_x^\alpha = -\frac{1}{\cos(\alpha\pi/2)} \lim_{\omega \rightarrow 0} |\omega|^\alpha \sum_{j=0}^{\infty} \binom{\alpha}{2j} \omega^{-2j} \partial_x^{2j} \quad (13.50)$$

$$= -\frac{1}{\cos(\alpha\pi/2)} \lim_{\omega \rightarrow 0} |\omega|^\alpha {}_2F_1\left(\frac{1}{2} - \frac{\alpha}{2}, -\frac{\alpha}{2}; \frac{1}{2}; \frac{1}{\omega^2} \partial_x^2\right) \quad (13.51)$$

with the same eigenfunctions and eigenvalue spectrum (13.36)-(13.38).

Hence we have demonstrated, that indeed there exist distinct differential representations, which in the limit $\omega \rightarrow 0$ lead to the same eigenvalue spectrum.

With (13.35) and (13.51) we have presented two different realizations of a differential representation of the Riesz derivative as a limiting case of two different series expansions in terms of integer derivatives.

At least in the case of the trigonometric functions $\sin(kx)$ and $\cos(kx)$ and therefore for every Fourier series these series are convergent and valid for all $\alpha \in \mathbb{R}$ and thus are more robust than their integral counterparts, where the range of allowed α values is restricted to $0 < \alpha < 2$.

13.3 Manifest covariant differential representation of the Riesz derivative on \mathbb{R}^N

A straightforward extension of e.g. (13.51) to the N-dimensional case is given by

$$\overset{\triangle}{\text{RZ}} \Delta_N^{\alpha/2} = -\frac{1}{\cos(\alpha\pi/2)} \lim_{\omega \rightarrow 0} |\omega|^\alpha {}_2F_1\left(\frac{1}{2} - \frac{\alpha}{2}, -\frac{\alpha}{2}; \frac{1}{2}; \frac{\Delta}{\omega^2}\right) \quad (13.52)$$

with the N-dimensional Laplace-operator Δ in Cartesian coordinates on \mathbb{R}^N

$$\Delta\Psi = \sum_{n=1}^N \partial_{x_n}^2 \Psi \quad N \in \mathbb{N} \quad (13.53)$$

The eigenfunctions and the eigenvalue spectrum of this differential representation of the N-dimensional Riesz derivative are then given by:

$$\overset{\triangle}{\text{RZ}} \Delta_N^{\alpha/2} \prod_{n=1}^N \exp(ik_n x_n) = -\left(\sum_{n=1}^N k_n^2\right)^{\alpha/2} \prod_{n=1}^N \exp(ik_n x_n) \quad (13.54)$$

which coincides with the standard result using the standard integral representation.

In a similar approach we may extend (13.35) to the N-dimensional case:

$$\overset{\triangle}{\text{RZ}} \Delta_N^{\alpha/2} = \lim_{\omega \rightarrow 0} -|\omega|^\alpha \sum_{j=0}^{\infty} \binom{\alpha/2}{j} |\omega|^{-2j} (-1)^j \Delta^j \quad (13.55)$$

Since the Laplace-operator applied on an arbitrary analytic function may be derived for any set of coordinates, where the metric tensor g_{ij} is known

[Adler *et al.* (1975)] e.g. for a scalar field Ψ :

$$\Delta\Psi = \nabla^j \nabla_j \Psi \quad (13.56)$$

$$= g^{ij} \nabla_i \nabla_j \Psi \quad i, j = 1, \dots, N \quad (13.57)$$

$$= g^{ij} (\partial_i \partial_j - \left\{ \begin{matrix} k \\ ij \end{matrix} \right\} \partial_k) \Psi \quad (13.58)$$

$$= \frac{1}{\sqrt{g}} \partial_i g^{ij} \sqrt{g} \partial_j \Psi \quad (13.59)$$

where $\left\{ \begin{matrix} k \\ ij \end{matrix} \right\}$ is the Christoffel symbol

$$\left\{ \begin{matrix} k \\ ij \end{matrix} \right\} = \frac{1}{2} g^{kl} (\partial_i g_{jl} + \partial_j g_{il} - \partial_l g_{ij}) \quad (13.60)$$

g is the determinant of the metric tensor, $g = \det g_{ij}$ and ∇_n is the covariant derivative, defined for a tensor of rank k as

$$\nabla_n T_{b_1 b_2 \dots b_s}^{a_1 a_2 \dots a_r} = T_{b_1 b_2 \dots b_s || n}^{a_1 a_2 \dots a_r} \quad (13.61)$$

$$= \partial_n T_{b_1 b_2 \dots b_s}^{a_1 a_2 \dots a_r}$$

$$+ \left\{ \begin{matrix} a_1 \\ np \end{matrix} \right\} T_{b_1 b_2 \dots b_s}^{pa_2 \dots a_r} + \left\{ \begin{matrix} a_2 \\ np \end{matrix} \right\} T_{b_1 b_2 \dots b_s}^{a_1 p \dots a_r} + \dots + \left\{ \begin{matrix} a_r \\ np \end{matrix} \right\} T_{b_1 b_2 \dots b_s}^{a_1 a_2 \dots p} \\ - \left\{ \begin{matrix} p \\ b_1 n \end{matrix} \right\} T_{pb_2 \dots b_s}^{a_1 a_2 \dots a_r} - \left\{ \begin{matrix} p \\ b_2 n \end{matrix} \right\} T_{b_1 p \dots b_s}^{a_1 a_2 \dots a_r} - \dots - \left\{ \begin{matrix} p \\ b_s n \end{matrix} \right\} T_{b_1 b_2 \dots p}^{a_1 a_2 \dots a_r}$$

$$a_1, \dots, a_r, b_1, \dots, b_s, c, p \in 1, 2, \dots, N \quad (13.62)$$

The simplest cases are

(rank 0) scalar fields ψ

$$\nabla_n \psi = \psi_{||n} = \psi_{|n} = \partial_n \psi \quad (13.63)$$

(rank 1) contravariant or covariant vector fields ψ^m or ψ_m

$$\nabla_n \psi^m = \psi_{||n}^m = \partial_n \psi^m + \left\{ \begin{matrix} m \\ np \end{matrix} \right\} \psi^p \quad (13.64)$$

$$\nabla_n \psi_m = \psi_{m||n} = \partial_n \psi_m - \left\{ \begin{matrix} p \\ mn \end{matrix} \right\} \psi_p$$

(rank 2) tensor fields ψ^{mq} , $\psi^m{}_q$ or ψ_{mq}

$$\nabla_n \psi^{mq} = \psi_{||n}^{mq} = \partial_n \psi^{mq} + \left\{ \begin{matrix} m \\ np \end{matrix} \right\} \psi^{pq} + \left\{ \begin{matrix} q \\ np \end{matrix} \right\} \psi^{mp} \quad (13.65)$$

$$\nabla_n \psi^m{}_q = \psi^m{}_{q||n} = \partial_n \psi^m{}_q + \left\{ \begin{matrix} m \\ np \end{matrix} \right\} \psi^p{}_q - \left\{ \begin{matrix} p \\ mn \end{matrix} \right\} \psi^m{}_p$$

$$\nabla_n \psi_{mq} = \psi_{mq||n} = \partial_n \psi_{mq} - \left\{ \begin{matrix} p \\ mn \end{matrix} \right\} \psi_{mp} - \left\{ \begin{matrix} p \\ qn \end{matrix} \right\} \psi_{pq}$$

From (13.63) and (13.65) we can easily verify (13.56).

A first direct practical consequence of using either of these differential representations follows from the fact, that the eigenfunctions of the free standard Schrödinger equation ψ_0 in curvilinear coordinates $\vec{\chi}$ [Moon and Spencer (1988)]

$$-\mathcal{D}\Delta\psi_0(\vec{\chi}) = e_0\psi_0(\vec{\chi}) \quad (13.66)$$

are solutions of the free fractional Schrödinger equation too:

$$-\mathcal{D}_{\alpha/2}\Delta^{\alpha/2}\psi_0(\vec{\chi}) = E\psi_0(\vec{\chi}) \quad (13.67)$$

As a consequence, the eigenvalues of the free fractional Schrödinger equation using the differential representation of the Riesz derivative definition follow directly as

$$E = \mathcal{D}_{\alpha/2}|e_0|^{\alpha/2} \quad (13.68)$$

without any effort. In this generality, a result of fundamental importance for the investigation of the properties of second order fractional wave equations in curvilinear coordinates.

With (13.52) and (13.55) we have therefore presented two optional candidates which may considered for a differential representation of a valid covariant realization of the Riesz fractional derivative of a tensor of rank k on the Riemannian space.

It is important to mention, that these representations are realized as series in terms of standard derivatives and therefore determine a local version of the fractional derivative, since information is required only within an ϵ -region around x . The use of a fractional derivative does not automatically imply nonlocality.

As a consequence, using the differential representations of the Riesz derivative, it seems a valid procedure to generate piecewise steady solutions of a Riesz type fractional Schrödinger equation even though in a way this contradicts Feynman's view of a path integral formulation of quantum mechanics.

Consequently while in standard quantum mechanics Schrödinger's wave equation as a local view and Feynman's path integral approach as a non-local view lead to equivalent results, in fractional quantum mechanics this equivalence obviously is lost and leads to different results [Laskin (2002); Luchko (2013)].

Hence using the Riesz fractional derivative given in terms of either the integral or the differential representation indeed makes a difference in e.g.

fractional wave equations. Emphasizing fundamentally different aspects of a local or nonlocal approach to physical problems the use of the Riesz fractional derivative in either form revives the discussion of concepts like action-at-a-distance.

To be clear in the argument, the Riesz derivative is known as an integral operator and therefore is nonlocal and the resulting eigenfunctions for the e.g. fractional Schrödinger equation differ for the free and e.g. infinite potential well case. On the other hand, the proposed local versions are local and therefore the free and potential well eigenfunctions are the same. The consequence is simple: The proposed local form is not conformal with the original Riesz derivative but defines an alternative new type of a fractional derivative.

We also conclude, that the standard approach introducing a fractional derivative ∂_x^α via the connection to fractional integrals $I^\alpha(x)$, see chapter 5

$$\partial_x^\alpha = I^{-\alpha}(x) \quad (13.69)$$

with the well known consequence of being nonlocal, is only one option to give a reasonable definition of a fractional derivative. As a consequence, the presented differential realizations of a Riesz type derivative may be preferably considered as new definitions of a new type of fractional derivatives.

13.4 The integral representation of the regularized Liouville derivative

In the last section we have presented some properties of the Riesz derivative, which is an example for a symmetric summation of the standard second derivative approximation based on central differences. Now we want to investigate the corresponding first derivative. The integral representation is given by (5.79),(8.52)

$${}_{\text{RL}}^{\infty} \partial_x^\alpha f(x) = I^\alpha \partial_x f(x) = I^\alpha f'(x) \quad (13.70)$$

$$= 2\Gamma(\alpha) \frac{\cos(\pi\alpha/2)}{\pi} \int_0^\infty d\xi \xi^{-\alpha} \frac{f'(x+\xi) + f'(x-\xi)}{2} \quad (13.71)$$

$$= 2\Gamma(1+\alpha) \frac{\cos(\pi\alpha/2)}{\pi} \int_0^\infty d\xi \xi^{-\alpha} \frac{f(x+\xi) - f(x-\xi)}{2\xi} \quad (13.72)$$

$0 < \alpha < 1$

which we call the regularized Liouville ${}_{\text{RL}}^{\infty} \partial_x^\alpha$ and asymmetric case of the Feller($\theta = 1$) derivative respectively. The eigenfunctions of this operator

are the trigonometric functions and the eigenvalues are given by

$${}_{\text{RL}}^{\infty} \partial_x^{\alpha} \sin(kx) = +\text{sign}(k)|k|^{\alpha} \cos(kx) \quad (13.73)$$

$${}_{\text{RL}}^{\infty} \partial_x^{\alpha} \cos(kx) = -\text{sign}(k)|k|^{\alpha} \sin(kx) \quad (13.74)$$

Equation (13.72) may be considered as a weighted sum of the simplest central difference approximation of the first derivative:

$$f'(x) = \frac{f(x + \xi) - f(x - \xi)}{2\xi} + o(\xi^3) \quad (13.75)$$

More sophisticated definitions of the regularized Liouville derivative as a result of higher order accuracy approximations of the standard first order derivative are given as a finite series over $2N + 1$ elements

$$f'(x) = \frac{1}{\xi} \sum_{n=-N}^N a_n f(x + n\xi) + o(\xi^{2N+1}) \quad (13.76)$$

with the properties, resulting from the requirement of a vanishing first derivative for a constant function and invariance under parity transformation $\Pi(\pm\xi)$ with negative parity:

$$a_0 = 0, \quad a_{-n} = -a_n \quad (13.77)$$

In table 13.2 we have compiled the lowest representations of these finite series for $N = 1, \dots, 12$.

Let us therefore investigate the following generalization of the regularized Liouville derivative: ${}_{\text{N}}^{\infty} \partial_x^{\alpha}$:

$$\begin{aligned} {}_{\text{N}}^{\infty} \partial_x^{\alpha} f(x) &= 2\Gamma(1 + \alpha) \frac{\cos(\pi\alpha/2)}{\pi} \\ &\times \int_0^{\infty} d\xi \xi^{-\alpha} \sum_{n=-N}^N a_n f(x + n\xi) \frac{1}{\xi} \end{aligned} \quad (13.78)$$

For $f(x) = \sin(kx)$ we first obtain with (13.77) and (13.14):

$$\begin{aligned} \sum_{n=-N}^N a_n \sin(k(x + n\xi)) &= \sum_{n=1}^N a_n (\sin(k(x + n\xi)) - \sin(k(x - n\xi))) \\ &= 2 \cos(kx) \sum_{n=1}^N a_n \sin(kn\xi) \end{aligned} \quad (13.79)$$

As a consequence for the generalized regularized Liouville derivative the eigenvalue spectrum follows from:

$${}_{\text{N}}^{\infty} \partial_x^{\alpha} \exp(ikx) = \kappa \exp(ikx) \quad (13.80)$$

$${}_{\text{N}}^{\infty} \partial_x^{\alpha} \sin(kx) = \kappa \cos(kx) \quad (13.81)$$

$${}_{\text{N}}^{\infty} \partial_x^{\alpha} \cos(kx) = -\kappa \sin(kx) \quad (13.82)$$

Table 13.2 Coefficients a_n for a central difference approximation of the first derivative of the form $\sum_{n=-N}^N a_n f(x+n\xi)$ with $a_{-n} = -a_n$, calculated with [Fornberg (1988)].

N	a_1	a_2	a_3	a_4	a_5	a_6	a_7	a_8	a_9	a_{10}	a_{11}	a_{12}
1	$\frac{1}{2}$											
2	$\frac{2}{3}$	$-\frac{1}{12}$										
3	$\frac{3}{4}$	$-\frac{3}{20}$	$\frac{1}{60}$									
4	$\frac{4}{15}$	$-\frac{1}{5}$	$\frac{4}{105}$	$-\frac{1}{280}$								
5	$\frac{5}{6}$	$-\frac{5}{21}$	$\frac{5}{84}$	$-\frac{5}{504}$	$\frac{1}{1260}$							
6	$\frac{6}{7}$	$-\frac{15}{56}$	$\frac{5}{63}$	$-\frac{1}{56}$	$\frac{1}{385}$	$-\frac{1}{5544}$						
7	$\frac{7}{8}$	$-\frac{7}{24}$	$\frac{7}{72}$	$-\frac{7}{264}$	$\frac{7}{1320}$	$-\frac{7}{10296}$	$\frac{1}{24024}$					
8	$\frac{8}{9}$	$-\frac{14}{45}$	$\frac{56}{495}$	$-\frac{7}{198}$	$\frac{56}{6435}$	$-\frac{2}{1287}$	$\frac{8}{45045}$	$-\frac{1}{102960}$				
9	$\frac{9}{10}$	$-\frac{18}{55}$	$\frac{7}{55}$	$-\frac{63}{1430}$	$\frac{9}{715}$	$-\frac{2}{715}$	$\frac{9}{20020}$	$-\frac{9}{194480}$	$\frac{1}{437580}$			
10	$\frac{10}{11}$	$-\frac{15}{44}$	$\frac{20}{143}$	$-\frac{15}{286}$	$\frac{12}{715}$	$-\frac{5}{1144}$	$\frac{15}{17017}$	$-\frac{5}{38896}$	$\frac{5}{415701}$	$-\frac{1}{1847560}$		
11	$\frac{11}{12}$	$-\frac{55}{156}$	$\frac{55}{364}$	$-\frac{11}{182}$	$\frac{11}{520}$	$-\frac{11}{1768}$	$\frac{55}{37128}$	$-\frac{55}{201552}$	$\frac{11}{302328}$	$-\frac{11}{3527160}$	$\frac{1}{7759752}$	
12	$\frac{12}{13}$	$-\frac{33}{91}$	$\frac{44}{273}$	$-\frac{99}{1456}$	$\frac{198}{7735}$	$-\frac{11}{1326}$	$\frac{66}{29393}$	$-\frac{33}{67184}$	$\frac{22}{264537}$	$-\frac{3}{293930}$	$\frac{6}{7436429}$	$-\frac{1}{32449872}$

with:

$$\kappa = 4\Gamma(1+\alpha) \frac{\cos(\pi\alpha/2)}{\pi} \int_0^\infty d\xi \xi^{-1-\alpha} \sum_{n=1}^N a_n \sin(kn\xi) \quad (13.83)$$

For $n = 1$ we obtain the result $\kappa = \text{sign}(k)|k|^\alpha$.

For $n > 1$ since the integral covers the whole \mathbb{R}^+ , we may apply a coordinate transformation of the type $\nu\xi = \hat{\xi}$ to each term in the sum above. It then follows:

$$\begin{aligned} \kappa &= 4\Gamma(1+\alpha) \frac{\cos(\pi\alpha/2)}{\pi} \int_0^\infty d\xi \xi^{-1-\alpha} \sum_{n=1}^N n^\alpha a_n \sin(k\xi) \\ &= 4\Gamma(1+\alpha) \frac{\cos(\pi\alpha/2)}{\pi} \text{sign}(k)|k|^\alpha \int_0^\infty d\xi \xi^{-1-\alpha} \sum_{n=1}^N n^\alpha a_n \sin(\xi) \\ &= \text{sign}(k)|k|^\alpha \sum_{n=1}^N n^\alpha a_n, \quad 0 < \alpha < 1 \end{aligned} \quad (13.84)$$

or in short hand notation:

$$\kappa = -\zeta(\alpha, N)\text{sign}(k)|k|^\alpha \quad (13.85)$$

Therefore all generalized derivative definitions of type (13.78), which obey conditions (13.77) are equivalent and lead to same results. In that sense, the regularized Liouville definition of a symmetric first order fractional derivative is indeed unique and emphasizes the nonlocal aspects of a fractional derivative.

13.5 Differential representation of the regularized Liouville derivative

Differential representations of the Riesz derivative have been already given in the previous sections. In order to present the corresponding representations for the regularized Liouville derivative, we simply compare (13.6) and (13.72). We deduce the relation

$${}_{\text{RL}}\partial_x^\alpha = {}_{\text{RZ}}\partial_x^\alpha \partial^{-1} \quad (13.86)$$

which means, that the use of the regularized Liouville derivative is equivalent to an application of the standard integral followed by the Riesz derivative. Indeed for the eigenvalue spectrum of the regularized Liouville derivative we may deduce the relation:

$${}_{\text{RL}}\partial_x^\alpha \sin kx = \text{sign}(k)|k|^\alpha \cos(kx) \quad 0 < \alpha < 1 \quad (13.87)$$

$$= \frac{|k|^\alpha}{k} \cos(kx) = \frac{(k^2)^{\alpha/2}}{k} \cos(kx) \quad 0 < \alpha < 2 \quad (13.88)$$

Therefore we may use (13.35) to obtain a first valid differential representation:

$$\overset{\triangle}{_{\text{RL}}\partial_x^\alpha} = \lim_{\omega \rightarrow 0} -|\omega|^\alpha \sum_{j=0}^{\infty} \binom{\alpha/2}{j} |\omega|^{-2j} (i\partial_x)^{2j} (i\partial_x)^{-1} \quad (13.89)$$

$$= \lim_{\omega \rightarrow 0} -|\omega|^\alpha \sum_{j=1}^{\infty} \binom{\alpha/2}{j} |\omega|^{-2j} (i\partial_x)^{2j-1} \quad (13.90)$$

which explicitly emphasizes the fact that in the limit $\omega \rightarrow 0$ the term with $j = 0$ vanishes, since it is of order $\sim |\omega|^\alpha$. Therefore the leading term in the series is of order $\sim \partial_x$.

A second differential representation of the regularized Liouville derivative follows with (13.51):

$$\overset{\triangle}{\partial_x^\alpha} = -\frac{1}{\cos(\alpha\pi/2)} \lim_{\omega \rightarrow 0} |\omega|^\alpha \sum_{j=0}^{\infty} \binom{\alpha}{2j} \omega^{-2j} \partial_x^{2j} (-i\partial_x^{-1}) \quad (13.91)$$

$$= -\frac{1}{\cos(\alpha\pi/2)} \lim_{\omega \rightarrow 0} |\omega|^\alpha {}_2F_1\left(\frac{1}{2} - \frac{\alpha}{2}, -\frac{\alpha}{2}; \frac{1}{2}; \frac{1}{\omega^2} \partial_x^2\right) (-i\partial_x^{-1})$$

$$= \frac{1-\alpha}{\cos(\alpha\pi/2)} \lim_{\omega \rightarrow 0} |\omega|^{\alpha-2} {}_2F_1\left(\frac{3}{2} - \frac{\alpha}{2}, 1 - \frac{\alpha}{2}; \frac{3}{2}; \frac{1}{\omega^2} \partial_x^2\right) (i\partial_x) \quad 0 < \alpha < 2 \quad (13.92)$$

Applied to $\exp(ikx)$ leads to:

$$\overset{\triangle}{_{\text{RL}}\partial_x^\alpha} \exp(ikx) = \frac{1-\alpha}{\cos(\alpha\pi/2)} \lim_{\omega \rightarrow 0} |\omega|^{\alpha-2} {}_2F_1\left(\frac{3}{2} - \frac{\alpha}{2}, 1 - \frac{\alpha}{2}; \frac{3}{2}; -\frac{k^2}{\omega^2}\right) (-k) \times \exp(ikx) \quad (13.93)$$

$$= \frac{(k^2)^{\alpha/2}}{k} \exp(ikx) \quad (13.94)$$

$$= \text{sign}(k)|k|^{\alpha-1} \exp(ikx), \quad 0 < \alpha < 2 \quad (13.95)$$

$$= \text{sign}(k)|k|^\alpha \exp(ikx), \quad 0 < \alpha < 1 \quad (13.96)$$

and for the trigonometric functions

$$\overset{\triangle}{_{\text{RL}}\partial_x^\alpha} \sin(kx) = \text{sign}(k)|k|^\alpha \cos(kx) \quad (13.97)$$

$$\overset{\triangle}{_{\text{RL}}\partial_x^\alpha} \cos(kx) = -\text{sign}(k)|k|^\alpha \sin(kx), \quad 0 < \alpha < 1 \quad (13.98)$$

in accordance with the eigenvalue spectra of the integral representation of the regularized Liouville derivative.

13.6 Manifest covariant differential representation of the regularized Liouville derivative on \mathbb{R}^N

Let us first extend the one dimensional differential representation of the regularized Liouville derivative to the N-dimensional Euclidean space introducing a set of derivative operators:

$$\{\overset{\triangle}{\text{RL}}\partial_n^\alpha\} = \{\overset{\triangle}{\text{RL}}\partial_1^\alpha, \overset{\triangle}{\text{RL}}\partial_2^\alpha, \dots, \overset{\triangle}{\text{RL}}\partial_N^\alpha\} \quad n = 1, 2, \dots, N \quad (13.99)$$

where we introduced the abbreviation

$$\partial_n = \partial_{x_n} \quad n = 1, 2, \dots, N \quad (13.100)$$

With e.g. (13.92) we therefore have

$$\begin{aligned} \{\overset{\triangle}{\text{RL}}\partial_n^\alpha\} &= \left\{ \frac{1-\alpha}{\cos(\alpha\pi/2)} (i\partial_n) \lim_{\omega \rightarrow 0} |\omega|^{\alpha-2} {}_2F_1\left(\frac{3}{2} - \frac{\alpha}{2}, 1 - \frac{\alpha}{2}; \frac{3}{2}; \frac{\Delta}{\omega^2}\right) \right\} \\ &\quad n = 1, 2, \dots, N \end{aligned} \quad (13.101)$$

A possible candidate for an extension to the Riemannian curved space is then given by

$$\begin{aligned} \{\overset{\triangle}{\text{RL}}\partial_n^\alpha\} &= \left\{ \frac{1-\alpha}{\cos(\alpha\pi/2)} (i\nabla_n) \lim_{\omega \rightarrow 0} |\omega|^{\alpha-2} {}_2F_1\left(\frac{3}{2} - \frac{\alpha}{2}, 1 - \frac{\alpha}{2}; \frac{3}{2}; \frac{\Delta}{\omega^2}\right) \right\} \\ &\quad n = 1, 2, \dots, N \end{aligned} \quad (13.102)$$

where Δ is the covariant Laplace-operator $\Delta = \nabla^n \nabla_n$, which e.g. for scalar fields (rank 0 tensors) is given by (13.56) and ∇_n is the Riemann covariant derivative.

While the above candidate may be called Riemann type of the regularized Liouville derivative, the corresponding Caputo type interchanges the role of the covariant Laplace Δ and Riemann covariant derivative ∇_n and is of the form:

$$\begin{aligned} \{\overset{\triangle}{\text{RL}}\partial_n^\alpha\} &= \left\{ \frac{1-\alpha}{\cos(\alpha\pi/2)} \lim_{\omega \rightarrow 0} |\omega|^{\alpha-2} {}_2F_1\left(\frac{3}{2} - \frac{\alpha}{2}, 1 - \frac{\alpha}{2}; \frac{3}{2}; \frac{\Delta}{\omega^2}\right) (i\nabla_n) \right\} \\ &\quad n = 1, 2, \dots, N \end{aligned} \quad (13.103)$$

and will lead to similar results only if the commutator

$$[\Delta, \nabla_n] T_{b_1 b_2 \dots b_s}^{a_1 a_2 \dots a_r} = 0 \quad (13.104)$$

vanishes.

With the above definitions we are able to formulate covariant fractional derivatives of regularized Liouville or Feller($\theta = 1$) type in terms of the covariant Laplace-operator $\Delta = \nabla^\mu \nabla_\mu$ and covariant derivative ∇_μ acting on tensors of rank k on the Riemannian space.

Table 13.3 Properties of different free fractional Schrödinger equations. Replacing the Laplace-operator by either Riemann-, Caputo-, regularized Liouville or Riesz derivative we obtain different behaviors for the free solutions.

property	Riemann	Caputo	Feller($\theta = 1$)	Riesz
$\Delta^\alpha/2$	${}_{\text{R}}^{\text{R}} \partial_x^\alpha$	${}_{\text{C}}^{\text{C}} \partial_x^\alpha$	${}_{\text{RL}}^{\text{RL}} \partial_x^\alpha$	${}_{\text{RZ}}^{\text{RZ}} \partial_x^\alpha$
Hermiticity	${}_{\text{R}} \partial_x^\alpha {}_{\text{R}} \partial_{x\alpha}$ no	${}_{\text{C}} \partial_x^\alpha {}_{\text{C}} \partial_{x\alpha}$ no	${}_{\text{RL}} \partial_x^\alpha {}_{\text{RL}} \partial_{x\alpha}$ yes	${}_{\text{RZ}} \partial_x^\alpha {}_{\text{RZ}} \partial_{x\alpha}$ yes
Parity conservation	yes	yes	yes	yes
free waves $\psi^-(x)$	$x^{2\alpha-1} E_{2\alpha 2\alpha}(-x^2)$	$x^\alpha E_{2\alpha 1+\alpha}(-x^2)$	$\sin(x)$	$\sin x$
free waves $\psi^+(x)$	$x^{\alpha-1} E_{2\alpha \alpha}(-x^2)$	$E_{2\alpha}(-x^2)$	$\cos(x)$	$\cos(x)$
normalizable	yes	yes	no	no
translation invariance	no	no	yes	yes
confinement	yes	yes	no	no

Hence we have demonstrated that in both cases, for the Riesz as well as for the regularized Liouville fractional derivative definitions respectively, besides the well established integral representation there exist differential representations, which result in a local interpretation of a fractional derivative.

The use of any of these representations will lead to different results when applied e.g. in a fractional extension of the Schrödinger equation. In table 13.3 we have collected a set of resulting properties of eigenfunctions of the free fractional Schrödinger equation using different fractional derivative definitions. A major task in the following chapters is a comparison with experimental results to determine the quality of theoretical results for different definitions of a fractional Schrödinger equation.

13.7 Generalization of a fractional derivative

Finally we may speculate about extensions of the Riesz- and regularized Liouville integral representation of the fractional derivative. In order to evaluate the eigenvalue spectrum κ from (13.21) and (13.83) according to (13.22) and (13.84) we had to evaluate integrals of the type

$$\kappa = \int_0^\infty \frac{d\xi}{\xi} w(\xi) \quad (13.105)$$

$$= \zeta(\alpha) s(k) \int_0^\infty \frac{d\xi}{\xi} w(\xi/k) \quad (13.106)$$

with the specific fractional spectra $s(k) = |k|^\alpha$ and $s(k) = \text{sign}(k)|k|^\alpha$ respectively as a convolution integral with kernel

$$w(\xi) = \xi^{-\alpha} \quad (13.107)$$

More general the following scaling property holds

$$w(\xi/k) \equiv s(k)w(\xi) \quad (13.108)$$

which simply is a consequence of the infinite upper bound of the integral. We are left with the question, whether this relation determines the weight function uniquely. Setting e.g.

$$w(\xi/k) = w(\xi)/w(k) \quad (13.109)$$

indeed we are directly lead to (13.107).

But of course, every weight, which fulfills (13.108) is a valid realization.

A possible generalization may be introduced starting with the relation (15.1.8) from [Abramowitz and Stegun (1965)] for a special case of the hypergeometric function ${}_2F_1(a, b; c; z)$:

$${}_2F_1(a, b; b; z) = (1 - z)^{-a} \quad (13.110)$$

and therefore we may rewrite the weight (13.107) as:

$$w(\xi) = \xi^{-\alpha} = \lim_{\omega \rightarrow 0} \omega^{-\alpha} {}_2F_1(\alpha, b; b; -\xi/\omega) \quad (13.111)$$

$$= \lim_{\substack{\omega \rightarrow 0 \\ c \rightarrow b}} \omega^{-\alpha} {}_2F_1(\alpha, b; c; -\xi/\omega) \quad (13.112)$$

If we allow for extended spectral functions e.g. $s(k, b, c)$ we are lead to generalized fractional derivative definitions e.g. for the case $c \neq b$. The search for allowed families of generalized weight functions results in a generalized fractional calculus, see [Kiryakova (1994)].

Exercise 13.1

The differential representation of the fractional Schrödinger equation in spherical coordinates

Problem: Solve the fractional Schrödinger equation in spherical coordinates for the infinite potential well

$$V(r) = \begin{cases} 0 & r \leq R_0 \\ \infty & r > R_0 \end{cases} \quad (13.113)$$

where the fractional Laplace-operator is given by the differential representation of the Riesz fractional derivative.

Chapter 14

Fractional Spin — A Property of Particles Described with the Fractional Schrödinger Equation

Symmetries play an important role in physics. If a certain symmetry is present for a given problem, its solution will often be simplified [Greiner and Müller (1994); Frank et al. (2009)].

For example homogeneity of space, which means, that space has equal structure at all positions \vec{x} implies invariance under translations and therefore from a classical point of view conservation of momentum.

If we assume an isotropic space, which means, that space has a similar structure in all directions, this implies invariance of the system described under spatial rotations and consequently the conservation of angular momentum.

According to Noether's theorem, there always exists a conserved quantity, if the Euler-Lagrange equations are invariant under a specific coordinate transform [Noether (1918)].

In quantum mechanics a symmetry is described by an unitary operator U , which commutes with the Hamiltonian H . The existence of this symmetry operator implies the existence of a conserved observable. Let G be the Hermitian generator of U :

$$U = I - i\epsilon G + O(\epsilon^2) \quad (14.1)$$

Since U commutes with the Hamiltonian H , so does G :

$$[H, G] = 0 \quad (14.2)$$

and the conserved observable is the eigenvalue of G .

A fractional wave equation describes fractional particles, but the properties of space are not affected. We will therefore require, that symmetry properties of space will remain to be valid in the fractional case too. This implies, that e.g. the generator of a given symmetry operation should commute with the fractional Hamiltonian:

$$[H^\alpha, G] = 0 \quad (14.3)$$

As an example, we will investigate the properties of the fractional Schrödinger equation under rotations and will unveil an at first unexpected quantity, which we will call fractional spin.

14.1 Spin - the classical approach

Let us call a particle elementary, if it is described by a potential- and field-free wave equation. If in addition there is an internal structure, which is determined by additional quantum numbers, it may be revealed e.g. considering the behavior under rotations.

The generator for infinitesimal rotations about the z-axis

$$L_z = i\hbar(x\partial_y - y\partial_x) \quad (14.4)$$

commutes with the Hamiltonian H of the free ordinary Schrödinger equation

$$[L_z, H] = 0 \quad (14.5)$$

which indicates, that the particle described has no internal structure.

But the same operator L_z does not commute with the Dirac operator:

$$D = -i\hbar(\gamma^\mu\partial_\mu + m) \quad (14.6)$$

Instead it follows

$$[L_z, D] = \hbar^2(\gamma^x\partial_y - \gamma^y\partial_x) \quad (14.7)$$

Hence the invariance under rotations is lost. This is an indication for an internal structure of the particle described. There is an additional contribution, which results from the spin or intrinsic angular momentum of the particle.

In order to restore invariance of the wave equation under rotations we define the operator J of total angular momentum with z-component J_z :

$$J_z = L_z + S_z \quad (14.8)$$

which indeed commutes with the Dirac-operator

$$[J_z, D] = 0 \quad (14.9)$$

For the z-component of the intrinsic angular momentum S_z we obtain

$$S_z = -\frac{i\hbar}{4}[\gamma^x, \gamma^y] \quad (14.10)$$

and we conclude, that the Dirac equation may be used to describe the behavior of spin- $\frac{1}{2}$ particles.

14.2 Fractional spin

We will now proceed in a similar way to investigate the properties of particles, which are described with the fractional Schrödinger equation.

We will investigate the simplest case, the behavior of the 3-dimensional free fractional Schrödinger equation

$$H_{\text{free}}^{\alpha} \psi = -\frac{1}{2} mc^2 \left(\frac{\hbar}{mc} \right)^{2\alpha} (\partial_x^{2\alpha} + \partial_y^{2\alpha} + \partial_z^{2\alpha}) \psi = E\psi \quad (14.11)$$

under rotations in R^2 about the z-axis.

We start with a technical remark: According to the Leibniz product rule (3.39) the fractional derivative of the product $xf(x)$ is given by:

$$\partial_x^{\alpha} (xf(x)) = \sum_{j=0}^{\infty} \binom{\alpha}{j} (\partial_x^j x) \partial_x^{\alpha-j} f(x) \quad (14.12)$$

$$= (x\partial_x^{\alpha} + \alpha\partial_x^{\alpha-1}) f(x) \quad (14.13)$$

We define a generalized fractional angular momentum operator K^{α} with z-component K_z^{α}

$$K_z^{\alpha} = i \left(\frac{\hbar}{mc} \right)^{\alpha} mc (x\partial_y^{\alpha} - y\partial_x^{\alpha}) \quad (14.14)$$

The components $K_x^{\alpha}, K_y^{\alpha}$ are given by cyclic permutation of the spatial indices in (14.14). Using (14.12) the commutation relation with the Hamiltonian H_{free}^{α} of the free fractional Schrödinger equation (14.11) results as (setting $m = \hbar = c = 1$):

$$\begin{aligned} [-i2K_z^{\beta}, H_{\text{free}}^{\alpha}] &= [K_z^{\beta}, \partial_x^{2\alpha} + \partial_y^{2\alpha} + \partial_z^{2\alpha}] \\ &= [K_z^{\beta}, \partial_x^{2\alpha} + \partial_y^{2\alpha}] \\ &= K_z^{\beta}(\partial_x^{2\alpha} + \partial_y^{2\alpha}) - (\partial_x^{2\alpha} + \partial_y^{2\alpha})K_z^{\beta} \\ &= (x\partial_y^{\beta} - y\partial_x^{\beta})(\partial_x^{2\alpha} + \partial_y^{2\alpha}) - (\partial_x^{2\alpha} + \partial_y^{2\alpha})(x\partial_y^{\beta} - y\partial_x^{\beta}) \\ &= x\partial_x^{2\alpha}\partial_y^{\beta} + x\partial_x^{2\alpha+\beta} - y\partial_x^{2\alpha+\beta} - y\partial_x^{\beta}\partial_y^{2\alpha} \\ &\quad - (\partial_x^{2\alpha}x\partial_y^{\beta} - y\partial_x^{2\alpha+\beta} + x\partial_y^{2\alpha+\beta} - \partial_y^{2\alpha}y\partial_x^{\beta}) \\ &= x\partial_x^{2\alpha}\partial_y^{\beta} - y\partial_x^{\beta}\partial_y^{2\alpha} \\ &\quad - (x\partial_x^{2\alpha}\partial_y^{\beta} + 2\alpha\partial_x^{2\alpha-1}\partial_y^{\beta} - y\partial_x^{\beta}\partial_y^{2\alpha} - 2\alpha\partial_x^{\beta}\partial_y^{2\alpha-1}) \\ &= -2\alpha (\partial_x^{2\alpha-1}\partial_y^{\beta} - \partial_x^{\beta}\partial_y^{2\alpha-1}) \quad , \alpha, \beta \in \mathbb{C} \end{aligned} \quad (14.15)$$

Setting $\beta = 1$ we obtain for the z-component of the standard angular momentum operator L_z (14.4) the commutation relation

$$[L_z, H_{\text{free}}^{\alpha}] = [K_z^{\beta=1}, H_{\text{free}}^{\alpha}] = -i\alpha (\partial_x^{2\alpha-1}\partial_y - \partial_x\partial_y^{2\alpha-1}) \quad (14.16)$$

which obviously is not vanishing. Therefore particles described with the fractional Schrödinger equation (11.19) carry an additional internal structure for $\alpha \neq 1$.

We now define the fractional total angular momentum J^β with z-component J_z^β . Setting

$$\beta = 2\alpha - 1 \quad (14.17)$$

we obtain with $J_z^{2\alpha-1} = K_z^{2\alpha-1}$, and with (14.15)

$$[J_z^{2\alpha-1}, H_{\text{free}}^\alpha] = 0 \quad (14.18)$$

this operator commutes with the fractional free Hamiltonian. Therefore $J_z^{2\alpha-1}$ indeed is the fractional analogue of the standard z-component of the total angular momentum. Now we define the z-component of a fractional intrinsic angular momentum S_x^β with

$$J_z^{2\alpha-1} = L_z + S_z^{2\alpha-1} \quad (14.19)$$

The explicit form is given by

$$S_z^{2\alpha-1} = i(x(\partial_y^{2\alpha-1} - \partial_y) - y(\partial_x^{2\alpha-1} - \partial_x)) \quad (14.20)$$

This operator vanishes for $\alpha = 1$, whereas for $\alpha \neq 1$ it yields the z-component of a fractional spin.

Lets call the difference between fractional and ordinary derivative δp , or more precisely the components

$$\delta p_i = i(\partial_i^{2\alpha-1} - \partial_i) \quad (14.21)$$

Hence for $S_z^{2\alpha-1}$ we can write

$$S_z^{2\alpha-1} = x\delta p_y - y\delta p_x \quad (14.22)$$

The components of a fractional spin vector are then given by the cross product

$$\vec{S}^{2\alpha-1} = \vec{r} \times \delta \vec{p} \quad (14.23)$$

Therefore fractional spin describes an internal fractional rotation, which is proportional to the momentum difference between fractional and ordinary momentum. For a given α it has exactly one component.

With $J_x^{2\alpha-1} = K_x^{2\alpha-1}$ and $J_y^{2\alpha-1} = K_y^{2\alpha-1}$, the commutation relations for the total fractional angular momentum are given by

$$[J_x^{2\alpha-1}, J_y^{2\alpha-1}] = (2\alpha - 1) \frac{\hbar}{mc} J_z^{2\alpha-1} p_z^{2(\alpha-1)} \quad (14.24)$$

$$[J_y^{2\alpha-1}, J_z^{2\alpha-1}] = (2\alpha - 1) \frac{\hbar}{mc} J_x^{2\alpha-1} p_x^{2(\alpha-1)} \quad (14.25)$$

$$[J_z^{2\alpha-1}, J_x^{2\alpha-1}] = (2\alpha - 1) \frac{\hbar}{mc} J_y^{2\alpha-1} p_y^{2(\alpha-1)} \quad (14.26)$$

with components of the fractional momentum operator p^α or generators of fractional translations respectively given as

$$p_i^\alpha = i \left(\frac{\hbar}{mc} \right)^\alpha mc \partial_i^\alpha \quad (14.27)$$

Therefore in the general case $\alpha \neq 1$ an extended fractional rotation group is generated, which contains an additional fractional translation factor.

There is a unexpected relationship between the fractional angular momentum operators J_μ and the the Pauli-Lubanski vector W_μ and consequently the Lie algebra of fractional rotation group and the Lie algebra of Poincaré group are strongly related.

We conclude, that fractional elementary particles which are described with the fractional Schrödinger equation, carry an internal structure, which we call fractional spin, because analogies to e.g. electron spin are close.

Consequently, the transformation properties of the fractional Schrödinger equation are more related to the ordinary Pauli equation than to the ordinary ($\alpha = 1$) Schrödinger equation.

This page intentionally left blank

Chapter 15

Factorization

In the previous chapters we have presented a strategy to introduce a fractional extension for the nonrelativistic Schrödinger equation. Within the framework of canonical quantization we replaced the classical observables $\{x, p\}$ by fractional derivative operators.

In this section we will present an alternative direct approach, which will automatically lead to fractional derivative wave equations. This approach is solely based on symmetry considerations, namely an extension of the theoretical derivation of $SU(2)$ symmetric wave equations to the next complicated case of $SU(3)$ -symmetric wave equations by extending the concept of factorization of a given second-order operator.

Linearization of a relativistic second order wave equation was first considered by Dirac [Dirac (1928)]. Starting with the relativistic Klein-Gordon equation the derived Dirac equation gave a correct description of the spin and the magnetic moment of the electron.

The concept of linearization is important, since it provides a well defined mechanism to impose an additional $SU(2)$ symmetry onto a given set of symmetry properties of a second order wave equation.

Since linearization may be interpreted as a special case of factorization, namely to two factors, a natural generalization is a factorization to n factors.

Indeed we will find, that n -fold factorization of the Klein-Gordon equation automatically leads to fractional wave equations which describe particles with an internal $SU(N)$ -symmetry.

We will first recall the major results of a linearization of the relativistic Klein-Gordon equation for spin-0 particles leading to the relativistic Dirac-equation for spin- $\frac{1}{2}$ particles. In a next step we will show, that the new spin-property of the Dirac-equation is not the result of a relativistic

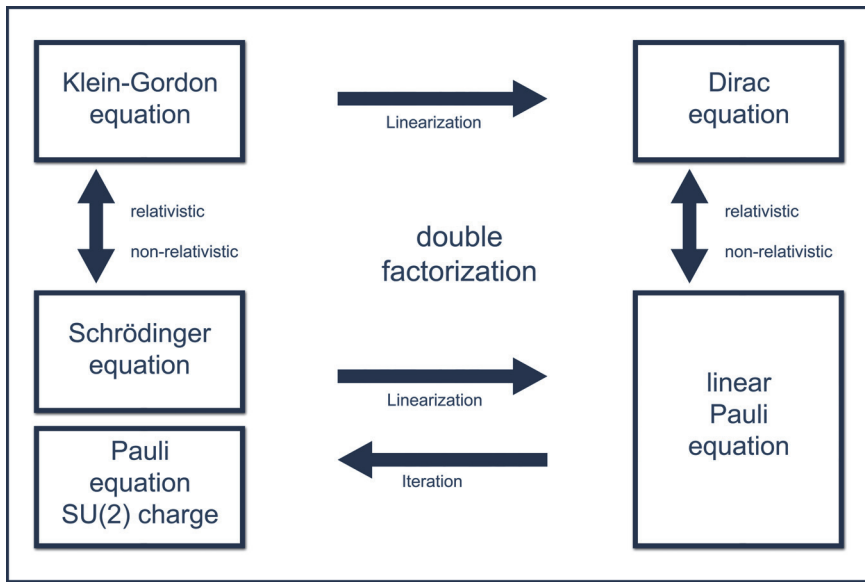


Fig. 15.1 Schematic view of the linearization procedure.

treatment, but a consequence of the linearization procedure. Following an idea of Levy-Leblond [Levy-Leblond (1967)] we will therefore present the linearization procedure for the nonrelativistic Schrödinger equation for an multi-dimensional Riemannian space, which yields a potential-free nonrelativistic Pauli-equation.

15.1 The Dirac equation

We start with the relativistic energy-momentum relation (setting $c = 1$)

$$E^2 = \vec{p}^2 + m^2 \quad (15.1)$$

Quantization with

$$E \rightarrow i\hbar\partial_t \quad (15.2)$$

$$p_i \rightarrow -i\hbar\partial_i \quad (15.3)$$

leads to the relativistic Klein-Gordon equation for particles with spin 0:

$$(-\hbar^2\partial^t\partial_t + \hbar^2\partial^i\partial_i - m^2)\phi = 0 \quad (15.4)$$

$$(\hbar^2\partial^\mu\partial_\mu - m^2)\phi = 0 \quad (15.5)$$

$$(\hbar^2\Box - m^2)\phi = 0 \quad (15.6)$$

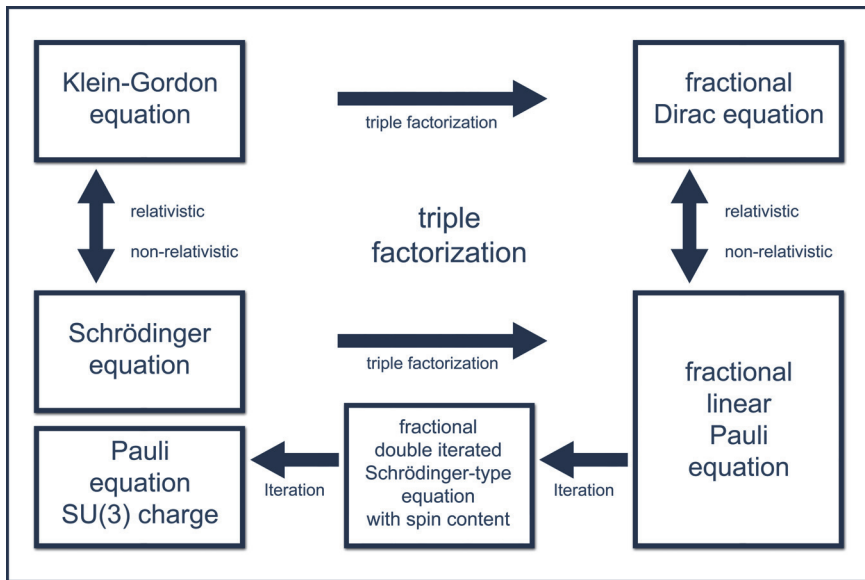


Fig. 15.2 Schematic view of the triple factorization procedure.

where we have introduced the d'Alembert-operator \square .

Dirac proposed a two-fold factorization of the d'Alembert-Operators introducing an operator D with the property

$$D D' = \hbar^2 \square - m^2 \quad (15.7)$$

The explicit form of this operator is given by:

$$D = i\hbar\gamma^\mu \partial_\mu + m \quad (15.8)$$

where the γ matrices fulfill the Clifford-algebra:

$$\gamma^\mu \gamma^\nu + \gamma^\nu \gamma^\mu = 2\delta^{\mu\nu} \quad (15.9)$$

where $\delta^{\mu\nu}$ is the Kronecker-delta.

The smallest representation of these γ -matrices is given as a triad of traceless 2×2 -Pauli-matrices σ_i :

$$\sigma_x = \begin{pmatrix} 0 & 1 \\ 1 & 0 \end{pmatrix} \quad \sigma_y = \begin{pmatrix} 0 & -i \\ i & 0 \end{pmatrix} \quad \sigma_z = \begin{pmatrix} 1 & 0 \\ 0 & -1 \end{pmatrix} \quad (15.10)$$

These matrices are generators of the unitary group SU(2). The four γ -matrices are then generated using the external vector product

$$\gamma^0 = \mathbf{1}_2 \otimes \sigma_z, \quad \gamma^i = \sigma_i \otimes \sigma_x \quad i = 1, 2, 3 \quad (15.11)$$

where $\mathbf{1}_2$ is the 2×2 unit matrix.

15.2 Linearization of the collective Schrödinger equation

For a given set of spatial collective coordinates $\{x^i, i = 1, \dots, d\}$, which span the d -dimensional Riemannian space R^d , the classical kinetic energy is defined by:

$$T = \frac{1}{2}mg_{ij}\dot{x}^i\dot{x}^j \quad (15.12)$$

where we have introduced the symmetric metric tensor g_{ij} .

Using the quantization method of Podolsky and Pauli [Podolsky (1928)], the corresponding Schrödinger equation reads:

$$\hat{S}\psi(x^i, t) = 0 \quad (15.13)$$

with the Schrödinger operator

$$\hat{S} = -\frac{\hbar^2}{2m}\Delta - i\hbar\partial_t \quad (15.14)$$

$$= -\frac{\hbar^2}{2m}g^{ij}\nabla_i\nabla_j - i\hbar\partial_t \quad (15.15)$$

$$= -\frac{\hbar^2}{2m}g^{ij}(\partial_i\partial_j - \left\{ \begin{array}{c} k \\ ij \end{array} \right\} \partial_k) - i\hbar\partial_t \quad (15.16)$$

$$= -\frac{\hbar^2}{2m}\frac{1}{\sqrt{g}}\partial_ig^{ij}\sqrt{g}\partial_j - i\hbar\partial_t \quad (15.17)$$

$$= -\frac{\hbar^2}{2m}\Delta - i\hbar\partial_t \quad (15.18)$$

where ∇_i denotes the Riemann covariant derivative, $\left\{ \begin{array}{c} k \\ ij \end{array} \right\}$ the Christoffel symbol and $g = \det g_{ij}$. This Schrödinger equation is quadratic in the spatial coordinates and linear in the time coordinate.

In the following, we will derive a pair of operators \hat{R}, \hat{R}' , which are linear in both spatial and time derivatives with the property:

$$\hat{R}\hat{R}' = \frac{2}{m}\hat{S} = \hat{S}' \quad (15.19)$$

The corresponding wave equation

$$\hat{R}\chi(x^i, t) = 0 \quad (15.20)$$

is the linearized Schrödinger equation, we are looking for. The ansatz:

$$\hat{R} = \alpha A\partial_t + \alpha B^i(x^i)\partial_i + C \quad (15.21)$$

$$\hat{R}' = \alpha A'\partial_t + \alpha B'^i(x^i)\partial_i + C' \quad (15.22)$$

with $\alpha = -\frac{i\hbar}{m}$, is general enough to treat a metric of the type:

$$g_{\mu\nu}dx^\mu dx^\nu = c^2dt^2 + g_{ij}dx^i dx^j, \quad \mu, \nu = 0, 1, \dots, d \quad (15.23)$$

For reasons of simplicity we will set $c = 1$.

The coordinate and time independent quantities A, A', C, C' and time independent $B(x), B'(x)$ will turn out to be spinors of mixed rank 2 and can be written as $2^N \times 2^N$ matrices. The minimal N is defined by the number of different matrices, which is $d+1$, necessary in R^d .

Inserting (15.21) and (15.22) into (15.19) yields the following conditions:

$$AA' = 0 \quad (15.24)$$

$$AB'^i + B^i A' = 0 \quad (15.25)$$

$$AC' + CA' = 2 \quad (15.26)$$

$$CB'^i + B^i C' = 0 \quad (15.27)$$

$$CC' = 0 \quad (15.28)$$

$$B^i B'^j + B^j B'^i = 2g^{ij} \quad (15.29)$$

$$B^i B'^j_{|i} = -g^{ik} \begin{Bmatrix} j \\ ik \end{Bmatrix} \quad (15.30)$$

$$\partial_t B'^i = 0 \quad (15.31)$$

These conditions may be written in compact form similar to the case of [Levy-Leblond (1967)], introducing the quantities:

$$\begin{aligned} B^0 &= \frac{1}{\sqrt{2}}(A + C) & B'^0 &= \frac{1}{\sqrt{2}}(A' + C') \\ B^{d+1} &= \frac{i}{\sqrt{2}}(A - C) & B'^{d+1} &= \frac{i}{\sqrt{2}}(A' - C') \end{aligned} \quad (15.32)$$

and the new extended metric:

$$\bar{g}_{\mu\nu}dx^\mu dx^\nu = d\bar{t}^2 + g_{ij}dx^i dx^j + d\bar{u}^2 \quad (15.33)$$

with the new variables \bar{t} and \bar{u} .

The matrices B^0 and B^{d+1} are linear combinations of A and C . Like A corresponds to the time coordinate t , C may be associated to an additional new coordinate u generating the mass m . Accordingly the new variables \bar{t} and \bar{u} may be regarded as proper linear combinations of t and u . The same argument holds for B'^0 and B'^{d+1} .

Then the conditions (15.24)-(15.31) are reduced to:

$$B^\mu B'^\nu + B^\nu B'^\mu = 2\bar{g}^{\mu\nu} \quad (15.34)$$

$$B^\mu B'^\nu_{|\mu} = -\bar{g}^{\mu\sigma} \begin{Bmatrix} \nu \\ \mu\sigma \end{Bmatrix} \quad \mu, \nu = 0, 1, \dots, d+1 \quad (15.35)$$

Since the Christoffel-symbols are symmetric with respect to μ and σ insertion of (15.34) into (15.35) leads to:

$$B^\mu(B'^\nu_{|\mu}) + B^\mu B'^\sigma \left\{ \begin{array}{c} \nu \\ \mu\sigma \end{array} \right\} = 0 \quad (15.36)$$

or equivalently

$$B^\mu \nabla_\mu B'^\nu = 0 \quad (15.37)$$

since B'^ν transforms as a tensor with rank 1. From condition (15.36) using

$$\nabla_\sigma \bar{g}^{\mu\nu} = \bar{g}^{\mu\nu}_{|\sigma} + \left\{ \begin{array}{c} \mu \\ \sigma\tau \end{array} \right\} \bar{g}^{\tau\nu} + \left\{ \begin{array}{c} \nu \\ \sigma\tau \end{array} \right\} \bar{g}^{\mu\tau} = 0 \quad (15.38)$$

we deduce that

$$(\nabla_\sigma B^\mu) B'^\nu + B^\mu (\nabla_\sigma B'^\nu) + (\nabla_\sigma B^\nu) B'^\mu + B^\nu (\nabla_\sigma B'^\mu) = 0 \quad (15.39)$$

Hence condition (15.37) is not fulfilled in general.

But we should keep in mind, that we may allow for B, B' besides tensorial transformation properties spinor transformations of the form:

$$\tilde{B}^\mu = MB^\mu M^{-1} \quad (15.40)$$

$$\tilde{B}'^\mu = MB'^\mu M^{-1} \quad (15.41)$$

where M is an arbitrary, nonsingular $2^N \times 2^N$ matrix.

Consequently we may define a spinor covariant derivative \mathcal{D}_μ . We want to keep condition (15.38) valid for the spinor covariant derivative:

$$\mathcal{D}_\sigma \bar{g}^{\mu\nu} = \nabla_\sigma \bar{g}^{\mu\nu} = 0 \quad (15.42)$$

or with (15.39)

$$(\mathcal{D}_\sigma B^\mu) B'^\nu + B^\mu (\mathcal{D}_\sigma B'^\nu) + (\mathcal{D}_\sigma B^\nu) B'^\mu + B^\nu (\mathcal{D}_\sigma B'^\mu) = 0 \quad (15.43)$$

Now we postulate that the spinor covariant derivative on the matrices B, B' vanishes [Schmutzler (1968)]

$$\mathcal{D}_\sigma B^\mu = 0 \quad (15.44)$$

$$\mathcal{D}_\sigma B'^\mu = 0 \quad (15.45)$$

Comparing (15.39) with (15.43), the difference between the tensor- and the spinor covariant derivative may be written as

$$\mathcal{D}_\sigma B'^\mu = B'^\mu_{|\sigma} + \left\{ \begin{array}{c} \mu \\ \sigma\tau \end{array} \right\} B'^\tau + T'_\sigma{}^\mu = 0 \quad (15.46)$$

$$\mathcal{D}_\sigma B^\mu = B^\mu_{|\sigma} + \left\{ \begin{array}{c} \mu \\ \sigma\tau \end{array} \right\} B^\tau + T_\sigma{}^\mu = 0 \quad (15.47)$$

where the objects $T_\sigma^\mu, T_\sigma'^\mu$ satisfy the relation

$$T_\sigma^\mu B'^\nu + B^\mu T_\sigma'^\nu + T_\sigma^\nu B'^\mu + B^\nu T_\sigma'^\mu = 0 \quad (15.48)$$

which is fulfilled introducing the generalized affine spinor connection or Fock-Ivanenko coefficient Γ_σ :

$$T_\sigma^\mu = [\Gamma_\sigma, B^\mu] \quad (15.49)$$

$$T_\sigma'^\mu = [\Gamma_\sigma, B'^\mu] \quad (15.50)$$

where Γ_σ is an at first arbitrary $2^N \times 2^N$ -matrix.

To fulfill condition (15.35), the quantities $T_\sigma^\mu, T_\sigma'^\mu$ or Γ_σ respectively have to vanish identically. In other words: The iteration of the linear equations yields the Schrödinger equation if and only if the matrices B, B' are invariant under global spinor transformations and thus transform as tensors of rank 1 only. Hence the spinor transformation M may not be coordinate dependent. Choosing

$$\begin{aligned} B^0 &= M\gamma^0 & B'^0 &= \gamma^0 M^{-1} \\ B^i &= M\gamma^i & B'^i &= \gamma^i M^{-1} \\ B^{d+1} &= iM & B'^{d+1} &= -iM^{-1} \end{aligned} \quad (15.51)$$

the conditions (15.34) and (15.35) are automatically fulfilled for any global spinor transformation M . According to (15.32) the matrices A, A', C, C' may be written as a function of M and γ^0 :

$$\begin{aligned} A &= M \frac{1}{\sqrt{2}}(\gamma^0 + 1_N) & A' &= \frac{1}{\sqrt{2}}(\gamma^0 - 1_N)M^{-1} \\ C &= M \frac{1}{\sqrt{2}}(\gamma^0 - 1_N) & C' &= \frac{1}{\sqrt{2}}(\gamma^0 + 1_N)M^{-1} \end{aligned} \quad (15.52)$$

where 1_N die $2^N \times 2^N$ - unit matrix.

The remaining relations (15.34) and (15.35) are then isomorph to the Clifford-algebra

$$\gamma^\mu \gamma^\nu + \gamma^\nu \gamma^\mu = 2\hat{g}^{\mu\nu} \quad \mu, \nu = 0, 1, \dots, d \quad (15.53)$$

or equivalently with the original metric (15.23) as a consequence of the flatness in \hat{t} .

The linear operators \hat{R}, \hat{R}' finally read:

$$\hat{R} = -\frac{i\hbar}{m} \frac{1}{\sqrt{2}}(\gamma^0 + 1_N) \partial_t - \frac{i\hbar}{m} \gamma^i \partial_i + \frac{1}{\sqrt{2}}(\gamma^0 - 1_N) \quad (15.54)$$

$$\hat{R}' = -\frac{i\hbar}{m} \frac{1}{\sqrt{2}}(\gamma^0 - 1_N) \partial_t - \frac{i\hbar}{m} \gamma^i \partial_i + \frac{1}{\sqrt{2}}(\gamma^0 + 1_N) \quad (15.55)$$

Which yields the linearized Schrödinger equation:

$$\left(-\frac{i\hbar}{m} \frac{1}{\sqrt{2}}(\gamma^0 + 1_N) \partial_t - \frac{i\hbar}{m} \gamma^i \partial_i + \frac{1}{\sqrt{2}}(\gamma^0 - 1_N) \right) \chi = 0 \quad (15.56)$$

or equivalently as a result of the property $\hat{R}\hat{R}' = \hat{R}'\hat{R}$:

$$\left(-\frac{i\hbar}{m} \frac{1}{\sqrt{2}}(\gamma^0 - 1_N) \partial_t - \frac{i\hbar}{m} \gamma^i \partial_i + \frac{1}{\sqrt{2}}(\gamma^0 + 1_N) \right) \chi' = 0 \quad (15.57)$$

15.3 The fractional Dirac equation

We will now apply the method of factorization to the next complex case of three factors. Hence we search for an operator ${}^\alpha D$ with the property:

$${}^\alpha D {}^\alpha D' {}^\alpha D'' = \hbar^2 \square - m^2 \quad (15.58)$$

With the ansatz

$${}^\alpha D = \hbar^\alpha \gamma_\alpha^\mu \partial_\mu^\alpha + m^\alpha \quad (15.59)$$

where the index α indicates that the matrix dimensions depend on α , the following conditions have to be fulfilled:

$$3\alpha = 2 \quad (15.60)$$

$$\gamma_\alpha^\mu \gamma_\alpha^\nu \gamma_\alpha^\sigma + \gamma_\alpha^\mu \gamma_\alpha^\sigma \gamma_\alpha^\mu + \gamma_\alpha^\nu \gamma_\alpha^\mu \gamma_\alpha^\sigma + \gamma_\alpha^\nu \gamma_\alpha^\sigma \gamma_\alpha^\mu + \gamma_\alpha^\sigma \gamma_\alpha^\mu \gamma_\alpha^\nu + \gamma_\alpha^\sigma \gamma_\alpha^\nu \gamma_\alpha^\mu = 6 \delta^{\mu\nu\sigma} \quad (15.61)$$

And the explicit form of the triple factorized operator results as

$${}^{2/3} D = \hbar^{2/3} \gamma_{2/3}^\mu \partial_\mu^{2/3} + m^{2/3} \mathbf{1}_9 \quad (15.62)$$

which is indeed a fractional wave equation. $\mathbf{1}_9$ is the 9×9 unit matrix, as we will demonstrate in the following.

The smallest representation of the $\gamma_{2/3}$ -matrices is given in terms of traceless 3×3 matrices. We define the unit roots:

$$r_1 = e^{2\pi i \frac{1}{3}} = -\frac{1}{2} + \frac{\sqrt{3}}{2}i \quad (15.63)$$

$$r_2 = e^{2\pi i \frac{2}{3}} = -\frac{1}{2} - \frac{\sqrt{3}}{2}i \quad (15.64)$$

$$r_3 = e^{2\pi i} = 1 \quad (15.65)$$

A possible representation of the basis for all 3×3 -matrices is then given by:

$$\begin{aligned} \sigma_1 &= \begin{pmatrix} r_1 & 0 & 0 \\ 0 & r_2 & 0 \\ 0 & 0 & r_3 \end{pmatrix} & \sigma_2 &= \begin{pmatrix} r_2 & 0 & 0 \\ 0 & r_1 & 0 \\ 0 & 0 & r_3 \end{pmatrix} & \sigma_3 &= \begin{pmatrix} r_3 & 0 & 0 \\ 0 & r_3 & 0 \\ 0 & 0 & r_3 \end{pmatrix} \\ \sigma_4 &= \begin{pmatrix} 0 & r_1 & 0 \\ 0 & 0 & r_2 \\ r_3 & 0 & 0 \end{pmatrix} & \sigma_5 &= \begin{pmatrix} 0 & r_2 & 0 \\ 0 & 0 & r_1 \\ r_3 & 0 & 0 \end{pmatrix} & \sigma_6 &= \begin{pmatrix} 0 & r_3 & 0 \\ 0 & 0 & r_3 \\ r_3 & 0 & 0 \end{pmatrix} \\ \sigma_7 &= \begin{pmatrix} 0 & 0 & r_1 \\ r_2 & 0 & 0 \\ 0 & r_3 & 0 \end{pmatrix} & \sigma_8 &= \begin{pmatrix} 0 & 0 & r_2 \\ r_1 & 0 & 0 \\ 0 & r_3 & 0 \end{pmatrix} & \sigma_9 &= \begin{pmatrix} 0 & 0 & r_3 \\ r_3 & 0 & 0 \\ 0 & r_3 & 0 \end{pmatrix} \end{aligned} \quad (15.66)$$

24 different triples of these matrices fulfill condition (15.61), namely:

$$\begin{aligned} & \{1, 4, 5\} \{1, 4, 6\} \{1, 4, 9\} \{1, 5, 6\} \{1, 5, 8\} \{1, 6, 7\} \{1, 7, 8\} \{1, 7, 9\} \\ & \{1, 8, 9\} \{2, 4, 5\} \{2, 4, 6\} \{2, 4, 7\} \{2, 5, 6\} \{2, 5, 9\} \{2, 6, 8\} \{2, 7, 8\} \\ & \{2, 7, 9\} \{2, 8, 9\} \{4, 5, 9\} \{4, 6, 7\} \{4, 7, 9\} \{5, 6, 8\} \{5, 8, 9\} \{6, 7, 8\} \end{aligned} \quad (15.67)$$

6 of these 24 allowed combinations generate all three matrix diagonals, e.g. $\{\{1, 4, 9\}\}$. Every single of these 24 triplets may be chosen as a realization for a set of 3×3 extended Pauli-matrices.

From an arbitrarily chosen set e.g. $\{1, 4, 5\}$ the follow extended Pauli matrices explicitly result as:

$$\sigma_x = \begin{pmatrix} 0 & r_1 & 0 \\ 0 & 0 & r_2 \\ r_3 & 0 & 0 \end{pmatrix} \quad \sigma_y = \begin{pmatrix} 0 & r_2 & 0 \\ 0 & 0 & r_1 \\ r_3 & 0 & 0 \end{pmatrix} \quad \sigma_z = \begin{pmatrix} r_1 & 0 & 0 \\ 0 & r_2 & 0 \\ 0 & 0 & r_3 \end{pmatrix} \quad (15.68)$$

and the four $\gamma_{2/3}$ -matrices result as 9×9 -matrices with the explicit form

$$\gamma_{2/3}^0 = \mathbf{1}_3 \otimes \sigma_z \quad (15.69)$$

$$\gamma_{2/3}^i = \sigma_i \otimes \sigma_x \quad i = 1, 2, 3 \quad (15.70)$$

These matrices span a subspace of $SU(3)$.

Hence we have derived a fractional Dirac equation by a triple factorization of the d'Alembert operator. This procedure lead to two conditions: First a fractional derivative with $\alpha = 2/3$ is introduced. Second, the extended Clifford-Algebra (15.61) determines the structure of the γ -matrices to be generators of $SU(3)$.

For the first time in the history of physics a formal method is proposed which derives a wave equation, which correctly describes the dynamics of a particle with internal $SU(n)$ -symmetry.

The requirement of n-fold factorization of the d'Alembert-operator leads to fractional wave equations for $n > 2$.

To state this result more precisely: the extension of Diracs linearization procedure which determines the correct coupling of a $SU(2)$ symmetric charge to a 3-fold factorization of the d'Alembert-operator leads to a fractional wave equation with an inherent $SU(3)$ symmetry. This symmetry is formally deduced by the factorization procedure. In contrast to this formal derivation a standard Yang-Mills theory is merely a recipe, how to couple a phenomenologically deduced $SU(3)$ symmetry.

15.4 The fractional Pauli equation

There are two possible strategies to derive a nonrelativistic limit of the fractional Dirac equation: We could try a fractional extension of a Foldy-Wouthuysen transformation or alternatively, we could factorize the standard nonrelativistic Schrödinger equation.

Whether or not both methods lead to similar results, has not been examined yet.

In 1967, Levy-Leblond [Levy-Leblond (1967)] has linearized the standard nonrelativistic Schrödinger equation and obtained a linear wave equation with an additional SU(2) symmetry and we have presented a derivation for arbitrary number of dimensions in the last section. But until now this approach has not been extended to higher order.

In a first approach we will derive the explicit form of a fractional operator R , which, iterated 3 times, conforms with the ordinary, nonrelativistic Schrödinger operator:

$$RR'R'' = \left(-\frac{\hbar^2}{2m} \Delta - i\hbar\partial_t \right) \mathbf{1}_n \quad (15.71)$$

where $\mathbf{1}_n$ is the $n \times n$ unit matrix.

We use the following ansatz:

$$R = aA\partial_t^{\alpha_t} + bB^i\partial_i^{\alpha_i} + cC \quad (15.72)$$

$$R' = aA'\partial_t^{\alpha_t} + bB'^i\partial_i^{\alpha_i} + cC' \quad (15.73)$$

$$R'' = aA''\partial_t^{\alpha_t} + bB''^i\partial_i^{\alpha_i} + cC'' \quad (15.74)$$

with matrices $A, A', A'', B, B', B'', C, C', C''$, fractional derivative coefficients for time and space derivative α_t, α_i and scalar factors a, b, c , which will be determined in the following.

A triple iteration of (15.72) leads to the following determining equations:

$$\begin{aligned} A &= \frac{1}{\sqrt{3}}(\gamma^0 - r_1 \mathbf{1}_9) & B^i &= \gamma^i & C &= r_1 \mathbf{1}_3 \otimes \begin{pmatrix} 1 & 0 & 0 \\ 0 & 0 & 0 \\ 0 & 0 & 0 \end{pmatrix} \\ A' &= \frac{1}{\sqrt{3}}(\gamma^0 - r_2 \mathbf{1}_9) & B'^i &= \gamma^i & C' &= r_2 \mathbf{1}_3 \otimes \begin{pmatrix} 0 & 0 & 0 \\ 0 & 1 & 0 \\ 0 & 0 & 0 \end{pmatrix} \quad (15.75) \\ A'' &= \frac{1}{\sqrt{3}}(\gamma^0 - r_3 \mathbf{1}_9) & B''^i &= \gamma^i & C'' &= r_3 \mathbf{1}_3 \otimes \begin{pmatrix} 0 & 0 & 0 \\ 0 & 0 & 0 \\ 0 & 0 & 1 \end{pmatrix} \end{aligned}$$

with these specifications $RR'R''$ according to (15.71) it follows

$$RR'R'' = \left(a^2 c \partial_t^{2\alpha_t} + b^3 \sum_{i=1}^3 \partial_i^{3\alpha_i} \right) \mathbf{1}_9 \quad (15.76)$$

A term by term comparison with the nonrelativistic Schrödinger operator determines the fractional derivative coefficients:

$$\alpha_t = 1/2 \quad (15.77)$$

$$\alpha_i = 2/3 \quad (15.78)$$

and the scalar factors:

$$a = (-i\hbar)^{1/2} \left(\frac{1}{mc^2} \right)^{1/6} \quad (15.79)$$

$$b = - \left(\frac{\hbar^2}{2m} \right)^{1/3} \quad (15.80)$$

$$c = (mc^2)^{1/3} \quad (15.81)$$

Thus the fractional operators R, R', R'' are completely determined. As a remarkable fact we note the different fractional derivative coefficients for the fractional time and space derivative.

We therefore have proven, that the resulting SU(3) symmetry is neither a consequence of a relativistic treatment nor is it a specific property of linearization (which means, specific to first order derivatives of time and space respectively).

It is a consequence of the triple factorization solely.

We want to emphasize, that the factorization procedure even in the nonrelativistic case not only determines the symmetry group of the γ -matrices used, but also determines the dynamics of the system, forcing e.g. for a SU(3) symmetry fractional time ($\alpha_t = 1/2$) and space derivatives ($\alpha_i = 2/3$).

Finally, besides the fractional wave equation operator R and the triple iterated $RR'R''$, which corresponds to the ordinary Schrödinger operator, an additional type of wave equation, the twofold iterated $S^{(2)} = RR'$ emerges, which reads (including the additional phase factor c):

$$cRR' = a^2 c A A' \partial_t + b^2 c B^i B^j \partial_i^{2/3} \partial_j^{2/3} + \text{additional terms} \quad (15.82)$$

or, inserting the factors:

$$cS^{(2)} = -i\hbar A A' \partial_t - \frac{1}{2} \left(\frac{\hbar}{mc} \right)^{4/3} mc^2 \left(\frac{1}{2} \right)^{1/3} B^i B^j \partial_i^{2/3} \partial_j^{2/3} + \text{additional terms} \quad (15.83)$$

Table 15.1 A comparison of QED versus fQED, which for $\alpha = 2/3$ leads to a SU(3) symmetric wave equation.

parameter	QED	fQED
α	1	$\frac{2}{3}$
smallest representation rotational symmetry charge symmetry	$\sigma_x^{\alpha=1} = \begin{pmatrix} 0 & 1 \\ 1 & 0 \end{pmatrix}$	$\sigma_x^{\alpha=\frac{2}{3}} = \begin{pmatrix} 0 & 0 & r_1 \\ 0 & r_2 & 0 \\ r_3 & 0 & 0 \end{pmatrix}$
	$SO^{\alpha=1}(3) \equiv SO(3)$	$SO^{\alpha=\frac{2}{3}}(3)$
	SU(2)	SU(3)

Obviously $cS^{(2)}$ and the fractional Schrödinger equation (11.17), we derived in section 11.2, are closely related.

Let us summarize the results of this section: The extension of Dirac's linearization procedure of the d'Alembert-operator to a triple factorization formally leads to the requirement for derivatives of noninteger order $\alpha = 2/3$. This is a completely new approach to fractional calculus and its use in physics.

The classical approach considers fractional derivatives legitimated on the area of stochastic processes, fractional Brownian motion and anomalous diffusion respectively, where nonlocal aspects are an additional motivation to introduce fractional operators. Therefore complex classical multi-particle interactions are modeled using fractional derivatives.

In contrast to this classical approach, the new aspect is a formally correct treatment of higher symmetries and their dynamic description. The factorization generates in the simplest case SU(3) symmetric wave equations. As a direct consequence of the factorization conditions the resulting wave equations have the remarkable property to be of fractional nature in the derivative operators. Nonlocality is not a necessary requisite. In table 15.1 we compare the properties of the resulting wave equations for double (leading to QED) and triple (leading to fractional QED) factorization.

It should also be emphasized, that there is no additional free parameter in the theory. In the case of quantum electrodynamics, we must set $\alpha = 1$ to obtain a SU(2) charge symmetry, for triple iterated fractional quantum electrodynamics we must set $\alpha = 2/3$ to obtain a SU(3) symmetric charge symmetry.

It seems quite suggestive, to identify the fractional QED for $\alpha = 2/3$ as an alternative approach besides standard quantum chromodynamics (QCD). Whether this is a promising hypothesis, can only be proven by a comparison of derived theoretical results with experimental findings.

Therefore in the following chapters we will derive the necessary prerequisites to support this idea. Since this is a complex task, as a motivation for the reader, let us mention already, that e.g. the experimental excitation spectrum of charmonium will be described with an excellent accuracy within the framework of a fractional extension of the standard rotation group setting

$$\alpha_{\text{experimental}} \approx 0.648 \quad (15.84)$$

which we think is too close to $\alpha = 2/3$ to be considered merely as an accidental coincidence.

Factorization is the key mechanism to formally introduce SU(n) invariant wave equations. As a consequence of this procedure, these wave equations carry fractional derivative operators.

This is the way, how fractional calculus enters the physics building through the main entrance and this is the reason, why a physicist should become acquainted with this fundamental concept. A physicist may lead a simple, modest life ignoring exotic subjects like anomalous diffusion or fractional Brownian motion, which are classical fields of application of fractional calculus, but he should not ignore fractional wave equations, especially if he is interested in the foundations of the relationship between symmetry and dynamical behavior.

Therefore in the next chapter we will investigate fundamental aspects of a fractional group theory and present the fractional extension of the standard rotation group.

Exercise 15.1

Commutation relations for the matrix-representation of $U(d)$

Problem: The i $d \times d$ -matrices

$$\sigma^i = \{A_l^k\}, \quad i, 1, \dots, d^2 \quad k, l = 1, \dots, d \quad \text{modulo } d \quad (15.85)$$

with the elements a_{mn}

$$A_l^k(a_{mn}) = e^{\frac{2\pi i}{d} km} \delta_{m,n+l}, \quad m, n = 1, \dots, d \quad \text{modulo } d \quad (15.86)$$

where $e^{\frac{2\pi i}{d}} = \sqrt[d]{1}$, k is the phase and l measures the off-diagonality determine a specific matrix-representation of the unitary group $U(d)$.

Give the commutation relations $[\sigma^i, \sigma^{i'}]$ and $\{\sigma^i, \sigma^{i'}\}$.

Exercise 15.2

Linearization of a $2\lambda + 1$ dimensional free collective Schrödinger equation

Problem: The surface of a liquid drop may be expanded in spherical harmonics $Y_{\lambda\mu}$ introducing the surface variables $\alpha_{\lambda\mu}$ with a given multipolarity λ [Eisenberg and Greiner (1987)]:

$$R = R_0(1 + \sum_{\lambda,\mu}(-1)^\mu \alpha_{\lambda-\mu} Y_{\lambda\mu}) \quad (15.87)$$

From the behavior under rotations in \mathbb{R}^3 of the $Y_{\lambda\mu}$ follows, that the surface variables $\alpha_{\lambda\mu}$ behave like components of a spherical tensor of rank λ :

$$\alpha_{\lambda\mu}^{[\lambda]} = \sum_{\nu} D_{\nu\mu}^{\lambda} \alpha_{\lambda\nu}^{[\lambda]} \quad (15.88)$$

The corresponding canonical momenta $\pi_{\lambda\mu}$ are then defined via

$$\pi_{\lambda\mu} = -i\hbar\partial_{\alpha_{\lambda\mu}} \quad (15.89)$$

with the transformation property

$$\pi_{\lambda\mu}^{[\lambda]} = \sum_{\nu} D_{\mu\nu}^{\lambda*} \pi_{\lambda\nu}^{[\lambda]} \quad (15.90)$$

In lowest order, the corresponding kinetic energy term is given as a second order derivative operator, where the momenta of rank λ are coupled to a spherical tensor of rank 0:

$$T_2 = [\pi^{[\lambda]} \otimes \pi^{[\lambda]}]^{[0]} \quad (15.91)$$

which is the basic input for a description of the dynamic behavior of the liquid drop surface vibrations in term of a collective $2\lambda + 1$ dimensional Schrödinger equation e.g.:

$$(-1)^\lambda \frac{\sqrt{2\lambda+1}}{2B_\lambda} [\pi^{[\lambda]} \otimes \pi^{[\lambda]}]^{[0]} + (-1)^\lambda \frac{\sqrt{2\lambda+1}C_\lambda}{2} [\alpha^{[\lambda]} \otimes \alpha^{[\lambda]}]^{[0]} \quad (15.92)$$

Introducing spherical spinors γ determine the correct form of a linearized version of the kinetic energy.

Chapter 16

Symmetries

The complexity of a general problem may be drastically reduced if we are able to recognize inherent symmetries or if a classification according to an already known symmetry is possible.

If, e.g. a symmetric hexagon is inscribed into a circle, a clockwise rotation of 60° about the center leaves its form invariant. The same result follows from any multiple of 60° . Furthermore two consecutive rotations may be described by a single one with 120° . The same holds for counter clockwise rotations. From the listed properties we may combine all these rotations into one discrete rotation group.

There are additional discrete operations which leave the shape of the hexagon invariant e.g. reflections at a symmetry axis.

Consequently we may describe a hexagon only by its symmetry properties.

If we fix the hexagon at its boundaries and investigate the vibrational characteristics of this hexagonal membrane, we have to solve a second order differential equation. We expect, that the symmetry properties mentioned above are still valid for the fundamental mode. This means, that the solution of the wave equation is invariant for rotations about 60° .

Considerations of this type are very important, since they reduce the complexity of a given problem and in many cases are necessary to obtain a valid solution.

The extension from discrete to continuous symmetries, e.g. a rotation with arbitrary angle, a shift with arbitrary length parameter or a measurement at any time leads to the concept of continuous groups, which are called Lie groups [Greiner and Müller (1994)], [Steeb (2007)].

Prominent examples are the components of the classical angular momentum $\vec{L} = \{L_x, L_y, L_z\}$, which are defined as

$$\vec{L} = \vec{r} \times \vec{p} \quad (16.1)$$

They obey the commutation relations

$$[L_x, L_y] = L_z \quad [L_x, L_z] = -L_y \quad [L_y, L_z] = L_x \quad (16.2)$$

and consequently form a non-Abelian group.

The Casimir operator Operator Λ_3^2 commutes with all elements of this group simultaneously:

$$\Lambda_3^2 = L_x^2 + L_y^2 + L_z^2 \quad (16.3)$$

$$[\Lambda_3^2, L_x] = 0 \quad [\Lambda_3^2, L_y] = 0 \quad [\Lambda_3^2, L_z] = 0 \quad (16.4)$$

16.1 Characteristics of fractional group theory

The transition from classical mechanics to quantum mechanics is realized within the framework of canonical quantization by replacing the classical observables $\{x, p\}$ by the corresponding quantum mechanical observables $\{\hat{x}, \hat{p}\}$, which are realized as derivative operators.

In quantum mechanics, calculations are performed using these operators. For example, we obtain for the commutation relation $[\hat{x}, \hat{p}]$

$$\begin{aligned} [\hat{x}, \hat{p}] &= [x, -i\hbar\partial_x] \\ &= -i\hbar(x\partial_x - \partial_xx) \\ &= -i\hbar(x\partial_x - 1 - x\partial_x) \\ &= i\hbar \end{aligned} \quad (16.5)$$

where we have used the Leibniz' product rule.

We want to emphasize that the commutation relations were calculated independently of a specific function set $|\nu\rangle$ they are acting on. Therefore we obtain results, which are valid in general for any reasonable realization of the underlying Hilbert space.

In order to realize the transition to fractional quantum mechanics within the framework of canonical quantization the classical observables $\{x, p\}$ are replaced by (11.10) and (11.11). For the commutation relations $[\hat{X}, \hat{P}]$ are given as

$$[\hat{X}, \hat{P}] = -i\hbar[\hat{x}^\alpha, \hat{D}^\alpha] \quad (16.6)$$

In the following we will show, that commutation relations may not be calculated independently of a specific function set any more. Instead, the results derived are only valid for a given function set, the operators act on.

As an illustrative example we will apply the fractional derivative according to Riemann and will calculate the explicit action of the commutation relations on the specific function set $|\nu\rangle = \hat{x}^{\alpha\nu}$. We obtain:

$$\begin{aligned} -i\hbar[\hat{x}^\alpha, {}_R\hat{D}^\alpha]|\nu\rangle &= -i\hbar\left(\hat{x}^\alpha \frac{\Gamma(1+\nu\alpha)}{\Gamma(1+(\nu-1)\alpha)}|\nu-1\rangle - {}_R\hat{D}^\alpha|\nu+1\rangle\right) \\ &= -i\hbar\left(\frac{\Gamma(1+\nu\alpha)}{\Gamma(1+(\nu-1)\alpha)} - \frac{\Gamma(1+(\nu+1)\alpha)}{\Gamma(1+\nu\alpha)}\right)|\nu\rangle \end{aligned} \quad (16.7)$$

With the abbreviation

$${}_Rc(\nu, \alpha) = \frac{\Gamma(1+(\nu+1)\alpha)}{\Gamma(1+\nu\alpha)} - \frac{\Gamma(1+\nu\alpha)}{\Gamma(1+(\nu-1)\alpha)} \quad (16.8)$$

the commutation relations (16.6) based on the fractional derivative according to Riemann result as:

$$[\hat{X}, {}_R\hat{P}]|\nu\rangle = i\hbar {}_Rc(\nu, \alpha)|\nu\rangle \quad (16.9)$$

We obtain the important result that, in contrast to classical quantum mechanics, within the framework of fractional quantum mechanics all calculations depend on the specific representation of the Hilbert space, the fractional operators act on.

The minimum requirement for a fractional operator algebra is the explicit knowledge of the corresponding set of eigenfunctions.

Hence if we present the result of our derivation as

$$[\hat{X}, {}_R\hat{P}] = i\hbar {}_Rc(\nu, \alpha) \quad (16.10)$$

this relation is valid only on the set of square integrable eigenfunctions $|\nu\rangle$.

For the same commutation relations with the Liouville definition of the fractional derivative on the set of eigenfunctions $|\nu\rangle = |x|^{-\alpha\nu}, x < 0$ we obtain:

$$\begin{aligned} -i\hbar[\hat{x}^\alpha, {}_L\hat{D}^\alpha]|\nu\rangle &= -i\hbar\left(\hat{x}^\alpha \frac{\Gamma((\nu+1)\alpha)}{\Gamma(\nu\alpha)}|\nu+1\rangle - {}_L\hat{D}^\alpha|\nu-1\rangle\right) \\ &= -i\hbar \text{sign}(x) \left(|x|^\alpha \frac{\Gamma((\nu+1)\alpha)}{\Gamma(\nu\alpha)}|\nu+1\rangle - {}_L\hat{D}^\alpha|\nu-1\rangle\right) \\ &= -i\hbar \text{sign}(x) \left(\frac{\Gamma((\nu+1)\alpha)}{\Gamma(\nu\alpha)} - \frac{\Gamma(\nu\alpha)}{\Gamma((\nu-1)\alpha)}\right)|\nu\rangle \end{aligned} \quad (16.11)$$

and hence

$${}_Lc(\nu, \alpha) = \text{sign}(x) \left(\frac{\Gamma(\nu\alpha)}{\Gamma((\nu-1)\alpha)} - \frac{\Gamma((\nu+1)\alpha)}{\Gamma(\nu\alpha)} \right) \quad x < 0 \quad (16.12)$$

$$= \frac{\Gamma((\nu+1)\alpha)}{\Gamma(\nu\alpha)} - \frac{\Gamma(\nu\alpha)}{\Gamma((\nu-1)\alpha)} \quad (16.13)$$

Finally, applying the fractional derivative according to Caputo the eigenfunctions of the commutation relations are given by $|\nu\rangle = x^{\nu\alpha}$ and therefore we may proceed

$${}_Cc(\nu, \alpha) = \begin{cases} \frac{\Gamma(1+(\nu+1)\alpha)}{\Gamma(1+\nu\alpha)} - \frac{\Gamma(1+\nu\alpha)}{\Gamma(1+(\nu-1)\alpha)} & \nu \neq 0 \\ \frac{\Gamma(1+(\nu+1)\alpha)}{\Gamma(1+\nu\alpha)} & \nu = 0 \end{cases} \quad (16.14)$$

Obviously the sets of eigenfunctions for the different commutation relations are eigenfunctions of the fractional one dimensional Euler operator $j_1^E = \hat{x}^\alpha \hat{D}^\alpha$ as well. The corresponding eigenvalues follow as:

$${}_Rj_1^E = \frac{\Gamma(1+\nu\alpha)}{\Gamma(1+(\nu-1)\alpha)} \quad (16.15)$$

$${}_Cj_1^E = \begin{cases} \frac{\Gamma(1+\nu\alpha)}{\Gamma(1+(\nu-1)\alpha)} & \nu \neq 0 \\ 0 & \nu = 0 \end{cases} \quad (16.16)$$

$${}_Lj_1^E = -\frac{\Gamma((\nu+1)\alpha)}{\Gamma(\nu\alpha)} \quad (16.17)$$

We conclude that an extension from standard group theory to fractional group theory is confronted with some additional difficulties. Despite this fact a group theoretical approach for a classification of multiplets of fractional extensions of standard groups will turn out to be a powerful tool to solve problems.

Especially nontrivial symmetries in multi-dimensional spaces, like fractional rotational symmetry in \mathbb{R}^3 may successfully be investigated. Instead of solving the fractional Schrödinger equation in hyper-spherical coordinates directly, group theoretical methods provide elegant methods and strategies, to determine the eigenvalue spectrum of such highly symmetric problems analytically.

This will be explicitly shown in the next section.

16.2 The fractional rotation group SO_N^α

The components of the classical angular momentum in \mathbb{R}^3 are given by

$$L_{ij} = x_i p_j - x_j p_i \quad i, j = 1, 2, 3 \quad (16.18)$$

The canonical quantization procedure (11.7), (11.8) determines the transition from classical mechanics to quantum mechanics we obtain the corresponding angular momentum operators

$$\hat{L}_{ij} = \hat{x}_i \hat{p}_j - \hat{x}_j \hat{p}_i \quad i, j = 1, 2, 3 \quad (16.19)$$

which are the generators of infinitesimal rotations in the i, j plane.

Within the framework of fractional calculus we will propose a generalization to fractional rotations. For that purpose we replace in (16.19) according to (11.10) and (11.11) the classical operators by the fractional generalization

$$\hat{x}_i \rightarrow \hat{X}_i \quad (16.20)$$

$$\hat{p}_i \rightarrow \hat{P}_i \quad (16.21)$$

and define the generators of infinitesimal fractional rotations in the i, j plane in \mathbb{R}^N with $(i, j = 1, \dots, 3N)$ as:

$$\begin{aligned} L_{ij}^\alpha &= \hat{X}_i \hat{P}_j - \hat{X}_j \hat{P}_i \\ &= -i\hbar \left(\hat{x}_i^\alpha \hat{D}_j^\alpha - \hat{x}_j^\alpha \hat{D}_i^\alpha \right) \end{aligned} \quad (16.22)$$

In order to calculate the commutation relations of the fractional angular momentum operators, we introduce the function set f :

$$\{f(\hat{x}_1^\alpha, \hat{x}_2^\alpha, \dots, \hat{x}_{3N}^\alpha) = \prod_i^{3N} \hat{x}_i^{\nu\alpha}\} \quad (16.23)$$

On this function set the commutation relations for the generators L_{ij}^α are isomorphic to the fractional extension $SO^\alpha(3N)$ of the standard rotation group $SO(3N)$:

$$[L_{ij}^\alpha, L_{mn}^\alpha] = i\hbar c(\nu, \alpha) (\delta_{im} L_{jn}^\alpha + \delta_{jn} L_{im}^\alpha - \delta_{in} L_{jm}^\alpha - \delta_{jm} L_{in}^\alpha) \quad (16.24)$$

where $c(\nu, \alpha)$ denotes the commutation relation

$$c(\nu, \alpha) = [\hat{x}_i^\alpha, \hat{D}_i^\alpha] \quad i = 1, \dots, 3N \quad (16.25)$$

Hence we may derive the eigenvalue spectrum of the fractional angular momentum operators in a similar manner as for the standard rotation group [Louck and Galbraith (1972)].

We define a set of Casimir operators Λ_k^2 , where the index k indicates the Casimir operator associated with $SO^\alpha(k)$:

$$\Lambda_k^2 = \frac{1}{2} \sum_{i,j}^k (L_{ij}^\alpha)^2 \quad k = 2, \dots, 3N \quad (16.26)$$

Indeed these operators fulfill the commutation relations:

$$[\Lambda_{3N}^2, L_{ij}^\alpha] = 0 \quad (16.27)$$

and successively

$$[\Lambda_k^2, \Lambda_{k'}^2] = 0. \quad (16.28)$$

The multiplets of $SO^\alpha(3N)$ may be therefore classified according to the group chain

$$SO^\alpha(3N) \supset SO^\alpha(3N-1) \supset \dots \supset SO^\alpha(3) \supset SO^\alpha(2) \quad (16.29)$$

We use Einstein's summation convention and introduce the metric of the Euclidean space to be $g_{ij} = \delta_{ij}$ for raising and lowering indices.

The explicit form of the Casimir operators is then given by

$$\begin{aligned} \Lambda_k^2 = & +\hat{X}^i \hat{X}_i \hat{P}^j \hat{P}_j - i\hbar c(\nu, \alpha) (k-1) \hat{X}^j \hat{P}_j - \hat{X}^i \hat{X}^j \hat{P}_i \hat{P}_j \\ & i, j = 1, \dots, k \end{aligned} \quad (16.30)$$

The classical homogeneous Euler operator is defined as $x_1 \partial_{x_1} + x_2 \partial_{x_2} + \dots + x_k \partial_{x_k}$.

We introduce a generalization of the classical homogeneous Euler operator J_k^e for fractional derivative operators

$$J_k^e = \hat{x}^{\alpha i} \hat{D}_i^\alpha \quad i = 1, \dots, k \quad (16.31)$$

With the generalized homogeneous Euler operator the Casimir operators are given explicitly:

$$\Lambda_k^2 = +\hat{X}^i \hat{X}_i \hat{P}^j \hat{P}_j + \hbar^2 \left(c(\nu, \alpha) (k-2) J_k^e + J_k^e J_k^e \right) \quad i, j = 1, \dots, k \quad (16.32)$$

From this equation follows, that the Casimir operator is diagonal on a function set f , if the generalized homogeneous Euler operator is diagonal on f and if f fulfills the Laplace-equation

$$\hat{D}^{\alpha i} \hat{D}_i^\alpha f = 0 \quad (16.33)$$

We will show, that the generalized homogeneous Euler operator is diagonal, if f fulfills an extended fractional homogeneity condition, which we will derive in the following. For that purpose, we first verify, that the generalized homogeneous Euler operator is diagonal on a homogeneous function in the one dimensional case.

As an example we will apply the Riemann fractional derivative. For other derivative definitions the procedure is similar.

With $\hat{\lambda}^\alpha = \text{sign}(\lambda) |\lambda|^\alpha$ the following scaling property, which is valid for the fractional derivative [Oldham and Spanier (1974)] will be used:

$$\hat{D}_{\hat{\lambda}^\alpha} f(\hat{\lambda}^\alpha \hat{x}^\alpha) = \hat{x}^\alpha \hat{D}_{\hat{\lambda}^\alpha \hat{x}^\alpha}^\alpha f(\hat{\lambda}^\alpha \hat{x}^\alpha) \quad (16.34)$$

Homogeneity of a function in one dimension implies:

$$f(\hat{\lambda}^\alpha \hat{x}^\alpha) = \hat{\lambda}^{\alpha \nu} f(\hat{x}^\alpha) \quad \nu \alpha > -1 \quad (16.35)$$

We apply the Riemann derivative to (16.35) with (16.34) we obtain:

$$\hat{x}^\alpha \hat{D}_{\hat{\lambda}^\alpha \hat{x}^\alpha}^\alpha f(\hat{\lambda}^\alpha \hat{x}^\alpha) = \frac{\Gamma(1 + \nu \alpha)}{\Gamma(1 + (\nu - 1)\alpha)} \hat{\lambda}^{\alpha(\nu - 1)} f(\hat{x}^\alpha) \quad (16.36)$$

Which for $\hat{\lambda}^\alpha = 1$ reduces (16.36) to:

$$\hat{x}^\alpha \hat{D}_{\hat{x}^\alpha}^\alpha f(\hat{x}^\alpha) = \frac{\Gamma(1 + \nu \alpha)}{\Gamma(1 + (\nu - 1)\alpha)} f(\hat{x}^\alpha) \quad (16.37)$$

The left-hand side of (16.37) is nothing else but the generalized homogeneous Euler operator (16.31) in one dimension $J_{k=1}^e$.

Hence we have demonstrated that a one dimensional homogeneous function is an eigenfunction of the fractional Euler operator.

Therefore, for the multi-dimensional case, on a function set of the form

$$\{f(\hat{x}_1^\alpha, \hat{x}_2^\alpha, \dots, \hat{x}_k^\alpha) = \sum_{\nu_i} a_{\nu_1 \nu_2 \dots \nu_k} \hat{x}_1^{\alpha \nu_1} \hat{x}_2^{\alpha \nu_2} \dots \hat{x}_k^{\alpha \nu_k}\} \quad (16.38)$$

the Euler operator J_k^e is diagonal, if the ν_i fulfill the following condition:

$$\sum_{i=1}^k \frac{\Gamma(1 + \nu_i \alpha)}{\Gamma(1 + (\nu_i - 1)\alpha)} = \frac{\Gamma(1 + \nu \alpha)}{\Gamma(1 + (\nu - 1)\alpha)} \quad (16.39)$$

This is the fractional homogeneity condition.

Hence we define the Hilbert space H^α of all functions f , which fulfill the fractional homogeneity condition (16.39), satisfy the Laplace equation $\bar{D}^i \bar{D}_i f = 0$ and are normalized in the interval $[-1, 1]$.

We propose the quantization condition:

$$\nu = n \quad n = 0, 1, 2, \dots \quad (16.40)$$

Where n is a non-negative integer. This specific choice reduces to the classical quantization condition for the case $\alpha = 1$.

On this Hilbert space H^α , the generalized homogeneous Euler operator J_k^e is diagonal and has the eigenvalues $l_k(\alpha, n)$

$$l_k(\alpha, n) = \frac{\Gamma(1 + n\alpha)}{\Gamma(1 + (n - 1)\alpha)} \quad n = 0, 1, 2, \dots \quad (16.41)$$

The eigenvalues of the Casimir operators on H^α follow as:

$$\Lambda_2 f = \hbar l_2(\alpha, n) f \quad (16.42)$$

$$\Lambda_k^2 f = \hbar^2 l_k(\alpha, n) \left(l_k(\alpha, n) + c(n, \alpha) (k - 2) \right) f \quad k = 3, \dots, 3N \quad (16.43)$$

with

$$l_k(\alpha, n) \geq l_{k-1}(\alpha, n) \geq \dots \geq |\pm l_2(\alpha, n)| \geq 0 \quad (16.44)$$

We have derived an analytic expression for the full spectrum of the Casimir operators for the $SO^\alpha(3N)$, which may be interpreted as a projection of function set (16.38) onto function set (16.23) determined by the fractional homogeneity condition (16.39).

For the special case of only one particle ($N = 1$), we can introduce the quantum numbers J and M , which now denote the J -th and M -th eigenvalue $l_3(\alpha, J)$ and $l_2(\alpha, M)$ of the generalized homogeneous Euler operators J_3^e and J_2^e respectively.

The eigenfunctions are fully determined by these two quantum numbers $f = |JM\rangle$.

With the definitions $\hat{J}_z(\alpha) = \Lambda_2 = L_{12}^\alpha$ and $\hat{J}^2(\alpha) = \Lambda_3^2 = L_{12}^{\alpha 2} + L_{13}^{\alpha 2} + L_{23}^{\alpha 2}$ it follows

$$\begin{aligned} \hat{J}_z(\alpha) |JM\rangle &= \pm \hbar \frac{\Gamma(1 + |M|\alpha)}{\Gamma(1 + (|M| - 1)\alpha)} |JM\rangle \\ M &= \pm 0, \pm 1, \pm 2, \dots, \pm J \end{aligned} \quad (16.45)$$

$$\begin{aligned} \hat{J}^2(\alpha) |JM\rangle &= \hbar^2 \frac{\Gamma(1 + (J + 1)\alpha)}{\Gamma(1 + (J - 1)\alpha)} |JM\rangle \\ J &= 0, +1, +2, \dots \end{aligned} \quad (16.46)$$

For $\alpha = 1$ equations (16.45) and (16.46) reduce to the classical values

$$\hat{J}_z(\alpha = 1) |JM\rangle = \hbar M |JM\rangle \quad M = 0, \pm 1, \pm 2, \dots, \pm J \quad (16.47)$$

$$\hat{J}^2(\alpha = 1) |JM\rangle = \hbar^2 J(J + 1) |JM\rangle \quad J = 0, +1, +2, \dots \quad (16.48)$$

and $\hat{J}^2(\alpha = 1)$, $\hat{J}_z(\alpha = 1)$ reduce to the classical operators \hat{J}^2 , \hat{J}_z used in standard quantum mechanical angular momentum algebra [Edmonds (1957); Rose (1995)].

The complete eigenvalue spectrum of the Casimir operators of the fractional rotation group has been calculated algebraically for the Riemann fractional derivative.

It is important to mention, that there are two different eigenvalues for $M = 0$ as a consequence of the nonvanishing derivative of a homogeneous

function of degree $n = 0$. This is a special property of the Riemann fractional derivative definition.

To illustrate this point we present the Cartesian representation of the eigenfunction f for the simple case $\alpha = \frac{1}{2}$ and $n = 2$ explicitly:

$$f(\alpha = 1/2, n = 2, x, y) = |\pm 0\rangle = y^{-\frac{1}{2}} \pm ix^{-\frac{1}{2}} \quad (16.49)$$

Indeed it follows:

$$l_2(\alpha = 1/2, n = 2) |\pm 0\rangle = \frac{1}{\Gamma(1/2)} |\pm 0\rangle \quad (16.50)$$

$$L_z^{\alpha=1/2} |\pm 0\rangle = \pm \frac{1}{\Gamma(1/2)} |\pm 0\rangle \quad (16.51)$$

The calculation of the eigenvalue spectrum of the Casimir operators for different fractional derivative definitions follows the same procedure.

On the basis of the Caputo derivative we obtain for the eigenvalue spectrum of the fractional Euler operator:

$$l_k(\alpha, n) = \begin{cases} \frac{\Gamma(1+n\alpha)}{\Gamma(1+(n-1)\alpha)} & n = 1, 2, \dots \\ 0 & n = 0 \end{cases} \quad (16.52)$$

which differs from the Riemann definition only in the case $n = 0$ and for the sequence of eigenvalues for the Casimir operators we obtain:

$$\hat{J}_z(\alpha) |JM\rangle = \begin{cases} \pm \hbar \frac{\Gamma(1+|M|\alpha)}{\Gamma(1+(|M|-1)\alpha)} |JM\rangle & M = \pm 1, \pm 2, \dots, \pm J \\ 0 & M = 0 \end{cases} \quad (16.53)$$

$$\hat{J}^2(\alpha) |JM\rangle = \begin{cases} \hbar^2 \frac{\Gamma(1+(J+1)\alpha)}{\Gamma(1+(J-1)\alpha)} |JM\rangle & J = +1, +2, \dots \\ 0 & J = 0 \end{cases} \quad (16.54)$$

Therefore we have classified the multiplets of the fractional extension of the standard rotation group $SO^\alpha(3N)$.

Now we may search for a realization of $SO^\alpha(3)$ symmetry in nature. Promising candidates for a still unrevealed $SO^\alpha(3)$ symmetry are the ground state band spectra of even-even nuclei. Therefore we will introduce the fractional symmetric rigid rotor model in the next chapter and discuss some of its applications.

Exercise 16.1

Invariant commutation relations of canonically conjugated operators

Problem: Show that the canonically conjugated operators

$$X = x^\alpha \partial_x^\beta \quad (16.55)$$

$$P = \partial_x^\alpha x^\beta \quad \alpha + \beta = 1 \quad (16.56)$$

where ∂_x^α is the Riemann fractional derivative, fulfill the commutation relation

$$[X, P] = \beta - \alpha \quad (16.57)$$

which is independent from a specific choice of the underlying function space.

Exercise 16.2

Asymptotic expansion of the eigenvalue spectrum of the fractional $SO^\alpha(2)$ and $SO^\alpha(3)$

Problem: What is the asymptotic expansion of the spectrum of the Casimir operators for $|M|\alpha \gg 1$ and $J\alpha \gg 1$ respectively.

$$\hat{J}_z(\alpha) |JM\rangle = \pm \hbar \frac{\Gamma(1 + |M|\alpha)}{\Gamma(1 + (|M| - 1)\alpha)} |JM\rangle \quad (16.58)$$

$$\hat{J}^2(\alpha) |JM\rangle = \hbar^2 \frac{\Gamma(1 + (J + 1)\alpha)}{\Gamma(1 + (J - 1)\alpha)} |JM\rangle \quad (16.59)$$

Hint: Use the Stirling's formula (A.54)

Chapter 17

The Fractional Symmetric Rigid Rotor

As a first application of the fractional rotation group the ground state excitation spectra of even-even nuclei will be successfully interpreted with a fully analytic fractional symmetric rigid rotor model.

In a generalized, unique approach the fractional symmetric rigid rotor treats rotations, the γ -unstable limit, vibrations and the linear potential limit similarly as fractional rotations. They all are included in the same symmetry group, the fractional $SO^\alpha(3)$. This is an encouraging unifying point of view and a new powerful approach for the interpretation of nuclear ground state band spectra.

The results derived may be applied to other branches of physics as well, e.g. molecular spectroscopy.

17.1 The spectrum of the fractional symmetric rigid rotor

The fractional stationary Schrödinger equation is given as

$$H\Psi = E\Psi \quad (17.1)$$

The requirement of invariance under fractional rotations in \mathbb{R}^3 completely determines the structure of the fractional Hamiltonian up to a constant A_0 :

$$H = m_0 + A_0\Lambda_3^2(SO^\alpha(3)) \quad (17.2)$$

$$= m_0 + A_0 \hat{J}^2(\alpha) \quad (17.3)$$

where the constant m_0 acts as a counter term for the zero-point contribution of the fractional rotational energy and constant A_0 is a measure for the level spacing.

In the last section we have demonstrated, that the Hamiltonian is diagonal on a function set $|JM\rangle$ diagonal.

Furthermore the Hamiltonian commutes with the parity operator Π , $[H, \Pi] = 0$.

For $\alpha = 1$ the function set $|JM\rangle$ reduces to the set of spherical harmonics Y_{JM} in Cartesian representation. The eigenvalues of the parity operator Π are then given by:

$$\begin{aligned}\Pi Y_{JM}(x_1, x_2, x_3) &= Y_{JM}(-x_1, -x_2, -x_3) \\ &= (-1)^J Y_{JM}(x_1, x_2, x_3)\end{aligned}\quad (17.4)$$

Hence the wave function Y_{JM} is invariant under parity transformation Π , if J is restricted to even, non-negative integers $J = 0, 2, 4, \dots$. In a collective geometric model, this symmetry is interpreted as the geometry of the symmetric rigid rotor model [Eisenberg and Greiner (1987)].

Whether or not the behavior (17.4) is still valid for the function set $|JM\rangle$ with arbitrary α cannot be proven directly with the methods developed so far.

Nevertheless, restricting J to be an even, non-negative integer $J = 0, 2, 4, \dots$ for arbitrary α , implies a symmetry, which we call in analogy to the case $\alpha = 1$ the fractional symmetric rigid rotor, even though this term lacks a direct geometric interpretation for $\alpha \neq 1$.

Hence we define the spectrum of a fractional symmetric rigid rotor:

$$E = E_J^\alpha = m_0 + A_0 \hbar^2 \frac{\Gamma(1 + (J+1)\alpha)}{\Gamma(1 + (J-1)\alpha)} \quad , \quad J = 0, 2, 4, \dots \quad (17.5)$$

where we have used the Riemann version of the fractional Casimir operator. We will present convincing arguments, why this variant of a fractional derivative is the right choice for the fractional rigid rotor spectrum. In figure 17.1 this level spectrum is plotted as a function of α .

As a general trend the higher angular momentum energy values are decreasing for $\alpha < 1$. This behavior is a well established observation for nuclear low energy rotational band structures [Eisenberg and Greiner (1987)].

In a classical geometric picture of the nucleus [Bohr (1952); Eisenberg and Greiner (1987)] this phenomenon is interpreted as a change of the nuclear shape under rotations, causing an increasing moment of inertia and therefore a decrease of rotational bands.

Within the framework of the fractional model presented so far the moment of inertia is fixed (since A_0 is a constant) but the same effect

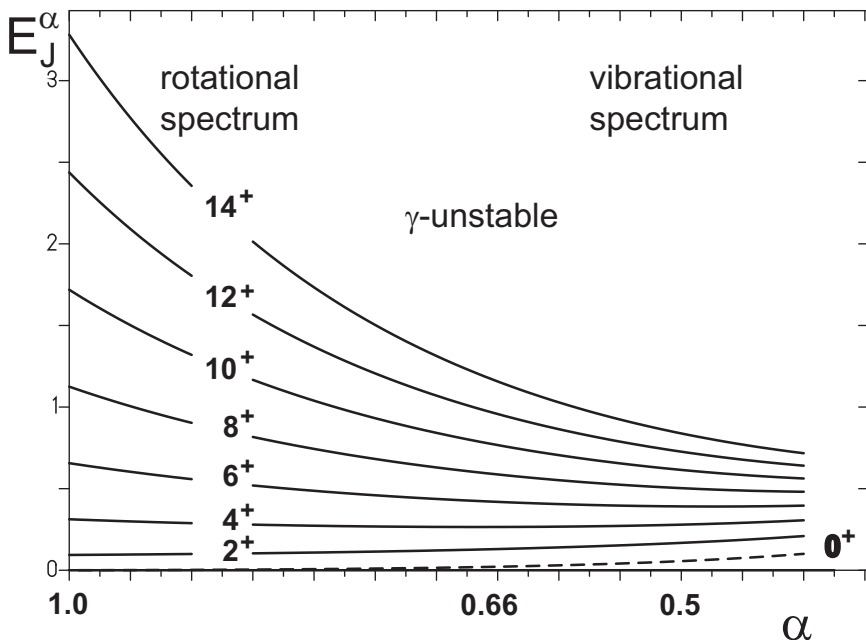


Fig. 17.1 The energy level spectrum E_J^α according to (17.5) for the fractional symmetric rigid rotor. The dotted line 0^+ shows the ground state energy for the Riemann fractional derivative. If we had used the Caputo derivative instead, the ground state energy was exactly 0.

now results as an inherent property of the fractional derivatives angular momentum.

Another remarkable characteristic of the fractional symmetric rigid rotor spectrum is due to the fact, that the relative spacing between different levels is changing with α (see figure 17.2).

In classical geometric models there are distinct analytically solvable limits, e.g. the rotational, vibrational and so called γ -unstable limits.

These limits are characterized by their independence of the potential energy from γ . In that case, the five dimensional Bohr Hamiltonian is separable [Bohr (1952); Fortunato (2005)].

With the collective coordinates β , γ and the three Euler angles θ_i the product ansatz for the wave function

$$\Psi(\beta, \gamma, \theta_i) = f(\beta)\Phi(\gamma, \theta_i) \quad (17.6)$$

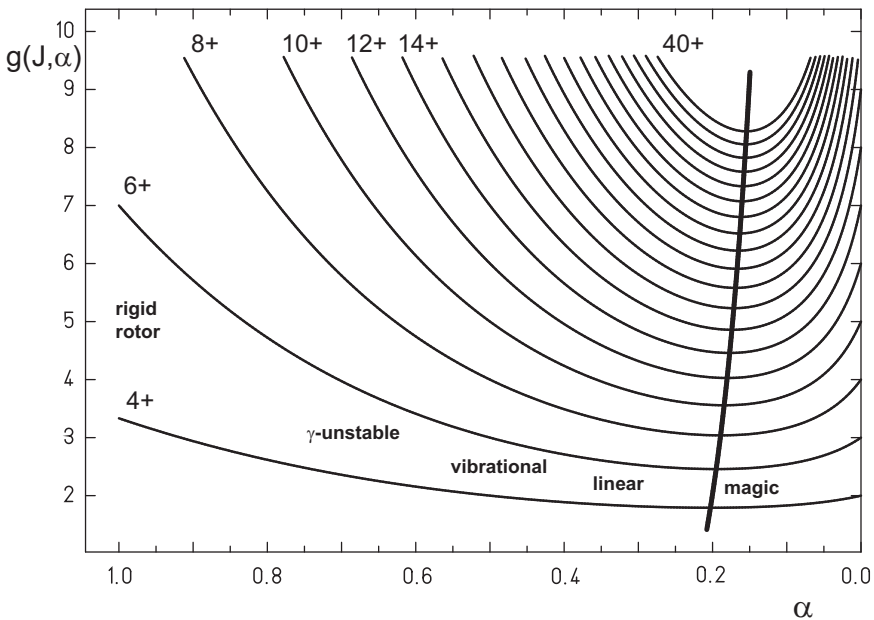


Fig. 17.2 Relative energy levels $g(J, \alpha) = (E_J^\alpha - E_0^\alpha)/(E_2^\alpha - E_0^\alpha)$ with E_J^α from (17.5) for the fractional symmetric rigid rotor. The thick line indicates the minimum ratio for a given J as a function of α .

leads to a differential equation for β , expressed in canonical form:

$$\left\{ \frac{\hbar^2}{2B} \left(-\frac{\partial^2}{\partial \beta^2} + \frac{(\tau+1)(\tau+2)}{\beta^2} \right) + V(\beta) \right\} (\beta^2 f(\beta)) = E(n_\beta, \tau) (\beta^2 f(\beta)) \quad (17.7)$$

The ground state spectra of nuclei, based on γ independent potentials, are then determined by the conditions [Fortunato (2005)]:

$$\begin{aligned} n_\beta &= 0 \\ 2\tau &= J \quad , \quad \tau = 0, 1, 2, \dots \end{aligned} \quad (17.8)$$

In the following we will prove, that the above mentioned limits are included within the fractional symmetric rigid rotor spectrum as special cases at distinct α -values. This is a further indication, that the fractional symmetric rigid rotor model may be successfully applied to low energy excitation spectra of nuclei.

17.2 Rotational limit

In the geometric collective model the rotational limit is described by the symmetric rigid rotor [Bohr (1954); Eisenberg and Greiner (1987)]:

$$E = \frac{1}{2} \frac{\hbar^2}{\Theta} J(J+1) \quad , \quad J = 0, 2, 4, \dots \quad (17.9)$$

This limit is trivially included in the fractional symmetric rigid rotor spectrum for $\alpha = 1$.

$$\begin{aligned} E_J^{\alpha=1} &= m_0 + A_0 \hbar^2 \frac{\Gamma(1+(J+1))}{\Gamma(1+(J-1))} \\ &= m_0 + A_0 \hbar^2 \frac{(J+1)!}{(J-1)!} \\ &= m_0 + A_0 \hbar^2 J(J+1) \quad , \quad J = 0, 2, 4, \dots \end{aligned} \quad (17.10)$$

Setting $m_0 = 0$ and $A_0 = 1/(2\Theta)$ completes the derivation.

Remarkably enough, reading (17.9) backwards is an application of the original Euler concept for a fractional derivative, since Euler suggested a replacement of $n!$ for the discrete case by $\Gamma(1+n)$ for the fractional case [Euler (1738)].

17.3 Vibrational limit

In the geometric collective model the vibrational limit is described by a harmonic oscillator potential [Eisenberg and Greiner (1987)].

$$V(\beta) = \frac{1}{2} C \beta^2 \quad (17.11)$$

where C is the stiffness in β -direction. The level spectrum is given by

$$E = \hbar\omega(N + 5/2) \quad (17.12)$$

with $\omega = \sqrt{C/B}$ and

$$N = 2n_\beta + \tau \quad , \quad N = 0, 1, 2, 3, \dots \quad (17.13)$$

Therefore the ground state band $E^{g.s.}$ is given according to the conditions (17.8) by

$$E^{g.s.}(\tau) = \hbar\omega(\tau + 5/2) \quad \tau = 0, 1, 2, \dots \quad (17.14)$$

We will now prove, that for $\alpha = 1/2$ the spectrum for the fractional symmetric rigid rotor corresponds to this vibrational type ground state spectrum

$$\begin{aligned} E_J^{\alpha=1/2} &= m_0 + A_0 \hbar^2 \frac{\Gamma\left(1 + \frac{1}{2}(J+1)\right)}{\Gamma\left(1 + \frac{1}{2}(J-1)\right)} \\ &= m_0 + A_0 \hbar^2 \frac{\Gamma(1 + J/2 + \frac{1}{2})}{\Gamma(1 + J/2 - \frac{1}{2})} \\ &= m_0 + A_0 \hbar^2 \frac{\Gamma(1 + J/2 + \frac{1}{2})}{\Gamma(J/2 + \frac{1}{2})} \\ &= m_0 + A_0 \hbar^2 (J/2 + \frac{1}{2}) \quad , \quad J = 0, 2, 4, \dots \end{aligned} \tag{17.15}$$

where we have used $\Gamma(1+z) = z\Gamma(z)$.

Since $J = 2\tau$ for the ground state band we get:

$$E_J^{\alpha=1/2} = m_0 + A_0 \hbar^2 (\tau + \frac{1}{2}) \quad , \quad \tau = 0, 1, 2, \dots \tag{17.16}$$

Setting $m_0 = 2\hbar\omega$ and $A_0 = \omega/\hbar$ completes the derivation.

It should at least be mentioned, that the above few lines mark the realization of an old alchemist's dream: the transmutation of a given group to another (here from SO(n) to U(n)). This was also the ambitious aim of q-deformed Lie algebras [Gupta *et al.* (1992)], but was missed until now.

The appearance of the correct equidistant level spacing including the zero-point energy contribution of the harmonic oscillator eigenvalues (17.16) is due to the fact, that the Riemann fractional derivative does not vanish when applied to a constant function. Instead, for the fractional symmetric rigid rotor based on the Riemann fractional derivative there always exists a zero-point energy for $\alpha \neq 1$ of the form

$$\hat{J}^2(\alpha)|00\rangle = \hbar^2 \frac{\Gamma(1+\alpha)}{\Gamma(1-\alpha)}|00\rangle \tag{17.17}$$

If we had chosen the Caputo derivative definition, for $\alpha = 1/2$ we would have obtained an equidistant spectrum too, but the zero-point energy would have been $E_0^{\alpha=1/2} = 0$ and consequently would have been too small.

Hence the consistence with the spectrum of the harmonic oscillator including the zero-point energy is a strong argument for our specific choice of the Riemann fractional derivative definition.

17.4 Davidson potential - the so called γ -unstable limit

A third analytically solvable case exists, which is based on the Davidson potential [Davidson (1932)], which originally was proposed to describe an interaction in diatomic molecules.

The potential is of the form

$$V(\beta) = \frac{1}{8}C\beta_0^2 \left(\frac{\beta}{\beta_0} - \frac{\beta_0}{\beta} \right)^2 \quad (17.18)$$

where β_0 (the position of the minimum) and C (the stiffness in β -direction at the minimum) are the parameters of the model.

For $\beta_0 = 0$ this potential is equivalent to the harmonic oscillator potential.

In the general case, the energy level spectrum is given by

$$E(n_\beta, \tau) = \hbar\omega(n_\beta + \frac{1}{2} + \frac{1}{2}a_\tau) - \frac{1}{4}C\beta_0^2 \quad (17.19)$$

with

$$a_\tau = \frac{1}{2}\sqrt{\sqrt{BC}\beta_0^4 + (2\tau + 3)^2} \quad (17.20)$$

For the ground state band we get

$$E^{g.s.}(\tau) = \hbar\omega \left(\frac{1}{2} + \frac{1}{2}a_\tau \right) - \frac{1}{4}C\beta_0^2 \quad (17.21)$$

For $\beta_0 > 0$ we expand the square root in a_τ in a Taylor-Series

$$a_\tau = \frac{1}{2}\sqrt{\sqrt{BC}\beta_0^2} \left(1 + \frac{1}{2} \frac{(2\tau + 3)^2}{\sqrt{BC}\beta_0^4} + \dots \right) \quad (17.22)$$

Shifting τ by

$$\tau = \hat{\tau} - 3/2 \quad (17.23)$$

causes the linear term to vanish and the resulting level scheme is of the form

$$E^{g.s.}(\hat{\tau}) = c_0 + c_1\hat{\tau}^2 + \dots \quad (17.24)$$

Therefore the γ -unstable Davidson potential is characterized by the condition, that the linear term in a shifted series expansion in τ vanishes.

In order to determine the corresponding fractional coefficient α , we shift the fractional energy spectrum by $-3/2$ and expand in a Taylor series at

$J/2 = \tau = 0$ (Ψ and Ψ^1 denote the di- and tri-gamma function):

$$\begin{aligned} E_{\tau-\frac{3}{2}}^\alpha &= m_0 + A_0 \hbar^2 \frac{\Gamma(1-\alpha/2)}{\Gamma(1-5\alpha/2)} \\ &\quad \times \left[1 - \alpha \left(\Psi(1-5\alpha/2) - \Psi(1-\alpha/2) \right) \tau \right. \\ &\quad + \frac{\alpha^2}{2} \left\{ \left(\Psi(1-5\alpha/2) - \Psi(1-\alpha/2) \right)^2 \right. \\ &\quad \left. \left. - \left(\Psi^1(1-5\alpha/2) - \Psi^1(1-\alpha/2) \right) \right\} \tau^2 + \dots \right] \end{aligned} \quad (17.25)$$

The linear term in τ has to vanish. Therefore α is determined by the condition α :

$$\Psi(1-5\alpha/2) = \Psi(1-\alpha/2) \quad (17.26)$$

which is fulfilled for $\alpha \approx 0.66$.

Hence for a sufficiently large β_0 the ground state band spectrum of the γ -unstable Davidson potential is reproduced within the fractional symmetric rigid rotor at $\alpha \approx 2/3$.

17.5 Linear potential limit

The hitherto discussed three special cases, which are known to be analytically solvable in geometric and IBM-models respectively were found to be realized within proposed fractional rotor model using a fractional derivative parameter in the range $1/2 \leq \alpha \leq 1$. But the domain of allowed fractional derivative parameters is at least extendible down to $\alpha = 0$. Therefore our interest is attracted to fractional derivative parameters with $\alpha < 1/2$. As an intuitive guess we may assume, that this region may be interpreted in terms of a geometric model using potentials which increase weaker than a harmonic oscillator potential:

$$V(\beta) \sim |\beta|^\nu \quad \nu < 2, \nu \in \mathbb{R} \quad (17.27)$$

In view of fractional calculus therefore the investigation of the properties of e.g. a linear potential is an obvious extension of the well established geometric model potentials. Since geometric models are subject of interest for more than 50 years now, it is surprising that potentials of the type (17.27) did not play any role and were never considered even for academic reasons only.

An investigation of potentials of type (17.27) is a natural consequence of a fractional extension of $SO^\alpha(N)$. For geometric models this subject is an open task. This is a nice example for the fact, that on one hand even in this research area there are still open questions and on the other hand, that a concept based on fractional calculus indeed may stimulate research in other areas.

Hence the linear potential was proposed and studied theoretically as late as 2005 by Fortunato [Fortunato (2005)].

Although it has not been used for a description of nuclear ground state band spectra yet, it will turn out to be useful for an understanding of nuclear spectra near closed shells discussed in the following section.

The potential is of the form

$$V(\beta) = C|\beta| \quad (17.28)$$

where C (the stiffness in β -direction) is the main parameter of the model.

The level spectrum is given approximately by [Fortunato (2005)]:

$$E(n_\beta, \tau) = \frac{3}{2}C\beta_0 + (n_\beta + \frac{1}{2})\sqrt{\frac{3C}{\beta_0}} \quad (17.29)$$

with

$$\beta_0 = \left(2(\tau+1)(\tau+2)/C\right)^{1/3} \quad (17.30)$$

The ground state band level spectrum is given according to conditions (17.8) by

$$E^{g.s.}(\tau) = \frac{3}{2}C\beta_0 + \frac{1}{2}\sqrt{\frac{3C}{\beta_0}} \quad (17.31)$$

We therefore are able to define the relative energy levels $f(\tau)$ in units $E^{g.s.}(1) - E^{g.s.}(0)$, which are independent of parameter C .

$$f(\tau) = \frac{E^{g.s.}(\tau) - E^{g.s.}(0)}{E^{g.s.}(1) - E^{g.s.}(0)} \quad (17.32)$$

An expansion in a Taylor series at $\tau = 1$ yields:

$$f(\tau) = 1 + 0.895(\tau - 1) - 0.076(\tau - 1)^2 + 0.018(\tau - 1)^3 + \dots \quad (17.33)$$

An equivalent expression for the fractional rotational energy is given by:

$$g(\tau, \alpha) = \frac{E_{2\tau}^\alpha - E_0^\alpha}{E_2^\alpha - E_0^\alpha} \quad \tau \in \mathbb{N} \quad (17.34)$$

A Taylor series expansion at $\tau = 1$ followed by a comparison of the linear terms of $f(\tau)$ and $g(\tau, \alpha)$ leads to the condition

$$\frac{2\alpha\Gamma(1-\alpha)\Gamma(3\alpha)\left(2+3\alpha\Psi(\alpha)-\Psi(3\alpha)\right)}{\Gamma^2(1+\alpha)-\Gamma(1-\alpha)\Gamma(1+3\alpha)}=0.895 \quad (17.35)$$

There are two solutions given by:

$$\alpha_1 = 0.33 \quad (17.36)$$

$$\alpha_2 = 0.11 \quad (17.37)$$

Hence below the vibrational region at $\alpha \approx 1/2$ there exists a region at $\alpha \approx 1/3$, which corresponds to the linear potential model in a geometric picture.

17.6 The magic limit

In figure 17.2 an additional region is visible, which attracts our attention. Near $\alpha \approx 0.2$ a minimum occurs for the relative level spacing. Of course this immediately raises the question, if we can assign a model potential in this case too.

The answer will be given in terms of an approximation of the effective potential in terms of the shifted harmonic oscillator:

Starting with a model potential of the form

$$V(\beta) = C\beta^\nu \quad \nu \geq 0 \quad (17.38)$$

according to (17.7) the effective potential is given by:

$$V_{\text{eff}}(\beta) = C\beta^\nu + \frac{(\tau+1)(\tau+2)}{\beta^2} \quad (17.39)$$

The minimum of the potential at β_0 may be calculated from the requirement:

$$\frac{d}{d\beta} V_{\text{eff}}(\beta) |_{\beta=\beta_0} = 0 \quad (17.40)$$

We obtain

$$\beta_0 = \left(\frac{2(\tau+1)(\tau+2)}{\nu C} \right)^{\frac{1}{\nu+2}} \quad (17.41)$$

A series expansion of the effective potential at β_0 up to second order in β leads to:

$$V_{\text{eff}}(\beta) \approx c_0 + \frac{1}{2}\omega^2(\beta - \beta_0)^2 \quad (17.42)$$

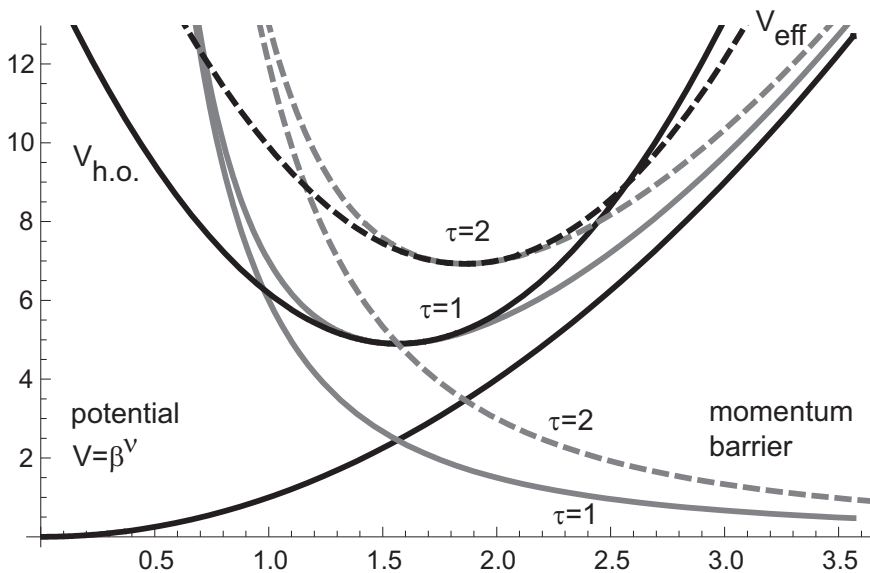


Fig. 17.3 An approximation for the geometric model potential $V = \beta^\nu$ for an analytic calculation of the level spectrum. Gray lines correspond to the angular momentum barrier, the sum of these two terms which is the effective potential V_{eff} and the harmonic approximation $V_{\text{h.o.}}$. Thick lines correspond to $\tau = 1$ and dashed lines indicate $\tau = 2$.

The constants c_0 and ω^2 result as

$$c_0 = C \left(1 + \frac{\nu}{2}\right) \beta_0^\nu \quad (17.43)$$

$$\omega^2 = C \frac{\nu(\nu+2)}{2} \beta_0^{\nu-2} \quad (17.44)$$

Energy eigenvalues in units \hbar are then given as

$$E(n_\beta, \tau, n) = c_0 + \left(n_\beta + \frac{1}{2}\right)\omega \quad (17.45)$$

In figure 17.3 we present the single terms of the effective potential and the harmonic approximation for different angular momenta τ .

For the ground state band we obtain according to conditions (17.8)

$$E^{g.s.}(\tau) = c_0 + \frac{1}{2}\omega \quad (17.46)$$

The special case of the linear potential ($\nu = 1$) presented in the previous section has been investigated by Fortunato using the same method of harmonic approximation.

Let us present the relative energy values $f(\tau)$ in units $E^{g.s.}(1) - E^{g.s.}(0)$, which are independent of the parameter C .

$$f(\tau, \nu) = \frac{E^{g.s.}(\tau) - E^{g.s.}(0)}{E^{g.s.}(1) - E^{g.s.}(0)} \quad (17.47)$$

The minimum for the relative level spacing for the fractional rigid rotor can be deduced from figure 17.2 as $\alpha \approx 0.2$ and $R(4^+/2^+) = 1.79$ results.

Within the framework of the geometric model we now will search for a value for ν which leads to a similar ratio.

Indeed it follows that in the limit $\nu \rightarrow 0$ the ratio

$$\lim_{\nu \rightarrow 0} f(\tau = 2^+, \nu) = 1.72 \quad (17.48)$$

We obtain the remarkable result, that we may associate within the limitations of the analytic harmonic approximation the minimum of the relative level spacing at $\alpha \approx 0.2$ with a vanishing collective potential in the geometric model.

In other words, if the macroscopic collective potential vanishes, the spectrum is dominated by microscopic effects like shell- and pairing corrections. This situation is indeed realized near atomic nuclei with magic proton and neutron numbers respectively.

Therefore the validity of fractional symmetric rigid rotor model by far exceeds the scope of a collective geometric model.

Let us summarize the results:

A change of the fractional derivative coefficient α may be interpreted within a geometric collective model as a change of the potential energy surface.

In a generalized, unique approach the fractional symmetric rigid rotor treats rotations at $\alpha \approx 1$, the γ -unstable limit at $\alpha \approx 2/3$, vibrations at $\alpha \approx 1/2$, the linear potential limit at $\alpha \approx 1/3$ and even the magic limit similarly as fractional rotations. They all are included in the same symmetry group, the fractional $SO^\alpha(3)$. This is an encouraging unifying point of view and a new powerful approach for the interpretation of nuclear ground state band spectra.

Of course the results derived may be applied to other branches of physics as well, e.g. molecular spectroscopy.

In the following section we will apply the fractional rotor model to experimental data.

17.7 Comparison with experimental data

In the previous section we have shown, that the rotational, vibrational and γ -unstable limit of geometric collective models are special cases of the fractional symmetric rigid rotor spectrum.

The fractional derivative coefficient α acts like an order parameter and allows a smooth transition between these idealized cases.

Of course, a smooth transition between rotational and e.g. vibrational spectra may be achieved by geometric collective models too. A typical example is the Gneuss-Greiner model [Gneuss and Greiner (1971)] with a more sophisticated potential. Critical phase transitions from vibrational to rotational states have been studied for decades using e.g. coherent states formalism or within the framework of the IBM-model [Casten *et al.* (1993); Feng *et al.* (1981); Haapakoski *et al.* (1970); Raduta *et al.* (2005); Raduta *et al.* (2010)]. But in general, within these models, results may be obtained only numerically with extensive effort, while the fractional rotor model leads to analytic results for intermediate cases too.

Especially the intermediate cases are important, because there are only very few nuclei, whose spectra may correspond to the idealized limits.

In the following we will prove, that the full range of low energy ground state band spectra of even-even nuclei is accurately reproduced within the framework of the fractional symmetric rigid rotor model.

For a fit of the experimental spectra E_J^{exp} we will use (17.5)

$$E_J^\alpha = m_0 + a_0 \frac{\Gamma(1 + (J+1)\alpha)}{\Gamma(1 + (J-1)\alpha)} \quad , \quad J = 0, 2, 4, \dots \quad (17.49)$$

with the slight modification, that \hbar^2 has been included into the definition of a_0 , so that m_0 and a_0 may both be given in units of [keV].

As a first application we will analyze typical rotational, γ -unstable, vibrational and linear type spectra.

In the upper row of figure 17.4 the energy levels of the ground state bands are plotted for ^{156}Gd , ^{196}Pt , ^{110}Cd and ^{218}Po which represent typical rotational-, γ -unstable-, vibrational and linear type spectra.

The fractional coefficients α , deduced from the experimental data, are remarkably close to the theoretically expected idealized limits of the fractional symmetric rigid rotor.

From the experimental data, we can roughly distinguish a rotational region for $1 \geq \alpha \geq 0.8$, a γ -unstable region for $0.8 \geq \alpha \geq 0.6$, a vibrational

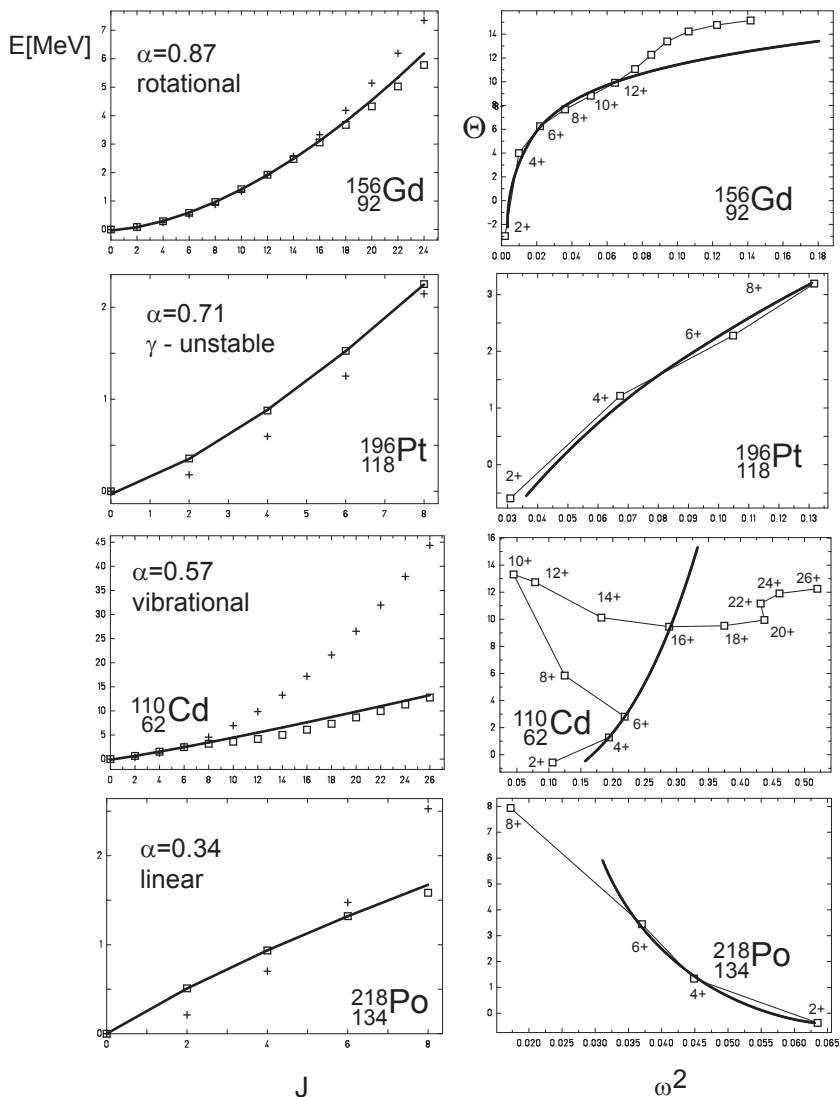


Fig. 17.4 The left column shows energy levels of the ground state bands for ^{156}Gd , ^{196}Pt , ^{110}Cd and ^{218}Po for increasing J . Squares indicate the experimental values, + symbols indicate the optimum fit of the classical symmetric rigid rotor and the curves give the best fit for the fractional symmetric rigid rotor. In the right column the corresponding back bending plots are shown.

region for $0.6 \geq \alpha \geq 0.4$ and a linear potential region for $0.4 \geq \alpha \geq 0.2$. Experimental results are reproduced very well for all regions within the framework of the fractional symmetric rigid rotor model.

Since for higher angular momenta commencing microscopic effects limit the validity of the macroscopic fractional symmetric rigid rotor model fits, in the lower row of figure 17.4 the corresponding back bending plots are shown. With these plots, the maximum angular momentum J_{max} for a valid fit may be determined. In table 17.1 the optimum parameter sets (α, a_0, m_0) as well as the average root mean square deviation ΔE are listed. In general, the difference between experimental and calculated energies is less than 2%.

This means, that the error is better than a factor 3 to 6 compared to the results of a standard Taylor series expansion up to second order in J .

As a second application of the fractional symmetric rigid rotor, we study systematic isotopic effects for osmium isotopes. Optimum fit parameter sets are given in the second part of table 17.1, the corresponding back bending plots are given in figure 17.5. In table 17.2 the results for the fitted ground state band energies of the fractional symmetric rigid rotor model according to (17.49) are compared to the experimental levels for ^{176}Os .

Obviously below the beginning of alignment effects the spectra are reproduced very well within the fractional symmetric rigid rotor model. The fractional coefficient α listed in table 17.1 increases slowly for increasing nucleon numbers. Consequently, we observe a smooth transition of the osmium isotopes from the γ -unstable to the rotational region.

As a third application, we investigate the systematics of the ground state energy level structure near closed shells. For that purpose, in figure 17.6 a series of spectra of radium isotopes near the magic neutron number $N = 126$ are plotted.

Starting with radium ^{224}Ra , the full variety of possible spectral types emerges while approaching the magic ^{214}Ra .

While ^{224}Ra and ^{222}Ra are pure rotors, ^{220}Ra shows a perfect γ -unstable type spectrum. ^{218}Ra presents a spectrum of an almost ideal vibrational type. ^{216}Ra is even closer to the magic ^{214}Ra and represents a new class of nuclear spectra.

In a geometric picture, this spectrum may be best interpreted as a linear potential spectrum as proposed in section 17.5. Typical candidates for this kind of spectrum are nuclei in close vicinity of magic numbers like $^{218}_{134}\text{Po}_{84}$, $^{154}_{84}\text{Yb}_{70}$, $^{134}_{80}\text{Xe}_{54}$, $^{96}_{56}\text{Zr}_{40}$ or $^{88}_{50}\text{Sr}_{38}$.

Finally, the experimental ground state spectrum of the magic nucleus ^{214}Ra shows a clustering of energy values: for low angular momenta α tends towards zero, which becomes manifest through almost degenerated energy levels while for higher angular momenta the spectrum tends to the vibrational type. In a classical picture this is interpreted as the dominating influence of microscopic shell effects. Within the framework of catastrophe theory this observation could be interpreted as a bifurcation as well.

Therefore the fractional symmetric rigid rotor model is not well suited for a description of the full spectrum of a nucleus with magic proton or neutron numbers. But all other nuclear spectra are described with a high

Table 17.1 Listed are the optimum parameter sets (α , a_0 , m_0 according to (17.49)) for the fractional symmetric rigid rotor for different nuclids. The maximum valid angular momentum J_{max} below the onset of alignment effects are given as well as the root mean square error ΔE between experimental and fitted energies in %.

nuclid	α	a_0 [keV]	m_0 [keV]	J_{max}	$\Delta E[\%]$
$^{156}_{92}\text{Gd}64$	0.863	31.90	-43.65	14	2.23
$^{196}_{118}\text{Pt}78$	0.710	175.06	-83.69	10	0.44
$^{110}_{62}\text{Cd}48$	0.570	607.91	-405.80	6	0
$^{218}_{134}\text{Po}84$	0.345	1035.69	-671.03	8	0.12
$^{164}_{88}\text{Os}76$	0.624	339.423	-128.448	6	0
$^{166}_{90}\text{Os}76$	0.634	282.411	-118.024	10	2.74
$^{168}_{92}\text{Os}76$	0.723	158.584	-54.499	12	1.33
$^{170}_{94}\text{Os}76$	0.743	125.128	-39.968	10	1.35
$^{172}_{96}\text{Os}76$	0.767	89.010	-23.656	8	1.21
$^{174}_{98}\text{Os}76$	0.771	63.388	-17.656	24	0.73
$^{176}_{100}\text{Os}76$	0.808	51.231	-23.064	18	1.22
$^{178}_{102}\text{Os}76$	0.816	49.882	-22.792	14	2.16
$^{180}_{104}\text{Os}76$	0.841	45.309	-18.662	12	2.50
$^{182}_{106}\text{Os}76$	0.903	32.002	-7.159	10	1.29
$^{184}_{108}\text{Os}76$	0.904	31.690	-12.902	14	1.39
$^{186}_{110}\text{Os}76$	0.882	40.433	-19.155	14	1.82
$^{188}_{112}\text{Os}76$	0.875	44.567	-14.629	12	1.58
$^{190}_{114}\text{Os}76$	0.847	58.055	-17.748	12	1.34
$^{192}_{116}\text{Os}76$	0.835	63.774	-15.437	12	0.71
$^{214}_{126}\text{Ra}88$	-0.007	374408	-376529	8	2.53
$^{214}_{126}\text{Ra}88$	0.548	344.107	305.766	24	8.27
$^{216}_{128}\text{Ra}88$	0.181	3665.36	-2887.88	10	4.22
$^{218}_{130}\text{Ra}88$	0.536	321.622	-160.787	30	1.25
$^{220}_{132}\text{Ra}88$	0.696	83.603	-25.966	30	0.26
$^{222}_{134}\text{Ra}88$	0.831	33.221	-5.67	6	0
$^{224}_{136}\text{Ra}88$	0.841	27.295	-8.849	12	1.57

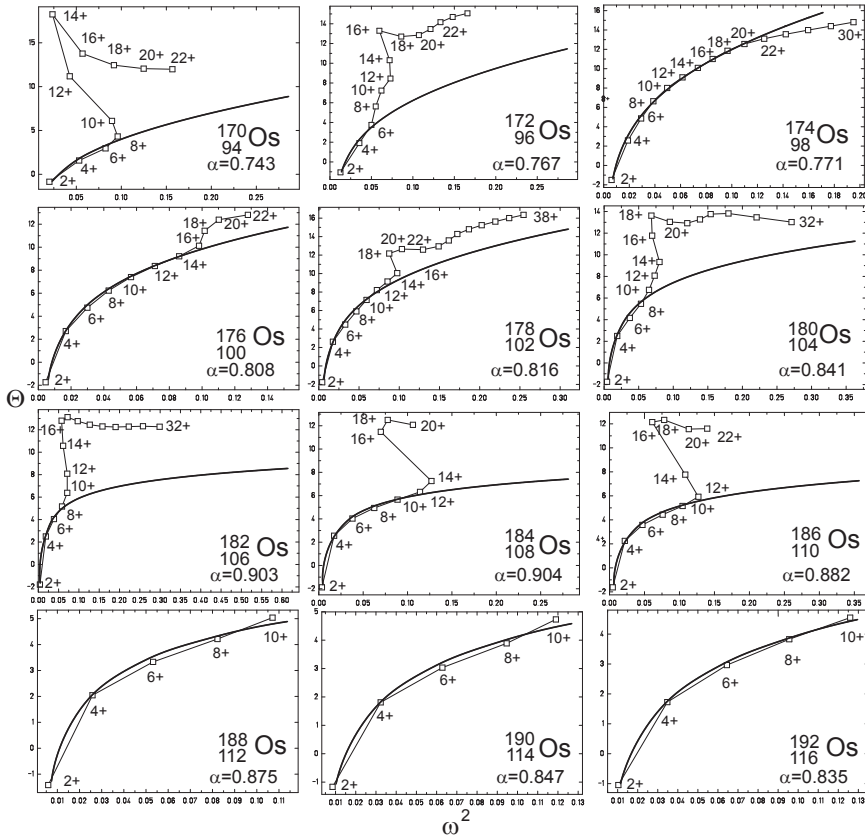


Fig. 17.5 For a set of osmium isotopes back bending plots are shown. Squares indicate experimental values. The thick line is the optimum fit result for the fractional symmetric rigid rotor. Optimum fit parameter sets are given in table 17.1. For the fit all angular momenta below the onset of microscopic alignment effects are included.

grade of accuracy within the framework of the fractional symmetric rigid rotor.

As a remarkable fact α reduces smoothly within the interval $1 \geq \alpha \geq 0$ while approaching a magic number, e.g. $N = 126$. Therefore, α is an appropriate order parameter for such sequences of ground state band spectra.

As a fourth application we analyze some general aspects, which are common to all even-even nuclei. Experimental ground state band spectra up to at least $J = 4^+$ are currently known for 490 even-even nuclei. For

Table 17.2 Energy levels for ^{176}Os with optimum parameter set from table 17.1 for the fractional symmetric rigid rotor E_J^α according to (17.49) compared with the experimental values E_J^{exp} and relative error ΔE in % for different angular momenta J . Note that for $J > 14\hbar$ beginning microscopic alignment effects are ignored in the fractional symmetric rigid rotor model and therefore the error is increasing.

$J[\hbar]$	E_J^α [keV]	E_J^{exp} [keV]	$\Delta E[\%]$
0^+	-13.1	0.0	-
2^+	144.9	135.1	-7.29
4^+	404.4	395.3	-2.31
6^+	744.8	742.3	0.33
8^+	1155.4	1157.5	0.17
10^+	1629.6	1633.8	0.25
12^+	2162.3	2167.7	0.24
14^+	2749.8	2754.6	0.17
(16^+)	3389.2	3381.4	-0.23
(18^+)	4077.8	4019.1	-1.46
(20^+)	4813.6	4683.2	-2.78
(22^+)	5594.8	5398.8	-3.63

these nuclei a full parameter fit according (17.49) was performed. The resulting distribution $n(\alpha)$ of fitted α values in 0.1 steps is plotted in figure 17.7.

This distribution is not evenly spread. Most of even-even nuclei exhibit rotational type ground state band spectra followed by γ -unstable and vibrational type spectra. There is a distribution gap at $\alpha \approx 0.3$. This is the region, where in a geometrical picture nuclear spectra corresponding to the linear potential model are expected.

About 8% of even-even nuclear spectra are best described with $\alpha \approx 0.2$. The sequence of radium isotopes, presented in figure 17.6 reflects the general distribution of spectra for even-even nuclei.

An interesting feature may be deduced from the observation, that $n(\alpha)$ is almost linear in the region $0.3 \leq \alpha \leq 0.8$.

Hence, with the proton number Z and the neutron number N , we define the distance $R(Z, N)$ in the (Z, N) -plane, from the next magic proton or neutron number respectively to be

$$R(Z, N) = \sqrt{(Z - Z_{\text{magic}})^2 + (N - N_{\text{magic}})^2} \quad (17.50)$$

The linearity of $n(\alpha)$ implies a linear dependence of α from R

$$\alpha(Z, N) = c_0 + c_1 R(Z, N) \quad , \quad 0.25 \leq \alpha \leq 0.85 \quad (17.51)$$

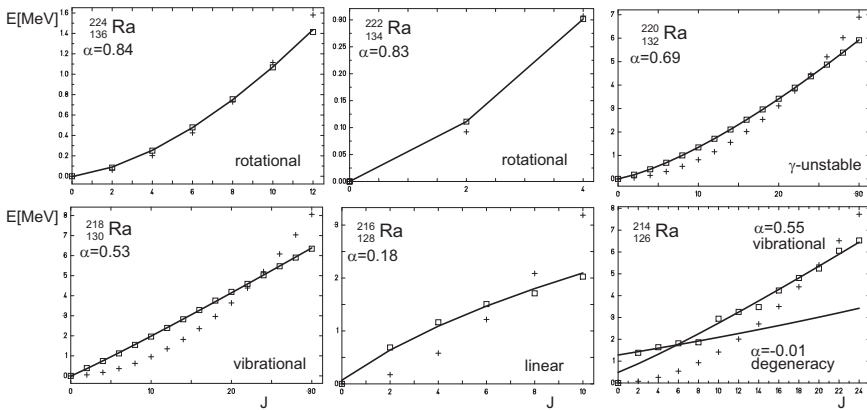


Fig. 17.6 The change of energy level structure of ground state bands near closed shells is illustrated for the magic neutron number $N = 126$ with a set of radium isotopes. Squares indicate experimental energy values. Crosses indicate the optimum fit with the standard symmetric rigid rotor model. The thick line is the optimum fit result for the fractional symmetric rigid rotor. Optimum fit parameter sets are given in the lower part of table 17.1. For ^{214}Ra , two different fits for low and higher angular momentum indicate the different spectral regions for magic nucleon numbers.

which is a helpful relation to determine an estimate of α for a series of nuclei.

Therefore the series of α values for osmium isotopes, given in table 17.1 may be understood even quantitatively:

The series of $^{164}_{88}\text{Os}$ to $^{182}_{104}\text{Os}$ is closer to the $N = 82$ magic shell and therefore shows an increasing sequence in α . A least square fit yields $c_0 = 0.528$ and $c_1 = 0.0143$ with an average error in α less than 3%

The series $^{184}_{106}\text{Os}$ to $^{192}_{116}\text{Os}$ is closer to the $N = 126$ shell and therefore shows a descending sequence in α . A least square fit yields $c_0 = 0.744$ and $c_1 = 0.008$ with an error in α less than 1%.

In figure 17.8 these results are presented graphically. We can deduce a prediction for $\alpha(^{166}_{90}\text{Os}) = 0.671$ and $\alpha(^{168}_{92}\text{Os}) = 0.695$. From these predicted α values the ratio

$$R_{4+/2+}^\alpha = \frac{E_{4+}^\alpha - E_{0+}^\alpha}{E_{2+}^\alpha - E_{0+}^\alpha} \quad (17.52)$$

may be derived.

For $^{166}_{90}\text{Os}$ a value of $R_{4+/2+} = 2.29$ and for $^{168}_{92}\text{Os}$ a value of $R_{4+/2+} = 2.35$ results. In the meantime, these predictions have been verified by experiment (see optimum α values in table 17.1) and are noted in figure 17.8

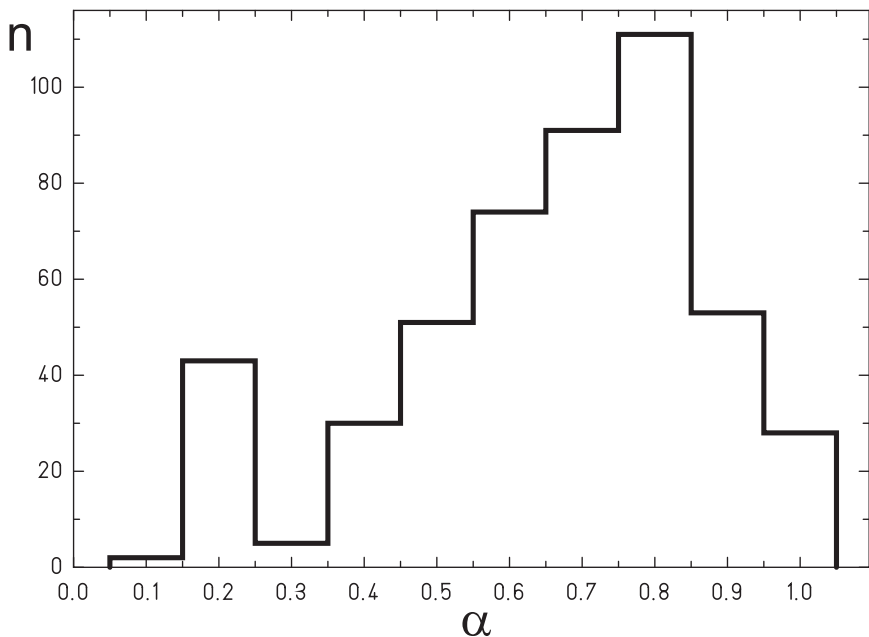


Fig. 17.7 The distribution $n(\alpha)$ of α -values from a fit of 490 ground state band spectra of even-even nuclei, accumulated in intervals $\Delta\alpha = 0.1$ from $^{84}_{4}\text{Be}_4$ to $^{256}_{156}\text{Fm}_{100}$ and $^{254}_{152}\text{No}_{102}$ respectively.

by filled squares. Within the expected error bounds a nice agreement of experimentally deduced α values with the predictions is obtained.

Furthermore, the sequence of osmium isotopes, presented in figure 17.8 indicates the position of the next magic neutron number $N = 126$. The nucleus $^{184}_{106}\text{Os}$ with the maximum α value in the sequence of osmium isotopes, is positioned just between the two magic numbers $N = 82$ and $N = 126$ and may be used for an estimate for the next magic neutron number. Therefore, we propose an alternative approach to the search for super heavy elements. Instead of a direct synthesis of super heavy elements [Oganessian *et al.* (2004); Hofmann and Münzenberg (2000); Oganessian *et al.* (2010); Düllmann *et al.* (2010)] a systematic survey of α values of the ground state band spectra of even-even nuclei with $N > 158$ and $Z > 98$ could reveal indirect information about the next expected magic numbers $Z = 114$ and $N = 184$. The currently available experimental data do not suffice to determine these magic numbers accurately.

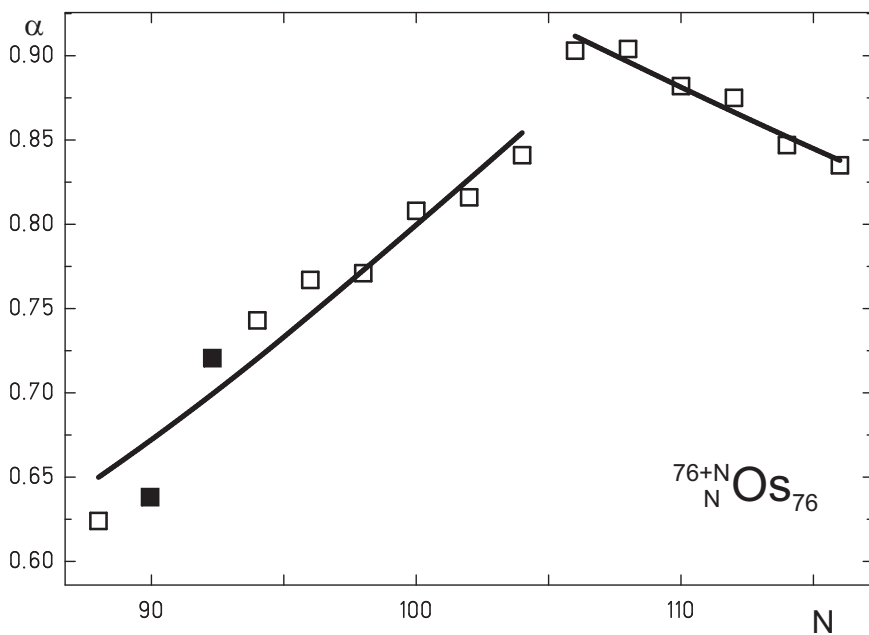


Fig. 17.8 Plot of fitted α parameters for a set of osmium isotopes as a function of increasing neutron number N . Squares indicate the optimum α listed in table 17.1, full squares indicate values, which were not available at the time of the first publication. Thick lines are fits according to equation (17.51).

From the results presented we draw the conclusion, that the full variety of low energy ground state spectra of even-even nuclei is described with a high grade of accuracy from a generalized point of view within the framework of the fractional symmetric rigid rotor.

The great advantage of the fractional symmetric rigid rotor model compared to the classical geometric models is, that nuclear ground state band spectra are described analytically with minimal effort according to equation (17.49) and with an excellent accuracy.

We also obtained a surprising physical interpretation of the nonvanishing value of the derivative of a constant function, which is a specific property of the Riemann type of a fractional derivative: In quantum mechanics this value has to be interpreted as the nonvanishing zero-point energy in quantum systems, which is a direct consequence of Heisenberg's uncertainty relation [Heisenberg (1927)].

This page intentionally left blank

Chapter 18

q-deformed Lie Algebras and Fractional Calculus

In the previous sections we have demonstrated, that the extension of the standard rotation group $SO(N)$, whose elements are the standard angular momentum operators to the fractional rotation group $SO^\alpha(N)$, whose elements are the fractional angular momentum operators leads to extended symmetries. In this case from a pure rotational symmetry to fractional rotation symmetry, which besides rotations also includes vibrational degrees of freedom.

The transition from a classical symmetry group to the analogue fractional symmetry group always implies a generalization of the classical symmetry and allows for a broader description of natural phenomena.

There is a different branch of physics which deals with exactly the same subject, too. This is the theory of q-deformed Lie algebras, which may be interpreted as extended versions of standard Lie groups.

The combination of concepts and methods developed in different branches of physics, has always led to new insights and improvements. The intention of this chapter is to show, that the concept of q-deformed Lie algebras and the methods developed in fractional calculus are strongly related (both are based on a generalized derivative definition) and may be combined leading to a new class of fractional deformed Lie algebras.

An interesting question of physical relevance is if deformed Lie algebras are not only suitable for describing small deviations from Lie symmetries, but in addition can bridge different Lie symmetries. We will demonstrate that fractional q-deformed Lie algebras show exactly this behavior.

18.1 q-deformed Lie algebras

q-deformed Lie algebras are extended versions of the usual Lie algebras [Bonatsos and Daskaloyannis (1999); Pashaev and Nalci (2012)]. They provide us with an extended set of symmetries and therefore allow the description of physical phenomena, which are beyond the scope of usual Lie algebras. In order to describe a q-deformed Lie algebra, we introduce a parameter q and define a mapping of ordinary numbers x to q-numbers e.g. via:

$$[x]_q = \frac{q^x - q^{-x}}{q - q^{-1}} \quad (18.1)$$

which in the limit $q \rightarrow 1$ yields the ordinary numbers

$$\lim_{q \rightarrow 1} [x]_q = x \quad (18.2)$$

and furthermore we obtain as a special value

$$[0]_q = 0 \quad (18.3)$$

Based on q-numbers a q-derivative may be defined via:

$$D_x^q f(x) = \frac{f(qx) - f(q^{-1}x)}{(q - q^{-1})x} \quad (18.4)$$

With this definition for a function $f(x) = x^n$ we get

$$D_x^q x^n = [n]_q x^{n-1} \quad (18.5)$$

This is a first common aspect of q-deformation and fractional calculus: they both introduce a generalized derivative operator.

As an example for q-deformed Lie algebras we introduce the q-deformed harmonic oscillator. The creation and annihilation operators a^\dagger , a and the number operator N generate the algebra:

$$[N, a^\dagger] = a^\dagger \quad (18.6)$$

$$[N, a] = -a \quad (18.7)$$

$$aa^\dagger - q^{\pm 1} a^\dagger a = q^{\mp N} \quad (18.8)$$

with the definition (18.1) equation (18.8) may be rewritten as

$$a^\dagger a = [N]_q \quad (18.9)$$

$$aa^\dagger = [N + 1]_q \quad (18.10)$$

Defining a vacuum state with $a|0\rangle = 0$, the action of the operators $\{a, a^\dagger, N\}$ on the basis $|n\rangle$ of a Fock space, defined by a repeated action of the creation operator on the vacuum state, is given by:

$$N|n\rangle = n|n\rangle \quad (18.11)$$

$$a^\dagger|n\rangle = \sqrt{[n+1]_q}|n+1\rangle \quad (18.12)$$

$$a|n\rangle = \sqrt{[n]_q}|n-1\rangle \quad (18.13)$$

The Hamiltonian of the q-deformed harmonic oscillator is defined as

$$H = \frac{\hbar\omega}{2}(aa^\dagger + a^\dagger a) \quad (18.14)$$

and the eigenvalues on the basis $|n\rangle$ result as

$$E^q(n) = \frac{\hbar\omega}{2}([n]_q + [n+1]_q) \quad (18.15)$$

There is a common aspect in the concepts of fractional calculus and q-deformed Lie algebras: they both extend the definition of the standard derivative operator.

Therefore we will try to establish a connection between the q-derivative (18.4) and the fractional derivative definition. To be conformal with the requirements (18.3) and (18.5), we will apply the Caputo derivative D_x^α :

$$D_x^\alpha f(x) = \begin{cases} \frac{1}{\Gamma(1-\alpha)} \int_0^x d\xi (x-\xi)^{-\alpha} \frac{\partial}{\partial\xi} f(\xi) & 0 \leq \alpha < 1 \\ \frac{1}{\Gamma(2-\alpha)} \int_0^x d\xi (x-\xi)^{1-\alpha} \frac{\partial^2}{\partial\xi^2} f(\xi) & 1 \leq \alpha < 2 \end{cases} \quad (18.16)$$

For a function set $f(x) = x^{n\alpha}$ we obtain:

$$D_x^\alpha x^{n\alpha} = \begin{cases} \frac{\Gamma(1+n\alpha)}{\Gamma(1+(n-1)\alpha)} x^{(n-1)\alpha} & n > 0 \\ 0 & n = 0 \end{cases} \quad (18.17)$$

Let us now interpret the fractional derivative parameter α as a deformation parameter in the sense of q-deformed Lie algebras. Setting $|n\rangle = x^{n\alpha}$ we define:

$$[n]_\alpha |n\rangle = \begin{cases} \frac{\Gamma(1+n\alpha)}{\Gamma(1+(n-1)\alpha)} |n\rangle & n > 0 \\ 0 & n = 0 \end{cases} \quad (18.18)$$

Indeed it follows

$$\lim_{\alpha \rightarrow 1} [n]_\alpha = n \quad (18.19)$$

The more or less abstract q-number is now interpreted within the mathematical context of fractional calculus as the fractional derivative parameter α with a well-understood meaning.

The definition (18.18) looks just like one more definition for a q-deformation. But there is a significant difference which makes the definition based on fractional calculus unique.

Standard q-numbers are defined more or less heuristically. There exists no physical or mathematical framework, which determines their explicit structure. Consequently, many different definitions have been proposed in the literature (see e.g. [Bonatsos and Daskaloyannis (1999)]).

In contrast to this diversity, the q-deformation based on the definition of the fractional derivative is uniquely determined, once a set of basis functions is given.

As an example we will derive the q-numbers for the fractional harmonic oscillator in the next section.

18.2 The fractional q-deformed harmonic oscillator

In the following we will present a derivation of a fractional q-number, which is independent of the specific choice of a fractional derivative definition.

The classical Hamilton function of the harmonic oscillator is given by

$$H_{\text{class}} = \frac{p^2}{2m} + \frac{1}{2}m\omega^2x^2 \quad (18.20)$$

Following the canonical quantization procedure we replace the classical observables $\{x, p\}$ by the fractional derivative operators $\{\hat{X}, \hat{P}\}$ according to (11.10) and (11.11). The quantized Hamilton operator H^α results:

$$H^\alpha = \frac{\hat{P}^2}{2m} + \frac{1}{2}m\omega^2\hat{X}^2 \quad (18.21)$$

The stationary Schrödinger equation is given by

$$H^\alpha\Psi = \left(-\frac{1}{2m}\left(\frac{\hbar}{mc}\right)^{2\alpha}m^2c^2D_x^\alpha D_x^\alpha + \frac{1}{2}m\omega^2\left(\frac{\hbar}{mc}\right)^{2(1-\alpha)}x^{2\alpha}\right)\Psi = E\Psi \quad (18.22)$$

Introducing the variable ξ and the scaled energy E' :

$$\xi^\alpha = \sqrt{\frac{m\omega}{\hbar}}\left(\frac{\hbar}{mc}\right)^{1-\alpha}x^\alpha \quad (18.23)$$

$$E = \hbar\omega E' \quad (18.24)$$

we obtain the stationary Schrödinger equation for the fractional harmonic oscillator in the canonical form

$$H^\alpha \Psi_n(\xi) = \frac{1}{2}(-D_\xi^{2\alpha} + |\xi|^{2\alpha}) \Psi_n(\xi) = E'(n, \alpha) \Psi_n(\xi) \quad (18.25)$$

In contrast to the classical harmonic oscillator this fractional Schrödinger equation has not been solved analytically until now. Since we are interested in an analytic expression for the energy levels, we will use the Bohr-Sommerfeld quantization rule to obtain an analytic approximation [Laskin (2002)]:

$$2\pi\hbar(n + \frac{1}{2}) = \oint pd\xi \quad (18.26)$$

from (18.25) it follows for the momentum

$$|p| = (2E' - |\xi|^{2\alpha})^{\frac{1}{2\alpha}} \quad (18.27)$$

For classical turning points the condition $p = 0$ holds. Motion in the classical sense therefore is allowed for $|\xi| \leq (2E')^{\frac{1}{2\alpha}}$. For (18.26) it follows explicitly:

$$2\pi\hbar(n + \frac{1}{2}) = 4 \int_0^{(2E')^{\frac{1}{2\alpha}}} pd\xi = 4 \int_0^{(2E')^{\frac{1}{2\alpha}}} (2E' - |\xi|^{2\alpha})^{\frac{1}{2\alpha}} d\xi \quad (18.28)$$

The integral may be solved:

$$E'(n, \alpha) = \left(\frac{1}{2} + n\right)^\alpha \pi^{\alpha/2} \left(\frac{\alpha \Gamma(\frac{1+\alpha}{2\alpha})}{\Gamma(\frac{1}{2\alpha})}\right)^\alpha \quad n = 0, 1, 2, \dots \quad (18.29)$$

This is the analytic approximation for the energy spectrum of the fractional harmonic oscillator. Furthermore this expression is independent of a specific choice of the fractional derivative definition.

In view of q-deformed Lie algebras, we can use this analytic result to derive the corresponding q-number. With (18.15) the q-number is determined by the recursion relation:

$$[n+1]_\alpha = 2E'(n, \alpha) - [n]_\alpha \quad (18.30)$$

Let us recall, that this recurrence relation is fulfilled in case of $\alpha \in \mathbb{N}$ by the Euler polynomials and consequently we have to extend their definition in a reasonable way to the fractional case.

In order to solve this problem, an appropriate choice for the initial condition is necessary. The obvious choice $[0]_\alpha = 0$ for the initial condition

leads to an oscillatory behavior for $[n]_\alpha$ for $\alpha < 1$. If we require a monotonically increasing behavior of $[n]_\alpha$ for increasing n , an adequate choice for the initial condition is

$$[0]_\alpha = 2^{1+\alpha} \pi^{\alpha/2} \left(\frac{\alpha \Gamma(\frac{1+\alpha}{2\alpha})}{\Gamma(\frac{1}{2\alpha})} \right)^\alpha \left(\zeta(-\alpha, \frac{1}{4}) - \zeta(-\alpha, \frac{3}{4}) \right) \quad (18.31)$$

which you will agree in after having had a look at exercise 18.1. The explicit solution is then given by

$$\begin{aligned} [n]_\alpha &= 2^{1+\alpha} \pi^{\alpha/2} \left(\frac{\alpha \Gamma(\frac{1+\alpha}{2\alpha})}{\Gamma(\frac{1}{2\alpha})} \right)^\alpha \left(\zeta(-\alpha, \frac{1}{4} + \frac{n}{2}) - \zeta(-\alpha, \frac{3}{4} + \frac{n}{2}) \right) \\ &= \pi^{\alpha/2} \left(\frac{\alpha \Gamma(\frac{1+\alpha}{2\alpha})}{\Gamma(\frac{1}{2\alpha})} \right)^\alpha E_\alpha(n + \frac{1}{2}) \end{aligned} \quad (18.32)$$

where $\zeta(s, x)$ is the incomplete Riemann or Hurwitz zeta function, which is defined as:

$$\zeta(s, x) = \sum_{k=0}^{\infty} (k+x)^{-s} \quad (18.33)$$

and for $\alpha = m \in 0, 1, 2, \dots$ it is related to the Bernoulli polynomials B_m via:

$$\zeta(-m, x) = -\frac{1}{(m+1)} B_{m+1}(x) \quad (18.34)$$

and $E_\alpha(z)$ denotes the fractional extension of the Euler polynomials [Euler (1768)] as given in (A.282).

Of course, the vacuum state $|0\rangle$ is no more characterized by a vanishing expectation value of the annihilation operator, but is defined by a zero expectation value of the number operator, which is the inverse function of the fractional q-number (18.32):

$$N|0\rangle = ([n]_\alpha)^{-1}|0\rangle = n|0\rangle = 0 \quad (18.35)$$

Following an idea of Goldfain [Goldfain (2008a)] we may interpret the fractional derivative as a simultaneous description of a particle and a corresponding gauge field. Interpreting the vacuum state as a particles absent, but gauge field present state, the nonvanishing expectation value of the annihilation operator indicates the presence of the gauge field, while the number operator only counts for particles.

Setting $\alpha = 1$ leads to $[n]_{\alpha=1} = n$ and consequently, the standard harmonic oscillator energy spectrum $E'(n, \alpha = 1) = (1/2 + n)$ results. For $\alpha = 2$ it follows

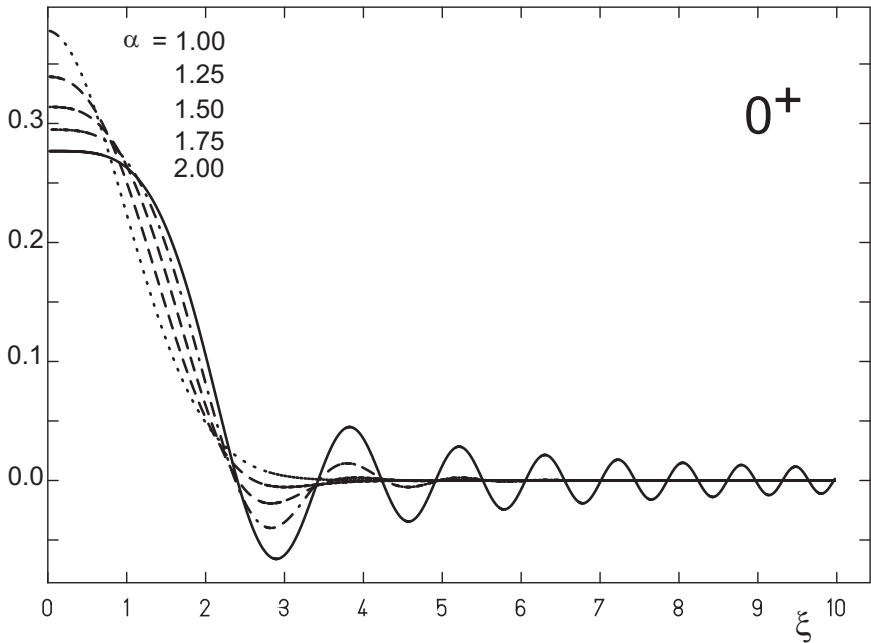


Fig. 18.1 Plot of the ground-state wave function $\Psi_{0+}(\xi)$ of the fractional harmonic oscillator (18.25), solved numerically with the Caputo fractional derivative (18.16) for different α . Numerical methods see e.g. [Diethelm *et al.* (2005)].

$$E'(n, \alpha = 2) = 4\pi \left(\frac{\Gamma(\frac{3}{4})}{\Gamma(\frac{1}{4})} \right)^2 \left(\frac{1}{2} + n \right)^2 \quad (18.36)$$

$$= \frac{8\pi^3}{\Gamma(\frac{1}{4})^4} \left(\frac{1}{4} + n + n^2 \right) \quad (18.37)$$

$$= \frac{2\pi^3}{\Gamma(\frac{1}{4})^4} + \frac{8\pi^3}{\Gamma(\frac{1}{4})^4} (n(n+1)) \quad (18.38)$$

which matches, besides a nonvanishing zero point energy contribution, a spectrum of rotational type $E_{\text{rot}} \equiv l(l+1)$, $l = 0, 1, 2, \dots$. Unlike applications of ordinary q-numbers, this result is not restricted to a finite number n , but is valid for all n . This is a significant enhancement and it allows us to apply this model for high-energy excitations, too.

We obtained two idealized limits for the energy spectrum of the fractional harmonic oscillator. For $\alpha = 1$ a vibration type spectrum is

Table 18.1 Listed are the optimum parameter sets (α , a_0^{vib} , m_0^{vib} according to (18.39)) for the fractional harmonic oscillator for different nuclids. The maximum angular momentum J_{max} for a valid fit below the onset of alignment effects is given as well as the root mean square error ΔE between experimental and fitted energies in %. The values may be compared with table 17.1.

nuclid	α	$a_0^{\text{vib}} [\text{keV}]$	$m_0^{\text{vib}} [\text{keV}]$	J_{max}	$\Delta E [\%]$
$^{156}_{92}\text{Gd}_{64}$	1.795	15.736	-14.136	14	1.48
$^{196}_{118}\text{Pt}_{78}$	1.436	91.556	-39.832	10	0.16
$^{110}_{62}\text{Cd}_{48}$	1.331	197.119	-87.416	6	0
$^{218}_{134}\text{Po}_{84}$	0.801	357.493	-193.868	8	0.06

generated, while for $\alpha = 2$ a rotational spectrum results. The fractional derivative coefficient α acts like an order parameter and allows for a smooth transition between these idealized limits.

Therefore the properties of the fractional harmonic oscillator seem to be well suited to describe e.g. the ground-state band spectra of even-even nuclei. We define

$$E_J^{\text{vib}}(\alpha, m_0^{\text{vib}}, a_0^{\text{vib}}) = m_0^{\text{vib}} + a_0^{\text{vib}}([J]_\alpha + [J+1]_\alpha)/2 \quad J = 0, 2, 4, \dots \quad (18.39)$$

where m_0^{vib} mainly acts as a counter term for the zero-point energy and a_0^{vib} is a measure for the level spacing.

Using (18.39) for a fit of the experimental ground-state band spectra of ^{156}Gd , ^{196}Pt , ^{110}Cd and ^{218}Po , which represent typical rotational-, γ -unstable-, vibrational and linear type spectra, in table 18.1 the optimum parameter sets are listed. Below the onset of microscopic alignment effects all spectra are described with an accuracy better than 2% and are of similar accuracy like the results presented for the symmetric fractional rotor in the last chapter.

Therefore the fractional q-deformed harmonic oscillator indeed describes the full variety of ground-state bands of even-even nuclei with remarkable accuracy.

The proposed fractional q-deformed harmonic oscillator is a fully analytic model, which may be applied with minimum effort not only to the limiting idealized cases of the pure rotor and pure vibrator respectively, but covers all intermediate configurations as well.

In the next section we will demonstrate the equivalence of the proposed fractional q-deformed harmonic oscillator and the corresponding fractional q-deformed symmetric rotor.

18.3 The fractional q-deformed symmetric rotor

In the previous section we have derived the q-number associated with the fractional harmonic oscillator. Interpreting equation (18.32) as a formal definition, the Casimir operator $C(\mathrm{SU}_\alpha(2))$

$$C(\mathrm{SU}_\alpha(2)) = [J]_\alpha [J+1]_\alpha \quad J = 0, 1, 2, \dots \quad (18.40)$$

of the group $\mathrm{SU}_\alpha(2)$ is determined. This group is generated by the operators J_+ , J_0 and J_- , satisfying the commutation relations:

$$[J_0, J_\pm] = \pm J_\pm \quad (18.41)$$

$$[J_+, J_-] = [2J_0]_\alpha \quad (18.42)$$

Consequently we are able to define the fractional q-deformed symmetric rotor as

$$E_J^{\text{rot}}(\alpha, m_0^{\text{rot}}, a_0^{\text{rot}}) = m_0^{\text{rot}} + a_0^{\text{rot}} [J]_\alpha [J+1]_\alpha \quad J = 0, 2, 4, \dots \quad (18.43)$$

where m_0^{rot} mainly acts as a counter term for the zero-point energy and a_0^{rot} is a measure for the level spacing.

For $\alpha = 1$, E^{rot} reduces to $E^{\text{rot}} = m_0^{\text{rot}} + a_0^{\text{rot}} J(J+1)$, which is the spectrum of a symmetric rigid rotor. For $\alpha = 1/2$ we obtain:

$$\lim_{J \rightarrow \infty} (E_{J+2}^{\text{rot}} - E_J^{\text{rot}}) = a_0^{\text{rot}} \pi / 2 = \text{const} \quad (18.44)$$

which is the spectrum of a harmonic oscillator. We define the ratios

$$R_{J,\alpha}^{\text{vib}} = \frac{(E_J^{\text{vib}} - E_0^{\text{vib}})}{(E_2^{\text{vib}} - E_0^{\text{vib}})} \quad (18.45)$$

$$R_{J,\alpha}^{\text{rot}} = \frac{(E_J^{\text{rot}} - E_0^{\text{rot}})}{(E_2^{\text{rot}} - E_0^{\text{rot}})} \quad (18.46)$$

which only depend on J and α .

A Taylor series expansion at $J = 2$ and $\alpha = 1$ leads to:

$$\begin{aligned} R_{J,\alpha}^{\text{vib}} &= 1 + (J-2)(0.10 - 0.04(J-2)) \\ &\quad + (\alpha-1)(J-2)(0.101 - 0.020(J-2)) \end{aligned} \quad (18.47)$$

$$\begin{aligned} R_{J,\alpha/2}^{\text{rot}} &= 1 + (J-2)(0.11 - 0.04(J-2)) \\ &\quad + (\alpha-1)(J-2)(0.095 - 0.016(J-2)) \end{aligned} \quad (18.48)$$

A comparison of these series leads to the remarkable result

$$R_{J,\alpha}^{\text{vib}} \simeq R_{J,\alpha/2}^{\text{rot}} \quad + o(J^3, \alpha^2) \quad (18.49)$$

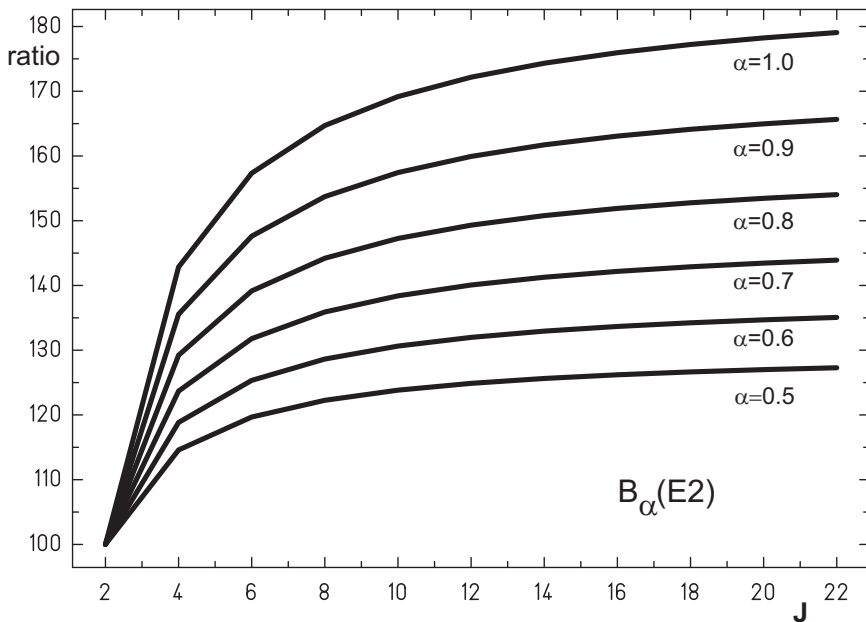


Fig. 18.2 $B(E2)$ -values for the fractional q-deformed $SU_\alpha(2)$ symmetric rotor according to (18.50), normalized with $100/B_\alpha(E2; 2^+ \rightarrow 0^+)$.

Therefore the fractional q-deformed harmonic oscillator (18.39) and the fractional q-deformed symmetric rotor (18.43) generate similar spectra. As a consequence, a fit of the experimental ground-state band spectra of even-even nuclei with (18.39) and (18.43) respectively leads to comparable results. There is no difference between rotations and vibrations any more, the corresponding spectra are mutually connected via relation (18.49).

Finally we may consider the behavior of $B(E2)$ -values for the fractional q-deformed symmetric rotor. Using the formal equivalence with q-deformation, these values are given by [Raychev *et al.* (1990)]:

$$B_\alpha(E2; J+2 \rightarrow J) = \frac{5}{16\pi} Q_0^2 \frac{[3]_\alpha [4]_\alpha [J+1]_\alpha^2 [J+2]_\alpha^2}{[2]_\alpha [2J+2]_\alpha [2J+3]_\alpha [2J+4]_\alpha [2J+5]_\alpha} \quad (18.50)$$

In figure 18.2 these values are plotted, normalized with $100/B_\alpha(E2; 2^+ \rightarrow 0^+)$. Obviously there is a saturation effect for increasing J .

18.4 Half integer representations of the fractional rotation group $SO^\alpha(3)$

Up to now we have investigated the ground-state excitation spectra of even-even nuclei. The next step of complication arises if the proton or neutron number is odd. In classical models it is expected, that excitations of both collective and single-particle type will be possible and in general will be coupled. Approximately, the even-even nucleus is treated as a collective core, whose internal structure is not affected by one more particle moving on its surface. In the strong-coupling model, the corresponding strong coupling Hamiltonian H_{sc} is decomposed into a collective, single-particle and interaction term [Eisenberg and Greiner (1987)]:

$$H_{sc} = H_{coll}^0 + H_{sp}^0 + H_{ii} \quad (18.51)$$

For $K = 1/2$ ground-state bands the energy level spectrum is known analytically [Eisenberg and Greiner (1987)]:

$$E_{K=1/2}(I) = m_0 + c_0 I(I+1) + a_0 (-1)^{I+1/2} (I+1/2) \quad I = 1/2, 3/2, 5/2, \dots \quad (18.52)$$

where a_0 is called the decoupling parameter and m_0 and c_0 in units (keV) are parameters to be fitted with experimental data.

In view of a q-deformed Lie algebra of the standard rotation group $SO(3)$ this result may be interpreted as an expansion in terms of Casimir operators:

$$E_{K=1/2}(I) = m_0 + c_0 C(SO(3)_q) + a_0 (-1)^{I+1/2} C(SO(2)_q) \quad (18.53)$$

$$= m_0 + c_0 [I]_q [I+1]_q + a_0 (-1)^{I+1/2} [I+1/2]_q \quad (18.54)$$

Consequently the investigation of the ground-state band spectra of even-odd and odd-even nuclei respectively is a test of whether or not half-integer representations of the fractional q-deformed rotation group are realized in nature.

Furthermore, in view of fractional calculus, we may use the explicit form (18.32) of the q-number associated with the fractional harmonic oscillator:

$$E_{K=1/2}(I) = m_0 + c_0 C(SO(3)_\alpha) + a_0 (-1)^{I+1/2} C(SO(2)_\alpha) \quad (18.55)$$

$$= m_0 + c_0 [I]_\alpha [I+1]_\alpha + a_0 (-1)^{I+1/2} [I+1/2]_\alpha \quad (18.56)$$

In figure 18.3 we show a fit of the experimental values for the $K = 1/2^-$ band of the nucleus $^{183}\text{W}_{74}$ with (18.56). With $\alpha = 1.02$, $m_0 = -6.077$, $c_0 = 11.76$ and $a_0 = 2.09$ the rms-error is less than 1%. This is a first

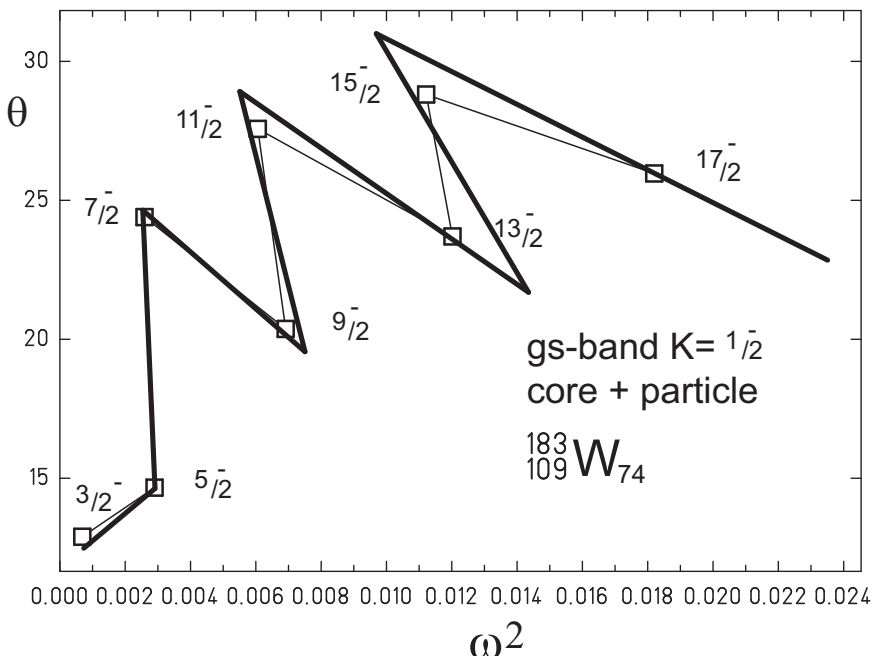


Fig. 18.3 Back bending plot for $^{183}\text{W}_{74}$ for the $K = 1/2^-$ ground-state band. Thick line is the fit result according to (18.56). Squares indicate the experimental values.

indication, that half-integer representations of the fractional rotation group may be indeed realized in nature.

In this chapter we have demonstrated, that we are able to describe the strong relation between rotations and vibrations on the basis of two different approaches.

On one hand we presented the fractional symmetric rotor which contains as the classical limit $\alpha = 1$ the standard rotation spectrum and generates a vibrational spectrum for the semi-derivative $\alpha = \frac{1}{2}$.

On the other hand we have shown, that the fractional harmonic oscillator exhibits the vibrational spectrum in the limit $\alpha = 1$, while for $\alpha = 2$ we obtain a rotational spectrum.

Therefore, within the fractional calculus, the difference between $SO(3)$ and $U(1)$ is annihilated. Instead a generalized view is established, which allows to interpret vibrations as a specific limit of fractional rotations and vice versa, rotations may be interpreted as a specific limit of fractional vibrations.

The similarity of intentions applying q-deformed Lie algebras and the use of a fractional extension of well known standard groups respectively may also be interpreted as a guide for the future development of fractional calculus.

A vast amount of results has already been presented in the past. The concept of q-deformed Lie algebras was applied to problems in different branches of physics.

A possible extension of these research areas within the framework of a fractional group theory could lead to a broader understanding of both concepts and could provide new insights into the structure and variety of extended symmetries in nature.

In the next chapter we will present an example for an application of the fractional harmonic oscillator as a generalized model for a deeper understanding of infra-red spectra of diatomic molecules.

Exercise 18.1

Fractional Euler polynomials

Problem: The Euler polynomials E_n are generated by (see (23.1.1) [Abramowitz and Stegun (1965)])

$$E_n(z) = \lim_{w \rightarrow 0} \partial_w^n \frac{2e^{zw}}{1 + e^w} \quad (18.57)$$

where the first few are given as

$$E_0(z) = 1 \quad (18.58)$$

$$E_1(z) = z - 1/2 \quad (18.59)$$

$$E_2(z) = z^2 - z \quad (18.60)$$

The Euler polynomials fulfill the relation

$$E_n(1 + z) + E_n(z) = 2z^n \quad (18.61)$$

Extend the definition of the Euler polynomials from $n \in \mathbb{N}$ to the fractional case $\alpha \in \mathbb{R}$ and prove, that the fractional Euler polynomials fulfill the fractional version of (18.61):

$$E_\alpha(1 + z) + E_\alpha(z) = 2z^\alpha \quad (18.62)$$

This page intentionally left blank

Chapter 19

Infrared Spectroscopy of Diatomic Molecules

Besides Newton's Principia, Huygens' treatise [Huygens (1673)] on the pendulum clock may be considered as one of the most influential works in physics. Since then, the description of periodical motion in terms of the classical harmonic oscillator is a standard example for an exactly solvable problem in classical mechanics.

In nonrelativistic quantum mechanics an arbitrary potential may be approximated using a harmonic expansion around the equilibrium position. Therefore it is the ideal tool to model vibrational degrees of freedom in many different quantum systems.

Consequently one of the first applications of the quantum harmonic oscillator was the analytic description of the vibrational energy contribution in quantum mechanical models of diatomic molecules [Herzberg (1951); Whitten et al. (2013)].

To establish the standard model for a successful description of excitation spectra of diatomic molecules in addition to vibrations, rotational degrees of freedom have to be considered, so that the total energy of such a system is given in the simplest approximation mainly as a sum of both contributions (including e.g. anharmonic corrections and a rot-vib interaction term):

$$E_{\text{tot}} = E_{\text{vib}} + E_{\text{rot}} \quad (19.1)$$

Here we propose an alternative approach based on fractional calculus, which overcomes the traditional distinction between rotational and vibrational degrees of freedom by introducing a more universal description, which treats rotations and vibrations simultaneously within the generalized framework of fractional oscillations.

The fractional calculus allows for an extended, smooth derivative definition, which may be used to determine generalized symmetries, which go beyond the $U(1)$ -symmetry of the standard harmonic oscillator.

In the following, we will first present the main results of a numerical solution of the fractional Schrödinger equation with the fractional harmonic oscillator potential.

We will then propose a fractional analogue to the standard rot-vib model used for a description of spectra of diatomic molecules. As a first application, we will use this model to describe the IR-spectrum of hydrogen chloride.

19.1 The fractional quantum harmonic oscillator

In the last chapter, we obtained the stationary Schrödinger equation for the fractional harmonic oscillator in the canonical form as:

$$H^\alpha \Psi_n(\xi) = \frac{1}{2} (-\hat{D}_\xi^{2\alpha} + |\xi|^{2\alpha}) \Psi_n(\xi) = E(n, \alpha) \Psi_n(\xi) \quad (19.2)$$

In contrast to the standard quantum harmonic oscillator [Greiner (2009)], the quantum harmonic oscillator in hyperspherical coordinates for arbitrary integer dimension [Erdélyi *et al.* (1953); Herrmann *et al.* (1989a)] and the radial part of the Schrödinger equation for the quantum harmonic oscillator in fractional space dimension respectively [Eid *et al.* (2011)], the Schrödinger equation (19.2) containing fractional derivatives has not been solved analytically until now.

An approximate solution for the energy levels has been derived by Laskin [Laskin (2002)] within the framework of WKB-approximation, which is independent from a specific choice of a fractional derivative type:

$$E_{\text{WKB}}(n, \alpha) = \left(n + \frac{1}{2} \right)^\alpha \pi^{\alpha/2} \left(\frac{\alpha \Gamma(\frac{1+\alpha}{2\alpha})}{\Gamma(\frac{1}{2\alpha})} \right)^\alpha \quad n = 0, 1, 2, \dots \quad (19.3)$$

We have already emphasized, that these levels allow for a smooth transition from vibrational to rotational types of spectra, depending on the value of the fractional derivative coefficient α .

$$E_{\text{WKB}}(n, \alpha \approx 1) \sim n + \frac{1}{2} \quad n = 0, 1, 2, \dots \quad (19.4)$$

$$E_{\text{WKB}}(n, \alpha \approx 2) \sim (n + \frac{1}{2})^2 = n(n + 1) + 1/4 \quad (19.5)$$

The multiplicity for both vibrational and rotational energy levels is 1. This implies that an additional symmetry restriction applies for rotational type degrees of freedom as a consequence of the fractional approach. In order to give a geometric interpretation, let us recall, that for $\alpha = 2$ in the classical approach rotational states $|LM\rangle$ are classified according to the group chain

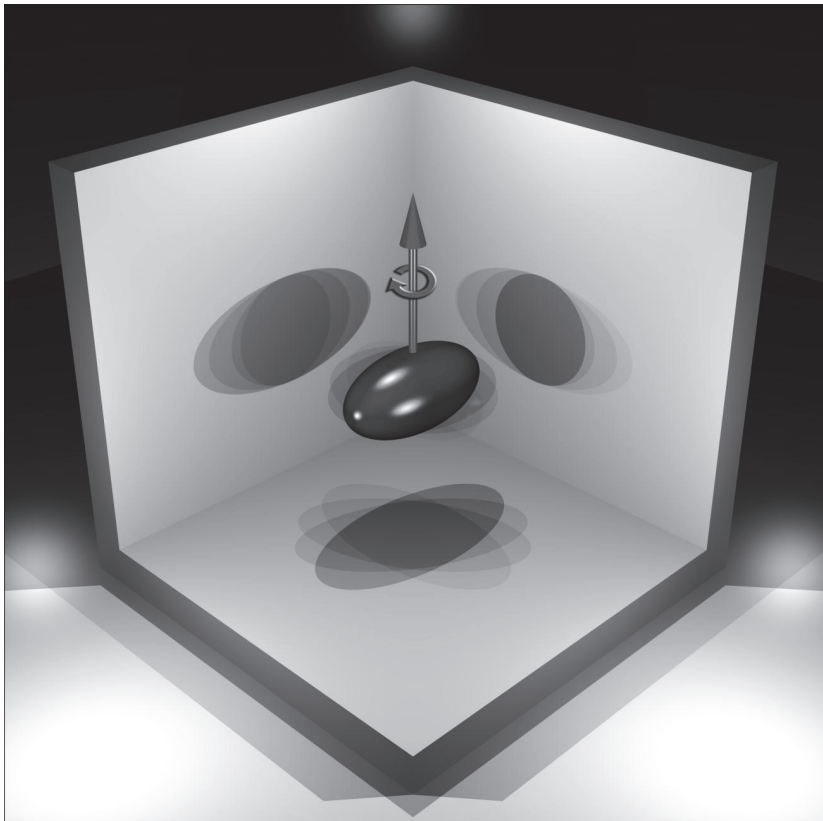


Fig. 19.1 Geometric interpretation of the group transmutation $SO(3) \rightarrow_{\text{sym}} SO(3) \rightarrow U(1)$: The rotational state $|LM\rangle$, characterized by two quantum numbers L, M may be projected from 3-dimensional space onto the 2-dimensional x-y plane fixing the rotation axis imposing the additional symmetry requirement $M = +L$ which may then be interpreted (besides a nonexisting zero-point energy contribution) as a vibrational degree of freedom with fixed phase relation [Lissajous (1857)] in both dimensions $|n\rangle \equiv |nn\rangle$ determined by a single quantum number $n = L$. The same argument holds for $SO(3) \leftarrow_{\text{sym}} SO(3) \leftarrow U(1)$, see discussion of (19.25)ff.

$SO(3) \supset SO(2)$ by the two quantum numbers L, M . Thus the additional symmetry may be imposed as a geometric constraint by fixing the rotation axis in space setting e.g. $M = +L$.

This additional symmetry requirement reduces the multiplicity of a $SO(3)$ multiplet for given $L = n$ from $2n + 1$ to 1 and the corresponding rotational states $|nn\rangle$ are characterized by a single quantum number n .

Table 19.1 Parameters in the ${}_{R,C}\Psi_n^\pm(\xi, \alpha)$ series expansion (19.6) and validity ranges of the fractional parameter α , which fulfills the requirement of normalizability of the wave function.

type	parity	τ	π	normalizable	$\Psi(\xi \approx 0)$
Riemann	even	$\alpha - 1$	0	$0.5 \leq \alpha \leq 2$	$o(\xi^{\alpha-1})$
Riemann	odd	$\alpha - 1$	α	$0.25 \leq \alpha \leq 2$	$o(\xi^{2\alpha-1})$
Caputo	even	0	0	$0 \leq \alpha \leq 2$	$o(\xi^0)$
Caputo	odd	0	α	$0 \leq \alpha \leq 2$	$o(\xi^\alpha)$

Hence the symmetry of the fractional quantum harmonic oscillator bridges two different Lie-algebras, it is the transmutation of one group into another, an idea, which also motivated the development of q-deformed Lie-algebras.

Therefore the fractional harmonic oscillator may be a useful tool to describe rot-vib spectra, with α in the range of $1 \leq \alpha \leq 2$. The fractional harmonic oscillator could be of similar importance as its classical counterpart, an exact solution is of fundamental interest.

The main results from a numerical solution of the canonical Schrödinger equation of the fractional quantum harmonic oscillator (19.2) using the Riemann and Caputo fractional derivative definition are presented in the next section. This step introduces an extended symmetry group which covers the classical range $U(1) \rightarrow_{\text{sym}} SO(3)$.

19.2 Numerical solution of the fractional quantum harmonic oscillator

For a numerical solution of (19.2), we expand the wave function in a fractional Taylor-series on the positive semi-axis $\xi \geq 0$. Furthermore the wave function should be an eigenfunction of the parity operator Π :

$${}_{R,C}\Psi_n^\pm(\xi, \alpha) = \xi^\tau \xi^\pi \sum_{i=0}^N a_i(E) \xi^{2\alpha i} \quad \xi > 0 \quad (19.6)$$

$$\Pi_{R,C}\Psi_n^\pm(\xi, \alpha) = \pm {}_{R,C}\Psi_n^\pm(\xi, \alpha) \quad (19.7)$$

where the parameters τ and π determining the type (Riemann or Caputo) of the fractional derivative definition used and parity of the wave function are listed in table 19.1. The \pm index indicates the parity for n even and odd respectively.

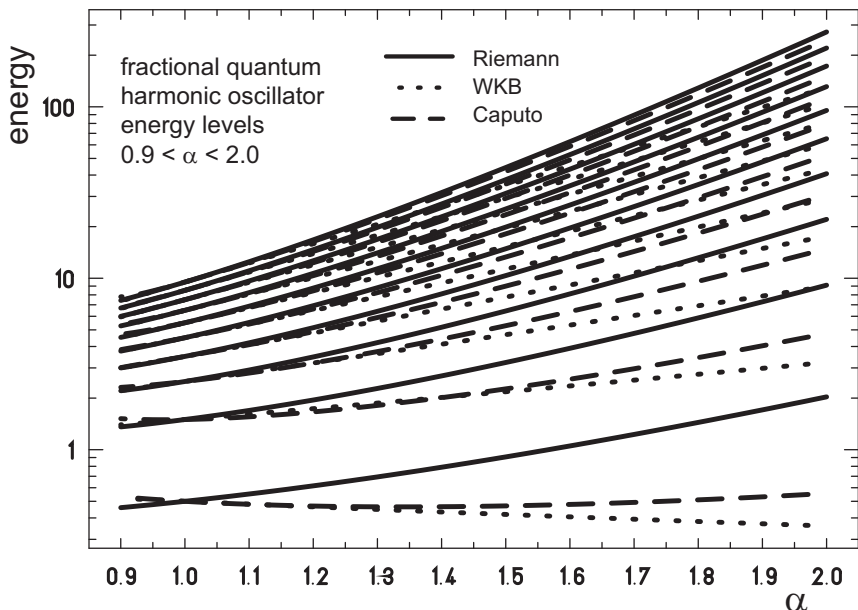


Fig. 19.2 Logarithmic plot of the first 10 energy levels of the fractional quantum harmonic oscillator in the range $0.90 \leq \alpha \leq 2$ based on the Riemann (thick lines), Caputo (dashed lines) and WKB-approximation (dotted lines) of the fractional derivative definition.

The coefficients $a_i(E)$ are determined using a standard shooting method: From the requirement, that the wave function should vanish at infinity for a given eigenvalue E_n follows a determining condition for sufficiently large distance ξ_{det} :

$$\lim_{E \rightarrow E_n} {}_{\text{R,C}}\Psi_n^{\pm}(\xi_{\text{det}}, \alpha, E) = 0 \quad (19.8)$$

which allows for an iterative procedure to calculate E_n with arbitrary precision.

For practical calculations, we determined the eigenvalues with a precision of 32 significant digits with the settings $20 \leq \xi_{\text{det}} \leq 40$, $1000 \leq N \leq 10000$, depending on α and $\Delta\alpha = 0.01$.

The major restriction for the range of allowed α values is the requirement of normalizability of the wave function obtained. From

$$\int_{-\infty}^{\infty} d\xi_{\text{R,C}} \Psi_n^{\pm}(\xi, \alpha) {}_{\text{R,C}}\Psi_n^{\pm}(\xi, \alpha)^* < \infty \quad (19.9)$$

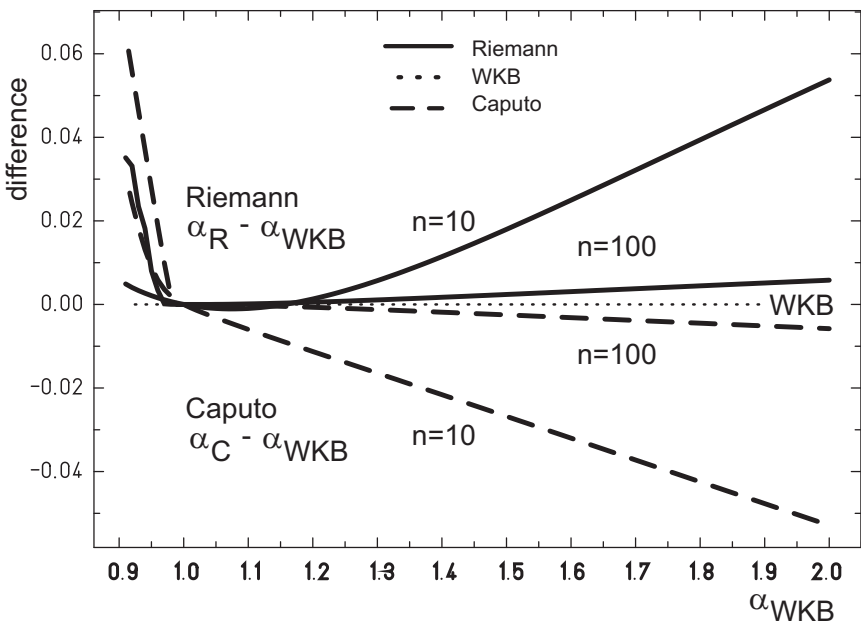


Fig. 19.3 Result of a least square fit of energy level spectra based on the Riemann (thick lines) and Caputo (dashed lines) derivative definition with the WKB-approximation (dotted line) (19.3). Plotted is the difference of α values for a given number of energy levels ($n = 10, 100$) with fitted α_{WKB} .

follows an upper bound $\alpha \leq 2$. Of course, for $\alpha > 2$ condition (19.8) may still be used as an equivalent of a box-normalization condition, but the results are no solutions of the harmonic oscillator potential any more.

In figure 19.2 we compare the resulting energy level spectra to the WKB-approximation. While in the vicinity of $\alpha = 1$ differences are negligible, for larger α values especially for low lying energies the calculated spectra differ significantly, but as a first remarkable result we obtain similar to the case of WKB-approximation the expected smooth transition from vibrational to rotational type of spectrum using the Riemann and Caputo fractional derivative definition respectively.

The results of a fit of the energy levels with the WKB-approximation are plotted in figure 19.3. We may deduce, that for increasing number of energy levels n , equation (19.3) approximates the energy values better.

From this figure we may also deduce, that rotational spectra, which are characterized by $\alpha_{WKB} = 2$ are reproduced using the Caputo derivative for

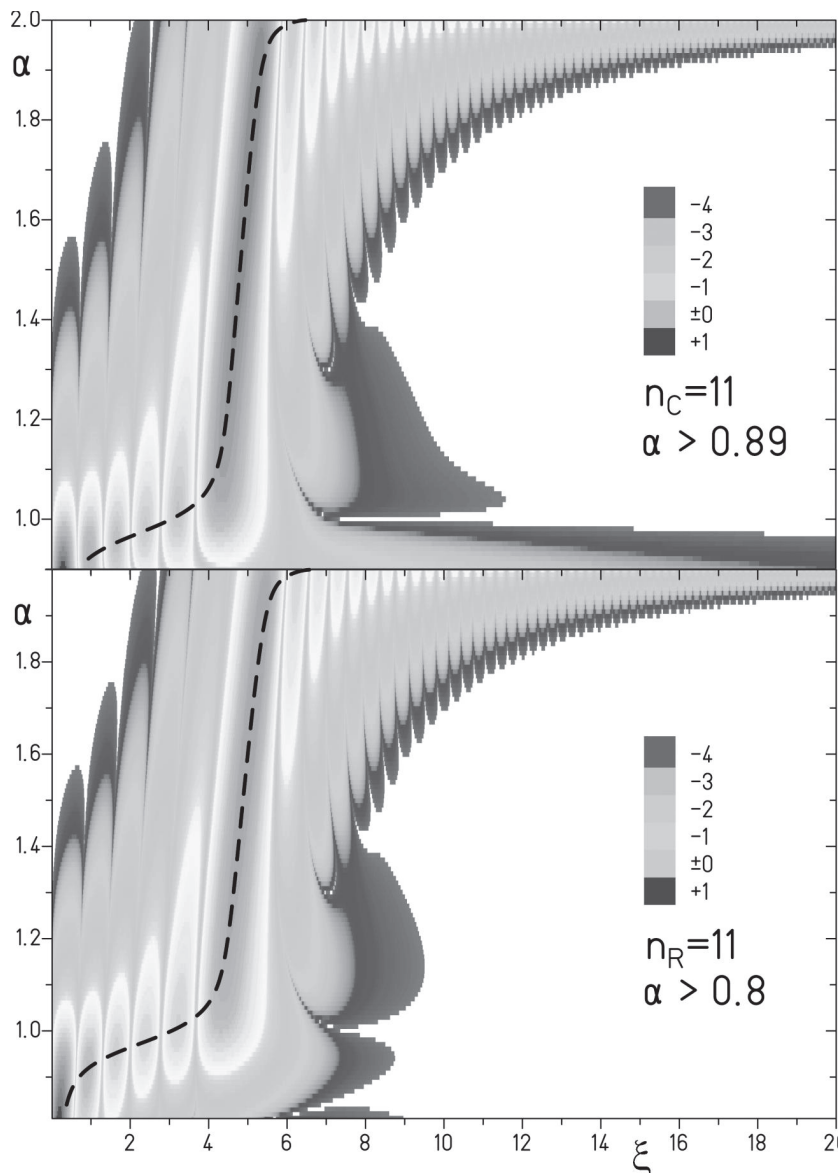


Fig. 19.4 Logarithmic probability density $|\Psi_{n=11}^-(\xi, \alpha)|^2$ for the solution of the fractional quantum harmonic oscillator based on the Caputo (top) and Riemann (bottom) definition of the fractional derivative in the full range of allowed α values for real energy eigenvalues. The dashed line indicates the expectation value for the modified position operator $\langle \hat{\xi} \rangle$.

a slightly smaller α value, $\alpha_C < 2$, while for the Riemann derivative we have to use a slightly larger α value, $\alpha_R > 2$ and therefore using the Riemann fractional derivative definition implies the need for box normalization, if we want to generate the exact level spacing of rotational type.

The behavior of the eigenfunctions $\Psi_n^\pm(\xi, \alpha)$ differs significantly in the region $1 \leq \alpha \leq 2$ and $\alpha < 1$. As an example, in figure 19.7 we have plotted the occupation probability for the eigenfunction $\Psi_{n=11}^-(\xi, \alpha)$ for the Caputo and Riemann solution.

Introducing the modified position operator $\bar{\xi} = \theta(\xi)\xi$, its expectation value

$$\langle \bar{\xi} \rangle = \int_0^\infty d\xi_{R,C} \Psi_n^\pm(\xi, \alpha) \xi_{R,C} \Psi_n^\pm(\xi, \alpha)^* \quad (19.10)$$

yields the position information on the positive semi-axis. This value is almost constant for $\alpha > 1$. For increasing α only the side maxima are changing from inside to outside and therefore mark a smooth transition from Hermite-type to Bessel-type polynomials. In contrast for $\alpha < 1$, the position value tends very fast to zero which means, that the wave function becomes strongly located at the origin in this case.

As a consequence, the energy diagram for $\alpha < 1$ is dominated by the kinetic term, since for the potential near the origin

$$\lim_{\xi \rightarrow 0} |\xi|^{2\alpha} = 0 \quad (19.11)$$

holds.

This means, that the solutions of the fractional Schrödinger equation for the harmonic oscillator and the solutions for the free fractional Schrödinger equation more and more coincide for $\alpha < 1$, a behavior, which we expect for any potential, which vanishes at the origin.

The eigenfunctions of the free fractional Schrödinger equation are known analytically and are given in terms of the Mittag-Leffler functions $E_\alpha(z)$ and $E_{\alpha,\beta}(z)$ as:

$${}_C\Psi_n^{+free}(\xi, \alpha) = E_{2\alpha}(-\xi^{2\alpha}) \quad (19.12)$$

$${}_C\Psi_n^{-free}(\xi, \alpha) = \xi^\alpha E_{2\alpha, 1+\alpha}(-\xi^{2\alpha}) \quad (19.13)$$

$${}_R\Psi_n^{+free}(\xi, \alpha) = \xi^{\alpha-1} E_{2\alpha, \alpha}(-\xi^{2\alpha}) \quad (19.14)$$

$${}_R\Psi_n^{-free}(\xi, \alpha) = \xi^{2\alpha-1} E_{2\alpha, 2\alpha}(-\xi^{2\alpha}) \quad (19.15)$$

and the corresponding eigenvalues are determined in box-normalization from the zeros of these functions. For $\alpha < 1$ there exists only a finite number of zeros and therefore the energy spectrum is limited [Hilfer and Seybold (2006); Seybold and Hilfer (2008)].

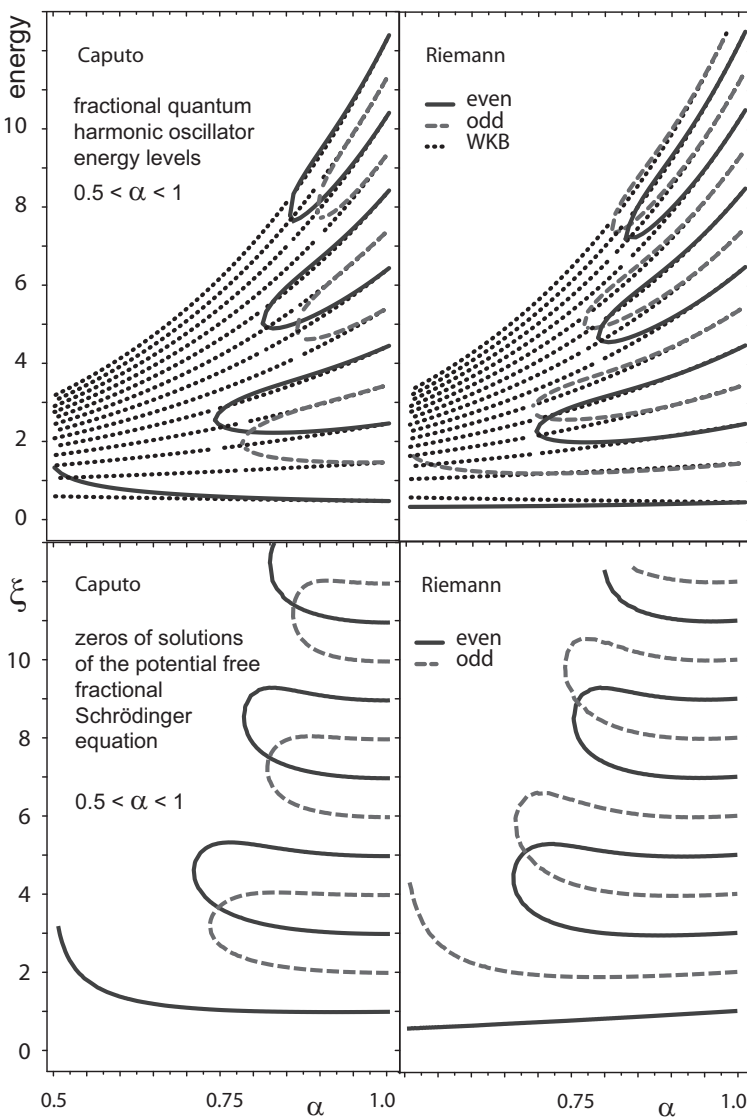


Fig. 19.5 In the upper row energy levels in the range $0.5 < \alpha < 1$ for the Caputo (left column) and Riemann (right column) fractional quantum harmonic oscillator are plotted. Thick lines indicate positive parity, dashed lines indicate odd parity of the corresponding solution. For decreasing α , the number of real eigenvalues is reduced. Dotted lines show the WKB-approximation E_{WKB} . The lower row shows the zeros of eigenfunctions for the potential free fractional Schrödinger equation.

In the upper row of figure 19.5 we show the lowest energy levels for the fractional harmonic oscillator for $\alpha < 1$. This spectrum is limited to a finite number of levels, which may now be understood in comparison to the plot of zeros of the solutions of the free fractional Schrödinger equation presented in the lower row of figure 19.5.

It can be deduced, that the onset of real eigenvalues for a given α of the fractional harmonic oscillator and the occurrence of a zero in the potential free solution agree qualitatively.

Since the free fractional Schrödinger equation is formally equivalent to the classical fractional harmonic oscillator differential equation we may conclude, that in the special case of the harmonic oscillator the transition from fractional classical mechanics to fractional quantum mechanics is smooth.

We have thus demonstrated, that the fractional quantum harmonic oscillator extends the symmetry of the standard harmonic oscillator and allows for a generalized description of rotational and vibrational degrees of freedom.

Since we want to emphasize this unifying point of view, an appropriate area of application is molecular spectroscopy, where an interplay between vibrations and rotations is observed.

Therefore we will investigate the properties of infrared spectra of diatomic molecules in the next section using the fractional quantum harmonic oscillator.

19.3 The infrared-spectrum of HCl

Traditionally diatomic molecules are treated in lowest order as rigid rotors with a fixed bond length, which in addition are able to perform vibrations around this equilibrium position.

For higher excitations, anharmonic contributions and the influence of centrifugal stretching are taken into account via a series expansion, which we present here up to third order:

$$\begin{aligned} E_{\text{rot-vib}}(\nu, J) &= E_{\text{rot}} + E_{\text{vib}} \\ &= B_\nu J(J+1) + D_\nu J^2(J+1)^2 \\ &\quad + \hbar\omega_e \left(\nu + \frac{1}{2} \right) + \hbar\omega_e x_e \left(\nu + \frac{1}{2} \right)^2 + \hbar\omega_e y_e \left(\nu + \frac{1}{2} \right)^3 \end{aligned} \tag{19.16}$$

where the constants B_ν and D_ν add a rot-vib coupling via:

$$B_\nu = B_e - \alpha_e \left(\nu + \frac{1}{2} \right) \quad (19.17)$$

$$D_\nu = D_e - \beta_e \left(\nu + \frac{1}{2} \right) \quad (19.18)$$

which results in a seven parameter energy formula to determine the energy levels in the rot-vib model.

Now we introduce the fractional quantum harmonic oscillator model, which describes rotational and vibrational spectra from a unifying point of view. As we pointed out in the previous section, depending on the value of the fractional derivative parameter α we may generate both types of spectra:

$$E_{\text{rot}}(J) = E(\alpha \approx 2, J) \quad (19.19)$$

$$E_{\text{vib}}(\nu) = E(\alpha \approx 1, \nu) \quad (19.20)$$

Thus we propose the fractional analogue of the standard rot-vib-model:

$$\begin{aligned} E_{\text{rot-vib}}^{\text{fractional}}(\nu, J) &= E_{\text{rot}} + E_{\text{vib}} + E_{\text{coupling}} \\ &= \tilde{B}_e E(\alpha_J \approx 2, J) + \hbar \tilde{\omega}_e E(\alpha_\nu \approx 1, \nu) \\ &\quad + \tilde{\alpha}_e E(\alpha_J \approx 2, J) E(\alpha_\nu \approx 1, \nu) + g_0 \end{aligned} \quad (19.21)$$

with six parameters α_J , \tilde{B}_e , α_ν , $\hbar \tilde{\omega}_e$, $\tilde{\alpha}_e$, g_0 . A least square fit of the fractional rot-vib model energies with the standard rot-vib model energies yields the parameter sets listed in table 19.2.

In order to emphasize the property of the fractional rot-vib model to realize rotational type spectra, we want to explore the lowest energy photon absorption processes in the infrared region. In that case from $\Delta J = \pm 1$, we obtain two branches (R and P) with the properties:

$$\Delta E_R(J) = E(\nu = 1, J + 1) - E(\nu = 0, J) \quad J = 0, \dots \quad (19.22)$$

$$\Delta E_P(J) = E(\nu = 1, J - 1) - E(\nu = 0, J) \quad J = 1, \dots \quad (19.23)$$

These transition energies may be directly compared to the experimental spectrum.

The corresponding intensities I_j for a given transition are determined in the standard case by the Boltzmann-distribution

$$I_j = (2J + 1)e^{-E_{\text{rot}}/(k_B T)} = (2J + 1)e^{-B_\nu J(J+1)/(k_B T)} \quad (19.24)$$

where k_B is the Boltzmann constant. The factor $(2J + 1)$ is a result of the multiplicity of a given rotational state.

Table 19.2 Parameter sets to determine the energy levels of H³⁵Cl for the standard rot-vib-model (19.16) in the first row [Herzberg (1951)] and for the proposed generalized fractional model (19.21) for WKB, Riemann and Caputo definition of the fractional derivative. Finally the rms-error is given.

standard	B_e	α_e	D_e	β_e
	10.59341	0.30718	$5.3194 * 10^{-4}$	$7.51 * 10^{-6}$
	$\hbar\omega_e$	$\hbar\omega_e x_e$	$\hbar\omega_e y_e$	rms-error
	2990.946	52.8186	0.2243	3.8%
WKB	\tilde{B}_e	$\tilde{\alpha}_e$	g_0	$\hbar\tilde{\omega}_e$
	7.406	0.202	152.016	2707.77
	α_J	α_ν		rms-error
	1.997	1.051		3.3%
Riemann	\tilde{B}_e	$\tilde{\alpha}_e$	g_0	$\hbar\tilde{\omega}_e$
	2.588	0.080	10.355	3095.36
	α_J	α_ν		rms-error
	2.081	0.937		3.8%
Caputo	\tilde{B}_e	$\tilde{\alpha}_e$	g_0	$\hbar\tilde{\omega}_e$
	5.264	0.155	-64.973	2938.77
	α_J	α_ν		rms-error
	1.91	0.914		3.8%

In the case of the fractional rot-vib model this implies the following generalization:

$$I_j^{\text{fractional}} = (2(\alpha_J - 1)J + 1)e^{-E_{\text{rot}}/(k_B T)} \quad (19.25)$$

For varying α the factor

$$m = 2(\alpha - 1)J + 1 \quad (19.26)$$

may now be interpreted physically as a smooth transition of multiplicities m from 1 to $2J+1$ in the range $1 \leq \alpha \leq 2$; Hence (21.77) indeed completes the proper transition from $U(1)$ to $SO(3)$. Furthermore we obtain a physical explanation for the limited number of energy levels in the case $\alpha < 1$:

From the requirement that the multiplicity of a given state J should be a positive real number, $m > 0$, which means, within the framework of a possible particle-hole formalism we restrict to a description of particles only, using (21.77) a condition follows for the finite set of allowed J values $J \in \{0, \dots, J_{\max}\}$:

$$J_{\max} < \frac{1}{2(1-\alpha)}, \quad \alpha < 1 \quad (19.27)$$

which in the limiting case $\alpha \rightarrow \frac{1}{2}$ reduces to only one allowed level with $J = 0$.

This is in qualitative agreement with numerical results presented in figure 19.5 and a strong argument for the validity and physical justification of our choice of the Riemann and Caputo definition of the fractional derivative.

These considerations establish a connection between continuous, fractional space dimension D and the fractional quantum harmonic oscillator with order parameter α as

$$D = 2\alpha - 1, \quad \frac{1}{2} < \alpha \leq 2 \quad (19.28)$$

which sets an upper limit to the space dimension $D \leq 3$ as a consequence of the requirement of normalizability of the wave function and a lower limit of $D \geq 0$, where we observe a dimensional freezing of vibrational degrees of freedom for a point particle and therefore gives an alternative answer to Ehrenfest's thought-provoking question [Ehrenfest (1917)] 100 years after.

With intensities (19.25) and assuming an exponential distribution for every transition we are able to fit the experimental spectrum [NIST (2012)]. The results are presented in figure 19.6.

The overall error is less than 4%. As a remarkable fact, the experimental spectrum is reproduced in the case of the Riemann fractional harmonic oscillator with $\alpha_J > 2$, which means, the corresponding eigenfunctions are only box-normalizable.

Consequently, only the Caputo fractional rot-vib model describes the experiment within the allowed parameter range.

It is remarkable, that in the case of the fractional rigid rotor, which is an alternative description of rot-vib systems, just the opposite conclusion was drawn: The Caputo derivative based version was discarded and only the Riemann rotor model was acceptable, since only in this case the zero-point energy contribution of vibrational modes was treated correctly.

It has been demonstrated, that the fractional quantum harmonic oscillator generates an energy spectrum, which, besides vibrational degrees of freedom also shows rotational type spectra. The fractional parameter α allows for a smooth transition between these two extreme cases.

Therefore vibrations and rotations may be treated equivalently in a unified generalized rot-vib model, which may be successfully used to reproduce the infrared spectra of diatomic molecules, which has been demonstrated for the case of hydrogen chloride.

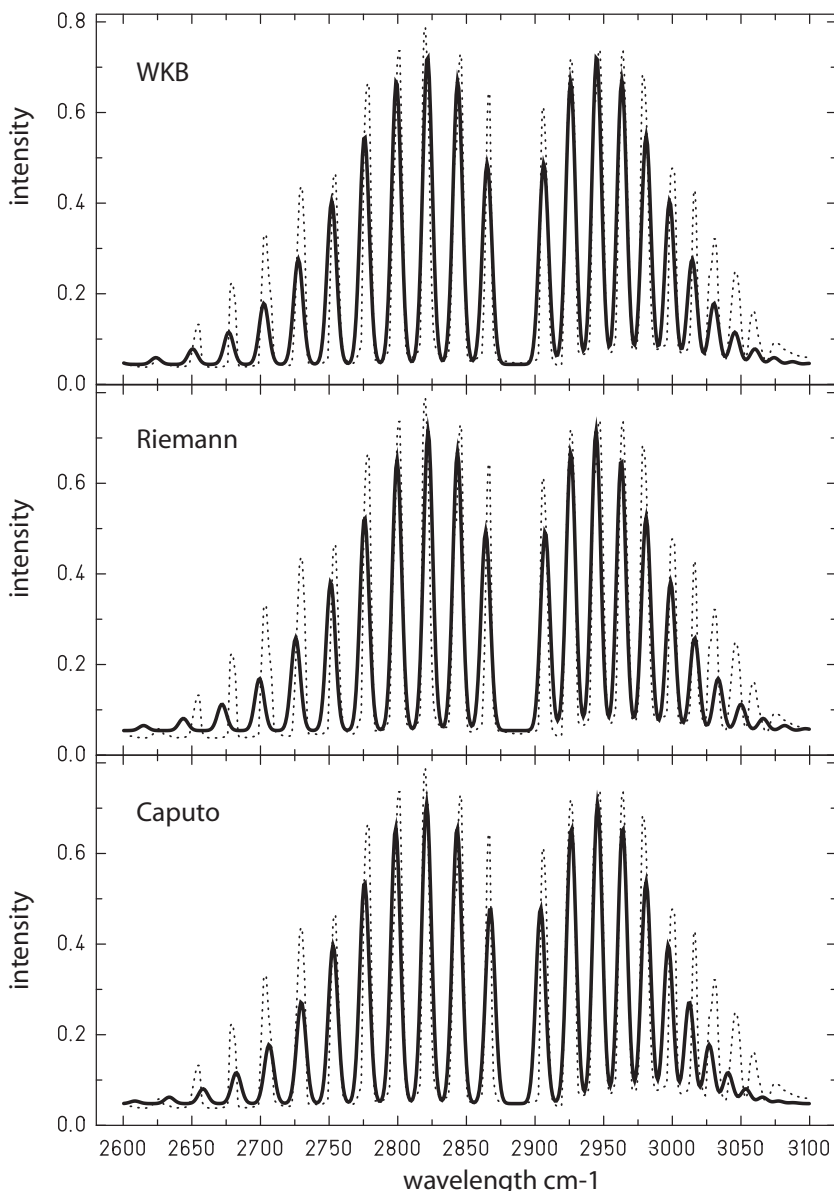


Fig. 19.6 Fit results for the infrared spectrum of H^{35}Cl in the wavelength range from 2600–3100 [cm^{-1}]. Dotted lines are the experimental values from [NIST (2012)]. From top to bottom the result for the energy levels of the fractional rot-vib-model (19.21) using the WKB-approximation, the Riemann and the Caputo fractional derivative definition.

It has also been shown, that the WKB-approximation is a useful tool to approximate higher energy levels, but in the low energy region the exact solutions using the Riemann and Caputo derivative definitions differ significantly and cover a much broader area of useful applications.

We presented first results for the fractional quantum harmonic oscillator. The results encourage further studies in this field, especially the knowledge of eigenvalues and eigenfunctions for higher energy levels will be useful to describe highly excited rotational molecular states, an area, which has been made accessible recently, see e.g. [Villeneuve *et al.* (2000); Yuan *et al.* (2011)].

Finally we collected arguments in support of the idea, that a promising field of future research is the formulation of a quantum statistical extension of fractional thermodynamics [Abe (1997); Hilfer (2000)] in terms of the fractional extension of the partition function Z using the fractional generalization of a Hamiltonian H^α :

$$Z^\alpha = \text{Tr}(m(\alpha)e^{-\beta H^\alpha}) \quad (19.29)$$

with the additional fractional multiplicity $m(\alpha)$, which emphasizes the connection between fractional calculus and fractional space dimensions. Closer examinations on this subject will be presented in Chapter 26.

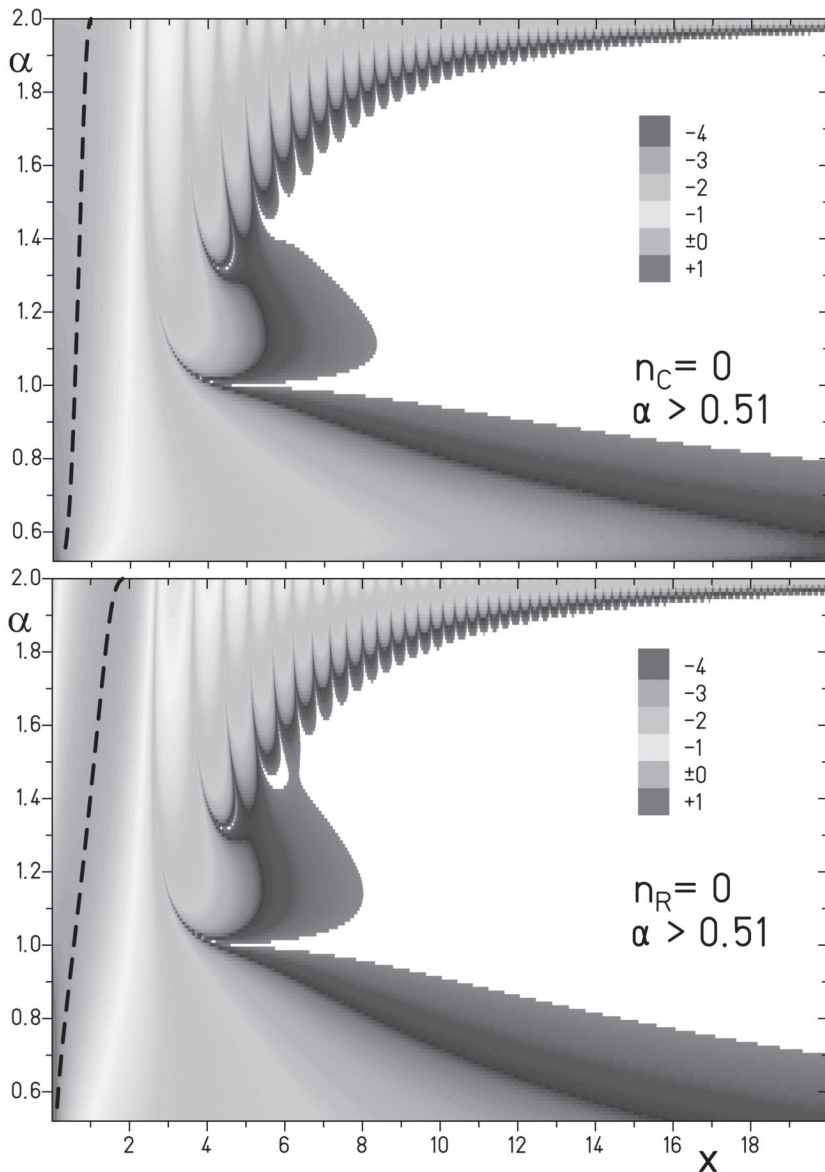


Fig. 19.7 Logarithmic probability density $|\Psi_{n=0}^+(\xi, \alpha)|^2$ for the solution of the fractional quantum harmonic oscillator based on the Caputo (top) and Riemann (bottom) definition of the fractional derivative in the full range of allowed α values for real energy eigenvalues. The dashed line indicates the expectation value for the modified position operator $\langle \hat{\xi} \rangle$.

With kind permission from [Herrmann (2013a)] © Gam. Ori. Chron. Phys.

Table 19.3 A comparison of the fractional harmonic oscillator ground state energy values for $r.c\Psi(n = 0)^+$ using the WKB approximation E_{WKB} , the Riemann- and Caputo derivative definition in the range $0.50 \leq \alpha \leq 1.00$.

With kind permission from [Herrmann (2013a)] © Gam. Ori. Chron. Phys.

Table 19.4 A comparison of the fractional harmonic oscillator ground state energy values for $r_c \Psi(n=0)^+$ using the WKB approximation E_{WKB} , the Riemann- and Caputo derivative definition in the range $1.00 \leq \alpha \leq 1.50$.

With kind permission from [Herrmann (2013a)] © Gam. Ori. Chron. Phys.

Table 19.5 A comparison of the fractional harmonic oscillator ground state energy values for $r_c \Psi(n = 0)^+$ using the WKB approximation E_{WKB} , the Riemann- and Caputo derivative definition in the range $1.50 \leq \alpha \leq 2.00$.

With kind permission from [Herrmann (2013a)] © Gam. Ori. Chron. Phys.

α	E_{WKB}	E_C	E_R
1.50	0.419207	0.4701976098702006714507470909667	0.9077988195496354977790899151313
1.51	0.417841	0.4709463141699638543214800976246	0.920905983934370075800341634143
1.52	0.416483	0.4717360695408179429601155283752	0.9342858593019137328852879828535
1.53	0.415133	0.4725665974667356895003981567567	0.9479330659756106497595506103507
1.54	0.413790	0.4734376376638116037500042365835	0.9618568104520960493326179999178
1.55	0.412454	0.4743489475037181117036217329112	0.9760628160961782919915607366141
1.56	0.411126	0.4753003014669489358324080466701	0.9905569406675935002838531946466
1.57	0.409805	0.4762914906242127624100496416336	1.005345179468094080565881524498
1.58	0.408492	0.477322322144466600820061816679	1.02043366856992199640041142152
1.59	0.407185	0.4783926188280173565029722321264	1.035828688127706165171376178108
1.60	0.405885	0.4795022186637699969622332005363	1.051536665775880253607250023383
1.61	0.404593	0.4806509744086689748388036604991	1.067564180113775549461486180581
1.62	0.403307	0.4818387531888543618853554267370	1.083917964280603528382046733787
1.63	0.402028	0.4830654361210108541225978321980	1.100604909622604261262886760268
1.64	0.400756	0.4843309179530144223197434132186	1.11763206945469996371293129314
1.65	0.399490	0.4856351067228854127772431439365	1.135006662919057822708772416798
1.66	0.398231	0.4869779234351360484476340332214	1.152736078943032794436575617902
1.67	0.396978	0.4883593017536554654450321371001	1.170827880299029401645433786911
1.68	0.395732	0.489779187710326890766944836228	1.189289807768891719879423390403
1.69	0.394492	0.4912375394286196031716172145575	1.208129784415502782589015002215
1.70	0.393258	0.492734326861443177053470685588	1.227355919964348609756909143290
1.71	0.392031	0.4942695315935934242092322033297	1.246976515297878029305237183148
1.72	0.390810	0.4958431463511586367842246198056	1.267000067065567472804396155251
1.73	0.389594	0.4974551752882913951576141830202	1.287435272412680046170116542483
1.74	0.388385	0.4991056332657855198631759381816	1.308291033803790463118024489016
1.75	0.387182	0.5007945459059298851079562626725	1.329576464133231946904662340016
1.76	0.385985	0.5025219493521409280301054954171	1.351300891558708018886408820559
1.77	0.384794	0.5042878900899039253825782534463	1.373473865006401267093534460686
1.78	0.383608	0.50609242477757959998303333494	1.396105159406002792670491291655
1.79	0.382428	0.5079356200866574808042733295384	1.419204781226180136969848436436
1.80	0.381254	0.5098175525510608025423658551463	1.442782974125098169585982284893
1.81	0.380085	0.5117383084251296506877588309922	1.466850224746706742087839692107
1.82	0.378923	0.5136979835499297129748269912617	1.491417268666610960119148958278
1.83	0.377765	0.5156966832275533798201854110253	1.516495096491444776617852643223
1.84	0.376613	0.5177345221030982076541504219531	1.542094960115776342101111395484
1.85	0.375467	0.5198116240540249500660399623598	1.568228379140684247558116214615
1.86	0.374235	0.5219281220866135602470621784258	1.594907147458257547162032251652
1.87	0.373189	0.5240841582392508359502106823655	1.622143340006389339890453344777
1.88	0.372059	0.5262798834922977762197613977604	1.649949319698353811900802828261
1.89	0.370933	0.5285154576842983038704950375655	1.678337744531780088422485631992
1.90	0.369813	0.53079104944343038315103559015727	1.707321574881763110967093844504
1.91	0.368698	0.533106836071002604974173444442	1.736914080982982141553557822643
1.92	0.367588	0.5354630035621354468908990810396	1.767128850605831501977073484111
1.93	0.366483	0.5378597464629559883363843388855	1.797979796931705887432166272661
1.94	0.365383	0.5402972678519724201482062272823	1.829481166632724157564922018372
1.95	0.364288	0.5427757792853815941588799491900	1.8616475481613221014921092057368
1.96	0.363198	0.5452955007510841842506321903441	1.894493880255285544622431786429
1.97	0.362112	0.5478566606284439496195723998265	1.928035460663979327088950877404
1.98	0.361032	0.5504594956527436203691888072089	1.962287955101624868272708187245
1.99	0.359956	0.553104250884200077631988425195	1.997267406433717543221178644731
2.00	0.358885	0.5557911796814089078908930833120	2.032990244102781246490346396776

This page intentionally left blank

Chapter 20

Fractional Spectroscopy of Hadrons

The calculation of the hadron spectrum is a task of central interest in quantum chromodynamics (QCD), which describes the dynamics of particles which are subject to strong interaction forces. This requires enormous efforts and computer power [Dürr et al. (2008)], that is one reason, why different approximate strategies have been established, which reduce the complexity of the problem.

Most prominent representatives are nonrelativistic potential models, which are very easy to handle. A standard Schrödinger equation is solved with an appropriately chosen model potential. Minimum requirements for such potentials are, that for small distances the one gluon exchange potential should be simulated while for large distances the quark confinement should be modeled.

A simple ansatz is given with a rotational symmetric potential [Eichten et al. (1975)]

$$V(r) = -\frac{\bar{\alpha}_s}{r} + \kappa r \quad (20.1)$$

where a running coupling constant $\bar{\alpha}_s$ and a force constant κ are parameters of this model. For a realistic treatment of fine- and hyperfine-structure of spectra it is necessary, to introduce additional spin-spin, spin-orbit and tensor interaction terms [Godfrey and Isgur (1985); Barnes et al. (1995); Li and Chao (2009)].

Such potential models describe the low energy excitation spectrum of meson and baryon spectra with reasonable accuracy. But in the meantime more and more recently discovered particles do not fit very well into the calculated term schemes [Zhu (2005); Stancu (2010); Pakhlova et al. (2010)].

In this section we want to demonstrate that fractional calculus provides excellent contributions for a successful description and understanding of hadron spectra.

We want to remind, that the solutions of a free fractional Schrödinger equation, presented in chapter 11 are localized in a very small region of space. A direct consequence of this behavior may be quark confinement. Furthermore we have demonstrated, that this behavior of free, fractional and localized solutions of a fractional Schrödinger equation may be simulated using a standard Schrödinger equation with a linear potential.

Therefore we assume, that the experimental hadron spectra may be successfully be described with a free fractional Schrödinger equation. A specific additional potential term is not necessary.

That this hope is justified will be shown in the next sections.

20.1 Phenomenology of the baryon spectrum

In order to classify the multiplets of the fractional rotation group $SO^\alpha(3)$ we derived the group chain

$$SO^\alpha(3) \supset SO^\alpha(2) \quad (20.2)$$

In the last section we presented a successful interpretation of low energy excitation spectra for even-even nuclei based of the fractional symmetric rotor model, which is based on the Casimir operator $L^2(\alpha)$ of $SO^\alpha(3)$. Until now we have ignored a possible influence of the Casimir operator $L_z(\alpha)$ of $SO^\alpha(2)$. We start with a model Hamilton operator H^α

$$H^\alpha = m_0 + a_0 L^2(\alpha) + b_0 L_z(\alpha) \quad (20.3)$$

where coefficients m_0 , a_0 and b_0 are free parameters. A complete classification of multiplets of this operator may be realized, introducing the Casimir operators (16.45) and (16.46). The levels are uniquely determined for a given set of L and M :

$$E_R^\alpha = m_0 + a_0 \frac{\Gamma(1 + (L+1)\alpha)}{\Gamma(1 + (L-1)\alpha)} \pm b_0 \frac{\Gamma(1 + |M|\alpha)}{\Gamma(1 + (|M|-1)\alpha)} \quad (20.4)$$

Note that for $\alpha = 1$ the Casimir operators and the corresponding eigenvalues reduce to the well known results of standard quantum mechanical angular momentum algebra [Edmonds (1957)].

$$E_R^{\alpha=1} = m_0 + a_0 L(L+1) + b_0 M \quad (20.5)$$

Let us recall, that the motion of an electron around the atomic nucleus under the influence of a constant magnetic field B_z , which is known as normal Zeeman effect [Zeeman (1897)] ignoring a spin dependency is described in

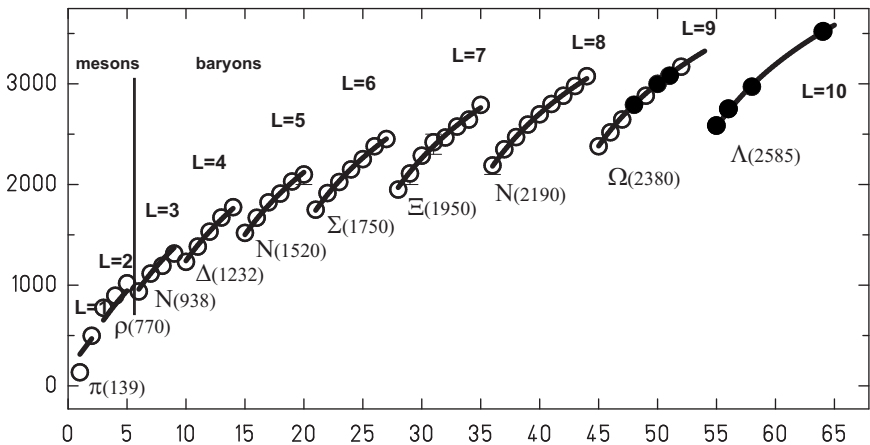


Fig. 20.1 A comparison of the experimental baryon spectrum [Behringer *et al.* (2012)] with a fit with E_R^α from (20.4), which generates the full spectrum of the fractional rotation group $SO^\alpha(3)$. Circles denote the experimental mass, theoretical values are drawn as lines for a given L . Band heads are labeled with the corresponding particle name and mass. Since this figure has been first published [Herrmann (2007a)], additional particles have been discovered, which we show with filled circles. For $L = 1, 2$ the calculated predictions for baryon masses are compared with the masses of mesons.

this way as a dependence on the angular momentum L and its projection onto the z-axis M . We are led to the conclusion, that parameter b_0 may be interpreted as the fractional analogue to a magnetic field.

Hence we interpret (20.4) as a description of a nonrelativistic spin-0 particle in constant fractional magnetic field with strength b_0 .

If we associate this particle with a quark and the fractional magnetic field with a color magnetic field, we obtain a simple analytic fractional model, which should allow a description of the hadron spectrum.

This assumption is motivated by results obtained with the phenomenological quark bag models [Creutz (1974); Chodos *et al.* (1974); Vasak *et al.* (1983)] and by ab initio calculations in lattice QCD [Wilson (1974); Cardoso *et al.* (2009)], where a color flux tube with almost constant color magnetic field between quarks is observed [Casher *et al.* (1979); Takahashi *et al.* (2002)].

Since we expect a similar result for self consistent solutions of the nonlinear QCD field equations, the fractional Zeeman-effect serves as a simple, idealized model for a first test, whether the hadron spectrum may be reproduced at all within the framework of a fractional Abelian field theory.

Therefore we will use formula (20.4) for a fit of the experimental baryon spectrum [Behringer *et al.* (2012)].

The optimum fit parameter set with an r.m.s error of 0.84% results as:

$$\alpha = 0.112 \quad (20.6)$$

$$m_0 = -17171.6[\text{MeV}] \quad (20.7)$$

$$a_0 = 10971.8[\text{MeV}] \quad (20.8)$$

$$b_0 = 8064.6[\text{MeV}] \quad (20.9)$$

In figure 20.1 the experimental versus fitted values are shown. In table 20.1 name, proposed quantum numbers L and M , experimental mass $E^{\exp}[\text{MeV}]$ taken from [Behringer *et al.* (2012)], fitted mass $E_R^\alpha[\text{MeV}]$ according to (20.4) and error $\Delta E[\%]$ are listed.

Remarkable enough, the overall error for the fitted baryon spectrum $L = 3, \dots, 10$ is less than 1%. A general trend is an increasing error for small masses which possibly indicates the limitations of a nonrelativistic model.

For the fractional symmetric rigid rotor we have demonstrated in section 17.5 that the limit $\alpha = 0.11$ corresponds in a geometric picture to the case of a linear potential. Therefore the optimum fit value for $\alpha = 0.112$ represents the correct linear type for the long range potential used in phenomenological quark models.

In addition, the $\alpha = 0.112$ value corresponds in the sense of the relativistic theory (see chapter 11) to an inherent $SU(18)$ symmetry, which optimistically may be interpreted as the direct product:

$$SU(18) = SU(N = 6)^{\textit{flavor}} \otimes SU(3)^{\textit{color}} \quad (20.10)$$

and is therefore an indirect indication for the maximum number of different quark flavors to be found in nature.

In the lower part of table 20.1 the proposed (L, M) values for $\Lambda_c(2880)$ up to Λ_b give a rough estimate for the number of particles, which are still missing in the experimental spectrum.

For $L = 1, 2$ we can compare the theoretical mass predictions for baryons with the experimental meson spectrum, see upper part of table 20.1 and left part of figure 20.1. The results are surprisingly close to the experimental masses, despite the fact that mesons and baryons are different constructs.

This means, that the relative strength of the fractional magnetic field $b_0 = B_q/m_q$, $\{q \in u, d, s, c\}$ is of similar magnitude in mesonic ($q\bar{q}$) and baryonic qqq systems.

Table 20.1 A comparison of the experimental baryon spectrum with the mass formula (20.4). Listed are name, proposed quantum numbers L and M , experimental mass $E^{\text{exp}}[\text{MeV}]$, fitted mass $E_R^\alpha[\text{MeV}]$ and error $\Delta E[\%]$. For $L = 1$ and $L = 2$ the predicted baryon masses are compared with experimental meson masses. * indicates the status of a particle.

name	L	M	$E^{\text{exp}}[\text{MeV}]$	$E_R^\alpha[\text{MeV}]$	$\Delta E[\%]$
π^0	1	0	135	313.90	132.57
K_s^0	1	1	498	470.45	-5.46
$\rho(770)$	2	0	776	652.41	-15.87
$K^*(892)^0$	2	1	896	808.96	-9.71
$\phi(1020)$	2	2	1019	945.76	-7.19
N	3	0	938	959.39	2.28
Λ	3	1	1116	1115.94	0.02
Σ^0	3	2	1193	1252.74	5.04
Ξ^0	3	3	1315	1374.16	4.51
$\Delta(1232)$	4	0	1232	1240.53	0.69
$\Sigma^0(1385)$	4	1	1384	1397.08	0.97
$\Xi(1530)$	4	2	1532	1533.87	0.14
Ω^-	4	3	1672	1655.29	-1.00
$\Lambda(1800)$	4	4	1775	1764.44	-0.60
$\Lambda(1520)$	5	0	1520	1500.10	-1.28
$\Lambda(1670)$	5	1	1670	1656.65	-0.80
$\Xi(1820)$	5	2	1823	1793.45	-1.62
$\Delta(1910)$	5	3	1910	1914.87	0.25
$\Sigma(2030)$	5	4	2030	2024.01	-0.29
$\Lambda(2100)$	5	5	2100	2123.14	1.10
$\Sigma(1750)$	6	0	1750	1741.42	-0.49
$\Sigma(1915)$	6	1	1915	1897.97	-0.89
$\Xi(2030)$	6	2	2025	2034.76	0.48
$\Delta(2150) (*)$	6	3	2150	2156.18	0.29
$\Omega(2250)$	6	4	2252	2265.33	0.59
$\Omega(2380) (**)$	6	5	2380	2364.46	-0.65
$\Sigma_c(2452)$	6	6	2452	2455.27	0.13
$\Xi(1950)$	7	0	1950	1967.06	0.88
$\Lambda(2110)$	7	1	2110	2123.61	0.65
Λ_c	7	2	2286	2260.41	-1.14
$\Delta(2420)$	7	3	2420	2381.83	-1.58
$\Xi_c^+(2467)$	7	4	2467	2490.97	0.97
$\Xi_c^{'+}(2575)$	7	5	2576	2590.10	0.56
$\Xi_c^0(2645)$	7	6	2645	2680.92	1.35
$\Xi_c^0(2790)$	7	7	2791	2764.73	-0.94

Table 20.2 A comparison of the experimental baryon spectrum with the mass formula (20.4). Table 20.1 continued.

name	L	M	$E^{\text{exp}}[\text{MeV}]$	$E_R^\alpha[\text{MeV}]$	$\Delta E[\%]$
$N(2190)$	8	0	2190	2179.12	-0.50
$\Lambda(2350)$	8	1	2350	2335.67	-0.61
$\Xi_c^0(2471)$	8	2	2471	2472.47	0.06
$\Lambda_c^+(2593)$	8	3	2595	2593.89	-0.06
Ω_c^0	8	4	2698	2703.03	0.21
$\Sigma_c^0(2800)$	8	5	2800	2802.16	0.08
$\Lambda_c^+(2880)(***)$	8	6	2882	2892.98	0.38
$\Xi(2980)(***)$	8	7	2978	2976.79	-0.06
$\Xi_c(3080)(***)$	8	8	3076	3054.61	-0.70
$\Omega^-(2380)(**)$	9	0	2380	2379.27	-0.03
$\Sigma_c(2520)(***)$	9	1	2518	2535.82	0.69
$\Sigma_c(2645)(***)$	9	2	2646	2672.62	1.00
$\Xi_c^0(***)$	9	3	2792	2794.04	0.20
$\Lambda_c(2880)(***)$	9	4	2882	2903.18	0.74
$\Sigma(3000)(*)$	9	5	3000	3002.31	0.10
$\Xi_c^0(***)$	9	6	3080	3093.13	0.43
$\Sigma(3170)(*)$	9	7	3170	3176.94	0.22
	9	8		3254	
	9	9		3327	
$\Lambda(2585)(**) \quad \Delta(2750)(**)$	10	0	2585	2568.9	0.66
	10	1	2750	2725	0.92
	10	2		2862	
$\Xi_c^0(***)$	10	3	2971	2983	0.40
	10	4		3092	
	10	5		3191	
	10	6		3282	
	10	7		3366	
	10	8		3444	
$\Xi_{cc}^+(*)$	10	9	3519	3517.06	-0.05
Ω_{cc}	11	8	3637	3627.63	
Ω_{ccc}	15	15	4681	4702.20	
$\Lambda_b^0(***)$	20	20	5620	5612.75	-0.13

Summarizing the results of this section we conclude, that the fractional Zeeman effect, which describes the motion of a fractional charged particle in a constant fractional magnetic field serves as a reasonable nonrelativistic model for an understanding of the full baryon spectrum.

This result has far reaching consequences: For the first time the terms “particle described by a fractional wave equation” and “fractional magnetic field” have successfully been associated with the entities quark, which follows a $SU(n)^{\text{flavor}}$ symmetry and color, which follows a $SU(3)^{\text{color}}$ symmetry.

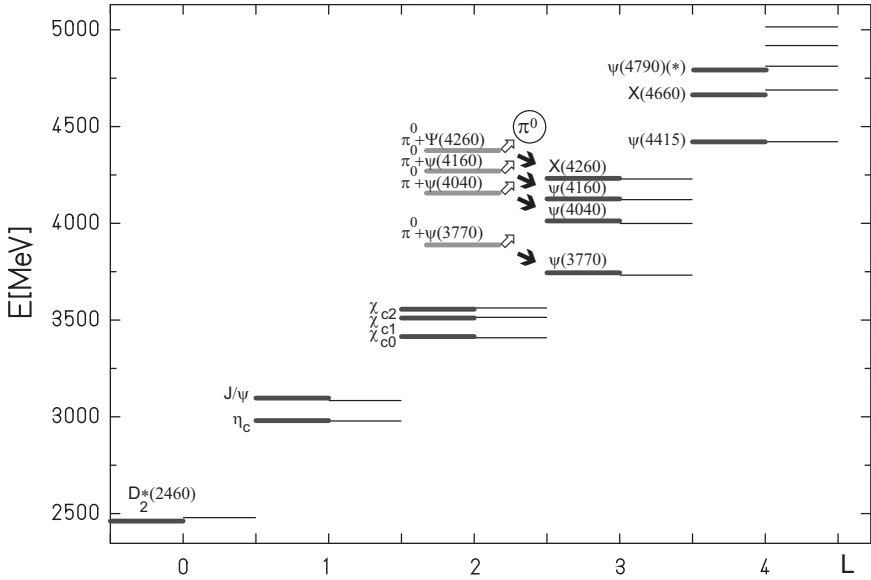


Fig. 20.2 Ground state bands of the charmonium spectrum. The experimental values are given as thick lines and theoretical values as small lines. Particles are labeled according to the quantum numbers of the fractional rotation group $SO^\alpha(3)$. While the overall agreement is very good, only for the multiplet $L = 3$ the theoretical predictions deviate by 133 [MeV]. Therefore we propose the following production process: First an excited short lived hybrid of type $u\bar{u}cc^*$ and $d\bar{d}c\bar{c}^*$ respectively is produced, which decays into a pion and a long lived experimentally observed final state. This is indicated by gray lines for the theoretical mass of the predicted short lived hybrid state, arrows sketch the decay process.

20.2 Charmonium

So far, the presented results lead to the conclusion, that a fractional rotation group $SO^\alpha(3)$ based on the Riemann fractional derivative definition determines an inherent symmetry of the baryon excitation spectrum.

From this encouraging result immediately follows the question, whether the same symmetry is realized for mesonic excitation spectra too. In this section, we will present explicit evidence for that suggestion. But there is one fundamental difference: meson excitation spectra will be reproduced with an excellent degree of precision, if we apply the Caputo definition of the fractional derivative.

As a consequence, for $M = 0$ and $L = 0$ there will be a reduction of the corresponding energy levels in comparison with the levels obtained with the Riemann definition, while all other energy levels there will be no difference. But it is exactly this specific lowering of energy levels, that we observe in all meson spectra without exception.

To start our investigation of meson excitation levels, we will first describe the charmonium spectrum as the most prominent example:

In analogy to (20.4) based on the Caputo definition of the fractional derivative we propose the following mass formula in order to classify the multiplets of $SO^\alpha(3)$:

$$E_C^\alpha = m_0 \quad (20.11)$$

$$+ \begin{cases} a_0 \frac{\Gamma(1+(L+1)\alpha)}{\Gamma(1+(L-1)\alpha)} \pm b_0 \frac{\Gamma(1+|M|\alpha)}{\Gamma(1+(|M|-1)\alpha)} & L \neq 0 \text{ and } M \neq 0 \\ a_0 \frac{\Gamma(1+(L+1)\alpha)}{\Gamma(1+(L-1)\alpha)} & L \neq 0 \text{ and } M = 0 \\ 0 & L = 0 \text{ and } M = 0 \end{cases}$$

In figure 20.2 we present the ground state spectrum of charmonium, the experimental values according to [Behringer *et al.* (2012)] are plotted with thick lines. In table 20.3 these values and the proposed quantum numbers L, M for a complete classification of multiplets according to the fractional rotation group are given.

We want to emphasize, that the presentation for reasons of simplicity is restricted to the ground state excitation spectrum of charmonium, higher order excitations like η_c' will be associated with higher radial excitations and therefore will be ignored in a first attempt.

For a given $L = \text{const}$ multiplet the mass formula reduces to:

$$E_C^\alpha(\tilde{m}_0, b_0, \alpha) = \tilde{m}_0 \pm \begin{cases} b_0 \frac{\Gamma(1+|M|\alpha)}{\Gamma(1+(|M|-1)\alpha)} & M \neq 0 \\ 0 & M = 0 \end{cases} \quad (20.12)$$

with three parameters \tilde{m}_0 , b_0 and α . Let us apply (20.12) for $L = 2$ to the χ_c triplet, we have three determining equations for the parameters. Therefore we obtain:

$$\tilde{m}_0 = \chi_{c0} = 3414.75[\text{MeV}] \quad (20.13)$$

$$b_0 = 106.03[\text{MeV}] \quad (20.14)$$

$$\alpha = 0.677 \quad (20.15)$$

Table 20.3 Comparison of experimental and theoretical masses according to (20.11) for the ground state band of charmonium. The values above |41⟩ are predictions of the theoretical model.

$ LM\rangle$	Name	m_{exp}	m_{th}
$ 00\rangle$	$D_2^*(2460)$	2461.10 ± 1.6	2461.63
$ 10\rangle$	η_c	2981.0 ± 1.2	2989.58
$ 11\rangle$	J/ψ	3096.916 ± 0.011	3086.63
$ 20\rangle$	χ_{c0}	3414.75 ± 0.31	3419.65
$ 21\rangle$	χ_{c1}	3510.66 ± 0.07	3516.70
$ 22\rangle$	χ_{c2}	3556.20 ± 0.09	3559.16
$ 30\rangle$	$\psi(3770)$	3773.15 ± 0.33	3763.12
$ 31\rangle$	$\psi(4040)$	4039 ± 1	4034.12
$ 32\rangle$	$\psi(4160)$	4153 ± 3	4152.68
$ 33\rangle$	$X(4260)$	4263 ± 9	4254.87
$ 40\rangle$	$\psi(4415)$	4421 ± 4	4413.10
$ 41\rangle$	$X(4660)$	4664 ± 12	4684.09
$ 42\rangle$	$\psi(4790)(*)$	4790	4802.66
$ 43\rangle$	X	-	4904.85
$ 44\rangle$	X	-	4996.81
$ 50\rangle$	X	-	4961.84
$ 51\rangle$	X	-	5232.84
$ 52\rangle$	X	-	5351.40
$ 53\rangle$	X	-	5453.59
$ 54\rangle$	X	-	5545.56
$ 55\rangle$	X	-	5630.34
$ 60\rangle$	X	-	5539.31
$ 61\rangle$	X	-	5810.30
$ 62\rangle$	X	-	5928.86
$ 63\rangle$	X	-	6031.05
$ 64\rangle$	X	-	6123.02
$ 65\rangle$	X	-	6207.80
$ 66\rangle$	X	-	6287.16

Hence we are confronted with a first encouraging result: The fractional derivative parameter α obtained from experimental data is very close to $\alpha = \frac{2}{3}$. From our derivation of a fractional Dirac equation we already found, that $\alpha = \frac{2}{n}$, which results from a n-fold factorization of the Klein-Gordon equation implies the existence of an inherent $SU(n)$ symmetry of the corresponding fractional wave equation. Therefore a symmetric fractional rotation group with $\alpha \approx 2/3$ implies an isomorphism with the group $SU(3)$ and is a first experimental evidence for a $SU(3)$ symmetric charge in particle physics.

Furthermore for $L = 3$ we interpret the ψ triplet as state $|30\rangle$, $|31\rangle$ and $|32\rangle$ and obtain another set of parameters:

$$\tilde{m}_0 = \psi(3770)|30\rangle = 3775.2[\text{MeV}] \quad (20.16)$$

$$b_0 = 293.8[\text{MeV}] \quad (20.17)$$

$$\alpha = 0.644 \quad (20.18)$$

This triplet is located above the $D - D^*$ meson threshold.

Within experimental errors, both α values are identical. This observation supports the assumption, that the spectrum may be interpreted using one unique α . The difference between both triplets is mainly absorbed by the magnetic field strength parameter b_0 , which suddenly increases by a factor 2.8. This may be directly related to the observation of a similar change of magnitude in the ratio R of cross-sections

$$R = \frac{\sigma(e^+e^- \rightarrow \text{Hadrons})}{\sigma(e^+e^-\mu^+\mu^-)} \quad (20.19)$$

which increases from $R = 2$ to $R = 5$ in this energy region.

The complete charmonium spectrum is therefore described by two distinct parameter sets below and above the threshold respectively:

$$E_C^\alpha = \begin{cases} E_C^\alpha(m_0, b_0^1, \alpha) & E < \text{threshold} \\ E_C^\alpha(m_0, b_0^2, \alpha) & E > \text{threshold} \end{cases} \quad (20.20)$$

Therefore we will apply b_0^1 and b_0^2 as two distinct fractional magnetic field strength parameters below and above the threshold respectively.

In addition, if our assumption of an inherent fractional rotation symmetry of the charmonium spectrum is valid, the experimentally observed triplet of ψ particles is not complete, because the state $|33\rangle$ is missing.

Using the parameter set (20.16) we are able to predict the mass of the $|33\rangle$ state, which turns out to be in excellent agreement with the recently observed $X(4260)$ (formerly known as $Y(4260)$ [Aubert *et al.* (2005)]) particle:

$$X(4260)_{\text{th}} = \psi|33\rangle = 4252.04[\text{MeV}] \quad (20.21)$$

This result also indicates, that the fractional magnetic field for a given $L = \text{const}$ multiplet is indeed a constant. Furthermore the proposed fractional model based on the fractional symmetry group $SO^\alpha(3)$ is the first one to give a reasonable classification for $X(4260)$ as a member of the $L = 3$ quartet.

Until now all standard models making use of phenomenological model potentials failed to explain the existence of $X(4260)$. This failure also

inspired several investigations to interpret $X(4260)$ not as a simple charmonium excitation, but e.g. as a hybrid state [Zhu (2005)].

A complete fit of experimental data for the charmonium spectrum using (20.20) leads to a surprising result: The full spectrum is reproduced with excellent accuracy, but there is one exception: The theoretical masses for members of the multiplet $L = 3$ deviate from the experimental values by an amount of 133[MeV]. This is very close to the rest mass of the pion π^0 .

We therefore suppose, that all members of the particle family $\psi(3770)$, $\psi(4040)$, $\psi(4160)$ and $X(4260)$ are generated via the same mechanism:

In a first step, a short lived hybrid state is formed e.g. $(u\bar{u}cc^*)$ and $(d\bar{d}cc^*)$ respectively: The mass of this hybrid state is exactly predicted by our model (20.11). Within a very short period of time this excited state decays into a pion and a long lived excited final state, which is observed experimentally:

$$X(3905) \rightarrow \pi^0 + \psi(3770) \quad (20.22)$$

$$X(4173) \rightarrow \pi^0 + \psi(4040) \quad (20.23)$$

$$X(4287) \rightarrow \pi^0 + \psi(4160) \quad (20.24)$$

$$X(4393) \rightarrow \pi^0 + X(4260) \quad (20.25)$$

In march 2013 the BESIII collaboration published results [BESIII Collaboration (2013)], which may be interpreted as decays of type:

$$X(4260) \rightarrow \pi^0 \pi^0 \pi^0? + Z_c(3900)^* \quad (20.26)$$

where $Z_c(3900)$ may be considered as an excited state of the $X(3872)$ state, which support the idea, that even the above long lived states are possibly objects of hybrid type. Using this hypothesis with the parameters

$$m_0 = 2461.63[\text{MeV}] \quad (20.27)$$

$$a_0 = 453.60[\text{MeV}] \quad (20.28)$$

$$b_0^1 = 107.85[\text{MeV}] \quad (20.29)$$

$$b_0^2 = 301.17[\text{MeV}] \quad (20.30)$$

$$\alpha = 0.648 \quad (20.31)$$

we calculate the theoretical masses, which are listed in table 20.3 and agree with the experiment to a very high degree. Especially interesting is the state $|00\rangle$, which is not included within the framework of conventional potential models. We predict a particle with mass $m_0 = 2461.76[\text{MeV}]$. Indeed there exists a possible candidate in this energy region, which is $D_2^*(2460)$ a charmed meson.

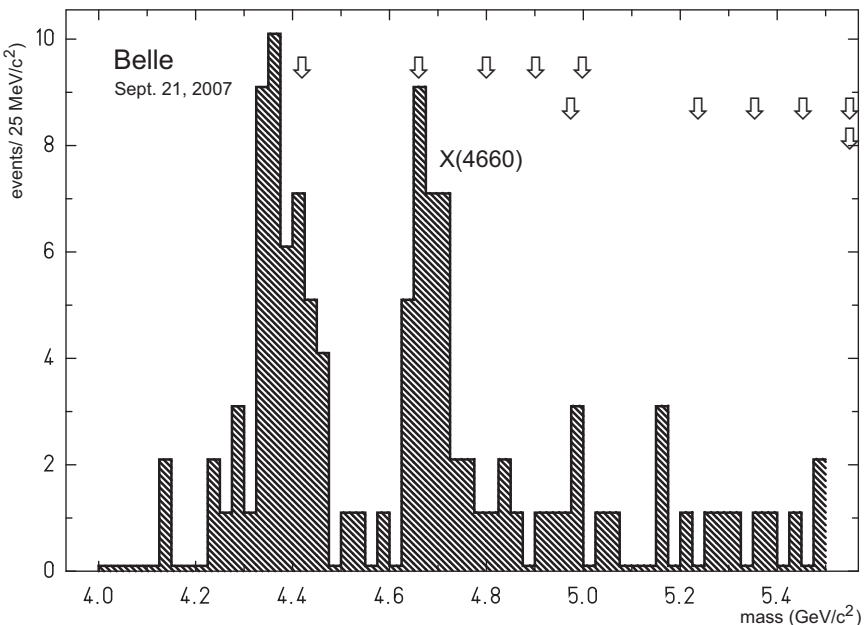


Fig. 20.3 Results from the Belle collaboration from September 2007 [Wang *et al.* (2007)]. A new particle at $X(4660)$ is detected. Within the fractional level spectrum listed in table 20.3 this particle was predicted as the $|41\rangle$ -state of the fractional rotation group.

Hence the symmetry of the fractional rotation group covers not only pure $c\bar{c}$ candidates but includes other charmed mesons as well.

In September 2007 the Belle collaboration, an international team of researchers at the High Energy Accelerator Research organization (KEK) in Tsukuba, Japan, found a new resonance at $X(4660)$, which may be directly identified as the $|41\rangle$ -state of a fractional multiplet. This assignment also supports the assumption, that states above the meson-threshold may be characterized using a single unique magnetic field parameter b_0^2 .

Figure 20.3 shows the results of the experiments performed by the Belle collaboration. The $X(4660)$ peak may be easily recognized. With arrows we marked additional positions of theoretically predicted peaks, which are also listed in the lower part of table 20.3.

There is increasing evidence for a resonance $\psi(5S)$ at 4790[MeV] [Beveren *et al.* (2009); Segovia *et al.* (2010)], which could be interpreted as a realization of the $|42\rangle$ -state with a predicted mass of 4802.66[MeV].

Table 20.4 Optimum parameter sets $\{m_0, a_0, b_0\}$ and rms-error in percent for a fit with experimental meson spectra. Since the experimental situation is not sufficient to determine all parameters simultaneously, in the lower part of this table all predicted parameters are labeled with (*).

meson	name	α	m_0	a_0	b_0	$\Delta [\%]$
$u\bar{u} \pm d\bar{d}$	pions (light mesons)	0.842	149.26	292.66	137.85	3.40
$u\bar{s} \pm s\bar{u}$	kaons	0.814	489.73	281.56	399.15	0.48
$s\bar{s}$	strangeonium	0.751	534.96	278.96	132.57	1.24
$s\bar{c} \pm c\bar{s}$	D_s -mesons	0.716	1617.06	276.97	156.85	0.02
$c\bar{c}$	charmonium	0.648	2461.63	453.60	$\begin{cases} 107.85 \\ 301.16 \end{cases}$	0.18
$b\bar{b}$	bottomonium	0.736	8978.68	323.37		
$u\bar{c}, c\bar{u}$	D -mesons	0.75*	1528.23	258.10	154.72	0.0*
$u\bar{b}, b\bar{u}$	B -mesons	0.80*	4906.38	260.01	49.36	0.0*
$s\bar{b}, b\bar{s}$	B_s -mesons	0.75*	4919.72	336.49	49.83	0.0*
$c\bar{b}, b\bar{c}$	B_c -mesons	0.71*	5819.36	365*	51*	0.0*

The current status of research leaves it merely as a speculation, whether three events are already a significant accumulation, to assert the existence of the $|50\rangle$ -state to 4961[MeV] and of the $|60\rangle$ -state to 5539[MeV]. Hence a new generation of experiments should be performed.

In this section we have collected a large number of arguments, which all demonstrate, that the charmonium spectrum may be understood consistently on the basis of a fractional rotation group with $\alpha \approx 2/3$.

Recently discovered particles $X(4260)$ and $X(4660)$ may be reproduced within the experimental errors.

There is no other model worldwide, which describes the properties of the charmonium spectrum with similar accuracy.

20.3 Phenomenology of meson spectra

The charmonium spectrum is just one example of all possible mesonic quark-anti quark states. In this section we will demonstrate, that a simultaneous description of all mesonic ground state excitation spectra may be obtained with the mass formula (20.11) if we associate the quantum numbers $|LM\rangle$ with the corresponding mesonic excitation states.

In a first simplified approach we will treat the up- and down-quarks as similar and will investigate the ground state excitation spectra of mesons of the family $\{u, s, c, b\}$. In figures 20.4-20.8 these spectra are plotted.

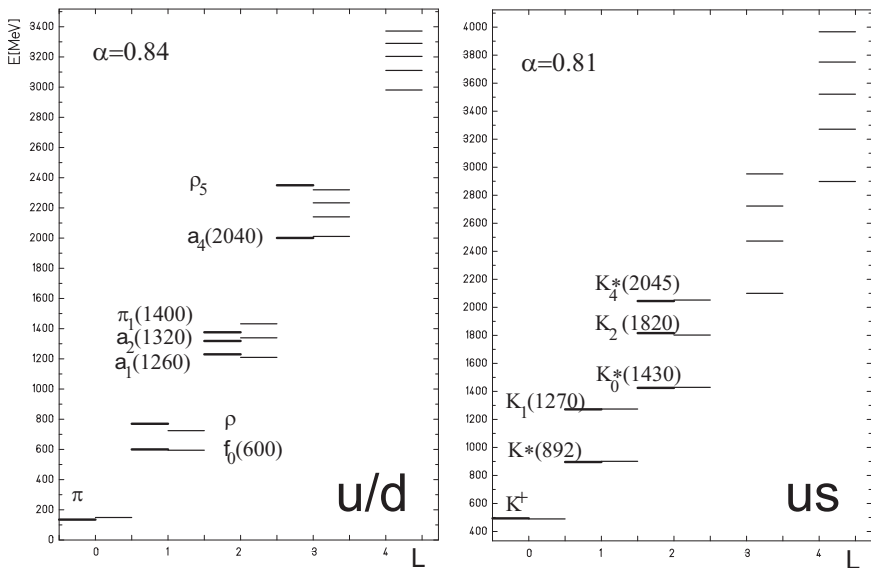


Fig. 20.4 Ground state meson excitation spectra for $u\bar{u}$ (light mesons) and $u\bar{s}$ (kaons). Thick lines represent experimental data [Behringer *et al.* (2012)]. Names and experimental masses are given. Thin lines denote the theoretical masses according to (20.11), values listed in table 20.5.

The free parameters $\{m_0, a_0, b_0\}$ of the fractional model (20.11) were determined by a fit with the experimental data. For light mesons the experimental data base is broad enough. Consequently there are no problems using a fit procedure. In fact, the situation is much easier to handle than in the special case of charmonium, discussed in the previous chapter, since the determination of a single fractional magnetic field strength parameter b_0 suffices to describe the experimental data sufficiently.

For heavy quarks we have only a limited number of experimental data. Consequently it is essential to deduce systematic trends in order to specify appropriate parameter values. Using conventional phenomenological models a survey of strangeonium, charmonium and bottomonium states did not reveal a systematic trend for the parameter sets derived [Henriquez (1979)].

The fundamental new aspect for an interpretation of meson spectra within the framework of a fractional rotation group is the fact, that systematic trends for the parameters may be recognized and may be used for an universal description of all possible mesonic ground state excitations.

From table 20.4 a systematic trend for the optimum fractional derivative parameter α for different mesonic systems may be deduced. These values are explained quantitatively, if we attribute to every quark and anti-quark respectively a multiplicative quantum number α_q , which we call fractional hypercharge in analogy to the standard hyper-charge property associated with quarks:

$$\alpha_u = \sqrt{\frac{6}{7}} \quad \alpha_s = \sqrt{\frac{6}{8}} \quad \alpha_c = \sqrt{\frac{6}{9}} \quad \alpha_b = \sqrt{\frac{6}{8}} \quad (20.32)$$

Assigning these values to every single quark α follows from the product

$$\alpha = \alpha_{q_1 \bar{q}_2} = \alpha_{q_1} \alpha_{\bar{q}_2} \quad (20.33)$$

As a consequence, using (20.33) we predict α -values for quark-antiquark combinations, where the experimental basis is yet too small to determine all parameters of the model (20.11) simultaneously. These predicted α -values are labeled with (*) in table 20.4.

The assumption of a fractional hyper-charge reduces the number of free parameters of the model by one, which allows to calculate the spectra of $u\bar{c}$, $u\bar{b}$ and $s\bar{b}$ mesons on the basis of available experimental data. As a consequence, all meson ground state excitation spectra except $c\bar{b}$ may be determined. Since for $c\bar{b}$ -mesons until now only the B_c -meson has been verified experimentally, for this meson the number of model parameters has to be reduced to one.

A comparison of the optimum parameter sets for different quark-antiquark combinations reveals common aspects:

For all mesons except charmonium the parameter a_0 is of similar magnitude of order 280[MeV] with a weak tendency to higher values for heavy mesons.

In addition, the value for the fractional magnetic field strength b_0 for all mesons except kaons is about 150 [MeV]. Furthermore there seems to exist a saturation limit for the field strength $b_0 = B/m_q$ which is reached for charmonium. For bottomonium which is about three times heavier, the fitted b_0 turns out to be 55 [MeV], which is about 1/3 of the charmonium value. Most probably an additional enhancement of the field strength could exceed the critical energy density for the creation of a light quark-antiquark pair e.g. a pion.

Consequently in view of a fractional mass formula (20.11) the different meson spectra have a great deal in common and systematic trends may be used to estimate the spectrum of $c\bar{b}$ -mesons.

Table 20.5 Complete listing of ground state meson excitations according to (20.11) with parameters from table 20.4. For a given level in the first line identified particles and experimental masses in brackets, in the second line theoretical fit/prediction. All masses are given in MeV.

level / $ LM $	$u\bar{u}$	$u\bar{s}$	$s\bar{s}$	$u\bar{c}$	$s\bar{c}$	$c\bar{c}$	$u\bar{b}$	$s\bar{b}$	$c\bar{b}$	$b\bar{b}$	
00> exp. 00 th.	$\pi^0(134.976)$ 149.26	$K^+(493.667)$ 489.73	$\eta(547.51)$ 534.96	$f_2(1252)$ 1528.23	$\eta_2(1617)$ 1617.06	$D_2^*(2461.1)$ 2461.63	$[B_2^*(5818)]$		8978.68		
							4906.38	4919.72	5819.36		
10> exp. 10 th.	$f_0(600)$ 595.76	$K^*(896)$ 900.88	$K(892)$ 906.50	$D(1864.5)$ 1856.51	$D_s(1968.2)$ 1968.53	$\eta_c(2980.4)$ 2989.58	$B(5279.1)$ 5279.10	$B_s(5367)$ 5367.00	$B_c(6277)$ 6277.00	$\eta_b(9388.90)$ 9400.27	
11> exp. 11 th.	$\rho(775.5)$ 725.79	$K_1(1272)$ 1274.15	$\phi(1019.46)$ 1028.38	$D^*(2006.79)$ 2011.92	$D_s^*(2112)$ 2111.55	$J/\psi(3096.92)$ 3086.63	$B^*(5325.1)$ 5325.10	$B_s^*(5412.8)$ 5412.80	$\Upsilon(1s)(9460.3)$ 6323.51	9451.42	
20> exp. 20 th.	$a_1(1230)$ 1211.16	$K_0^*(1425)$ 1428.80	$f_1(1281.8)$ 1311.68	$D_{s0}^*(2317)$		$\chi_{c0}(3414.76)$ 3419.65	$B_2^*(5743)$ 5743.00	$B_{sJ}^*(5853)$ 5853.00	$\chi_{b0}(9859.44)$ 6719.15	9841.41	
21> exp. 21 th.	$a_2(1318.3)$ 1341.19	$K_2(1816)$ 1802.07	$f_1(1426.3)$ 1433.56	$-D_{s1}^*(2458.9)$		$\chi_{c1}(3510.66)$ 3516.70	5789.00		5898.80	6765.56	$\chi_{b1}(9892.78)$ 9892.56
22> exp. 22 th.	$\pi_1(1376)$ 1434.13	$K_4^*(2045)$ 2052.06	$f_0(1507)$ 1503.73	$D_s^*(2461.1)$ 2457.79	$D_{s2}^*(2572.6)$ 2535.35	$\chi_{c2}(3556.2)$ 3559.16	$[B_2^*(5818)]$ 5818.94	B_{s2}^* 5925.08	B_{c2}^* 6789.42	$\chi_{b2}(9912.1)$ 9920.90	
30> exp. 30 th.	$a_4(2001)$ 2012.74	2099.90		$\phi_3(1854)$ 1800.25	$D^*(2640)$ 2642.85	$[D_{s1}^*(2690)]$ 2724.73	$\psi(3772.92)$ 3763.12	$B_s^{**}(10355.2)$		10366.7	
31> exp. 31 th.	$\rho(2149)$ 2142.77	2473.17		$f_2(1944)$ 1922.13	2798.25		2867.75	$\psi(4039)$ 4034.12	6372.60	6484.17	7279.79
											10417.8
32> exp. 32 th.			$f_2(2011)$		2887.42		2943.03	$\psi(4153)$ 4152.68	6402.53	6510.45	7303.65
											10446.2
33> exp. 33 th.	$\rho_5(2350)$ 2321.99	2952.46		$f_4(2044)$ 2055.05	$D_{sJ}(3040)$		$X(4259)$ 4254.87	6429.85		6533.94	7324.63
											10471.3
40> exp. 40 th.	2982.63		$f_2(2339)$		3134.97		$\psi(4421)$ 4413.10	7015.83		7108.88	7807.95
											10963.5
41> exp. 41 th.	3112.66		$f_0(2465)$		3290.37		$X(4660)$ 4684.09	7061.83		7154.68	$\Upsilon(11019)$ 7854.36
											11014.6
42> exp. 42 th.	3205.60		3521.53		3379.54		$\psi(4790)(*)$ 4802.66	7091.76		7180.96	7878.22
											11042.9
43> exp. 43 th.	3291.88		3750.83		3261.13		3467.66 4904.85	7119.08		7204.44	7899.20
											11068.1
44> exp. 44 th.	3373.90		3966.94		2673.19		3532.94 4996.81	7144.73		7226.17	7918.37
											11091.3
error %	3.40	0.48	1.24	*0.00		0.02	0.18	*0.00		*0.00	0.09

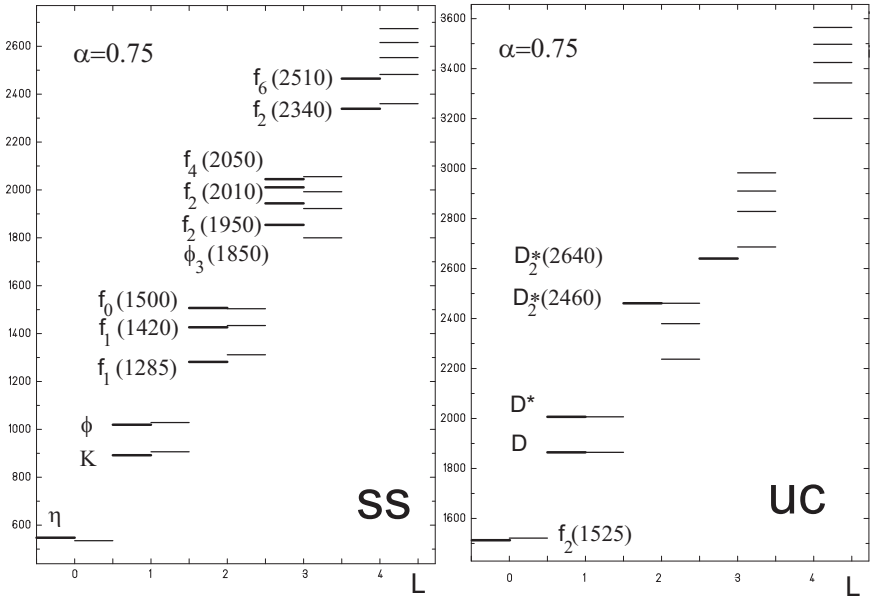


Fig. 20.5 Ground state meson excitation spectra for $s\bar{s}$ (strangeonium) and $u\bar{c}$ (D -mesons). Thick lines represent experimental data [Behringer *et al.* (2012)]. Names and experimental masses are given. Thin lines denote the theoretical masses according to (20.11), values listed in table 20.5.

- From our considerations on a maximum magnetic field strength we deduce the following systematics for the magnetic field strength for the family of $Q_j\bar{b}$ mesons:

$$b_0 = c_0 m_b + c_1 m_{Q_j} \quad j = u, s, c, b \quad (20.34)$$

where c_0, c_1 are parameters and $m_{Q_j} = 4^j$ is the mass of the constituent quark (see discussion in the following section). It follows $b_0 = 51$ [MeV] for the $c\bar{b}$ meson.

- We assume a similar trend in the a_0 parameter for charmed and bottom mesons. We propose the relation:

$$\frac{a_0(c\bar{b})}{a_0(s\bar{b})} = \frac{a_0(s\bar{c})}{a_0(u\bar{c})} \quad (20.35)$$

With the values from table 20.4, $a_0 = 365.00$ [MeV] follows for the $c\bar{b}$ meson.

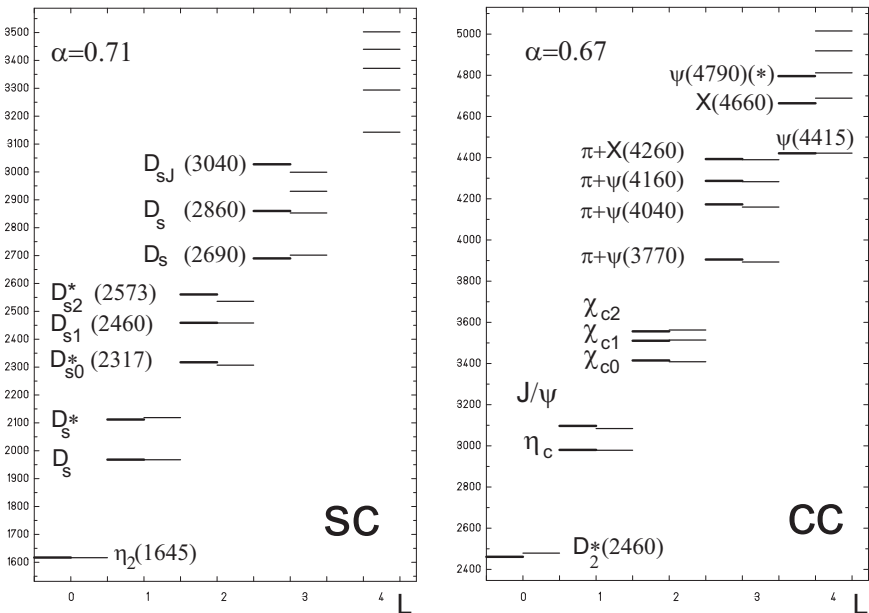


Fig. 20.6 Ground state meson excitation spectra for $s\bar{c}$ (D_s -mesons) and $c\bar{c}$ (charmonium). Thick lines represent experimental data [Behringer *et al.* (2012)]. Names and experimental masses are given. Thin lines denote the theoretical masses according to (20.11).

With these assumptions the ground state spectra of all possible quark-antiquark combinations may be calculated. The resulting masses are presented in table 20.5.

Based on the fractional mass formula (20.11) we found a general systematic in the ground state excitation spectra of mesons. Consequently we were able to classify all ground state excitation states for all possible mesons up to the bottom-quark as multiplets of the fractional rotation group $SO^\alpha(3)$.

The application of our fractional model reveals some unexpected characteristics: The predicted energies for the ground states $|00\rangle$ cannot be described with standard phenomenological potential models and are therefore an important indicator for the validity of the fractional concept.

Since we apply the Caputo fractional derivative, the ground state masses are directly determined by parameter m_0 . We find a first family of well known mesons which we successfully associate with the calculated ground state masses.

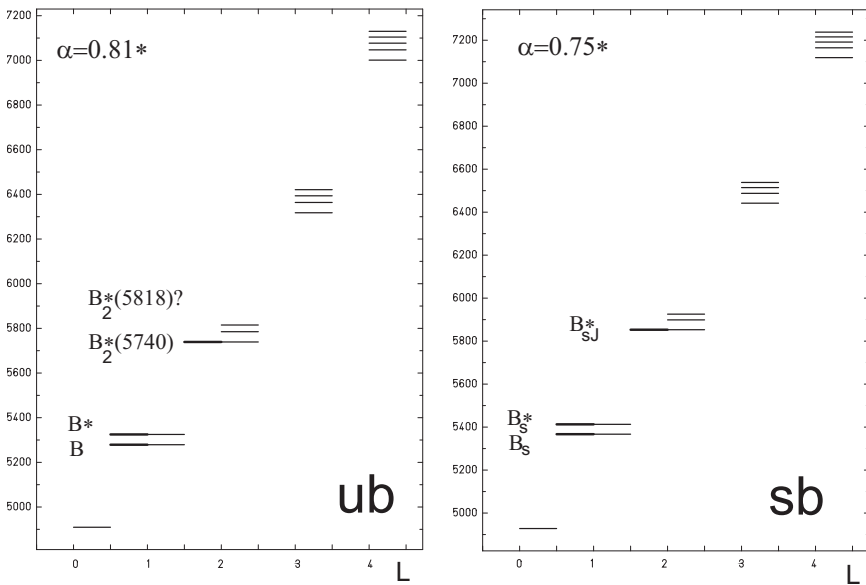


Fig. 20.7 Ground state meson excitation spectra for $u\bar{b}$ (B -mesons) and $s\bar{b}$ (B_s -mesons). Thick lines represent experimental data [Behringer *et al.* (2012)]. Names and experimental masses are given. Thin lines denote the theoretical masses according to (20.11).

- The ground state $|00\rangle$ of the $u\bar{u}$ system is predicted as 149[MeV]. Consequently we assign a pion with experimentally deduced mass of 135[MeV].
- The ground state $|00\rangle$ of the $u\bar{s}$ system is predicted as 489[MeV], which very well corresponds to the experimental mass of the K^+ kaon with 493[MeV].
- The ground state $|00\rangle$ of the $s\bar{s}$ is predicted as 534[MeV]. The lightest meson with a dominant $s\bar{s}$ content is the η -meson with an experimental mass of 547[MeV].

This family of ground states of light mesons is characterized by $J^P = 0^-$ and leaves the quark content of the meson unchanged.

For heavier mesons we propose experimental candidates for predicted ground states, which unexpectedly modify the quark content of the meson-family considered:

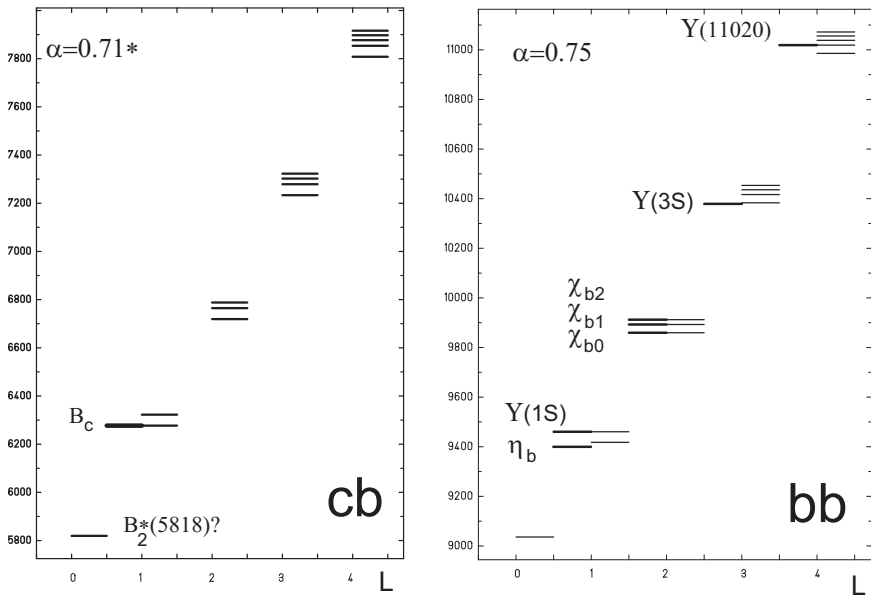


Fig. 20.8 Ground state meson excitation spectra for $c\bar{b}$ (B_c -mesons) and $b\bar{b}$ (bottomonium). Thick lines represent experimental data [Behringer *et al.* (2012)]. Names and experimental masses are given. Thin lines denote the theoretical masses according to (20.11).

- The ground state $|00\rangle$ of the $u\bar{c}$ is predicted as 1528.23[MeV]. The only meson which corresponds to this value is $f_2(1525)$ with a dominant $u\bar{u}$ content and an experimental mass 1525[MeV].
- The ground state $|00\rangle$ of the $s\bar{c}$ is predicted as 1617.06[MeV]. The only meson which corresponds to this value is $\eta_2(1624)$ with a dominant $u\bar{s}$ content and an experimental mass 1617[MeV].
- The ground state $|00\rangle$ of the $c\bar{c}$ is predicted as 2461.63[MeV]. The only meson which corresponds to this value is $D_2^*(2460)$ with a dominant $u\bar{c}$ content and an experimental mass 2461.1[MeV].

This family of ground states is characterized by a $J^P = 2^+$ value and may be constructed by replacing the \bar{c} quark by \bar{u} quark for a given meson. Therefore the fractional model generates a connection between different meson families. Distinct meson spectra seem to be more related, than assumed until now.

The proposed classification scheme is also useful to make predictions: For the ground state of charmonium we have associated the $|22\rangle$ -state of $u\bar{c}$, which is the $D_2^*(2640)$ meson with $J^p = 2^+$. For the analogous $|22\rangle$ -state of $u\bar{b}$ -mesons we predict $B_2^*(5818)$ with a mass of 5818.94 [MeV] and $J^p = 2^+$. This state may be associated with the $|00\rangle$ ground state of $c\bar{b}$ -mesons, replacing the \bar{c} quark by an \bar{u} quark, as already observed for the ground states of charmed mesons. This ground state has a predicted mass of 5819.36[MeV]. Within expected errors, this is an excellent agreement and pronounces the similarity of charm- and bottom-mesons in view of the proposed fractional mass formula.

Furthermore this is a first direct indication, that two different quark families $\{u, d, s\}$ and $\{c, b, t\}$ with sum of charges 0 and 1 respectively exist, which differ significantly in their $|00\rangle$ ground state properties. This may be interpreted as an indication, that in a fractional theory the quarks are grouped in triplets, while the standard model prefers generations of doublets ($\{u, d\}$, $\{s, c\}$ and $\{b, t\}$).

In addition, this interpretation allows a deeper understanding of the strength of the fractional magnetic field, parametrized with b_0 and listed in table 20.4:

For the triplet $\{u, d, s\}$ this strengths is of the type $nm_\pi, n \in \mathbb{N}$ with $m_\pi \approx 133$ [MeV] with the combinations

$$b_0(u\bar{u} \pm d\bar{d}) = 1 \times m_\pi \quad (20.36)$$

$$b_0(u\bar{s} \pm s\bar{u}) = 3 \times m_\pi \quad (20.37)$$

$$b_0(s\bar{s}) = 1 \times m_\pi \quad (20.38)$$

And for the second family triplet $\{c, b, t\}$ this strengths is of the type $nm_x, n \in \mathbb{N}$ with $m_x \approx 55$ [MeV] with the combinations

$$b_0(s\bar{c} \pm c\bar{s}) = 3 \times m_x \quad (20.39)$$

$$b_0(c\bar{c}) = 2 \times m_x \quad \text{and} \quad 2 \times 3 \times m_x \quad (20.40)$$

$$b_0(b\bar{b}) = 1 \times m_x \quad (20.41)$$

$$b_0(u\bar{c} \pm c\bar{u}) = 3 \times m_x \quad (20.42)$$

$$b_0(u\bar{b} \pm b\bar{u}) = 1 \times m_x \quad (20.43)$$

$$b_0(s\bar{b} \pm b\bar{s}) = 1 \times m_x \quad (20.44)$$

$$b_0(c\bar{b} \pm b\bar{c}) = 1 \times m_x^* \quad (20.45)$$

These b_0 -values approximate the fitted values up to a few MeV. This error corresponds to the estimated influence of electromagnetic effects, which are

ignored in the presented idealized fractional $SO(3)^\alpha \supset SO(2)^\alpha$ -model and once more underlines the connection between quark-families.

Summarizing our results we have demonstrated, that a fractional model may indeed explain the excitation spectra of all possible quark-antiquark combinations with an accuracy of better than 2%.

20.4 Metaphysics: about the internal structure of quarks

Finally we may speculate about an internal structure of quarks. We have calculated the ground state masses m_0 for all possible excitation spectra of mesons.

Let us assume that m_0 is the sum of the masses of two hypothetical constituent quarks (Q_i):

$$m_0(Q_1, Q_2) = m_{Q_1} + m_{Q_2} \quad (20.46)$$

We perform a fit procedure of parameter m_0 from table 20.4 according to (20.46) and obtain:

$$Q_u \approx 75[\text{MeV}] \quad (20.47)$$

$$Q_s \approx 302[\text{MeV}] \quad (20.48)$$

$$Q_c \approx 1210[\text{MeV}] \quad (20.49)$$

$$Q_b \approx 4800[\text{MeV}] \quad (20.50)$$

A remarkable coincidence is the fact that $Q_s \approx 4Q_u$, $Q_c \approx 4Q_s$, $Q_b \approx 4Q_c$, the mass of every constituent quark is four times its predecessor. We obtain a rule

$$Q_j = m_u 4^j, \quad j = 1, 2, \dots \quad (20.51)$$

with $m_u = 18.92[\text{MeV}]$.

From this result we may speculate, that quarks exhibit an internal structure. Four constituents with mass m_u constitute an up-constituent quark, 16 built up a strange-constituent quark etc. Therefore we naively guess, that this is a hint for an internal SU(4)-symmetry.

Furthermore we can make predictions for heavier quarkonia. We obtain

$$b^* \bar{b}^*(j=5) \approx 38.4 \pm 5.0[\text{GeV}], \quad \alpha^* = \sqrt{\frac{6}{7}} \quad (20.52)$$

$$b^* \bar{b}^*(j=6) \approx 153.6 \pm 20[\text{GeV}], \quad \alpha^* = 1 \quad (20.53)$$

So we are left with the problem, why these quarkonia have not been observed yet. Hence it is quite instructive to scan the energy region in the

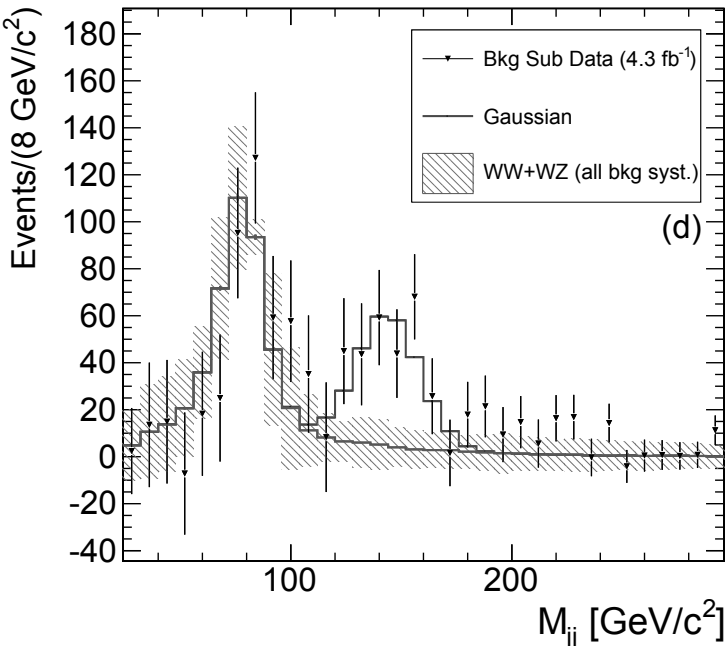


Fig. 20.9 In April, 2011 the CDF-collaboration reported evidence for the detection of a new particle at $\approx 144 \text{ GeV}$ [Aaltonen *et al.* (2011)]: The dijet invariant mass distribution for the sum of electron and muon events is shown after subtraction of fitted background components with the exception of resonant contribution to M_{jj} including WW and WZ production and the hypothesized narrow Gaussian contribution. The uncertainty band corresponds to background statistical uncertainty. (With kind permission from Aaltonen T. *et al.*, (CDF-collaboration) Phys. Rev. Lett. **106** (2011) 171801, ©American Physics Society).

vicinity of these quarkonia. Let us first mention, that confinement is a natural property of free solutions of a fractional wave equation with $\alpha < 1$. Therefore the constituents of the $j = 6$ quarkonia are predicted to be quarks, which are not confined. As a consequence they are free particles. It is at least remarkable, that indeed there are direct observations of top-events near $173[\text{GeV}]$. Therefore within the framework of fractional calculus, the top-quark could be interpreted as a $j = 6$ quarkonium state.

The proposed fractional model predicts the existence of single top-quarks as a consequence of deconfinement for $\alpha^* = 1$. What at the first glance seems to be a strong argument against the fractional model in the meantime turned out as a nice success, since free top-quarks have been

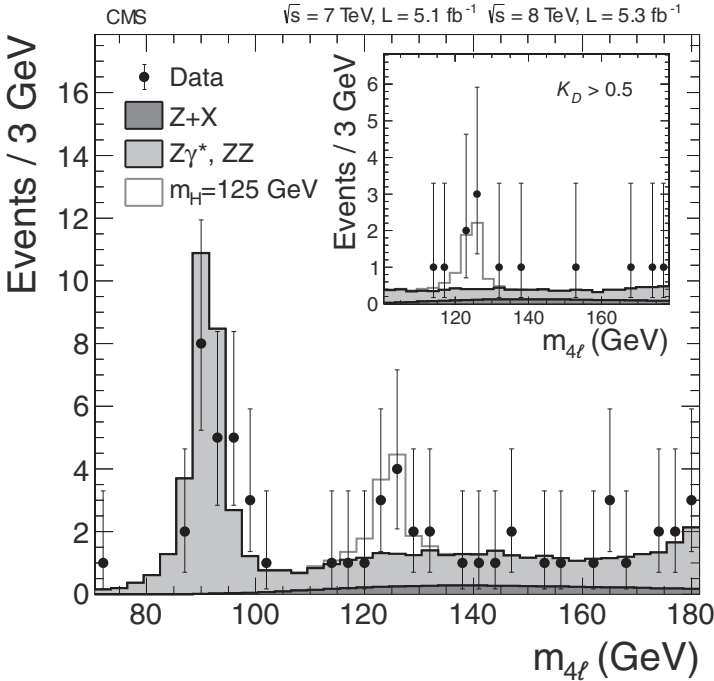


Fig. 20.10 Another candidate for a sixth quark family: Distribution of the four-lepton invariant mass for the $ZZ \rightarrow 4l$ analysis. The points represent the data, the filled histograms represent the background, and the open histogram shows the signal expectation for a Higgs boson of mass $m_H = 125$ GeV, added to the background expectation. The inset shows the m_{4l} distribution after selection of events with $K_D > 0.5$, as described in [CMS (2012)].

observed for the first time undoubtedly by two different collaborations in 2009 [Aaltonen *et al.* (2009); Abazov *et al.* (2009)].

It is at least a surprising coincidence that within the above given energy range at about 150 [GeV] there have been several more or less serious observations of possible particles: To be even more highly speculative let us remind, that the CDF-collaboration [Aaltonen *et al.* (2011)] in April, 2011, claimed the unexpected discovery of a new particle at ≈ 144 GeV (see figure 20.9) which sadly enough could not be verified by other groups yet.

Finally, the experiments at CERN, culminating in the claim for the discovery of the Higgs-particle, may be interpreted still quite differently as any other particle with $J = 0$, see figure 20.10. Future will tell.

Summarizing our results, we found strong evidence, that the full excitation spectrum for baryons may successfully be interpreted as a fractional rotation spectrum based on the Riemann definition of the fractional derivative. Furthermore we have demonstrated, that the full variety of mesonic excitations may be interpreted as a fractional rotation spectrum too, if we apply the Caputo definition of the fractional derivative.

It is also remarkable, that the experimental hadron spectrum may be described quite successfully with the fractional mass formulas with $M \geq 0$. We did not find any evidence for particles with $M < 0$. This is an indication, that chirality plays an important role in hadron physics.

The only difference between baryons and mesons within the framework of fractional calculus is the presence and absence of a zero-point energy contribution to the fractional rotational energy respectively, which we will interpret in the next chapter according to Racah's SU(2) pairing model as a pairing gap.

This is a first indication, that Caputo- and Riemann fractional derivative describe distinct fundamental physical properties, which are directly related to fermionic and bosonic systems respectively.

Until now, we have investigated the properties of a single fractional particle. In the next section, we will give an additional surprising interpretation for a mixed Caputo-/Riemann- fractional derivative system with three independent particles.

This page intentionally left blank

Chapter 21

Magic Numbers in Atomic Nuclei

We have demonstrated that both fractional extensions of the standard rotation group $SO(N)$ based on the Riemann and the Caputo fractional derivative definition respectively may successfully be used to describe excitation spectra of baryons and mesons respectively. Baryons are composite particle combinations of three quarks, while mesons are built up by a quark and an antiquark. As a consequence, baryons are fermions and obey the Pauli-exclusion principle and Fermi-Dirac statistics, while mesons are bosons, which obey the Bose-Einstein statistics.

If we want to learn about the physical meaning of the difference between the Riemann- and Caputo based fractional derivative definition it will be helpful to investigate the properties of higher dimensional rotation groups.

We have already mentioned, that the fractional rotation group describes not only rotational but also vibrational degrees of freedom. In section 19.1 we gave a geometric interpretation of the group chain

$$SO(3)^{\alpha=1/2} \rightarrow U(1) \quad (21.1)$$

Our investigation of the properties of higher dimensional fractional rotation groups may therefore in a first approach concentrate on a 9-dimensional space, since it follows

$$\begin{aligned} SO(9)^{\alpha=1/2} &\rightarrow SO(3)^{\alpha=1/2} \otimes SO(3)^{\alpha=1/2} \otimes SO(3)^{\alpha=1/2} \\ &\rightarrow U(1) \otimes U(1) \otimes U(1) \rightarrow U(3) \end{aligned} \quad (21.2)$$

which corresponds to the 3-dimensional oscillator, which serves as a standard model in many different branches of physics.

Indeed we will find, that there are four different decompositions of the 9-dimensional mixed fractional rotation group. For each decomposition we will determine the magic numbers associated with this symmetry. As an astounding result we will realize, that two of these four sequences of magic

numbers are already realized in nature as magic nucleon numbers and as magic cluster numbers respectively, which are given by

$$\text{magic numbers in nuclei } 2, 8, 20, 28, 50, 82, 126, \dots \quad (21.3)$$

$$\text{magic numbers in metal clusters } 2, 8, 18, 34, 58, 92, 138, \dots \quad (21.4)$$

A fundamental understanding of magic numbers for e.g. protons and neutrons may be achieved if the underlying corresponding symmetry of the nuclear many body system is determined. Therefore a group theoretical approach seems appropriate.

Group theoretical methods have been successfully applied to problems in nuclear physics for decades. Elliott [Elliott (1958)] has demonstrated, that an average nuclear potential given by a three dimensional harmonic oscillator corresponds to a $SU(3)$ symmetry. Low lying collective states have been successfully described within the IBM-model [Iachello and Arima (1987)], which contains as one limit the five dimensional harmonic oscillator, which is directly related to the Bohr-Mottelson Hamiltonian.

Consequently the following derivation is the first reasonable explanation for magic numbers based on group theoretical arguments.

21.1 The four decompositions of the mixed fractional $SO^\alpha(9)$

The 9-dimensional Schrödinger equation

$$-\frac{\hbar^2}{2m} \sum_{i=1}^9 \frac{\partial^2}{\partial x_i^2} \Psi(x_1, \dots, x_9) = E\Psi(x_1, \dots, x_9) \quad (21.5)$$

may be considered as the quantum mechanical description of a single particle in a 9-dimensional space. Alternatively we may interpret this equation as a description of $N = 3$ independent particles in three dimensional space:

$$-\frac{\hbar^2}{2m} \sum_{j=1}^{N=3} \sum_{i=1}^3 \frac{\partial^2}{\partial x_{ij}^2} \Psi(x_{11}, \dots, x_{33}) = E\Psi(x_{11}, \dots, x_{33}) \quad (21.6)$$

In spherical coordinates this equation is separable. The angular part is a direct product of spherical harmonics $Y_{L_j M_j}$ which are eigenfunctions of

the Casimir operators C_j^2 and C_j^3 of $SO(2)$ and $SO(3)$ respectively:

$$\begin{aligned} C_1^3(SO(3))|L_1 M_1 L_2 M_2 L_3 M_3\rangle &= L_1(L_1 + 1)|L_1 M_1 L_2 M_2 L_3 M_3\rangle \\ L_1 &= 0, 1, \dots \end{aligned} \quad (21.7)$$

$$\begin{aligned} C_1^2(SO(2))|L_1 M_1 L_2 M_2 L_3 M_3\rangle &= M_1|L_1 M_1 L_2 M_2 L_3 M_3\rangle \\ M_1 &= -L_1, \dots, 0, \dots, +L_1 \end{aligned} \quad (21.8)$$

$$\begin{aligned} C_2^3(SO(3))|L_1 M_1 L_2 M_2 L_3 M_3\rangle &= L_2(L_2 + 1)|L_1 M_1 L_2 M_2 L_3 M_3\rangle \\ L_2 &= 0, 1, \dots \end{aligned} \quad (21.9)$$

$$\begin{aligned} C_2^2(SO(2))|L_1 M_1 L_2 M_2 L_3 M_3\rangle &= M_2|L_1 M_1 L_2 M_2 L_3 M_3\rangle \\ M_2 &= -L_2, \dots, 0, \dots, +L_2 \end{aligned} \quad (21.10)$$

$$\begin{aligned} C_3^3(SO(3))|L_1 M_1 L_2 M_2 L_3 M_3\rangle &= L_3(L_3 + 1)|L_1 M_1 L_2 M_2 L_3 M_3\rangle \\ L_3 &= 0, 1, \dots \end{aligned} \quad (21.11)$$

$$\begin{aligned} C_3^2(SO(2))|L_1 M_1 L_2 M_2 L_3 M_3\rangle &= M_3|L_1 M_1 L_2 M_2 L_3 M_3\rangle \\ M_3 &= -L_3, \dots, 0, \dots, +L_3 \end{aligned} \quad (21.12)$$

In terms of a group theoretical approach the 9-dimensional rotation group G may be decomposed into a chain of subalgebras:

$$G \supset SO(3) \supset SO(3) \supset SO(3) \quad (21.13)$$

In the previous chapters we have discussed two different options for a possible extension to fractional rotation groups, namely

$$SO(n) \rightarrow \begin{cases} {}_{\text{R}}SO^{\alpha}(n) & \text{Riemann} \\ {}_{\text{C}}SO^{\alpha}(n) & \text{Caputo} \end{cases} \quad (21.14)$$

Consequently for a fractional extension of the 9-dimensional rotation group G^{α} now four different decompositions exist with the following chain of subalgebras:

$${}_{\text{RRR}}G \supset {}_{\text{R}}SO^{\alpha}(3) \supset {}_{\text{R}}SO^{\alpha}(3) \supset {}_{\text{R}}SO^{\alpha}(3) \quad (21.15)$$

$${}_{\text{CRR}}G \supset {}_{\text{C}}SO^{\alpha}(3) \supset {}_{\text{R}}SO^{\alpha}(3) \supset {}_{\text{R}}SO^{\alpha}(3) \quad (21.16)$$

$${}_{\text{CCR}}G \supset {}_{\text{C}}SO^{\alpha}(3) \supset {}_{\text{C}}SO^{\alpha}(3) \supset {}_{\text{R}}SO^{\alpha}(3) \quad (21.17)$$

$${}_{\text{CCC}}G \supset {}_{\text{C}}SO^{\alpha}(3) \supset {}_{\text{C}}SO^{\alpha}(3) \supset {}_{\text{C}}SO^{\alpha}(3) \quad (21.18)$$

Until now we have always assumed, that a fractional differential equation is based on a uniquely determined fractional derivative. Now we investigate rotation groups with mixed fractional derivative type.

We will demonstrate, that a new fundamental symmetry is established which will be used to determine the magic numbers in atomic nuclei and in electronic clusters accurately from a generalized point of view.

For that purpose, we will first introduce the necessary notation for a simultaneous treatment of mixed fractional rotation groups and will derive the corresponding level spectrum analytically.

21.2 Notation

We will investigate the spectrum of multi-dimensional fractional rotation groups for two different definitions of the fractional derivative, namely the Riemann- and Caputo fractional derivative. Both types are strongly related.

Starting with the definition of the fractional Riemann integral

$${}_{\text{R}}I^{\alpha} f(x) = \begin{cases} ({}_{\text{R}}I_{+}^{\alpha} f)(x) = \frac{1}{\Gamma(\alpha)} \int_0^x d\xi (x - \xi)^{\alpha-1} f(\xi) & x \geq 0 \\ ({}_{\text{R}}I_{-}^{\alpha} f)(x) = \frac{1}{\Gamma(\alpha)} \int_x^0 d\xi (\xi - x)^{\alpha-1} f(\xi) & x < 0 \end{cases} \quad (21.19)$$

where $\Gamma(z)$ denotes the Euler Γ -function, the fractional Riemann derivative is defined as the result of a fractional integration followed by an ordinary differentiation:

$${}_{\text{R}}\partial_x^{\alpha} = \frac{\partial}{\partial x} {}_{\text{R}}I^{1-\alpha} \quad (21.20)$$

It is explicitly given by:

$${}_{\text{R}}\partial_x^{\alpha} f(x) = \begin{cases} ({}_{\text{R}}\partial_x^{\alpha} f)(x) = \frac{1}{\Gamma(1-\alpha)} \frac{\partial}{\partial x} \int_0^x d\xi (x - \xi)^{-\alpha} f(\xi) & x \geq 0 \\ ({}_{\text{R}}\partial_x^{\alpha} f)(x) = \frac{1}{\Gamma(1-\alpha)} \frac{\partial}{\partial x} \int_x^0 d\xi (\xi - x)^{-\alpha} f(\xi) & x < 0 \end{cases} \quad (21.21)$$

The Caputo definition of a fractional derivative follows an inverted sequence of operations (21.20). An ordinary differentiation is followed by a fractional integration

$${}_{\text{C}}\partial_x^{\alpha} = {}_{\text{R}}I^{1-\alpha} \frac{\partial}{\partial x} \quad (21.22)$$

This results in:

$${}_{\text{C}}\partial_x^{\alpha} f(x) = \begin{cases} ({}_{\text{C}}\partial_x^{\alpha} f)(x) = \frac{1}{\Gamma(1-\alpha)} \int_0^x d\xi (x - \xi)^{-\alpha} \frac{\partial}{\partial \xi} f(\xi) & x \geq 0 \\ ({}_{\text{C}}\partial_x^{\alpha} f)(x) = \frac{1}{\Gamma(1-\alpha)} \int_x^0 d\xi (\xi - x)^{-\alpha} \frac{\partial}{\partial \xi} f(\xi) & x < 0 \end{cases} \quad (21.23)$$

Applied to a function set $f(x) = x^{n\alpha}$ using the Riemann fractional derivative definition (21.21), we obtain:

$${}_{\text{R}}\partial_x^{\alpha} x^{n\alpha} = \frac{\Gamma(1+n\alpha)}{\Gamma(1+(n-1)\alpha)} x^{(n-1)\alpha} \quad (21.24)$$

$$= {}_{\text{R}}[n] x^{(n-1)\alpha} \quad (21.25)$$

where we have introduced the abbreviation ${}_{\text{R}}[n]$.

For the Caputo definition of the fractional derivative it follows for the same function set:

$$\begin{aligned} {}_{\text{C}}\partial_x^\alpha x^{n\alpha} &= \begin{cases} \frac{\Gamma(1+n\alpha)}{\Gamma(1+(n-1)\alpha)} x^{(n-1)\alpha} & n > 0 \\ 0 & n = 0 \end{cases} \\ &= {}_{\text{C}}[n] x^{(n-1)\alpha} \end{aligned} \quad (21.26)$$

where we have introduced the abbreviation ${}_{\text{C}}[n]$.

Both derivative definitions only differ in the case $n = 0$:

$${}_{\text{C}}[n] = {}_{\text{R}}[n] - \delta_{n0} {}_{\text{R}}[0] \quad (21.27)$$

$$= {}_{\text{R}}[n] - \delta_{n0} \frac{1}{\Gamma(1-\alpha)} \quad (21.28)$$

where δ_{mn} denotes the Kronecker- δ . We will rewrite equations (21.25) and (21.26) simultaneously, introducing the short hand notation

$${}_{\text{R,C}}\partial_x^\alpha x^{n\alpha} = {}_{\text{R,C}}[n] x^{(n-1)\alpha} \quad (21.29)$$

We now introduce the fractional angular momentum operators or generators of infinitesimal rotations in the i, j plane on the N -dimensional Euclidean space:

$${}_{\text{R,C}}L_{ij}(\alpha) = i\hbar(x_i^{\alpha} {}_{\text{R,C}}\partial_j^\alpha - x_j^{\alpha} {}_{\text{R,C}}\partial_i^\alpha) \quad (21.30)$$

which result from canonical quantization of the classical angular momentum definition. The commutation relations of the fractional angular momentum operators are isomorphic to the fractional extension of the rotational group $SO(N)$

$$\begin{aligned} {}_{\text{R,C}}[L_{ij}(\alpha), L_{kl}(\alpha)] &= i\hbar {}_{\text{R,C}}f_{ijkl}{}^{mn}(\alpha) {}_{\text{R,C}}L_{mn}(\alpha) \\ i, j, k, l, m, n &= 1, 2, \dots, N \end{aligned} \quad (21.31)$$

with structure coefficients ${}_{\text{R,C}}f_{ijkl}{}^{mn}(\alpha)$. Their explicit form depends on the function set the fractional angular momentum operators act on and on the fractional derivative type used.

According to the group chain

$${}_{\text{R,C}}SO^\alpha(3) \supset {}_{\text{R,C}}SO^\alpha(2) \quad (21.32)$$

there are two Casimir operators Λ_i , namely $\Lambda_2 = L_z(\alpha) = L_{12}(\alpha)$ and $\Lambda_3 = L^2(\alpha) = L_{12}^2(\alpha) + L_{13}^2(\alpha) + L_{23}^2(\alpha)$. We introduce the two quantum

numbers L and M , which completely determine the eigenfunctions $|LM\rangle$. It follows

$${}_{R,C} L_z(\alpha) |LM\rangle = \hbar \operatorname{sign}(M) {}_{R,C} [|M|] |LM\rangle \quad (21.33)$$

$$M = -L, -L+1, \dots, \pm 0, \dots, L$$

$${}_{R,C} L^2(\alpha) |LM\rangle = \hbar^2 {}_{R,C} [L] {}_{R,C} [L+1] |LM\rangle \quad (21.34)$$

$$L = 0, 1, 2, \dots$$

where $|M|$ denotes the absolute value of M . In addition, on the set of eigenfunctions $|LM\rangle$, the parity operator Π is diagonal and has the eigenvalues

$$\Pi |LM\rangle = (-1)^L |LM\rangle \quad (21.35)$$

Near $\alpha \approx 1$ there is a region of a rotational type of spectrum, while for $\alpha \approx 1/2$, the levels are nearly equidistant, which corresponds to a vibrational type of spectrum.

In addition, for decreasing $\alpha < 1$ higher angular momenta are lowered.

Only in the case $L = 0$ the spectra differ for the Riemann- and Caputo derivative. While for the Caputo derivative

$${}_C L^2(\alpha) |00\rangle = 0 \quad (21.36)$$

because ${}_C[0] = 0$, using the Riemann derivative for $\alpha \neq 1$ there is a non-vanishing contribution

$${}_R L^2(\alpha) |00\rangle = \hbar^2 {}_R[0] {}_R[1] |00\rangle = \hbar^2 \frac{\Gamma(1+\alpha)}{\Gamma(1-\alpha)} |00\rangle \quad (21.37)$$

In analogy to Racah's SU(2) model of a pairing interaction [Racah (1942)] we may therefore interpret (21.37) as a pairing energy contribution, which in case of using the Caputo derivative definition for $L = 0$ leads to a lowering of the ground state energy.

In the next section we will demonstrate, that near the semi-derivative $\alpha \approx 1/2$ we may interpret the ${}_{R,C} SO^\alpha(3)$ as a spherical representation of $U(1)$ and $U(1) \otimes U(1)_{\text{pairing}}$ respectively

$${}_R SO^{\alpha=1/2}(3) \supset U(1) \quad (21.38)$$

$${}_C SO^{\alpha=1/2}(3) \supset U(1) \otimes U(1)_{\text{pairing}} \quad (21.39)$$

if some specific symmetry requirements are imposed.

21.3 The 9-dimensional fractional Caputo-Riemann-Riemann symmetric rotor

We use group theoretical methods to construct higher dimensional representations of the fractional rotation groups ${}_{\text{R,C}}SO^{\alpha}(3)$.

As an example of physical relevance we will investigate the properties of the 9-dimensional fractional rotation group ${}_{\text{CRR}}G$ (21.16) with the following chain of subalgebras:

$${}_{\text{CRR}}G \supset {}_{\text{C}}SO^{\alpha}(3) \supset {}_{\text{R}}SO^{\alpha}(3) \supset {}_{\text{R}}SO^{\alpha}(3) \quad (21.40)$$

We associate a Hamiltonian H , which can now be written in terms of the Casimir operators of the algebras appearing in the chain and can be analytically diagonalized in the corresponding basis. The Hamiltonian is explicitly given as:

$$H = \frac{\omega_1}{\hbar} {}_{\text{C}}L_1^2(\alpha) + \frac{\omega_2}{\hbar} {}_{\text{R}}L_2^2(\alpha) + \frac{\omega_3}{\hbar} {}_{\text{R}}L_3^2(\alpha) \quad (21.41)$$

with the free parameters $\omega_1, \omega_2, \omega_3$ and the basis is $|L_1 M_1 L_2 M_2 L_3 M_3\rangle$. Furthermore, we demand the following symmetries:

First, the wave functions should be invariant under parity transformations, which according to (21.35) leads to the conditions

$$L_1 = 2n_1 \quad L_2 = 2n_2 \quad L_3 = 2n_3, \quad n_1, n_2, n_3 = 0, 1, 2, 3, \dots \quad (21.42)$$

second, we require

$${}_{\text{C}}L_{z_1}(\alpha)|L_1 M_1 L_2 M_2 L_3 M_3\rangle = +\hbar_{\text{C}}[L_1]|L_1 M_1 L_2 M_2 L_3 M_3\rangle \quad (21.43)$$

$${}_{\text{R}}L_{z_2}(\alpha)|L_1 M_1 L_2 M_2 L_3 M_3\rangle = +\hbar_{\text{R}}[L_2]|L_1 M_1 L_2 M_2 L_3 M_3\rangle \quad (21.44)$$

$${}_{\text{R}}L_{z_3}(\alpha)|L_1 M_1 L_2 M_2 L_3 M_3\rangle = +\hbar_{\text{R}}[L_3]|L_1 M_1 L_2 M_2 L_3 M_3\rangle \quad (21.45)$$

which leads to the conditions

$$M_1 = 2n_1 \quad M_2 = 2n_2 \quad M_3 = 2n_3, \quad n_1, n_2, n_3 = 0, 1, 2, 3, \dots \quad (21.46)$$

and reduces the multiplicity of a given $|2n_1 M_1 2n_2 M_2 2n_3 M_3\rangle$ set to 1.

With these conditions, the eigenvalues of the Hamiltonian (21.41) are given as

$$\begin{aligned} E(\alpha) &= \hbar\omega_1 {}_{\text{C}}[2n_1] {}_{\text{C}}[2n_1 + 1] \\ &\quad + \hbar\omega_2 {}_{\text{R}}[2n_2] {}_{\text{R}}[2n_2 + 1] + \hbar\omega_3 {}_{\text{R}}[2n_3] {}_{\text{R}}[2n_3 + 1] \end{aligned} \quad (21.47)$$

$$= \sum_{i=1}^3 \hbar\omega_i \frac{\Gamma(1 + (2n_i + 1)\alpha)}{\Gamma(1 + (2n_i - 1)\alpha)} - \delta_{n_1 0} \hbar\omega_1 \frac{\Gamma(1 + \alpha)}{\Gamma(1 - \alpha)} \quad (21.48)$$

$$n_1, n_2, n_3 = 0, 1, 2, \dots$$

on a basis $|2n_1 2n_1 2n_2 2n_2 2n_3 2n_3\rangle$.

This is the major result of our derivation. We call this model the Caputo-Riemann-Riemann symmetric rotor.

In the next section we will investigate the properties of this model near the semi-derivative $\alpha = 1/2$ and will present a surprising coincidence with the magic numbers of nuclei.

21.4 Magic numbers of nuclei

The experimental evidence for discontinuities in the sequence of atomic masses, α - and β - decay systematic and binding energies of nuclei suggests the existence of a set of magic proton and neutron numbers, which can be described successfully by single particle shell models with a heuristic spin-orbit term [Goeppert-Mayer (1948); Haxel *et al.* (1949)]. The most prominent representative is the phenomenological Nilsson model [Nilsson (1955)] with an anisotropic oscillator potential:

$$V(x_i) = \sum_{i=1}^3 \frac{1}{2} m \omega_i^2 x_i^2 - \hbar \omega_0 \kappa (2\vec{l}\vec{s} + \mu l^2) \quad (21.49)$$

Although these models are flexible enough to reproduce the experimental results, they lack a deeper theoretical justification, which becomes obvious, when extrapolating the parameters κ , μ , which determine the strength of the spin orbit and l^2 term to the region of super heavy elements [Hofmann and Münzenberg (2000)]. Hence it seems tempting to describe the experimental data with alternative methods. Typical examples are microscopic Hartree-Fock calculations with a uniform nucleon-nucleon interaction of e.g. Skyrme type [Vautherin and Brink (1972)] or relativistic mean field theories [Rufa *et al.* (1988); Bender *et al.* (2001)], where nucleons are described by the Dirac-equation and the interaction is mediated by mesons. Although a spin orbit force is unnecessary in these models, different parametrizations predict different shell closures [Rutz *et al.* (1997); Kruppa *et al.* (2000)].

Therefore the problem of a theoretical foundation of magic numbers remains an open question since Elsasser [Elsasser (1933)] raised the problem more than 80 years ago.

There are two points, which make an approach within the framework of fractional group theory promising. First, since the beginning of a theoretical foundation of strong interaction, a nonlocal component has been considered as a vital ingredient for a realistic treatment of e.g. nucleon-

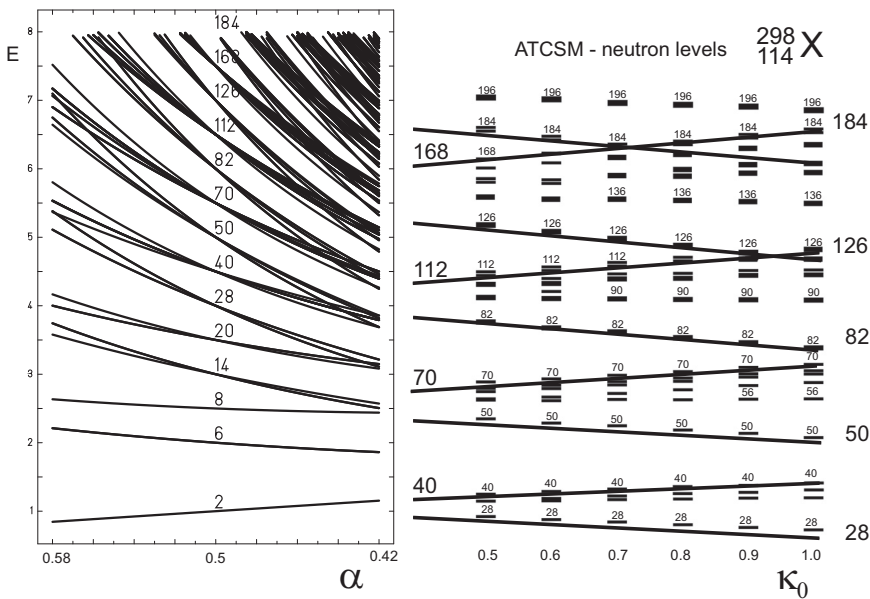


Fig. 21.1 On the left the energy spectrum $E(\alpha)$ from (21.48) for the spherical case (21.50) in units of $\hbar\omega_0$ for the Caputo-Riemann-Riemann symmetric rotor near the ideal vibrational case $\alpha = 1/2$ is presented. The right diagram shows the neutron energy levels for the spherical nucleus $^{298}_{114}X$ calculated within the framework of the asymmetric two center shell model (ATCSM) [Maruhn and Greiner (1972)], which exactly corresponds to the Nilsson shell model (21.49) near the ground state as a function of increasing strength of the spin-orbit term ($\kappa_0 \kappa \vec{l} \cdot \vec{s}$) increasing from 50% to 100% of the recommended κ value, while the μl^2 value is kept constant. The transition from magic numbers of the standard 3-dimensional harmonic oscillator levels (21.53) to the shifted set of magic numbers (21.56) is pointed out with thick lines. Left and right figure therefore show a similar behavior for the energy levels.

nucleon interaction. Especially the LS -term in effective interaction models has been introduced as a specific realization of nonlocality [Baumgärtner and Schuck (1968); Ring and Schuck (2008)].

Since e.g. the fractional generators for a fractional extension of a standard Lie-group introduces a new facet of nonlocality, a fractional approach seems an interesting option.

Furthermore we will demonstrate, applying the Caputo-Riemann-Riemann symmetric rotor (21.47), that a new fundamental dynamic symmetry is established, which determines the magic numbers for protons and neutrons and furthermore describes the ground state properties like binding

energies and ground state quadrupole deformations of nuclei with reasonable accuracy.

On the left of figure 21.1 we have plotted the energy levels of the Caputo-Riemann-Riemann fractional symmetric rotor (21.47) in the vicinity of $\alpha \approx 1/2$ for the case

$$\omega_1 = \omega_2 = \omega_3 = \omega_0 \quad (21.50)$$

which we denote as the spherical case.

For the idealized case $\alpha = 1/2$, using the relation $\Gamma(1+z) = z\Gamma(z)$ the level spectrum (21.47) is simply given by:

$$E(\alpha = 1/2) = \hbar\omega_0(n_1 + n_2 + n_3 + \frac{3}{2} - \frac{1}{2}\delta_{n_1 0}) \quad (21.51)$$

According to (21.38) and (21.39) near $\alpha = 1/2$ the quantum numbers n_i may be interpreted as eigenvalues of the U(1) number operator. For $n_1 \neq 0$ the energy spectrum (21.51) is the well known spectrum of the 3-dimensional harmonic oscillator. We introduce the quantum number N as

$$N = n_1 + n_2 + n_3 \quad (21.52)$$

Assuming a 2-fold spin degeneracy of the energy levels, we obtain a first set $n_{\text{magic } 1}$ of magic numbers n_{magic}

$$n_{\text{magic } 1} = \frac{1}{3}(N+1)(N+2)(N+3) \quad N = 1, 2, 3, \dots \quad (21.53)$$

$$= 8, 20, 40, 70, 112, 168, 240, \dots \quad (21.54)$$

which correspond to the standard 3-dimensional harmonic oscillator at energies

$$E = \hbar\omega_0(N + 3/2) \quad (21.55)$$

In addition, for $n_1 = 0$, which corresponds to the $|002n_22n_22n_32n_3\rangle$ states with a $2\sum_{n=0}^N n = N(N+1)$ -fold multiplicity, we obtain a second set $n_{\text{magic } 2}$ of magic numbers

$$n_{\text{magic } 2} = n_{\text{magic } 1} - N(N+1) \quad N = 0, 1, 2, 3, \dots \quad (21.56)$$

$$= \frac{1}{3}(N+1)((N+2)(N+3) - 3N) \quad (21.57)$$

$$= \frac{1}{3}(N+1)((N+1)^2 + 5) \quad (21.58)$$

$$= 2, 6, 14, 28, 50, 82, 126, 184, 258, \dots \quad (21.59)$$

at energies

$$E = \hbar\omega_0(N + 1) \quad (21.60)$$

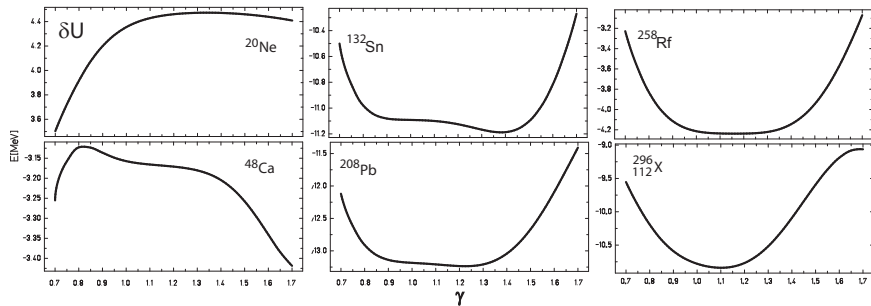


Fig. 21.2 As a test of the plateau condition $\partial U / \partial \gamma = 0$ for the Strutinsky shell correction method, the total shell correction energy $\delta U = \delta U_P + \delta U_N$ is plotted as a function of γ for different nuclei.

which is shifted by the amount $-\frac{1}{2}\hbar\omega_0$ compared to the standard 3-dimensional harmonic oscillator values.

From figure 21.1 it follows, that for $\alpha < 1/2$ the second set $n_{\text{magic} 2}$ of energy levels falls off more rapidly than the levels of set $n_{\text{magic} 1}$. As a consequence for decreasing α the magic numbers $n_{\text{magic} 1}$ die out successively. On the other hand, for $\alpha > 1/2$ the same effect causes the magic numbers $n_{\text{magic} 1}$ to survive.

We want to emphasize, that the described behavior for the energy levels in the region $\alpha < 1/2$ may be directly compared to the influence of a ls -term in phenomenological shell models. As an example, on the right-hand side of figure 21.1 a sequence of neutron levels for the super heavy element $^{298}_{114}X$ calculated with the asymmetric two center shell model (ATCSM) [Maruhn and Greiner (1972)], which exactly corresponds to the Nilsson shell model near the spherical ground state, with increasing strength of the ls -term from 50% to 100% is plotted. It shows, that the $n = 168$ gap breaks down at about 70% and the $n = 112$ gap at about 90% of the recommended κ -value for the ls -term. This corresponds to an $\alpha \approx 0.46$ value, since in the Caputo-Riemann-Riemann symmetric rotor the $n = 168$ gap breaks down at $\alpha = 0.466$, the $n = 112$ gap at $\alpha = 0.460$ and the $n = 70$ gap vanishes at $\alpha = 0.453$.

21.5 Ground state properties of nuclei

We will use the Caputo-Riemann-Riemann symmetric rotor (21.47) as a dynamic shell model for a description of the microscopic part of the total

energy E_{tot} of the nucleus.

$$E_{\text{tot}} = E_{\text{macroscopic}} + E_{\text{microscopic}} \quad (21.61)$$

$$= E_{\text{macroscopic}} + \delta U + \delta P \quad (21.62)$$

where δU and δP denote the shell- and pairing energy contributions.

For the macroscopic contribution we use the finite range liquid drop model (FRLDM) proposed by Möller [Möller *et al.* (1993)] using the original parameters, except the value for the constant energy contribution a_0 , which will be used as a free parameter for a fit with the experimental data.

As the primary deformation parameter we use the ellipsoidal deformation Q :

$$Q = \frac{b}{a} = \frac{\omega_3}{\omega_1} = \frac{\omega_3}{\omega_2} \quad (21.63)$$

where a, b are the semiaxes of a rotational symmetric ellipsoid. Consequently a value $Q < 1$ describes prolate and a value of $Q > 1$ describes oblate shapes. In order to relate the ellipsoidal deformation Q to the quadrupole deformation ϵ_2 used by Möller, we use the relation:

$$Q = 1 - 1.43085\epsilon_2 + 0.707669\epsilon_2^2 \quad (21.64)$$

which is a result from a least square fit and quadratic approximation of equipotential surfaces.

Furthermore we extend the original FRLDM-model introducing an additional curvature energy term $V_R(Q)$, which describes the interaction of the nucleus with the collective curved coordinate space [Herrmann (2008a)]:

$$V_R(Q) = -a_R B_R A^{-5/3} \quad (21.65)$$

where A is the nucleon number, a_R is the curvature parameter given in [MeV] and the relative curvature energy $B_R(Q)$ given as:

$$B_R(Q) = 9 Q^{16/3} \left(\frac{199 - 288 \ln(2)}{(2 + Q^2)(266 - 67Q^2 + 96(Q^2 - 4) \ln(2))} \right)^2 \quad (21.66)$$

which is normalized relative to a sphere $B_R(Q = 1) = 1$.

Therefore the total energy may be split into

$$E_{\text{tot}} = E_{\text{mac}} + E_{\text{mic}} \quad (21.67)$$

where

$$E_{\text{mac}}(a_0, a_R) = \text{FRLDM}(a_0, Q = 1) + V_R(Q = 1, a_R) \quad (21.68)$$

$$\begin{aligned} E_{\text{mic}}(a_0, a_R, Q) = & +\delta U + \delta P + \text{FRLDM}(a_0, Q) + V_R(Q, a_R) \\ & - (\text{FRLDM}(a_0, Q = 1) + V_R(Q = 1, a_R)) \end{aligned} \quad (21.69)$$

with two free parameters a_0, a_R , which will be used for a least square fit with the experimental data.

For calculation of the shell corrections we use the Strutinsky method [Strutinsky (1967b); Strutinsky (1968)]. Since we expect that the shell corrections are the dominant contribution to the microscopic energy, for a first comparison with experimental data we will neglect the pairing energy term.

In order to calculate the shell corrections, we introduce the following parameters:

$$\hbar\omega_0 = 38A^{-\frac{1}{3}}[\text{MeV}] \quad (21.70)$$

$$\omega_1 = \omega_0 Q^{-\frac{1}{3}} \quad (21.71)$$

$$\omega_2 = \omega_0 Q^{-\frac{1}{3}} \quad (21.72)$$

$$\omega_3 = \omega_0 Q^{\frac{2}{3}} \quad (21.73)$$

$$\alpha_Z = \begin{cases} 0.46 + 0.000220 Z & Z > 50 \\ 0.2469 + 0.00448 Z & 28 < Z \leq 50 \\ 0.2793 + 0.00332 Z & Z \leq 28 \end{cases} \quad (21.74)$$

$$\alpha_N = \begin{cases} 0.41 + 0.000200 N & N > 50 \\ 0.3118 + 0.00216 N & 28 < N \leq 50 \\ 0.2793 + 0.00332 N & N \leq 28 \end{cases} \quad (21.75)$$

$$\gamma = 1.1 \hbar\omega_0 \quad (21.76)$$

$$m = 4 \quad (21.77)$$

$$a_0 = 2.409[\text{MeV}] \quad (21.78)$$

$$a_R = 15.0[\text{MeV}] \quad (21.79)$$

Input parameters are the number of protons Z , number of neutrons N , the nucleon number $A = N + Z$, and the ground state quadrupole deformation ϵ_2 .

The values obtained include:

- the frequencies (21.71),(21.72),(21.73), which are related to the quadrupole deformation ϵ_2 via (21.64),
- the fractional derivative coefficients for protons (21.74) and neutrons (21.75) which determine the level spectrum for protons and neutrons for the proton and neutron part of the shell correction energy respectively from a fit of the set of nuclides $^{56}_{28}\text{Ni}$, $^{100}_{50}\text{Sn}$, $^{132}_{50}\text{Sn}$, $^{208}_{82}\text{Pb}$ and from the requirement, that the neutron shell correction for $^{100}_{50}\text{Sn}$ should amount about $-5.1[\text{MeV}]$,

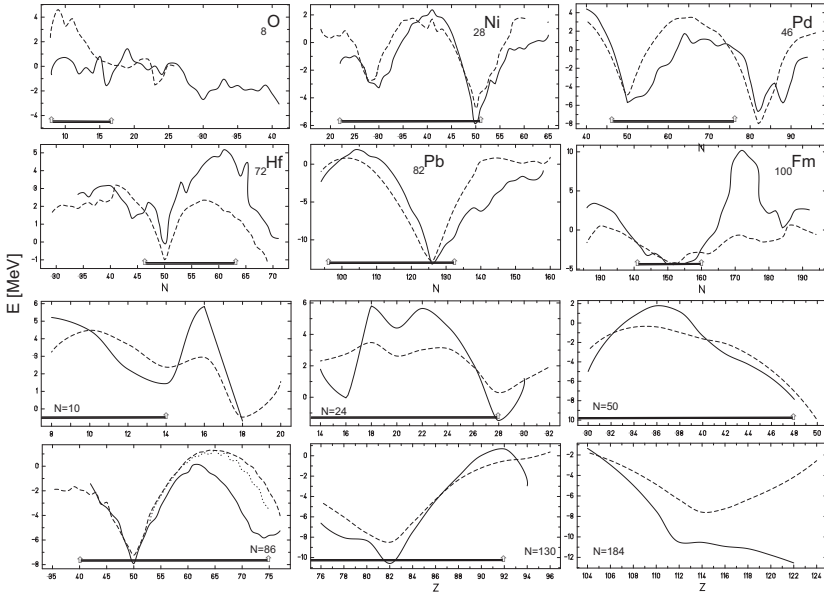


Fig. 21.3 Comparison of calculated shell corrections δU from the Caputo-Riemann-Riemann symmetric rotor (21.48) with the parameter set (21.70)-(21.77) (thick line) with the tabulated E_{mic} from Möller [Möller *et al.* (1993)] (dashed line). Upper two rows show values for a given Z as a function of N , lower two rows for a given N as a function of Z . Bars indicate the experimentally known region. The original ϵ_2 values from [Möller *et al.* (1993)] are used, which is the main source of error.

- (21.76) from the plateau condition $\partial U / \partial \gamma = 0$ (see figure 21.2) and
- (21.77) the order of included Hermite polynomials for the Strutinsky shell correction method. Finally
- $\hbar\omega_0, a_0, a_R$ from a fit of the experimental mass excess given in [Audi *et al.* (2003)].

We compare our results for the microscopic energy contribution E_{mic} with data from Möller et al. [Möller *et al.* (1993)] and use their tabulated ϵ_2 values. They have not only listed data for experimental masses but also predictions for regions, not yet confirmed by experiment.

In figure 21.3 we compare the calculated δU values with the tabulated E_{mic} , which is justified for almost spherical shapes ($\epsilon_2 \approx 0$). The results agree very well within the expected errors (which are estimated ≈ 2 [MeV] for the pairing energy and 0.5 [MeV] for E_{mic}), especially in the region of experimentally known nuclei.

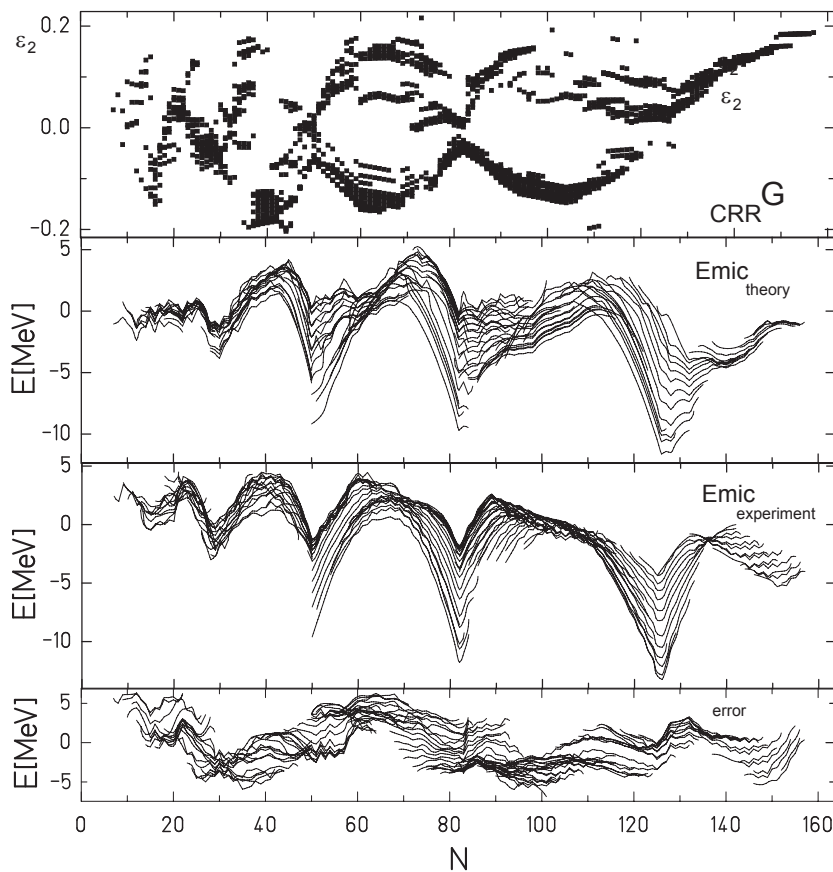


Fig. 21.4 Comparison of calculated E_{mic} from the Caputo-Riemann-Riemann symmetric rotor (21.48) with the parameter set (21.70)-(21.79), minimized with respect to ϵ_2 with the experimental masses from Audi [Audi *et al.* (2003)] as a function of N . From top to bottom the minimized ϵ_2 values, theoretical E_{mic} , experimental microscopic contribution from the difference of experimental mass excess and macroscopic FRFLDM energy and error in [MeV] are plotted.

A remarkable difference between the calculated shell correction and tabulated E_{mic} from Möller occurs for spherical super heavy elements ($N = 184$, last picture in figure 21.3).

While phenomenological shell models predict a pronounced minimum in the shell correction energy for $Z = 114$ [Myers and Swiatecki (1966); Mosel and Greiner (1969); Nihti *et al.* (2010)] the situation is quite different

for the rotor model, where two magic shell closures at $Z = 112$ and $Z = 126$ are given, but the $Z = 112$ shell closure is not strong enough to produce a local minimum in the shell correction energy plot as a function of Z . Instead, between $Z = 112$ and $Z = 126$, a slightly falling energy plateau emerges, which makes the full region promising candidates for stable, long-lived super heavy elements.

While this result contradicts predictions made with phenomenological shell models, it supports recent results obtained with relativistic mean field models [Bender *et al.* (2001)], which predict a similar behavior in the region of super heavy elements as the proposed rotor model.

In figure 21.4 we have covered the complete region of available experimental data for nuclides and compare the calculated theoretical microscopic energy contribution minimized with respect to the deformation with the experimental values. The influence of shell closures is very clear. The rms-error is about 2.4[MeV]. The maximum deviation occurs between closed magic shells.

Therefore in the next section we will introduce a generalization of the proposed fractional rotor model, which not only determines the magic numbers accurately but in addition determines the fine structure of the single particle spectrum correctly.

21.6 Fine structure of the single particle spectrum - the extended Caputo-Riemann-Riemann symmetric rotor

In the previous section we have demonstrated, that the Caputo-Riemann-Riemann symmetric rotor correctly determines the magic numbers in the single particle spectra for neutrons and protons. However, there remains a significant difference between calculated and experimental ground state masses for nuclei with nucleon numbers far from magic shell closures. This indicates that the fine structure of the single particle levels is not yet correctly reproduced.

We therefore propose the following generalization of the Caputo-Riemann-Riemann symmetric rotor group:

$${}_{\text{C}3\text{C}2\text{R}3\text{R}3}G \supset {}_{\text{C}}SO^{\alpha}(3) \supset {}_{\text{C}}SO^{\alpha}(2) \supset {}_{\text{R}}SO^{\alpha}(3) \supset {}_{\text{R}}SO^{\alpha}(3) \quad (21.80)$$

with the Casimir operators (21.33) and (21.34) it follows for the Hamiltonian H :

$$H = \frac{\omega_1}{\hbar} {}_{\text{C}}L_1^2(\alpha) + B\omega_0 {}_{\text{C}}L_{z1}(\alpha) + \frac{\omega_2}{\hbar} {}_{\text{R}}L_2^2(\alpha) + \frac{\omega_3}{\hbar} {}_{\text{R}}L_3^2(\alpha) \quad (21.81)$$

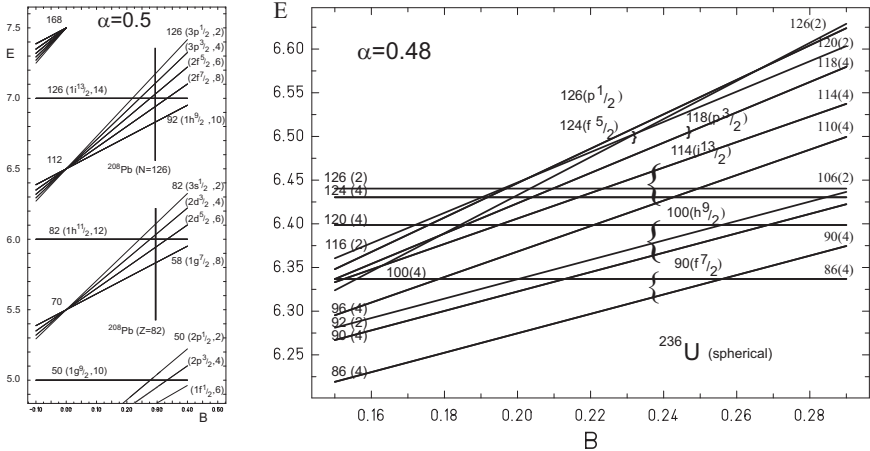


Fig. 21.5 For $\alpha = 1/2$, on the left side the level spectrum for the extended Caputo-Riemann-Riemann symmetric rotor (21.83) is plotted as a function of the fractional magnetic field strength B . The levels are labeled according to the corresponding $[Nl j_z]$ Nilsson scheme and the multiplicity is given. The level sequence reproducing the experimental data for lead is given for $N = 126$ and $Z = 82$, see also [Rufa *et al.* (1988)]. For $\alpha = 0.48$ the resulting level sequence near $N \approx 126$ is plotted on the right. At $B \approx 0.25$ the resulting spectrum coincides with the corresponding spherical Nilsson level spectrum. Brackets indicate the proposed appropriate combinations of rotor levels.

with the free parameters $\omega_1, \omega_2, \omega_3, B$, where B may be called fractional magnetic field strength in units $[\hbar\omega_0]$, since this Hamiltonian is the extension of the fractional Zeeman effect to 9-dimensional space.

Demanding the same symmetries (21.42), (21.43) as in the case of the symmetric Caputo-Riemann-Riemann rotor, the eigenvalues of the Hamiltonian (21.81) are given as

$$\begin{aligned} E(\alpha) &= \hbar\omega_1 c[2n_1]_c[2n_1 + 1] + B\hbar\omega_0 c[2n_1] \\ &\quad + \hbar\omega_2 r[2n_2]_r[2n_2 + 1] + \hbar\omega_3 r[2n_3]_r[2n_3 + 1] \end{aligned} \quad (21.82)$$

$$\begin{aligned} &= \sum_{i=1}^3 \hbar\omega_i \frac{\Gamma(1 + (2n_i + 1)\alpha)}{\Gamma(1 + (2n_i - 1)\alpha)} - \delta_{n_1 0} \hbar\omega_1 \frac{\Gamma(1 + \alpha)}{\Gamma(1 - \alpha)} \\ &\quad + B\hbar\omega_0 \frac{\Gamma(1 + 2n_1\alpha)}{\Gamma(1 + (2n_1 - 1)\alpha)} - \delta_{n_1 0} B\hbar\omega_0 \frac{1}{\Gamma(1 - \alpha)} \\ &\quad n_1, n_2, n_3 = 0, 1, 2, \dots \end{aligned} \quad (21.83)$$

on a basis $|2n_1 2n_1 2n_2 2n_2 2n_3 2n_3\rangle$.

We call this model the extended Caputo-Riemann-Riemann symmetric rotor. The additional ${}_c L_{z_1}(\alpha)$ term yields a level splitting of the harmonic oscillator set of magic numbers $n_{\text{magic } 1}$ (21.53), while the multiplicity of the $n_{\text{magic } 2}$ set (21.56) remains unchanged, since this set is characterized by $n_1 = 0$. This is exactly the behavior needed to describe the experimentally observed fine structure, as can be deduced from the right-hand side of figure 21.1.

In order to clearly demonstrate the influence of the additional term, we first investigate the level spectrum for the spherical (21.50) and idealized case $\alpha = 1/2$.

The level spectrum (21.83) simply results as:

$$\begin{aligned} E(\alpha = 1/2) &= \hbar\omega_0(n_1 + n_2 + n_3 + \frac{3}{2} - \frac{1}{2}\delta_{n_1 0}) \\ &\quad + B\hbar\omega_0 \left(\frac{n_1!}{\Gamma(1/2 + n_1)} - \frac{1}{\Gamma(1/2)}\delta_{n_1 0} \right) \end{aligned} \quad (21.84)$$

$$\begin{aligned} &= \hbar\omega_0(n_1 + n_2 + n_3 + \frac{3}{2} - \frac{1}{2}\delta_{n_1 0}) \\ &\quad + \frac{B\hbar\omega_0}{\sqrt{\pi}} \left(\frac{(2n_1)!!}{(2n_1 - 1)!!} - \delta_{n_1 0} \right) \end{aligned} \quad (21.85)$$

where !! denotes the double factorial.

On the left side of figure 21.5 this spectrum is plotted in units [$\hbar\omega_0$]. Single levels are labeled according to the Nilsson-scheme and multiplicities are given in brackets. For small fractional field strength B the resulting spectrum exactly follows the schematic level diagram of a phenomenological shell model with spin-orbit term, as demonstrated e.g. by Goeppert-Mayer [Goeppert-Mayer (1948)].

A small deviation from the ideal $\alpha = 1/2$ value reproduces the experimental spectra accurately:

For $\alpha = 0.48$ the resulting level spectrum is given on the right-hand side of figure 21.5. Obviously there is an interference of two effects:

First, for $\alpha \neq 1/2$ now the degenerated levels of both magic sets split up and second the fractional magnetic field B acts on the subset $n_{\text{magic } 1}$.

For $B \approx 0.25$ the spectrum may be directly compared with the spherical Nilsson level scheme. For example, for neutrons between $82 \leq N \leq 126$, this level scheme is given as $2f\frac{7}{2}$, $1h\frac{9}{2}$, $1i\frac{13}{2}$, $3p\frac{3}{2}$, $2f\frac{5}{2}$, $3p\frac{1}{2}$, see e.g. results of [Scharnweber *et al.* (1970)], which corresponds to a sequence of sub-shells at 90, 100, 114, 118, 124, 126. This sequence is correctly reproduced with the extended Caputo-Riemann-Riemann symmetric rotor.

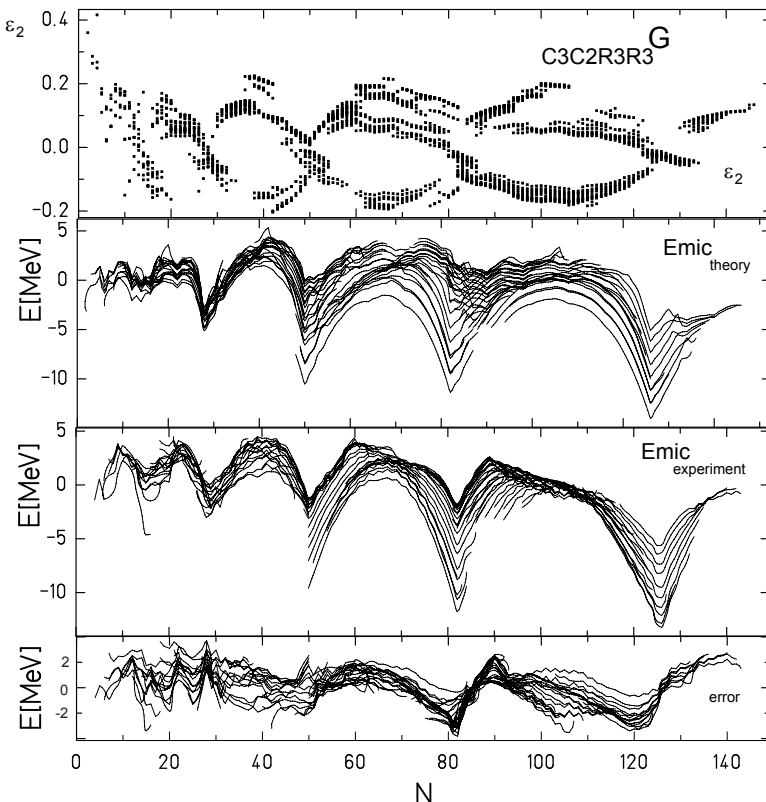


Fig. 21.6 Comparison of calculated E_{mic} from the extended Caputo-Riemann-Riemann symmetric rotor (21.83) with the parameter set (21.86)-(21.89), minimized with respect to ϵ_2 with the experimental masses from Audi [Audi *et al.* (2003)] as a function of N . From top to bottom the minimized ϵ_2 values, theoretical and experimental masses and error in [MeV] are plotted.

With the parameter set, which is obtained by a fit with the experimental masses of Ca-, Sn- and Pb-isotopes

$$\hbar\omega_0 = 28A^{-\frac{1}{3}}[\text{MeV}] \quad (21.86)$$

$$\alpha_Z = \begin{cases} 0.480 + 0.00022 Z & Z > 50 \\ 0.324 + 0.00332 Z & Z \leq 50 \end{cases} \quad (21.87)$$

$$\alpha_N = \begin{cases} 0.446 + 0.00022 N & N > 29 \\ 0.356 + 0.00332 N & N \leq 29 \end{cases} \quad (21.88)$$

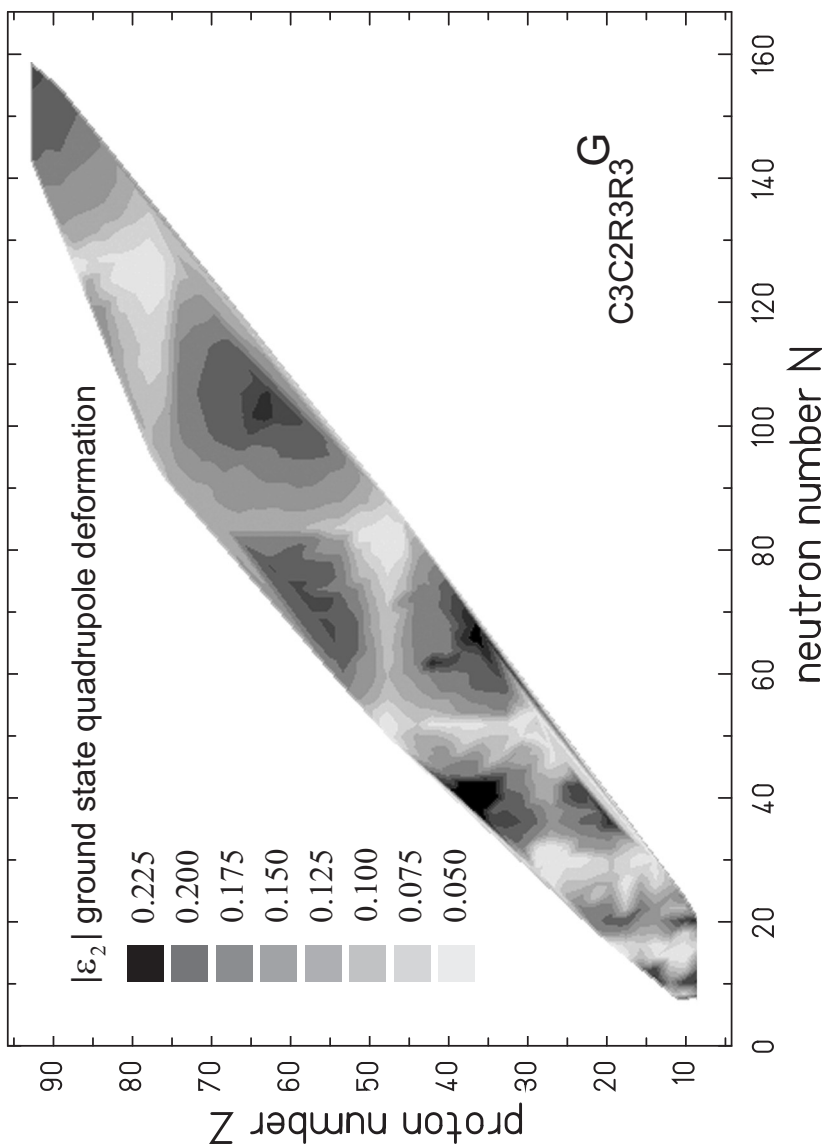


Fig. 21.7 Absolute value of the ground state quadrupole deformations ϵ_2 minimizing the total energy for the extended Caputo-Riemann-Riemann symmetric rotor (21.83) with parameter set (21.86)-(21.89) for even-even nuclei. Gray levels indicate the increasing deformation from white ($|\epsilon_2| \leq 0.05$) to black ($|\epsilon_2| \geq 0.225$).

$$B = \begin{cases} 0 & Z < 40 \\ 0.0235 Z - 0.94 & 40 \leq Z < 50 \\ 0.235 & Z \geq 50 \end{cases} \quad (21.89)$$

the experimental masses are reproduced with an rms-error of 1.7[MeV]. Results are given in figures 21.6 and 21.7.

The deformation parameters, obtained by minimization of the total energy, are to a large extent consistent with values given in [Möller *et al.* (1993)], e.g. for $^{264}\text{Hs}_{108}$ we obtain $\epsilon_2 = 0.22$, which conforms with Möller's ($\epsilon_2 = 0.2$) and Rutz's results [Rutz *et al.* (1997)]. However, there occur discrepancies mostly for exotic nuclei. For example our calculations determine the nucleus ^{42}Si to be almost spherical ($\epsilon_2 = -0.03$), which conforms with recent experimental findings [Fridmann *et al.* (2005)], while Möller predicts a definitely oblate shape ($\epsilon_2 = -0.3$).

Finally, defining a nucleus with $\epsilon_2 > 0.05$ as prolate and with $\epsilon_2 < -0.05$ as oblate the amount of prolate shapes is about 74% of all deformed nuclei. This is close to the value of 82% [Tajima and Suzuki (2001)], obtained with the Nilsson model using the standard parameters.

21.7 Triaxiality

A systematic investigation of properties of triaxial clusters up to now has been carried out only rudimentary. The main reason for this is the fact, that current models in use cannot be solved analytically for triaxial shapes. A numerical solution consumes a large amount of computer power and time and therefore is costly.

As a consequence first systematic studies on triaxial shapes of nuclei based on the finite range droplet model using a phenomenological Woods-Saxon-potential were published by Möller *et al.* in September 2008 [Möller *et al.* (2008)].

On the other hand based on the fractional symmetry group we have just derived an alternative universal model, which describes the ground state properties of clusters with high precision and as an important fact is fully analytically solvable. With this model high precision potential energy surfaces (PES) of triaxial nuclei may be calculated with minimum effort and no simplifications are necessary. Therefore this model is well suited to investigate the general properties and systematic trends for triaxially deformed nuclei.

The great advantage of the fractional approach is the fact that the microscopic corrections of binding energies are given analytically. As a consequence, calculations using the fractional approach are about a factor 10^6 (one million times) faster compared to traditional methods applied for triaxial deformations.

As an example, we investigate the properties of the ruthenium isotopes ($Z=44$), which are just located in the Z-region, where the influence of the B-field becomes important. A least square fit with experimental ground state masses results in an optimized parameter set:

$$\alpha_Z = 0.470 \quad (21.90)$$

$$\alpha_N = 0.456 \quad (21.91)$$

$$B = -0.08 \quad (21.92)$$

and the relation between the set $(\omega_a, \omega_b, \omega_c)$ and (β, γ) is given by [Eisenberg and Greiner (1987)]:

$$\epsilon = 0.95\beta \quad (21.93)$$

$$\omega_1 = 1 - \frac{2}{3}\epsilon(\cos \gamma + \frac{2}{3}\pi) \quad (21.94)$$

$$\omega_2 = 1 - \frac{2}{3}\epsilon(\cos \gamma) \quad (21.95)$$

$$\omega_3 = 1 - \frac{2}{3}\epsilon(\cos \gamma - \frac{2}{3}\pi) \quad (21.96)$$

so that for $\gamma = 0^\circ$ we have prolate and for $\gamma = 60^\circ$ we have oblate shapes. For $\gamma = 30^\circ$ we have maximal triaxial shapes.

Table 21.1 Comparison of Möllers results with the fractional model. β_M , γ_M and ΔE_M in units [MeV] from [Möller *et al.* (2008)]. β , γ and ΔE in units [MeV] from a fit with parameter set (21.90)-(21.92). ΔE is the energy gain with respect to the rotationally symmetric shape.

nucleus	β_M	γ_M	ΔE_M	β	γ	ΔE
⁹⁸ Ru	0.11	0.0	0.0	0.162	3.0	0.02
¹⁰⁰ Ru	0.16	0.0	0.0	0.171	11.4	0.29
¹⁰² Ru	0.24	27.5	0.18	0.135	46.8	0.30
¹⁰⁴ Ru	0.26	27.5	0.38	0.171	35.4	0.40
¹⁰⁶ Ru	0.26	27.5	0.41	0.165	44.4	0.46
¹⁰⁸ Ru	0.29	25.0	0.63	0.171	43.8	0.51
¹¹⁰ Ru	0.29	22.5	0.47	0.171	47.4	0.50
¹¹² Ru	0.26	60.0	0.0	0.153	52.8	0.12
¹¹⁴ Ru	0.26	60.0	0.0	0.147	53.4	0.10

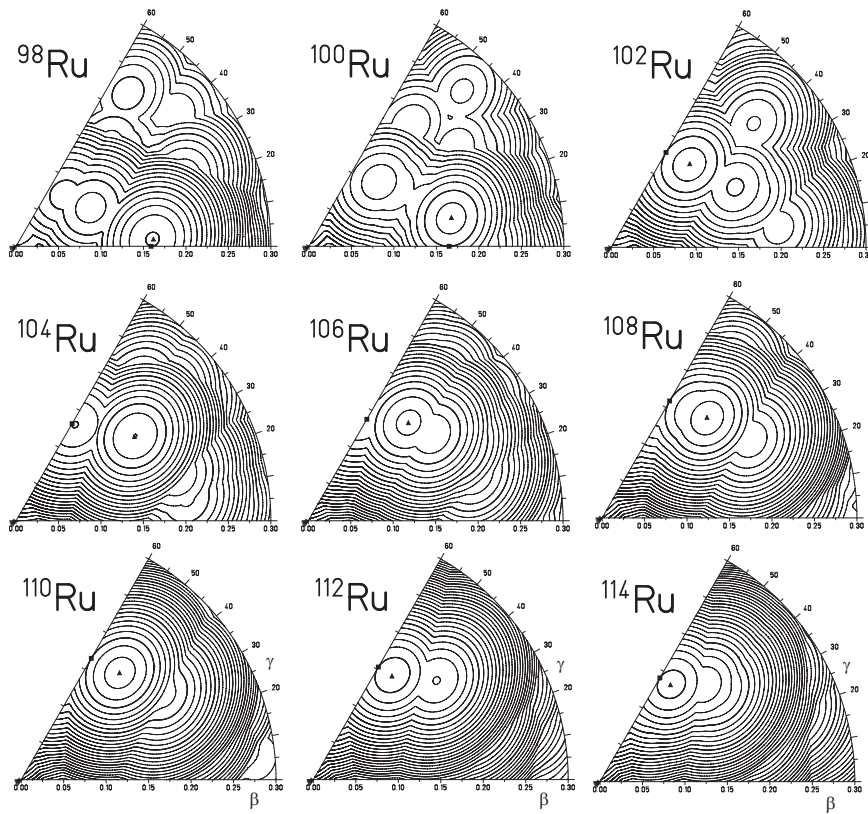


Fig. 21.8 Potential energy surfaces (PES) for a set of triaxially deformed ruthenium-isotopes ($Z = 44$) calculated with the fractional model using parameter set (21.90)-(21.92). Energy values are normalized to the rotational symmetric prolate or oblate minimum and are given in 0.2 MeV step contours. Thick lines indicate integer values of the energy (0,1,2, ... MeV). Black filled squares indicate the rotationally symmetric minimum, while black filled triangles show the position of the global minimum. The transition from prolate to oblate shapes is reproduced in accordance with results presented in [Möller *et al.* (2008)].

In table 21.1 we compare Möller's results with our fit using parameter set (21.90)-(21.92). Listed are the minimizing parameter sets (β, γ) for a given shape and the energy gain with respect to the rotationally symmetric shape. There is a qualitative agreement.

It should be mentioned, that Möller's minimization parameter set includes hexadecupole deformations (ϵ_4) too, which are ignored using our simplified approach. Furthermore we have neglected the influence of pairing

forces. Consequently, we can not expect a quantitative agreement. Nevertheless, the transition from prolate to oblate shapes is reproduced very well for both cases, see also results from [Troltenier *et al.* (1991)], based on the general collective model (GCM).

In figure 21.8 the corresponding potential energy surface (PES) are plotted. These results may be directly compared with [Möller *et al.* (2008)]. The resolution in β and γ is 100 times 100 points, shell corrections have been calculated for every single point separately, no interpolation was done.

Summarizing the results presented, the proposed extended Caputo-Riemann-Riemann symmetric rotor describes the ground state properties of nuclei with reasonable accuracy. We have demonstrated, that the nuclear shell structure may indeed be successfully described on the basis of a dynamical symmetry model.

The advantages of this model, compared to phenomenological shell and relativistic mean field models respectively are obvious:

Magic numbers are predicted, they are not the result of a fit with a phenomenological ls -term. The experimentally observed ground state properties of nuclei occur at a very small deviation from the ideal vibrational case $\alpha = 1/2$. There are no potential-terms or parametrized Skyrme-forces involved and finally, single particle levels are given analytically.

Therefore we have demonstrated, that a dynamic symmetry, generated by mixed fractional type rotation groups is indeed realized in nature.

Of course, there are other areas of physics, where magic numbers have been observed.

In the next chapter we will demonstrate, that the Caputo-Caputo-Riemann decomposition of the 9-dimensional fractional rotation group (21.17) generates a dynamic symmetry group, which determines the magic numbers in metal clusters accurately. Furthermore a comparison with experimental data will lead to the conclusion, that a fractional phase transition occurs near cluster size $200 \leq N \leq 300$.

21.8 Discussion

21.8.1 *Curvature interaction in the collective Riemannian space*

question:

You introduced an interaction with the curvature of the collective Riemannian space. Can you give an example of practical application, where this new term becomes evident?

answer:

The use of collective models for a description of collective aspects of nuclear motion within the framework of fractional calculus has been demonstrated in section 10.1.

There we have shown, that the collective Schrödinger equation

$$\hat{S}_0 \Psi(q^i, t) = \left(-\frac{\hbar^2}{2} \frac{1}{\sqrt{B}} \partial_i B^{ij} \sqrt{B} \partial_j - i\hbar \partial_t + V_0 \right) \Psi(q^i, t) = 0 \quad (21.97)$$

with B_{ij} is the mass tensor and $B = \det B_{ij}$ is the determinant of the mass tensor, is the central starting point for a discussion of nuclear collective phenomena.

Here we want to emphasize the fact, that via the relation

$$B_{ij} = m_A g_{ij} = m_u A g_{ij} \quad (21.98)$$

(m_A is the mass of the nucleus, $m_u = 931.5$ MeV is the mass unit and A is the number of nucleons) the collective masses may be interpreted geometrically, defining the metric tensor g_{ij} , which fully determines the geometric properties of the collective Riemannian space.

Hence the collective Schrödinger equation may be written as

$$\hat{S}_0 \Psi(q^i, t) = \left(-\frac{\hbar^2}{2m_A \sqrt{g}} \partial_i g^{ij} \sqrt{g} \partial_j - i\hbar \partial_t + V_0 \right) \Psi(q^i, t) = 0 \quad (21.99)$$

emphasizing the one to one correspondence of collective masses and collective space.

An alternative approach to derive the collective Schrödinger equation starts with the Lagrangian density \mathcal{L}_0

$$\mathcal{L}_0 = \frac{\hbar^2}{2m_A} g^{ij} (\partial_i \Psi^*) (\partial_j \Psi) + \frac{i\hbar}{2} (\Psi^* \frac{\partial \Psi}{\partial t} - \frac{\partial \Psi^*}{\partial t} \Psi) - \Psi^* V_0 \Psi \quad (21.100)$$

Variation with respect to Ψ^* and Ψ yields the above Schrödinger equation.

From this point of view, it is remarkable, that until now obvious extensions of this Lagrange density have been discussed in other branches of physics, e.g. cosmology or string theory, but, until now, have been neglected within the framework of nuclear collective models.

As one obvious extension let us investigate the influence of nonvanishing curvature in collective space: For that purpose, we consider an additional interaction with the collective metric, which is determined by the collective mass parameters.

We extend the Lagrangian density

$$\mathcal{L} = \mathcal{L}_0 - \frac{\hbar^2}{2m_A}\xi\Psi^*R\Psi \quad (21.101)$$

introducing the Einstein curvature scalar R as an invariant measure for collective curvature. The coupling strength is parametrized with ξ .

Variation of this Lagrangian density results in an additional potential term

$$V = V_0 + \frac{\hbar^2}{2m_A}\xi R \quad (21.102)$$

Since the collective mass parameters are known, R can be calculated. As a starting point the Riemann curvature tensor is given by

$$R^\alpha_{\eta\beta\gamma} = \partial_\gamma\Gamma^\alpha_{\beta\eta} - \partial_\beta\Gamma^\alpha_{\eta\gamma} + \Gamma^\alpha_{\tau\gamma}\Gamma^\tau_{\beta\eta} - \Gamma^\alpha_{\tau\beta}\Gamma^\tau_{\gamma\eta} \quad (21.103)$$

with the Christoffel symbols of second kind [Adler *et al.* (1975)]

$$\Gamma^\mu_{\kappa\sigma} = \frac{1}{2}g^{\nu\mu}(\partial_\kappa g_{\nu\sigma} + \partial_\sigma g_{\nu\kappa} - \partial_\nu g_{\kappa\sigma}) \quad (21.104)$$

The Riemann curvature tensor may be contracted to get the Ricci tensor

$$R_{\eta\gamma} = R^\alpha_{\eta\alpha\gamma} \quad (21.105)$$

and finally we obtain the Einstein curvature scalar R via:

$$R = R^\eta_\eta \quad (21.106)$$

The explicit form of this curvature term depends on the specific choice of collective coordinates.

In order to examine the consequences and physical interpretation of this additional new term we choose the symmetric two-center shell model including elliptical deformations [Scharnweber *et al.* (1970)], which can be solved fully analytically. This model is widely used in the description of symmetric fusion reactions and contains the Nilsson model as a limiting case, which will turn out to be a useful property for a physical interpretation. As an illustrative, exactly solvable scenario we consider the nuclear shape given by two intersecting rotationally symmetric ellipsoids. Introducing two collective coordinates q^i namely, the ellipsoidal deformation $Q = b/a$ and the total elongation L the shape $P(z, q^i)$ is given by (see figure 21.9):

$$P(z, q^i) = Q\sqrt{a^2 - (z \mp z_1)^2} \quad (21.107)$$

where the geometric quantities semi axis a and center position of ellipsoids z_1 are determined by the definition of L and by the requirement of volume

$$Q = b/a$$

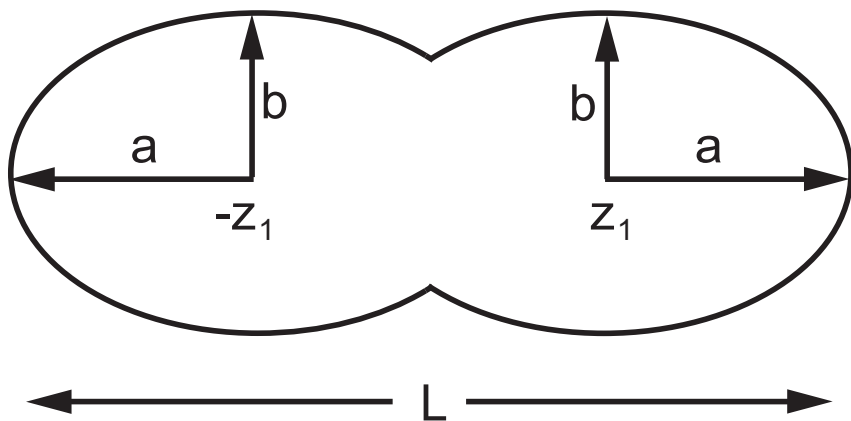


Fig. 21.9 Geometry of the symmetric two-center shell model.

conservation, which yields in the case of connected fragments with $R_0 = r_0 A^{1/3}$:

$$L = 2(a + z_1) \quad (21.108)$$

$$\text{volume} = (4/3)\pi R_0^3 = 2(2/3)\pi Q^2 \left(a^3 + \frac{3}{2}a^2 z_1 - \frac{1}{2}z_1^3 \right) \quad (21.109)$$

These equations may be simplified introducing the dimensionless quantities

$$\alpha = Q^{2/3} a/R_0 \quad (21.110)$$

$$\gamma_1 = Q^{2/3} z_1/R_0 \quad (21.111)$$

$$\lambda = Q^{2/3} L/(2R_0) \quad (21.112)$$

Equations (21.110)-(21.112) define a transformation to a new set of coordinates (λ, Q) , where the range from spherical compound nucleus $\lambda = 1$ up to the scission point configuration $\lambda = 4^{1/3}$ is independent from Q . Results depend on λ only. We obtain:

$$\alpha = \frac{2 + \lambda^3}{3 \lambda^2} \quad (21.113)$$

$$\gamma_1 = \frac{2(\lambda^3 - 1)}{3 \lambda^2} \quad (21.114)$$

Thus, the shape geometry is fully determined for a given set of collective coordinates (λ, Q) . $1 \leq \lambda \leq 4^{1/3}$ describes connected fragments, where

$\lambda = 1$ is the compound nucleus and $\lambda = 4^{1/3}$ is the scission point and $\lambda > 4^{1/3}$ describes separated fragments. $Q < 1$ describes prolate and $Q > 1$ oblate shapes.

We now apply the Werner-Wheeler-formalism [Werner and Wheeler (1958)] to calculate the collective masses B_{ij} , which are directly correlated to the metric tensor g_{ij} according to (21.98). We choose this method, since masses are determined by shape geometry only and the procedure itself is well defined. Using the abbreviation

$$\Theta = \ln \left(\frac{4 - \lambda^3}{4 + 2\lambda^3} \right) \quad (21.115)$$

the components of the metric tensor g_{ij} result as

$$g_{\lambda\lambda} = \frac{R_0^2 (2 + \lambda^3)^2}{324 Q^{4/3} \lambda^{12}} \times \left(3(Q^2 - 16)\lambda^9 + 4(Q^2 - 4)[24\lambda^3 - 3\lambda^6 + (\lambda^3 - 4)^2(2 + \lambda^3)\Theta] \right) \quad (21.116)$$

$$g_{\lambda Q} = -\frac{R_0^2}{108 Q^{7/3} \lambda^2} (2 + \lambda^3) (6\lambda^3 + Q^2(4 - \lambda^3)) \quad (21.117)$$

$$g_{QQ} = \frac{R_0^2}{810 Q^{10/3} \lambda} (12\lambda^3(5 + \lambda^3) + Q^2(40 - 5\lambda^3 + \lambda^6)) \quad (21.118)$$

A coordinate transformation from the coordinate set (λ, Q) to the original (L, Q) using

$$g_{ij} = \frac{\partial x^m}{\partial x^i} \frac{\partial x^n}{\partial x^j} g_{mn} \quad (21.119)$$

yields the final result for connected shapes in the range $1 \leq \lambda \leq 4^{1/3}$

$$g_{LL} = \frac{(2 + \lambda^3)^2}{1296 \lambda^{12}} \times \left(3(Q^2 - 16)\lambda^9 + 4(Q^2 - 4)[8\lambda^3(3 - \lambda^3) + (4 - \lambda^3)^2(2 + \lambda^3)\Theta] \right) \quad (21.120)$$

$$g_{LQ} = \frac{R_0 (2 + \lambda^3)}{1944 Q^{5/3} \lambda^{11}} \times \left(3\lambda^3[(Q^2 + 14)\lambda^9 + 8(Q^2 - 4)(16 + 6\lambda^3 - 3\lambda^6)] + 8(Q^2 - 4)(-8 - 2\lambda^3 + \lambda^6)^2\Theta \right) \quad (21.121)$$

$$g_{QQ} = \frac{R_0^2}{7290 Q^{10/3} \lambda^{10}} \times \left((48 + 69Q^2)\lambda^{15} + (Q^2 - 4)[15\lambda^3(256 + 224\lambda^3 - 31\lambda^9) + 40(\lambda^3 - 4)^2(2 + \lambda^3)^3\Theta] \right) \quad 1 \leq \lambda \leq 4^{1/3} \quad (21.122)$$

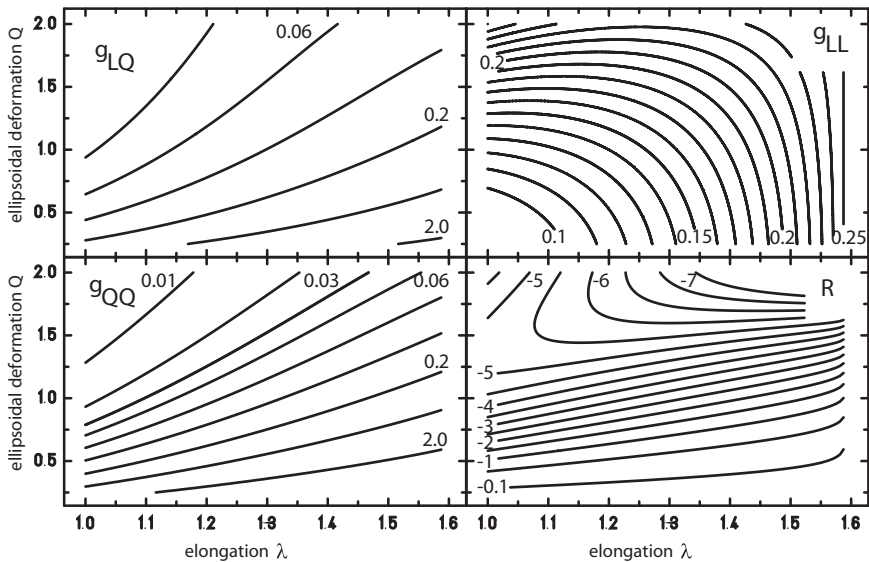


Fig. 21.10 Metric tensor components g_{LQ} (upper left), g_{LL} (upper right), g_{QQ} (lower left) and curvature scalar R (lower right) for the symmetric two-center shell model, normalized setting $R_0 = 1$.

A similar calculation for separated fragments with $\lambda \geq 4^{1/3}$ yields

$$g_{LL} = \frac{1}{4} \quad (21.123)$$

$$g_{LQ} = \frac{R_0/3}{2^{1/3} Q^{5/3}} \quad (21.124)$$

$$g_{QQ} = \frac{2^{1/3} (12 + Q^2) R_0^2}{45 Q^{10/3}} \quad \lambda > 4^{1/3} \quad (21.125)$$

Given the metric tensor g_{ij} , the curvature scalar $R(L, Q)$ can easily be calculated.

Figure 21.10 shows the elements of the metric tensor g_{ij} and the resulting curvature scalar R . For connected fragments with $\lambda \leq 4^{1/3}$ a non-vanishing curvature scalar $R(L, Q)$ exists. This is a direct consequence of the volume conservation condition (see (21.109)).

For prolate and moderately oblate shapes ($Q \leq 1.7$) with a fixed Q , the curvature scalar starts with a negative value, which tends to 0 with increasing λ up to the scission point. For oblate shapes ($Q \geq 1.7$) with a fixed Q , R decreases with increasing λ down to the scission point.

For separated fragments we obtain $R = 0$. This discontinuity of the curvature scalar at the scission point is a direct consequence of the underlying simple geometry, the derivative of the shape is not defined at the contact point of the two ellipsoids. This can be avoided by smoothing the shape appropriately, resulting in a smooth curvature term at the scission point, but the resulting model has to be solved numerically.

The curvature minimizing shape is not a sphere, but a slightly deformed, oblate shape, due to the fact, that the subject of our considerations is not the curvature of a given shape, but curvature of the collective space, generated by the Werner-Wheeler-masses.

In case of a single deformed ellipsoid ($\lambda = 1$), R is explicitly given as:

$$R(Q) = \frac{-720 Q^{16/3} (-25 + 36 \ln(2)) (-67 + 96 \ln(2))}{R_0^2 (2 + Q^2)^2 [-2 + (Q^2 - 4) (-67 + 96 \ln(2))]^2} \quad (21.126)$$

and finally, for a sphere this reduces to R_{sphere} :

$$R_{\text{sphere}} = -4.3599 \frac{1}{R_0^2} \quad (21.127)$$

Since R is an invariant (transforms as a scalar) under coordinate transformations, the shape may be described by any appropriate set of coordinates, which obey the transformation rule given in (21.119). Consequently, for the symmetric two-center shell model, which we discussed here as an example, the coordinate sets $(L, Q), (\lambda, Q), (\lambda, \beta = 1/Q)$ or $(\Delta z, \beta)$ where Δz is the two-center distance, are equivalent. They lead to different mass parameters, but yield the same R . In that sense, the curvature scalar is a unique, outstanding property of a given shape geometry.

In order to get an estimate for the curvature coupling constant, we will now investigate the influence of an additional curvature term by a fit of experimentally known ground state masses of nuclei.

For reasons of simplicity, we assume the ground state of nuclei being of ellipsoidal form only, neglecting higher order multipoles. Therefore the shapes are described by $(\lambda = 1, Q)$, depending on only one collective coordinate Q .

We define the relative curvature energy B_R with respect to the spherical compound nucleus ($\lambda = 1, Q = 1$) as

$$B_R = R(\lambda = 1, Q) / R_{\text{sphere}} \quad (21.128)$$

$$= 9 Q^{16/3} \left(\frac{199 - 288 \ln(2)}{(2 + Q^2)[266 - 67Q^2 + 96(Q^2 - 4) \ln(2)]} \right)^2 \quad (21.129)$$

Table 21.2 Determination of volume-energy a_v , volume-asymmetry k_v , surface-energy a_s , surface-asymmetry k_s and curvature energy a_R constants within the original FRLDM, FRLDM2003 fitted with AME2003 experimental masses and FRLDMC, which corresponds to FRLDM plus curvature term and resulting root-mean-square deviations Δ_{rms} from AME2003 experimental data.

constants	FRLDM	FRLDM2003	FRLDMC
a_v	16.00126 MeV	16.00496 MeV	16.01890 MeV
k_v	1.92240 MeV	1.93167 MeV	1.92882 MeV
a_s	21.18466 MeV	21.18770 MeV	21.25974 MeV
k_s	2.345 MeV	2.35968 MeV	2.34955 MeV
a_R	-	-	529.95850 MeV
Δ_{rms}	0.821 MeV	0.815 MeV	0.764 MeV

An additional curvature potential term V_R is defined

$$V_R(a_R, Q) = +\frac{\hbar^2}{2m_A} \xi R_{\text{sphere}} B_R \quad (21.130)$$

$$= -a_R B_R A^{-5/3} \quad (21.131)$$

where we have introduced the curvature-energy constant a_R , which will be determined now.

Our choice for an appropriate macroscopic model is the finite range liquid drop model FRLDM. It is widely used and documented in detail [Möller *et al.* (1993)].

We shall vary only a subset of parameters, namely, the volume-energy a_v , the volume-asymmetry k_v , the surface-energy a_s and the surface-asymmetry k_s constants, which generate the major contributions for the calculated masses, keeping all other parameters at their original values.

We define the finite range liquid drop model with curvature (FRLDMC):

$$\text{FRLDMC}(a_v, k_v, a_s, k_s, a_R, Q) = \text{FRLDM}(a_v, k_v, a_s, k_s, Q) + V_R(a_R, Q) \quad (21.132)$$

Theoretical masses m_{th} are then obtained, including the microscopic corrections E_{mic}

$$m_{\text{th}} = \text{FRLDMC} + E_{\text{mic}} \quad (21.133)$$

and are compared with the AME2003 experimental masses [Audi *et al.* (2003)]. For conversion from quadrupole moments β_2 to ellipsoidal deformations Q we use the relation

$$Q = 1 + \frac{3}{2} \sqrt{\frac{5}{4\pi}} \beta_2 \quad (21.134)$$

Table 21.3 Determination of volume-energy a_v , surface-energy a_s , charge-asymmetry c_a and curvature energy a_R constants within the original FRDM, FRDM2003 fitted with AME2003 experimental masses and FRDMC, which corresponds to FRDM plus curvature term and resulting root-mean-square deviations Δ_{rms} from AME2003 experimental data.

constants	FRDM	FRDM2003	FRDMC
a_v	16.247 MeV	16.2401 MeV	16.2467 MeV
a_s	22.92 MeV	22.8812 MeV	22.9159 MeV
c_a	0.436 MeV	0.4368 MeV	0.4332 MeV
a_R	-	-	172.676 MeV
Δ_{rms}	0.679 MeV	0.674 MeV	0.655 MeV

As a measure for the quality of the fit, we tabulate the root mean square deviation

$$\Delta_{\text{rms}} = \sqrt{\frac{1}{N} \sum^N (m_{\text{exp}} - m_{\text{th}})^2} \quad (21.135)$$

Results are listed in table 21.2. The first column tabulates the original FRLDM parameter set, followed by results for FRLDM2003, which corresponds to an actualized FRLDM-parameter set for AME2003 masses and finally results for FRLDMC, which corresponds to the original FRLDM including the curvature term are presented.

The corresponding Δ_{rms} -values indicate a significant improvement of the new, extended FRLDMC-model. Especially for light nuclei and in the region of trans-lead elements results improvements are significant, as shown in table 21.4, where errors for different Z -regions are listed.

For light nuclei this is due to the $A^{-5/3}$ behavior of the curvature energy, since this term contributes most to the total binding energy for light nuclei, e.g. for $^{16}\text{O} = 5.21$ MeV, while for heavy nuclei, this term becomes negligible e.g. for $^{208}\text{Pb} = 0.07$ MeV. The improvement indicates, that the additional Riemann curvature term is a useful extension for a collective model.

Since overestimating masses for heavy nuclei is a known shortcoming of FRLDM, Möller *et al.* [Möller *et al.* (1993)] introduced the finite range droplet model (FRDM), whose major improvement is an additional empirical exponential term of the form

$$-CA \exp^{-\gamma A^{1/3}} \bar{\epsilon} \quad (21.136)$$

Using original parameters, this term simulates an A -dependence, which is close to the collective curvature term, derived in this work. Therefore

Table 21.4 Root-mean-square deviations Δ_{rms} from AME2003 experimental data in MeV for different Z -Regions.

Z/model	8-20	20-40	40-60	60-80	80-100	≥ 100
FRLDM	1.716	0.857	0.568	0.654	0.746	1.091
FRLDMC	1.307	0.900	0.582	0.814	0.494	0.508
FRDM	1.447	0.871	0.579	0.449	0.388	0.512
FRDMC	1.287	0.887	0.547	0.448	0.407	0.487

we expect a reduced influence of an additional curvature term within the framework of FRDM.

To proof this hypothesis, we define the finite range drop model with curvature (FRDMC) and vary with respect to the subset of most important parameters, a_v volume-energy, a_s surface-energy and c_a charge-asymmetry constants, keeping all other parameters fixed at their original values.

$$\text{FRDMC}(a_v, a_s, c_a, a_R, Q) = \text{FRDM}(a_v, a_s, c_a, Q) + V_R(a_R, Q) \quad (21.137)$$

Once again theoretical masses m_{th} and experimental masses were fitted. Results are listed in table 21.3.

As expected, the curvature-energy constant a_R is reduced by a factor 3, which results in an absolute contribution to the total binding energy of about 1.7 MeV for ^{16}O .

For light and trans-fermium nuclei we achieve a significant improvement with the extended FRDMC, compared to the original FRDM. The additional curvature term makes the FRDMC the best model available for the description of ground state masses in the full range of the nuclear table.

Thus, within both extended models, the FRLDMC and the FRDMC, the existence of a curvature term is supported. The coupling strength ξ , derived from fits, setting $r_0 = 1.16$ fm results as $\xi = 7.8$ for FRLDMC and $\xi = 2.5$ for FRDMC respectively.

Based on a purely geometric interpretation of collective mass-parameters, the collective curvature scalar term has been introduced. For the geometry of the symmetric two-center shell model this term has been derived analytically. Interpreting this term as an additional potential term with the explicit form $V \sim A^{-5/3}$, we have investigated the influence of this term within the framework of two new macroscopic models: The finite range liquid drop model with curvature (FRLDMC) and the finite range droplet model with curvature (FRDMC).

Significant improvements have been found especially for light nuclei and for trans-fermium elements. Thus, the new models allow a more precise description of nuclear ground state properties.

Therefore the collective curvature scalar as a manifestation of interaction with curved collective space, plays an important role, e.g. for strong asymmetric fission, cluster-radioactivity or prediction of super-heavy element properties.

On the other hand, the curvature energy is a nice example for an energy contribution, which cannot be handled by a Riesz-potential within the allowed fractional parameter range $0 < \alpha < 3$, see Chapter 10.

Chapter 22

Magic Numbers in Metal Clusters

Since 1984, an increasing amount of experimental data [Knight et al. (1984); Martin et al. (1991); Pellarin et al. (1994)] confirms an at first unexpected shell structure in fermion systems, realized as magic numbers in metal clusters.

The observation of varying binding energy of the valence electron, moving freely in a metallic cluster, has initiated the development of several theoretical models. Besides *ab initio* calculation, the most prominent representatives are the jellium model and, in analogy to methods already in use in nuclear physics, phenomenological shell models with modified potential terms like the Clemenger-Nilsson model or deformed Woods-Saxon potential [Clemenger (1985); Bjornholm et al. (1990); de Heer (1993); Brack (1993); Engel et al. (1993); Moriarty (2001); Reinhard and Suraud (2004); Haberland et al. (2005); Poenaru and Plonski (2008); Poenaru et al. (2010a)].

Although these models describe the experimental data with reasonable accuracy, they do not give a theoretical explanation for the observed sequence of magic numbers. Therefore the problem of a theoretical foundation of the magic numbers is still an open question.

In the last chapter we have demonstrated, that the magic numbers in atomic nuclei are the result of a fractional dynamic symmetry, which is determined by a specific decomposition of the 9-dimensional mixed fractional rotation group.

On the basis of this encouraging result, we will demonstrate, that a more fundamental understanding of magic numbers found for metal clusters may be achieved applying an alternative decomposition of the same 9-dimensional fractional rotation group.

22.1 The Caputo-Caputo-Riemann symmetric rotor - an analytic model for metallic clusters

According to the group chain (21.17) we associate the Hamiltonian:

$$H = \frac{\omega_1}{\hbar} {}_{\text{C}}L_1^2(\alpha) + \frac{\omega_2}{\hbar} {}_{\text{C}}L_2^2(\alpha) + \frac{\omega_3}{\hbar} {}_{\text{R}}L_3^2(\alpha) \quad (22.1)$$

with the free parameters $\omega_1, \omega_2, \omega_3$ and the basis is $|L_1 M_1 L_2 M_2 L_3 M_3\rangle$.

Imposing the same symmetries as in section 21.3 we obtain the corresponding level spectrum:

$$\begin{aligned} E(\alpha) &= \hbar\omega_1 {}_{\text{C}}[2n_1]_{\text{C}}[2n_1 + 1] + \hbar\omega_2 {}_{\text{C}}[2n_2]_{\text{C}}[2n_2 + 1] \\ &\quad + \hbar\omega_3 {}_{\text{R}}[2n_3]_{\text{R}}[2n_3 + 1] \end{aligned} \quad (22.2)$$

$$\begin{aligned} &= \sum_{i=1}^3 \hbar\omega_i \frac{\Gamma(1 + (2n_i + 1)\alpha)}{\Gamma(1 + (2n_i - 1)\alpha)} \\ &\quad - \delta_{n_1 0} \hbar\omega_1 \frac{\Gamma(1 + \alpha)}{\Gamma(1 - \alpha)} - \delta_{n_2 0} \hbar\omega_2 \frac{\Gamma(1 + \alpha)}{\Gamma(1 - \alpha)} \end{aligned} \quad (22.3)$$

$$n_1, n_2, n_3 = 0, 1, 2, \dots$$

on a basis $|2n_1 2n_1 2n_2 2n_2 2n_3 2n_3\rangle$.

This is the major result of our derivation. We call this model the Caputo-Caputo-Riemann symmetric rotor. What makes this model remarkable once again is its behavior in the vibrational region near the semi-derivative $\alpha = 1/2$.

In figure 22.1 we have plotted the energy levels in the vicinity of $\alpha \approx 1/2$ for the spherical case (21.50).

For the idealized spherical case $\alpha = 1/2$, using the relation $\Gamma(1 + z) = z\Gamma(z)$ the level spectrum (22.2) is simply given by:

$$E(\alpha = 1/2) = \hbar\omega_0 \left(n_1 + n_2 + n_3 + \frac{3}{2} - \frac{1}{2}\delta_{n_1 0} - \frac{1}{2}\delta_{n_2 0} \right) \quad (22.4)$$

In order to determine the multiplets of (22.4), we first recall the properties of the well known spectrum of the spherical 3-dimensional harmonic oscillator.

$$E_{\text{HO}} = \hbar\omega_0(n_1 + n_2 + n_3 + 3/2) \quad (22.5)$$

We introduce the quantum number N as

$$N = n_1 + n_2 + n_3 \quad (22.6)$$

Assuming a 2-fold spin degeneracy of the energy levels, we obtain the multiplets of the spherical 3-dimensional harmonic oscillator with magic numbers for

$$n_{\text{HO}}(N) = \frac{1}{3}(N + 1)(N + 2)(N + 3) \quad N = 0, 1, 2, 3, \dots \quad (22.7)$$

$$= 2, 8, 20, 40, 70, 112, 168, 240, \dots \quad (22.8)$$

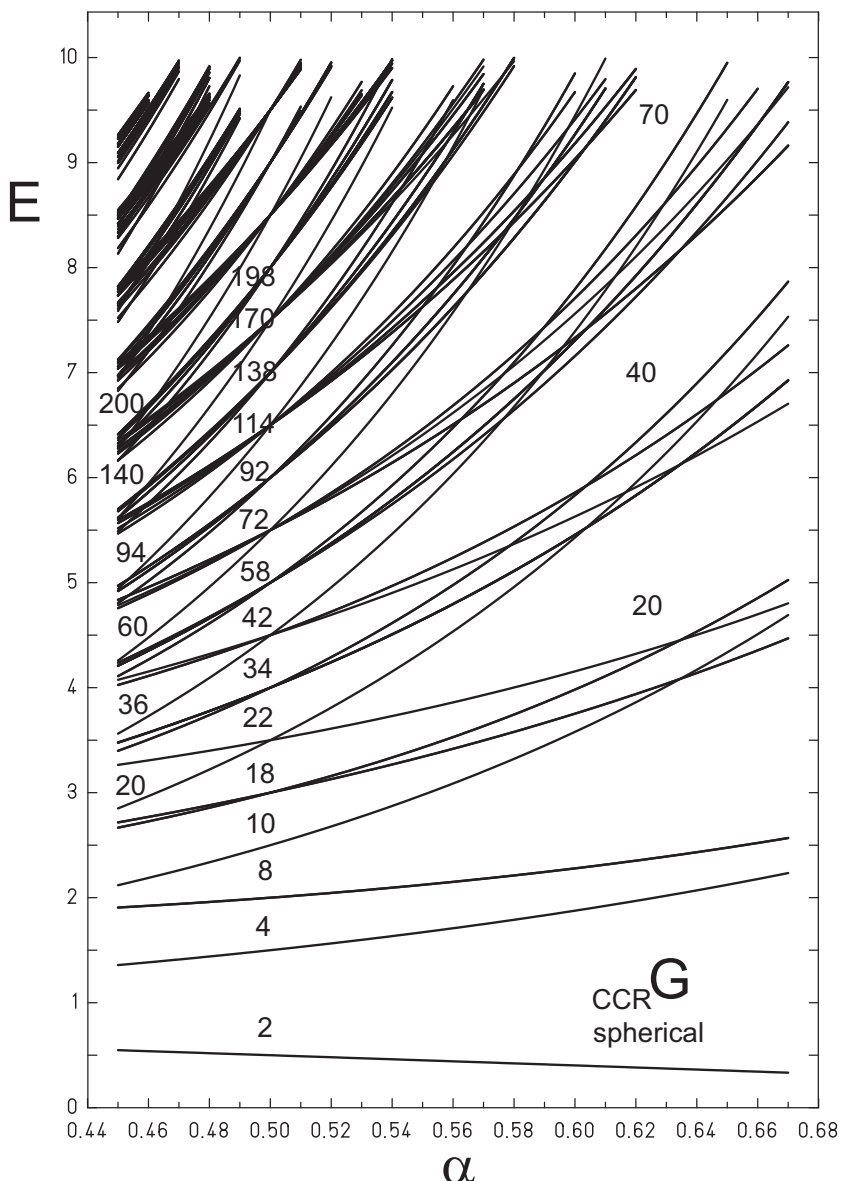


Fig. 22.1 Level diagram of the Caputo-Caputo-Riemann symmetric rotor (22.2) for the spherical case in the vicinity of $\alpha \approx 1/2$.

at energies

$$E(N)_{\text{HO}} = \hbar\omega_0(N + 3/2) \quad (22.9)$$

For the multiplets of (22.4) we distinguish two different sets of magic numbers, which we label with N_1 and N_2 :

For $n_1 = 0$ and $n_2 = 0$ the multiplicity of a harmonic oscillator shell for N at energy (22.9) is increased by exactly one state, the $|0000N+1N+1\rangle$ state, which originates from the $N+1$ shell. Therefore we obtain a first set ${}_{\text{CCR}}n_{\text{magic } 1}$ of magic numbers (including the state $|000000\rangle$) for which we assign $N = -1$:

$${}_{\text{CCR}}n_{\text{magic } 1}(N_1) = n_{\text{HO}}(N_1 - 1) + 2 \quad N_1 = 0, 1, 2, 3, \dots \quad (22.10)$$

$$= \frac{1}{3}N_1(N_1 + 1)(N_1 + 2) + 2 \quad (22.11)$$

$$= 2, 4, 10, 22, 42, 72, 114, 170, 242, 332, 442, \dots \quad (22.12)$$

at energies

$$E(N_1)_{\text{CCR}}n_{\text{magic } 1} = \hbar\omega_0(N_1 + 1/2) \quad (22.13)$$

In addition, for $n_1 = 0$, which corresponds to the $|002n_22n_22n_32n_3\rangle$ states and $n_2 = 0$ respectively, which corresponds to the $|2n_12n_1002n_32n_3\rangle$ states with a $\sum_{n=1}^{N+1} 2 = 2(N+1)$ -fold multiplicity for each set $n_1 = 0$ and $n_2 = 0$ we obtain a second set ${}_{\text{CCR}}n_{\text{magic } 2}$ of magic numbers

$${}_{\text{CCR}}n_{\text{magic } 2}(N_2) = {}_{\text{CCR}}n_{\text{magic } 1}(N_2 + 1) + 4(N_2 + 1) \quad (22.14)$$

$$N_2 = 0, 1, 2, 3, \dots$$

$$= \frac{1}{3}(N_2 + 1)(N_2 + 2)(N_2 + 3) + 2 + 4(N_2 + 1) \quad (22.15)$$

$$= 8, 18, 34, 58, 92, 138, 198, 274, \dots \quad (22.16)$$

at energies

$$E(N_2)_{\text{CCR}}n_{\text{magic } 2} = \hbar\omega_0(N_2 + 2) \quad (22.17)$$

In figure 22.1, the single particle levels are plotted. A remarkable feature is the dominant influence of the $|0000NN\rangle$ state. For $\alpha < 0.5$ the harmonic oscillator type magic numbers die out. As a consequence, for $\alpha \approx 0.48$ the set of magic numbers ${}_{\text{CCR}}n_{\text{magic } 2}$ is shifted by 1, which leads to the series $2, 4, 9, 19, 35, 59, 93, 139, \dots$. For $\alpha \approx 0.46$ the $|0000NN\rangle$ state has completely reached the ${}_{\text{CCR}}n_{\text{magic } 2}$ multiplet, which in a stable series of magic numbers at $2, 4, 10, 20, 36, 60, 94, 140, 200, \dots$

On the other hand for $\alpha > 0.55$ the levels are rearranged to form the set of magic numbers of the harmonic oscillator.

We conclude, that the Caputo-Caputo-Riemann symmetric rotor predicts a well defined set of magic numbers. This set is a direct consequence of the underlying dynamic symmetries of the three fractional rotation groups involved. It is indeed remarkable, that the same set of magic numbers is realized in nature as electronic magic numbers in metal clusters.

In the next section we will demonstrate, that the proposed analytical model is an appropriate tool to describe the shell correction contribution to the total binding energy of metal clusters.

22.2 Binding energy of electronic clusters

We will use the Caputo-Caputo-Riemann symmetric rotor (22.2) as a dynamic shell model for a description of the microscopic part of the total energy binding energy E_{tot} of the metal cluster:

$$E_{\text{tot}} = E_{\text{macroscopic}} + E_{\text{microscopic}} \quad (22.18)$$

$$= E_{\text{macroscopic}} + \delta U \quad (22.19)$$

where δU denotes the shell-correction contributions.

To make our argumentation as clear as possible, we will restrict our investigation to the spherical configuration, which will allow to discuss the main features of the proposed model in a simple context. We will compare our results with calculations for the most prominent metal cluster, the sodium (Na) cluster. From experimental data [Knight *et al.* (1984); Bjornholm *et al.* (1990); Martin *et al.* (1991)], the following sequence of magic numbers is deduced:

$$\begin{aligned} n_{\text{magic Na}} = \{ & 2, 8, 20, 40, 58, 92, 138, 198 \pm 2, 263 \pm 5, 341 \pm 5, \\ & 443 \pm 5, 557 \pm 5, 700 \pm 15, 840 \pm 15, 1040 \pm 20, \\ & 1220 \pm 20, 1430 \pm 20 \} \end{aligned} \quad (22.20)$$

For a graphical representation of the experimental magic numbers we introduce the two quantities:

$$\Theta = i / (n_{\text{magic Na}}(i+1) - n_{\text{magic Na}}(i)) \quad (22.21)$$

$$\omega = n_{\text{magic Na}}(i+1) - n_{\text{magic Na}}(i) \quad (22.22)$$

where i denotes the array-index in (22.20).

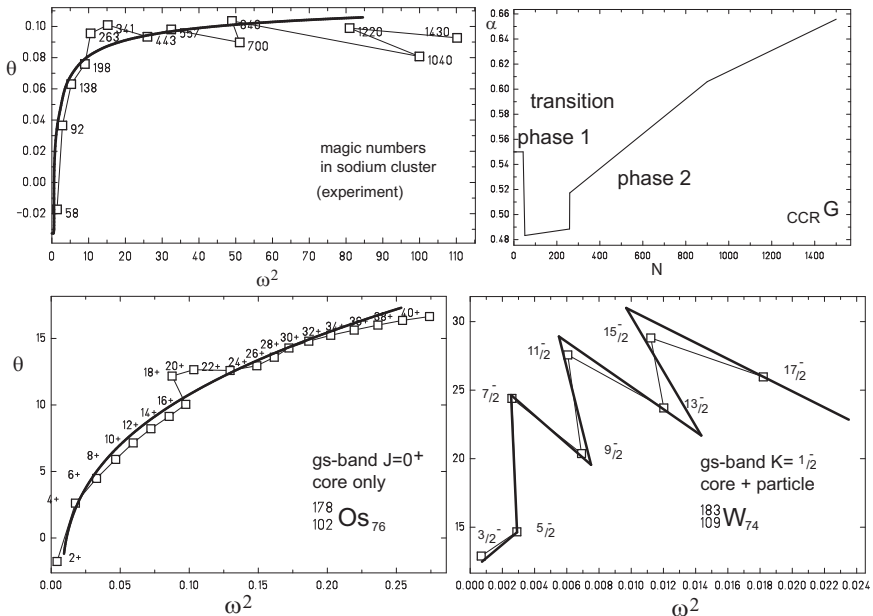


Fig. 22.2 Back bending plots of experimentally determined magic numbers for $(\text{Na})_N$ clusters from [Knight *et al.* (1984); Bjornholm *et al.* (1990); Martin *et al.* (1991)], ground state excitation spectrum for $^{178}\text{Os}_{76}$ from chapter 17.7 and ground state excitation spectrum of $^{109}\text{W}_{74}$ from chapter 18.4. Squares indicate the experimental values. The sequence of experimentally observed magic numbers may be categorized for $N < 58$ to be purely vibrational, for $N < 200$ to be equivalent to an excitation spectrum of purely rotational type, the thick line indicating a fit with a fractional rigid rotor spectrum, for $200 \leq N \leq 300$ a region of back bending type (compare with the plotted ground state band spectrum for $^{178}\text{Os}_{76}$) and finally, for $N > 300$ a region with almost constant θ and a behavior similar to excitation spectra of ug-nuclei (compare with the plotted excitation spectrum of $^{109}\text{W}_{74}$). In the upper right the corresponding proposed $\alpha(N)$ from (22.27) is plotted.

Interpreting Θ as a moment of inertia and ω a rotational frequency, figure 22.2 is a back bending plot of the experimental magic numbers.

We distinguish different regions of magic numbers:

For cluster size $N < 58$ we have purely vibrational magic numbers, while for $N < 200$ the plot shows a typical rotor spectrum. In the region $200 < N < 300$ a typical back bending phenomenon is observed. For illustrative purposes in figure 22.2 the same phenomenon is documented within the framework of nuclear physics for the ground state rotation spectrum of $^{178}\text{Os}_{76}$. For $N > 300$ the moment of inertia becomes nearly constant and

the graph may be compared with the rotational $K = \frac{1}{2}$ band of the ug-nucleus $^{183}_{109}\text{W}_{74}$, which is a typical example of a core plus single particle motion in nuclear physics.

These different structures in the sequence of electric magic numbers are reflected in the choice of the fractional derivative coefficient α . For $\mathcal{N} < 200$, α shows a simple behavior similar to the case of magic nucleon numbers, it varies in the vicinity of $\alpha \approx 1/2$. For the special case of sodium clusters, the lowest four magic numbers are reproduced with $\alpha > 1/2$, while up to $\mathcal{N} = 198$ $\alpha < 1/2$ is sufficient. Within the back bending region there is a sudden change in α , which we call a fractional second order phase transition, followed by a linear increase of the α value for larger cluster sizes. The resulting dependence $\alpha(\mathcal{N})$ is shown in figure 22.2.

In order to compare our calculated shell correction with published results, we use the Strutinsky method [Strutinsky (1967b); Strutinsky (1968)] with the following parameters:

$$\hbar\omega_0 = 3.96\mathcal{N}^{-\frac{1}{3}} [\text{eV}] \quad (22.23)$$

$$\omega_1 = 1 \quad (22.24)$$

$$\omega_2 = 1 \quad (22.25)$$

$$\omega_3 = 1 \quad (22.26)$$

$$\alpha = \begin{cases} 0.55 & \mathcal{N} < 43 \\ 0.908 - 0.000834\mathcal{N} & \mathcal{N} < 51 \\ 0.482 + 0.000025\mathcal{N} & \mathcal{N} < 260 \\ 0.069 + 0.000139(\mathcal{N} - 260) & \mathcal{N} < 900 \\ 0.062 + 0.000083(\mathcal{N} - 260) & \mathcal{N} \geq 900 \end{cases} \quad (22.27)$$

$$\gamma = 1.1 \hbar\omega_0 \left({}_{\text{R}}[\mathcal{N}^{1/3} + 1] - {}_{\text{R}}[\mathcal{N}^{1/3}] \right)^3 \quad (22.28)$$

$$m = 4 \quad (22.29)$$

(22.28) follows from the plateau condition $\partial U / \partial \gamma = 0$ and (22.29) is the order of included Hermite polynomials for the Strutinsky shell correction method.

In figure 22.3 the resulting shell correction δU is plotted. Magic numbers are reproduced correctly within the experimental errors. Furthermore we obtain a nearly quantitative agreement with published results for the shell correction term obtained e.g. with the spherical Woods-Saxon potential [Bjornholm *et al.* (1990); Nishioka *et al.* (1990)].

Summarizing the results presented so far, the proposed Caputo-Caputo-Riemann symmetric rotor describes the magic numbers and microscopic

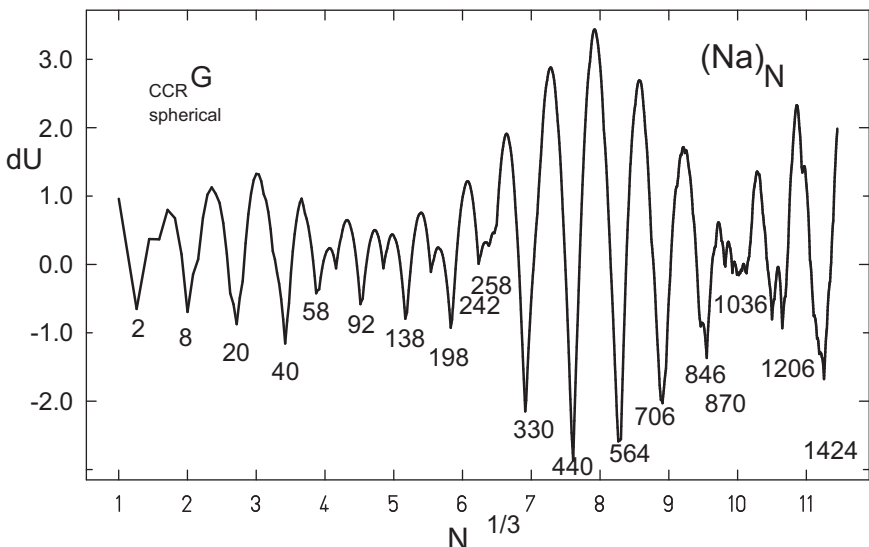


Fig. 22.3 Calculated shell correction dU as a function of cluster size \mathcal{N} for the Caputo-Caputo-Riemann fractional symmetric spherical rotor with parameter set (22.23)-(22.29). This graph should be directly compared with [Bjornholm *et al.* (1990)].

part of the total binding energy for metal clusters with reasonable accuracy. We have demonstrated, that the cluster shell structure may indeed be successfully described on the basis of a dynamical symmetry model.

The behavior of metallic clusters is dominated by electromagnetic forces, while in nuclei the long range part of strong forces is important. Therefore it has been shown that two out of the four different decompositions (21.15)-(21.18) of the 9-dimensional fractional rotation group generate dynamical symmetries, which dominate the ground state properties of atomic nuclei and metallic clusters.

22.3 Metaphysics: magic numbers for clusters bound by weak and gravitational forces respectively

We have demonstrated, that the Caputo-Caputo-Riemann rotor (22.2) correctly determines the magic numbers of metal clusters and that the Caputo-Riemann-Riemann rotor (21.47) is an appropriate tool to describe the ground state properties of nuclei with reasonable accuracy. Both models

differ only in the mixing ratio of fractional derivatives. The phenomena described, differ only in the interaction type of the constituents which build up the cluster. The behavior of metallic clusters is dominated by electromagnetic forces, while in nuclei the long range part of strong forces is important.

Therefore we postulate, that the group decomposition (21.15)

$${}_{\text{RRR}}G \supset {}_{\text{R}}SO^{\alpha}(3) \supset {}_{\text{R}}SO^{\alpha}(3) \supset {}_{\text{R}}SO^{\alpha}(3) \quad (22.30)$$

will determine the magic number of a cluster, which is dominated by a gravitational type of interaction between its constituents.

The Hamiltonian ${}_{\text{RRR}}H$

$${}_{\text{RRR}}H = \frac{\omega_1}{\hbar} {}_{\text{R}}L_1^2(\alpha) + \frac{\omega_2}{\hbar} {}_{\text{R}}L_2^2(\alpha) + \frac{\omega_3}{\hbar} {}_{\text{R}}L_3^2(\alpha) \quad (22.31)$$

with the free deformation parameters $\omega_1, \omega_2, \omega_3$ on a basis $|L_1 M_1 L_2 M_2 L_3 M_3\rangle$ may be diagonalized and with the symmetries (21.42) and (21.43) a level spectrum

$$\begin{aligned} E(\alpha) &= \hbar\omega_1 {}_{\text{R}}[2n_1]_R [2n_1 + 1] + \hbar\omega_2 {}_{\text{R}}[2n_2]_R [2n_2 + 1] \\ &\quad + \hbar\omega_3 {}_{\text{R}}[2n_3]_R [2n_3 + 1] \end{aligned} \quad (22.32)$$

$$= \sum_{i=1}^3 \hbar\omega_i \frac{\Gamma(1 + (2n_i + 1)\alpha)}{\Gamma(1 + (2n_i - 1)\alpha)} \quad (22.33)$$

$$n_1, n_2, n_3 = 0, 1, 2, \dots$$

on a basis $|2n_1 2n_1 2n_2 2n_2 2n_3 2n_3\rangle$ results.

For the idealized spherical case $\alpha = 1/2$ this spectrum is simply given by:

$$E(\alpha = 1/2) = \hbar\omega_0 \left(n_1 + n_2 + n_3 + \frac{3}{2} \right) \quad (22.34)$$

which is the spectrum of the deformed harmonic oscillator. In the spherical case, magic numbers are determined by:

$$n_{\text{RRR}} = \frac{1}{3}(N + 1)(N + 2)(N + 3) \quad N = 0, 1, 2, 3, \dots \quad (22.35)$$

$$= 2, 8, 20, 40, 70, 112, 168, 240, \dots \quad (22.36)$$

at energies

$$E(N)_{\text{RRR}} = \hbar\omega_0(N + 3/2) \quad (22.37)$$

This result may be compared with solutions for an independent particle shell model, where the potential is determined by a uniformly distributed

gravitational charge (mass) distribution $\rho(r) = q/V$ inside a sphere. This potential is given by

$$V(r) = \int \int \int \frac{\rho(r')}{|r - r'|} d^3 r' \quad (22.38)$$

$$= q \left(\frac{r^2}{2R_0^3} - \frac{3}{2R_0} \right) \quad r < R_0 \quad (22.39)$$

and leads to a radial Schrödinger equation for the harmonic oscillator.

Therefore we are led to the prediction, that for microscopic clusters with gravitational type of interaction of the constituents there will be variations in the binding energy per mass unit according to (22.35). We cannot predict the value of the mass unit, but since the magnitude of shell corrections for metal clusters is of order eV and for nuclear shell corrections of order MeV, we assume the magnitude of shell corrections for gravity dominated clusters to be of order TeV, which amounts about 1000 proton masses or $10^{-23}[\text{kg}]$.

Consequently we are left with the fourth decomposition of the 9-dimensional fractional rotation group (21.18)

$${}_{\text{ccc}}G \supset {}_{\text{c}}SO^\alpha(3) \supset {}_{\text{c}}SO^\alpha(3) \supset {}_{\text{c}}SO^\alpha(3) \quad (22.40)$$

The Hamiltonian ${}_{\text{ccc}}H$

$${}_{\text{ccc}}H = \frac{\omega_1}{\hbar} {}_{\text{c}}L_1^2(\alpha) + \frac{\omega_2}{\hbar} {}_{\text{c}}L_2^2(\alpha) + \frac{\omega_3}{\hbar} {}_{\text{c}}L_3^2(\alpha) \quad (22.41)$$

with the free deformation parameters $\omega_1, \omega_2, \omega_3$ on a basis $|L_1 M_1 L_2 M_2 L_3 M_3\rangle$ may be diagonalized and with the symmetries (21.42) and (21.43) a level spectrum

$$\begin{aligned} E(\alpha) = & \hbar\omega_1 {}_{\text{c}}[2n_1]_c [2n_1 + 1] + \hbar\omega_2 {}_{\text{c}}[2n_2]_c [2n_2 + 1] \\ & + \hbar\omega_3 {}_{\text{c}}[2n_3]_c [2n_3 + 1] \end{aligned} \quad (22.42)$$

$$\begin{aligned} & = \sum_{i=1}^3 \hbar\omega_i \frac{\Gamma(1 + (2n_i + 1)\alpha)}{\Gamma(1 + (2n_i - 1)\alpha)} \\ & - \delta_{n_1 0} \hbar\omega_1 \frac{\Gamma(1 + \alpha)}{\Gamma(1 - \alpha)} - \delta_{n_2 0} \hbar\omega_2 \frac{\Gamma(1 + \alpha)}{\Gamma(1 - \alpha)} - \delta_{n_3 0} \hbar\omega_3 \frac{\Gamma(1 + \alpha)}{\Gamma(1 - \alpha)} \\ & n_1, n_2, n_3 = 0, 1, 2, \dots \end{aligned} \quad (22.43)$$

on a basis $|2n_1 2n_1 2n_2 2n_2 2n_3 2n_3\rangle$ results.

We call this model the Caputo-Caputo-Caputo symmetric rotor. For the idealized spherical case $\alpha = 1/2$ this spectrum is simply given by:

$$E(\alpha = 1/2) = \hbar\omega_0 \left(n_1 + n_2 + n_3 + \frac{3}{2} - \frac{1}{2}\delta_{n_1 0} - \frac{1}{2}\delta_{n_2 0} - \frac{1}{2}\delta_{n_3 0} \right) \quad (22.44)$$

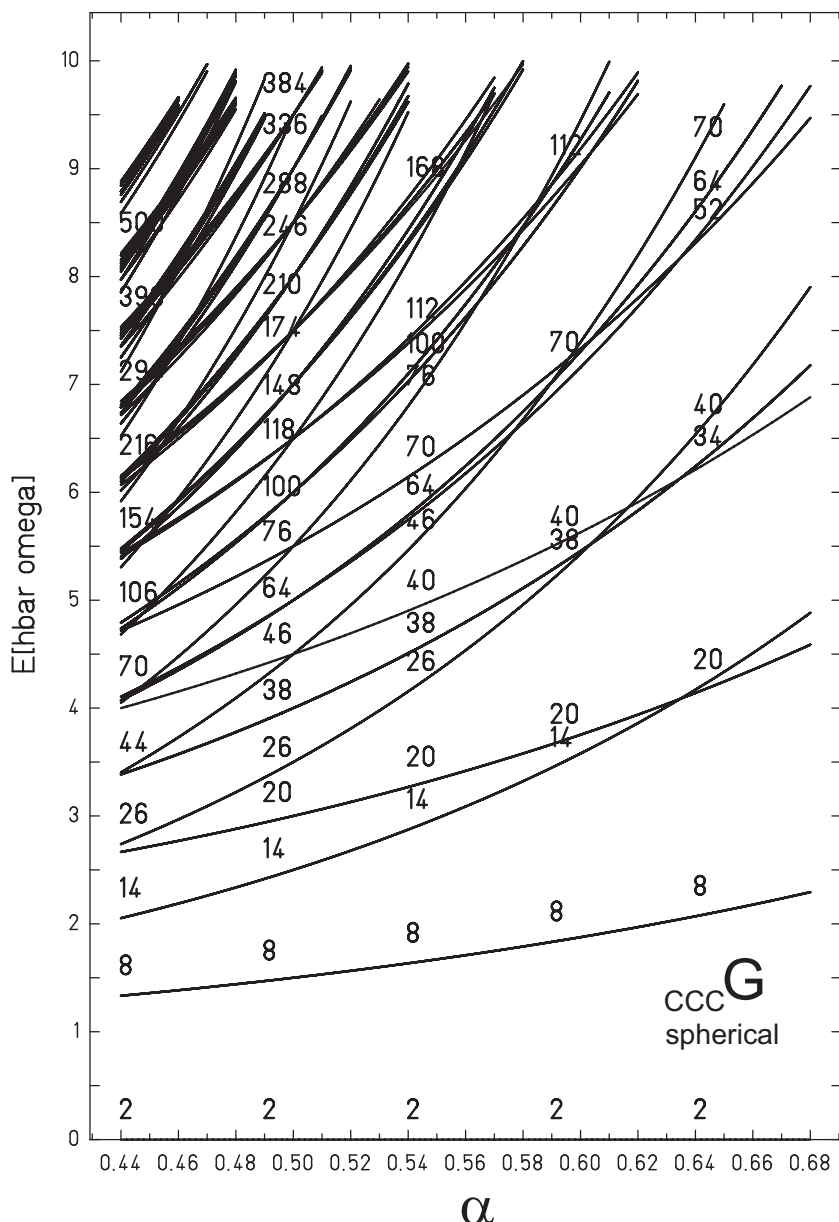


Fig. 22.4 Level diagram of the Caputo-Caputo-Caputo symmetric rotor for the spherical case in the vicinity of $\alpha \approx 1/2$.

Table 22.1 Sequence of magic numbers for the four different decompositions of $SO(9)^{\alpha=1/2}$. Braces indicate equivalent magic numbers from the harmonic oscillator sequence.

group	cluster type	.	2	8	20	40	70	112	168	240
$RRR G$	gravity?	.	2	8	20	40	70	112	168	240
$CRR G$	strong	(2)	6	14	28	50	82	126	184	258
$CCR G$	electro-magnetic	(2)	8	18	34	58	92	138	198	274
$CCC G$	weak?	(2)	(8)	20	38	64	100	148	210	288

We obtain a first set $_{CCC}n_{\text{magic } 1}$ of magic numbers

$$_{CCC}n_{\text{magic } 1} = n_{HO} + 6 \quad N = 0, 1, 2, 3, \dots \quad (22.45)$$

$$= \frac{1}{3}(N+1)(N+2)(N+3) + 6 \quad (22.46)$$

$$= 8, 14, 26, 46, 76, 118, 174, 246, 336, 446, \dots \quad (22.47)$$

at energies

$$E(N)_{CCC}n_{\text{magic } 1} = \hbar\omega_0(N+3/2) \quad (22.48)$$

In addition we obtain a second set $_{CCC}n_{\text{magic } 2}$ of magic numbers

$$_{CCC}n_{\text{magic } 2} = _{CCC}n_{\text{magic } 1} + 6N \quad N = 1, 2, 3, \dots \quad (22.49)$$

$$= \frac{1}{3}(N+1)(N+2)(N+3) + 6(N+1) \quad (22.50)$$

$$= 20, 38, 64, 100, 148, 210, 288, \dots \quad (22.51)$$

at energies

$$E(N)_{CCC}n_{\text{magic } 2} = \hbar\omega_0(N+1) \quad (22.52)$$

Finally, the state $|000000\rangle$ with a 2-fold multiplicity has energy $E = 0$ and therefore does fit into one of the two derived series.

Consequently we are led to the prediction, that for microscopic clusters with weak interaction type of the constituents there will be variations in the binding energy per charge unit according to (22.49). We estimate the order of magnitude of shell corrections for weak interaction dominated clusters to be $10^{-6}[\text{eV}]$, which seems reasonable for e.g. a neutrino-cluster.

Summarizing the results presented in this section, we have associated the four different decompositions (21.15)-(21.18) of the 9-dimensional mixed fractional rotation group with the four fundamental types of interaction found in nature. We found common aspects determining the magic numbers for each group. There are always two different sets of magic numbers, one set is a shifted harmonic oscillator set, the other set is specific to the group

considered. For the spherical and idealized case $\alpha = 1/2$ the four different sequences of magic number sets are simply the result of the presence or absence of a Kronecker-delta.

Our investigations lead to the conclusion, that mixed fractional derivative type field theories may play an important role in a unified theory including all four fundamental interactions.

This page intentionally left blank

Chapter 23

Fractors — Fractional Tensor Calculus

No specific theory of fractional tensor calculus exists up to now. In the following we propose notations, which may be of use for a formulation of such a theory. Especially we propose to interpret the fractional derivative parameter α as an extension of tensor calculus on a level similar to spin, which leads to the definition of spinors [Schmutzler (1968)].

Consequently the objects considered in fractional tensor calculus may be called fractors.

23.1 Covariance for fractional tensors

Especially the fractional derivative and in general the quantities being investigated, are elements of a direct product space of the discrete coordinate space, whose discrete coordinate indices are denoted by $\mu, \nu, \dots = 0, \dots, 3$ and the continuous space of fractional derivatives, which are labeled with $\alpha, \beta, \dots \in \mathbb{R}$. These are real numbers, which in the case $\alpha < 0$ or $\beta < 0$ are interpreted as a fractional integral of order α and β respectively.

For the covariant fractional derivatives of order α we introduce the short hand notations

$$\frac{\partial^\alpha}{\partial(x^\mu)^\alpha} f = \partial_\mu^\alpha f = f|_\mu^\alpha \quad (23.1)$$

Einstein's summation convention for tensors e.g.

$$\partial_\mu = g_{\mu\nu} \partial^\nu = \sum_{\nu=0}^3 g_{\mu\nu} \partial^\nu \quad (23.2)$$

is extended to the continuous case for the fractional derivative coefficients

$$\partial_\alpha = g_{\alpha\beta} \partial^\beta = \int_{\beta=-\infty}^{+\infty} d\beta \hat{g}(\alpha, \beta) \partial^\beta \quad (23.3)$$

where $\hat{g}(\alpha, \beta)$ is an appropriately chosen function of the two variables α, β .

Hence we define the generalized metric tensor

$$\eta_{\alpha\beta}^{\mu\nu} = \text{diag}\{-1, 1, 1, 1\}\delta(\alpha - \beta) \quad (23.4)$$

where $\delta(\alpha - \beta)$ is the Dirac delta function for raising and lowering of indices.

Therefore the fractional derivative objects are formally described in a manner similar to the case of spinor objects. A quantity like e.g. $F_{\mu\nu}^\alpha$ transforms as a tensor of rank 2 in coordinate space and as a vector in the sense of (23.3) in fractional derivative space, which in analogy to spinors we may call a fractor of rank one.

With these definitions, the contravariant fractional derivative follows as:

$$\partial_\alpha^\mu f = f_\alpha^{|\mu} = \eta_{\alpha\beta}^{\mu\nu} \partial_\nu^\beta f \quad (23.5)$$

A scalar quantity like the Lagrange density of a fractional electromagnetic field is then generated by contracting the indices in the usual way:

$$\mathcal{L}_{\text{fEM}} = -\frac{1}{4} F_{\mu\nu}^\alpha F_\alpha^{\mu\nu} \quad (23.6)$$

23.2 Singular fractional tensors

Finally, we have to resolve an ambiguity, which is specific to fractional tensor calculus. For $\alpha = 0$ the use of the fractional derivative introduces an index and therefore

$$\partial_\mu^0 f = f \quad (23.7)$$

obviously violates the principle of covariance, since the tensor rank differs for left and right hand side of (23.7). Consequently we introduce the Kronecker delta δ_0^μ :

$$\delta_0^\mu \partial_\mu^0 f = \delta_0^0 \partial_0^\mu f = f \quad (23.8)$$

and perform a pseudo-summation, which is reduced to a single term. We introduce the abbreviations

$$\delta_0^\mu \partial_\mu^0 = \delta^{(\mu)} \quad (23.9)$$

$$\delta_\mu^0 \partial_0^\mu = \delta_{(\mu)} \quad (23.10)$$

and call (μ) a pseudo index, where summation is performed, but the tensor properties in fractional coordinate space are not affected.

The Kronecker delta may be generalized to

$$\delta_{(\mu)}^\tau \partial_\tau^\alpha f = \partial_{(\mu)}^\alpha f \quad (23.11)$$

where $\partial_{(\mu)}^\alpha f$ transforms like a scalar in fractional coordinate space, but the derivative with respect to μ is performed. With this definition, the Kronecker delta will be used like

$$\delta_{(\mu)}^{\tau\sigma} \partial_\tau^\alpha \partial_\sigma^{-\beta} f = \delta_{(\mu)}^\tau \partial_\tau^{\alpha-\beta} f = \partial_{(\mu)}^{\alpha-\beta} f \quad (23.12)$$

Hence introducing the Kronecker delta extends manifest covariant tensor calculus in a reasonable way to fractional derivative tensors.

This page intentionally left blank

Chapter 24

Fractional Fields

The dynamical behavior of fields may be deduced with appropriately chosen equations of motion, which in general will be a complex system of interdependent components.

Introducing a Lagrangian density, which is a function of the fields and their derivatives allows for an elegant description from a generalized point of view, since it is a scalar quantity, from which the field equations may be deduced using a variation principle.

Hence a Lagrangian density serves as a starting point to model a dynamic field theory.

Classical examples for Lagrangian densities, which play an important role in physics include:

- *The Lagrangian density of the electromagnetic field has two terms, one for the electric charge density J_μ coupled to an external potential A_μ and another term with the electromagnetic field strength tensor $F_{\mu\nu}$:*

$$\mathcal{L}_{EM} = J^\mu A_\mu - \frac{1}{4} F_{\mu\nu} F^{\mu\nu} \quad (24.1)$$

- *The Lagrangian density for a free Dirac-field is given by:*

$$\mathcal{L}_D = \bar{\psi}(i\gamma^\mu \partial_\mu + m)\psi \quad (24.2)$$

- *For the simplest version of quantum hadrodynamics of relativistic nuclear matter [Serot and Walecka (1986)] the Walecka model is defined starting with a Lagrangian density for the nucleon (ψ), the neutral scalar (ϕ) and the vector (ω^μ) mesonic fields:*

$$\begin{aligned} \mathcal{L}_W = & i\bar{\psi}\partial_\mu\gamma^\mu\psi - M\bar{\psi}\psi + \bar{\psi}(g_s\phi - g_v\omega_\mu\gamma^\mu)\psi \\ & + \frac{1}{2}[\partial_\mu\phi\partial^\mu\phi - m_s^2\phi^2] - \frac{1}{4}\mathcal{F}^{\mu\nu}\mathcal{F}_{\mu\nu} + \frac{1}{2}m_v^2\omega^2 \end{aligned} \quad (24.3)$$

where M , m_s , m_v are the masses of the nucleon, scalar and vector mesons, respectively; g_s , g_v are the coupling constants and $\mathcal{F}^{\mu\nu} = \partial^\mu\omega^\nu - \partial^\nu\omega^\mu$.

- Last not least, the Landau-Ginzburg model of super conductivity, which is one of the ancestors of the non-Abelian Higgs-model [Higgs (1964)] is based on a Lagrangian density of the form:

$$\mathcal{L}_{LG} = \frac{1}{4}F^{\mu\nu}F_{\mu\nu} + (D_\mu\phi)(D^\mu\phi) + V(|\phi|) \quad (24.4)$$

where the gauge covariant derivative D_μ is given as

$$D_\mu\phi = \partial_\mu\phi - igA_\mu\phi \quad (24.5)$$

and the potential $V(|\phi|)$ models a self-interaction

e.g. $V(|\phi|) = \phi^4$.

In modern theory the Lagrangian density is the formal tool to model dynamic properties of fields.

Since we want to investigate the properties of fractional fields, a formulation in terms of fractional Lagrangian densities could be helpful and is a research area of increasing interest [Baleanu and Muslih (2005); Agrawal (2007); El-Nabulsi and Torres (2008); Baleanu and Trujillo (2010); Odziewicz et al. (2013c)].

Fractional Lagrangian densities are functions of fractional fields and their fractional derivatives. Hence we will first derive appropriate fractional Euler-Lagrange equations using an extended variation principle.

We will then demonstrate, that the proposed procedure may be applied to the free fields, e.g. for the Dirac matter field leading to the fractional Dirac equation and e.g. for a fractional gauge field, which leads to a fractional extension of the Maxwell equations.

In the next chapter we will then extend the principle of local gauge invariance to fractional fields and will indeed determine the exact form of a gauge invariant coupling of the fractional gauge field to the fractional matter field. The result is a fractional gauge invariant extension of the standard QED.

24.1 Fractional Euler-Lagrange equations

The covariant expression for the action S is defined as the time integral of the Lagrangian L

$$S = \int L dt \quad (24.6)$$

where the Lagrangian is related to the Lagrangian density \mathcal{L} by

$$L = \int \mathcal{L} d^3x \quad (24.7)$$

As long as the Lagrangian density is a function of the field ϕ and its derivatives $\phi_{|\mu}$, the classical Euler-Lagrange-equations follow from the vanishing variation of the action

$$\delta S = 0 \quad (24.8)$$

as

$$\frac{\partial}{\partial \phi} \mathcal{L} - \partial_\mu \frac{\partial \mathcal{L}}{\partial \phi_{|\mu}} = 0 \quad (24.9)$$

We now want to extend this formalism to fractional fields. We will investigate a simple example and derive the fractional Euler-Lagrange-equations for a Lagrangian density, which contains as independent variables the field ϕ and its fractional derivatives $\phi_{|\mu}^\alpha$. Starting point is the fractional action:

$$S = \int \mathcal{L}(\phi, \phi_{|\mu}^\alpha) d^3x dt \quad (24.10)$$

We will determine the variation of the action by the limiting procedure

$$\delta S = \lim_{h \rightarrow 0} \frac{\Delta S}{h} \quad (24.11)$$

with

$$\Delta S = \int \left(\mathcal{L}(\phi + h \delta\phi, \phi_{|\mu}^\alpha + h \delta(\phi_{|\mu}^\alpha)) - \mathcal{L}(\phi, \phi_{|\mu}^\alpha) \right) d^3x dt \quad (24.12)$$

A series expansion up to first order in h leads to

$$\Delta S = \int \left(h \frac{\partial \mathcal{L}}{\partial \phi} \delta\phi + h \sum_{\mu=0}^4 \frac{\partial \mathcal{L}}{\partial \phi_{|\mu}^\alpha} \delta\phi_{|\mu}^\alpha \right) d^3x dt \quad (24.13)$$

or

$$\frac{\Delta S}{h} = \int \left(\frac{\partial \mathcal{L}}{\partial \phi} \delta\phi + \sum_{\mu=0}^4 \frac{\partial \mathcal{L}}{\partial \phi_{|\mu}^\alpha} \delta\phi_{|\mu}^\alpha \right) d^3x dt \quad (24.14)$$

For reasons of simplicity we will ignore surface effects and therefore we demand, that the Lagrangian density vanishes at infinity. In addition we use the property of the scalar product:

$$\int_{-\infty}^{+\infty} f g_{|\mu}^\alpha dx_\mu = \mp \int_{-\infty}^{+\infty} f_{|\mu}^\alpha g dx_\mu \quad (24.15)$$

The minus sign holds for odd fractional derivatives (Liouville-, Fourier-, 3., 5., ... order). The plus sign for all even fractional derivatives (Riesz-, 4., 6., ... order).

Hence partial integration of (24.14) leads to:

$$\frac{\Delta S}{h} = \int \left(\frac{\partial \mathcal{L}}{\partial \phi} \delta \phi \mp \sum_{\mu=0}^4 \partial_{\mu}^{\alpha} \left(\frac{\partial \mathcal{L}}{\partial \phi_{|\mu}^{\alpha}} \right) \delta \phi \right) d^3 x dt \quad (24.16)$$

$$= \int \left(\frac{\partial \mathcal{L}}{\partial \phi} \mp \sum_{\mu=0}^4 \partial_{\mu}^{\alpha} \left(\frac{\partial \mathcal{L}}{\partial \phi_{|\mu}^{\alpha}} \right) \right) \delta \phi d^3 x dt \quad (24.17)$$

According to (24.8) for $h \rightarrow 0$ we obtain the fractional Euler-Lagrange-equations

$$\frac{\partial \mathcal{L}}{\partial \phi} \mp \sum_{\mu=0}^4 \partial_{\mu}^{\alpha} \left(\frac{\partial \mathcal{L}}{\partial \phi_{|\mu}^{\alpha}} \right) = 0 \quad (24.18)$$

As an example we propose a Lagrangian density for a free fractional Dirac-field:

$$\mathcal{L}_D^{\text{free}} = \bar{\Psi} (i \gamma_{\alpha}^{\mu} \partial_{\mu}^{\alpha} + \mathbf{1}_{\alpha} m^{\alpha}) \Psi \quad (24.19)$$

where $\mathbf{1}_{\alpha}$ indicates a $n \times n$ unit matrix with dimension $n = (2/\alpha)^2$. Using (24.18) the variation with respect to $\bar{\Psi}$ results in the fractional Dirac equation

$$(i \gamma_{\alpha}^{\mu} \partial_{\mu}^{\alpha} + \mathbf{1}_{\alpha} m^{\alpha}) \Psi = 0 \quad (24.20)$$

The hitherto presented strategy for a derivation of Euler-Lagrange-equations may be easily extended to more complex Lagrangian density types (see e.g. [Muslih (2010b)]).

For Lagrangian densities of type

$$\mathcal{L} = \mathcal{L}(\phi, \phi_{|\mu}^{\alpha}, \phi_{|\mu}^{-\alpha}, \phi_{|\mu}^{-\alpha+1}, \dots, \phi_{|\mu}^{-\alpha+k}) \quad (24.21)$$

we obtain a corresponding set of extended fractional Euler-Lagrange-equations:

$$\frac{\partial \mathcal{L}}{\partial \phi} \mp \partial_{\mu}^{\alpha} \frac{\partial \mathcal{L}}{\partial (\phi_{|\mu}^{\alpha})} \mp \sum_{n=0}^k (-1)^n \partial_{\mu}^{-\alpha+n} \frac{\partial \mathcal{L}}{\partial (\phi_{|\mu}^{-\alpha+n})} = 0 \quad (24.22)$$

24.2 The fractional Maxwell equations

In this section we will demonstrate that the direct fractional extension of the ordinary Lagrange density for the electromagnetic field determines fractional Maxwell equations and consequently leads to fractional wave equations for the electric and magnetic field respectively.

We will first derive these equations for a general fractional derivative and will then discuss a specific use of the Riemann- and Caputo fractional derivative definition in the next section. We define the fractional extension of the standard field strength tensor

$$F_{\mu\nu}^\alpha = \partial_\nu^\alpha A_\mu - \partial_\mu^\alpha A_\nu \quad (24.23)$$

The potential A_μ is not uniquely determined. Adding a four-gradient of an arbitrary scalar function $\phi^\alpha(x, y, z, t)$

$$A'_\mu = A_\mu + \partial_\mu^\alpha \phi = A_\mu + \phi_{|\mu}^\alpha \quad (24.24)$$

because of

$$\partial_\mu^\alpha \partial_\nu^\alpha \phi = \partial_\nu^\alpha \partial_\mu^\alpha \phi \quad (24.25)$$

leaves the form of the field strength tensor unchanged and is therefore called a local gauge transformation.

The Lagrange density for a fractional electromagnetic field \mathcal{L}_{fEM} is given by

$$\mathcal{L}_{\text{fEM}} = -\frac{1}{4} F_{\mu\nu}^\alpha F_\alpha^{\mu\nu} \quad (24.26)$$

A variation of \mathcal{L}_{fEM} with respect to the fractional potential A_μ leads to the fractional inhomogeneous Maxwell equations

$$\partial_\mu^\alpha F_\alpha^{\mu\nu} = 0 \quad (24.27)$$

since the four-current j^ν is vanishing in the absence of external sources. We have to show, that the definition of the fractional field strength tensor (24.23) and the corresponding derived field equations (24.27) lead to reasonable results. As a typical example we will derive fractional wave equations which may be used for a description of fractional electromagnetic fields.

Therefore in the following we will derive the vacuum solutions for the fractional Maxwell equations.

We set $\vec{E} = \{E_1, E_2, E_3\}$ and $\vec{B} = \{B_1, B_2, B_3\}$ and present the explicit form for the field strength tensor:

$$F_\alpha^{\mu\nu} = \begin{pmatrix} 0 & -E_1 & -E_2 & -E_3 \\ E_1 & 0 & -B_3 & B_2 \\ E_2 & B_3 & 0 & -B_1 \\ E_3 & -B_2 & B_1 & 0 \end{pmatrix} \quad (24.28)$$

We insert into (24.27):

$$\nabla^\alpha \vec{E} = 0 \quad (24.29)$$

$$\nabla^\alpha \times \vec{B} = \partial_t^\alpha \vec{E} \quad (24.30)$$

where we have introduced the del or nabla operator $\nabla^\alpha = \{\partial_1^\alpha, \partial_2^\alpha, \partial_3^\alpha\}$.

The homogeneous Maxwell equations may be derived by introducing the dual field strength tensor $\mathcal{F}^{\alpha,\mu\nu}$ which is given with the Levi-Civitta symbol $\epsilon_{\mu\nu\rho\sigma}$ as:

$$\mathcal{F}_{\mu\nu}^\alpha = \frac{1}{2} \epsilon_{\mu\nu\rho\sigma} F^{\alpha,\rho\sigma} \quad (24.31)$$

With the condition

$$\partial_\alpha^\mu \mathcal{F}_{\mu\nu}^\alpha = 0 \quad (24.32)$$

and with

$$F_{\mu\nu}^\alpha = \begin{pmatrix} 0 & E_1 & E_2 & E_3 \\ -E_1 & 0 & -B_3 & B_2 \\ -E_2 & B_3 & 0 & -B_1 \\ -E_3 & -B_2 & B_1 & 0 \end{pmatrix} \quad (24.33)$$

we obtain:

$$\nabla^\alpha \vec{B} = 0 \quad (24.34)$$

$$\nabla^\alpha \times \vec{E} = -\partial_t^\alpha \vec{B} \quad (24.35)$$

The relations (24.29),(24.30),(24.34),(24.35) are the fractional Maxwell equations for the vacuum.

Since we intend to derive a wave equation for the fractional electromagnetic field, we will eliminate \vec{E} and \vec{B} respectively from these equations.

We illustrate the procedure for an elimination of \vec{E} :

An application of the curl-operator to (24.30)

$$\nabla^\alpha \times (\nabla_\alpha \times \vec{B}) = \partial_t^\alpha (\nabla_\alpha \times \vec{E}) \quad (24.36)$$

and inserting (24.35) leads to:

$$\nabla^\alpha \times (\nabla_\alpha \times \vec{B}) = -\partial_t^\alpha \partial_t^\alpha \vec{B} \quad (24.37)$$

Let us introduce the fractional Laplace operator Δ_α^α and the fractional d'Alembert operator \square_α^α .

$$\Delta_\alpha^\alpha = \partial_x^\alpha \partial_\alpha^x + \partial_y^\alpha \partial_\alpha^y + \partial_z^\alpha \partial_\alpha^z \quad (24.38)$$

$$\square_\alpha^\alpha = \Delta_\alpha^\alpha - \partial_t^\alpha \partial_\alpha^t \quad (24.39)$$

Using the identity $\nabla^\alpha \times (\nabla_\alpha \times \vec{B}) = \nabla^\alpha(\nabla_\alpha \cdot \vec{B}) - \Delta_\alpha^\alpha \vec{B}$ and because of $\nabla^\alpha \vec{B} = 0$ we obtain for (24.37):

$$\Delta_\alpha^\alpha \vec{B} = \partial_t^\alpha \partial_\alpha^t \vec{B} \quad (24.40)$$

$$\square_\alpha^\alpha \vec{B} = 0 \quad (24.41)$$

In a similar procedure we may eliminate \vec{B} from the fractional Maxwell equations and obtain:

$$\Delta_\alpha^\alpha \vec{E} = \partial_t^\alpha \partial_\alpha^t \vec{E} \quad (24.42)$$

$$\square_\alpha^\alpha \vec{E} = 0 \quad (24.43)$$

Therefore both vectors \vec{E} and \vec{B} fulfill the same type of a fractional wave equation.

Hence we have demonstrated that the use of the fractional Lagrange density (24.26) leads to a fractional wave equation.

Of course, an interesting question is the physical interpretation and relevance of the proposed fractional Maxwell-equations.

Therefore in the next section we will investigate the properties of fractional interacting fields. We will apply the principle of local gauge invariance to determine the interaction term of a fractional Dirac matter field with a fractional electromagnetic gauge field.

We will obtain a fractional generalization of quantum electrodynamics, which for $\alpha = 1$ reduces to classical QED, which describes with a very high accuracy the interaction of electrons with photons.

Since QED is the most successful theory ever, we will not explore the fractional QED in the vicinity of $\alpha \approx 1$. But for $\alpha \neq 1$ we expect a quantum theory, which extends the standard QED to fractional QED, which describes an interaction of a fractional matter field with a fractional gauge field. Hence the coupling of more complex charge types is described with such a fractional field theory.

We will give a physical interpretation of the proposed fractional fields in terms of quantum chromodynamics (QCD) and will identify the fractional matter field with quarks and the fractional gauge field with gluons.

24.3 Discussion

24.3.1 Lagrangian density for a space fractional Schrödinger equation

question:

What is the correct Lagrangian density for the space fractional Schrödinger equation using e.g. the Riesz derivative definition?

answer:

For reasons of simplicity we restrict our derivation to one space dimension.

Let us first recall, that for a Lagrangian density for a classical field $\Psi(x, t)$ of type

$$\mathcal{L} = \mathcal{L}(\Psi, \Psi_x^{(1)}, \Psi_x^{(2)}, \dots, \Psi_x^{(N)}, \Psi_t) \quad (24.44)$$

with the abbreviations

$$\Psi_x^{(n)} = \partial_x^n \Psi(x, t) \quad n = 1, 2, \dots, N \quad (24.45)$$

$$\Psi_t = \partial_t \Psi(x, t) \quad (24.46)$$

the Euler-Lagrange-equations are explicitly given as [Greiner and Maruhn (1997a)]:

$$\frac{\partial \mathcal{L}}{\partial \Psi} + \sum_{n=1}^k (-1)^n \partial_x^n \frac{\partial \mathcal{L}}{\partial (\Psi_x^{(n)})} - \partial_t \frac{\partial \mathcal{L}}{\partial (\Psi_t)} = 0 \quad (24.47)$$

The classical Schrödinger equation including a potential term $V(x, t)$

$$i\hbar \Psi_t = \left(-\frac{\hbar^2}{2m} \partial_x^2 + V(x, t) \right) \Psi \quad (24.48)$$

is resulting from the following Lagrangian density for the classical Schrödinger field $\Psi(x, t)$

$$\mathcal{L}(\Psi, \Psi_x^{(1)}, \Psi_t) = \frac{i\hbar}{2} (\Psi^* \Psi_t - \Psi_t^* \Psi) - \frac{\hbar^2}{2m} (\partial_x \Psi^*) (\partial_x \Psi) + V(x, t) \Psi^* \Psi \quad (24.49)$$

which immediately follows, treating $\Psi(x, t)$ and $\Psi^*(x, t)$ as two independent fields, since (24.47) reduces to the set:

$$\frac{\partial \mathcal{L}}{\partial \Psi} - \partial_x \frac{\partial \mathcal{L}}{\partial (\Psi_x^{(1)})} - \partial_t \frac{\partial \mathcal{L}}{\partial (\Psi_t)} = 0 \quad (24.50)$$

$$\frac{\partial \mathcal{L}}{\partial \Psi^*} - \partial_x \frac{\partial \mathcal{L}}{\partial (\Psi_x^{*(1)})} - \partial_t \frac{\partial \mathcal{L}}{\partial (\Psi_t^*)} = 0 \quad (24.51)$$

which then generates the Schrödinger equation (24.48) and its complex conjugate.

In analogy to this classical approach we will now derive the space fractional Schrödinger equation from an appropriately defined Lagrange density. We will use as a specific realization of the fractional derivative the Riesz definition and set in analogy to (24.49);

$$\begin{aligned} {}_{\text{RZ}}\mathcal{L}(\Psi, {}_{\text{RZ}}\Delta^{\alpha/2}\Psi, \Psi_t) &= \frac{i\hbar}{2}(\Psi^*\Psi_t - \Psi_t^*\Psi) \\ &\quad - (\mathcal{D}_{\alpha/4}{}_{\text{RZ}}\Delta^{\alpha/4}\Psi^*)(\mathcal{D}_{\alpha/4}{}_{\text{RZ}}\Delta^{\alpha/4}\Psi) \\ &\quad + V(x, t)\Psi^*\Psi \quad 0 < \alpha < 2 \end{aligned} \quad (24.52)$$

where \mathcal{D}_α is a constant in units [MeV m $^\alpha$ s $^{-\alpha}$], and ${}_{\text{RZ}}\Delta^{\alpha/2}$ is the Riesz derivative. For our purpose, we will use the differential representation (13.51):

$${}_{\text{RZ}}\Delta^{\alpha/2} = -\frac{1}{\cos(\alpha\pi/2)} \lim_{\omega \rightarrow 0} |\omega|^\alpha \sum_{j=0}^{\infty} \binom{\alpha}{2j} \omega^{-2j} \partial_x^{2j} \quad (24.53)$$

$$= -\frac{1}{\cos(\alpha\pi/2)} \lim_{\omega \rightarrow 0} |\omega|^\alpha {}_2F_1\left(\frac{1}{2} - \frac{\alpha}{2}, -\frac{\alpha}{2}; \frac{1}{2}; \frac{1}{\omega^2} \partial_x^2\right) \quad (24.54)$$

In the limiting case $\alpha = 2$ we obtain:

$$\lim_{\alpha \rightarrow 2} {}_{\text{RZ}}\Delta^{\alpha/2} = \lim_{\alpha \rightarrow 2} -\frac{1}{\cos(\alpha\pi/2)} \lim_{\omega \rightarrow 0} |\omega|^\alpha \sum_{j=0}^{\infty} \binom{\alpha}{2j} \omega^{-2j} \partial_x^{2j} \quad (24.55)$$

$$= \lim_{\substack{\alpha \rightarrow 2 \\ \omega \rightarrow 0}} |\omega|^\alpha \sum_{j=0}^1 \binom{2}{2j} \omega^{-2j} \partial_x^{2j} \quad (24.56)$$

$$= \lim_{\substack{\alpha \rightarrow 2 \\ \omega \rightarrow 0}} |\omega|^\alpha + |\omega|^{\alpha-2} \partial_x^2 \quad (24.57)$$

$$= \lim_{\omega \rightarrow 0} \omega^2 + \partial_x^2 \quad (24.58)$$

$$= \partial_x^2 \quad (24.59)$$

For all other cases $\alpha < 2$ we have a series of even higher order derivatives, starting with ∂_x^2 :

$${}_{\text{RZ}}\Delta^{\alpha/2} = -\frac{1}{\cos(\alpha\pi/2)} \lim_{\omega \rightarrow 0} |\omega|^\alpha \sum_{j=0}^{\infty} \binom{\alpha}{2j} \omega^{-2j} \partial_x^{2j} \quad (24.60)$$

$$= -\frac{1}{\cos(\alpha\pi/2)} \lim_{\omega \rightarrow 0} |\omega|^\alpha \sum_{j=1}^{\infty} \binom{\alpha}{2j} \omega^{-2j} \partial_x^{2j} \quad (24.61)$$

$$= -\lim_{\omega \rightarrow 0} \frac{1}{\cos(\alpha\pi/2)} (c_2(\alpha, \omega) \partial_x^2 + c_4(\alpha, \omega) \partial_x^4 + \dots) \quad (24.62)$$

Therefore we may write the fractional Lagrangian density (24.78) as a series expansion in terms of even standard derivatives, which we demonstrate for Ψ^* :

$${}_{\text{RZ}}\mathcal{L} = \frac{i\hbar}{2}(\Psi^*\Psi_t - \Psi_t^*\Psi) - V(x, t)\Psi^*\Psi \quad (24.63)$$

$$\begin{aligned} & -\mathcal{D}_{\alpha/2}({}_{\text{RZ}}\Delta^{\alpha/4}\Psi^*)({}_{\text{RZ}}\Delta^{\alpha/4}\Psi) \\ & = \frac{i\hbar}{2}(\Psi^*\Psi_t - \Psi_t^*\Psi) - V(x, t)\Psi^*\Psi \end{aligned} \quad (24.64)$$

$$\begin{aligned} & -\mathcal{D}_{\alpha/2}\left(\frac{1}{\cos(\alpha\pi/4)} \lim_{\omega \rightarrow 0} |\omega|^{\alpha/2} \sum_{j=1}^{\infty} \binom{\alpha/2}{2j} \omega^{-2j} \partial_x^{2j} \Psi^*\right)({}_{\text{RZ}}\Delta^{\alpha/4}\Psi^*) \\ & = \frac{i\hbar}{2}(\Psi^*\Psi_t - \Psi_t^*\Psi) - V(x, t)\Psi^*\Psi \end{aligned} \quad (24.65)$$

$$-\mathcal{D}_{\alpha/2} \lim_{\omega \rightarrow 0} \left(\frac{1}{\cos(\alpha\pi/4)} |\omega|^{\alpha/2} \sum_{j=1}^{\infty} \binom{\alpha/2}{2j} \omega^{-2j} \Psi_x^{(2j)*} \right) ({}_{\text{RZ}}\Delta^{\alpha/4}\Psi^*)$$

Therefore ${}_{\text{RZ}}\mathcal{L}$ is a Lagrangian density of type (24.44). Considering Ψ^* and Ψ as independent fields, a variation for e.g. Ψ^* with

$$\frac{\partial \mathcal{L}}{\partial \Psi^*} = \frac{i\hbar}{2}\Psi_t - V\Psi \quad (24.66)$$

$$\frac{\partial \mathcal{L}}{\partial (\Psi_t^*)} = -\frac{i\hbar}{2}\Psi \quad (24.67)$$

$$\frac{\partial \mathcal{L}}{\partial (\Psi_x^{(2j)*})} = -\mathcal{D}_{\alpha/2} \lim_{\omega \rightarrow 0} \frac{1}{\cos(\alpha\pi/4)} |\omega|^{\alpha/2} \binom{\alpha/2}{2j} \omega^{-2j} \quad (24.68)$$

and furthermore for every term according to the Euler-Lagrange equations (24.47)

$$\partial_t \frac{\partial \mathcal{L}}{\partial (\Psi_t^*)} = -\frac{i\hbar}{2}\Psi_t \quad (24.69)$$

$$\begin{aligned} \sum_{j=0} \partial_x^{2j} \frac{\partial \mathcal{L}}{\partial (\Psi_x^{(2j)*})} & = -\mathcal{D}_{\alpha/2} \sum_{j=0} \lim_{\omega \rightarrow 0} \frac{1}{\cos(\alpha\pi/4)} |\omega|^{\alpha/2} \binom{\alpha/2}{2j} \omega^{-2j} \partial_x^{2j} \\ & = -\mathcal{D}_{\alpha/2} {}_{\text{RZ}}\Delta^{\alpha/4} \end{aligned} \quad (24.70)$$

which results in a wave equation for Ψ :

$$i\hbar\Psi_t = -\mathcal{D}_{\alpha/2} {}_{\text{RZ}}\Delta^{\alpha/4} \times {}_{\text{RZ}}\Delta^{\alpha/4}\Psi + V\Psi \quad (24.71)$$

which, as long as

$${}_{\text{RZ}}\Delta^{\alpha/4} \times {}_{\text{RZ}}\Delta^{\alpha/4} = {}_{\text{RZ}}\Delta^{\alpha/2} \quad 0 < \alpha < 2 \quad (24.72)$$

holds, yields the Schrödinger type equation:

$$i\hbar\Psi_t = -\mathcal{D}_{\alpha/2_{\text{RZ}}}\Delta^{\alpha/2}\Psi + V\Psi \quad (24.73)$$

The same wave equation may be formally obtained, if we consider the following Euler-Lagrange equations for the Riesz derivative, which are the result of an independent variation of the Lagrangian density with respect to the fields Ψ and Ψ^* respectively with the Riesz derivative directly (see e.g. [Agrawal (2007)] for this result derived based on the integral representation of the Riesz derivative):

$$\sum_{n=0}^N ({}_{\text{RZ}}\Delta^{\alpha/2})^n \frac{\partial \mathcal{L}}{\partial(\Psi_x^{(\tilde{n})})} - \partial_t \frac{\partial \mathcal{L}}{\partial(\Psi_t)} = 0 \quad (24.74)$$

$$\sum_{n=0}^N ({}_{\text{RZ}}\Delta^{\alpha/2})^n \frac{\partial \mathcal{L}}{\partial(\Psi_x^{(\tilde{n})}*}) - \partial_t \frac{\partial \mathcal{L}}{\partial(\Psi_t^*)} = 0 \quad (24.75)$$

where

$$\Psi_x^{(\tilde{n})} = ({}_{\text{RZ}}\Delta^{\alpha/2})^n \Psi \quad (24.76)$$

and

$$\Psi_x^{(\tilde{n})*} = ({}_{\text{RZ}}\Delta^{\alpha/2})^n \Psi^* \quad (24.77)$$

Since the Riesz derivative is an even operator with respect to the scalar product (24.15), there are no sign changes in the Euler-Lagrange equations.

The approach, we just presented, implicitly benefits from the similarity of the fractional Schrödinger equation and the standard Schrödinger equation. But as we already know, the behavior of the fractional Schrödinger equation under rotations is more related to the classical Pauli-Equation.

Therefore, if we intend to emphasize a more Dirac-like approach, we may start with a model Lagrangian density of the form:

$$\begin{aligned} {}_{\text{RZ}}\mathcal{L}(\Psi, {}_{\text{RZ}}\Delta^{\alpha/2}\Psi, \Psi_t) &= \frac{i\hbar}{2}(\Psi^*\Psi_t - \Psi_t^*\Psi) - V(x, t)\Psi^*\Psi \\ &\quad + \Psi^*(\mathcal{D}_{\alpha/2_{\text{RZ}}}\Delta^{\alpha/2}\Psi) \end{aligned} \quad (24.78)$$

which, if varied with respect to Ψ^* yields the same Schrödinger equation (24.73).

$$i\hbar\Psi_t = -\mathcal{D}_{\alpha/2_{\text{RZ}}}\Delta^{\alpha/2}\Psi + V\Psi \quad (24.79)$$

This page intentionally left blank

Chapter 25

Gauge Invariance in Fractional Field Theories

Historically the first example for a quantum field theory is quantum electrodynamics (QED), which successfully describes the interaction between electrons and positrons with photons [Pauli (1941); Sakurai (1967)]. The interaction type of this quantum field theory between the electromagnetic field and the electron Dirac field is determined by the principle of minimal gauge invariant coupling of the electric charge.

For more complex charge types, this principle may be extended to non-Abelian gauge theories or Yang-Mills field theories [Yang and Mills (1954)]. A typical example is quantum chromodynamics (QCD), which describes a hadronic interaction by gauge invariant coupling of quark fields with gluon fields.

Hence local gauge invariance seems to be a fundamental principle for studying of the dynamics of particles [Abers and Lee (1973)].

In the following we will apply the concept of local gauge invariance to fractional fields and will outline the basic structure of a quantum field theory based on fractional calculus.

This concept is motivated by the observation that the fractional Dirac-equation for $\alpha = 2/3$ describes particles which obey an inherent $SU(3)$ -symmetry. Since the only mechanism currently used to introduce a symmetry like $SU(n)$ involves non-Abelian gauge fields as proposed by Yang-Mills, the study of gauge invariant fractional wave equations is a new, interesting alternative approach.

Free fractional fields have been studied already in the previous chapter [Goldfain (2006); Lim (2006a)]. Different approaches exist on interacting fractional fields [Herrmann (2007a); Lim and Tao (2008)]. In this chapter we will apply the principle of local gauge invariance to fractional wave equations and derive the resulting interaction up to order $o(\bar{g})$ in the coupling constant.

The result will be a fractional extension of quantum electrodynamics (QED), which for the limit $\alpha = 1$ reduces to standard QED. But for $\alpha \neq 1$ it describes the interaction of a fractional particle field with a fractional gauge field.

As a first application, we will derive the energy spectrum of a non-relativistic fractional particle in a fractional constant magnetic field. The resulting mass formula is in lowest order equivalent to the mass formulas previously derived with group theoretical methods and has been successfully applied in the last chapters for an interpretation of meson and baryon spectra.

25.1 Gauge invariance in first order of the coupling constant \bar{g}

In the previous chapter we have presented an example for a fractional free field, the relativistic fractional Dirac field and for a fractional gauge field, the fractional electromagnetic field.

We now postulate, that the principle of local gauge invariance is valid for fractional wave equations, too.

The requirement of invariance of the fractional Lagrangian density for the Dirac field under local gauge transformations should uniquely determine the type of the interaction with a fractional gauge field.

We therefore will investigate the transformation properties of the fractional analogue of the free QED-Lagrangian $\mathcal{L}_{FQED}^{free}$:

$$\mathcal{L}_{FQED}^{free} = \bar{\Psi}(i\gamma_\alpha^\mu \partial_\mu^\alpha + \mathbf{1}_\alpha m^\alpha)\Psi - \frac{1}{4}F_{\mu\nu}^\beta F_\beta^{\mu\nu} \quad (25.1)$$

where $\alpha = 2/n$ and β both denote derivatives of fractional order. $\mathbf{1}_\alpha$ indicates a $n \times n$ unit matrix with dimension $n = (2/\alpha)^2$.

Special cases are: for $\alpha = 1$ a fractional electric field couples to the standard Dirac field, for $\beta = 1$ a standard electric field couples to a fractional Dirac field. For $\alpha = \beta$ both fractional fields are of similar type. For $\alpha = \beta = 1$ the Lagrangian density (25.1) reduces to the QED Lagrangian density.

Under local gauge transformations the following transformation properties hold:

$$\bar{\Psi}' = \bar{\Psi}e^{-i\bar{g}\phi(x)} \quad (25.2)$$

$$\Psi' = e^{i\bar{g}\phi(x)}\Psi \quad (25.3)$$

$$A'_\mu = A_\mu + \phi_{|\mu}^\beta \quad (25.4)$$

The transformation properties of the fractional derivative operator ∂_μ^α may be deduced from:

$$\bar{\Psi}' \gamma_\alpha^\mu \partial_\mu^\alpha \Psi' = \bar{\Psi}' \gamma_\alpha^\mu \partial_\mu^\alpha e^{i\bar{g}\phi} \Psi \quad (25.5)$$

$$= \bar{\Psi}' \gamma_\alpha^\mu (e^{i\bar{g}\phi} \partial_\mu^\alpha + [\partial_\mu^\alpha, e^{i\bar{g}\phi}]) \Psi \quad (25.6)$$

$$= \bar{\Psi} \gamma_\alpha^\mu (\partial_\mu^\alpha + e^{-i\bar{g}\phi} [\partial_\mu^\alpha, e^{i\bar{g}\phi}]) \Psi \quad (25.7)$$

The commutator reflects the nonlocality for the fractional derivative. Since there is no fractional analogue to the chain rule, which is known for the standard derivative, this commutator cannot be evaluated directly.

Therefore we will restrict our derivation to gauge invariance up to first order in the coupling constant \bar{g} only, which corresponds to an infinitesimal gauge transformation.

We obtain:

$$e^{-i\bar{g}\phi} [\partial_\mu^\alpha, e^{i\bar{g}\phi}] = (1 - i\bar{g}\phi) [\partial_\mu^\alpha, 1 + i\bar{g}\phi] \quad (25.8)$$

$$= (1 - i\bar{g}\phi) [\partial_\mu^\alpha, i\bar{g}\phi] \quad (25.9)$$

$$= i\bar{g} [\partial_\mu^\alpha, \phi] + o(\bar{g}^2) \quad (25.10)$$

We define the fractional charge connection operator $\hat{\Gamma}_\mu^{\alpha\beta}$, which in a fractional charge tangent space is the analogue to the fractional Christoffel symbols in a fractional coordinate tangent space or the fractional Fock-Ivanenko coefficients in a fractional spinor tangent space:

$$\hat{\Gamma}_\mu^{\alpha\beta}(\xi_\mu) = \delta_{(\mu)}^{\sigma\tau} [\partial_\sigma^\alpha, (\partial_\tau^\beta \xi_\mu)] \quad (25.11)$$

$$= \delta_{(\mu)}^{\sigma\tau} [\partial_\sigma^\alpha, \xi_{|\tau}^{-\beta}] \quad (25.12)$$

with the Kronecker delta $\delta_{(\mu)}^{\sigma\tau}$, where (μ) indicates that a summation over μ is performed, which reduces the sum (25.11) to a single term (25.12). But on the other hand (μ) should be ignored, when the transformation properties in fractional coordinate space are determined. Therefore the vector character of $\hat{\Gamma}_\mu^{\alpha\beta}(\xi_\mu)$ is conserved in the fractional coordinate space.

This operator is linear

$$\hat{\Gamma}_\mu^{\alpha\beta}(\xi_\mu + \zeta_\mu) = \hat{\Gamma}_\mu^{\alpha\beta}(\xi_\mu) + \hat{\Gamma}_\mu^{\alpha\beta}(\zeta_\mu) \quad (25.13)$$

It should be emphasized, that $\hat{\Gamma}_\mu^{\alpha\beta}(\xi_\mu)$ is an operator and therefore does not transform as a simple c-number. But up to first order in \bar{g} the relation

$$\bar{\Psi}' \gamma_\alpha^\mu i\bar{g} \hat{\Gamma}_\mu^{\alpha\beta'}(\xi_\mu) \Psi' = \bar{\Psi} \gamma_\alpha^\mu i\bar{g} \hat{\Gamma}_\mu^{\alpha\beta}(\xi_\mu) \Psi + o(\bar{g}^2) \quad (25.14)$$

holds. Hence the fractional derivative operator ∂_μ^α transforms as

$$\bar{\Psi}' \gamma_\alpha^\mu \partial_\mu^\alpha \Psi' = \bar{\Psi} \gamma_\alpha^\mu (\partial_\mu^\alpha + i\bar{g} \hat{\Gamma}_\mu^{\alpha\beta}(\phi_{|\mu}^\beta)) \Psi + o(\bar{g}^2) \quad (25.15)$$

Therefore we define the covariant fractional derivative D_μ^α as

$$D_\mu^\alpha = \partial_\mu^\alpha - i\bar{g}\hat{\Gamma}_\mu^{\alpha\beta}(A_\mu) \quad (25.16)$$

It transforms as

$$D_\mu^{\alpha'} = \partial_\mu^\alpha + i\bar{g}\hat{\Gamma}_\mu^{\alpha\beta}(\phi_{|\mu}^\beta) - i\bar{g}\hat{\Gamma}_\mu^{\alpha\beta'}(A_\mu') \quad (25.17)$$

With the covariant fractional derivative D_μ^α it follows from (25.14) and from the linearity of the fractional charge connection operator $\hat{\Gamma}_\mu^{\alpha\beta}$, that the Lagrangian density \mathcal{L}_{FQED} for the fractional extension of QED

$$\mathcal{L}_{FQED} = \bar{\Psi}(i\gamma_\alpha^\mu D_\mu^\alpha + \mathbf{1}_\alpha m^\alpha)\Psi - \frac{1}{4}F_{\mu\nu}^\beta F_\beta^{\mu\nu} \quad (25.18)$$

is invariant under local gauge transformations up to first order in the coupling constant \bar{g} .

Variation of \mathcal{L}_{FQED} with respect to $\bar{\Psi}$ leads to the Dirac equation for the fractional Dirac field Ψ :

$$(i\gamma_\alpha^\mu \partial_\mu^\alpha + \mathbf{1}_\alpha m^\alpha)\Psi = -\bar{g}\gamma_\alpha^\mu \hat{\Gamma}_\mu^{\alpha\beta}(A_\mu)\Psi \quad (25.19)$$

Variation of \mathcal{L}_{FQED} with respect to the four-potential A_μ leads to the fractional Maxwell equations

$$\partial_\mu^\beta F_\beta^{\mu\nu} = -\bar{g}\bar{\Psi}\gamma_\alpha^\nu (\delta_{(\nu)}^{\sigma\tau} \partial_\tau^{-\beta} \partial_\sigma^\alpha)\Psi \quad (25.20)$$

$$= -\bar{g}\bar{\Psi}\gamma_\alpha^\nu (\delta_{(\nu)}^{\sigma} \partial_\sigma^{\alpha-\beta})\Psi \quad (25.21)$$

$$= -\bar{g}\bar{\Psi}\gamma_\alpha^\nu \partial_{(\nu)}^{\alpha-\beta}\Psi \quad (25.22)$$

with $\delta_{(\nu)}^{\sigma\tau}$ the Kronecker delta, where (ν) indicates, that the term $(\delta_{(\nu)}^{\sigma\tau} \partial_\tau^{-\beta} \partial_\sigma^\alpha)$ transforms like a scalar in fractional coordinate space but summation is performed in (25.20), which yields a single term $\partial_{(\nu)}^{\alpha-\beta}$ in (25.22), which for $\alpha = \beta$ becomes 1, while for $\alpha > \beta$ fractional differentiation and for $\alpha < \beta$ fractional integration is performed.

The term on the right side of (25.20) is the variation of

$$\mathcal{L}_\Gamma = \bar{g}\bar{\Psi}\gamma_\alpha^\mu \hat{\Gamma}_\mu^{\alpha\beta}(A_\mu)\Psi \quad (25.23)$$

with respect to the four potential A_μ and may be derived using the Leibniz product rule for fractional derivatives:

$$\mathcal{L}_\Gamma = \bar{g}\bar{\Psi}\gamma_\alpha^\mu \hat{\Gamma}_\mu^{\alpha\beta}(A_\mu)\Psi \quad (25.24)$$

$$= \bar{g}\bar{\Psi}\gamma_\alpha^\mu (\delta_{(\mu)}^{\sigma\tau} [\partial_\sigma^\alpha, A_{\mu|\tau}^{-\beta}])\Psi$$

$$= \bar{g}\bar{\Psi}\gamma_\alpha^\mu (\delta_{(\mu)}^{\sigma\tau} (\partial_\sigma^\alpha A_{\mu|\tau}^{-\beta} - A_{\mu|\tau}^{-\beta} \partial_\sigma^\alpha))\Psi$$

$$= \bar{g}\bar{\Psi}\gamma_\alpha^\mu \left(\delta_{(\mu)}^{\sigma\tau} \left(\sum_{k=0}^{\infty} \binom{\alpha}{k} A_{\mu|\tau}^{-\beta+k} \partial_\sigma^{\alpha-k} - A_{\mu|\tau}^{-\beta} \partial_\sigma^\alpha \right) \right) \Psi$$

$$= \bar{g}\bar{\Psi}\gamma_\alpha^\mu \left(\delta_{(\mu)}^{\sigma\tau} \sum_{k=1}^{\infty} \binom{\alpha}{k} A_{\mu|\tau}^{-\beta+k} \partial_\sigma^{\alpha-k} \right) \Psi \quad (25.25)$$

where the fractional binomial is given by:

$$\binom{\alpha}{k} = \frac{\Gamma(1+\alpha)}{\Gamma(1+k)\Gamma(1+\alpha-k)} \quad (25.26)$$

Therefore \mathcal{L}_Γ is a function of type (24.21). Applying the corresponding Euler-Lagrange equations (24.22) to (25.25) yields

$$\sum_{k=1}^{\infty} (-1)^k \partial_\tau^{-\beta+k} \frac{\partial \mathcal{L}_\Gamma}{\partial (A_{\mu|\tau}^{-\beta+k})} \quad (25.27)$$

$$= \bar{g} \bar{\Psi} \gamma_\alpha^\mu (\delta_{(\mu)}^{\sigma\tau} \partial_\tau^{-\beta} \partial_\sigma^\alpha) \sum_{k=1}^{\infty} \binom{\alpha}{k} (-1)^k \partial_\tau^{-\beta+k} \partial_\sigma^{\alpha-k} \Psi \quad (25.28)$$

$$= \bar{g} \bar{\Psi} \gamma_\alpha^\mu (\delta_{(\mu)}^{\sigma\tau} \partial_\tau^{-\beta} \partial_\sigma^\alpha) \sum_{k=1}^{\infty} \binom{\alpha}{k} (-1)^k \Psi \quad (25.29)$$

$$= -\bar{g} \bar{\Psi} \gamma_\alpha^\mu (\delta_{(\mu)}^{\sigma\tau} \partial_\tau^{-\beta} \partial_\sigma^\alpha) \Psi \quad (25.30)$$

Hence the coupling term in (25.20) is derived.

The nonlinear field equations (25.19) and (25.20) completely determine the interaction of the fractional Dirac field with the fractional gauge field up to first order in $o(\bar{g})$. We have proven, that the principle of local gauge invariance still is effective for fractional fields.

Furthermore, besides the mechanism proposed by Yang-Mills, now an alternative approach for implementing an inherent $SU(n)$ -symmetry exists. While in a Yang-Mills theory, the $SU(n)$ -symmetry is explicitly introduced via a non-Abelian gauge field, now the same symmetry is introduced implicitly via the fractional Dirac equation leaving the symmetry of the fractional gauge field Abelian. Therefore equations (25.18), (25.19) and (25.20) serve as an alternative formulation of a gauge field theory of e.g. for $\alpha = \beta = 2/3$ the strong interaction of hadrons.

For $\alpha = 1, \beta = 1$ these equations reduce to the standard QED equations. For $\alpha \neq 1, \beta \neq 1$ the major extensions are: the electric field A_μ extends from a c-number to a nonlocal operator, which we called the fractional charge connection operator. The γ_α^μ -matrices obey an extended Clifford algebra, which reflects the transition from $SU(2)$ to $SU(n > 2)$. This makes the fractional QED an interesting candidate to describe properties of particles, which obey an inherent $SU(n)$ symmetry.

To help to get this idea accepted we investigate in the following section the fractional extension of the classical Zeeman effect.

25.2 The fractional Riemann-Liouville-Zeeman effect

In the previous section, we have applied a local gauge transformation to a free fractional Dirac field and obtained a fractional interaction with the fractional gauge field. Of course, this method is neither restricted to spinor fields nor does it rely on Lorentz-covariant wave equations, but may be applied to other free fields as well.

In this section, we will present a simple example to illustrate the validity of the proposed mechanism to generate an interaction for fractional fields. We will investigate the fractional analogue of the classical Zeeman effect, which describes the level splitting of a charged particle in an external constant magnetic field.

For that purpose, we will first derive the fractional nonrelativistic Schrödinger equation including the interaction term.

The Lagrangian density \mathcal{L}_{FS}^{free} for the free fractional Schrödinger field is given by

$$\mathcal{L}_{FS}^{free} = -\frac{1}{2m}(\partial_\alpha^i \Psi)^*(\partial_i^\alpha \Psi) + i\Psi^* \partial_t \Psi \quad (25.31)$$

Local gauge invariance up to first order in \bar{g} is achieved by a replacement of the fractional derivative by

$$D_\mu^\alpha = \{D_t, D_i^\alpha\} = \{\partial_t + i\bar{g}V, \partial_i^\alpha - i\bar{g}\hat{\Gamma}_i^{\alpha\beta}(A_i)\} \quad (25.32)$$

$$= \{D_t, \vec{D}^\alpha\} = \{\partial_t + i\bar{g}V, \nabla^\alpha - i\bar{g}\hat{\vec{\Gamma}}^{\alpha\beta}\} \quad (25.33)$$

Therefore the free Lagrangian density (25.31) is extended to

$$\mathcal{L}_{FS} = -\frac{1}{2m}(D_\alpha^i \Psi)^*(D_i^\alpha \Psi) + i\Psi^*(\partial_t + i\bar{g}V)\Psi \quad (25.34)$$

Variation of \mathcal{L}_{FS} with respect to Ψ^* yields the fractional Schrödinger equation including an interaction with an external gauge field:

$$-\frac{1}{2m}((\partial_i^\alpha - i\bar{g}\hat{\Omega}_i^{\alpha\beta})D_\alpha^i - i(\partial_t + i\bar{g}V))\Psi = 0 \quad (25.35)$$

or

$$-\frac{1}{2m}(\partial_i^\alpha \partial_\alpha^i - i\bar{g}(\hat{\Omega}_i^{\alpha\beta} \partial_\alpha^i + \partial_\alpha^i \hat{\Omega}_i^{\alpha\beta}))\Psi = i(\partial_t + i\bar{g}V)\Psi \quad (25.36)$$

with

$$\hat{\Omega}_i^{\alpha\beta}(A_i) = -\delta_{(i)}^{\sigma\tau} \sum_{k=1}^{\infty} \binom{\alpha}{k} (-1)^k \partial_\sigma^{\alpha-k} A_{i|\tau}^{-\beta+k} \quad (25.37)$$

which results from the variation of $\hat{\Gamma}_i^{\alpha\beta}(A_i)\Psi^*$.

In order to simplify the procedure, we intend to describe a fractional particle in a corresponding fractional constant external magnetic field and set $\alpha = \beta$.

The fractional charge connection operator is then given according to (25.25) by

$$\hat{\Gamma}_i^{\alpha\alpha} = \sum_{k=1}^{\infty} \binom{\alpha}{k} (\partial_i^{-\alpha+k} A_i) \partial_i^{\alpha-k} \quad (25.38)$$

and

$$\hat{\Omega}_i^{\alpha\alpha} = - \sum_{k=1}^{\infty} \binom{\alpha}{k} (-1)^k \partial_i^{\alpha-k} (\partial_i^{-\alpha+k} A_i) \quad (25.39)$$

In order to evaluate these series, we apply the Riemann-Liouville fractional derivative

$$\partial^{\alpha} x^{\nu} = \frac{\Gamma(1+\nu)}{\Gamma(1+\nu-\alpha)} x^{\nu-\alpha} \quad (25.40)$$

where $\Gamma(z)$ denotes the Euler Γ -function.

We now introduce the external field \vec{A} :

$$\vec{A} = \left\{ -\frac{1}{2} B y^{2\alpha-1} x^{\alpha-1} z^{\alpha-1}, \frac{1}{2} B x^{2\alpha-1} y^{\alpha-1} z^{\alpha-1}, 0 \right\} \quad (25.41)$$

which for $\alpha = 1$ reduces to $\{-\frac{1}{2} B y, \frac{1}{2} B x, 0\}$ and is therefore the fractional analogue for a constant magnetic field, because

$$\vec{B} = \{B_x, B_y, B_z\} = \nabla^{\alpha} \times \vec{A} = \{0, 0, B x^{\alpha-1} y^{\alpha-1} z^{\alpha-1}\} \quad (25.42)$$

Since $1/\Gamma(0) = 0$ it follows:

$$\partial_x^{\alpha} B_z = \partial_y^{\alpha} B_z = \partial_z^{\alpha} B_z = 0 \quad (25.43)$$

Therefore the fractional magnetic field is indeed constant within the context of the Riemann-Liouville fractional derivative definition.

Hence we obtain

$$\partial^{-\alpha+1} \vec{A} = \Gamma(\alpha) \left\{ -\frac{1}{2} B y^{2\alpha-1} z^{\alpha-1}, \frac{1}{2} B x^{2\alpha-1} z^{\alpha-1}, 0 \right\} \quad (25.44)$$

and consecutively

$$\partial^k (\partial^{-\alpha+1} \vec{A}) = 0 \quad (25.45)$$

As a consequence, the infinite series in (25.38) and (25.39) reduce to a single term.

$$\begin{aligned} \hat{\Gamma}_i^{\alpha\alpha} &= \Gamma(1+\alpha) \frac{B}{2} \left\{ -z^{\alpha-1} y^{2\alpha-1} \partial_x^{\alpha-1}, z^{\alpha-1} x^{2\alpha-1} \partial_y^{\alpha-1}, 0 \right\} \\ &= \hat{\Omega}_i^{\alpha\alpha} \end{aligned} \quad (25.46)$$

We introduce the fractional analogue of the z-component of the angular momentum operator $\hat{L}_z(\alpha)$

$$\hat{L}_z(\alpha) = i(y^\alpha \partial_x^\alpha - x^\alpha \partial_y^\alpha) \quad (25.47)$$

With this definition we obtain

$$\nabla_\alpha \hat{\tilde{\Gamma}}^{\alpha\alpha} = \hat{\tilde{\Omega}}^{\alpha\alpha} \nabla_\alpha \quad (25.48)$$

and

$$\nabla_\alpha \hat{\tilde{\Gamma}}^{\alpha\alpha} = \hat{\tilde{\Omega}}^{\alpha\alpha} \nabla_\alpha = i\Gamma(1+\alpha) \frac{B}{2} z^{\alpha-1} \hat{L}_z(2\alpha-1) \quad (25.49)$$

The fractional Schrödinger equation (25.35) reduces to

$$-\frac{1}{2m} (\Delta_\alpha^\alpha + \bar{g}\Gamma(1+\alpha)Bz^{\alpha-1} \hat{L}_z(2\alpha-1))\Psi = -i\partial_t\Psi \quad (25.50)$$

where $\Delta_\alpha^\alpha = \nabla^\alpha \nabla_\alpha$. With the product ansatz $\Psi = e^{-iEt}\psi$ a stationary Schrödinger equation for the energy spectrum results in:

$$H\psi = -\frac{1}{2m} (\Delta_\alpha^\alpha + \bar{g}\Gamma(1+\alpha)Bz^{\alpha-1} \hat{L}_z(2\alpha-1))\psi = E\psi \quad (25.51)$$

With (25.51) we have derived the nonrelativistic fractional Schrödinger equation for a spinless particle moving in a constant external fractional magnetic field, which is gauge invariant up to first order in \hat{g} . We want to emphasize, that for a different choice of the fractional derivative definition a different Hamiltonian results, e.g. for the Caputo fractional derivative definition $z^{\alpha-1}$ has to be replaced by 1.

The derived equation is a fractional integro-differential equation, a solution may be obtained by iteration. In lowest order approximation, we set

$$z^{\alpha-1} \hat{L}_z(2\alpha-1) \approx \rho \hat{L}_z(\alpha) \quad (25.52)$$

with the constant ρ and obtain

$$H^0\psi^0 = -\frac{1}{2m} (\Delta_\alpha^\alpha + \bar{g}\Gamma(1+\alpha)B\rho \hat{L}_z(\alpha))\psi = E_R^0\psi^0 \quad (25.53)$$

Since $\hat{L}_z(\alpha)$ is the Casimir operator of the fractional rotation group $SO^\alpha(2)$, for an analytic solution a group theoretical approach is appropriate.

In order to classify the multiplets only, the Hamiltonian (25.53) may be rewritten as a linear combination of the Casimir operators $\hat{L}^2(\alpha)$ of $SO^\alpha(3)$ which corresponds in a classical picture to the fractional angular momentum and $\hat{L}_z(\alpha)$ of $SO^\alpha(2)$ which corresponds to the z-projection of the angular

momentum. The eigenfunctions are determined by two quantum numbers $|LM\rangle$

$$H^0|LM\rangle = m_0 + a_0 \hat{L}^2 + b_0 \hat{L}_z |LM\rangle \quad (25.54)$$

The eigenvalues of the Casimir operators based on the Riemann-Liouville fractional derivative definition are given by (16.47) and (16.48)

$$\begin{aligned} \hat{L}_z(\alpha) |LM\rangle &= \pm \frac{\Gamma(1+|M|\alpha)}{\Gamma(1+(|M|-1)\alpha)} |LM\rangle \\ M &= 0, \pm 1, \pm 2, \dots, \pm L \end{aligned} \quad (25.55)$$

$$\begin{aligned} \hat{L}^2(\alpha) |LM\rangle &= \frac{\Gamma(1+(L+1)\alpha)}{\Gamma(1+(L-1)\alpha)} |LM\rangle \\ L &= 0, +1, +2, \dots \end{aligned} \quad (25.56)$$

Note that for $\alpha = 1$ the Casimir operators and the corresponding eigenvalues reduce to the well known results of standard quantum mechanical angular momentum algebra [Edmonds (1957)].

With (25.55) and (25.56) the level spectrum of the multiplets is determined

$$E_R^0 = m_0 + a_0 \frac{\Gamma(1+(L+1)\alpha)}{\Gamma(1+(L-1)\alpha)} \pm b_0 \frac{\Gamma(1+|M|\alpha)}{\Gamma(1+(|M|-1)\alpha)} \quad (25.57)$$

Thus we have derived in lowest order an analytic expression (25.57) for the splitting of the energy levels of a nonrelativistic charged spinless particle in a constant fractional magnetic field.

Using this result we may establish a connection with the previously presented results for an interpretation of the hadron spectrum. There we used a heuristic group theoretical approach, which now is justified on the basis of the derived model for the fractional Zeeman-effect.

With reference to (25.51) we may conclude that a constant fractional magnetic field generates an additional term of the form

$$\frac{1}{2m^{2\alpha-1}} \bar{g}\alpha\Gamma(2-\alpha)Bz^{\alpha-1}\hat{L}_z(2\alpha-1) \quad (25.58)$$

According to our derivation presented in chapter 10 the term $\hat{L}_z(2\alpha-1)$ may be interpreted as a projection of the total angular momentum

$$\hat{L}_z(2\alpha-1) = \hat{L}_z + \hat{S}_z(2\alpha-1) \quad (25.59)$$

and consequently the fractional magnetic field acts on two components simultaneously: the angular momentum and the fractional spin.

These results indicate, that a fractional QED based on the Lagrangian density (25.18) with a small coupling constant \bar{g} and an Abelian gauge field

and QCD based on the standard QCD Lagrangian density with a strong coupling constant \bar{g} and a non-Abelian gauge field may probably describe the same phenomena.

Therefore the step to interacting fractional fields based on the principle of local gauge invariance opens up a new exciting research area in high energy and particle physics.

Chapter 26

On the Origin of Space

Fractional calculus introduces the concepts of nonlocality and memory in order to model complex dynamical behavior [Miller and Ross (1993); Samko and Ross (1993a); Podlubny (1999); Hilfer (2000)]. Literally spoken, we have learned, that the present is influenced by the past in more than one way. Within the framework of fractional calculus it really makes a difference how an actual state is achieved.

Alternatively, fractional calculus may be described as an extension of the concept of a derivative operator from integer order n to arbitrary order α , where α is a real or complex value [Leibniz (1695)]:

$$\frac{d^n}{dx^n} \rightarrow \frac{d^\alpha}{dx^\alpha} \quad (26.1)$$

In this chapter we want to introduce a further facet, which emerges naturally from a new point of view based on fractional calculus with variable order. It is the fascinating idea of an evolutionary development of dynamic processes, which are described by differential equations, which themselves evolve dynamically in evolutionary scenarios; an idea, that dates back to the early 90s of the last century [Samko and Ross (1993a); Ramirez and Ciombra (2010); Odzijewicz et al. (2011); Odzijewicz et al. (2013c)] and which may be realized introducing a time and/or space dependence for α .

$$\alpha \rightarrow \alpha(x, t) \quad (26.2)$$

The governing differential equations, which until now remained form invariant within an ever changing environment, now themselves take part in a global evolutionary process.

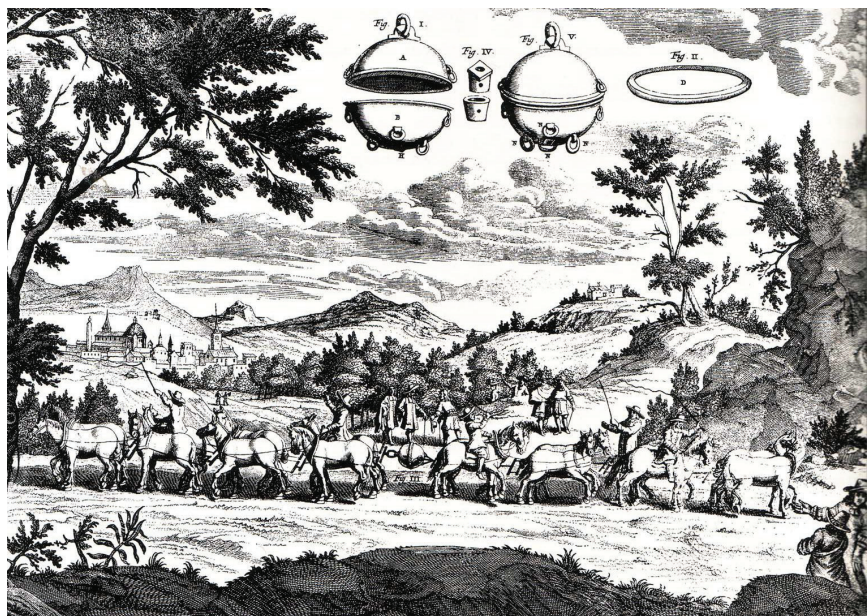


Fig. 26.1 Illustration of Guericke's experiment from 1654 as a demonstration of the existence of the vacuum, which was doubted by Aristotle. Copper plate from [Guericke (1672)].

With respect to this concept, we will also take a look into the future of fractional calculus and we anticipate developments that have yet to be achieved. The time has come to present an unconventional approach to the still open question of all questions, on the origin and the evolutionary genesis of space.

26.1 The interplay between matter and space

In times of Aristotle matter and space were interdependent quantities, where one could not exist without the other. This holistic view allowed an understanding of phenomena like *horror vacui*, but needed a revision to conform with e.g. von Guericke's experiments [Guericke (1672)] in the second half of the 17th century.

As a fundamental assumption in Newtonian physics the concept of matter was established as an independent quality in an absolute space and time,

which left themselves reduced to passive containers of a dynamically developing material world.

This tendency to interpret space as a passive container for dynamically interacting particles becomes most obvious in quantum theory, where the vacuum state, which initially was characterized by the absence of any particles, since the days of Dirac, serves more and more as a waste deposit for dispensable virtual matter of all kind.

In Einstein's theory of general relativity the hitherto disjunct concepts of space, time and matter are once again connected via the field equations

$$R_{\mu\nu} - \frac{1}{2}g_{\mu\nu}R = \kappa T_{\mu\nu} \quad (26.3)$$

which relate a property of space-time called curvature with a property of matter collected in the energy-momentum tensor. In the case of matter absent, these equations reduce to the vacuum field equations

$$R_{\mu\nu} - \frac{1}{2}g_{\mu\nu}R = 0 \quad (26.4)$$

or equivalently $R_{\mu\nu} = 0$, which generates a flat space.

Hence in Einstein's field theory besides curvature there is no other property of space affected. Especially the number of space and time dimensions is invariant (3+1) under any Lorentz-transformation, which results in a very static picture of space and time at the end.

The first serious attempt to overcome the paradigm of a fixed number of space dimensions was realized by Kaluza [Kaluza (1919)] and Klein [Klein (1926)] introducing a 5-dimensional theory of relativity, which allowed for a simultaneous treatment of gravity and electro-magnetism.

The Kaluza-Klein theory may be considered as one of the ancestors of string theory, which gained increasing interest, after it was shown, that a higher dimensional realization introducing extra dimensions avoids divergences in a perturbation expansion. Of course, to be comparable with experimental observations, a mechanism to reduce a multi-dimensional theory to a 3-dimensional in space had to be introduced as compactification.

There have been several approaches to generalize Einstein's field equations, e.g. introducing torsion terms [Cartan (1922); Kibble (1961)] or employing gauge fields for a new theory of gravitation [Lasenby *et al.* (1998)]. Recent developments are models of generalized teleparallel gravity [Jamil *et al.* (2012); Karami *et al.* (2013)]. But, despite a few occasional attempts [Bolzano (1843); Poincaré (1912); Tangherlini (1963); He (1990); Ellis *et al.* (1992); Bars (2000); Calcagni (2011); Merali (2013)], up to now there is no generally accepted theory, which explains the observed number

of space dimensions and Ehrenfest's [Ehrenfest (1917)] question, why space has three dimensions, is still unanswered. Furthermore, there is no dynamic theory, which rationalizes the genesis of 3-dimensional space.

Instead e.g. the classical big bang model starts with an object with very small size but right from the beginning the number of space dimensions is fixed to a value, which remains unchanged till today.

At this point fractional calculus comes into focus as a possible candidate to overcome some of the restrictions of hitherto discussed approaches.

From a historical point of view, up to now, there have been two different strategies to apply fractional calculus methods in cosmology: the first one is a replacement of the partial derivatives in the Einstein field equations with the corresponding fractional derivatives [Roberts (2009)]; the second technique derives the fractional extension of the field equations and geodesic equations starting with the least action principle and replacing the usual integral with a fractional integral [El-Nabulsi (2010); Chakraborty *et al.* (2012); El-Nabulsi (2013)].

We will propose a completely different approach, which is based on fractional calculus with variable order. We will collect arguments, that space and especially the space dimension d is a dynamic quality. Considering space as a quantum phenomenon, it evolves smoothly from a point-like vacuum fluctuation with $d = 0$ up to its final form $d = 3$, where d is a real number. Therefore interpreting $d \in \mathbb{R}$ instead of $d \in \mathbb{N}$ seems a necessary prerequisite and is a natural legitimization for the use of a fractional concept. This is our first argument for a fractional approach.

Furthermore space dimension is considered a dynamic quality $d = d(t)$, which clearly emphasizes the evolutionary aspect of space genesis. This is the second argument for a fractional approach and in the following we will model this behavior by investigating the properties of a fractional wave equation with time dependent $\alpha = \alpha(t)$.

Besides the known mechanisms for an explanation of an inflating universe, we propose in the following an evolutionary approach, where space is permanently generated starting from a dimensionless infinitely small seed up to its final $d = 3$ form which may be compared to gas bubbles in boiling water.

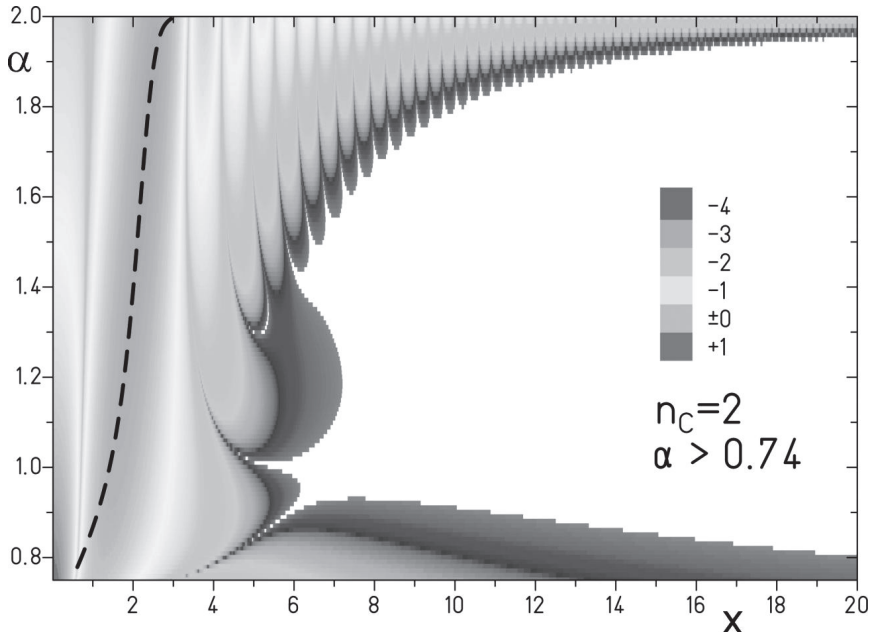


Fig. 26.2 Logarithmic probability density $|\Psi_{n=2}^+(x(t), \alpha)|^2$ for the solution of the fractional quantum harmonic oscillator based on the Caputo definition of the fractional derivative in the full range of allowed α values for real energy eigenvalues. The dashed line indicates the expectation value for the size operator $s = 2\bar{x}$, with $\bar{x} = H(x)x$, (with $H(x)$ is the Heaviside step function), its expectation value $\langle \bar{x} \rangle = \int_0^\infty dx \Psi_n^\pm(x, \alpha) x \Psi_n^\pm(x, \alpha)^*$ yields the position information on the positive semi-axis.

With kind permission from [Herrmann (2013a)] © Gam. Ori. Chron. Phys.

26.2 Fractional calculus with time dependent α in the adiabatic limit

Since we consider the genesis of space as a quantum phenomenon, we describe this process with the simple model of the fractional quantum harmonic oscillator:

$$H^{\alpha(t)}\Psi(x, t) = \left(\frac{1}{2}\left(-({}_c\hat{D}_x^{\alpha(t)})^2 + (|x|^{\alpha(t)})^2\right)\right)\Psi(x, t) = -i\hbar\partial_t\Psi(x, t) \quad (26.5)$$

using the Caputo fractional derivative ${}_c\hat{D}_x^\alpha$, which is related to the Riemann fractional derivative ${}_R\hat{D}_x^\alpha$ according to Chapter 3:

$${}_c\hat{D}_x^\alpha = {}_R\hat{D}_x^{\alpha-1}\partial_x \quad (26.6)$$

$$= \frac{1}{\Gamma(2-\alpha)}|x|^{1-\alpha} :_1F_1(1-\alpha; 2-\alpha; -x\partial_x) : \partial_x \quad (26.7)$$

where the hypergeometric function ${}_1F_1(a; b; x)$ is interpreted as a series expansion in terms of integer derivatives, where : $(x\partial_x)^n := x^n \partial_x^n$ is the normal ordered product and with time dependent $\alpha(t)$, where the set $\{x, t\}$ marks two different space- and time-like variables.

In order to simplify the procedure, we assume complete adiabaticity, which means, that the system has always time enough to occupy the equilibrium state. In that case, we may treat the time t as a parameter and the problem is reduced to the solution of a one dimensional stationary Schrödinger equation in x , where t parametrizes the solutions.

An approximate solution for the stationary energy levels, which is valid in the neighborhood of $\alpha \approx 1$ has been derived by Laskin [Laskin (2002)] within the framework of WKB-approximation, which is independent from a specific choice of a fractional derivative type:

$$E_{\text{WKB}}(n, \alpha) = \left(n + \frac{1}{2}\right)^\alpha \pi^{\alpha/2} \left(\frac{\alpha \Gamma(\frac{1+\alpha}{2\alpha})}{\Gamma(\frac{1}{2\alpha})}\right)^\alpha \quad n = 0, 1, 2, \dots \quad (26.8)$$

We have already emphasized, that these levels allow for a smooth transition from vibrational to rotational types of spectra, depending on the value of the fractional derivative coefficient α .

$$E_{\text{WKB}}(n, \alpha \approx 1) \sim n + \frac{1}{2} \quad n = 0, 1, 2, \dots \quad (26.9)$$

$$E_{\text{WKB}}(n, \alpha \approx 2) \sim (n + \frac{1}{2})^2 = n(n + 1) + 1/4 \quad (26.10)$$

Indeed the solutions of the fractional quantum harmonic oscillator cover vibrational as well as rotational degrees of freedom from a generalized view as fractional vibrations [Herrmann (2007b)].

Exact eigenfunctions and eigenvalues have been obtained numerically recently [Herrmann (2013a)]. As an example, in figure 26.2 we have plotted a typical eigenfunction ($\Psi_{n=2}^+(x, \alpha)$). The eigenfunctions, normalizable only for $\alpha \leq 2$, determine a Hilbert space and are used to calculate a measure of the time dependent size $s/2 = \langle \bar{x} \rangle$ given in terms of the modified position expectation value

$$\langle \bar{x}(t) \rangle = \langle H(x(t))x(t) \rangle = \int_0^\infty dx \Psi_n^\pm(x, \alpha(t)) x \Psi_n^\pm(x, \alpha(t))^* \quad (26.11)$$

where $H(x)$ is the Heaviside step function.

The time development of a space element with size s starts for $\alpha = 0.5$ with $s(\alpha = 0.5) = 0$ for the ground state Ψ_0^+ and above $\alpha = 1$ it increases slowly, but becomes divergent for $\alpha > 2$. Therefore when α becomes time dependent,

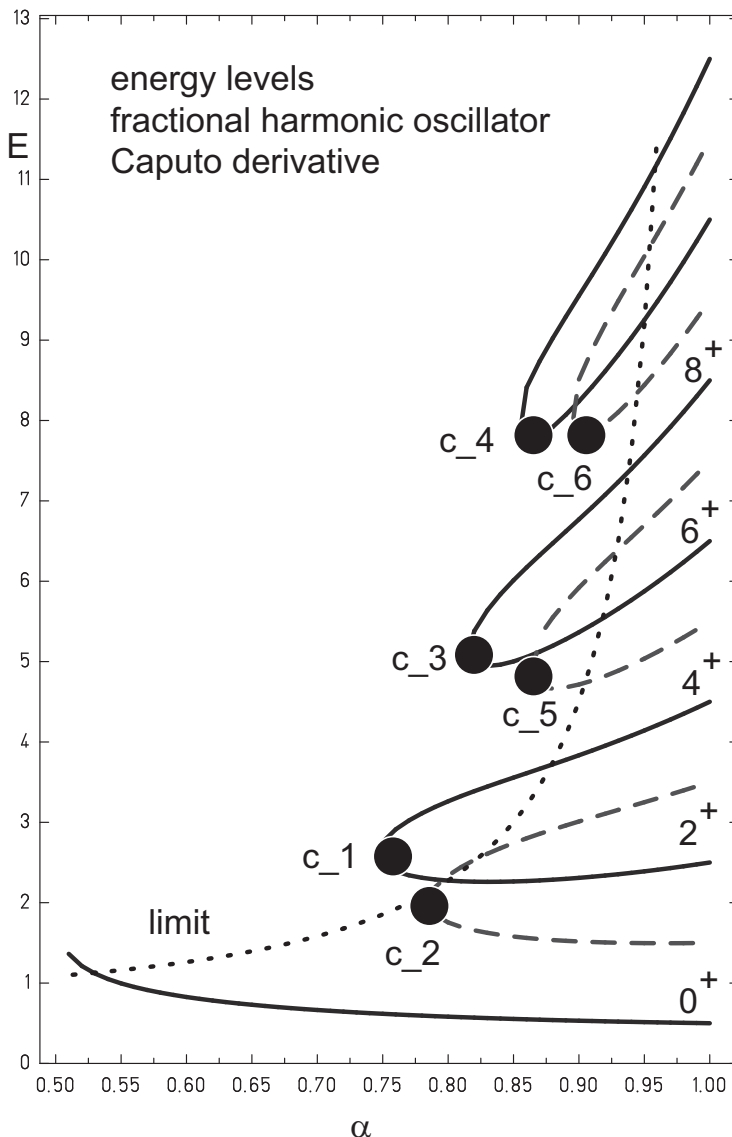


Fig. 26.3 The energy spectrum (in units $[\hbar\omega]$) for the fractional quantum harmonic oscillator using the Caputo derivative. Thick lines indicate positive parity, dotted lines indicate negative parity. Bullets depict the bifurcation points (c_i) determined numerically (see table 26.1). Pointed line according to (26.22) shows a first crude guess for bifurcation points from the requirement, that the occupation probability for a given state should be a positive number.

the expectation value $\langle \bar{x}(t) \rangle$ may then be considered as a measure of the size development of a space element with time and may be compared to a bursting soap bubble.

In figure 26.3 we present the exact energy spectrum for the fractional quantum harmonic oscillator using the Caputo derivative definition for the range $0.5 \leq \alpha \leq 1$.

For $\alpha < 1$ we obtain only a limited number of eigenvalues. In the limiting case $\alpha = 0.5$ we are left with only a single energy level. Below $\alpha = 1/2$ the fractional quantum harmonic oscillator using the Caputo derivative definition has no real eigenvalues any more.

Based on the stationary fractional quantum harmonic oscillator in Chapter 19 the infrared spectrum of HCl has been reproduced successfully [Herrmann (2012a)]. It has also been demonstrated, that the transition from vibrational ($\alpha \approx 1$) to rotational type ($\alpha \approx 2$) of spectra may be interpreted within the context of the fractional quantum harmonic oscillator as a transition from one- $d \approx 1$ to three-dimensional $d \approx 3$ space, as long as the corresponding multiplicities are correctly implemented.

Therefore in the following we will consider the consequences of a time dependence of $\alpha = \alpha(t)$, which implies a time development of the space dimension $d = d(t)$:

26.3 The model and possible consequences for an application in cosmology

We know, that the infrared spectra of diatomic molecules may be reproduced based on the level spectrum of the fractional quantum harmonic oscillator by defining the relative intensities I_n^α as a Boltzmann distribution weighted with the degeneracy of the n-th energy level [Herrmann (2012a)], where $\beta = 1/(k_B T)$:

$$I_n^\alpha = (2(\alpha - 1)n + 1)e^{-\beta E_n} \quad (26.12)$$

Which clearly demonstrates the unifying aspects of the fractional ansatz, since it combines the standard vibrational as well as the standard rotational elements as special cases

$$I_n^{\text{vib}} = e^{-\beta(n+1/2)}, \quad \alpha = 1 \quad (26.13)$$

$$I_n^{\text{rot}} = (2n + 1)e^{-\beta n(n+1)}, \quad \alpha = 2 \quad (26.14)$$

if we associate n with the vibrational quantum number for the standard one dimensional quantum harmonic oscillator and with the total angular momentum quantum number L with degeneracy $2L + 1$ for rotations in \mathbb{R}^3 .

Table 26.1 Bifurcation points (c_i) corresponding to the lowest excited states for the energy levels of the fractional quantum harmonic oscillator using the Caputo derivative. Points are sorted for increasing α and determined as the lowest real energy E_c for a given $\alpha = \alpha_c$, the corresponding fractional dimension d_c is given according to (26.18).

c_i	levels	α_c	E_c	d_c
1	$2^+ - 4^+$	0.7463952	2.6065	0.4927904
2	$1^- - 3^-$	0.7847781	2.0067	0.5695562
3	$6^+ - 8^+$	0.8156782	5.1369	0.6313564
4	$10^+ - 12^+$	0.8501847	7.8612	0.7003694
5	$5^- - 7^-$	0.8603896	4.9009	0.7207792
6	$9^- - 11^-$	0.8919590	7.9842	0.7839180

For a practical application, the spectra of diatomic molecules are reproduced with high accuracy setting $\alpha \approx 2$ for rotational spectra and $\alpha \approx 1$ for vibrational spectra and therefore prove the validity of the fractional approach in the close vicinity of $\alpha = 1, 2$ only.

Now we want to investigate this approach for the full range of allowed α -values, especially $\alpha \ll 1$ and parametrize with time t .

In order to calculate the time dependent spectral response of a space element, we therefore postulate that the dimensionality of a given space element is directly related to the multiplicity of the occupation probability $p_n^{\alpha(t)}$ for a given state $\psi_n(x, t)$.

$$p_n^{\alpha(t)} = m(d(t), n) \frac{1}{Z^{\alpha(t)}} e^{-\beta E_n^{\alpha(t)}} \quad (26.15)$$

as a product of a thermalized level distribution with a dimension dependent multiplicity factor $m(d(t), n)$, which determines the dimension dependent degeneracy of the n -th eigenvalue and with the extended canonical ensemble $Z^{\alpha(t)}$

$$Z^{\alpha(t)} = \text{Tr}(m(d(t), n) e^{-\beta H^{\alpha(t)}}) \quad (26.16)$$

where $\beta = 1/(k_B T)$ and the multiplicity m is defined as

$$m = (d(t) - 1)n + 1 \quad (26.17)$$

and the connection between dimension d and the fractional parameter α is given as:

$$d(t) = 2\alpha(t) - 1, \quad \frac{1}{2} \leq \alpha \leq 2 \quad (26.18)$$

Indeed, with these settings, for the special case $d \in \mathbb{N}$ we obtain the multiplicities

$$m(d=1) = 1 \quad (26.19)$$

$$m(d=2) = n+1 \quad (26.20)$$

$$m(d=3) = 2n+1 \quad (26.21)$$

which is conformal with classical quantum mechanics, if we agree, that the fractional quantum harmonic oscillator bridges the two different Lie algebras $U(1) \rightarrow O(3)$ and n counts the multiplets of the corresponding Casimir-operators \hat{N} and \hat{L}^2 as outlined in e.g. [Herrmann (2007b); Herrmann (2012a)]. By the way, the explicit properties of the group elements and Casimir-operator for $d = 2$ have not been investigated yet.

Consequently, we obtain a first natural explanation for the upper limit $d = 3$ of allowed space dimensions from the requirement of normalizability of the solutions of the fractional quantum harmonic oscillator, which requires $\alpha \leq 2$. This is a fascinating answer to Ehrenfest's question [Ehrenfest (1917)].

Equation (26.17) also leads to a natural explanation for the limited number of levels for small α : From the requirement that the multiplicity of a given state n should be a positive real number, $m > 0$, which means, within the framework of a possible particle-hole, or better space-antispace formalism (since we discuss a property of space, not matter) we restrict to a description of space only, using (26.17) a condition follows for the finite set of allowed n values $n \in \{0, \dots, n_{\max}\}$:

$$n_{\max} < \frac{1}{2(1 - \alpha(t))}, \quad \alpha < 1 \quad (26.22)$$

which in the limiting case $\alpha \rightarrow \frac{1}{2}$ reduces to only one allowed level with $n = 0$. Consequently we obtain a natural explanation for the lower limit of allowed space dimension, since below $\alpha = 0.5$ there are no solutions for the fractional quantum harmonic oscillator, which according to (26.18) leads to the lower limit of $d = 0$.

In figure 26.3 this limiting function (26.22) is plotted with pointed lines and it shows a qualitative agreement with the exact data.

From the time dependence of $\alpha = \alpha(t)$ and the assumed correspondence of α with the space dimension d according to (26.18) we now propose an evolution of the space dimension as a function of time which is mediated by e.g.

$$\alpha(t) = \frac{1}{2} + \frac{3}{2} \arctan(t) \quad 0 \leq t \leq \infty \quad (26.23)$$

which of course is a heuristic approach. In a complete theory, which may be a possible direction of future research, the behavior of $\alpha(t)$ should be self consistently derived from a governing variation principle.

The expansion of the universe may be explained within the framework of this model: In an initially mainly homogeneous environment space elements with an initial space dimension $d = 0$ are seeded, which evolve with time to $d = 3$ standard space dimension, generating a foamy structure of the universe (see (26.11) for a size estimate as a function of $\alpha(t)$).

In figure 26.4 the distribution of space and matter for a small slice of space shows exactly this foamy structure. Space dominated regions are considered as matter free, shown as white areas, while matter dominated areas may be considered as boundaries and are presented in dark color. The white regions are therefore permanent sources of space generation and cause a major contribution to the expansion of the universe.

26.4 On the detectability of dynamic space evolution

The space dimension may be probed experimentally by a measurement of an intensity distribution of light as a function of an incident light ray:

The minimum requirement for photon absorption and emission processes respectively is the existence of at least two energy levels: a ground state and a first excited state. From figure 26.3 we may deduce the bifurcation points for a given α_c giving the onset of a real eigenvalue for increasing α . In table 26.1 these values are listed for increasing α .

Through the genesis of space starting with $\alpha = 0.50, d = 0$ we therefore have a threshold space dimension of about $\alpha_c = 0.7463952, d_c = 0.4927904$, which is the minimum space dimension, allowing for excitation ($0^+ \rightarrow 2^+$) and radiation ($2^+ \rightarrow 0^+$) processes. Below this threshold this space element is dark.

The threshold dimension d_c may be considered as

$$d_c = 1/2 - \text{perturbation} \quad (26.24)$$

Within that context, we want to make the following remark: a fractional derivative may be written as a Taylor-series of standard integer derivatives.

For the Caputo fractional derivative we have already derived (26.6), therefore it will be no surprise, that the above numerically calculated threshold dimension d_c introducing Sommerfeld's fine structure constant $\alpha_S \approx 1/137.036 = e^2/(\hbar c)$ may be compared with the following quantity

D_c , which describes the perturbation as an infinite geometric series expansion in α_S :

$$D_c = \frac{1}{2} - \text{perturbation} \quad (26.25)$$

$$= \frac{1}{2} - \alpha_S + \alpha_S^2 - \alpha_S^3 \dots \quad (26.26)$$

$$= \sum_{n=0}^{\infty} (-\alpha_S)^n - \frac{1}{2} \quad (26.27)$$

$$= \frac{1}{1 + \alpha_S} - \frac{1}{2} \quad (26.28)$$

$$\approx 0.492756 \quad (26.29)$$

which agrees with d_c up to 10^{-5} .

This may be interpreted as an indication,

- that the fractional quantum harmonic oscillator with the Caputo fractional derivative *per se* describes an electro-magnetic charge type or alternatively may be used to give a very good estimate for the fine structure constant α_S . Hence for a first time the fine structure constant is derived from first principles, which was a demand stated by Dirac more than 50 years ago [Dirac (1963); Dirac (1984)].

As a consequence, we are directly led to the conclusion, that electro-magnetic interaction is rather a property of space than of matter. Furthermore, e.g. the constancy of the speed of light in the vacuum may be understood immediately, assuming it a property of space, instead of matter.

Even more generally we may speculate

- that the solution of a fractional differential equation compared to the standard path integral approach used in QED and QCD respectively, already includes higher order perturbations, which could be considered as a future research area of major importance.

26.5 Meta physics: on the connection between dark matter and dark energy

At this point of discussion, we may introduce two possible candidates of common interest. In current cosmology there exist two miraculous contributions: dark energy and dark matter.

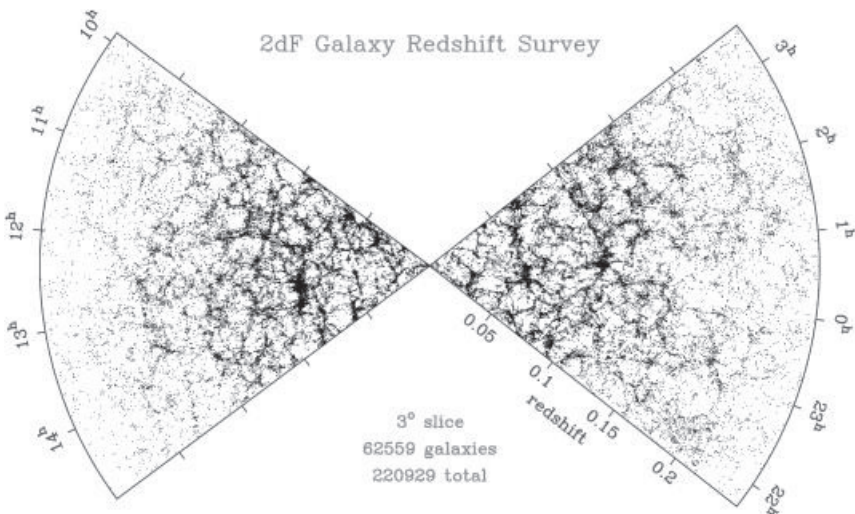


Fig. 26.4 Results of the 2dF redshift galaxy survey. Here one of the redshift slices for different spectral types is shown. It is a graphical presentation of our interpretation of space genesis and inflation of the universe. Space dominated regions are considered as matter free and shown as white areas, while matter dominated areas may be considered as boundaries and are presented in dark color. In a classical approach, space dominated regions may be considered as dominated by dark energy E_d while matter dominated regions may be interpreted as a surface of a space generating region, emulating a compressive contribution which may be interpreted classically as the influence of a dark matter M_d . Credits go to the “the 2dF Galaxy Redshift Survey team”.

With kind permission, see Colless et al. [Colless *et al.* (2001)], source from: <http://www2.aaq.gov.au/2dFGRS>.

Dark energy was first introduced as a necessary attribution for the explanation for the accelerated expansion of the universe, deduced from the observed redshift of distant galaxies [Riess *et al.* (1998)].

Dark matter has been considered to explain e.g. the observations of Rubin *et al.* [Zwicky (1933); Rubin *et al.* (1976a); Rubin *et al.* (1976b)] about the rotation velocity of stars in galaxies.

It is quite interesting, that both contributions carry the property darkness, which is just a phrase for the nonobservability of these entities using standard approaches, which means e.g. nonexistent emission or reflection of light.

In the above presented fractional model darkness in the early stage of space creation is a natural outcome of a threshold space dimension, above which the minimum requirement for visibility, a single additional

real eigenvalue, is fulfilled. It seems therefore tempting to associate regions of space genesis with high concentrations of dark energy E_d , while matter dominated regions may be considered as a manifestation of a boundary effect with a compressive contribution which is interpreted classically as the influence of so called dark matter M_d .

The fractional ansatz therefore connects the concepts of dark energy and dark matter as a unified concept of space generation. In a foamy large scale structure of the universe, the empty areas are considered as sources of expanding space and may be responsible for a concentration of matter at the boundaries of those space bubbles, which simulates the influence of an imaginary matter contribution.

The proposed fractional model also predicts a time development of the ratio of dark energy E_d and dark matter M_d of increasing type

$$\lim_{t \rightarrow \infty} \frac{E_d}{M_d} \rightarrow \infty \quad (26.30)$$

since the time development of the dark energy E_d within the framework of our fractional approach depends on a volume $E_d \sim R(t)^3$ and of dark matter M_d depends on a surface $M_d(t) \sim R(t)^2$ for large t , where $R(t)$ is a time dependent measure of the size of a given space generating region and consequently corresponds to the total size of the universe for a given time t , which is in accordance with current cosmological models.

In this chapter the creation of space as an evolutionary process has been described within the framework of fractional calculus with time dependent varying order.

A model was presented, which describes space generation as a dynamic process, where the dimension d of space evolves smoothly with time within the range $0 \leq d(t) \leq 3$.

The proposed model gives a direct explanation for the dimension bounds: the lower bound of dimension results from the requirement of positive (> 0) intensity value for an occupied energy level, while the upper bound follows from the requirement of normalizability of the calculated eigenfunctions.

Furthermore a minimum threshold for the space dimension was deduced $d_c \approx 1/2$, which is necessary to establish an interaction with external probe particles (e.g. light). Below this threshold, no absorption or emission processes are possible and as a consequence, this object cannot be detected with spectral methods.

This property is of fundamental importance for a successful application of the proposed model in cosmology: the fractional approach combines the

concepts of dark energy and dark matter within the unified concept of dynamic space generation.

Though the hitherto presented fractional approach is still a raw concept, we wanted to demonstrate the potential of an extended fractional calculus, based on a varying fractional parameter $\alpha(t)$, when applied to questions in cosmology. Many efforts have still to be made to obtain a reliable, consistent model of the universe. But we may already conclude, that genetic models, based on evolutionary fractional differential equations, will play an increasingly important role in cosmology.

This page intentionally left blank

Chapter 27

Outlook

In this book we have given a concise introduction to methods and strategies used within the fractional calculus. We have demonstrated, that this specific approach may be a powerful alternative for a description of phenomena in high energy and particle physics.

In addition we have shown, that the application of fractional group theory leads to a vast amount of intriguing and valuable results.

One reason for this success is the strategy, to interpret concrete experimental data and strictly verify the theoretical results with experimental findings.

Important achievements are:

- Exact prediction of the masses of $X(4260)$ and $X(4660)$ in the charmonium-spectrum, which were verified experimentally afterwards. Prediction of $B_2^*(5818)$ as an excited state of the B -meson, which still is to be verified by the experiment.
- The first application of fractional calculus in nuclear theory: a successful description of ground state band excitations in even-even nuclei.
- A derivation of the exact form of interacting fractional fields in lowest order of the coupling constant and a first application: a high precision mass formula for baryon masses based on the Riemann fractional derivative and a similar mass formula for a simultaneous calculation of all possible mesons based on the Caputo fractional derivative.
- A generalized treatment of vibrations and rotations and a direct application in infrared spectroscopy.
- Deduction of the fractional dynamic symmetry group, which simultaneously describes the magic numbers in nuclei and metal clusters.

Furthermore we have presented a large amount of practical applications of the fractional concept in different branches of physics.

Many open problems still need to be solved on the way to a consistent formulation of fractional calculus, e.g. a covariant realization of nonlocal operators is a necessary prerequisite.

During the process of writing this book the development of fractional calculus of course keeps evolving.

For example, besides some remarks in the last chapter, in this book we restricted the presentation of fractional calculus to a constant fractional derivative parameter α . Today we can already estimate, that a generalization of this concept to a derivative of varying order will lead to new insights when applied to systems, where the dynamics is a function of a time and position dependent fractional derivative $\alpha = \alpha(x, t)$ [Samko and Ross (1993a); Sun *et al.* (2009); Ramirez and Ciombra (2010)]. This would allow to determine an evolution of the governing differential equations used to describe a complex dynamical system.

This is only one of many examples, where fractional calculus will find its way to establish new strategies to explore previously unknown fields of application. Hence fractional calculus continues to keep ahead in a vividly developing research area. New questions will be raised and new problems will successfully be solved using the fractional approach.

Appendix A

Solutions to Exercises

Exercise 2.1: Fractional binomials

Problem: Prove the identity

$$(-1)^j \binom{j-q-1}{j} = \binom{q}{j} \quad q \in \mathbb{R} \wedge q \notin \mathbb{N}, j \in \mathbb{N} \quad (\text{A.1})$$

Solution: With the definition of the fractional binomial (2.10) we obtain

$$(-1)^j \binom{j-q-1}{j} = \binom{q}{j} \quad (\text{A.2})$$

$$(-1)^j \frac{\Gamma(j-q)}{\Gamma(1+j)\Gamma(-q)} = \frac{\Gamma(1+q)}{\Gamma(1+j)\Gamma(1+q-j)} \quad (\text{A.3})$$

$$(-1)^j \frac{\Gamma(j-q)}{\Gamma(-q)} = \frac{\Gamma(1+q)}{\Gamma(1+q-j)} \quad (\text{A.4})$$

$$(-1)^j \frac{1}{\Gamma(1+q)\Gamma(-q)} = \frac{1}{\Gamma(j-q)\Gamma(1-(j-q))} \quad (\text{A.5})$$

inserting the reflection formula (2.11) we get

$$(-1)^j \sin(-\pi q) = \sin(\pi(j-q)) \quad (\text{A.6})$$

Since (see e.g. (4.3.34) [Abramowitz and Stegun (1965)])

$$\sin(z_1 + z_2) = \sin(z_1) \cos(z_2) + \cos(z_1) \sin(z_2) \quad (\text{A.7})$$

we obtain the result

$$(-1)^j \sin(-\pi q) = \sin(-\pi q) \cos(\pi j) + \cos(-\pi q) \sin(\pi j) \quad (\text{A.8})$$

$$= (-1)^j \sin(-\pi q) \quad \text{q.e.d} \quad (\text{A.9})$$

Exercise 2.2: Solution of the cubic equation in terms of hypergeometric functions

Problem: The general solution of the cubic equation

$$x^3 + ax^2 + bx + c = 0 \quad (\text{A.10})$$

given in radicals was first published by Cardano [Cardano (1545)].

An alternative approach, which is more appropriate in view of a generalization to higher order equations, gives the solutions in terms of hypergeometric functions:

Applying a Tschirnhausen transformation [Tschirnhausen (1683)] of type

$$x \Rightarrow \alpha x + \beta \quad (\text{A.11})$$

the cubic equation may be transformed to an equivalent, but easier to handle form:

$$x^3 - x - q = 0, \quad q = \left(\frac{2a^3}{27} - \frac{ab}{3} + c \right) / \sqrt{\left(b - \frac{a^3}{3} \right)^3} \quad (\text{A.12})$$

where the general solutions x_i with $i \in \{1, 2, 3\}$ are a function of only one variable $x_i = f_i(q)$.

Prove that one solution of (A.12) is given by:

$$x_1(q) = -q {}_2F_1(1/3, 2/3; 3/2; \frac{27}{4}q^2) \quad (\text{A.13})$$

Solution: We have to prove, that the solution satisfies the equation:

$$x_1^3 - x_1 - q = 0, \quad q \in \mathbb{C} \quad (\text{A.14})$$

For that purpose, we rewrite the hypergeometric function in a more appropriate form. With (15.1.15) from [Abramowitz and Stegun (1965)]

$${}_2F_1(a, 1-a; 3/2; \sin^2(z)) = \frac{\sin((2a-1)z)}{(2a-1)\sin(z)} \quad (\text{A.15})$$

we obtain:

$$x_1(q) = -q {}_2F_1(1/3, 2/3; 3/2; \frac{27}{4}q^2) \quad (\text{A.16})$$

$$= -\frac{2}{\sqrt{3}} \sin\left(\frac{1}{3}p\right), \quad p = \arcsin\left(\frac{\sqrt{27}}{2}q\right) \quad (\text{A.17})$$

This yields for the cubic x_1^3 :

$$x_1^3(q) = -\frac{8}{3\sqrt{3}} \sin^3\left(\frac{1}{3}p\right) \quad (\text{A.18})$$

$$= \frac{2}{3\sqrt{3}} \{-4 \sin^3\left(\frac{1}{3}p\right)\} \quad (\text{A.19})$$

With (4.3.27) from [Abramowitz and Stegun (1965)]

$$\sin(z) = 3 \sin(z/3) - 4 \sin^3(z/3) \quad (\text{A.20})$$

we finally obtain:

$$x_1^3(q) = \frac{2}{3\sqrt{3}} \{\sin(p) - 3 \sin\left(\frac{1}{3}p\right)\} \quad (\text{A.21})$$

$$= q - \frac{2}{\sqrt{3}} \sin\left(\frac{1}{3}p\right) \quad (\text{A.22})$$

$$= q + x_1 \quad \text{q.e.d} \quad (\text{A.23})$$

Therefore we have proven, that (A.13) indeed solves the cubic equation (A.12).

As a motivation it should be mentioned, that a solution of the quintic [Klein (1884)]

$$x^5 - x - q = 0 \quad (\text{A.24})$$

is given in terms of a hypergeometric function as:

$$x_1(q) = -q {}_4F_3(1/5, 2/5, 3/5, 4/5; 2/4, 3/4, 5/4; \frac{3125}{256}q^4) \quad (\text{A.25})$$

which clearly demonstrates, that higher order equations of type (A.24) are always solvable via a series expansion in q and are given in terms of hypergeometric functions.

Exercise 3.1: The Riemann derivative of $x^\alpha/(1-x)$

Problem: Calculate the fractional derivative according to Riemann for

$$f(x) = \frac{x^\alpha}{1-x} \quad |x| < 1 \quad (\text{A.26})$$

Solution: The problem may be solved elegantly, rewriting the denominator in (A.26) as the result of a summation of a geometric series

$$\sum_{k=0}^{\infty} x^k = \frac{1}{1-x} \quad |x| < 1 \quad (\text{A.27})$$

since we may apply the Riemann fractional derivative for a power series in x term by term:

$$\partial_x^\alpha f(x) = \partial_x^\alpha \frac{x^\alpha}{1-x} \quad (\text{A.28})$$

$$= \partial_x^\alpha \sum_{k=0}^{\infty} x^{\alpha+k} \quad (\text{A.29})$$

$$= \sum_{k=0}^{\infty} \frac{\Gamma(1+\alpha+k)}{\Gamma(1+k)} x^k \quad (\text{A.30})$$

$$= \Gamma(1+\alpha) \sum_{k=0}^{\infty} \frac{\Gamma(1+\alpha+k)}{\Gamma(1+k)\Gamma(1+\alpha)} x^k \quad (\text{A.31})$$

$$= \Gamma(1+\alpha) \sum_{k=0}^{\infty} \binom{\alpha+k}{k} x^k \quad (\text{A.32})$$

$$= \Gamma(1+\alpha) \sum_{k=0}^{\infty} \binom{-\alpha-1}{k} (-1)^k x^k \quad (\text{A.33})$$

$$= \Gamma(1+\alpha) \frac{1}{(1-x)^{1+\alpha}} \quad (\text{A.34})$$

where we have used (2.10), (A.1) and (3.28).

Exercise 3.2: The Riemann derivative of $x^p/(1-x)$

Problem: Calculate the fractional derivative according to Riemann for

$$f(x) = \frac{x^p}{1-x} \quad |x| < 1, p \in \mathbb{R}, p > -1 \quad (\text{A.35})$$

Solution: The solution may be realized using the geometric series

$$\sum_{k=0}^{\infty} x^k = \frac{1}{1-x} \quad |x| < 1 \quad (\text{A.36})$$

and by a term by term differentiation of the series:

$$\partial_x^\alpha \frac{x^p}{1-x} = \partial_x^\alpha \sum_{k=0}^{\infty} x^{p+k} \quad (\text{A.37})$$

$$= \sum_{k=0}^{\infty} \frac{\Gamma(1+p+k)}{\Gamma(1+p+k-\alpha)} x^{k+p-\alpha} \quad (\text{A.38})$$

$$= x^{p-\alpha} \frac{\Gamma(1+p)}{\Gamma(1+p-\alpha)} \times \sum_{k=0}^{\infty} \frac{\Gamma(1+p+k)}{\Gamma(1+p)} \frac{\Gamma(1+p-\alpha)}{\Gamma(1+p-\alpha+k)} x^k \quad (\text{A.39})$$

$$= x^{p-\alpha} \frac{\Gamma(1+p)}{\Gamma(1+p-\alpha)} \times \sum_{k=0}^{\infty} \frac{\Gamma(1+p+k)}{\Gamma(1+p)} \frac{\Gamma(1+p-\alpha)}{\Gamma(1+p-\alpha+k)} \frac{k!}{k!} x^k \quad (\text{A.40})$$

$$= x^{p-\alpha} \frac{\Gamma(1+p)}{\Gamma(1+p-\alpha)} \times \sum_{k=0}^{\infty} \frac{\Gamma(1+k)}{\Gamma(1)} \frac{\Gamma(1+p+k)}{\Gamma(1+p)} \frac{\Gamma(1+p-\alpha)}{\Gamma(1+p-\alpha+k)} \frac{x^k}{k!} \quad (\text{A.41})$$

$$= x^{p-\alpha} \frac{\Gamma(1+p)}{\Gamma(1+p-\alpha)} {}_2F_1(1, 1+p; 1+p-\alpha; x) \quad (\text{A.42})$$

where we have used (2.19).

Exercise 3.3: Eigenvalues and eigenfunctions of the Caputo fractional derivative

Problem: The eigenvalues $s(k)$ and the eigenfunctions $\Psi(k, t)$ of the Caputo derivative ${}_C\partial_t$ are solutions of the differential equation

$${}_C\partial_t \Psi(k, t) = s(k)\Psi(k, t) \quad (\text{A.43})$$

Show that the solution of this differential equation for $t \geq 0$ and $k \geq 0$ is given by the Mittag-Leffler function (2.14)

$$\Psi(k, t) = E_\alpha(k^\alpha t^\alpha) \quad (\text{A.44})$$

and the eigenvalues are given by

$$s(k) = k^\alpha \quad (\text{A.45})$$

Solution: We write the Mittag-Leffler function as a series expansion and apply the Caputo fractional derivative to each single term in this series:

$${}_C\partial_t E_\alpha((kt)^\alpha) = {}_C\partial_t \sum_{n=0}^{\infty} \frac{k^{n\alpha} t^{n\alpha}}{\Gamma(1+n\alpha)} \quad (\text{A.46})$$

$$= \sum_{n=1}^{\infty} \frac{k^{n\alpha}}{\Gamma(1+n\alpha)} \frac{\Gamma(1+n\alpha)}{\Gamma(1+(n-1)\alpha)} t^{(n-1)\alpha} \quad (\text{A.47})$$

$$= k^\alpha \sum_{n=1}^{\infty} \frac{k^{(n-1)\alpha}}{\Gamma(1+(n-1)\alpha)} t^{(n-1)\alpha} \quad (\text{A.48})$$

$$= k^\alpha \sum_{n=0}^{\infty} \frac{k^{n\alpha}}{\Gamma(1+n\alpha)} t^{n\alpha} \quad (\text{A.49})$$

$$= k^\alpha E_\alpha((kt)^\alpha) \quad \text{q.e.d} \quad (\text{A.50})$$

For the special case the semi-derivative $\alpha = 1/2$ we obtain:

$$E_{\frac{1}{2}}(\sqrt{kt}) = e^{kt}(1 + \operatorname{erf}(\sqrt{kt})) \quad (\text{A.51})$$

Exercise 3.4: Asymptotic behavior of the the Grünwald-Letnikov fractional derivative

Problem: Prove that the asymptotic behavior of the weights in the Grünwald-Letnikov derivative

$$\partial_x^\alpha f(x) = \lim_{h \rightarrow 0} \frac{\Delta^\alpha f(x)}{h^\alpha} = \lim_{h \rightarrow 0} \left(\sum_{m=0}^{\infty} \binom{\alpha}{m} (-1)^m f(x - mh) \right) / h^\alpha \quad (\text{A.52})$$

is approximately given by:

$$(-1)^m \binom{\alpha}{m} \sim \frac{-\alpha}{\Gamma(1-\alpha)} \frac{1}{m^{1+\alpha}} \quad m \rightarrow \infty \quad (\text{A.53})$$

Solution: The basic idea for a solution is a proper approximation of the $\Gamma(z)$ function by Stirling's formula [Stirling (1730); Feller (1968)]. With (6.1.39) from [Abramowitz and Stegun (1965)]:

$$\Gamma(b+z) \sim \sqrt{2\pi} \exp(-z) z^{z+b-1/2} \quad (\text{A.54})$$

with (3.13) [Abramowitz and Stegun (1965)]:

$$\binom{n}{k} = (-1)^k \binom{k-n-1}{k} \quad (\text{A.55})$$

and with (4.2.21) [Abramowitz and Stegun (1965)]:

$$\lim_{m \rightarrow \infty} \left(1 + \frac{z}{m}\right)^m = e^z \quad (\text{A.56})$$

we may evaluate the left side of (A.53) to:

$$(-1)^m \binom{\alpha}{m} = \binom{m-\alpha-1}{m} \quad (\text{A.57})$$

$$= \frac{1}{\Gamma(-\alpha)} \frac{\Gamma(m-\alpha)}{\Gamma(1+m)} \quad (\text{A.58})$$

$$\sim \frac{-\alpha}{\Gamma(1-\alpha)} \frac{\sqrt{2\pi} e^{-(m-\alpha)} (m-\alpha)^{m-\alpha-1/2}}{\sqrt{2\pi} e^{-m} m^{m+1/2}} \quad (\text{A.59})$$

$$\sim \frac{-\alpha}{\Gamma(1-\alpha)} \frac{e^\alpha (1-\alpha/m)^{m-\alpha-1/2}}{m^{1+\alpha}} \quad (\text{A.60})$$

$$\sim \frac{-\alpha}{\Gamma(1-\alpha)} \frac{e^\alpha (1-\alpha/m)^m}{m^{1+\alpha}} \quad (\text{A.61})$$

$$\sim \frac{-\alpha}{\Gamma(1-\alpha)} \frac{1}{m^{1+\alpha}} \quad m \rightarrow \infty, \quad \text{q.e.d} \quad (\text{A.62})$$

Exercise 4.1: Eigenfunctions for a first order fractional differential equation with purely imaginary fractional coefficient α

Problem: We know that an exponential growth may be modeled by the standard first order differential equation:

$$\partial_t f(t) = k f(t) \quad (\text{A.63})$$

where the solution is given by $f(t) = e^{kt}$.

This ansatz was extended by Liouville for fractional derivatives

$$\partial_t^\alpha f(t) = k^\alpha f(t), \quad k > 0, t > 0, \alpha \in \mathbb{C} \quad (\text{A.64})$$

with the same eigenfunction $f(t) = e^{kt}$, which may be interpreted from a physicists point of view as the fractional generalization of exponential growth, which seems a natural explanation for $\alpha \in \mathbb{R}$.

But what are the characteristics of the eigenfunctions of the following purely imaginary fractional differential equation with $\alpha = i = \sqrt{-1}$

$$\partial_t^i f(t) = k f(t), \quad k > 0, t > 0 \quad (\text{A.65})$$

Hint: Use the Liouville definition of a fractional derivative and the Moivre formula:

$$e^{i\phi} = \cos(\phi) + i \sin(\phi) \quad (\text{A.66})$$

Solution: We first calculate the fractional derivative according to Liouville of the exponential test function

$$\partial_t^i e^{\nu t} = \nu^i e^{\nu t} \quad (\text{A.67})$$

This is a solution of the imaginary differential equation (A.65) if ν fulfills the condition

$$\nu^i = k \quad (\text{A.68})$$

and therefore

$$\nu = k^{-i} \quad (\text{A.69})$$

Using Moivres formula, we obtain for the real and imaginary part of k^{-i} :

$$k^{-i} = (e^{\ln(k)})^{-i} = e^{i(-\ln(k))} = \cos(\ln(k)) - i \sin(\ln(k)) \quad (\text{A.70})$$

and the eigenfunction is given as

$$e^{\{\cos(\ln(k)) - i \sin(\ln(k))\}t} \quad (\text{A.71})$$

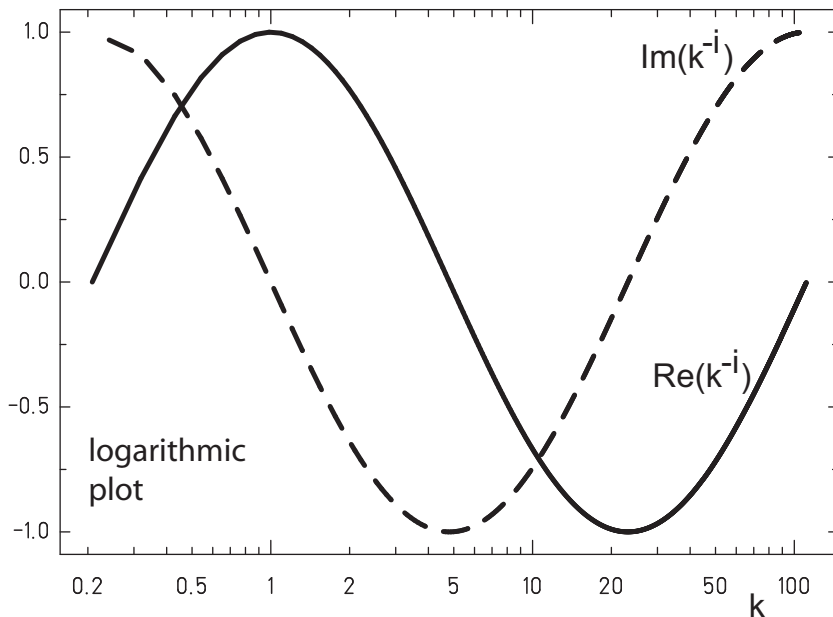


Fig. A.1 Logarithmic plot of k^{-i} , real part ($\cos(\ln(k))$) (thick line) and imaginary part $-\sin(\ln(k))$ (dashed line) in the interval $e^{-\frac{\pi}{2}} \leq k \leq e^{+\frac{3\pi}{2}}$ which covers the range of a full period 2π .

We may deduce, that the behavior of the eigenfunction depends on the value of k . In case of vanishing imaginary part indeed we have an exponential growth, but also decay for distinct values of k :

$$\sin(\ln(k)) = 0 \Rightarrow \ln(k) = \pm n\pi \Rightarrow k = e^{\pm n\pi}, \quad n \in \mathbb{N} \quad (\text{A.72})$$

and the eigenfunction takes the simple form

$$e^{\cos(\ln(k))t} = e^{\cos(\pm n\pi)t} = e^{\pm t} \quad (\text{A.73})$$

In addition, for vanishing real part, there remains a completely imaginary solution:

$$\cos(\ln(k)) = 0 \Rightarrow \ln(k) = \pm(2n+1)\frac{\pi}{2} \Rightarrow k = e^{\pm(2n+1)\pi/2}, \quad n \in \mathbb{N} \quad (\text{A.74})$$

and the eigenfunction takes the simple form

$$e^{-i \sin(\ln(k))t} = e^{-i \sin(\pm(2n+1)\pi/2)t} = e^{\pm it} \quad (\text{A.75})$$

which therefore determines an oscillatory part of the eigenfunction.

It should be noted, that for $k > 0$ there exists an infinite number of different k-values, which fulfill conditions (A.72) and (A.74) respectively, since for $k < e$:

$$\lim_{k \rightarrow 0} \ln(k) = -\infty \quad (\text{A.76})$$

In figure A.1 we show a logarithmic plot for the real and imaginary part of k^{-i} , which are nothing else but:

$$\operatorname{Re}(k^{-i}) = \cos(\ln(k)) \quad (\text{A.77})$$

$$\operatorname{Im}(k^{-i}) = -\sin(\ln(k)) \quad (\text{A.78})$$

As a consequence, if we insist to model exponential growth, only a discrete spectrum of k-values is allowed. But the same differential equation also describes exponential decay or even more surprising oscillations, if we use different sets of k-values.

We also observe a realization of self similar solutions for a set of k-values within

$$2\pi n \leq |\ln(k)| \leq 2\pi(n+1) \quad n \in \mathbb{N} \quad (\text{A.79})$$

where the interval length for different k tends to zero while k reaches 0.

Obviously oscillatory processes are not necessarily described by second order differential equations, the solutions of a first order fractional differential equation show a similar behavior.

Another point is quantization. Let us apply the imaginary fractional differential equation as a simple model for a light emitting source in a dusty surrounding e.g. a dwarf star in a far distant dark nebula. What is the spectrum of this object observed from a very large distance. If k is the wavelength, at first all frequencies are emitted, but all light rays with an imaginary contribution die out on their way. Finally we are left with a discrete spectrum at distinct k values:

$$k = e^{\pm 2n\pi} \quad n \in \mathbb{N} \quad (\text{A.80})$$

From now on, whenever you observe a spectrum of this type, hopefully you recall this exercise.

We may conclude, that a fractional differential equation describes in general a much broader variety of physical behavior, than its integer pendant. On the other hand, it may be misleading to simply generalize results, which have been derived for the integer case of a differential equation.

Exercise 5.1: The Laplace transform of the Mittag-Leffler function

Problem: The Laplace transform of a function $f(t)$ is given by:

$$\mathcal{F}(s) = \int_0^\infty dt e^{-st} f(t) \quad s \in \mathbb{R}^+ \quad (\text{A.81})$$

What is the Laplace transform of the Mittag-Leffler function $E_\alpha(\nu t^\alpha)$, $\nu \in \mathbb{R}^+$?

Solution: By direct integration we obtain:

$$\int_0^\infty dt e^{-st} E_\alpha(\nu t^\alpha) = \int_0^\infty dt e^{-st} \sum_{k=0}^\infty \frac{(\nu t^\alpha)^n}{\Gamma(1+\alpha n)} \quad (\text{A.82})$$

$$= \sum_{k=0}^\infty \frac{\nu^n}{\Gamma(1+\alpha n)} \int_0^\infty dt e^{-st} t^{\alpha n} \quad (\text{A.83})$$

With the substitution $u = st$ follows

$$\int_0^\infty dt e^{-st} E_\alpha(\nu t^\alpha) = \sum_{k=0}^\infty \frac{\nu^n}{\Gamma(1+\alpha n)} \frac{1}{s^{1+\alpha n}} \int_0^\infty du e^{-u} u^{\alpha n} \quad (\text{A.84})$$

$$= \sum_{k=0}^\infty \frac{\nu^n}{\Gamma(1+\alpha n)} \frac{1}{s^{1+\alpha n}} \Gamma(1+\alpha n) \quad (\text{A.85})$$

$$= \sum_{k=0}^\infty \frac{\nu^n}{s^{1+\alpha n}} \quad (\text{A.86})$$

since the integral is nothing else but the definition of the Γ -function. Finally the summation of the series is easily done, when interpreted as a geometric series

$$\sum_{k=0}^\infty \frac{\nu^n}{s^{1+\alpha n}} = \frac{1}{s} \sum_{k=0}^\infty \left(\frac{\nu}{s^\alpha}\right)^n \quad (\text{A.87})$$

$$= \frac{1}{s} \frac{1}{1 - \nu/s^\alpha} \quad (\text{A.88})$$

$$= \frac{s^{\alpha-1}}{s^\alpha - \nu} \quad (\text{A.89})$$

Exercise 5.2: The Caputo derivative of $\ln(1 + x)$

Problem: Calculate the fractional derivative according to Caputo for

$$f(x) = \ln(1 + x) \quad |x| < 1 \quad (\text{A.90})$$

Hint: Use a Taylor series expansion

Solution: The Taylor series expansion of a function $f(x)$ at $x = 0$ is given by:

$$f(x) = \sum_{n=0}^{\infty} \frac{f^{(n)}(0)}{n!} x^n \quad (\text{A.91})$$

The derivatives for the logarithm are given in closed form as:

$$\partial_x^n \ln(1 + x) = (-1)^{n-1} (n-1)! \frac{1}{(1+x)^n}, \quad n \in \mathbb{N} \quad (\text{A.92})$$

The Taylor series for the logarithm results as

$$\ln(1 + x) = x - \frac{x^2}{2} + \frac{x^3}{3} \dots \quad (\text{A.93})$$

$$= \sum_{n=0}^{\infty} (-1)^n \frac{x^{n+1}}{n+1} \quad (\text{A.94})$$

The Caputo derivative follows by a term by term differentiation of the series

$$\partial_x^\alpha \ln(1 + x) = \partial_x^\alpha \sum_{n=0}^{\infty} (-1)^n \frac{x^{n+1}}{n+1} \quad (\text{A.95})$$

$$= \sum_{n=0}^{\infty} (-1)^n \frac{\Gamma(1+n+1)}{\Gamma(1+n+1-\alpha)} \frac{x^{n+1-\alpha}}{n+1} \quad (\text{A.96})$$

$$= x^{1-\alpha} \sum_{n=0}^{\infty} (-1)^n \frac{\Gamma(1+n)}{\Gamma(2+n-\alpha)} x^n \quad (\text{A.97})$$

$$= x^{1-\alpha} \frac{1}{\Gamma(2-\alpha)} \sum_{n=0}^{\infty} (-1)^n \frac{\Gamma(2-\alpha)\Gamma(1+n)}{\Gamma(2+n-\alpha)} x^n \quad (\text{A.98})$$

$$= x^{1-\alpha} \frac{1}{\Gamma(2-\alpha)} \sum_{n=0}^{\infty} n! n! \frac{\Gamma(2-\alpha)}{\Gamma(2+n-\alpha)} \frac{(-x)^n}{n!} \quad (\text{A.99})$$

$$= x^{1-\alpha} \frac{1}{\Gamma(2-\alpha)} {}_2F_1(1, 1; 2-\alpha; -x) \quad (\text{A.100})$$

which is the final result. It should be mentioned, since $f(0) = 0$, there was no fractional derivative for x^0 necessary. Consequently the Riemann fractional derivative yields the same result.

Exercise 5.3: Low level fractionality for $\ln(1 + x)$

Problem: For $f(x) = \ln(1 + x)$ compare the low level fractional derivative of Caputo type with the exact solution from exercise (5.2).

Hint: The following integral might be of help [Gradshteyn and Ryzhik (1980)]:

$$\int d\xi \frac{\ln(x - \xi)}{(1 + \xi)^2} = -\frac{(x - \xi) \ln(x - \xi) + (1 + \xi) \ln(1 + \xi)}{(1 + x)(1 + \xi)} \quad (\text{A.101})$$

Solution: For the low level fractional derivative we have

$$\alpha = 1 - \epsilon \quad \epsilon \ll 1 \quad (\text{A.102})$$

First of all, the exact solution for the Caputo fractional derivative for the logarithmic function is given according the last exercise by:

$${}_C\partial_x^\alpha \ln(1 + x) = \frac{x^\epsilon}{\Gamma(1 + \epsilon)} {}_2F_1(1, 1; 1 + \epsilon; -x) \quad (\text{A.103})$$

and for the approximation we already derived (with γ is the Euler- γ)

$${}_C\partial_x^{1-\epsilon} f(x) = f'(x) + \epsilon \left\{ f'(0) \ln(x) + \gamma f'(x) + \int_0^x f''(\xi) \ln(x - \xi) d\xi \right\} \quad (\text{A.104})$$

For the logarithm function we obtain:

$$f(x) = \ln(1 + x) \quad (\text{A.105})$$

$$f'(x) = \frac{1}{1 + x} \quad (\text{A.106})$$

$$f''(x) = -\frac{1}{(1 + x)^2} \quad (\text{A.107})$$

We have to evaluate

$$\begin{aligned} \int_0^x f''(\xi) \ln(x - \xi) d\xi &= - \int_0^x \frac{1}{(1 + \xi)^2} \ln(x - \xi) d\xi \\ &= \frac{(x - \xi) \ln(x - \xi) + (1 + \xi) \ln(1 + \xi)}{(1 + x)(1 + \xi)} \Big|_{\xi=0} \end{aligned} \quad (\text{A.108})$$

where we have used (A.101). Since

$$\lim_{x \rightarrow 0} x \ln(x) = 0, \quad (\text{A.109})$$

the logarithmic singularity at $\xi = x$ may be easily removed (the first term vanishes):

$$\lim_{\xi \rightarrow x} \frac{(x - \xi) \ln(x - \xi) + (1 + \xi) \ln(1 + \xi)}{(1 + x)(1 + \xi)} = \frac{\ln(1 + x)}{1 + x} \quad (\text{A.110})$$

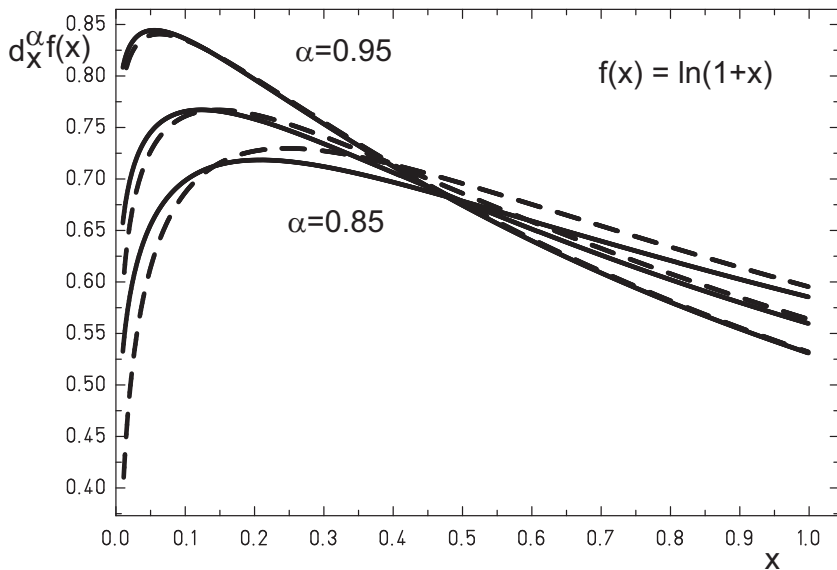


Fig. A.2 Comparison of the exact (thick line) and low level approximation (dashed line) of the Caputo fractional derivative of the logarithm $f(x) = \ln(1 + x)$ for different $\alpha = 0.95, 0.90, 0.85$. For $\alpha = 1$ we have $f'(x) = 1/(1 + x)$.

So we obtain:

$$-\int_0^x \frac{1}{(1+\xi)^2} \ln(x-\xi) d\xi = \frac{\ln(1+x)}{1+x} - \frac{x \ln(x)}{1+x} \quad (\text{A.111})$$

$$= \frac{\ln(x^{-x}(1+x))}{1+x} \quad (\text{A.112})$$

Therefore the final result for the low level approximation of the Caputo fractional derivative of $\ln(1 + x)$ is:

$${}_c\partial_x^{1-\epsilon} \ln(1+x) = \frac{1}{1+x} + \epsilon \left\{ \ln(x) + \frac{\gamma}{1+x} + \frac{\ln(x^{-x}(1+x))}{1+x} \right\} \quad (\text{A.113})$$

In figure A.2 we compare the exact to the low level approximation for different α close to 1. In the limit for $\alpha \rightarrow 1$ we observe a smooth transition from fractional, to low level up to standard derivative definition.

Exercise 6.1: Eigenfunctions of the m-th order Caputo differential operator

Problem: For the m-th order differential equation

$$(\partial_t^\alpha)^m x(t) = -\omega^{m\alpha} x(t) \quad (\text{A.114})$$

give the m different solutions in terms of the Mittag-Leffler functions.

Solution: It is helpful to determine the solutions of the m-th integer order differential equation first.

For $m = 1$ we have:

$$\partial_t x(t) = -\omega x(t) \quad (\text{A.115})$$

with the solution:

$$x(t) = \exp(-\omega t) = \sum_{k=0}^{\infty} (-1)^k \frac{(\omega t)^k}{k!} \quad (\text{A.116})$$

which is known as exponential decay.

For $m = 2$ we have:

$$\partial_t^2 x(t) = -\omega^2 x(t) \quad (\text{A.117})$$

with two linearly independent solutions:

$$x_1(t) = \cos(\omega t) = \sum_{k=0}^{\infty} (-1)^k \frac{(\omega t)^{2k}}{(2k)!} \quad (\text{A.118})$$

$$x_2(t) = \sin(\omega t) = \sum_{k=0}^{\infty} (-1)^k \frac{(\omega t)^{2k+1}}{(2k+1)!} \quad (\text{A.119})$$

with the property:

$$\partial_t x_1(t) = -x_2(t) \quad (\text{A.120})$$

$$\partial_t x_2(t) = x_1(t) \quad (\text{A.121})$$

which are known as oscillatory solutions.

In the fractional differential equation case we already solved (see exercise 3.3)

$$\partial_t^\alpha x(t) = -\omega^\alpha x(t) \quad (\text{A.122})$$

with the solution

$$s_{1,0}^\alpha = \sum_{k=0}^{\infty} (-1)^k \frac{(\omega t)^{k\alpha}}{\Gamma(1+k\alpha)} = E_\alpha(-(\omega t)^\alpha) \quad (\text{A.123})$$

and for $m = 2$ we derived for the fractional harmonic oscillator

$$(\partial_t^\alpha)^2 x(t) = -\omega^{2\alpha} x(t) \quad (\text{A.124})$$

with the solution

$$s_{2,0}^\alpha = \sum_{k=0}^{\infty} (-1)^k \frac{(\omega t)^{2k\alpha}}{\Gamma(1+2k\alpha)} = E_{2\alpha}(-(\omega t)^{2\alpha}) \quad (\text{A.125})$$

$$s_{2,1}^\alpha = \sum_{k=0}^{\infty} (-1)^k \frac{(\omega t)^{2k\alpha+\alpha}}{\Gamma(1+2k\alpha+\alpha)} = (\omega t)^\alpha E_{2\alpha,1+\alpha}(-(\omega t)^{2\alpha}) \quad (\text{A.126})$$

Therefore it is promising to start with the ansatz

$$s_{m,n}^\alpha = \sum_{k=0}^{\infty} (-1)^k \frac{(\omega t)^{mk\alpha+n\alpha}}{\Gamma(1+mk\alpha+n\alpha)} \quad n = 0, 1, \dots, m-1 \quad (\text{A.127})$$

$$= (\omega t)^{n\alpha} E_{m\alpha,1+n\alpha}(-(\omega t)^{m\alpha}) \quad (\text{A.128})$$

Indeed we have

$$\partial_t^\alpha s_{m,n}^\alpha = \sum_{k=0}^{\infty} (-1)^k \frac{\omega^{mk\alpha+n\alpha} t^{mk\alpha+n\alpha-\alpha}}{\Gamma(1+mk\alpha+n\alpha-\alpha)} \quad (\text{A.129})$$

$$= \omega^\alpha \sum_{k=0}^{\infty} (-1)^k \frac{(\omega t)^{mk\alpha+(n-1)\alpha}}{\Gamma(1+mk\alpha+(n-1)\alpha)} \quad (\text{A.130})$$

$$= \omega^\alpha s_{m,n-1}^\alpha \quad n = 1, \dots, m-1 \quad (\text{A.131})$$

and

$$\partial_t^\alpha s_{m,0}^\alpha = \sum_{k=1}^{\infty} (-1)^k \frac{\omega^{mk\alpha+n\alpha} t^{mk\alpha+-\alpha}}{\Gamma(1+mk\alpha-\alpha)} \quad (\text{A.132})$$

$$= (-1)\omega^\alpha \sum_{k=0}^{\infty} (-1)^k \frac{(\omega t)^{mk\alpha+(m-1)\alpha}}{\Gamma(1+mk\alpha+(m-1)\alpha)} \quad (\text{A.133})$$

$$= -\omega^\alpha s_{m,m-1}^\alpha \quad (\text{A.134})$$

and it follows

$$(\partial_t^\alpha)^m s_{m,n}^\alpha = -\omega^{m\alpha} s_{m,n}^\alpha \quad n, 0, 1, \dots, m-1 \quad (\text{A.135})$$

Therefore (A.127) indeed solves the fractional differential equation (A.114).

The case $m = 3$ is of special interest, since it is an open question, if the behavior of solutions contains the exponential decay, which was observed for $m = 1$ as well as oscillatory contributions, which were observed for $m = 2$.

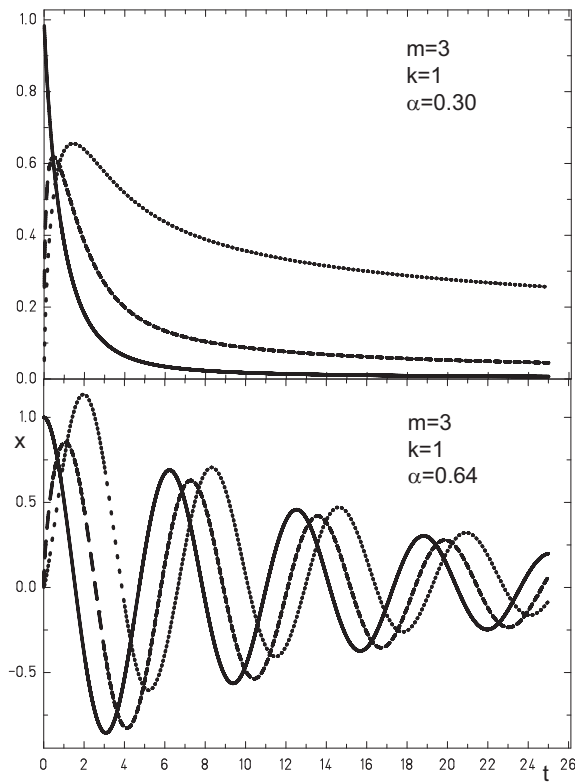


Fig. A.3 Solutions of the third order linear fractional differential equation (A.114) for $\alpha = 0.30$ (top) and $\alpha = 0.64$ (bottom). Thick line indicates $s_{3,0}$, dashed line is $s_{3,1}$ and dotted line is $s_{3,2}$.

For the special case $\alpha = 1/3$ we obtain:

$$s_{3,0}^{1/3} = E_1(-\omega t) \quad (\text{A.136})$$

$$= \exp(-\omega t) \quad (\text{A.137})$$

$$s_{3,1}^{1/3} = (\omega t)^{\frac{1}{3}} E_{1,4/3}(-\omega t) \quad (\text{A.138})$$

$$= \exp(-\omega t) \frac{\Gamma(1/3) - \Gamma(1/3, -\omega t)}{(-1)^{\frac{1}{3}} \Gamma(1/3)} \quad (\text{A.139})$$

$$s_{3,2}^{1/3} = (\omega t)^{\frac{2}{3}} E_{1,5/3}(-\omega t) \quad (\text{A.140})$$

$$= \exp(-\omega t) \frac{\Gamma(2/3) - \Gamma(2/3, -\omega t)}{(-1)^{\frac{2}{3}} \Gamma(2/3)} \quad (\text{A.141})$$

with the asymptotic behavior

$$\lim_{t \rightarrow \infty} s_{3,0}^{1/3} = \exp(-\omega t) \quad (\text{A.142})$$

$$\lim_{t \rightarrow \infty} s_{3,1}^{1/3} = \exp(-\omega t) \quad (\text{A.143})$$

$$\lim_{t \rightarrow \infty} s_{3,2}^{1/3} = \exp(-\omega t) \quad (\text{A.144})$$

For the special case $\alpha = 2/3$ we obtain:

$$s_{3,0}^{2/3} = E_2(-(\omega t)^2) \quad (\text{A.145})$$

$$= \cos(\omega t) \quad (\text{A.146})$$

$$s_{3,1}^{2/3} = (\omega t)^{\frac{2}{3}} E_{2,5/3}(-(\omega t)^2) \quad (\text{A.147})$$

$$= (\omega t)^{\frac{2}{3}} \frac{1}{\Gamma(5/3)} {}_1F_2(1; 5/6, 4/3; -\frac{1}{4}\omega^2 t^2) \quad (\text{A.148})$$

$$s_{3,2}^{2/3} = (\omega t)^{\frac{4}{3}} E_{2,7/3}(-(\omega t)^2) \quad (\text{A.149})$$

$$= (\omega t)^{\frac{4}{3}} \frac{1}{\Gamma(7/3)} {}_1F_2(1; 7/6, 5/3; -\frac{1}{4}\omega^2 t^2) \quad (\text{A.150})$$

with the asymptotic behavior

$$\lim_{t \rightarrow \infty} s_{3,0}^{2/3} = \cos(\omega t) \quad (\text{A.151})$$

$$\lim_{t \rightarrow \infty} s_{3,1}^{2/3} = \cos(\omega t - \frac{\pi}{3}) \quad (\text{A.152})$$

$$\lim_{t \rightarrow \infty} s_{3,2}^{2/3} = \cos(\omega t - \frac{2\pi}{3}) \quad (\text{A.153})$$

For the special case $\alpha = 1$ we obtain:

$$s_{3,0}^1 = E_3(-(\omega t)^3) \quad (\text{A.154})$$

$$= \frac{1}{3} \exp(-\omega t) \left(1 + 2 \exp\left(\frac{3}{2}\omega t\right) \cos\left(\frac{\sqrt{3}}{2}\right) \right) \quad (\text{A.155})$$

$$s_{3,1}^1 = \omega t E_{3,2}(-(\omega t)^3) \quad (\text{A.156})$$

$$= \frac{1}{3} \exp(-\omega t) \left(-1 + 2 \exp\left(\frac{3}{2}\omega t\right) \sin\left(\frac{\pi}{6} + \frac{\sqrt{3}}{2}\omega t\right) \right) \quad (\text{A.157})$$

$$s_{3,2}^1 = (\omega t)^2 E_{3,3}(-(\omega t)^3) \quad (\text{A.158})$$

$$= \frac{1}{3} \exp(-\omega t) \left(-1 + 2 \exp\left(\frac{3}{2}\omega t\right) \sin\left(\frac{\pi}{6} - \frac{\sqrt{3}}{2}\omega t\right) \right) \quad (\text{A.159})$$

which illustrates the exponential growth with an oscillatory admixture of solutions for $\alpha > 2/3$.

In figure A.3 we have sketched the three solutions near the discussed special cases.

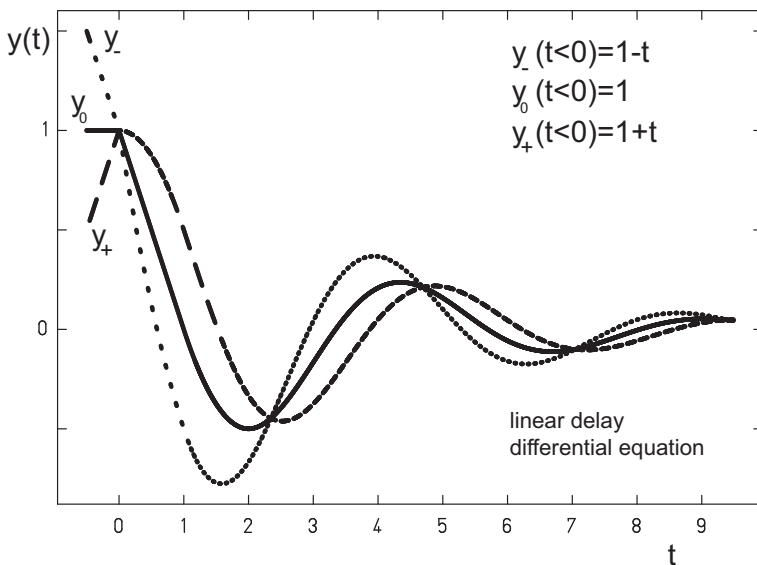


Fig. A.4 Solutions of the linear delay differential equation (A.160) for three different initial functions for $t \leq 0$: Thick line $y_0(t) = 1$, dashed line $y_+(t) = 1 + t$ and dotted line $y_-(t) = 1 - t$.

Exercise 8.1: A linear delay differential equation

Problem: Give an analytic solution for $y(t)$ in the interval $t \in [0, 4a]$ of the following delay differential equation

$$\partial_t y(t) = -y(t - a), \quad t > 0, a \in \mathbb{R} \quad (\text{A.160})$$

where $y(t)$ is given by

$$y(t) = 1, \quad t \leq 0 \quad (\text{A.161})$$

For reasons of simplicity set the interval length to $a = 1$.

Solution: The solution is given by a step by step procedure: For t in the interval $[0, a]$ we get by direct integration

$$y(t) = y(0) - \int_0^t dt y(t - a) = - \int_0^t dt y(t - a) = - \int_0^t dt = 1 - t \quad (\text{A.162})$$

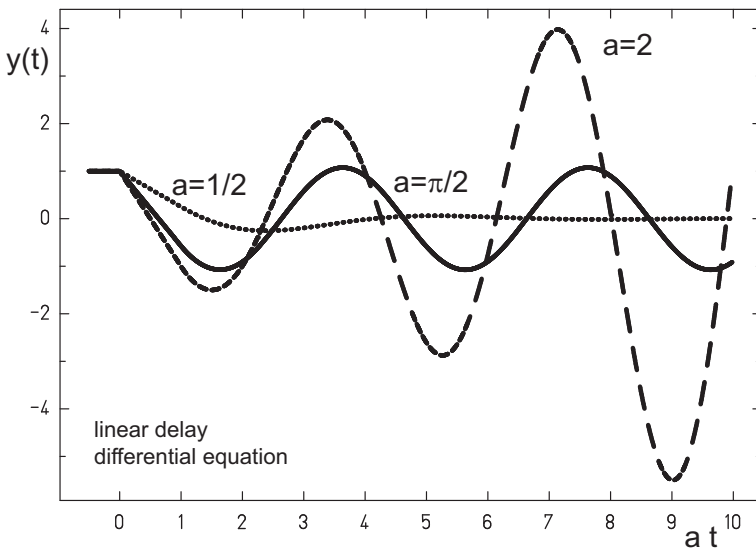


Fig. A.5 Solutions delay intervals. Thick line $a = \pi/2$, dashed line $a = 2$ and dotted line $a = 1/2$.

and subsequently

$$y_n(t) = y_{n-1}((n-1)a) - \int_{(n-1)a}^t dt y_{n-1}(t-a), \quad t \in [(n-1)a, na] \quad (\text{A.163})$$

which may be solved using an appropriate software tool for analytical integration or directly, setting $a = 1$:

$$y_n(t) = \begin{cases} 1 & t \leq 0 \\ 1-t & 0 < t \leq 1 \\ \frac{3}{2} - 2t + \frac{1}{2}t^2 & 1 < t \leq 2 \\ \frac{17}{6} - 4t + \frac{3}{2}t^2 - \frac{1}{6}t^3 & 2 < t \leq 3 \\ \frac{149}{24} - \frac{17}{2}t + \frac{15}{4}t^2 - \frac{2}{3}t^3 + \frac{1}{24}t^4 & 3 < t \leq 4 \end{cases} \quad (\text{A.164})$$

From interval to interval the solution is given by a polynomial of increasing order. Therefore this seems a nice way to define orthogonal polynomials (e.g. in this special case there is a close relationship to the Laguerre polynomials). But in general, there will be no closed solution, especially if the initial function is complicated enough.

In figure A.4 we compare the derived solution to solutions with different initial functions.

The result may be directly compared to our previously presented findings on the fractional harmonic oscillator, where in the case of the Caputo derivative the result was given in terms of Mittag-Leffler functions. In both cases we find a decreasing oscillatory behavior.

Finally we suggest some numerical experiments:
If we increase the interval length a , the damping of the oscillation is reduced, see figure A.5. For $a = \pi/2$ we obtain a solution, which oscillates with a constant amplitude. For $a > \pi/2$ the solution is growing with t . This behavior we know already from the fractional harmonic oscillator.

Exercise 9.1: A geometric interpretation of a generalized nonlocal integral

Problem: We may consider a fractional integral in \mathbb{R}^2 as a blur operator in two dimensions; a subject we have just discussed. We had demonstrated that for increasing α in the limiting case of $\lim \alpha \rightarrow 2$ the Riesz fractional integral may be interpreted physically as a synonym for a pinhole camera with finite more and more increasing circular cut off radius a . Since the camera pinhole is circular, the result of acting to any function $f(x, y)$ is invariant under rotations of the camera objective.

The 2-dimensional approach may also be useful for a geometric interpretation of a generalized fractional calculus [Kiryakova (1994)], where the fractional integral depends on more than one parameter:

$$I^\alpha f(x) \Rightarrow I^{\alpha, \gamma} f(x) \quad (\text{A.165})$$

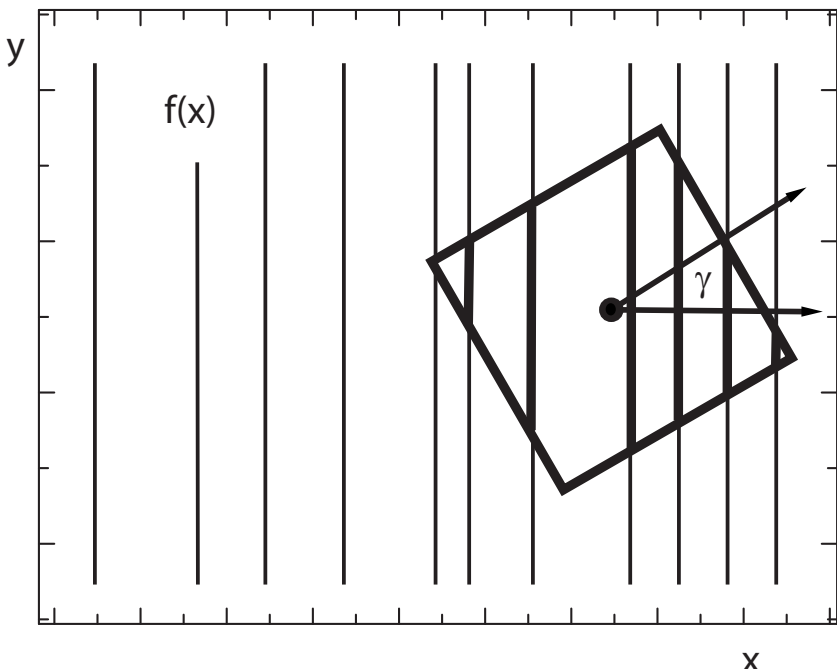


Fig. A.6 Area of integration for a quadratic pinhole of size a rotated by the angle γ . Vertical lines sketch the contours of a given function $f(x)$. Thick lines indicate the interior of the integration area.

Typical examples of this class of fractional operators are the Erdélyi-Kober operators (5.108), (5.110).

We choose the pinhole camera as a model for a nonlocal operator (with the simple weight function $w(h) = H(a/2 - |h|)$, $H(x)$ being the Heaviside step function), which has the advantage to be fully analytically solvable. Investigating the case of a pinhole camera with a quadratic pinhole shape of size a , introduces an additional parameter γ , which may be interpreted as an rotation angle γ , see figure A.6.

In this case, such an operator acting on a function $f(x, y)$ has the form

$$I(a, \gamma)f(x, y) = \frac{1}{a^2} \int_{-a/2}^{+a/2} dh_x \int_{-a/2}^{+a/2} dh_y \\ \times f(x + \cos(\gamma)h_x + \sin(\gamma)h_y, y - \sin(\gamma)h_x + \cos(\gamma)h_y) \quad (\text{A.166})$$

Acting on a function depending on only one variable $f(x, y) = f(x)$ the integral is simply given by:

$$I(a, \gamma)f(x) = \frac{1}{a^2} \int_{-a/2}^{+a/2} dh_x \int_{-a/2}^{+a/2} dh_y f(x + \cos(\gamma)h_x + \sin(\gamma)h_y) \quad (\text{A.167})$$

which may be interpreted as a generalized nonlocal integral depending on an additional parameter γ with a well defined geometric meaning.

Prove that $f(x) = \cos(kx)$ is an eigenfunction of this operator and determine the eigenvalues $\kappa(\alpha, \gamma)$.

Compare the result with the rotationally invariant pinhole camera with circular cutoff R_0 , which is given by:

$$I^0(a)f(x) = \frac{1}{\pi R_0^2} \int_{-R_0}^{+R_0} dh_x \int_{-\sqrt{R_0^2 - h_x^2}}^{+\sqrt{R_0^2 - h_x^2}} dh_y f(x + h_x) \quad (\text{A.168})$$

Solution: We have to evaluate

$$I(a, \gamma) \cos(kx) = \frac{1}{a^2} \int_{-a/2}^{+a/2} dh_x \int_{-a/2}^{+a/2} dh_y \cos(k(x + \cos(\gamma)h_x + \sin(\gamma)h_y)) \quad (\text{A.169})$$

which is not difficult, if we apply (4.3.16) and (4.3.17) from [Abramowitz and Stegun (1965)]

$$\sin(z_1 + z_2) = \sin(z_1) \cos(z_2) + \cos(z_1) \sin(z_2) \quad (\text{A.170})$$

$$\cos(z_1 + z_2) = \cos(z_1) \cos(z_2) - \sin(z_1) \sin(z_2) \quad (\text{A.171})$$

and hence

$$I(a, \gamma) \cos(kx) = \frac{1}{a^2} \int_{-a/2}^{+a/2} dh_x \int_{-a/2}^{+a/2} dh_y \\ \times (+ \cos(kx) \cos(k(\cos(\gamma)h_x + \sin(\gamma)h_y)) \\ - \sin(kx) \sin(k(\cos(\gamma)h_x + \sin(\gamma)h_y))) \quad (\text{A.172})$$

$$= \frac{1}{a^2} \int_{-a/2}^{+a/2} dh_x \int_{-a/2}^{+a/2} dh_y \\ \times (+ \cos(kx) \{ \cos(\cos(\gamma)kh_x) \cos(\sin(\gamma)kh_y) \\ - \sin(\cos(\gamma)kh_x) \sin(\sin(\gamma)kh_y) \} \\ - \sin(kx) \{ \sin(\cos(\gamma)kh_x) \cos(\sin(\gamma)kh_y) \\ + \cos(\cos(\gamma)kh_x) \sin(\sin(\gamma)kh_y) \}) \quad (\text{A.173})$$

$$= \frac{1}{a^2} \int_{-a/2}^{+a/2} dh_x \\ \times (\cos(kx) \{ \cos(\cos(\gamma)kh_x) \frac{\sin(\sin(\gamma)kh_y)}{\sin(\gamma)k} \\ + \sin(\cos(\gamma)kh_x) \frac{\cos(\sin(\gamma)kh_y)}{\sin(\gamma)k} \} \\ - \sin(kx) \{ \sin(\cos(\gamma)kh_x) \frac{\sin(\sin(\gamma)kh_y)}{\sin(\gamma)k} \\ - \cos(\cos(\gamma)kh_x) \frac{\cos(\sin(\gamma)kh_y)}{\sin(\gamma)k} \})|_{h_y=-a/2}^{h_y=+a/2} \quad (\text{A.174})$$

$$= \frac{1}{a^2} \int_{-a/2}^{+a/2} dh_x \\ \times 2(\cos(kx) \cos(\cos(\gamma)kh_x) \frac{\sin(\sin(\gamma)ka/2)}{\sin(\gamma)k} \\ - \sin(kx) \sin(\cos(\gamma)kh_x) \frac{\sin(\sin(\gamma)ka/2)}{\sin(\gamma)k}) \quad (\text{A.175})$$

$$= \frac{1}{a^2} \\ \times 2(\cos(kx) \frac{\sin(\cos(\gamma)kh_x) \sin(\sin(\gamma)ka/2)}{\cos(\gamma)k \sin(\gamma)k} \\ + \sin(kx) \frac{\cos(\cos(\gamma)kh_x) \sin(\sin(\gamma)ka/2)}{\cos(\gamma)k \sin(\gamma)k})|_{h_x=-a/2}^{h_x=+a/2} \quad (\text{A.176})$$

$$= \frac{4}{a^2} \cos(kx) \frac{\sin(\cos(\gamma)ka/2) \sin(\sin(\gamma)ka/2)}{\cos(\gamma)k \sin(\gamma)k} \quad (\text{A.177})$$

and finally

$$I(a, \gamma) \cos(kx) = \cos(kx) \left\{ \frac{\sin(\cos(\gamma)ka/2)}{\cos(\gamma)ka/2} \frac{\sin(\sin(\gamma)ka/2)}{\sin(\gamma)ka/2} \right\} \quad (\text{A.178})$$

Therefore, $\cos(kx)$ is indeed an eigenfunction of the operator $I(a, \gamma)$ and the eigenvalue spectrum is given by

$$\kappa(a, \gamma) = \frac{\sin(\cos(\gamma)ka/2)}{\cos(\gamma)ka/2} \frac{\sin(\sin(\gamma)ka/2)}{\sin(\gamma)ka/2} \quad (\text{A.179})$$

with the properties

$$\lim_{\gamma \rightarrow 0} \kappa(a, \gamma) = \kappa(a) = \frac{\sin(ka/2)}{ka/2} \quad (\text{A.180})$$

$$\lim_{a \rightarrow 0} \kappa(a) = 1 \quad (\text{A.181})$$

In order to compare this result with a pinhole with circular shape and equivalent surface we choose

$$R_0 = \frac{a}{\sqrt{\pi}} \quad (\text{A.182})$$

and evaluate

$$I^0(a, \gamma) \cos(kx) = \frac{1}{\pi R_0^2} \int_{-R_0}^{+R_0} dh_x \int_{-\sqrt{R_0^2 - h_x^2}}^{+\sqrt{R_0^2 - h_x^2}} dh_y \cos(kx + kh_x) \quad (\text{A.183})$$

$$= \frac{2}{\pi R_0^2} \int_{-R_0}^{+R_0} dh_x \sqrt{R_0^2 - h_x^2} \times (\cos(kx) \cos(kh_x) - \sin(kx) \sin(kh_x)) \quad (\text{A.184})$$

$$= \cos(kx) \frac{4}{\pi R_0^2} \int_0^{+R_0} dh_x \sqrt{R_0^2 - h_x^2} \cos(kh_x) \quad (\text{A.185})$$

Substituting $h_x = R_0 t$, the integral represents the Bessel function J_ν , see (9.1.20) [Abramowitz and Stegun (1965)]

$$J_\nu(z) = \frac{2(z/2)^\nu}{\sqrt{\pi}\Gamma(\nu + 1/2)} \int_0^1 dt \cos(zt)(1-t^2)^{\nu-1/2} \quad (\text{A.186})$$

for the special case $\nu = 1$ and therefore

$$I^0(a) \cos(x) = \frac{2}{|k|R_0} J_1(|k|R_0) \cos(kx) \quad (\text{A.187})$$

Consequently $\cos(kx)$ is an eigenfunction of the circular pinhole operator and the eigenvalue spectrum is given by

$$\kappa^0(R_0) = \frac{2}{|k|R_0} J_1(|k|R_0) \quad (\text{A.188})$$

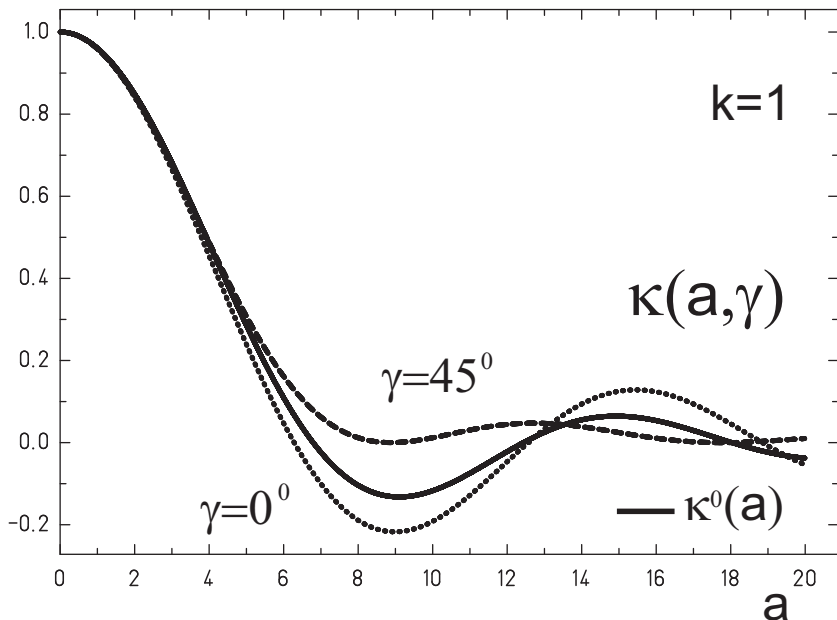


Fig. A.7 Eigenvalue spectra κ^0 and κ for operators $I^0(a, \gamma)$ and $I(a, \gamma)$ Setting $k = 1$ graphs for the quadratic pinhole rotated by $\gamma = 0$ (dotted line), $\gamma = \pi/4$ (dashed line) and the circular pinhole (thick line).

with the property

$$\lim_{R_0 \rightarrow 0} \kappa^0(R_0) = 1 \quad (\text{A.189})$$

In figure A.7 the corresponding spectra with a given pinhole size a are compared for $k = 1$. For small pinhole size a results are similar. For increasing pinhole size a we observe deviations for different γ . Therefore different orientations of the quadratic pinhole result in different spectra.

Exercise 10.1: Momentum dependence of nonlocal potentials

Problem: Nonlocal potentials play an important role in nuclear physics. Show that nonlocality and momentum dependence of potentials are equivalent concepts.

Hint: Expand the wave function in a Taylor series.

Solution: Following [Baumgärtner and Schuck (1968)] we first define the potential operator V applied to a state $|\sigma\rangle$. For reasons of simplicity we restrict the derivation to a one dimensional problem:

$$\langle x|V|\sigma\rangle = \int \langle x|V|x'\rangle \langle x'|\sigma\rangle dx' = \int V(x, x')\psi_\sigma(x')dx' \quad (\text{A.190})$$

Only for the very special case

$$V(x, x') = V(x)\delta(x - x') \quad (\text{A.191})$$

the potential is called local and (A.190) reduces to:

$$\langle x|V|\sigma\rangle = V(x)\psi_\sigma(x) \quad (\text{A.192})$$

But in general also values of the wave function ψ_σ in the neighborhood x' of x contribute and therefore such a potential is called nonlocal.

We expand $\psi_\sigma(x')$ at position x as a Taylor-series in $x' - x$:

$$\psi_\sigma(x') = \psi_\sigma(x) + (x' - x)\partial_x\psi_\sigma(x) + (x' - x)^2\frac{1}{2!}\partial_x^2\psi_\sigma(x)\dots \quad (\text{A.193})$$

$$= e^{(x'-x)\partial_x}\psi_\sigma(x) \quad (\text{A.194})$$

$$= e^{(x'-x)(-i/\hbar)\hat{p}}\psi_\sigma(x) \quad (\text{A.195})$$

where $\hat{p} = i\hbar\partial_x$ is the momentum operator.

Inserting (A.193) into (A.190) yields:

$$\langle x|V|\sigma\rangle = \int V(x, x')e^{(x'-x)(-i/\hbar)\hat{p}}\psi_\sigma(x)dx' \quad (\text{A.196})$$

$$= \hat{V}(x, p)\psi_\sigma(x) \quad \text{q.e.d} \quad (\text{A.197})$$

It is quite interesting, that nonlocality in nuclear physics has a long and successful tradition entering via a nonlocal potential energy, while within the framework of fractional calculus nonlocality enters via the kinetic part of the total energy,

$$\hat{H} = \hat{T} + \hat{V} \quad (\text{A.198})$$

which seems a surprisingly irritating new concept for many physicists. But since we have just shown, that nonlocal potentials imply an additional momentum dependence, we consider it as only a small step to investigate nonlocal kinetic terms in the Hamiltonian directly.

In that sense, a nonlocal potential may be considered as an additional contribution to the kinetic part of the Hamiltonian, while a nonlocal kinetic energy term may be considered as an additional and of course very special nonlocal potential. In other words, a nonlocal contribution to the total energy may be interpreted as an intermediate term W collecting both aspects (kinetic and potential energy) simultaneously.

$$\hat{H}_{\text{nonlocal}}(x, p) = \hat{T}_{\text{local}}(p) + \hat{W}_{\text{nonlocal}}(x, p) + \hat{V}_{\text{local}}(x) \quad (\text{A.199})$$

We might even speculate, whether or not a fractional approach with

$$\hat{H}_{\text{nonlocal}}(x, p) = \hat{W}_{\text{nonlocal}}(x, p) \quad (\text{A.200})$$

would be sufficient to model a large variety of different physical problems in an elegant and generalized way.

In the following chapters we will therefore present some results, which hopefully help to obtain a deeper understanding of this concept, which actually emerges as a new vista on a wide area of physical problems.

Exercise 13.1: The differential representation of the fractional Schrödinger equation in spherical coordinates

Problem: Solve the fractional Schrödinger equation in spherical coordinates for the infinite potential well

$$V_{\text{sph}}(r) = \begin{cases} 0 & r \leq R_0 \\ \infty & r > R_0 \end{cases} \quad (\text{A.201})$$

where the fractional Laplace-operator is given by the differential representation of the Riesz fractional derivative.

Solution: In a first step we recollect information to solve the standard Schrödinger equation in spherical coordinates. Spherical coordinates in \mathbb{R}^3 are defined as

$$x = r \cos(\phi) \sin(\theta) \quad (\text{A.202})$$

$$y = r \sin(\phi) \sin(\theta) \quad (\text{A.203})$$

$$z = r \cos(\theta) \quad (\text{A.204})$$

With (13.56) the Laplace-operator follows as:

$$\Delta(r, \phi, \theta) = \frac{1}{r^2} \partial_r r^2 \partial_r + \frac{1}{r^2 \sin(\theta)} \partial_\theta \sin(\theta) \partial_\theta + \frac{1}{r^2 \sin(\theta)} \partial_\phi^2 \quad (\text{A.205})$$

The free stationary Schrödinger equation is then given by:

$$-\frac{\hbar^2}{2m} \Delta(r, \phi, \theta) \Psi(r, \phi, \theta) = E \Psi(r, \phi, \theta) \quad (\text{A.206})$$

This equation is separable. With the ansatz

$$\Psi(r, \phi, \theta) = R(r) Y_{lm}(\phi, \theta) \quad (\text{A.207})$$

we obtain a set of ordinary differential equations

$$-\frac{1}{\sin(\theta)} \left\{ \partial_\theta \sin(\theta) \partial_\theta + \partial_\phi^2 \right\} Y_{lm}(\phi, \theta) = l(l+1) Y_{lm}(\phi, \theta) \quad (\text{A.208})$$

$$-\frac{\hbar^2}{2m} \left\{ \frac{1}{r^2} \partial_r r^2 \partial_r + \frac{l(l+1)}{r^2} \right\} R(r) = E R(r) \quad (\text{A.209})$$

where $Y_{lm}(\phi, \theta)$ denote the spherical harmonics

$$Y_{lm}(\phi, \theta) = \sqrt{\frac{2l+1}{4\pi} \frac{(l-m)!}{(l+m)!}} P_l^m(\cos(\theta)) e^{im\phi} \quad l = 0, 1, 2, \dots \quad -l \leq m \leq l$$

Table A.1 Zeros $\zeta_{n,l}$ of the spherical Bessel function in units $[\pi]$, with $\zeta_{n,l} \leq 10[\pi]$, normalized to $k = 1$. For the Riesz semi-derivative $\alpha = 1$, according to (A.217) the zeros are up to a factor identical to the energy values.

l/n	1	2	3	4	5	6	7	8	9	10
0	1.	2.	3.	4.	5.	6.	7.	8.	9.	10.
1	1.4303	2.45902	3.47089	4.47741	5.48154	6.48439	7.48647	8.48807	9.48933	
2	1.83457	2.89503	3.92251	4.93845	5.94891	6.9563	7.96182	8.9661	9.96951	
3	2.22433	3.31587	4.36022	5.38696	6.40497	7.41797	8.42782	9.43553		
4	2.60459	3.72579	4.78727	5.82547	6.85175	7.87103	8.8858	9.89751		
5	2.97805	4.12737	5.20587	6.25579	7.29074	8.31672	9.33684			
6	3.34634	4.52235	5.61752	6.67924	7.72308	8.75603	9.78178			
7	3.71055	4.91193	6.02338	7.09683	8.14964	9.18973				
8	4.07143	5.297	6.42428	7.50934	8.57114	9.61845				
9	4.42954	5.67822	6.8209	7.91739	8.98816					
10	4.7853	6.05612	7.21377	8.3215	9.40117					
11	5.13903	6.43111	7.60332	8.72209	9.81056					
12	5.49099	6.80355	7.98991	9.11951						
13	5.84139	7.17369	8.37384	9.51406						
14	6.1904	7.54178	8.75535	9.906						
15	6.53816	7.90802	9.13468							
16	6.8848	8.27256	9.51199							
17	7.23041	8.63556	9.88746							
18	7.57509	8.99713								
19	7.91891	9.3574								
20	8.26195	9.71646								
21	8.60425									
22	8.94588									
23	9.28688									
24	9.62728									
25	9.96713									

and

$$R(r) = j_l(kr) \quad k = \sqrt{\frac{2mE}{\hbar^2}} \quad (\text{A.210})$$

is the spherical Bessel function.

The wave function should vanish at the boundary $r = R_0$ and therefore we obtain a discrete energy spectrum

$$E_{n,l} = \frac{\hbar^2}{2mR_0} \zeta_{n,l}^2 \quad (\text{A.211})$$

where $\zeta_{n,l}$ is the n-th zero of the spherical Bessel function $j_l(kr)$. Since $j_0(z) = \sin(z)/z$, the zeros for s-waves ($l = 0$) are known analytically $\zeta_{n,0} = n\pi$. For nonvanishing angular momentum $l > 0$ the zeros are determined numerically. In table A.1 we have collected all zeros $\zeta_{n,l}^2 \leq 10\pi$, normalized to $k = 1$.

In order to determine the spectrum of the corresponding fractional Schrödinger equation in spherical coordinates

$$(-\mathcal{D}_{\alpha/2 \text{ RZ}} \Delta^{\alpha/2} + V_{\text{sph}}(r)) \Psi(r, \phi, \theta) = E(\alpha) \Psi(r, \phi, \theta) \quad (\text{A.212})$$

we use the differential representation of the Riesz derivative:

$${}_{\text{RZ}}\Delta^{\alpha/2} = \lim_{\omega \rightarrow 0} -|\omega|^\alpha \sum_{j=0}^{\infty} \binom{\alpha/2}{j} |\omega|^{-2j} (-1)^j \Delta^j \quad (\text{A.213})$$

and use the fact, that the eigenfunctions and the eigenspectrum of the Laplace operator are known:

$$\Delta^j \Psi(r, \phi, \theta) = \left(-\frac{2m}{\hbar^2} E_{n,l}\right)^j \Psi(r, \phi, \theta) = \left(-\frac{\zeta_{n,l}^2}{R_0}\right)^j \Psi(r, \phi, \theta) \quad (\text{A.214})$$

It is straightforward to determine the spectrum

$$\begin{aligned} -\mathcal{D}_{\alpha/2} {}_{\text{RZ}}\Delta^{\alpha/2} \Psi(r, \phi, \theta) &= \mathcal{D}_{\alpha/2} \lim_{\omega \rightarrow 0} |\omega|^\alpha \sum_{j=0}^{\infty} \binom{\alpha/2}{j} |\omega|^{-2j} (-1)^j \left(-\frac{\zeta_{n,l}^2}{R_0}\right)^j \Psi(r, \phi, \theta) \\ &= \mathcal{D}_{\alpha/2} \lim_{\omega \rightarrow 0} \left(\omega^2 + \frac{\zeta_{n,l}^2}{R_0}\right)^{\alpha/2} \Psi(r, \phi, \theta) \end{aligned} \quad (\text{A.215})$$

$$= \mathcal{D}_{\alpha/2} \left(\frac{\zeta_{n,l}^2}{R_0}\right)^{\alpha/2} \Psi(r, \phi, \theta) \quad (\text{A.216})$$

and therefore the fractional energy spectrum is given by:

$$E(\alpha) = \mathcal{D}_{\alpha/2} \left(\frac{\zeta_{n,l}^2}{R_0}\right)^{\alpha/2} \quad (\text{A.217})$$

In the same way we also may derive the spectrum of a fractional rotation group ${}_{\text{RZ}}SO^\alpha(3)$. With (A.208) and since the spherical harmonics are eigenfunctions of the local representation of the 2-dimensional fractional Riesz Laplace-operator, which we define to be the Casimir-operator of this group, as well:

$${}_{\text{RZ}}\Delta^{\alpha/2} Y_{lm}(\phi, \theta) = \{l(l+1)\}^{\alpha/2} Y_{lm}(\phi, \theta) \quad (\text{A.218})$$

which is a nice prequel for results, which will be presented in the following chapters.

Of course it should be emphasized, that all presented solutions are only valid for the differential representation of the Riesz derivative. The integral representation is nonlocal and the solutions would differ for the free and the infinite potential well significantly.

Exercise 15.1: Commutation relations for the matrix-representation of $U(d)$

Problem: The i $d \times d$ -matrices

$$\sigma^i = \{A_l^k\}, \quad i, 1, \dots, d^2 \quad k, l = 1, \dots, d \quad \text{modulo } d \quad (\text{A.219})$$

with the elements a_{mn}

$$A_l^k(a_{mn}) = e^{\frac{2\pi i}{d} km} \delta_{m,n+l}, \quad m, n = 1, \dots, d \quad \text{modulo } d \quad (\text{A.220})$$

where $e^{\frac{2\pi i}{d}} = \sqrt[d]{1}$, k is the phase and l measures the off-diagonality determine a specific matrix-representation of the unitary group $U(d)$.

Give the commutation relations $[\sigma^i, \sigma^{i'}]$ and $\{\sigma^i, \sigma^{i'}\}$.

Solution: We first calculate the product

$$A_l^k A_{l'}^{k'} = \sum_{n'} e^{\frac{2\pi i}{d} km} \delta_{m,n'+l} e^{\frac{2\pi i}{d} k' n'} \delta_{n',n+l'} \quad (\text{A.221})$$

$$= e^{\frac{2\pi i}{d} (km + k'(m-l))} \delta_{m,n+l+l'} \quad (\text{A.222})$$

$$= e^{-\frac{2\pi i}{d} k'l} e^{\frac{2\pi i}{d} (k+k')m} \delta_{m,n+l+l'} \quad (\text{A.223})$$

$$= e^{-\frac{2\pi i}{d} k'l} A_{l+l'}^{k+k'} \quad \text{modulo } d \quad (\text{A.224})$$

If follows immediately

$$[A_l^k, A_{l'}^{k'}] = (e^{-\frac{2\pi i}{d} k'l} - e^{-\frac{2\pi i}{d} kl'}) A_{l+l'}^{k+k'} \quad (\text{A.225})$$

$$\{A_l^k, A_{l'}^{k'}\} = (e^{-\frac{2\pi i}{d} k'l} + e^{-\frac{2\pi i}{d} kl'}) A_{l+l'}^{k+k'} \quad \text{modulo } d \quad (\text{A.226})$$

As a consequence, all calculations with matrices σ^i are reduced to c-number calculus.

Exercise 15.2: Linearization of a $2\lambda + 1$ dimensional free collective Schrödinger equation

Problem: The surface of a liquid drop may be expanded in spherical harmonics $Y_{\lambda\mu}$ introducing the surface variables $\alpha_{\lambda\mu}$ with a given multipolarity λ [Eisenberg and Greiner (1987)]:

$$R = R_0(1 + \sum_{\lambda,\mu}(-1)^{\mu}\alpha_{\lambda-\mu}Y_{\lambda\mu}) \quad (\text{A.227})$$

From the behavior under rotations in \mathbb{R}^3 of the $Y_{\lambda\mu}$ follows, that the surface variables $\alpha_{\lambda\mu}$ behave like components of a spherical tensor of rank λ :

$$\alpha_{\lambda\mu}^{[\lambda]} = \sum_{\nu} D_{\nu\mu}^{\lambda} \alpha_{\lambda\nu}^{[\lambda]} \quad (\text{A.228})$$

The corresponding canonical momenta $\pi_{\lambda\mu}$ are then defined via

$$\pi_{\lambda\mu} = -i\hbar\partial_{\alpha_{\lambda\mu}} \quad (\text{A.229})$$

with the transformation property

$$\pi_{\lambda\mu}^{[\lambda]} = \sum_{\nu} D_{\mu\nu}^{\lambda*} \pi_{\lambda\nu}^{[\lambda]} \quad (\text{A.230})$$

In lowest order, the corresponding kinetic energy term is given as a second order derivative operator, where the momenta of rank λ are coupled to a spherical tensor of rank 0:

$$T_2 = [\pi^{[\lambda]} \otimes \pi^{[\lambda]}]^{[0]} \quad (\text{A.231})$$

which is the basic input for a description of the dynamic behavior of the liquid drop surface vibrations in term of a collective $2\lambda + 1$ dimensional Schrödinger equation e.g.:

$$(-1)^{\lambda} \frac{\sqrt{2\lambda+1}}{2B_{\lambda}} [\pi^{[\lambda]} \otimes \pi^{[\lambda]}]^{[0]} + (-1)^{\lambda} \frac{\sqrt{2\lambda+1}C_{\lambda}}{2} [\alpha^{[\lambda]} \otimes \alpha^{[\lambda]}]^{[0]} \quad (\text{A.232})$$

Introducing spherical spinors γ determine the correct form of a linearized version of the kinetic energy.

Solution: We introduce a spherical spinor $\gamma^{[\lambda]}$ of rank λ and set

$$T_1 = [\gamma^{[\lambda]} \otimes \pi^{[\lambda]}]^{[0]} \quad (\text{A.233})$$

which is linear in π . Postulating the kinetic energy T_1 as a real quantity we obtain:

$$\pi_{\lambda\mu}^* = (-1)^{\mu+1} \pi_{\lambda\mu} \quad (\text{A.234})$$

$$\gamma_{\lambda\mu}^* = (-1)^{\mu+1} \gamma_{\lambda\mu} \quad (\text{A.235})$$

and the transformation property

$$\gamma_{\lambda\mu}^{[\lambda]} = \sum_{\nu} D_{\mu\nu}^{\lambda*} \gamma_{\lambda\nu}^{[\lambda]} \quad (\text{A.236})$$

The spherical representation of the γ -matrices are determined via the requirement

$$[T_1 \otimes T_1]^{[0]} = T_2 \quad (\text{A.237})$$

which explicitly yields

$$\begin{aligned} T_2 &= \frac{(-1)^{\lambda+1}}{\sqrt{2\lambda+1}} \sum_{\mu} \pi_{\lambda\mu} \pi_{\lambda\mu}^* \\ T_1 &= \frac{(-1)^{\lambda+1}}{\sqrt{2\lambda+1}} \sum_{\mu} \gamma_{\lambda\mu} \pi_{\lambda\mu}^* \\ T_1 T_1 &= \frac{(-1)^{\lambda+1}}{\sqrt{2\lambda+1}} \frac{(-1)^{\lambda+1}}{\sqrt{2\lambda+1}} \sum_{\mu\nu} \gamma_{\lambda\mu} \pi_{\lambda\mu}^* \gamma_{\lambda\nu} \pi_{\lambda\nu}^* \\ &= \frac{(-1)^{\lambda+1}}{\sqrt{2\lambda+1}} \frac{(-1)^{\lambda+1}}{\sqrt{2\lambda+1}} \sum_{\mu\nu} \gamma_{\lambda\mu}^* \gamma_{\lambda\nu} \pi_{\lambda\mu} \pi_{\lambda\nu}^* \end{aligned} \quad (\text{A.238})$$

From this calculation follows

$$\frac{(-1)^{\lambda+1}}{\sqrt{2\lambda+1}} (\gamma_{\lambda\mu}^* \gamma_{\lambda\nu} + \gamma_{\lambda\nu} \gamma_{\lambda\mu}^*) = 2\delta_{\mu\nu} \quad (\text{A.239})$$

This is the Clifford algebra for the spherical spinors.

Once the transformation properties for spherical spinors are known, we may apply a certain projection description onto \mathbb{R}^3 coupling the spherical tensors to rank 1 to obtain the angular momentum operators:

$$\begin{aligned} L_{1\mu} &= M[\alpha \times \pi^*]^{[1]} \\ S_{1\mu} &= N[\gamma^* \times \gamma^*]^{[1]} \end{aligned} \quad (\text{A.240})$$

where M and N are at first arbitrary normalization constants. Especially for the z-component we obtain:

$$\begin{aligned} L_z &= \sum_{\mu=1}^{\lambda} (\lambda+1-\mu) L_{2\lambda+2-\mu\mu} \\ S_z &= \sum_{\mu=1}^{\lambda} (\lambda+1-\mu) S_{2\lambda+2-\mu\mu} \end{aligned} \quad (\text{A.241})$$

For direct evaluation we use the Cartesian representation:

$$S_z = \sum_{\mu=1}^{\lambda} \mu S_{\mu} \quad (\text{A.242})$$

with the diagonal multiplet classification operators S_n , which are given by (σ_z is the diagonal 2×2 Pauli-matrix and $\mathbf{1}_2$ is the 2×2 unit matrix):

$$\begin{aligned} S_1 &= \frac{\hbar}{2} \sigma_z \otimes \mathbf{1}_2 \otimes \cdots \otimes \mathbf{1}_2 \\ S_2 &= \frac{\hbar}{2} \mathbf{1}_2 \otimes \sigma_z \otimes \cdots \otimes \mathbf{1}_2 \\ &\vdots \quad \vdots \quad \vdots \\ S_N &= \frac{\hbar}{2} \mathbf{1}_2 \otimes \mathbf{1}_2 \otimes \cdots \otimes \sigma_z \end{aligned} \quad (\text{A.243})$$

For a given λ we obtain 2^{λ} eigenvalues E_n^{λ} of the diagonal operator S_z

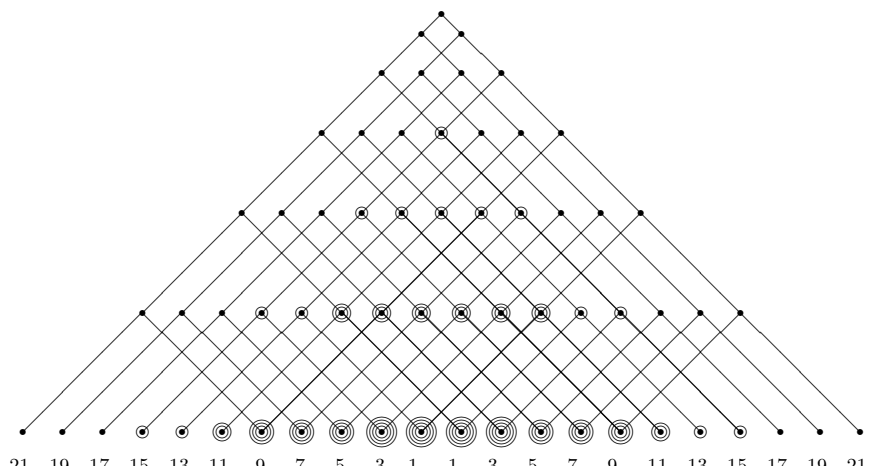
$$\{E_n^{\lambda}\} = \frac{\hbar}{2} \left\{ \sum_{\mu=1}^{\lambda} \pm \mu \right\} \quad (\text{A.244})$$

where every element E_n^{λ} corresponds to the sum for one of 2^{λ} given sign-permutations. These eigenvalues are centered at 0 and in units $\frac{\hbar}{2}$ integer numbers which we call N^{λ} .

The upper and lower extremes are given with multiplicity one for complete positive and negative sign sequence respectively and is given by:

$$N_{max}^{\lambda} = -N_{min}^{\lambda} = \frac{\lambda(\lambda+1)}{2} \quad (\text{A.245})$$

A geometric solution for the multiplicities in (A.244) is given below:



A geometric solution of the eigenvalue spectrum of (A.244) in units $\frac{\hbar}{2}$.

Table A.2 Branching ratios for $SO(2\lambda + 1)$ to $SO(3)$. For $\lambda \geq 9$ spin degeneracies are observed. Compare with [Armstrong and Judd (1970)].

$\lambda = 0$	1	2	3	4	5	6	7	8	9
0	$\frac{1}{2}$	$\frac{3}{2}$	3	5	$\frac{15}{2}$	$\frac{21}{2}$	14	18	$\frac{45}{2}$
			0	2	$\frac{9}{2}$	$\frac{15}{2}$	11	15	$\frac{39}{2}$
					$\frac{5}{2}$	$\frac{11}{2}$	9	13	$\frac{35}{2}$
					$\frac{9}{2}$	8	12		$\frac{33}{2}$
					$\frac{3}{2}$	7	11		$\frac{31}{2}$
						5	10		$\frac{29}{2}$
						4	9		$\frac{27}{2}, \frac{27}{2}$
						2	8		$\frac{25}{2}$
							7		$\frac{23}{2}$
							6		$\frac{21}{2}, \frac{21}{2}$
							5		$\frac{19}{2}$
							4		$\frac{17}{2}, \frac{17}{2}$
							3		$\frac{15}{2}, \frac{15}{2}$
							0		$\frac{13}{2}$
									$\frac{11}{2}$
									$\frac{9}{2}, \frac{9}{2}$
									$\frac{5}{2}$
									$\frac{3}{2}$

The corresponding multiplicities for a given spin value for the projection of $SO(2\lambda + 1)$ to $SO(3)$ are then given by

$$S_{N_{max}^\lambda}^\lambda = 1$$

$$S_{n-2}^\lambda = p_n^\lambda - p_{n-2}^\lambda \quad \forall n \in N_{max}^\lambda, N_{max}^\lambda - 2, \dots, 1 \text{ resp. } 0 \quad (\text{A.246})$$

and yield the listed spin values for the first few λ in table A.2.

We can give a rough estimate to show, that the level of degeneracy for a given spin value is getting larger for increasing λ . This happens, if the number of allowed states in the interval $N_{min}^\lambda \leq n \leq N_{max}^\lambda$ is smaller than the 2^λ different elements in (A.244):

$$2^\lambda \gg \frac{1}{2} \sum_{n=0}^{\lambda(\lambda+1)} n \approx \frac{1}{4} \lambda^4 \quad (\text{A.247})$$

which becomes true for $\lambda \gg 12$.

We obtain the result, that the linearized collective Schrödinger equation introduces a new quantity, which we call collective spin.

For example, for quadrupole vibrations, which are described in the 5-dimensional space spanned by the collective coordinates $\{\alpha_{2-2}, \alpha_{2-1}, \alpha_{20}, \alpha_{21}, \alpha_{22}\}$ the linearized equation describes spin $3/2$ particles.

Since linearization is the simplest version of factorization, the factorization of the collective Schrödinger equation with more than two factors is still an open task and could yield insights into a theory of more complex charge symmetries (like $SU(3)$) in multi-dimensional space $\mathbb{R}^{2\lambda+1}$.

Exercise 16.1: Invariant commutation relations of canonically conjugated operators

Problem: Show that the canonically conjugated operators

$$X = x^\alpha \partial_x^\beta \quad (\text{A.248})$$

$$P = \partial_x^\alpha x^\beta \quad \alpha + \beta = 1 \quad (\text{A.249})$$

where ∂_x^α is the Riemann fractional derivative, fulfill the commutation relation

$$[X, P] = \beta - \alpha \quad (\text{A.250})$$

which is independent from a specific choice of the underlying function space.

Solution: To prove the independence of the commutation relation, it is sufficient to calculate its influence on a test function

$$x^\nu = |\nu\rangle \quad (\text{A.251})$$

which results in

$$[X, P]|\nu\rangle = (XP - PX)|\nu\rangle \quad (\text{A.252})$$

$$= (x^\alpha \partial_x^\beta \partial_x^\alpha x^\beta - \partial_x^\alpha x^\beta x^\alpha \partial_x^\beta)|\nu\rangle \quad (\text{A.253})$$

$$= (x^\alpha \partial_x x^\beta - \partial_x^\alpha x \partial_x^\beta)|\nu\rangle \quad (\text{A.254})$$

$$= x^\alpha \partial_x |\nu + \beta\rangle - \partial_x^\alpha x \frac{\Gamma(1 + \nu)}{\Gamma(1 + \nu - \beta)} |\nu - \beta\rangle \quad (\text{A.255})$$

$$= x^\alpha (\nu + \beta) |\nu + \beta - 1\rangle - \partial_x^\alpha x \frac{\Gamma(1 + \nu)}{\Gamma(1 + \nu - \beta)} |\nu - \beta + 1\rangle$$

$$= (\nu + \beta) |\nu\rangle - \frac{\Gamma(1 + \nu)}{\Gamma(1 + \nu - \beta)} \frac{\Gamma(1 + \nu - \beta + 1)}{\Gamma(1 + \nu)} |\nu\rangle \quad (\text{A.256})$$

$$= (\nu + \beta) |\nu\rangle - (\nu - \beta + 1) |\nu\rangle \quad (\text{A.257})$$

$$= (\beta - \alpha) |\nu\rangle \quad \text{q.e.d} \quad (\text{A.258})$$

which indeed is independent from ν and therefore the commutation relation is invariant for any Taylor-series in x .

Exercise 16.2: Asymptotic expansion of the eigenvalue spectrum of the fractional $SO^\alpha(2)$ and $SO^\alpha(3)$

Problem: What is the asymptotic expansion of the spectrum of the Casimir operators for $|M|\alpha \gg 1$ and $J\alpha \gg 1$ respectively.

$$\hat{J}_z(\alpha) |JM\rangle = \pm \hbar \frac{\Gamma(1 + |M|\alpha)}{\Gamma(1 + (|M|-1)\alpha)} |JM\rangle \quad (\text{A.259})$$

$$\hat{J}^2(\alpha) |JM\rangle = \hbar^2 \frac{\Gamma(1 + (J+1)\alpha)}{\Gamma(1 + (J-1)\alpha)} |JM\rangle \quad (\text{A.260})$$

Hint: Use the Stirling's formula (A.54)

Solution: With Stirling's formula we obtain:

$$\hat{J}_z(\alpha) |JM\rangle = \pm \hbar \frac{\Gamma(1 + |M|\alpha)}{\Gamma(1 + (|M|-1)\alpha)} |JM\rangle \quad (\text{A.261})$$

$$= \pm \hbar \frac{\Gamma(1 + |M|\alpha)}{\Gamma(1 - \alpha + |M|\alpha)} |JM\rangle \quad (\text{A.262})$$

$$= \pm \hbar \frac{\sqrt{2\pi} \exp(-|M|\alpha) (|M|\alpha)^{|M|\alpha+1-1/2}}{\sqrt{2\pi} \exp(-|M|\alpha) (|M|\alpha)^{|M|\alpha+1-\alpha-1/2}} |JM\rangle$$

$$= \pm \hbar |M|^\alpha \alpha^\alpha |JM\rangle \quad |M|\alpha \gg 1 \quad (\text{A.263})$$

and similarly

$$\hat{J}^2(\alpha) |JM\rangle = \hbar^2 \frac{\Gamma(1 + (J+1)\alpha)}{\Gamma(1 + (J-1)\alpha)} |JM\rangle \quad (\text{A.264})$$

$$= \hbar^2 \frac{\Gamma(1 + (J+1)\alpha)}{\Gamma(1 - \alpha + (J+1)\alpha)} \frac{\Gamma(1 + J\alpha)}{\Gamma(1 - \alpha + J\alpha)} |JM\rangle \quad (\text{A.265})$$

$$= \hbar^2 \frac{\sqrt{2\pi} \exp(-(J+1)\alpha) ((J+1)\alpha)^{(J+1)\alpha+1-1/2}}{\sqrt{2\pi} \exp(-(J+1)\alpha) ((J+1)\alpha)^{(J+1)\alpha+1-\alpha-1/2}}$$

$$\times \frac{\sqrt{2\pi} \exp(-J\alpha) (J\alpha)^{J\alpha+1-1/2}}{\sqrt{2\pi} \exp(-J\alpha) (J\alpha)^{J\alpha+1-\alpha-1/2}} |JM\rangle \quad (\text{A.266})$$

$$= \hbar^2 J^\alpha (J+1)^\alpha \alpha^{2\alpha} |JM\rangle \quad J\alpha \gg 1 \quad (\text{A.267})$$

which may be compared with (A.218).

Exercise 18.1: Fractional Euler polynomials

Problem: The Euler polynomials E_n are generated by (see (23.1.1) [Abramowitz and Stegun (1965)])

$$E_n(z) = \lim_{w \rightarrow 0} \partial_w^n \frac{2e^{zw}}{1 + e^w} \quad (\text{A.268})$$

where the first few are given as

$$E_0(z) = 1 \quad (\text{A.269})$$

$$E_1(z) = z - 1/2 \quad (\text{A.270})$$

$$E_2(z) = z^2 - z \quad (\text{A.271})$$

The Euler polynomials fulfill the relation

$$E_n(1 + z) + E_n(z) = 2z^n \quad (\text{A.272})$$

Extend the definition of the Euler polynomials from $n \in \mathbb{N}$ to the fractional case $\alpha \in \mathbb{R}$ and prove, that the fractional Euler polynomials fulfill the fractional version of (A.272):

$$E_\alpha(1 + z) + E_\alpha(z) = 2z^\alpha \quad (\text{A.273})$$

Solution: The strategy for a solution is based on the idea, to interpret the generating function of the Euler polynomials as the sum of a geometric series [Euler (1768)]:

$$\sum_{n=0}^{\infty} q^n = \frac{1}{1-q} \quad |q| < 1 \quad (\text{A.274})$$

we obtain:

$$E_n(z) = \lim_{w \rightarrow 0} 2 \sum_{n=0}^{\infty} (-1)^n \partial_w^n e^{(z+n)w} \quad w < 0, z \geq 0 \quad (\text{A.275})$$

This rule may now easily be extended to the noninteger case

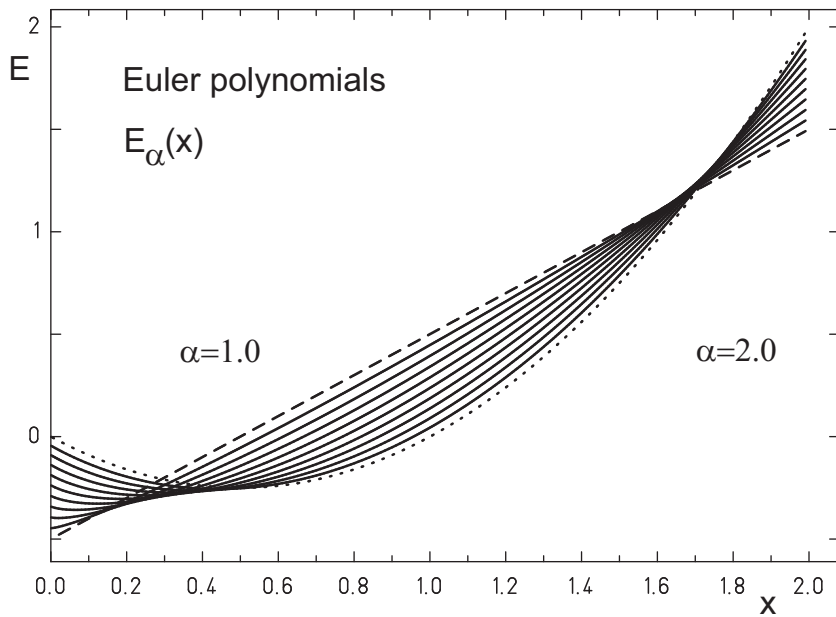


Fig. A.8 Fractional Euler polynomials $E_\alpha(x)$ for $1.0 \leq \alpha \leq 2.0$ (dashed) line.

$$E_\alpha(z) = \lim_{w \rightarrow 0} 2 \sum_{n=0}^{\infty} (-1)^n \partial_w^\alpha e^{(z+n)w} \quad (\text{A.276})$$

$$= \lim_{w \rightarrow 0} 2 \sum_{n=0}^{\infty} (-1)^n (z+n)^\alpha e^{(z+n)w} \quad (\text{A.277})$$

$$\begin{aligned} &= \lim_{w \rightarrow 0} 2 \left(\sum_{n=0}^{\infty} (z+2n)^\alpha e^{(z+n)w} \right. \\ &\quad \left. - \sum_{n=0}^{\infty} (z+2n+1)^\alpha e^{(z+n)w} \right) \quad (\text{A.278}) \end{aligned}$$

$$\begin{aligned} &= \lim_{w \rightarrow 0} 2^{1+\alpha} \left(\sum_{n=0}^{\infty} (n+z/2)^\alpha e^{(z+n)w} \right. \\ &\quad \left. - \sum_{n=0}^{\infty} (n+(1+z)/2)^\alpha e^{(z+n)w} \right) \quad (\text{A.279}) \end{aligned}$$

$$= 2^{1+\alpha} \left(\sum_{n=0}^{\infty} (n+z/2)^\alpha - \sum_{n=0}^{\infty} (n+(1+z)/2)^\alpha \right) \quad (\text{A.280})$$

Inserting the definition of the Hurwitz ζ function

$$\zeta(s, z) = \sum_{n=0}^{\infty} (n+z)^{-s} \quad (\text{A.281})$$

leads to the result

$$E_{\alpha}(z) = 2^{1+\alpha} (\zeta(-\alpha, z/2) - \zeta(-\alpha, (1+z)/2)) \quad (\text{A.282})$$

With this *ad hoc* extension of the Euler polynomials to the fractional case, where we have applied the Liouville fractional derivative, we obtain

$$\begin{aligned} E_{\alpha}(1+z) + E_{\alpha}(z) \\ = 2^{1+\alpha} (\zeta(-\alpha, (1+z)/2) - \zeta(-\alpha, 1+z/2) \\ + \zeta(-\alpha, z/2) - \zeta(-\alpha, (1+z)/2)) \end{aligned} \quad (\text{A.283})$$

$$= 2^{1+\alpha} (\zeta(-\alpha, z/2) - \zeta(-\alpha, 1+z/2)) \quad (\text{A.284})$$

$$= 2^{1+\alpha} \left(\sum_{k=0}^{\infty} (k+z/2)^{\alpha} - \sum_{k=0}^{\infty} (k+z/2+1)^{\alpha} \right) \quad (\text{A.285})$$

$$= 2^{1+\alpha} \left(\left(\frac{z}{2}\right)^{\alpha} + \sum_{k=0}^{\infty} (k+z/2+1)^{\alpha} - \sum_{k=0}^{\infty} (k+z/2+1)^{\alpha} \right)$$

$$= 2z^{\alpha} \quad \text{q.e.d} \quad (\text{A.286})$$

which is independent from a specific fractional derivative definition.

Bibliography

- Aaltonen T. *et al.* (CDF-collaboration) (2009) *Observation of electroweak single top-quark production* arXiv:0903.0885 [hep-ex], Phys. Rev. Lett. **103** 092002 (8 pages), doi:10.1103/PhysRevLett.103.092002
- Aaltonen T. *et al.* (CDF-collaboration) (2011) *Invariant mass distribution of jet pairs produced in association with a W boson in p̄p collisions at $\sqrt{s} = 1.96$ TeV* arXiv:1104.0699v2 [hep-ex], Phys. Rev. Lett. **106** 171801, doi:10.1103/PhysRevLett.106.171801
- Abazov, V. M. *et al.* (DO Collaboration) (2009) *Observation of single top quark production* arXiv:0903.0850 [hep-ex], Phys. Rev. Lett. **103** 092001 (7 pages), doi:10.1103/PhysRevLett.103.092001
- Abbott, P. C. (2000) *Generalized Laguerre polynomials and quantum mechanics* J. Phys. A: Math. Theor. **33** 7659–7660, doi:10.1088/0305-4470/33/42/401
- Abe, S. (1997) *A note on the q-deformation-theoretic aspect of the generalized entropies in nonextensive physics* Phys. Lett. A **224** 326–330, doi:10.1016/S0375-9601(96)00832-8
- Abel, N. H. (1823) *Solution de quelques problemes a l'aide d'integrales definies, oeuvres completes* Vol. **1** Grondahl, Christiana, Norway, 16–18
- Abers, E. S. and Lee, B. W. (1973) *Gauge theories* Physics Reports C **9** 1–141, doi:10.1016/0370-1573(73)90027-6
- Abramowitz, M. and Stegun, I. A. (1965) *Handbook of mathematical functions* Dover Publications, New York
- Adler, R., Bazin, M. and Schiffer, M. (1975) *Introduction to general relativity* McGraw-Hill, New York
- Agrawal, O. P. (2002) *Formulation of Euler-Lagrange equations for fractional variational problems* Journal of Mathematical Analysis and Applications **272** 368–379, doi:10.1016/S0022-247X(02)00180-4
- Agrawal, O. P. (2007) *Fractional variational calculus in terms of Riesz fractional derivatives* J. Phys. A: Math. Theor. **40** 6287–6303, doi:10.1088/1751-8113/40/24/003
- Agrawal, O. P. (2010) *Generalized variational problems and Euler-Lagrange equations* Comput. Math. Appl. **59** 1852–1864, doi:10.1016/j.camwa.2009.08.029

- Amore, P., Fernandez, F. M., Hofmann, C. P. and Saenz, A. (2009) *Collocation method for fractional quantum mechanics* arXiv:0912.2562v1[quant-ph], J. Math. Phys. (2010) **51** 122101, doi:10.1063/1.3511330
- Arminjon, M. and Reifler, F. (2011) *Equivalent forms of Dirac equations in curved spacetimes and generalized de Broglie relations* arXiv:1103.3201v3 [gr-qc]
- Armstrong, L. and Judd, B. R. (1970) *Quasi-particles in atomic shell theory* Proc. Roy. Soc. **315** (1520) 27–37, doi:10.1098/rspa.1970.0027
- Aubert, B. et al. (2005) *Observation of a broad structure in the $\pi^+\pi^-J/\Psi$ mass spectrum around 4.26 GeV/ c^2* arXiv:hep-ex/0506081v2, Phys. Rev. Lett. **95** 142001, doi:10.1103/PhysRevLett.95.142001
- Audi, G., Wapstra, A. H. and Thibault, C. (2003) *The AME 2003 atomic mass evaluation* Nucl. Phys. A **729** 337–676, doi:10.1016/j.nuclphysa.2003.11.003
- Audi, G., Wang, M., Wapstra, A. H., Kondev, F. G., MacCormick, M., Xu, X. and Pfeiffer, B. (2012) *The AME 2012 atomic mass evaluation* Chinese Physics C **36** 1287–2014, doi:10.1088/1674-1137/36/12/002
- Babusci, D., Dattoli, G. and Saccetti, D. (2010) *Integral equations, fractional calculus and shift operator* arXiv:1007.5211v1 [math-ph].
- Babusci, D., Dattoli, G. and Quattromini, M. (2011) *Relativistic equations with fractional and pseudodifferential operators* arXiv:1101.5066v2 [math-ph], Phys. Rev. A **83** 0621109, doi:10.1103/PhysRevA.83.062109
- Babusci, D., Dattoli, G., Quattromini, M. and Ricci, P. E. (2012) *Dirac factorization and fractional calculus* arXiv:1209.2276v1 [math-ph]
- Bacon, R. (1267) *Opus majus* Translated by Robert Belle Burke, Cambridge Library Collection - Physical Sciences, Cambridge University Press (2010)
- Balachandran, K. and Kokila, J. (2012) *On the controllability of fractional dynamic systems* Int. J. Appl. Math. Comput. Sci. **22** 523–531, doi:10.2478/v10006-012-0039-0
- Baleanu, D. and Muslih, S. (2005) *Lagrangian formulation of classical fields within Riemann Liouville fractional derivatives* arXiv:hep-th/0510071v1, Physica Scripta **72** 119–121, doi:10.1238/Physica.Regular.072a00119
- Baleanu, D. and Trujillo, J. J. (2010) *A new method of finding the fractional Euler-Lagrange and Hamilton equations within Caputo fractional derivatives* Commun. Nonlin. Sci. Numer. Simul. **15** 1111–1115, doi:10.1016/j.cnsns.2009.05.023
- Baleanu, D., Tenreiro Machado, J. A. and Luo, A. C. J. (2011) *Fractional dynamics and control* Springer, Berlin, Heidelberg, New York
- Baleanu, D., Diethelm, K., Scalas, E. and Trujillo, J. J. (2012) *Fractional calculus models and numerical methods (Series on Complexity, Nonlinearity and Chaos)* World Scientific Publ., Singapore
- Baltay, C. et al. (1979) *Confirmation of the existence of the Σ_c^{++} and Λ_c^+ charmed baryons and observation of the decay $\Lambda_c^+ \rightarrow \Lambda\pi^+$ and $\bar{K}^0 p$* Phys. Rev. Lett. **42** 1721–1724, doi:10.1103/PhysRevLett.42.1721

- Barnes, T., Close, F. E. and Swanson, E. S. (1995) *Hybrid and conventional mesons in the flux tube model: Numerical studies and their phenomenological implications* arXiv:hep-ph/9501405#, Phys. Rev. D**52** 5242–5256, doi:10.1103/PhysRevD.52.5242
- Bars, I. (2000) *Two-time physics in field theory* arXiv:hep-th/0003100, Phys. Rev. D**62** 046007, doi:10.1103/PhysRevD.62.046007
- Baumgärtner, G. and Schuck, P. (1968) *Kernmodelle* series: BI Hochschultaschenbücher (203/203a), Bibliographisches Institut, Mannheim, Germany
- Bayin, S. S. (2012a) *On the consistency of the solutions of the space fractional Schrödinger equation* arXiv:1203.4556v1 [math-ph], J. Math. Phys. **53** 042105, doi:10.1063/1.4705268
- Bayin, S. S. (2012b) *Comments on "On the consistency of the solutions of the space fractional Schrödinger equation"* arXiv:1208.1142v1 [quant-ph], J. Math. Phys. **53** 084101, doi:10.1063/1.4739758
- Beecham, Sir Th. and the Royal Philharmonic Orchestra, London (1947) *Händel: Messiah* 3 discs, Biddulph Records (1998), ASIN:B00000FDCF
- Behringer, J. et al. (2012) (Particle Data Group) *Review of particle physics* J. Phys. D**86** 010001, <http://pdg.lbl.gov>
- Belyaev, S. T. (1959) *Effect to pairing correlations on nuclear properties* Mat. Fys. Medd. Dan. Vid. Selsk. **31** (11)
- Bender, M., Nazarewicz, W. and Reinhard, P.-G. (2001) *Shell stabilization of super- and hyper-heavy nuclei without magic gaps* arXiv:nucl-th/0103065v1, Phys. Lett. B**515** 42–48, doi:10.1016/S0370-2693(01)00863-2
- Benedetti, D. (2008) *Fractal properties of quantum spacetime* arXiv:0811.1396v2 [hep-th], Phys. Rev. Lett. **102** (2009) 111303, doi:10.1103/PhysRevLett.102.111303
- BESIII Collaboration, Ablikim, M. et al. (2013) *Observation of a charged charmoniumlike structure in e+e- to pi+pi-J/psi at $\sqrt{s}=4.26$ GeV* arXiv:1303.5949 [hep-ex]
- Bessel, F. W. (1824) *Untersuchung des Theils der planetarischen Störung, welcher aus der Bewegung der Sonne entsteht* Abhandl. d. Berl. Akademie der Wissenschaften, 1–52
- van Beveren, E., Liu, X., Coimbra, R. and Rupp, G. (2009) *Possible ψ (5S), ψ (4D), ψ (6S), and ψ (5D) signals in $\Lambda_c\bar{\Lambda}_c$* arXiv:0809.1151v3 [hep-ph], Europhys. Lett. **85** 61002, doi:10.1209/0295-5075/85/61002
- Bissey, F., Cao, F.-G., Kitson, A. R., Signal, A. I., Leinweber, D. B., Lasscock, B. G. and Williams, A. G. (2006) *Gluon flux-tube distribution and linear confinement in baryons* arXiv:hep-lat/0606016, Phys. Rev. D **76** 114512 (2007), doi:10.1103/PhysRevD.76.114512
- Bjornholm, S., Borggreen, J., Echt, O., Hansen, K., Pedersen, J. and Rasmussen, H. D. (1990) *Mean-field quantization of several hundred electrons in sodium metal clusters* Phys. Rev. Lett. **65** 1627–1630, doi:10.1103/PhysRevLett.65.1627
- Bohr, N. and Wheeler, J. A. (1939) *The mechanism of nuclear fission* Phys. Rev. **56** 426–450, doi:10.1103/PhysRev.56.426
- Bohr, A. (1952) Mat. Fys. Medd. Dan. Vid. Selsk. **26** 14

- Bohr, A. (1954) *Rotational states in atomic nuclei* (Thesis, Copenhagen 1954)
- Bollini, C. G. and Giambiagi, J. J. (1993) *Arbitrary powers of d'Alembertian and the Huygens' principle* J. Math. Phys. **34** 610–621, doi:10.1063/1.530263
- Bolsterli, M., Fiset, E. O., Nix, J. R. and Norton, J. L. (1972) *New calculation of fission barriers for heavy and superheavy nuclei* Phys. Rev. C **5** 1050–1077, doi:10.1103/PhysRevC.5.1050
- Bolzano, B. (1843) *Versuch einer objektiven Begründung der Lehre von den drei Dimensionen des Raumes* Abhandlungen der k. böhmischen Gesellschaft der Wissenschaften, Prag **5**(3) 1–15
- Bombelli, R. (1572) *L'Algebra* Bologna, Italy
- Bonatsos, D. and Daskaloyannis, C. (1999) *Quantum groups and their applications in nuclear physics* arXiv:nucl-th/9909003v1, Prog. Part. Nucl. Phys. **43** 537–618, doi:10.1016/S0146-6410(99)00100-3
- Bonatsos, D., Lenis, D., Raychev, P. P. and Terziev, P. A. (2002) *Deformed harmonic oscillators in metal clusters: Analytic properties and supershells* arXiv:cond-mat/0203125v1, Phys. Rev. A **65** 033203, doi:10.1103/PhysRevA.65.033203
- Brack, M. (1993) *The physics of simple metal clusters: self-consistent jellium model and semi-classical approaches* Rev. Mod. Phys. **65** 677–732, doi:10.1103/RevModPhys.65.677
- Bronstein, I. N., Semendjajew, K. A., Musiol, G. and Mühlig, H. (2004) *Handbook of mathematics* 4th ed. Springer, Berlin, Heidelberg, New York
- Burkert, W. (1972) *Lore and science in ancient Pythagoreanism* Harvard University Press, Cambridge (Massachusetts), USA
- Butcher, J. C. (2008) *Numerical methods for ordinary differential equations* Wiley, Chichester, GB
- Caffarelli, L. and Silvestre, L. (2006) *An extension problem related to the fractional Laplacian* arXiv:math/0608640v2 [math.AP], Comm. Part. Diff. Eqs. **32** (2007) 1245–1260, doi:10.1080/03605300600987306
- Calcagni, G. (2011) *Geometry and field theory in multi-fractional spacetime* arXiv:1107.5041[hep-th], J. High Energy Phys. **2012** (2012) 65, doi:10.1007/JHEP01(2012)065
- Caputo, M. (1967) *Linear model of dissipation whose Q is almost frequency independent Part II* Geophys. J. R. Astr. Soc **13** 529–539, doi:10.1111/j.1365-246X.1967.tb02303.x
- Caputo, M. and Mainardi, F. (1971) *A new dissipation model based on memory mechanism* Pure and Appl. Geophys. (PAGEOPH) **91** 134–147, doi:10.1007/BF00879562 reprinted in Fract. Calc. Appl. Anal. **10** (2007) 309–324
- Cardano, H. (1545) *Ars magna sive de regulis algebraicis*
- Cardoso, M., Cardoso, N. and Biendo, P. (2009) *Lattice QCD computation of the colour fields for the static hybrid quark-gluon-antiquark system, and microscopic study of the Casimir-scaling* arXiv: 0912.3181v1[hep-lat] Phys. Rev. D **81** (2010) 034504, doi:10.1103/PhysRevD.81.034504
- Carrol, R. (2012) *On a fractional quantum potential* arXiv:1206.0900 [math-ph]
- Cartan, É. (1922) *Sur une généralisation de la notion de courbure de Riemann et les espaces à torsion* Comptes Rendus Acad. Sci. **174** 593–595

- Casher, A., Neuberger, H. and Nussinov, S. (1979) *Chromoelectric-flux-tube model of particle production* Phys. Rev. D **20** 179–188, doi:10.1103/PhysRevD.20.179
- Casten, R. F., Zamfir, N. V. and Brenner, D. S. (1993) *Universal anharmonic vibrator description of nuclei and critical nuclear phase transitions* Phys. Rev. Lett. **71** 227–230, doi:10.1103/PhysRevLett.71.227
- Chakraborty, S., Debnath, U. and Jamil, M. (2012) *Variable G correction for dark energy model in higher dimensional cosmology* Canadian Journal of Physics **90** 365–371, doi:10.1139/p2012-027
- Chandrasekhar, S. (1969) *Ellipsoidal figures of equilibrium* Dover Publications, New York
- Chang, S. (2011) *Fractional Brownian motion and blackbody radiation* Chinese Journal of Physics (CJP) **49** 752–758, doi:10.1109/icbbe.2011.5780232
- Chodos, A., Jaffe, R. L., Johnson, K., Thorn, C. B. and Weisskopf, V. F. (1974) *New extended mode of hadrons* Phys. Rev. D **9** 3471–3495, doi:10.1103/PhysRevD.9.3471
- Chowdhury, P. R., Samanta, C. and Basu, D. N. (2006) *α decay half-lives of new super-heavy elements* arXiv:nucl-th/0507054v2, Phys. Rev. C **73** 014612, doi:10.1103/PhysRevC.73.014612
- Chung, W. S. and Jung, M. (2013) *On the fractional damped oscillators and fractional forced oscillators* arXiv:1302.2847 [physics.gen-ph]
- Clemenger, K. (1985) *Ellipsoidal shell structure in free-electron metal clusters* Phys. Rev. B **32** 1359–1362, doi:10.1103/PhysRevB.32.1359
- CMS-Collaboration (2012) *Observation of a new boson at a mass of 125 GeV with the CMS experiment at the LHC* arXiv:1207.7235 [hep-ex], Phys. Lett. B **716** 30–61, doi:10.1016/j.physletb.2012.08.021
- Colless, M. M., Dalton, G. B., Maddox, S. J., Sutherland, W. J., Norberg, P., Cole, S. M., Bland-Hawthorn, J., Bridges, T. J., Cannon, R. D., Collins, C. A., Couch, W. J., Cross, N., Deeley, K., De Propris, R., Driver, S. P., Efstathiou, G., Ellis, R. S., Frenk, C. S., Glazebrook, K., Jackson, C. A., Lahav, O., Lewis, I. J., Lumsden, S., Madgwick, D. S., Peacock, J. A., Peterson, B. A., Price, I. A., Seaborne, M. and Taylor, K. (the 2dFGRS team) (2001) *The 2dF galaxy redshift survey: spectra and redshifts* arXiv:astro-ph/0106498, Mon. Not. R. Astron. Soc. **328** 1039–1063, doi:10.1046/j.1365-8711.2001.04902.x
- Cramer, J. D. and Nix, J. R. (1970) *Exact calculation of the penetrability through two-peaked fission barriers* Phys. Rev. C **2** 1048–1057, doi:10.1103/PhysRevC.2.1048
- Creutz, M. (1974) *Quark bags and local field theory* Phys. Rev. D **10** 1749–1752, doi:10.1103/PhysRevD.10.1749
- Cwiok, S., Rozmej, P., Sobczewski, A. and Patyk, Z. (1989) *Two fission modes of the heavy fermium isotopes* Nucl. Phys. A **2** 281–289, doi:10.1016/0375-9474(89)90703-3
- Darwin, C. (1859) *On the origin of species by means of natural selection* John Murray, London

- Davidson, P. M. (1932) *Eigenfunctions for calculating electronic vibrational intensities* Proc. R. Soc. **135** 459–472, <http://www.jstor.org/stable/95869>
- Davies, K. T. R., Sierk, A. J. and Nix J. R. (1976) *Effect of viscosity on the dynamics of fission* Phys. Rev. C **13** 2385–2403, doi:10.1103/PhysRevC.13.2385
- Dept, K., Herrmann, R., Greiner, W., Scheid, W. and Sandulescu, A. (1985) *Fission mass yields of excited-medium heavy nuclei studied within the fragmentation theory - the ^{172}Yb as an example* J. Phys. G: Nucl. Part. Phys. **11** 1087, doi:10.1088/0305-4616/11/9/015
- Dept, K., Greiner, W., Maruhn, J. A., Wang, H. J., Sandulescu, A. and Herrmann, R. (1990) *On the necking-in process in cluster decays* Intern. Journal of Modern Physics A, **5** 3901–3928, doi:10.1142/S0217751X90001677
- Descartes, R. (1664) *Le monde ou traité de la lumière* Le Gras, Paris
- Diaz, J. B. and Osler, T. J. (1974) *Differences of fractional order* Mathematics of computation. **28** 185–202, doi:10.1016/j.cma.2004.06.006
- Diethelm, K., Ford, N. J., Freed, A. D. and Luchko, Yu. (2005) *Algorithms for the fractional calculus: A selection of numerical methods* Comp. Methods. Appl. Mech. Engrg. **194** 743–773, doi:10.1016/j.cma.2004.06.006
- Diethelm, K. (2010) *The analysis of fractional differential equations* Springer, Berlin, Heidelberg, New York
- Dirac, P. A. M. (1928) *The quantum theory of the electron* Proc. Roy. Soc. (London) A **117** 610–624, <http://www.jstor.org/stable/94981>
- Dirac, P. A. M. (1930) *The principles of quantum mechanics* The Clarendon Press, Oxford
- Dirac, P. A. M. (1963) *The evolution of the physicist's picture of nature* Scientific American **208** (5) 47–56
- Dirac, P. A. M. (1984) *The requirements of fundamental physical theory* Eur. J. Phys. **5** 65–67, doi:10.1088/0143-0807/5/2/001
- Dominik, H. (1935) *Atomgewicht 500* Scherl, Berlin
- Dong, J. and Xu, M. (2007) *Some solutions to the space fractional Schrödinger equation using momentum representation method* J. Math. Phys. **48** 072105, doi:10.1063/1.2749172
- Dong, J. and Xu, M. (2008) *Space-time fractional Schrödinger equation with time-independent potentials* J. Math. Anal. Appl **344** 1005–1017, doi:10.1016/j.jmaa.2008.03.061
- Dong, J. (2013) *Levy path integral approach to the solution of the fractional Schrödinger equation with infinite square well* arXiv:1301.3009 [math-ph]
- Düllmann, Ch. E. et al. (2010) *Production and decay of element 114: high cross sections and the new nucleus ^{277}Hs* Phys. Rev. Lett. **104** 252701, doi:10.1103/PhysRevLett.104.252701
- Dürr, S., Fodor, Z., Frison, J., Hölbling, C., Hoffmann, R., Katz, S. D., Krieg, S., Kurth, T., Lellouch, L., Lippert, T., Szabo, K. K. and Vulvert, G. (2008) *Ab initio determination of light hadron masses* arXiv:0906.3599v1 [hep-lat], Science **322** 1224–1227, doi:10.1126/science.1163233

- Eab, C. H. and Lim, S. C. (2006) *Path integral representation of fractional harmonic oscillator* Phys. Lett. A **371** 303–316, doi:10.1016/j.physa.2006.03.029
- Eab, C. H. and Lim, S. C. (2010) *Fractional Langevin equation of distributed order* arXiv:1010.3327v2 [cond-mat.stat-mech], Physical Review E **83** 031136 (2011), doi:10.1103/PhysRevE.83.031136
- Edmonds, A. R. (1957) *Angular momentum in quantum mechanics* Princeton University Press, New Jersey.
- Ehrenfest, P. (1917) *In what way does it become manifest in the fundamental laws of physics that space has three dimensions?* Proc. Amsterdam Acad. **20** I, 200–209, reprinted in Klein, M. J. (Ed.) (1959) *Paul Ehrenfest - collected scientific papers* North Holland Publ. Co., Amsterdam
- Eichten, E., Gottfried, K., Kinoshita, T., Kogut, J., Lane, K. D. and Yan, T. M. (1975) *Spectrum of charmed quark-antiquark bound states* Phys. Rev. Lett. **34** 369–372, doi:10.1103/PhysRevLett.34.369 and Phys. Rev. Lett. **34** (1976) 1276, doi:10.1103/PhysRevLett.36.1276 *Interplay of confinement and decay in the spectrum of charmonium* Phys. Rev. Lett. **36** 500–504, doi:10.1103/PhysRevLett.36.500
- Eid, R., Muslih, S. I., Baleanu, D. and Rabei, E. (2009) *On fractional Schrödinger equation in α -dimensional fractional space* Nonlinear Analysis: Real World Applications **10** (2009) 1299–1304, doi:10.1016/j.nonrwa.2008.01.007
- Eid, R., Muslih, S. I., Baleanu, D. and Rabei, E. (2011) *Fractional dimensional harmonic oscillator* Rom. Journ. Phys. **56** 323–331
- Einstein, A. (1915) *Die Feldgleichungen der Gravitation* Sitzungsberichte der Preußischen Akademie der Wissenschaften zu Berlin: 844–847. in Simon, D. (Ed.) (2006) *Albert Einstein: Akademie-Vorträge: Sitzungsberichte der Preußischen Akademie der Wissenschaften 1914 - 1932* Wiley VCH-Verlag doi:10.1002/3527608958.ch5
- Einstein, A., Podolsky, B. and Rosen, N. (1935) *Can quantum-mechanical description of physical reality be considered complete?* Phys. Rev. **47** 777–780, doi:10.1103/PhysRev.47.777
- Eisenberg, J. M. and Greiner, W. (1987) *Nuclear models* North Holland, Amsterdam
- Elliott, J. P. (1958) *Collective motion in the nuclear shell model. I. Classification schemes for states of mixed configurations* Proc. Roy. Soc. London A **245** 128–145, <http://www.jstor.org/stable/100416>
- Ellis, J., Mavromatos, N. E. and Nanopoulos, D. V. (1992) *The origin of space-time as W-symmetry breaking in string theory* arXiv:hep-th/9205107, Phys. Lett. B **288** 23–30, doi:10.1016/0370-2693(92)91949-A
- El-Nabulsi, R. A. and Torres, D. F. M. (2008) *Fractional actionlike variational problems* arXiv:0804.4500v1 [math-ph], J. Math. Phys. **49** (5) 053521, doi:10.1063/1.2929662
- El-Nabulsi, R. A. (2009) *Complexified quantum field theory and mass without mass from multidimensional fractional actionlike variational approach with dynamical fractional exponents* Chaos, Solitons and Fractals, **42** 2384–2398, doi:10.1016/j.chaos.2009.03.115

- El-Nabulsi, R. A. (2010) *Fractional action-like variational approach, perturbed Einstein's gravity and new cosmology* Fizika B **19** 103–112
- El-Nabulsi, R. A. (2013) *Fractional derivatives generalization of Einstein's field equations* Indian J. Phys., **87** 195–200, doi:10.1007/s12648-012-0201-4
- Elsasser, W. M. (1933) *Sur le principe de Pauli dans les noyaux* J. Phys. Radium **4** 549–556, *ibid.* **5** (1934) 389–397, *ibid.* **5** (1934) 635–639, doi: 10.1051/jphysrad:01934005012063500 <http://hal.archives-ouvertes.fr/jpa-00233288>
- El-Sayed, A. M. A. and Gaber, M. (2006) *On the finite Caputo and finite Riesz derivatives* EJTP **3** (12)81–95
- Engel, E., Schmitt, U. R., Lüdde, H.-J., Toepfer, A., Wüst, E., Dreizler, R. M., Knospe, O., Schmidt, R. and Chattopadhyay, P. (1993) *Accurate numerical study of the stability of Na₁₉-cluster dimers* Phys. Rev. B **48** 1862–1869, doi:10.1103/PhysRevB.48.1862
- England, T. R. and Rider B. F. (1994) *Fission product yields per 100 fissions for ²³⁵U pooled fast neutron fission decay from Evaluation and compilation of fission product yields 1993* LA-UR-94-3106, ENDF-349, Los Alamos National Laboratory
- Erdélyi, A., Magnus, A., Oberhettinger, F. and Tricomi, F. G. (1953) *Higher transcendental functions* Vol. II, Bateman Manuscript Project, California Institute of Technology, McGraw Hill, New York
- Erzan, A. and Eckmann, J.-P. (1997) *q-analysis of fractal sets* Phys. Rev. Lett. **78** 3245–3248, doi:10.1103/PhysRevLett.78.3245
- Euler, L. (1738) *De progressionibus transcendentibus seu quarum termini generales algebraice dari nequeunt* Commentarii academiae scientiarum Petropolitanae **5** 36–57, reprinted in Opera omnia I.14, 1–24
- Euler, L. (1768) *Remarques sur un beau rapport entre les series des puissances tant directes que reciproques* Memoires de l' academie des sciences de Berlin **17** 83–106
- Falzon, F. and Giraudon, G. (1994) *Singularity analysis and derivative scale-space* in Proceedings CVPR '94, IEEE Computer Society Conference, 245–250, doi:10.1109/CVPR.1994.323836
- Farmelo, G. (2009) *The strangest man, the hidden life of Paul Dirac, mystic of the atom* Basic Books, NY.
- Feller, W. (1952) *On a generalization of Marcel Riesz' potentials and the semi-groups generated by them* Comm. Sem. Mathem. Universite de Lund, 72–81
- Feller, W. (1968) *An introduction to probability theory and Its applications* Vol. 1 3rd ed. pp 50–53, Wiley, New York
- Feng, D. H., Gilmore, R. and Deans, S. R. (1981) *Phase transitions and the geometric properties of the interacting boson model* Phys. Rev. C **23** 1254–1258, doi:10.1103/PhysRevC.23.1254
- Fermi, E. (1934) *Possible production of elements of atomic number higher than 92* Nature **133** 898–899, doi:10.1038/133898a0
- Feynman, R. P. (1949) *The theory of positrons* Phys. Rev. **76** 749–759, doi: 10.1103/PhysRev.76.749

- Fibonacci (1204) *Liber Abaci* translated by Sigler, L., Springer, Berlin, Heidelberg, New York (2002)
- Fink, H. J., Maruhn, J. A., Scheid, W. and Greiner, W. (1974) *Theory of fragmentation dynamics in nucleus-nucleus collisions* Z. Physik **268** 321–331, doi:10.1007/BF01669469
- Flerov, G. N. and Petrzhak, K. A. (1940) *Spontaneous fission of uranium* J. Phys. **3** 275–280
- Fornberg, B. (1988) *Generation of finite difference formulas on arbitrarily spaced grids* Math. Comp. **51** 699–706, <http://www.ams.org/mathscinet-getitem?mr=935077>
- Fortunato, L. (2005) *Solutions of the Bohr Hamiltonian, a compendium* arXiv:nucl-th/0411087v1, Eur. Phys. J. A **26** s01, 1–30, doi:10.1140/epjad/i2005-07-115-8
- Foster, J. G. and Müller, B. (2000) *Physics with two time dimensions* arXiv:1001.2485 [hep-th]
- Foster, D. and Krusch, S. (2013) *Negative baryon density and the folding structure of the $B = 3$ skyrmion* arXiv:1301.4197 [hep-th], J. Phys. A: Math. Theor. **46** 265401 (19pp), doi:10.1088/1751-8113/46/26/265401
- Fourier, J. B. J. (1822) *Théorie analytique de la chaleur* Cambridge University press (2009), Cambridge, UK.
- Frank, A., Jolie, J. and Van Isacker, P. (2009) *Symmetries in atomic nuclei* Springer, Berlin, Heidelberg, New York
- Frankel, S. and Metropolis, N. (1947) *Calculations in the liquid-drop model of fission* Phys. Rev. **72** 914–925
- Fridmann, J., Wiedenhöver, I., Gade, A., Baby, L. T., Bazin, D., Brown, B. A., Campbell, C. M., Cook, J. M., Cottle, P. D., Diffenderfer, E., Dinca, D.-C., Glasmacher, T., Hansen, P. G., Kemper, K. W., Lecouey, J. L., Mueller, W. F., Olliver, H., Rodriguez-Vieitez, E., Terry, J. R., Tostevin, J. A. and Yoneda, K. (2005) *Magic nucleus ^{42}Si* Nature **435** 922–924, doi:10.1038/nature03619
- GadElkarim, J. J., Magin, R. L., Meerschaert, M. M., Capuani, S., Palombo, M., Kumar, A. and Leov, A. D. (2013) *Fractional order generalization of anomalous diffusion as a multidimensional extension of the transmission line equation* IEEE Journal on Emerging and Selected Topics in Circuits and Systems **3**(3) 432–441, doi:0.1109/JETCAS.2013.2265795
- Garbaczewski, P. and Stephanowich, V. (2013) *Levy flights and nonlocal quantum dynamics* arXiv:1302.1478 [quant-ph], J. Math. Phys. **54** 072103, doi:10.1063/1.4814049
- Gauß, C. F. (1799) *Demonstratio nova theorematis omnem functionem algebraicam rationalem integrum unius variabilis in factores reales primi vel secundi gradus resolvi posse* dissertation, apud Fleckeisen, C. G., Helmstedt, Germany
- Gneuss, G. and Greiner, W. (1971) *Collective potential energy surfaces and nuclear structure* Nucl. Phys. A **171** 449–479, doi:10.1016/0375-9474(71)90596-3

- Godfrey, S. and Isgur, N. (1985) *Mesons in a relativized quark model with chrodynamics* Phys. Rev. D **32** 189–231, doi:10.1103/PhysRevD.32.189
- Godinho, C. F. L., Weberszpil, J. and Helayel-Neto, J. A. (2011) *Extending the d'Alembert solution to space-time modified Riemann-Liouville fractional wave equations* arXiv:1111.6266v3 [hep-th], Chaos, Solitons and Fractals **45** (2012) 765–771, doi:10.1016/j.chaos.2012.02.008
- Goeppert-Mayer, M. (1948) *On closed shells in nuclei* Phys. Rev. **74** 235–239, doi:10.1103/PhysRev.74.235 and Phys. Rev. **75** (1949) 1969–1970, doi:10.1103/PhysRev.75.1969
- Goldfain, E. (2006) *Complexity in quantum field theory and physics beyond the standard model* Chaos, Solitons and Fractals **28** 913–922, doi:10.1016/j.chaos.2005.09.012
- Goldfain, E. (2008a) *Fractional dynamics and the TeV regime of field theory* Commun. Nonlin. Sci. Numer. Simul. **13** 666–676.
- Goldfain, E. (2008b) *Fractional dynamics and the standard model for particle physics* Commun. Nonlin. Sci. Numer. Simul. **13** 1397–1404, doi:10.1016/j.cnsns.2006.12.007
- Gorenflo, R. and Mainardi, F. (1996) *Fractional oscillations and Mittag-Leffler functions* in: Proceedings of RAAM 1996, Kuwait University, 193–196
- Gorenflo, R. and Mainardi, F. (1997) *Fractional calculus: integral and differential equations of fractional order* in: Carpinteri, A. and Mainardi, F. (Eds.) *Fractals and Fractional Calculus in Continuous Mechanics* Springer, Berlin, Heidelberg, New York, 223–276
- Gorenflo, R., Luchko, J. and Luchko, Yu. (2002) *Computation of the Mittag-Leffler function $E_{\alpha,\beta}(z)$ and its derivative* Fract. Calc. Appl. Anal. **5** 491–518
- Gorenflo, R. et al. (2008) <http://www.fracalmo.org>
- Gradshteyn, I. S. and Ryzhik, I. M. (1980) *Table of integrals, series and products* Academic Press, New York
- Greenlees, P. T., Rubert, J., Piot, J., Gall, B. J. P., Andersson, L. L., Asai, M., Asfari, Z., Cox, D. M., Dechery, F., Dorvaux, O., Grahn, T., Hauschild, K., Henning, G., Herzan, A., Herzberg, R.-D., Heßberger, F. P., Jakobsson, U., Jones, P., Julin, R., Jutinen, S., Ketelhut, S., Khoo, T.-L., Leino, M., Ljungvall, J., Lopez-Martens, A., Lozeva, R., Nieminen, P., Pakarinen, J., Papadakis, P., Parr, E., Peura, P., Rahkila, P., Rinta-Antila, S., Ruotsalainen, P., Sandzelius, M., Saren, M., Scholey, C., Seweryniak, D., Sorri, J., Sulignano, B., Theisen, Ch., Uusitalo, J. and Venhart, M. (2012) *Shell-structure and pairing interaction in superheavy nuclei: Rotational properties of the $Z=104$ nucleus ^{256}Rf* Phys. Rev. Lett. **109** 012501, doi:10.1103/PhysRevLett.109.012501
- Greiner, M., Scheid, W. and Herrmann, R. (1988) *Collective spin by linearization of the Schrödinger equation for nuclear collective motion* Mod. Phys. Lett. A **3** 859–866, doi:10.1142/S0217732388001021
- Greiner, W. and Müller, B. (1994) *Quantum mechanics - symmetries* Springer, Berlin, Heidelberg, New York
- Greiner, W., Park, J. A. and Scheid, W. (1995) *Nuclear molecules* World Scientific

- Publ., Singapore
- Greiner, W. and Maruhn, J. A. (1997a) *Nuclear models* Springer, Berlin, Heidelberg, New York
- Greiner, W. and Reinhardt, J. (1997b) *Quantum field theory* Springer, Berlin, Heidelberg, New York
- Greiner, W., Neise, L. and Stöcker, H. (2001) *Thermodynamics and statistics* Springer, Berlin, Heidelberg, New York
- Greiner, W. (2008) *Quantum mechanics -an introduction* 4th ed. Springer, Berlin, Heidelberg, New York
- Greiner, W. (2009) *Quantum mechanics - an introduction* 4th ed. Springer, Berlin, Heidelberg, New York
- Grünwald, A. K. (1867) *Über begrenzte Derivationen und deren Anwendung* Z. angew. Math. und Physik **12** 441–480
- Grumann, J., Mosel, U., Fink, B. and Greiner, W. (1969) *Investigation of the stability of superheavy nuclei around $Z=114$ and $Z=164$* Z. Phys. **228** 371–386, doi:10.1007/BF01406719
- Guericke, O. von (1672) *Nova (ut vocantur) Magdeburgica de vacuo spatio* Schott, C. (Ed.) J. Janssonius, Waesberge, Amsterdam <http://web.archive.org/web/20110928171356/http://num-scd-ulp.u-strasbg.fr:8080/525/>
- Guo, X. and Xu, M. (2006) *Some physical applications of fractional Schrödinger equation* J. Math. Phys. **47** 082104, doi:10.1063/1.2235026
- Gupta, R. K., Cseh, J., Ludu, A., Greiner, W. and Scheid, W. (1992) *Dynamical symmetry breaking in $SU(2)$ model and the quantum group $SU(2)_q$* J. Phys. G: Nucl. Part. Phys. **18** L73–L82, doi:10.1088/0954-3899/18/3/003
- Haapakoski, P., Honkaranta, P. and Lipas, P. O. (1970) *Projection model for ground bands of even-even nuclei* Phys. Lett. B **31** 493–495, doi:10.1016/0370-2693(70)90071-7
- Haberland, H., Hippeler, T., Donges, J., Kostko, O., Schmidt, M. and von Isendorff, B. (2005) *Melting of sodium clusters: Where do the magic numbers come from?* Phys. Rev. Lett. **94** 035701 doi:10.1103/PhysRevLett.94.035701
- Hahn, O. and Straßmann, F. (1939) *Über den Nachweis und das Verhalten der bei der Bestrahlung des Urans mittels Neutronen entstehenden Erdalkalimetalle* Die Naturwissenschaften **27** 11–15, doi:10.1007/BF01488241
- Hall, A. R. (1952) *Ballistics in the seventeenth century* Cambridge University Press, Cambridge
- Hartwig, J. T., Larsson, D. and Silvestrov, S. D. (2006) *Deformations of Lie algebras using σ -derivations* J. Algebra **295** 314–361 doi:10.1016/j.jalgebra.2005.07.036
- Haubold, H. J., Mathai, A. M. and Saxena, R. K. (2009) *Mittag-Leffler functions and their applications* arXiv:0909.0230, Journal of Applied Mathematics, Hindawi, (2011) article-id: 298628, 51 pages, doi:10.1155/2011/298628
- Hawkins, E. and Schwarz, J. M. (2012) *Comment "On the consistency of solutions of the space fractional Schrödinger equation [J. Math. Phys. 53, 042105 (2012)] "* arXiv:1210.1447 [math-ph], J. Math. Phys. **54** (2013) 014101, doi:10.1063/1.4772533

- Haxel, F. P., Jensen, J. H. D. and Suess, H. D. (1949) *On the magic numbers in nuclei* Phys. Rev. **75** 1766–1766, doi:10.1103/PhysRev.75.1766.2
- He, X. F. (1990) *Fractional dimensionality and fractional derivative spectra of interband optical transitions* Phys. Rev. B **42** (18) 11751–11756 doi:10.1103/PhysRevB.42.11751
- Heer, W. A. de (1993) *The physics of simple metal clusters: experimental aspects and simple models* Rev. Mod. Phys. **65** 611–676, doi:10.1103/RevModPhys.65.611
- Heisenberg, W. (1927) *Über den anschaulichen Inhalt der quantentheoretischen Kinematik und Mechanik* Zeitschrift f. Physik **43** 172–198, doi:10.1007/BF01397280
- Henriquez, A. B. (1979) *A study of charmonium, upsilon and strangeonium systems* Z. Phys. C **2** 309–312, doi:10.1007/BF01545891
- Herrmann, R., Maruhn, J. A. and Greiner, W. (1986) *Towards a unified description of asymmetric nuclear shapes in structure, fission and cluster radioactivity* J. Phys. G.: Nuclear Physics **12** L285–L290, doi:10.1088/0305-4616/12/12/004
- Herrmann, R., Depta, K., Schnabel, D., Klein, H., Renner, W., Poenaru, D. N., Sandulescu, A., Maruhn, J. A. and Greiner, W. (1988) *Nuclear deformation, cluster-structure, fission and cluster radioactivity - A unifying point of view* in Märten, H. and Seeliger, D. (Eds.) (1988) *Physics and chemistry of fission, Proceedings of the XVIIIth international symposium on nuclear physics devoted to the fiftieth anniversary of the discovery of nuclear fission* Zentralinstitut für Kernforschung, Rossendorf/Dresden, ZfK-732, indc special 6, pp. 191–211, available online at IAEA, Vienna, Austria, nuclear data services, indc-special series - indc reports <http://www-nds.iaea.org/reports-new/indc-reports/indc.../indcspecial.pdf>
- Herrmann, R., Plunien, G., Greiner, M., Greiner, W. and Scheid, W. (1989a) *Collective spin from the linearization of the Schrödinger equation in multidimensional Riemannian spaces used in collective nuclear models* Int. J. Mod. Phys. A **4** 4961–4975, doi:10.1142/S0217751X89002107
- Herrmann, R. (1989b) *Einführung des Spinfreiheitsgrades im Riemannschen Raum kollektiver Modelle* PhD-Thesis, GSI-Report GSI-89-14 REP, GSI Darmstadt, Germany <http://hdl.handle.net/10068/273952>
- Herrmann, R. (2005a) *Continuous differential operators and a new interpretation of the charmonium spectrum* arXiv:nucl-th/0508033
- Herrmann, R. (2005b) *Properties of a fractional derivative Schrödinger type wave equation and a new interpretation of the charmonium spectrum* arXiv:math-ph/0510099
- Herrmann, R. (2006) *The fractional symmetric rigid rotor* arXiv:nucl-th/0610091v1, J. Phys. G: Nucl. Part. Phys. **34** 607–625, doi:10.1088/0954-3899/34/4/001
- Herrmann, R. (2007a) *Gauge invariance in fractional field theories* arXiv:0708.2262v1 [math-ph], Phys. Lett. A **372** (2008) 5515–5522, doi:10.1016/j.physleta.2008.06.063

- Herrmann, R. (2007b) *Common aspects of q -deformed Lie-algebras and fractional calculus* arXiv:0711.3701v1 [physics.gen-ph], arXiv:1007.1084v1 [physics.gen-ph], Physica A **389** (2010) 4613–4622, doi:10.1016/j.physa.2010.07.004
- Herrmann, R. (2008a) *Curvature interaction in collective space* arXiv:0801.0298 [nucl-th], Int. J. Mod. Phys. E **21** (12) (2012) 1250103 (10 pages), doi:10.1142/S0218301312501030
- Herrmann, R. (2008b) *Higher-dimensional mixed fractional rotation groups as a basis for dynamic symmetries generating the spectrum of the deformed Nilsson oscillator* arXiv:0806.2300v1 [physics.gen-ph], Physica A **389** (2010) 693–704, doi:10.1016/j.physa.2009.11.016
- Herrmann, R. (2009a) *Higher order fractional derivatives* arXiv:0906.2185v2 [physics.gen-ph].
- Herrmann, R. (2009b) *Fractional phase transition in medium size metal clusters* arXiv:0907.1953v1 [physics.gen-ph], Physica A **389** (2010) 3307–3315, doi:10.1016/j.physa.2010.03.033
- Herrmann, R. (2010) *Fractional quantum numbers deduced from experimental ground state meson spectra* arXiv:1003.5246v1 [physics.gen-ph]
- Herrmann, R. (2011) *Covariant fractional extension of the modified Laplace-operator used in 3D-shape recovery* arXiv:1111.1311v1 [cs.CV], Fract. Calc. Appl. Anal. **15** (2012) 332–343, doi:10.2478/s13540-012-0024-1
- Herrmann, R. (2012a) *Infrared spectroscopy of diatomic molecules - a fractional calculus approach* arXiv:1209.1630 [physics.gen-ph], Int. J. Mod. Phys. B **27** (2013) 1350019 (17 pages), doi:10.1142/S0217979213500197
- Herrmann, R. (2012b) *The fractional Schrödinger equation and the infinite potential well - numerical results using the Riesz derivative* arXiv:1210.4410 [math-ph], Gam. Ori. Chron. Phys. **1** (2013) 1–12
- Herrmann, R. (2013a) *Numerical solution of the fractional quantum mechanical harmonic oscillator based on the Riemann and Caputo derivative* Gam. Ori. Chron. Phys. **1** (2013) 13–176
- Herrmann, R. (2013b) *Uniqueness of the fractional derivative* arXiv:1303.2939 [physics.gen-ph]
- Herrmann, R. (2013c) *Folded potentials in cluster physics - a comparison of Yukawa and Coulomb potentials with Riesz fractional integrals* arXiv:1305.0890 [physics.gen-ph], J. Phys. A.: Math. Theor. **46** 405203 (12pp), doi:10.1088/1751-8113/46/40/405203
- Herrmann, R. (2013d) *On the origin of space* arXiv:1308.4587 [physics.gen-ph], Cent. Eur. J. Phys. **11**, doi:10.2478/s11534-013-0315-0
- Herzberg, G. (1951) *Molecular spectra and molecular structure I: structure of diatomic molecules* 2nd ed., D. Van Nostrand Company, New York, NY, USA
- Higgs, P. W. (1964) *Broken symmetries and the masses of gauge bosons* Phys. Rev. Lett. **13** 508–509, doi:10.1103/PhysRevLett.13.508
- Hilfer, R. (2000) *Applications of fractional calculus in physics* World Scientific Publ., Singapore

- Hilfer, R. and Seybold, H. J. (2006) *Computation of the generalized Mittag-Leffler function and its inverse in the complex plane* Integral transforms and special functions **17** 637–652, doi:10.1080/10652460600725341
- Hilfer, R. (2008) *Threefold introduction to fractional derivatives* in: Klages, R., Radons, G. and Sokolov I. (editors) *Anomalous transport, foundations and application* Wiley-VCH, Weinheim, Germany, 17–73.
- Hofmann, S., Ninov, V., Heßberger, F. P., Armbruster, P., Folger, H., Münzenberg, G., Schött, H. J., Popeko, A. G., Yeremin, A. V., Saro, S., Janik, R. and Leino, M. (1996) *The new element 112* Z. Phys. A **354** 229–230, doi:10.1007/BF02769517
- Hofmann, S. and Münzenberg, G. (2000) *The discovery of the heaviest elements* Rev. Mod. Phys. **72** 733–767, doi:10.1103/RevModPhys.72.733
- Hu, Y. and Kallianpur, G. (2000) *Schrödinger equations with fractional Laplacians* Appl. Math. Optim. **42** 281–290, doi:10.1007/s002450010014
- Hu, M. S., Agarwal, R. P. and Yang, X. J. (2012) *Local fractional Fourier series with application to wave equation in fractal vibrating string* Abstr. Appl. Anal. **2012** article-ID: 567401, 15 pages, doi:10.1155/2012/567401
- Hulet, E. K., Wild, J. F., Dougan, R. J., Lougheed, R. W., Landrum, J. H., Dougan, A. D., Schadel, M., Hahn, R. L., Baisden, P. A., Henderson, C. M., Dupzyk, R. J., Sümmerer, K. and Bethune, G. R. (1986) *Bimodal symmetric fission observed in the heaviest elements* Phys. Rev. Lett. **56** 313–316, doi:10.1103/PhysRevLett.56.313
- Hullmeine, U., Winsel, A. and Voss, E. (1989) *Effect of previous charge/discharge history on the capacity of the PbO₂/PbSO₄ electrode: the hysteresis or memory effect* J. of Power Sources **25** 27–47, doi:10.1016/0378-7753(89)80120-X
- Hunt, B. J. (2012) *Oliver Heaviside: A first-rate oddity* Phys. Today **65** 48–54, doi:10.1063/PT.3.1788
- Hurwitz, A. (1882) *Einige Eigenschaften der Dirichlet'schen Funktionen F(s) = $\sum(\frac{D}{n})\frac{1}{n^s}$, die bei der Bestimmung der Klassenanzahlen binärer quadratischer Formen auftreten* Z. für Math. und Physik **389** 86–101
- Huygens, C. (1673) *Horologium oscillatorium sive de motu pendulorum ad horologia aptato demonstrationes geometricae* F. Muguet, Paris, France, <http://ebooks.library.cornell.edu/cgi/t/text/text-idx?c=kmodd1;idno=km053>
- Iachello, F. and Arima, A. (1987) *The interacting boson model* Cambridge University Press, Cambridge.
- Ibe, O. C. (2013) *Elements of Random Walk and Diffusion Processes (Wiley Series in Operations Research and Management Science)* John Wiley and Sons, Hoboken, NJ, USA.
- Inglis, D. R. (1954) *Particle derivation of nuclear rotation properties associated with a surface wave* Phys. Rev. **96** 1059–1064, doi:10.1103/PhysRev.96.1059
- Iomin, A. (2007) *Accelerator dynamics of a fractional kicked rotor* arXiv:nlin/0609036 [nlin.CD], Phys. Rev. E **75** 037201, doi:10.1103/PhysRevE.75.037201

- Iomin, A. (2009) *Fractional time quantum mechanics* Phys. Rev. E **80** 022103, doi:10.1103/PhysRevE.80.022103
- Ishteva, M., Boyadjiev, L. and Scherer, R. (2005) *On the Caputo operator of fractional calculus and C-Laguerre functions* Mathematical Sciences Research Journal **9** 161–170
- Iwamoto, A. and Herrmann, R. (1991) *Evaporation of charged particles from highly deformed nucleus* Z. Phys. A.: Hadrons and Nuclei **338** 303–307, doi:10.1007/BF01288194
- Jackson, J. D. (1998) *Classical electrodynamics* 3rd ed. Wiley, New York
- Jamil, M., Momeni, D. and Myrzakulov, R. (2012) *Attractor solutions in $f(T)$ cosmology* arXiv:1202.4926 [physics.gen-ph], Eur. Phys. J. C D **72** 1959, doi:10.1140/epjc/s10052-012-1959-4
- Jeng, M., Xu, S.-L.-Y., Hawkins, E. and Schwarz, J. M. (2008) *On the nonlocality of the fractional Schrödinger equation* arXiv:0810.1543v1 [math-ph], J. Math. Phys. **51** (2010) 062102, doi:10.1063/1.3430552
- Jumarie, G. (2006) *Modified Riemann-Liouville derivative and fractional Taylor series of nondifferentiable functions further results* Computers and Mathematics with Applications **51** 1367–1376, doi:10.1016/j.camwa.2006.02.001
- Jumarie, G. (2009) *Table of some basic fractional calculus formulae derived from a modified Riemann-Liouville derivative for non-differentiable functions* Appl. Math. Lett. **22** 378–385, doi:10.1016/j.aml.2008.06.003
- Jumarie, G. (2013) *Riemann-Christoffel tensor in differential geometry of fractional order application to fractal space-time* Fractals **21** 1350004, doi:10.1142/S0218348X13500047
- Jumarie, G. (2014) *Fractional differential calculus via fractional difference theory and applications: A non-standard fractional calculus and its applications* World Scientific Publ., Singapore
- Kant, I. (1781) *Anmerkung zur dritten Antinomie* in: Die Antinomie der reinen Vernunft, Akademie Verlag, Berlin 1998
- Kalugampola, U. (2010) *New approach to a generalized fractional integral* arXiv:1010.0742v1 [math.CA], Appl. Math. Comp. **215** (2011) 860–865, doi:10.1016/j.amc.2011.03.062
- Kaluza, Th. (1919) *Zum Unitsproblem der Physik* Sitzungsberichte der Preussischen Akademie der Wissenschaften Physikalisch-mathematischer Klasse (1921) 966–972, <http://homepage.uibk.ac.at/~c705204/pdf/kaluza-1921.pdf>
- Karami, K., Jamil, M., Ghaffari, S., Fahimi, K. and Myrzakulov, R. (2013) *Holographic, new agegraphic, and ghost dark energy models in fractal cosmology* Canadian Journal of Physics **91** 770–776, doi:10.1139/cjp-2013-0293
- Kelson, I. (1964) *Dynamic calculation of fission of an axial symmetric liquid drop* Phys. Rev. **136** B1667–B1673, doi:10.1103/PhysRev.136.B1667
- Kepler, J. (1609) *Astronomia nova seu physica coelestis tradita commentariis de motibus stellae martis ex observationibus G.V. Tychoonis Brahe* Prague
- Kepler, J. (1619) *Harmonices mundi libri V* Linz, Austria

- Kerner, R. (1992) *Z_3 -grading and the cubic root of the Dirac equation* Classical Quantum Gravity **9** S137–S146, doi:10.1088/0264-9381/9/S/007
- Khanal, N., Wu, J. and Yuan, J. M. (2012) *Fifth-order complex Korteweg-de Vries-type equations* J. Phys. Math. A : Math. Theor. **45** 205202 (17pp), doi:10.1088/1751-8113/45/20/205202
- Kibble, T. W. B. (1961) *Lorentz invariance and the gravitational field* J. Math. Phys. **2** 212–223, doi:10.1063/1.1703702
- Kibble, T. W. B. and Berkshire, F. H. (2004) *Classical mechanics* 5th ed. Imperial College Press, London
- Kilbas, A. A., Srivastava, H. M. and Trujillo, J. J. (2003) *Fractional differential equations: A emergent field in applied and mathematical sciences* in Samko, S., Lebre, A. and Dos Santos, A. F. (Eds.) (2003) *Factorization, singular operators and related problems, Proceedings of the conference in honour of professor Georgii Litvinchuk* Springer, Berlin, Heidelberg, New York, 151–175
- Kilbas, A. A., Srivastava, H. M. and Trujillo, J. J. (2006) *Theory and applications of fractional differential equations* Elsevier, Amsterdam
- Kilbas, A. A., Koroleva, A. A. and Rogosin, S. S. (2013) *Multi-parameter Mittag-Leffler functions and their extension* Fract. Calc. Appl. Anal. **16** 378–404, doi:10.2478/s13540-013-0024-9
- Kiryakova, V. S. (1994) *Generalized fractional calculus and applications* Longman (Pitman Res. Notes in Math. Ser. **301**), Harlow; co-publ.: John Wiley and Sons, New York
- Kiryakova, V. S. (1997) *All the special functions are fractional differintegrals of elementary functions* J. Phys. A Math. Gen. **30** 5085–5104, doi:10.1088/0305-4470/30/14/019
- Kiryakova, V. S. (2008) *A brief story about the operators of the generalized fractional calculus* Fract. Calc. Appl. Anal. **11** 203–220, <http://hdl.handle.net/10525/1329>
- Kiryakova, V. S. and Luchko, Yu. (2013) *Riemann-Liouville and Caputo type multiple Erdélyi-Kober operators* Cent. Eur. J. Phys. **11** (5) doi:10.2478/s11534-013-0217-1
- Klafter, J., Lim, S. C. and Metzler, L. (Eds.) (2011) *Fractional dynamics: recent advances* World Scientific Publ., Singapore
- Klein, F. (1884) *Vorlesungen über das Ikosaeder und die Auflösung der Gleichungen vom fünften Grade* Teubner, Leipzig, Göttingen <http://archive.org/details/vorlesungenber00kleiuoft>
- Klein, O. (1926) *Quantentheorie und fünfdimensionale Relativitätstheorie* Z. Phys. **37** 895–906, doi:10.1007/BF01397481
- Klemm, A., Metzler, R. and Kimmich, R. (2001) *Diffusion on random site percolation clusters: Theory and NMR microscopy experiments with model objects* arXiv:cond-mat/0112098, Phys. Rev. E **65** (2002) 021112, doi:10.1103/PhysRevE.65.021112
- Klimek, M., Odzijewicz, T. and Malinowska, A. B. (2013) *Variational methods for the fractional Sturm-Liouville problem* arXiv:1304.6258 [math.OC]

- Knight, W. D., Clemenger, K., de Heer, W. A., Saunders, W. A., Chou, M. Y. and Cohen, M. L. (1984) *Electronic shell structure and abundances of sodium clusters* Phys. Rev. Lett. **52** 2141–2143, doi:10.1103/PhysRevLett.52.2141
- Kober, H. (1940) *On fractional integrals and derivatives* The Quarterly Journal of Mathematics (Oxford series) **11** (1), 193–211, doi:10.1093/qmath/os-11.1.193
- Kondej, S. and Vaz, J. (2012) *Fractional Schrödinger operator with delta potential localized on circle* J. Math. Phys. **53**, 033503, doi:10.1063/1.3691199
- Korteweg, D. J. and de Vries, G. (1895) *On the change of form of long waves advancing in a rectangular canal, and on a new type of long stationary waves* Philosophical Magazine **39** 422–443, doi:10.1080/14786449508620739
- Krammer, M. and Krasemann, H. (1979) *Quarkonia in quarks and leptons* Acta Physica Austriaca Suppl. XXI, 259–266
- Krappe, H. J. and Pomorski, K. (2012) *Theory of nuclear fission* Lecture notes on physics **838** Springer, Berlin, Heidelberg, New York, doi:10.1007/978-3-642-23515-3
- Krishnamurthy, H. R., Mani, H. S. and Verma, H. C. (1982) *Exact solution of the Schrödinger equation for a particle in a tetrahedral box* J. Phys. A: Math. Gen. **15** 2131–2138, doi:10.1088/0305-4470/15/7/024
- Krug, A. (1890) *Theorie der Derivationen* Akad. Wiss. Wien Denkschriften Math. Naturwiss. **57** 151–228
- Kruppa, A. T., Bender, M., Nazarewicz, W., Reinhard, P. G., Vertse, T. and Cwiok, S. (2000) *Shell corrections of superheavy nuclei in self-consistent calculations* Phys. Rev. C **61** 034313–034325, doi:10.1103/PhysRevC.61.034313
- Kwasnicki, M. (2010) *Eigenvalues of the fractional Laplace operator in the interval* arXiv:1012.1133 [math.SP] J. Funct. Anal. **262** (2012) 2379–2402, doi:10.1016/j.jfa.2011.12.004
- Lämmерzahl, C. (1993) *The pseudo-differential operator square root of the Klein-Gordon equation* J. Math. Phys. **34** 3918–3932, doi:10.1063/1.530015
- Lasenby, A., Doran, C. and Gull, S. (1998) *Gravity, gauge theories and geometric algebra* Phil. Trans. R. Soc. Lond. A **356** 487–582, doi:10.1098/rsta.1998.0178
- Laskin, N. (2000) *Fractals and quantum mechanics* Chaos **10** 780–791, doi:10.1063/1.1050284
- Laskin, N. (2002) *Fractional Schrödinger equation* Phys. Rev. E **66** 056108–0561014, doi:10.1103/PhysRevE.66.056108
- Laskin, N. (2010) *Principles of fractional quantum mechanics* arXiv:1009.5533v1 [math-ph]
- Laskin, N. (2013) *Fractional classical mechanics* arXiv:1302.0547 [math-ph]
- Lazo, M. J. (2011) *Gauge invariant fractional electromagnetic fields* arXiv:1108.3493v1[math-ph], Phys. Lett. A **375** 3541–3648, doi:10.1016/j.physleta.2011.08.033

- Lee, T. D., Oehme, R. and Yang, C. N. (1957) *Remarks on possible noninvariance under time reversal and charge conjugation* Phys. Rev. **106** 340–345, doi: 10.1103/PhysRev.106.340
- Leibniz, G. F. (1675) *Methodi tangentium inversae exempla* manuscript
- Leibniz, G. F. (1695) *Correspondence with l'Hospital* manuscript
- Lévy, P. (1997) *Non-local potentials with LS terms in algebraic scattering theory* J. Phys. A: Math. Gen. **30** 7243–7258, doi:10.1088/0305-4470/30/20/023
- Levy-Leblond, J. M. (1967) *Nonrelativistic particles and wave equations* Comm. Math. Phys. **6** 286–311, doi:10.1007/BF01646020 <http://projecteuclid.org/euclid.cmp/1103840281>
- Li, B.-Q. and Chao, K. T. (2009) *Higher charmonia and X,Y,Z states with screened potential* Phys. Rev. D**79** 094004, doi:10.1103/PhysRevD.79.094004
- Li, C., Chen, Y. Q. and Kurths, J. (Eds.) (2013) *Fractional calculus and its applications* Phil. Trans. R. Soc. A. **371** (1910), Royal Society Publ., London
- Li, M.-F., Ren, J.-R. and Zhu, T. (2010) *Fractional vector calculus and fractional special function* arXiv:1001.2889v1[math.ph]
- Li, M., Lim, S. C. and Chen, Z. (2011) *Exact solution of impulse response to a class of fractional oscillators and its stability* Math. Probl. Engin. article-ID: 657839, doi:10.1155/2011/657839
- Lighthill, M. J. (1958) *Introduction to Fourier analysis and generalized functions* Cambridge University Press, Cambridge
- Lim, S. C. and Muniandy, S. V. (2004) *Stochastic quantization of nonlocal fields* Phys. Lett. A **324** 396–405, doi:10.1016/j.physleta.2004.02.073
- Lim, S. C. (2006a) *Fractional derivative quantum fields at finite temperatures* Physica A **363** 269–281, doi:10.1016/j.physa.2005.08.005
- Lim, S. C. and Eab, C. H. (2006b) *Riemann-Liouville and Weyl fractional oscillator processes* Phys. Lett. A **335** 87–93, doi:10.1016/j.physleta.2006.02.014
- Lim, S. C., Li, M. and Teo, L. P. (2007) *Locally self-similar fractional oscillator processes* Fluct. Noise Lett., **7** L169–L179, doi:10.1142/S0219477507003817
- Lim, S. C. and Tao, L. P. (2008) *Topological symmetry breaking of self-interacting fractional Klein-Gordon field theories on toroidal spacetime* J. Phys. A: Math. Theor. **41** 145403, doi:10.1088/1751-8113/41/14/145403
- Lim, S. C. and Tao, L. P. (2009a) *Repulsive Casimir force from fractional Neumann boundary conditions* Phys. Lett. B **679** 130–137, doi:10.1016/j.physletb.2009.07.024
- Lim, S. C. and Tao, L. P. (2009b) *Three dimensional Casimir piston for massive scalar fields* arXiv:0807.3613v1 [hep-th], Annals. Phys. **324** 1676–1690, doi:10.1016/j.aop.2009.05.006
- Liouville, J. (1832) *Sur le calcul des différentielles à indices quelconques* J. École Polytechnique **13** 1–162
- Lissajous, J. A. (1857) *Mémoire sur l'étude optique des mouvements vibratoires* Mallet-Bachelier, Paris, France

- Liu, C.-S. (2010) *The essence of the generalized Newton binomial theorem* Commun. Nonlin. Sci. Numer. Simul. **15** 2766–2768, doi:10.1016/j.cnsns.2009.11.004
- Loss, R. D. and Corish, J. (2012) *Names and symbols of the elements with atomic numbers 114 and 116 (IUPAC recommendations 2012)* Pure Appl. Chem. **84** 1669–1672, doi:10.1351/PAC-REC-11-12-03
- Louck, J. D. and Galbraith, H. W. (1972) *Application of orthogonal and unitary group methods to the N-body problem* Rev. Mod. Phys. **44** 540–601, doi:10.1103/RevModPhys.44.540
- Luchko, Y. (2012) *Fractional wave equation and damped waves* arXiv:1205.1199 [math-ph], J. Math. Phys. **54** (2013) 031505, doi:10.1063/1.4794076
- Luchko, Y. (2013) *Fractional Schrödinger equation for a particle moving in a potential well* J. Math. Phys. **54** 012111, doi:10.1063/1.4777472
- Lustig, H.-J., Maruhn, J. A. and Greiner, W. (1980) *Transitions in the fission mass distributions of the fermium isotopes* J. Phys. G **6** L25–L36, doi:10.1088/0305-4616/6/2/001
- Lusztig, R. (1993) *Introduction to quantum groups* Birkhäuser Boston
- Mainardi, F. (1996) *Fractional relaxation-oscillation and fractional diffusion-wave phenomena* Chaos, Solitons and Fractals **7** (9), 1461–1477, doi:10.1016/0960-0779(95)00125-5
- Mainardi, F. and Gorenflo, R. (2000) *On Mittag-Leffler-type functions in fractional evolution processes* J. Comput. Appl. Math. **118** 283–299, doi:10.1016/S0377-0427(00)00294-6
- Mainardi, F. (2010) *Fractional calculus and waves in linear viscoelasticity: An introduction to mathematical models* World Scientific Publ., Singapore
- Mainardi, F. (2013) *On some properties of the Mittag-Leffler function $E_\alpha(-t^\alpha)$ completely monotone for $t > 0$ with $0 < \alpha < 1$* arXiv:1305.0161v2 [math-ph]
- Malinowska, A. B. (2012a) *On fractional variational problems which admit local transformations* arXiv:1203.2102v1 [math.OC], Journal of Vibration and Control 1077546312442697, first published on april 4, 2012, doi:10.1177/1077546312442697
- Malinowska, A. B. (2012b) *A formulation of the fractional Noether-type theorem for multidimensional Lagrangians* arXiv:1203.2107v1 [math.OC], Appl. Math. Lett. doi:10.1016/j.aml.2012.03.006
- Malkawi, E. (2013) *Transformation property of the Caputo fractional differential operator in two dimensional space* arXiv:1305.1264 [math-ph]
- Mandelbrot, B. (1982) *Fractal geometry of nature* W. H. Freeman, New York
- Marchant, T. R. and Smyth, N. F. (1990) *The extended Korteweg-de Vries equation and the resonant flow of a fluid over topology* J. Fluid Mech. **221** 263–288, doi:10.1017/S0022112090003561
- Marchaud, A. (1927) *Sur les dérivées et sur les différences des fonctions de variables réelles* J. Math. Pures et Appl. **6** 337–476, <http://eudml.org/doc/234901>
- Martens, G., Greiner, C., Leupold, S. and Mosel, U. (2003) *Chromofields of strings and baryons* arXiv:hep-ph/0303017v1, Eur.Phys.J. A **18** 223–226, doi:10.1140/epja/i2002-10303-6

- Martens, G., Greiner, C., Leupold, S. and Mosel, U. (2004) *Two- and three-body color flux tubes in the chromodielectric model* arXiv:hep-ph/0407215v2, Phys. Rev. D **70** 116010, doi:10.1103/PhysRevD.70.116010
- Martens, G., Greiner, C., Leupold, S. and Mosel, U. (2006) *Interactions of multi-quark states in the chromodielectric model* arXiv:hep-ph/0603100v2, Phys. Rev. D **73** 096004, doi:10.1103/PhysRevD.73.096004
- Martin, T. P., Bergmann, T., Göhlich, H. and Lange, T. (1991) *Electronic shells and shells of atoms in metallic clusters* Z. Phys. D **19** 25–29, doi:10.1007/BF01448248
- Martin, R. R. (2006) *Nuclear and particle physics* John Wiley and Sons, Hoboken, NJ, USA.
- Maruhn, J. A. and Greiner, W. (1972) *The asymmetric two center shell model* Z. Physik **251** 431–457, doi:10.1007/BF01391737
- Maruhn, J. A., Hahn, J., Lustig, H.-J., Ziegenhain, K.-H. and Greiner, W. (1980) *Quantum fluctuations within the fragmentation theory* Prog. Part. Nucl. Phys. **4** 257–271, doi:10.1016/0146-6410(80)90009-5
- Maxwell, J. C. (1873) *A treatise on electricity and magnetism* Clarendon Press, Oxford <http://www.archive.org/details/electricandmagne01maxwrich>
- May, R. M. (1975) *Stability and complexity in model ecosystems* 2nd ed. Princeton Univ. Press, Princeton
- Meerschaert, M. M. and Sikorskii, A. (2011) *Stochastic models for fractional calculus (de Gruyter Studies in Mathematics)* de Gruyter, Berlin.
- Meijer, C. S. (1941) *Multiplikationstheoreme für die Funktion $G_{p,q}^{m,n}(z)$* . Proc. Niederl. Akad. Wetenschau **44** 1062–1070.
- Meitner, L. and Fritsch, O. R. (1939) *Disintegration of uranium by neutrons: A new type of nuclear reaction* Nature **143** 239–240, doi:10.1038/143239a0
- Merali, Z. (2013) *Theoretical Physics: The origins of space and time* Nature **500** 516–519, doi:10.1038/500516a
- Messiah, A. (1968) *Quantum mechanics* John Wiley & Sons, North-Holland Pub. Co, New York
- Metzler, R., Barkai, E. and Klafter, J. (1999) *Deriving fractional Fokker-Planck equations from a generalised master equation* Europhys. Lett. **46** 431–436, doi:10.1209/epl/i1999-00279-7
- Metzler, R., and Klafter, J. (2004) *The restaurant at the end of the random walk: recent developments in the description of anomalous transport by fractional dynamics* J. Phys. A: Math. Gen. **37** R161R208, doi:10.1088/0305-4470/37/31/R01
- Mie, G. (1908) *Beiträge zur Optik trüber Medien, speziell kolloidaler Metall-ösungen* Ann. d. Physik **25** (3) 377–379, doi:10.1002/andp.19083300302
- Miller, K. and Ross, B. (1993) *An introduction to fractional calculus and fractional differential equations* Wiley, New York.
- Mittag-Leffler, M. G. (1903) *Sur la nouvelle function $E_\alpha(x)$* Comptes Rendus Acad. Sci. Paris **137** 554–558.
- Misner, C. W., Thorne, K. S. and Wheeler, J. A. (1973) *Gravitation* Freeman, San Francisco
- Möller, P. and Nix, J. R. (1981) *Nuclear mass formula with a Yukawa-plus-*

- exponential macroscopic model and a folded-Yukawa single-particle potential* Nucl. Phys. A **361** (1) 117–146, doi:10.1016/0375-9474(81)90473-5
- Möller, P., Nix, J. R., Myers, W. D. and Swiatecki, W. J. (1993) *Nuclear ground-state masses and deformations* arXiv:nucl-th/9308022v1, Atomic Data Nucl. Data Tables **59** (1995) 185–381, doi:10.1006/adnd.1995.1002
- Möller, P., Bengtsson, R., Carlsson, B. G., Olivius, P., Ichikawa, T., Sagawa, H. and Iwamoto, A. (2008) *Axial and reflection asymmetry of the nuclear ground state* Atomic Data and Nuclear Data Tables **94** 758–780, doi:10.1016/j.adt.2008.05.002
- Monje, C., Chen, Y., Vinagre, B. N. and Feliu-Batlle, G. (2010) *Fractional-order systems and controls: Fundamentals and applications* Springer, Berlin, Heidelberg, New York
- Moon, P. and Spencer, D. E. (1988) *Field theory handbook: Including coordinate systems, differential equations and their solutions* Springer, Berlin, Heidelberg, New York
- Moriarty, P. (2001) *Nanostructured materials* Rep. Prog. Phys. **64** 297–381, doi:10.1088/0034-4885/64/3/201
- Mosel, U. and Greiner, W. (1969) *On the stability of superheavy nuclei against fission* Z. Phys. A **222** 261–282, doi:10.1007/BF01392125
- Münster, S. (1551) *Rudimenta mathematica Petri*, Basel, 1 page 29. digital edition:Sächsische Landesbibliothek - Staats- und Universitätsbibliothek Dresden Math.59, misc.2, <http://digital.slub-dresden.de/id274384116>
- Muslih, S. I., Agrawal, O. P. and Baleanu, D. (2010a) *A fractional Dirac equation and its solution* J. Phys. A: Math. Theor. **43** 055203, doi:10.1088/1751-8113/43/5/055203
- Muslih, S. I. (2010b) *A formulation of Noethers theorem for fractional classical fields* arXiv:1003.0653v1 [math-ph]
- Myers, W. D. and Swiatecki, W. J. (1966) *Nuclear masses and deformations* Nucl. Phys. **81** 1–60, doi:10.1016/0029-5582(66)90639-0
- Naber, M. (2004) *Time fractional Schrödinger equation* arXiv:math-ph/0410028, J. Math. Phys. **45** 3339–3352, doi:10.1063/1.1769611
- Namias, V. (1980) *The fractional order Fourier transform and its application to quantum mechanics* IMA J. Appl. Math. **25** 241–265, doi:10.1093/imamat/25.3.241
- Nasrolahpour, H. (2013) *A note on fractional electrodynamics* Commun. Nonlin. Sci. Numer. Simul. **25** 5–15, doi:10.1016/j.cnsns.2013.01.005
- Newton, I. (1669) *De analysi per aequationes numero terminorum infinitas* manuscript.
- Newton, I. (1692) *a letter to Bentley, R.* in: Turnbull, H. W. (Ed.) *The correspondence of Isaac Newton* (1961) **3** 253–254
- Nishioka, H., Hansen, K. and Mottelson, B. R. (1990) *Supershells in metal clusters* Phys. Rev. B **42** 9377–9386, doi:10.1007/BF01448247
- National Institute of Standards and Technology (NIST) (2012) *Chemistry web-Book, NIST standard reference database number 69* <http://webbook.nist.gov/chemistry/>
- Nigmatullin, R. R. (1992) *Fractional integral and its physical interpretation* The-

- oret. Math. Phys. **90** 242–251, doi:10.1007/BF01036529
- Nilsson, S. G. (1955) Kgl. Danske Videnskab. Selsk. Mat.-Fys. Medd. **29** 431.
- Nilsson, S. G., Tsang, C. F., Sobczewski, A., Szymba, Z., Wycech, S., Gustafson, C., Lamm, I., Möller, P. and Nilsson, B. (1969) *On the nuclear structure and stability of heavy and super-heavy elements* Nucl. Phys. A **131** 1–66, doi:10.1016/0375-9474(69)90809-4
- Nishimoto, K. (1989) *Fractional calculus: Integrations and differentiations of arbitrary order* University of New Haven Press, New Haven.
- Nix, J. R., Sierk, A. J., Hofmann, H., Scheuter, F. and Vautherin, D. (1984) *Stationary Fokker-Planck equation applied to fission dynamics* Nucl. Phys. A **424** 239–261, doi:10.1016/0375-9474(84)90184-2
- Niyti, Gupta, R. K. and Greiner, W. (2010) *Establishing the island of stability for superheavy nuclei via the dynamical cluster-decay model applied to a hot fusion reaction $^{48}\text{Ca} + ^{238}\text{U} \rightarrow ^{286}112$* J. Phys. G: Nucl. Part. Phys. **37** 115103, doi:10.1088/0954-3899/37/11/115103
- Noddack, I. (1934) *Über das Element 93* Angewandte Chemie **47** 653–655, doi:10.1002/ange.19340473707
- Noether, E. (1918) *Invariante beliebiger Differentialausdrücke* Gött. Nachr. **1918** 37–44, <http://resolver.sub.uni-goettingen.de/purl?GDZPPN002504979> and *Invariante Variationsprobleme* ibid. 235–257, <http://resolver.sub.uni-goettingen.de/purl?GDZPPN00250510X>
- Nogin, V. A. and Samko, S. G. (1999) *Some applications of potentials and approximative inverse operators in multi-dimensional fractional calculus* Fract. Calc. Appl. Anal. **2** 205–228.
- Nomura, K., Shimizu, N. and Otsuka, T. (2008) *Mean-field derivation of the interacting boson model Hamiltonian and exotic nuclei* Phys. Rev. Lett. **101** 142501, doi:10.1103/PhysRevLett.101.142501
- Numerov, B. (1927) *Note on the numerical integration of $d^2x/dt^2 f(x, t)$* Astronomische Nachrichten **230** 359–364
- Odzijewicz, T., Malinkowska, A. B. and Torres, D. F. M. (2011) *Fractional variational calculus of variable order* arXiv:1110.4141 [math.OC], in *Advances in harmonic analysis and operator theory, The Stefan Samko anniversary volume* Almeida, A., Castro, L. and Speck, F. O. (Eds.) *Operator Theory: Advances and Applications* **229** (2013) 291–301, Birkhäuser Science, Springer, Berlin, Heidelberg, New York, doi:10.1007/978-3-0348-0516-2_16
- Odzijewicz, T., Malinkowska, A. B. and Torres, D. F. M. (2012) *Green's theorem for generalized fractional derivatives* arXiv:1205.4851[math.CA], Fract. Calc. Appl. Anal. **16** (2013) 64–75, doi:10.2478/s13540-013-0005-z
- Odzijewicz, T., Malinkowska, A. B. and Torres, D. F. M. (2013a) *Variable order fractional variational calculus for double integrals* arXiv:1209.1345 [math.OC], 51st IEEE Conference on Decision and Control (2012) 6873–6878, doi:10.1109/CDC.2012.6426489

- Odzijewicz, T., Malinkowska, A. B. and Torres, D. F. M. (2013b) *Noether's theorem for fractional variational problems of variable order* arXiv:1303.4075 [math.OC], Central European Journal of Physics, doi:10.1109/CDC.2012.6426489
- Odzijewicz, T., Malinkowska, A. B. and Torres, D. F. M. (2013c) *A generalized fractional calculus of variations* arXiv:1304.5282 [math.OC], Control and Cybernetics
- Oganessian, Yu. Ts., Utyonkov, V. K., Lobanov, Yu. V., Abdullin, F. Sh., Polyakov, A. N., Shirokovsky, I. V., Tsyganov, Yu. S., Gulbekian, G. G., Bogomolov, S. L., Gikal, B. N., Mezentsev, A. N., Iliev, S., Subbotin, V. G., Sukhov, A. M., Voinov, A. A., Buklanov, G. V., Subotic, K., Zagrebaev, V. I. and Itkis, M. G. (2004) *Measurements of cross sections for the fusion-evaporation reactions Pu-244 (Ca-48,xn) (292-x)114 and Cm-245 (Ca-48,xn) (293-x)116* Phys. Rev. C **69** 054607, doi:10.1103/PhysRevC.69.054607
- Oganessian, Yu. Ts., Abdullin, F. Sh., Bailey, P. D., Benker, D. E., Bennett, M. E., Dmitriev, S. N., Ezold, J. G., Hamilton, J. H., Henderson, R. A., Itkis, M. G., Lobanov, Yu. V., Mezentsev, A. N., Moody, K. J., Nelson, S. L., Polyakov, A. N., Porter, C. E., Ramayya, A. V., Riley, F. D., Roberto, J. B., Ryabinin, M. A., Rykaczewski, K. P., Sagaidak, R. N., Shaughnessy, D. A., Shirokovsky, I. V., Stoyer, M. A., Subbotin, V. G., Sudowe, R., Sukhov, A. M., Tsyganov, Yu. S., Utyonkov, V. K., Voinov, A. A., Vostokin, G. K. and Wilk, P. A. (2010) *Synthesis of a new element with atomic number Z = 117* Phys. Rev. Lett. **104** 142502, doi:10.1103/PhysRevLett.104.142502
- Ölander, A. (1932) *An electrochemical investigation of solid cadmium-gold alloys* Journal of the American Chemical Society **54** (10) 3819–3833, doi:10.1021/ja01349a004
- Oldham, K. B. and Spanier, J. (1974) *The fractional calculus* Academic Press, New York
- Ortigueira, M. D. and Machado, J. A. T. (2003) *Fractional signal processing and applications* Sign. Proc. **83** 2285–2286
- Ortigueira, M. D. (2003) *On the initial conditions in continuous-time fractional linear systems* Sign. Proc. **83** 2301–2309, doi:10.1016/S0165-1684(03)00183-X
- Ortigueira, M. D. and Coiti, F. (2004) *From differences to derivatives* Fract. Calc. Appl. Anal. **7** 459–471
- Ortigueira, M. D. (2006) *Riesz potential operators and inverses via fractional centred derivatives* International Journal of Mathematics and Mathematical Sciences, Article ID 48391, 1–12, doi:10.1155/IJMMS/2006/48391
- Ortigueira, M. D. (2008) *Fractional central differences and derivatives* Journal of Vibration and Control, **14** 1255–1266, doi:10.1177/1077546307087453
- Ortigueira, M. D. (2011a) *Fractional calculus for scientists and engineers* Springer, Berlin, Heidelberg, New York

- Ortigueira, M. D., Magin, R. and Trujillo, J. J. (2011b) *A regularized derivative* FSS 2011, Symposium on fractional signals and systems, IPC Coimbra, Portugal, 4–5 November, 2011
- Ortigueira, M. D. and Trujillo, J. J. (2012) *A unified approach to fractional derivatives* Commun. Nonlin. Sci. Numer. Simul. **17** 5151–5157, doi: 10.1016/j.cnsns.2012.04.021
- Osler, T. J. (1970) *Leibniz rule for fractional derivatives generalized and an application to infinite series* SIAM J. Appl Math. **18** 658–674, <http://www.jstor.org/stable/2099520>
- Pakhlova, G. V., Pakhlov, P. N. and Eidel'man, S. I. (2010) *Exotic charmonium* Phys. Usp. **180** 219–242, doi:10.3367/UFNe.0180.201003a.0225
- Parisi, G. and Wu, Y. (1981) *Perturbation theory without gauge fixing* Scientia Sinica **24** 483–496, reprinted in Damgaard, P. H. and Hüffel, H. (Eds.) (1988) *Stochastic quantization* World Scientific Publ., Singapore
- Pashaev, O. K. and Nalci, S. (2012) *Golden quantum oscillator and Binet-Fibonacci calculus* J. Phys. A: Math. Theor. **45** 015303, doi:10.1088/1751-8113/45/1/015303
- Pauli, W. (1933) *Handbuch der Physik* 2nd ed. **24** 120–133 Springer Heidelberg, Berlin, NY
- Pauli, W. (1941) *Relativistic field theories of elementary particles* Rev. Mod. Phys. **13** 203–232, doi:10.1103/RevModPhys.13.203
- Pellarin, M., Baguenard, B., Vialle, J. L., Lermé, J., Broyer, M., Miller, J. and Perez, A. (1994) *Evidence for icosahedral atomic shell structure in nickel and cobalt clusters. Comparison with iron clusters* Chem. Phys. Lett. **217** 349–356, doi:10.1016/0009-2614(93)E1474-U
- Perdew, J. P., Wang, Y. and Engel, E. (1991) *Liquid drop model for crystalline metallics: Vacancy-formation, cohesive and face-dependent surface energies* Phys. Rev. Lett. **66** 508–511, doi:10.1103/PhysRevLett.66.508
- Peyré, G., Bougleux, S. and Cohen, L. (2008) *Non-local regularization of inverse problems* in Forsyth, D., Torr, P. and Zisserman A. (Eds.) *Computer Vision ECCV 2008* 10th European Conference on Computer Vision, Marseille, France, October 12–18, 2008, Proceedings, Part III, pp. 57–68, Springer Berlin, Heidelberg, New York, doi:10.1007/978-3-540-88690-7_5
- Peyré, G., Bougleux, S. and Cohen, L. (2011) *Non-local regularization of inverse problems* Inverse Problems and Imaging **5** 511–530, doi:10.3934/ipi.2011.5.511
- Philoponus, I. (~530) *On Aristotle, Physics* translated by Osborne, C., Lacey, A. R., Edwards, M. J. , Lettinck, P. and Urmson, J. O., Duckworth, London (1993–2006)
- Plessis, N. du (1957) *Spherical fractional integrals* Trans. Amer. Math. Soc. **84** 262–272, <http://www.jstor.org/stable/1992901>
- Plutonium Project, The (1946) *Nuclei formed in fission: decay characteristics, fission yields, and chain relationships* J. Am. Chem. Soc. **68** 2411–2442, doi:10.1021/ja01215a600 and Rev. Mod. Phys. **18** 513–544 doi:10.1103/RevModPhys.18.513

- Plyushchay, M. S. and Rausch de Traubenberg, M. (2000) *Cubic root of Klein-Gordon equation* arXiv:hep-th/0001067v2, Phys. Lett. B **477** 276–284, doi: 10.1016/S0370-2693(00)00190-8
- Podlubny, I. (1999) *Fractional differential equations* Academic Press, New York
- Podlubny, I. (2001) *Geometric and physical interpretation of fractional integration and fractional differentiation* arXiv:math/0110241v1, Fract. Calc. Appl. Anal., **5** (2002) 367–386
- Podolsky, B. (1928) *Quantum-mechanically correct form of Hamiltonian function for conservative systems* Phys. Rev. , **32** 812–816, doi:10.1103/PhysRev.32.812
- Poenaru, D. N. and Plonski, I.-L. (2008) *Shell and pairing corrections for atomic cluster physics* Romanian Reports in Physics **60** 529–538
- Poenaru, D. N., Gherghescu, R. A. and Greiner, W. (2010a) *Individual and collective properties of fermions in nuclear and atomic cluster systems* J. Phys. G: Nucl. Part. Phys. **37** 085101, doi:10.1088/0954-3899/37/8/085101
- Poenaru, D. N. and Greiner, W. (2010b) *Cluster radio activity* in Beck, C. (Ed.) *Clusters in Nuclei I* 1–56, Springer, Berlin, Heidelberg, New York, doi: 10.1007/978-3-642-13899-7_1
- Poenaru, D. N., Gherghescu, R. A. and Greiner, W. (2012) *Simple relationships for α -decay half-lifes* J. Phys. G: Nucl. Part. Phys. **39** 015105 (9pp), doi: 10.1088/0954-3899/39/1/015105
- Poincaré, H. (1912) *Pourquoi l'espace a trois dimensions* Revue de métaphysique et de morale **20** 483–504, <http://www.univ-nancy2.fr/poincare/bhp/pdf/hp1912rm.pdf>
- Prudnikov, A. P., Brychkov, Yu. A. and Marichev, O. I. (1990) *Integrals and Series, Volume 3: More special functions* Gordon and Breach Science Publishers, New York
- Prusinkiewicz, P. and Lindenmayer, A. (1993) *The algorithmic beauty of plants* Springer, Berlin, Heidelberg, New York
- Rabei, E. M., Alhaloly, T. S. and Rousan, A. (2004) *Potentials of arbitrary forces with fractional derivatives* Int. Journ. Mod. Phys. A, **19** 3083–3092 doi: 10.1142/S0217751X04019408
- Rabei, E. M., Altarazi, I. M. A., Muslih, S. I. and Baleanu, D. (2007) *Fractional WKB approximation* arXiv:0704.0526v1 [math-ph], Nonlinear Dynamics **57** (2009) 171–175, doi:10.1007/s11071-008-9430-7
- Racah, G. (1942) *Theory of complex spectra* Phys. Rev. **61** 186–197, doi: 10.1103/PhysRev.61.186 Phys. Rev. **62** (1942) 438–462, doi:10.1103/PhysRev.62.438 Phys. Rev. **63** (1943) 367–382, doi:10.1103/PhysRev.63.367 Phys. Rev. **76** (1949) 1352–1365, doi:10.1103/PhysRev.76.1352
- Raduta, A. A., Gheorghe, A. C. and Faessler, A. (2005) *Remarks on the shape transition from spherical to deformed gamma unstable nuclei* J. Phys. G: Nucl. Part. Phys. **31** 337–353, doi:10.1088/0954-3899/31/5/005
- Raduta, A. A., Budaca, R. and Faessler, A. (2010) *Closed formulas for ground band energies of nuclei with various symmetries* J. Phys. G: Nucl. Part. Phys. **37** 085108, doi:10.1088/0954-3899/37/8/085108

- Rafeiro, H. and Samko, S. (2005) *On multidimensional analogue of Marchaud formula for fractional Riesz-type derivatives in domains in R^n* . Fract. Calc. Appl. Anal. **8** 393–402, <http://hdl.handle.net/10525/1265>
- Ramirez, L. E. S. and Coimbra, C. F. M. (2010) *On the selection and meaning of variable order operators for dynamic modeling* Int. J. Differential Equations **2010** Article ID 846107 (16 pages), doi:10.1155/2010/846107
- Ramirez, E. Minaya, Ackermann, D., Blaum, K., Block, M., Droese, C., Düllmann, Ch. E., Dworschak, M., Eibach, M., Eliseev, S., Haettner, E., Herfurth, F., Heßberger, F. P., Hofmann, S., Ketelaer, J., Marx, G., Mazzocco, M., Nesterenko, D., Novikov, Yu. N., Plaß, W. R., Rodriguez, D., Scheidenberger, C., Schweikhart, L., Thirolf, P. G. and Weber, C. (2012) *Direct mapping of nuclear shell effects in the heaviest elements* Science **337** 1207–1210, doi:10.1126/science.1225636
- Randall, L. and Sundrum, R. (1999) *An alternative to compactification* Phys. Rev. Lett. **83** 4690–4693 doi:0.1103/PhysRevLett.83.4690
- Raspini, A. (2000) *Dirac equation with fractional derivatives of order 2/3* Fizika B **9** 49–55, http://fizika.hfd.hr/fizika_b/bv00/b9p049.pdf
- Raspini, A. (2001) *Simple solutions of the fractional Dirac equation of order 2/3* Physica Scripta **64** 20–22, doi:10.1238/Physica.Regular.064a00020
- Raychev, P. P., Roussev, R. P. and Smirnov, Yu. F. (1990) *The quantum algebra $SU_q(2)$ and rotational spectra of deformed nuclei* J. Phys. G: Nucl. Part. Phys. **16** L137–L142, doi:10.1088/0954-3899/16/8/006
- Reinhard, P. G. and Surraud, E. (2004) *Introduction to cluster dynamics* Wiley-VCH, Weinheim, Germany
- Riemann, B. (1847) *Versuch einer allgemeinen Auffassung der Integration und Differentiation* in: Weber, H. and Dedekind, R. (Eds.) (1892) *Bernhard Riemann's gesammelte mathematische Werke und wissenschaftlicher Nachlass* Teubner, Leipzig, reprinted in *Collected works of Bernhard Riemann* Dover Publications (1953) 353–366
- Riess, A. G., Filippenko, A. V., Challis, P., Clocchiattia, A., Diercks, A., Garnavich, P. M., Gilliland, R. L., Hogan, C. J., Jha, S., Kirshner, R. P., Leibundgut, B., Phillips, M. M., Reiss, D., Schmidt, B. P., Schommer, R. A., Smith, R. C., Spyromilio, J., Stubbs, C., Suntzeff, N. B. and Tonry, J. (1998) *Observational evidence from supernovae for an accelerating universe and a cosmological constant* arXiv:astro-ph/9805201, Astron. J. **116** 1009–1038, doi:10.1086/300499
- Riesz, M. (1949) *L'intégrale de Riemann-Liouville et le problème de Cauchy* Acta Math. **81** 1–222
- Riewe, F. (1996) *Nonconservative Lagrangian and Hamiltonian mechanics* Phys. Rev. E **53** 1890–1899, doi:10.1103/PhysRevE.53.1890
- Riewe, F. (1997) *Mechanics with fractional derivatives* Phys. Rev. E **55** 3581–3592, doi:10.1103/PhysRevE.55.3581
- Ring, P. and Schuck, P. (2008) *The nuclear many-body problem* Springer Berlin, Heidelberg, New York
- Risken, H. (1989) *The Fokker-Planck equation - methods of solution and applications* 2nd ed. Springer, Berlin, Heidelberg, New York

- Roberts, M. D. (2009) *Fractional derivative cosmology* arXiv:0909.1171
- Rodriguez, M. E., Houndjo, M. J. S., Morneni, D. and Myrzakulov, R. (2013) *Planar Symmetry in $f(T)$ gravity* arXiv:1302.4372 [physics.gen-ph], Int. J. Mod. Phys. **22** 1350043, doi:10.1142/S0218271813500430
- Rose, H. J. and Jones, G. A. (1984) *A new kind of natural radioactivity* Nature **307** 245–247, doi:10.1038/307245a0
- Rose, M. E. (1995) *Elementary theory of angular momentum* Dover Publications, New York
- Ross, B. (1974) *Fractional calculus and its applications: Proceedings of the international conference* New Haven
- Ross, B. (1977) *Fractional calculus* Math. Mag. **50** 115–122, <http://www.jstor.org/stable/2689497>
- Rowling, J. K. (1999) *Harry Potter and the prisoner of Azkaban* Bloomsbury Publishing, UK
- Rozmey, P. and Bandrowski, B. (2010) *On fractional Schrödinger equation* Comput. Methods Sci. Technol. **16** 191–194
- Rubin, B. (1996) *Fractional integrals and potentials* Pitman Monographs and Surveys in Pure and Applied Mathematics, vol. 82, Longman, Harlow
- Rubin, B. (2012) *Weighted norm estimates for the Semenistyi fractional integrals and Radon transforms* arXiv:1210.5414 [math.FA]
- Rubin, V. C., Ford, W. K. Jr., Thonnard, N., Roberts, M. S. and Graham, J. A. (1976a) *Motion of the galaxy and the local group determined from the velocity anisotropy of distant Sc I galaxies. I. the data* Astronomical Journal, **81** 687–718, doi:10.1086/111942
- Rubin, V. C., Thonnard, N., Ford, W. K. and Roberts, M. S. (1976b) *Motion of the galaxy and the local group determined from the velocity anisotropy of distant SC I galaxies. II - The analysis for the motion* Astronomical Journal, **81** 718–737, doi:10.1086/111943
- Rufa, M., Reinhard, P. G., Maruhn, J. A., Greiner, W. and Strayer, M. R. (1988) *Optimal parametrization for the relativistic mean-field model of the nucleus* Phys. Rev. C **38** 390–409, doi:10.1103/PhysRevC.38.390
- Rutz, K., Bender, M., Bürvenich, T., Schilling, T., Reinhard, P. G., Maruhn, J. A. and Greiner, W. (1997) *Superheavy nuclei in self-consistent nuclear calculations* arXiv:nucl-th/9610032v1, Phys. Rev. C **56** 238–243, doi:10.1103/PhysRevC.56.238
- Ryabov, Ya. E. and Punzenko, A. (2002) *Damped oscillations in view of the fractional oscillator equation* Phys. Rev. B **66** 184201, doi:10.1103/PhysRevB.66.184201
- Sabatier, J., Agrawal, O. P. and Tenreiro Machado, J. A. (2007) *Advances in fractional calculus: Theoretical developments and applications in physics and engineering* Springer, Berlin, Heidelberg, New York
- Safdari, H., Vahabi, M. and Jafari, G. R. (2013) *Scattering from rough surfaces: A simple reflection phenomenon in fractional space* arXiv:1305.7029 [physics.optics]
- Sakurai, J. J. (1967) *Advanced quantum mechanics* Benjamin/Cummings, New York

- Samko, S. G. and Ross, B. (1993a) *Integration and differentiation to a variable fractional order* Integral Transforms and Special Functions **1** 277–300, doi: 10.1080/10652469308819027
- Samko, S. G., Kilbas, A. A. and Marichev, O. I. (1993b) *Fractional integrals and derivatives* Translated from the 1987 Russian original, Gordon and Breach, Yverdon
- Samko, S. G. (1995) *Fractional integration and differentiation of variable order* Anal. Math. **21** 213–236, doi:0.1007/BF01911126
- Sandev, T. and Tomovski, Z. (2010) *The general time fractional wave equation for a vibrating string* J. Phys. A: Math. Theor. **43** 055204, doi:10.1088/1751-8113/43/5/055204
- Sandulescu, A., Gupta, R. K., Scheid, W. and Greiner, W. (1976) *Synthesis of new elements within the fragmentation theory: Application to $Z = 104$ and 106 elements* Phys. Lett. B **60** 225–228, doi:10.1016/0370-2693(76)90286-0
- Sandulescu, A., Poenaru, D. N. and Greiner, W. (1980) *New type of decay of heavy nuclei intermediate between fission and alpha decay* Soviet Journal of Particles and Nuclei **11** 528–541
- Sato, Y., Takeuchi, S. and Kobayakawa, K. (2001) *Cause of the memory effect observed in alkaline secondary batteries using nickel electrode* J. of Power Sources **93** 20–24, doi:10.1016/S0378-7753(00)00506-1
- Scharnweber, D., Mosel, U. and Greiner, W. (1970) *Asymptotically correct shell model for nuclear fission* Phys. Rev. Lett. **24** 601–603, doi:10.1103/PhysRevLett.24.601
- Schlüter, P., Wietschorke, K. H. and Greiner, W. (1983) *The Dirac equation in orthogonal coordinate systems: I . The local representation* J. Phys. A: Math. Gen. **16** 1616, 1999–2016, doi:10.1088/0305-4470/16/9/024 and *The Dirac equation in orthogonal coordinate systems: II . The two center Dirac equation* J. Phys. A: Math. Gen. **16** 2017–2034, doi:10.1088/0305-4470/16/9/025
- Schmutzler, E. (1968) *Relativistische Physik* Teubner, Leipzig
- Schneider, V., Maruhn, J. A. and Greiner, W. (1986) *Cranking model mass parameters for the asymmetric two center shell model* Z. Phys. A **323** 111–118, doi:10.1007/BF01294562
- Secchi, S. and Squassina, M. (2013) *Soliton dynamics for the fractional Schrödinger equations* arXiv:1305.1804 [math.AP]
- Segovia, J., Entem, D. R. and Fernandez, F. (2010) *Charmonium narrow resonances in the string breaking region* J. Phys. G: Nucl. Part. Phys. **37** 075010, doi:10.1088/0954-3899/37/7/075010
- Semyanisty, V. I. (1960) *On some integral transformations in Euclidean space* (Russian) Dokl. Akad. Nauk CCCP, **134** 536–539
- Serot, B. D. and Walecka, J. D. (1986) *The relativistic nuclear many-body problem* in Negele, J. W. and Vogt, E. (editors) *Advances in Nuclear Physics* Vol. **16** Plenum Press, New York
- Seybold, H. J. and Hilfer, R. (2005) *Numerical results for the generalized Mittag-Leffler function* Fract. Calc. Appl. Anal. **8** 127–139

- Seybold, H. J. and Hilfer, R. (2008) *Numerical algorithm for calculating the generalized Mittag-Leffler function* Siam J. Numer. Anal. **47** 69–88, doi: 10.1137/070700280
- Shannon, C. E. (1949) *Communication in the presence of noise* Proc. Inst. of radio engineers, **37** (1), 10–21, doi:10.1109/JRPROC.1949.232969
- Sillion, F. X. and Puech, C. (1994) *Radiosity and global illumination* (The Morgan Kaufmann series in computer graphics and geometric modeling) Morgan Kaufmann Publishers Inc., San Francisco, CA
- Sneddon, I. N. (1966) *Mixed boundary value problem in potential theory* North-Holland Publ. Co., Amsterdam (1966)
- Sneddon, I. N. (1975) *The use in mathematical analysis of the Erdélyi-Kober operators and some of their applications* In: *Fractional Calculus and its applications* (Proc. Intern. Conf., New Haven, 1974) *Lecture notes in mathematics* **457** 37–79, Springer, Berlin Heidelberg New York (1975)
- Sobiczewski, A. and Pomorski, K. (2007) *Description of structure and properties of super-heavy nuclei* Prog. Part. Nucl. Phys. **58** 292–349, doi:10.1016/j.ppnp.2006.05.001
- Sousa, E. (2010) *How to approximate the fractional derivative of order $1 \leq \alpha \leq 2$* in Podlubny, I., Vinagre Jara, B. M., Chen, Y. Q., Feliu Batlle, V. and Tejado Balsera, I. (Eds.) *Proceedings of FDA10. The 4th IFAC workshop fractional differentiation and its applications* Badajoz, Spain, october 18–20, (2010)
- Spanier, J., Myland, J. and Oldham, K. B. (2008) *An atlas of functions* Springer, Berlin, Heidelberg, New York
- Sparavigna, A. C. (2009) *Using fractional differentiation in astronomy* arXiv.org:0910.2381
- Spencer, M. (1982) *Fundamentals of Light Microscopy* Cambridge University Press
- Stancu, F. I. (2010) *Can $Y(4140)$ be a $c\bar{c}s\bar{s}$ tetraquark?* J. Phys. G: Nucl. Part. Phys. **37** 075017, doi:10.1088/0954-3899/37/7/075017
- Stanislavsky, A. A. (2000) *Memory effects and macroscopic manifestation of randomness* Phys. Rev. E **61** 4752–4759, doi:10.1103/PhysRevE.61.4752
- Stanislavsky, A. A. (2004) *Fractional oscillator* Phys. Rev. E **70** 051103, doi: 10.1103/PhysRevE.70.051103
- Stanislavsky, A. A. (2006a) *The peculiarity of self-excited oscillations in fractional systems* Acta Physica Polonica B **37** (2), 319–329
- Stanislavsky, A. A. (2006b) *Hamiltonian formalism of fractional systems* Europ. Phys. J B **49** 93–101, doi:10.1140/epjb/e2006-00023-3
- Staszczak, A., Baran, A. and Nazarewicz, W. (2012) *Spontaneous fission modes and lifetimes of super-heavy elements in the nuclear density functional theory* arXiv:1208.1215 [nucl-th], Phys. Rev. C **87** 024320 (2013) [7 pages], doi:10.1103/PhysRevC.87.024320
- Steeb, W.-H. (2007) *Continuous symmetries, Lie algebras, differential equations and computer algebra* 2nd ed. World Scientific Publ., Singapore

- Stickler, B. (2013) *Some properties of the one-dimensional Lévy crystal* arXiv:1306.5874 [cond-mat.stat-mech] Phys. Rev. E **88** 012120, doi:10.1103/PhysRevE.88.012120
- Stirling, J. (1730) *Methodus differentialis, sive tractatus de summation et interpolation serierum infinitarum* London, English translation Tweddle, I. James *Stirling's methodus differentialis: An annotated translation of Stirling's text (sources and studies in the history of mathematics and physical sciences)* (2003) Springer, Berlin, Heidelberg, New York
- Struckmeyer, J. and Reichau, H. (2012) *General U(N) gauge transformations in the realm of covariant Hamiltonian field theory* arXiv:1205.5754v6 [hep-th], Proc. symposium on exciting physics: quarks and gluons, atomic nuclei, biological systems, networks, 13-20 november 2011, Makutsi Safari Farm, South Africa in Greiner, W. (Ed.) *Exciting interdisciplinary physics*, Frankfurt Institute for Advanced Studies (FIAS) (2013) Springer, Berlin, Heidelberg, New York
- Strutinsky, V. M. (1967a) *Microscopic calculation of the nucleon shell effects in the deformation energy of nuclei* Ark. Fysik **36** 629–632
- Strutinsky, V. M. (1967b) *Shell effects in nuclear masses and deformation energies* Nucl. Phys. A **95** 420–442, doi:10.1016/0375-9474(67)90510-6
- Strutinsky, V. M. (1968) *Shells in deformed nuclei* Nucl. Phys. **A122** 1–33, doi:10.1016/0375-9474(68)90699-4
- Stückelberg, E. C. G. (1941) *Un nouveau modèle de l'électron ponctuel en théorie classique* Helv. Phys. Acta **14** 51–80
- Sun, H. G., Chen, W. and Chen, Y. Q. (2009) *Variable-order fractional differential operators in anomalous diffusion modeling* Physica A **388** 4586–4592, doi:10.1016/j.physa.2009.07.024
- Svensmark, H. (2012) *Evidence of nearby supernovae affecting life on Earth* arXiv:1210.2963 [astro-ph.SR] Mon. Not. R. Astron. Soc. **423** 1234–1253, doi:10.1111/j.1365-2966.2012.20953.x
- Szwed, J. (1986) *The square root of the Dirac equation within super symmetry* Phys. Lett. B **181** 305–307, doi:10.1016/0370-2693(86)90051-1
- Tajima, N. and Suzuki, N. (2001) *Prolate dominance of nuclear shape caused by a strong interference between the effects of spin-orbit and l^2 terms of the Nilsson potential* Phys. Rev. C **64** 037301, doi:10.1103/PhysRevC.64.037301
- Takahashi, T. T., Suganuma, H., Nemoto, Y. and Matsufuru, H. (2002) *Detailed analysis of the three-quark potential in SU(3) lattice QCD* arXiv:hep-lat/0204011v1, Phys. Rev. D **65** 114509, doi:10.1103/PhysRevD.65.114509
- Tangherlini, F. R. (1963) *Schwarzschild field in n dimensions and the dimensionality of space problem* Nuovo Cimento **27** (3) 636–651 doi:10.1007/BF02784569
- Tarascon, J. M., Gozdz, A. S., Schmutz, C., Shokoohi, F. and Warren, P. C. (1996) *Performance of Bellcore's plastic rechargeable Lithium-ion batteries* Solid State Ionics **86–88** 49–54, doi:10.1016/0167-2738(96)00330-X

- Tarasov, V. E. and Zaslavsky, G. M. (2006) *Dynamics with low-level fractionality* arXiv:physics/0511138v1, Physica A **368** (2), 399–415, doi:10.1016/j.physa.2005.12.015
- Tarasov, V. E. (2007) *Fractional derivative as fractional power of derivative* arXiv:0711.2567 [nlin.CD], International Journal of Mathematics **18** (3), 281–299, doi:10.1142/S0129167X07004102
- Tarasov, V. E. (2008a) *Fractional vector calculus and fractional Maxwell's equations* arXiv:0907.2363v3 [math-ph], Ann. Physics **323** (11), 2756–2778, doi:10.1016/j.aop.2008.04.005
- Tarasov, V. E. (2008b) *Weyl quantization of fractional derivatives* arXiv:0907.2699 [math-ph], J. Math. Phys. **49** (10) 102112, doi:10.1063/1.3009533
- Tarasov, V. E. (2011) *Fractional dynamics: applications of fractional calculus to dynamics of particles, fields and media* Springer, Berlin, Heidelberg, New York
- Tarasov, V. E. (2013a) *Review of some promising fractional physical models* Int. J. Mod. Phys. B **27** (9) 1330005 (32 pages) doi:10.1142/S0217979213300053
- Tarasov, V. E. (2013b) *No violation of the Leibniz rule. No fractional derivative* Commun. Nonlin. Sci. Numer. Simul. **18** 2945–2948, doi:j.cnsns.2013.04.001
- Tarasov, V. E. (2013c) *Fractional gradient elasticity from spatial dispersion law* arXiv:1306.2572 [physics.class-ph]
- Tatom, F. B. (1995) *The relationship between fractional calculus and fractals* Fractals **3** 217–229, doi:10.1142/S0218348X95000175
- Taylor, B. (1715) *Methodus incrementorum directa et inversa* G. Innys, London, e.g. doi:10.3931/e-rara-4090
- Tenreiro Machado, J. A., Kiryakova, V. and Mainardi, F. (2011) *Recent history of fractional calculus* Commun. Nonlin. Sci. Numer. Simul. **16** 1140–1153, doi:10.1016/j.cnsns.2010.05.027
- Teo, L. P. (2009) *Finite temperature Casimir effect in Kaluza-Klein spacetime* arXiv:0901.2195v1 [hep-th], Nucl. Phys. B **819** 431–452, doi:10.1016/j.nuclphysb.2009.04.013
- Todd, S. and Latham, W. (1992) *Evolutionary art and computers* Academic Press, London
- Tofighi, A. (2003) *The intrinsic damping of the fractional oscillator* Physica A **329** 29–34, doi:10.1016/S0378-4371(03)00598-3
- Torres, D. F. M. and Malinowska, A. B. (2012) *Introduction to the fractional calculus of variations* Imperial College Press, London
- Treder, H. J. (1983) *On the correlations between the particles in the EPR-paradoxon* Annalen der Physik **495** 227–230, doi:10.1002/andp.19834950407
- Troltenier, D., Maruhn, J. A., Greiner, W., Velazquez Aguilar, V., Hess, P. O. and Hamilton, J. H. (1991) *Shape transitions and shape coexistence in the Ru and Hg chains* Z. Phys. A **338** 261–270, doi:10.1007/BF01288188
- Tschirnhausen, E W. (1683) *Methodus afferendi omnes terminos intermedios ex data aequatione* Acta Eruditorum (1683) 204–207

- Tseng, C.-C. and Lee, S.-L. (2012) *Design of linear phase FIR filters using fractional derivative constraints* Sign. Proc. **92** 1317–1327, doi:10.1016/j.sigpro.2011.11.030
- Tseng, C.-C. and Lee, S.-L. (2013) *Color image sharpening based on fractional differentiation and modulation transfer function* in 2013 IEEE 17th international symposium on consumer electronics (ISCE) 201–202, IEEE.
- Uchaikin, V., Sibatov, R. and Uchaikin, D. (2009) *Memory regeneration phenomenon in dielectrics: the fractional approach* Phys. Scr. **T136** 014002, doi:10.1088/0031-8949/2009/T136/014002
- Uchaikin, V. (2012) *Fractional derivatives for physicists and engineers* Springer Berlin, Heidelberg, New York
- Uchaikin, V. and Sibatov, R. (2013) *Fractional kinetics in solids: Anomalous charge transport in semiconductors, dielectrics and nanosystems* World Scientific Publ., Singapore
- Vacaru, S. I. (2010) *Fractional dynamics from Einstein gravity, general solutions, and black holes* arXiv:1004.0628v1 [math-ph], Int. J. Theor. Physics **51** (2012) 1338–1359, doi:10.1007/s10773-011-1010-9
- Vasak, D., Shanker, R., Müller, B. and Greiner, W. (1983) *Deformed solutions of the MIT quark bag model* J. Phys. G.: Nucl. Phys. **9** 511–520, doi:10.1088/0305-4616/9/5/004
- Vautherin, D. and Brink, D. M. (1972) *Hartree-Fock calculations with Skyrme's interaction* Phys. Rev. C **5** 626–647, doi:10.1103/PhysRevC.5.626
- Villeneuve, D. M., Aseyev, S., Dietrich, P., Ivanov, M. Yu. and Corkum, P. B. (2000) *Forced molecular rotations in an optical centrifuge* Phys. Rev. Lett. **8** 542–545 doi:10.1103/PhysRevLett.85.542
- Vinci, L. da (1488) *De materia Codex Atlanticus*, Ambrosiana Library, Milan, Italy, f. 460v
- Wang, X. L. et al. Belle Collaboration (2007) *Observation of two resonant structures in $e^+e^- \rightarrow \pi^+\pi^-\psi(2S)$ via initial-state radiation at Belle* arXiv:0707.3699v2 [hep-ex], Phys. Rev. Lett. **99** 142002, doi:10.1103/PhysRevLett.99.142002
- Wang, Z. and Markham, D. (2011) *Nonlocality of symmetric states* arXiv:1112.3695v2 [quant-ph], Phys. Rev. Lett. **108** 210407 (2012), doi:10.1103/PhysRevLett.108.210407
- Wang, Z. Y. (2012) *Time operator based on the highest weight representation of a centreless Virasoro algebra* arXiv:1205.5942v1 [quant-ph]
- Wang, G.-W., Liu, X.-Q. and Zhang, Y.-Y. (2013) *Lie symmetry analysis to the time fractional generalized fifth-order KdV equation* Commun. Nonlin. Sci. Numer. Simul. **18** 2321–2326, doi:10.1016/j.cnsns.2012.11.032
- Watanabe, Y. (1931) *Notes on the generalized derivative of Riemann-Liouville and its application to Leibniz's formula* Tohoku Math. J. **34** 8–41
- Weizsäcker, C. F. von (1935) *Zur Theorie der Kernmassen* Z. Phys. **96** 431–458
- Weizsäcker, C. F. von (1939) *Der zweite Hauptsatz und der Unterschied zwischen Vergangenheit und Zukunft* Annalen der Physik **428** 275–283, doi:10.1002/andp.19394280309

- Weizsäcker, C. F. von (1985) *Aufbau der Physik* Hanser, München, Germany, translation: Görnitz, T and Lyre, H. (Eds.) *The structure of physics* (2006), Springer, Berlin, Heidelberg, New York
- Wells, H. G. (1895) *The time machine* Heinemann edition, London
- Werner, F. G. and Wheeler, J. A. (1958) *Superheavy nuclei* Phys. Rev. **109** 126–144, doi:10.1103/PhysRev.109.126
- Westerlund, S. (1991) *Dead matter has memory!* Phys. Scr. **43** 174–179, doi:10.1088/0031-8949/43/2/011
- Weyl, H. (1917) *Bemerkungen zum Begriff des Differentialquotienten gebrochener Ordnung* Vierteljahrsschr. Naturforsch. Ges. Zürich **62** 296–302
- Weyl, H. (1919) *Eine neue Erweiterung der Relativitätstheorie* Ann. d. Phys. **364** 101–133, doi:10.1002/andp.19193641002
- Weyl, H. (1927) *Quantenmechanik und Gruppentheorie* Z. Phys. **A46** 1–46, doi:10.1007/BF02055756 reprinted in Zachos, C. K, Fairlie, D. B. and Curtright, T. L. (Eds.) (2006) *Quantum mechanics in phase space* World Scientific Publ., Singapore
- Whitrow, G. J. (1955) *Why physical space has three dimensions* Br. J. Philos. Sci. **6** 13–31, doi:10.1093/bjps/VI.21.13
- Whittaker, E. T. and Watson, G. N. (1965) *A course of modern analysis* Cambridge University Press, Cambridge
- Whitten, K. W., Davis, R. E., Peck, M. L. and Stanley, G. G. (2013) *Chemistry* 10th ed. Brooks/Cole, Cengage Learning
- Wienholtz, F., Beck, D. , Blaum, K., Borgmann, Ch., Breitenfeldt, M., Cakirli, R. B., George, S., Herfurth, F., Holt, J. D., Kowalska, M., Kreim, S., Lunney, D., Manea, V., Menendez, J., Neidherr, D., Rosenbusch, M., Schweikhard, L., Schwenk, A., Simonis, J., Stanja, J., Wolf, R. N. and Zuber, K. (2013) *Masses of exotic calcium isotopes pin down nuclear forces* Nature **498** 346–349, doi:10.1038/nature12226
- Wilson, K. G. (1974) *Confinement of quarks* Phys. Rev. D **10** 2445–2459, doi:10.1103/PhysRevD.10.2445
- Wiman, A. (1905) *Über den Fundamentalsatz in der Theorie der Funktionen $E_a(x)$* Acta Math. **29** 191–201, doi:10.1007/BF02403202
- Woods, P. J. and Davids, C. N. (1997) *Nuclei beyond the proton drip-line* Ann. Rev. Nucl. Part. Sci. **47** 541–590, doi:10.1146/annurev.nucl.47.1.541
- Wolf, G. (1980) *Selected topics on e^+e^- -physics* DESY 80/13
- Wolfram, S. (2013) *Wolfram Mathematica documentation center* <http://reference.wolfram.com/mathematica/guide/Mathematica.html>.
- Wu, X. Z., Depta, K., Herrmann, R., Maruhn, J. A. and Greiner, W. (1985) *Study of dynamics in ternary fission by solving classical equations of motion II* Nuevo Cimento, **87** 309–323, doi:10.1007/BF02902224
- Yang, C. N. and Mills, R. L. (1954) *Conservation of isotopic spin and isotopic gauge invariance* Phys. Rev. **96** 191–195, doi:10.1103/PhysRev.96.191
- Yang, X. J., Srivastava, H. M., He, J. H. and Baleanu, D. (2013) *Cantor-type cylindrical-coordinate method for differential equations with local fractional derivatives* Phys. Lett. A **96** 191–195, doi:10.1016/j.physleta.2013.04.012

- Yonggang, K. and Xiu'e, Z. (2010) *Some comparison of two fractional oscillators* Physica B **405** 369–373, doi:10.1016/j.physb.2009.08.092
- Young, D. A. (1978) *On the diffusion theory of phyllotaxis* J. Theor. Biology **71** 421–432, doi:0022-5193(78)90169-8
- Yuan, L., Teitelbaum, S. W., Robinson, A. and Mullin, A. S. (2011) *Dynamics of molecules in extreme rotational states* PNAS **108** 6872–6877, doi:10.1073/pnas.1018669108
- Závada, P. J. (2000) *Relativistic wave equations with fractional derivatives and pseudo-differential operators* arXiv:hep-th/0003126v2, J. Appl. Math. **2** 163–197, doi:10.1155/S1110757X02110102 <http://projecteuclid.org/euclid.jam/1049074993>
- Zeeman, P. (1897) *The effect of magnetisation on the nature of light emitted by a substance* Nature **55** 347–347, doi:10.1038/055347a0
- Zernike, M. (1935) *Das Phasenkontrastverfahren bei der mikroskopischen Beobachtung* Z. Tech. Phys. **16** 454–457
- Zhou, W.-X. and Sornette, D. (2002) *Generalized q-analysis of log-periodicity: Applications to critical rupture* arXiv:cond-mat/0201458v1 [cond-mat.stat-mech], Phys. Rev. E **66** 046111, doi:10.1103/PhysRevE.66.046111
- Zhou, W.-X. and Sornette, D. (2003) *Non-parametric analyses of log-periodic precursors to financial crashes* arXiv:cond-mat/0205531v1 [cond-mat.stat-mech], International Journal of Modern Physics C **14** 1107–1125, doi:10.1142/S0129183103005212
- Zhu, S. (2005) *The possible interpretations of Y (4260)* arXiv:hep-ph/0507025v2, Phys. Lett. B **625** 212–216, doi:10.1016/j.physletb.2005.08.068
- Zoia, A., Rosso, A. and Kardar, M. (2007) *Fractional Laplacian in bounded domains* arXiv:0706.1254 [cond-mat.stat-mech], Phys. Rev. E **76** 021116, doi:10.1103/PhysRevE.76.021116
- Zwicky, F. (1933) *Die Rotverschiebung von extragalaktischen Nebeln* Helv. Phys. Acta **6** 110–127, republication: *The redshift of extragalactic nebulae* General Relativity and Gravitation **41** (2009) 207–224, doi:10.1007/s10714-008-0707-4

Index

- 3-sphere model, 122
action, 358
 action-at-a-distance, 185
action principle, 358
angular momentum, 196
 algebra, 214
 Casimir operator, 214
 classical, 214
angular momentum barrier, 233
anti particle, 91
asymmetric two center shell model,
 312
ATCSM, 312
B(E2)-values, 254
backward differences, 22
baryon spectrum, 280
battery memory effect, 103
Belle collaboration, 290
Bernoulli polynomial, 250
Bessel function, 158
Bessel functions
 spherical, 426
beta function, 66
Binomial coefficient, 9
blur effect, 107, 117
Boltzmann-distribution, 269
boundary conditions
 Dirichlet, 78
 mixed, 78
 Neumann, 78
box normalization, 171
box-normalization, 266
canonical quantization, 217
Casimir operator, 218, 427
Casimir-operators, 310
Cauchy's formula of repeated
 integration, 46
causality, 23, 91
CDF-collaboration, 302
central differences
 first order approximations, 186
 second order approximations, 175
centrifugal stretching, 268
charge asymmetry, 123
charged sphere, 150
charmonium, 285
chirality, 303
Christoffel symbol, 183, 202
Christoffel symbols, 371
Clifford-algebra, 201
cluster physics, 155
cluster radioactivity, 123
collective
 masses, 329
 Schrödinger equation, 329
collective coordinates, 122
 charge asymmetry, 123
 mass asymmetry, 123
 neck, 123
 two center distance, 123
collective mass parameter, 124

- collective masses, 329
- commutation relation
 - Caputo, 216
 - Liouville, 215
 - Riemann, 215
- commutation relations, 214
- compactification, 381
- complementary error function, 12
- confocal microscopy, 107
- constituent quarks, 300
- cosine integral, 12, 66
- Coulomb potential, 121, 122, 125
- covariant derivative ∇_μ , 190
- covariant fractional derivative, 354
- cranking masses, 135
- cubic equation, 399
- curvature, 330
- curvilinear coordinates, 184
- damping, 71
- dark energy, 390
- dark matter, 390
- Davidson potential, 229
- delay differential equations, 96
- delayed response, 96
- derivative
 - anti-causal, 90
 - Caputo, 52
 - causal, 90
 - covariant, 184
 - Feller, 56
 - Fourier, 45
 - Grünwald-Letnikov, 23
 - higher order, 58, 59
 - Liouville, 48
 - Liouville, inverted, 50
 - Liouville-Caputo, 50, 51
 - Marchaud, 59
 - regularized Liouville, 57
 - Riemann, 49
 - Riemann, inverted operator
 - sequence, 52
 - Riesz, 54
 - symmetric, 90
- differences
 - backward, 22
- digamma function, 12
- Dirac field, 360
- Dirac's δ -function, 92
- Dirichlet formula, 66
- duality, 142
- dynamic symmetry, 328
- Einstein's filed equations, 381
- Einstein's summation convention, 144
- elasticity theory, 58
- electromagnetic field, 361
- energy
 - classical kinetic, 124
 - equivalent sequence, 92
 - error function, 11
 - Euler γ constant, 12
 - Euler angles, 225
 - Euler operator, 216, 218
 - Euler polynomials, 249, 257, 436
 - Euler-Lagrange equations, 358, 360, 367
 - evolutionary fractional differential equations, 379
 - excitation, 71
 - expectation value, 143
 - exponential growth, 404
 - exponential integral E_n , 12
 - exponential integral Ei , 12
- factorial, 8
- factorization, 206
- Fermi energy, 135
- field strength tensor, 361
- finite differences, 22
- fission
 - double humped barrier, 100
 - lifetime, 89
 - spontaneous, 88
- fission yield, 147
- Fock space, 247
- Fock-Ivanenko coefficient, 205
- Fock-Ivanenko coefficients, 371
- Fokker-Planck equation, 138
- folded Yukawa, 122
- Fourier transform, 44
- fQCD, 210

- fractals, 142
 fractional
 space, 209
 time, 209
 fractional derivative, 15
 backward differences, 22
 Caputo, 17, 18
 causal, 22
 covariance, 354
 covariant, 109, 184, 190
 curvilinear coordinates, 184
 differential representation, 26
 exponential function, 16
 Feller, 56, 98, 108
 finite differences, 22
 Fourier, 18
 friction, 36
 generalized, 192
 Grünwald-Letnikov, 22
 Liouville, 17, 98
 Liouville-Caputo, 99
 Liouville-Liouville, 99
 multi-dimensional, 110
 powers, 16
 Riemann, 18
 Riesz, 98, 109, 175
 \mathbb{R}^N , 184
 covariant, 184
 series expansion, 18, 19, 22, 179,
 189
 tensors, 190
 trigonometric functions, 16
 fractional friction, 36
 fractional integral
 geometric interpretation, 62
 fractional QED, 210, 363, 369
 fractional rotation group, 216, 280,
 427
 fractional rotator, 224
 fractional Schrödinger equation, 191
 fractional Schrödinger equation, 145
 fractional spin, 196, 377
 fractors, 354
 fragmentation theory, 122, 147
 friction, 33
 Stokes, 35
 functional differential equations, 96
 functions
 ζ -function, 178, 188
 Bernoulli polynomial, 250
 Bessel, 266
 beta function, 66
 complementary error function, 12
 cosine integral, 12
 digamma function, 12
 error function, 11
 Euler γ constant, 12
 Euler polynomials, 249
 exponential integral E_n , 12
 exponential integral Ei , 12
 gamma function, 8
 harmonic number, 12
 Heaviside step function, 23
 Hermite, 266
 Hurwitz function, 12, 250
 hypergeometric functions, 11
 incomplete gamma function, 12
 Meijer G-function, 13
 Mittag-Leffler, 266
 Mittag-Leffler function, 11
 polygamma function, 13
 sine integral, 13
 sinus hyperbolicus, 11
 gamma function, 8
 integral representation, 8
 gauge field, 250
 gauge invariance, 369
 gauge transformation, 361
 general collective model, 328
 generalized fractional calculus, 119,
 419
 generalized fractional derivative, 99
 generalized functions, 92
 generator, 193
 genetic fractional differential
 equations, 379
 Gneuss-Greiner model, 235
 good functions, 92
 gravitational potential, 121
 group chain, 218, 280

- hadrons, 279
- Hamilton function, 144
- Hamilton operator
 - fractional, 144
- Hamiltonian
 - $C_3C_2R_3R_3$, 320
 - $SO^\alpha(9)$, 311
 - $SO^\alpha(3)$, 280
- Bohr-Mottelson, 225
- CCC, 348
- CCR, 340
- classical, 193
- CRR, 311
- fractional, 144, 193, 223
- q-deformed harmonic oscillator, 247, 249
- RRR, 347
 - strong coupling model, 255
- handedness, 303
- harmonic approximation, 233
- harmonic oscillator, 39, 69
 - fractional, 70
- Heaviside step function, 23
- Hermitian generator, 193
- Hermiticity, 191
- Hilbert space, 142, 143
- homogeneity, 219
- horror vacui, 381
- Hurwitz function, 250
- Hybrid, 289
- hyper-spherical coordinates, 156
- hypergeometric function
 - derivative, 11
- hypergeometric functions, 11
- IBM model, 235
- impetus theory, 87
- incomplete gamma function, 12
- incomplete harmonic number, 12
- incomplete Hurwitz function, 12
- infrared spectra, 268
- initial conditions, 34
- Integral
 - Liouville, 46
 - Riemann, 46
- invariance
- rotational, 196
- translational, 191
- Kaluza-Klein theory, 381
- Klein-Gordon equation, 200
- Korteweg-de Vries equation, 58
 - extended, 58
- Lagrangian density, 330
 - Dirac, 357
 - electromagnetic, 357
 - fractional, 358
 - fractional Dirac, 360
 - fractional Maxwell, 361
 - free fractional Schrödinger, 374
 - Landau-Ginzburg, 358
 - Walecka, 357
- Laguerre polynomials, 24
- Laplace equation, 218
- Laplace transform, 68
- Leibniz product rule, 20, 195, 214
- Lie group
 - angular momentum, 214
 - fractional rotation group, 197, 216
 - Poincaré, 197
- linear potential, 147, 230
- linearization, 199
- linearized Schrödinger equation, 205
- locality, 90, 184, 210
- localized wave functions, 146
- low level fractionality, 63, 64
- low-pass filter, 110
- magic numbers
 - electronic clusters, 339
 - fractional infinite potential well, 153
 - gravitational interaction, 347
 - harmonic oscillator, 348
 - metal cluster, 306
 - neutrino clusters, 350
 - nuclear, 312
 - nuclei, 306
 - weak interaction, 348
- mass asymmetry, 123
- matrix representation, 116

- Maxwell equations, 361
Meijer G-function, 13
memory effect, 23
memory effects, 100
meson spectra, 291
mesons
 D, 292
 D_s, 292
 (*B*), 293
 (*B_c*), 293
 (*B_s*), 293
 bottomonium, 293
 charmonium, 292
 kaons, 292
 light unflavored, 292
 strangeonium, 292
metric tensor, 354
Mie scattering, 100
Mittag-Leffler function, 11, 73, 74
moment of inertia, 224
multiplicity, 270
neck, 123
Newton's law
 first, 34
 second, 34
Nilsson oscillator, 312
Noether's theorem, 193
nonlocality, 23, 133, 161
 ϵ , 91
 delayed response, 96
 discrete, 96
 functional differential equations, 96
 zero, 90
nonlocalization integral, 114
normalizability, 191, 263
normalization, 145, 163
numerics
 shooting method, 263
 Taylor series, 263
one gluon exchange, 279
operators
 infinitesimal rotation, 194
 space representation, 143
orthogonal polynomials, 24
osmium isotopes, 237
pairing, 234, 303
pairing corrections, 125
pairing gap, 310
parity, 78
parity conservation, 191
parity transformation, 224
particle-hole formalism, 270, 388
Pauli equation, 208
Pauli matrices, 201
Pauli-Lubanski vector, 197
photon absorption, 269
piecewise solution, 151
piecewise solutions, 104
pinhole camera, 117, 118, 418
Poincaré group, 197
polygamma function, 13
position operator, 266
potential
 box, 154
 Coulomb, 121, 122
 curvature, 330
 gravitational, 121
 harmonic oscillator, 154
 Nilsson, 125
 pairing, 131
 Riesz, 122
 single particle, 121
 sphere, 128, 154
 spin-orbit term, 125
 surface, 131
 symmetry, 131
 volume, 131
 Woods-Saxon, 122
 Yukawa, 122
potential energy surfaces, 326
potential minimum, 69
potential well, 150, 163
 spherical, 427
predicted particles
 B₂^{}(5818)*, 299
 X(4260), 291
 X(4660), 291
 $\psi(5S)(4790)$, 290
 $b^* \bar{b}^*(j = 5)38.4[\text{GeV}]$, 300

- $b^*\bar{b}^*(j=6)153.6[\text{GeV}]$, 300
- q-deformed harmonic oscillator, 246
q-deformed Lie algebra, 245
q-deformed symmetric rotor, 254
 $B(E2)$ -values, 254
- QCD, 210, 363, 369
- QED, 210, 363, 369
fractional, 363, 369
- quadratic pinhole camera, 118, 418
- quantization
canonical, 143
path-integrals, 143
phase space, 143
stochastic, 143
- quantization condition, 219
- quantum chromodynamics, 279, 369
- quantum mechanics, 69, 143
duality, 142
Hilbert space, 142
- quark confinement, 146, 279
- quarks, 146
- quintic equation, 399
- Racah's SU(2) pairing model, 310
- radium isotopes, 241
- RC-circuit, 101
- regular sequence, 92
- Riesz
Euler-Lagrange equations, 367
Riesz integral, 54
Riesz potential, 54
- rotation, 227
- rotation group
fractional, 217
- rotational spectrum, 227
- Ruthenium isotopes, 326
- scalar product, 56, 143, 359
- Schrödinger equation, 69
fractional, 144
fractional harmonic oscillator, 249
- shell corrections, 125, 234
- shell model of nuclei, 155
- sine integral, 13, 66
- sinus hyperbolicus, 11
 $\text{SO}^\alpha(3)$
half integer representation, 255
- $\text{SO}(9)$, 306
- SO_3 , 305
- solitons, 58
- space dimensions, 271
- space-antispace formalism, 388
- speed of light, 390
- spherical Bessel function, 426
- spherical Bessel functions
zeros, 426
- spherical harmonics, 426, 427
- spherical infinite potential well, 427
- spin
fractional, 196
spinors, 430
standard model, 299
- statistics
Bose-Einstein, 305
Fermi-Dirac, 305
- Stirling's formula, 403
- strong coupling model, 255
- $\text{SU}(2)$, 310
- super heavy elements, 242
- symmetries
geometric interpretation, 261
 $\text{SO}(3)$, 261
Casimir operators, 220
- $\text{SO}(9)$, 306
- $\text{SO}(n)$
Casimir operators, 220
- $\text{SU}(2)$, 199, 310
- $\text{SU}(3)$, 207
- $\text{U}(1)$, 261, 310
- $\text{U}(3)$, 305
- Taylor series expansion, 408
- temperature, 147
- tensor calculus, 353
- tensors, 190
- thermodynamics, 273
- time delay, 96
- translational invariance, 151, 191
- transmutation, 262
- triaxiality, 326

- Tschirnhausen transformation, 398
- tunnel effect, 88
- two center distance, 123
-
- U(1), 310
- U(1) number operator, 314
- U(3), 305
-
- vacuum state, 246
- vanishing collective potential, 234
- vibration, 228
- vibrational spectrum, 227
-
- wave equation
 - fractional, 77
 - regularized, 79
- membrane, 69
-
- string, 69
- vibrating string, 78
- zeros of solution, 85, 86
- weight, 92
- WKB-approximation, 89, 171, 249, 260, 384
- Woods-Saxon potential, 122
-
- X(4260), 289
-
- Yang-Mills field theory, 207
- Yukawa function, 124
- Yukawa single particle potential, 122
-
- Zeeman effect, 374
- zero-point energy, 228, 243, 303
- zeros, 81